UNCLASSIFIED

AD NUMBER

AD828948

NEW LIMITATION CHANGE

TO

Approved for public release, distribution unlimited

FROM

Distribution authorized to U.S. Gov't. agencies and their contractors; Critical Technology; MAR 1968. Other requests shall be referred to Naval Ship Engineering Center, Washington, DC 20360.

AUTHORITY

USNSEC ltr 11 Oct 1974

THIS PAGE IS UNCLASSIFIED

UNIVERSITY
OF
MARYLAND

AD828948

COLLEGE OF ENGINEERING
GLENN L. MARTIN INSTITUTE OF TECHNOLOGY
WIND TUNNEL OPERATIONS DEPARTMENT

BEST AVAILABLE COPY

College Park, Maryland

STATEMENT #2 UNCLASSIFIED

This document is subject to special export controls and each transmittal to foreign governments or foreign nationals may be made only with prior approval of NAVAL SHIP ENGINEERING CENTER
Code 6136-B
Washington, D. C. 20360

UNIVERSITY OF MARYLAND
WIND TUNNEL REPORT NO. 485

EFFECTS OF STREAMWISE GAPS, HULL FLOW AND PROPELLER SLIPSTREAM UPON THE AERODYNAMIC CHARACTERISTICS OF A FAMILY OF LOW-ASPECT RATIO, ALL-MOVEABLE CONTROL SURFACES

Prepared by: R. I. Windsor
R. I. Windsor

Approved by: Donald S. Gross
Donald S. Gross
Director, Wind Tunnel

PERFORMED UNDER NAVAL SHIP SYSTEMS COMMAND CONTRACT N00024-67-C-5149
PROJECT SERIAL NO. 5F-13-02-64; Task 1712

DDC
RECEIVED
MAR 26 1968
A

ABSTRACT

Effects of faired, streamwise gaps upon the free stream characteristics of a family of low-aspect-ratio, all-moveable control surfaces are presented. The family of control surfaces consisted of three aspect ratios (1, 2, and 3) and three sweep angles (0, 11, and 22.5 degrees), each having a NACA 0015 airfoil section and a taper ratio of 0.45. Gap effects were also investigated in conjunction with simulated hull effects. Propeller slipstream effects were determined for the minimum gap condition.

TABLE OF CONTENTS

	Page
INTRODUCTION	1
DESCRIPTION OF MODELS	1
TEST PROCEDURE	2
PRESENTATION OF DATA	3
DISCUSSION OF RESULTS	4
Free Stream Gap Effects	4
Free Stream Gap Effects Upon Lift	5
Free Stream Gap Effects Upon Drag	6
Free Stream Gap Effects Upon Chordwise Center of Pressure Location	6
Free Stream Gap Effects Upon Spanwise Center of Pressure Location	7
Summary of Free Stream Gap Effects	8
Gap Effects With Simulated Hull	8
Simulated Hull Flow and Propeller Slipstream Effects	9
CONCLUSIONS AND RECOMMENDATIONS	12
ACKNOWLEDGEMENTS	13
REFERENCES	14
TABLE	15
FIGURES	16

APPENDIX	A	Free Stream Characteristics for Various Gap Sizes	101
APPENDIX	B	Simulated Hull Flow Characteristics for Various Gap Sizes	185
APPENDIX	C	Combined Simulated Hull Flow and Propeller Slipstream Characteristics, Minimum Gap	255

INDEX OF FIGURES

Fig. No.	Title	Page
1	Basic Dimensions, AR = 1, Λ = 0°	16
2	Basic Dimensions, AR = 1, Λ = 11°	17
3	Basic Dimensions, AR = 1, Λ = 22.5°	18
4	Basic Dimensions, AR = 2, Λ = 0°	19
5	Basic Dimensions, AR = 2, Λ = 11°	20
6	Basic Dimensions, AR = 2, Λ = 22.5°	21
7	Basic Dimensions, AR = 3, Λ = 0°	22
8	Basic Dimensions, AR = 3, Λ = 11°	23
9	Basic Dimensions, AR = 3, Λ = 22.5°	24
10	Fairing Details, AR = 1, Λ = 0°	25
11	Fairing Details, AR = 3, Λ = 22.5°	26
12	Aspect Ratio 1, Λ = 11°, Control Surface Mounted on Tunnel Floor With Minimum Gap	27
13	Aspect Ratio 1, Λ = 22.5°, Control Surface With 4.5 in. Gap, α = 35°	27
14	Aspect Ratio 2, Λ = 0°, Control Surface With 12.0 in. Gap, α = 0°	28
15	Aspect Ratio 2, Λ = 11°, Control Surface With 4.5 in. Gap, α = 30°	28
16	Turning Vanes and Screen Installed at Leading Edge of Test Section to Simulate Hull Flow Conditions	29
17	Propeller and Drive Motor Installed With Turning Vanes and Screen	29
18	Free Stream Faired Gap Effects on Lift Coefficient, Aspect Ratio 1, Λ = 0°	30
19	Free Stream Faired Gap Effects on Lift Coefficient, Aspect Ratio 1, Λ = 11°	31
20	Free Stream Faired Gap Effects on Lift Coefficient, Aspect Ratio 1, Λ = 22.5°	32
21	Free Stream Faired Gap Effects on Lift Coefficient, Aspect Ratio 2, Λ = 0°	33
22	Free Stream Faired Gap Effects on Lift Coefficient, Aspect Ratio 2, Λ = 11°	34
23	Free Stream Faired Gap Effects on Lift Coefficient, Aspect Ratio 2, Λ = 22.5°	35
24	Free Stream Faired Gap Effects on Lift Coefficient, Aspect Ratio 3, Λ = 0°	36
25	Free Stream Faired Gap Effects on Lift Coefficient, Aspect Ratio 3, Λ = 11°	37
26	Free Stream Faired Gap Effects on Lift Coefficient, Aspect Ratio 3, Λ = 22.5°	38

INDEX OF FIGURES (continued)

Fig. No.	Title	Page
27	Free Stream, Faired Gap Effects on Drag Coefficient, Aspect Ratio 1, $\Lambda = 0°$	39
28	Free Stream, Faired Gap Effects on Drag Coefficient, Aspect Ratio 1, $\Lambda = 11°$	40
29	Free Stream, Faired Gap Effects on Drag Coefficient, Aspect Ratio 1, $\Lambda = 22.5°$	41
30	Free Stream, Faired Gap Effects on Drag Coefficient, Aspect Ratio 2, $\Lambda = 0°$	42
31	Free Stream, Faired Gap Effects on Drag Coefficient, Aspect Ratio 2, $\Lambda = 11°$	43
32	Free Stream, Faired Gap Effects on Drag Coefficient, Aspect Ratio 2, $\Lambda = 22.5°$	44
33	Free Stream, Faired Gap Effects on Drag Coefficient, Aspect Ratio 3, $\Lambda = 0°$	45
34	Free Stream, Faired Gap Effects on Drag Coefficient, Aspect Ratio 3, $\Lambda = 11°$	46
35	Free Stream, Faired Gap Effects on Drag Coefficient, Aspect Ratio 3, $\Lambda = 22.5°$	47
36	Free Stream, Faired Gap Effects on Chordwise Center of Pressure, Aspect Ratio 1, $\Lambda = 0°$	48
37	Free Stream, Faired Gap Effects on Chordwise Center of Pressure Aspect Ratio 1, $\Lambda = 11°$	49
38	Free Stream Faired Gap Effects on Chordwise Center of Pressure Aspect Ratio 1, $\Lambda = 22.5°$	50
39	Free Stream, Faired Gap Effects on Chordwise Center of Pressure Aspect Ratio 2, $\Lambda = 0°$	51
40	Free Stream, Faired Gap Effects on Chordwise Center of Pressure Aspect Ratio 2, $\Lambda = 11°$	52
41	Free Stream, Faired Gap Effects on Chordwise Center of Pressure, Aspect Ratio 2, $\Lambda = 22.5°$	53
42	Free Stream, Faired Gap Effects on Chordwise Center of Pressure, Aspect Ratio 3, $\Lambda = 0°$	54
43	Free Stream, Faired Gap Effects on Chordwise Center of Pressure, Aspect Ratio 3, $\Lambda = 11°$	55
44	Free Stream, Faired Gap Effects on Chordwise Center of Pressure, Aspect Ratio 3, $\Lambda = 22.5°$	56
45	Free Stream, Faired Gap Effects on Spanwise Center of Pressure Aspect Ratio 1, $\Lambda = 0°$	57
46	Free Stream, Faired Gap Effects on Spanwise Center of Pressure Aspect Ratio 1, $\Lambda = 11°$	58
47	Free Stream, Faired Gap Effects on Spanwise Center of Pressure Aspect Ratio 1, $\Lambda = 22.5°$	59

INDEX OF FIGURES (continued)

Fig. No.	Title	Page
48	Free Stream, Faired Gap Effects of Spanwise Center of Pressure, Aspect Ratio 3, $\Lambda = 0°$	60
49	Free Stream, Faired Gap Effects of Spanwise Center of Pressure, Aspect Ratio 3, $\Lambda = 11°$	61
50	Free Stream, Faired Gap Effects of Spanwise Center of Pressure, Aspect Ratio 3, $\Lambda = 22.5°$	62
51	Wake Velocity Diagram From Figure 11 of Reference 6	63
52	Wake Velocity Diagram For Simulated Hull Flow	64
53	Faired Gap Effects on Lift Coefficient For Simulated Hull Flow, Aspect Ratio 2, $\Lambda = 0°$	65
54	Faired Gap Effects on Drag Coefficient For Simulated Hull Flow, Aspect Ratio 2, $\Lambda = 0°$	66
55	Faired Gap Effects on Chordwise Center of Pressure For Simulated Hull Flow, Aspect Ratio 2 $\Lambda = 0°$	67
56	Faired Gap Effects on Spanwise Center of Pressure For Simulated Hull Flow, Aspect Ratio 2, $\Lambda = 0°$	68
57	Velocity Field at Rudder Leading Edge, From Figure 5 of Reference 7	69
58	Propeller Slipstream Velocity Survey at Rudder Leading Edge, Aspect Ratio 1	70
59	Propeller Slipstream Velocity Survey at Rudder Leading Edge, Aspect Ratio 2	71
60	Propeller Slipstream Velocity Survey at Rudder Leading Edge, Aspect Ratio 3	72
61	Comparison of Lift Coefficients For Free Stream, Simulated Hull Flow and Propeller Slipstream Conditions Aspect Ratio 1, $\Lambda = 0°$	73
62	Comparison of Lift Coefficients For Free Stream, Simulated Hull Flow and Propeller Slipstream Conditions Aspect Ratio 1, $\Lambda = 11°$	74
63	Comparison of Lift Coefficients For Free Stream, Simulated Hull Flow and Propeller Slipstream Conditions Aspect Ratio 1, $\Lambda = 22.5°$	75
64	Comparison of Lift Coefficients For Free Stream, Simulated Hull Flow and Propeller Slipstream Conditions Aspect Ratio 2, $\Lambda = 0°$	76
65	Comparison of Lift Coefficients For Free Stream, Simulated Hull Flow and Propeller Slipstream Conditions Aspect Ratio 2, $\Lambda = 11°$	77
66	Comparison of Lift Coefficients For Free Stream, Simulated Hull Flow and Propeller Slipstream Conditions Aspect Ratio 2, $\Lambda = 22.5°$	78

INDEX OF FIGURES (continued)

Fig. No.	Title	Page
67	Comparison of Lift Coefficients For free Stream, Simulated Hull Flow and Propeller Slipstream Conditions, Aspect Ratio 3, $\Lambda = 0°$	79
68	Comparison of Lift Coefficients For Free Stream, Simulated Hull Flow and Propeller Slipstream Conditions, Aspect Ratio 3, $\Lambda = 11°$	80
69	Comparison of Lift Coefficients For Free Stream, Simulated Hull Flow and Propeller Slipstream Conditions, Aspect Ratio 3, $\Lambda = 22.5°$	81
70	Comparison of Drag Coefficients For Free Stream, Simulated Hull Flow and Propeller Slipstream Conditions, Aspect Ratio 1, $\Lambda = 0°$	82
71	Comparison of Drag Coefficients For Free Stream, Simulated Hull Flow and Propeller Slipstream Conditions, Aspect Ratio 1, $\Lambda = 11°$	83
72	Comparison of Drag Coefficients For Free Stream, Simulated Hull Flow and Propeller Slipstream Conditions, Aspect Ratio 1, $\Lambda = 22.5°$	84
73	Comparison of Drag Coefficients For Free Stream, Simulated Hull Flow and Propeller Slipstream Conditions, Aspect Ratio 2, $\Lambda = 0°$	85
74	Comparison of Drag Coefficients For Free Stream, Simulated Hull Flow and Propeller Slipstream Conditions, Aspect Ratio 2, $\Lambda = 11°$	86
75	Comparison of Drag Coefficients For Free Stream, Simulated Hull Flow and Propeller Slipstream Conditions, Aspect Ratio 2, $\Lambda = 22.5°$	87
76	Comparison of Drag Coefficients For Free Stream, Simulated Hull Flow and Propeller Slipstream Conditions, Aspect Ratio 3, $\Lambda = 0°$	88
77	Comparison of Drag Coefficients For Free Stream, Simulated Hull Flow and Propeller Slipstream Conditions, Aspect Ratio 3, $\Lambda = 11°$	89
78	Comparison of Drag Coefficients For Free Stream, Simulated Hull Flow and Propeller Slipstream Conditions, Aspect Ratio 3, $\Lambda = 22.5°$	90
79	Comparison of Center of Pressure For Free Stream, Simulated Hull Flow and Propeller Slipstream Conditions, Aspect Ratio 1, $\Lambda = 0°$	91
80	Comparison of Center of Pressure For Free Stream, Simulated Hull Flow and Propeller Slipstream Conditions, Aspect Ratio 1, $\Lambda = 11°$	92

INDEX OF FIGURES (continued)

Fig. No.	Title	Page
81	Comparison of Center of Pressure For Free Stream, Simulated Hull Flow and Propeller Slipstream Conditions, Aspect Ratio 1, Λ = 22.5°	93
82	Comparison of Center of Pressure For Free Stream, Simulated Hull Flow and Propeller Slipstream Conditions, Aspect Ratio 2, Λ = 0°	94
83	Comparison of Center of Pressure For Free Stream, Simulated Hull Flow and Propeller Slipstream Conditions, Aspect Ratio 2, Λ = 11°	95
84	Comparison of Center of Pressure For Free Stream, Simulated Hull Flow and Propeller Slipstream Conditions, Aspect Ratio 2, Λ = 22.5°	96
85	Comparison of Center of Pressure For Free Stream, Simulated Hull Flow and Propeller Slipstream Conditions, Aspect Ratio 3, Λ = 0°	97
86	Comparison of Center of Pressure For Free Stream, Simulated Hull Flow and Propeller Slipstream Conditions, Aspect Ratio 3, Λ = 11°	98
87	Comparison of Center of Pressure For Free Stream, Simulated Hull Flow and Propeller Slipstream Conditions, Aspect Ratio 3, Λ = 22.5°	99

NOTATION

AR	Effective aspect ratio, two times geometric aspect ratio, $2\frac{b^2}{S}$
b	Control surface span, feet
c	Chord, measured parallel to plane of root section, feet
$\bar{c}$	Mean geometric chord, $\frac{c_t + c_r}{2}$, feet
C_D	Drag coefficient, $\frac{D}{qS}$
C_L	Lift coefficient, $\frac{L}{qS}$
$C_{\mathfrak{L}}$	Rolling moment coefficient, $\frac{\mathfrak{L}}{qSb}$
C_m	Pitching moment coefficient about the quarter chord point of the mean geometric chord, $\frac{M}{qS\bar{c}}$
C_n	Yawing moment coefficient, $\frac{N}{qS\bar{c}}$
$(CP)_{\bar{c}}$	Chordwise center of pressure measured from leading edge at mean geometric chord in per cent of the mean geometric chord, $(CP)_{\bar{c}} = 0.25 - \frac{C_m}{C_L \cos\alpha + C_D \sin\alpha}$
$(CP)_s$	Spanwise center of pressure measured from plane of root section in per cent of control surface span, $(CP)_s = \frac{C_{\mathfrak{L}} \cos\alpha - C_n \sin\alpha}{C_L \cos\alpha + C_D \sin\alpha}$
D	Drag force, pounds
L	Lift force, pounds
$\mathfrak{L}$	Rolling moment, foot pounds

M	Pitching moment, foot pounds
N	Yawing moment, foot pounds
q	Dynamic pressure, $1/2\ \rho V^2$, pounds per square foot
RN	Reynolds number, $\frac{\rho V \bar{c}}{\mu}$
s	Gap width, inches
S	Control surface area, $\bar{c}b$, square feet
V	Free stream velocity, feet per second
V_t	Tangential component of velocity measured in the plane of the propeller, feet per second
V_r	Radial component of velocity measured in the plane of the propeller, feet per second
V_{tr}	Transverse component of velocity, vector sum of V_t and V_r, feet per second
V_x	Velocity component in streamwise direction, feet per second
α	Angle of attack, degrees
λ	Taper ratio, c_t/c_r
Λ	Sweepback angle of quarter-chord line, degrees
μ	Coefficient of viscosity of air, pound second per square foot
ρ	Mass density of air, slugs per cubic foot

SUBSCRIPTS

r	Root
t	Tip

INTRODUCTION

Considerable information on the free stream characteristics of low-aspect-ratio control surfaces is available from various wind tunnel tests (Reference 1). The most comprehensive of these tests are those rported in Reference 2. While the information obtained from the wind tunnel tests is quite valuable to the control surface designer, it is not usually directly applicable to the design problem. The tunnel tests are usually conducted in a uniform flow field with minimum clearance between the root chord of the control surface and the tunnel boundary. Whereas, an actual control surface normally operates with an appreciable gap between the root chord and the ship hull in a stream that may be disturbed by the hull effects and propelier slipstream.

In recognition of the need for additional information on gap, hull and propeller slipstream effects, a three part wind tunnel test program was undertaken. A family of nine low-aspect-ratio, all moveable control surfaces was used for test purposes. Each surface had a NACA 0015 airfoil section, square tip and a taper ratio of 0.45. Effective aspect ratios of 1, 2, and 3 and quarter chord sweep angles of 0, 11 and 22.5 degrees were employed. Faired gaps of up to 40% of the planform mean chord were tested. Using these models, the test was broken into the following three parts:

1. Free stream gap effects
2. Gap with simulated hull flow
3. Combined simulated hull flow and propeller slipstream effects for the minimum gap configurations.

Throughout this report, the "aspect ratio" referred to is the effective aspect ratio when the model is mounted on the tunnel floor. In this type of installation, the control surface is considered as a reflection plane model (with the tunnel floor as the reflection plane) having an effective aspect ratio equal to twice the geometric aspect ratio.

DESCRIPTION OF MODELS

Nine all-moveable control surface models were constructed. Each model had a 30 in. mean geometric chord, NACA 0015 airfoil section, square tip and 0.45 taper ratio. Three models each of effective

aspect ratio 1, 2 and 3 were made. For each aspect ratio, models having quarter chord sweep angles of 0, 11 and 22.5 degrees were constructed. The model planforms are presented in Figures 1 - 9. Each surface was constructed in such a manner that a support strut could be attached at the root chord at the axis of rotation. The axis of rotation was perpendicular to the mean geometric chord at the 25% mean chord point. The length of the support strut could be varied to change the gap size.

All gaps employed during the test were faired gaps. That is, a fairing piece was positioned between the root chord of the surface and the tunnel floor. The fairing piece stayed aligned at zero angle with the free stream when the control surface was rotated. The fairing pieces were constructed as extensions of the control surfaces. Figures 10 and 11 are drawings showing the details of two of the fairings while photographs of the models and fairings are presented in Figures 12-15.

TEST PROCEDURE

The control surfaces were mounted on the floor of the 7.75 foot by 11 foot test section of the wind tunnel with the support strut located on the vertical axis of the balance system. Force and moment measurements were made using the wind tunnel six-component balance system. Gap fairing pieces were mounted on the tunnel floor but not attached to the balance system so that only those aerodynamic forces and moments acting on the control surface were recorded. The free stream gap effect runs were conducted at a dynamic pressure, q, of 43.235 pounds per square foot (indicated airspeed of 130 mph). The Reynolds number based upon the mean geometric chord length was 3.04×10^6.

Lift forces acting on the model mounted on the tunnel floor produced large rolling moments at the balance center (center line of test section). In order to keep the rolling moments from exceeding the balance limits at the desired Reynolds number, it was necessary to preload the balances. This was accomplished by placing a large static load on the balance turntable that produced a rolling moment that increased with angle of attack in the opposite direction of that caused by the model lift. Wind off static tare runs were made to obtain these corrections to the rolling moment.

Each of the nine control surfaces was tested to obtain the free stream gap effects. At least 6 gaps were tested for each surface. The gaps varied from a minimum of approximately 0.10 in. to 12 in. for the aspect-ratio 1 and 2 surfaces and up to 18 in. for the aspect ratio 3 surfaces. This corresponds to a maximum gap of 80% of the control surface span for the aspect ratio 1 surfaces and 40% of the span for the aspect ratio 2 and 3 surfaces.

After obtaining the free stream data, vanes and screen were installed at the entrance of the test section to produce a flow angularity and velocity gradient similar to that existing in actual conditions in the proximity of a ship hull. Figure 16 shows the vanes installed in the tunnel. The tunnel speed was adjusted to give the same velocity in the undisturbed flow as was used for the free stream tests. All of the control surfaces were tested for various gaps in this simulated hull flow.

To obtain slipstream effects, a 4 ft. diameter propeller was mounted between the hull simulation vanes and the control surface (Figure 17). Thus, the slipstream flow was superposed upon the simulated hull flow. For this condition, the nine control surfaces were tested only in the minimum gap position. To maintain the desired slipstream to free stream velocity ratio and not exceed the maximum propeller rpm, it was necessary to reduce the tunnel speed. This series of tests was conducted at a dynamic pressure of 18.92 pounds per square inch (indicated airspeed of 86 mph). The Reynolds number was 2.0×10^6. To obtain a direct comparison with the free stream conditions, test runs were made for the minimum gap in the free stream at this lower value of Reynolds Number.

The angle of attack range was zero to $\pm 45°$, except in a few instances where the model stalled at a slightly higher angle of attack.

PRESENTATION OF DATA

Results of the test are presented in nondimensional plotted form in Appendices A - C. These plots show lift and drag coefficients and chordwise and spanwise centers of pressure versus angle of attack. Data have been corrected for tunnel wall effects by computing the standard tunnel wall corrections for each control surface in the minimum gap configuration and applying these corrections to each run for that surface regardless of the gap size.

The effect of varying the gap size is shown in Figures 18-50 Whereas, Figures 61-87 show the effects of the hull simulation and propeller slipstream.

DISCUSSION OF RESULTS

FREE STREAM GAP EFFECTS

Due to the pressure differential across the gap on a lifting surface, air, or water in the case of ships, will leak through, thereby affecting the aerodynamic characteristics. Gap effects are treated theoretically in References 3 and 4. Theoretical results, neglecting the effects of viscosity, indicate large corrections to the pressures and velocities in the immediate vicinity of the gap. Theoretically, even small gaps result in very large loses in lift. However, in practical applications, viscous effects would alter the predicted theoretical results, especially when the gap is small.

Experimental data on gap effects suitable for control surfaces design is lacking. Due to the lack of experimental data, the author undertook an exploratory test (Reference 5) to determine experimentally the effects of a streamwise gap upon the aerodynamic characteristics of a representative all moveable control surface. The control surface used for this investigation had an effective aspect ratio of 2, a taper ratio of 0.45, quarter chord sweep of 22.5°, and a NACA 0015 airfoil section. Tests were conducted with an unfaired gap varying in size up to 4 inches or approximately 10 percent of the control surface span. Results of this study indicated that the gap effects upon the lift and drag values were considerably less than theoretical predictions, whereas, the effects upon the chordwise center of pressure shift were greater. This investigation resulted in the conclusion that it would be desirable to pursue the gap effect investigation for increased gap size and various surface geometries. The data presented in this report aid in fulfilling this need.

All gaps tested during this investigation were faired since this more nearly approximates the general condition for ship uses. The data presented in Reference 5 are for unfaired gaps.

Some of the control surfaces used in this investigation are similar to those used in the tests reported in Reference 2. The aerodynamic data for the minimum gap runs from this test should and do agree with the results presented in Reference 2. The force coefficients presented in the basic data (Appendix A) of this report are slightly lower, especially for the aspect ratio 1 surfaces. The reason the results of this

test are lower is that no correction for the boundary layer build up on the tunnel floor, at the control surface root chord, has been applied. This region of reduced velocity in the boundary layer exte is approximately 2.2 in. above the tunnel floor. This reduced velocity region covers a sizeable portion of the aspect ratio 1 control surfaces which have a span of only 15 in. The effects of the boundary layer are less noticeable for the aspect ratio 2 and 3 surfaces which have larger spans. This boundary layer correction has not been applied to data presented in this report, since this is part of the gap effects which are of interest.

Free Stream Gap Effects Upon Lift

Free stream gap effects upon the control surface lift are presented in Figures 18-26. The data presented in these figures are cross plots of the lift coefficient for selected values of angle of attack, α, versus gap size. Representative angles of attack below the stall, an angle of attack close to the stall angle (approximately $C_{L_{max.}}$) and angles above stall, where appropriate, were selected. At low angles of attack, the gap fairing essentially eliminates any gap effects. This is evidenced in the cross plots.

A study of the cross plots reveals that the gap effects change with variation in the quarter chord sweep angle, whereas, a change in aspect ratio has little or no influence upon the gap effects. At a quarter chord sweep angle of zero degrees, the lift coefficient drops off as the gap is increased up to 1.25 in. then increases with increase in gap up to about 4 in. then decreases slowly as the gap increases to the maximum tested. The minimum lift coefficient, a little over 90% of the value obtained at minimum gap, occurs at the 1.25 in. gap. At the maximum gap, the lift coefficient is approximately 95% of the minimum gap value. For the 11 degree sweep angle, the lift coefficient decreases for small gaps, then increases slightly before dropping off at the large gap. The value of the lift coefficient does not drop below about 94% of the minimum gap value for this sweep angle. For the 22.5 degree sweep angle, the lift coefficient drops off as the gap increases up to about 3 in., then remains essentially constant. The lift coefficient at maximum gap is approximately 94% of that at minimum gap. When viewed in the light of the large lift loses expected from theoretical considerations, the observed loses are very moderate even for the most severe case.

The cross plots for the aspect ratio 1 control surfaces indicate a combination of the gap effects and an increased velocity effect, obtained by moving the control surface out of the boundary layer into the free stream as the gap increases. This velocity effect is evident for the

low angle of attack curves where the gap effects are negated by the fairings.

Lift data for angles of attack above the stall angle are faired with dashed lines to indicate the uncertainty of the values obtained in the stalled situation.

Data are presented for positive angles of attack only, since the airfoil sections are symmetrical and the results should be the same in either direction.

Free Stream Gap Effects Upon Drag

Drag coefficients cross plotted against gap size are presented in Figures 27-35 for representative angles. Generally speaking, the drag coefficients increase with increasing gap size in the small gap region (up to 2 or 3 in.) then decrease steadily as the gap approaches the maximum value. The final drag coefficient for the maximum gap condition is usually close to the minimum gap value. Overall gap effects upon the drag are small with no noticeable changes due to quarter chord sweep angle or aspect ratio.

Minimum drag coefficients (α = 0°) decrease slightly with gap size for most of the configurations. Since the gaps are faired in all cases, a change in drag would not be expected at α = 0°. This reduction in drag is probably due to a reduction in the interference drag at the intersection of the model and the tunnel floor. In actual installations, this drag would still be present but would be acting upon the fairing piece instead of the control surface.

Curves for the angles of attack greater than the stall angle of attack are faired with dashed lines to indicate the uncertainty of these values.

Free Stream Gap Effects Upon Chordwise Center of Pressure Location

Cross plots of the chordwise center of pressure locations against gap size for selected angle of attack values are presented in Figures 36-44. As was noticed for the forces, the fairing pieces eliminate gap effects in the lower angle of attack range. For the aspect ratio 1 control surfaces, the chordwise center of pressure moves aft approximately 1.5 to 2 percent as the gap is increased from the minimum value to 2.0 or 2.5 in. As the gap size increases above this value, there is very little change in the center of pressure location. For the aspect ratio 2 and 3 control surfaces, the center

of pressure moves aft as the gap size is increased (up to 1.5 to 3.0 in., depending on the quarter chord sweep angle) then moves forward with increasing gap size. The maximum rearward center of pressure shift varies with the sweep angle, decreasing with increasing quarter chord sweep. The maximum center of pressure shift is about 4 percent and occurs at a 1.5 in. gap for a sweep angle of zero degrees. The chordwise center of pressure location for the maximum gap size tested was always aft of the minimum gap size location. However, this shift did not exceed 2 percent of the chord length for any of the control surfaces tested.

Free Stream Gap Effects Upon Spanwise Center of Pressure Location

Spanwise center of pressure location cross plots are presented in Figures 45-50. Before reviewing these, it is necessary to discuss the accuracy of the spanwise center of pressure calculations. As was mentioned previously, the control surfaces were mounted on the tunnel floor. This produced large rolling moments about the balance center, which is located on the test section center line. In order to keep the rolling moment balance from reaching the limit of its travel, large weights were placed on the balance turntable which produced a static variation with angle of attack that counterbalanced the aerodynamic rolling moment. Since this variation of rolling moment with angle was large, a small error in setting the angle produced appreciable errors in the rolling moment. In percent of total rolling moment experienced, the errors were quite small, but in the low angle of attack region where the aerodynamic forces are relatively small, the error becomes appreciable. It is estimated that the error in rolling moment is ±2.5 ft. lbs. With spanwise center of pressure defined as follows:

$$(CP)_s = \frac{C_\ell \cos\alpha - C_n \sin\alpha}{C_L \cos\alpha + C_D \sin\alpha}$$

it is seen that an error in rolling moment, C_ℓ, will cause a sizeable error in $(CP)_s$ at small values of angle of attack, α, where the lift and drag values are small. At larger values of α, lift and drag become greater decreasing the effect of the error in rolling moment. It is also evident that the error will be greater for the small aspect ratio control surface since the aerodynamic forces are smaller. For the aspect ratio 1 control surfaces, the error in $(CP)_s$ is considerable throughout the whole range of angle of attack. The data are presented in the plots of the basic data in Appendix A, but due to the scatter, no cross plots are presented. The data for the high angle of attack on the aspect ratio 2 surfaces are within ±1 percent and aspect ratio 3 data is not affected appreciably by the error in rolling moment.

A look at the spanwise center of pressure location cross plots shows that the gap effect is negligible in the data presented.

Summary of Free Stream Gap Effects

Free stream gap effects are considerably less than would be expected from theoretical considerations for the control surfaces tested. Aspect ratio appears to have no bearing upon the gap effects. There is a change in gap effects with variation in the quarter chord sweep angle, with the greatest effects occurring for zero sweep angle. Generally speaking, the maximum effects are in the region of small gaps (2 to 3 in.) with the effects diminishing as the gap increases. The fact that maximum gap effects occur in the 2 to 3 in. region (not a certain percent of span) may be a consequence of the boundary layer on the tunnel floor, which is approximately 2.20 in. thick. It is possible that a different boundary layer thickness may change the region of maximum gap effects. No attempt was made during this investigation to validate this statement.

GAP EFFECTS WITH SIMULATED HULL

For the purpose of hull simulation, it was decided to attempt to duplicate the wake velocity diagram of Figure 11 of Reference 6. This figure has been reproduced for convenience as Figure 51 in this report. Turning vanes and screens were installed in the entrance to the test section as shown in Figure 16 to produce the desired flow angularity and velocity gradient. The resulting flow distribution is presented in Figure 52. A comparison of Figures 51 and 52 shows that a reasonable simulation was obtained. A comparison of the streamwise components of velocity are presented in Table I.

With the simulated hull flow, gap effects become enmeshed with the velocity gradient effects. As the gap size is increased, the control surface moves into a higher average velocity stream. Since all force coefficients are based upon the free stream velocity, a reduced velocity near the hull results in reduced values of the coefficients. Therefore, the force coefficients increase as the gap size increases due to increased velocity over the control surface.

In the free stream investigation, it was found that gap effects on the configurations tested were relatively small. For this reason, only the data for the control surface exhibiting the greatest gap effects (aspect ratio 2, quarter chord sweep angle equal zero degrees) are presented in

the cross plots of Figures 53-56. As was noted previously in the free stream condition, gap effects at small angles of attack are negligible due to the fairing pieces.

Comparing Figures 21 and 53, the gap effects upon the lift coefficient in the small gap region, where velocity gradient effects are small, show the same characteristics for both free stream and simulated hull effects. As the gap is increased, the effects of the velocity gradient for the simulated hull flow are evidenced. The lift coefficient for the maximum gap tested is greater than that obtained for the minimum gap condition.

Comparing the drag values presented in Figures 30 and 54, shows the same relationships prevailing as mentioned for the lift coefficients. That is, gap effects are essentially the same for both conditions in the small gap region and velocity gradient effects predominate in the large gap region.

With chordwise center of pressure defined:

$$(CP)_{\frac{-}{c}} = .25 - \frac{C_m}{C_L \cos \alpha + C_D \sin \alpha} ,$$

velocity effects are present in both the numerator and denominator of the second term on the right, thereby eliminating the velocity gradient effects. This is seen to be the case by comparing Figures 39 and 55. The gap effects are seen to be essentially the same for both conditions.

Figure 56 shows that the gap effects upon the spanwise center of pressure location are negligible as was the case for the free stream investigation.

From the comparisons above, it may be noted that while the hull simulation does change the magnitude of the force coefficients, it has very little influence on the gap effects. These being essentially the same as for the free stream situation.

SIMULATED HULL FLOW AND PROPELLER SLIPSTREAM EFFECTS

In an effort to gain some insight of the propeller slipstream effects on the aerodynamic characteristics of the control surface, a propeller was mounted in the test section between the hull simulation vanes and the control surface being tested (See Figure 17). It was

desired to duplicate the flow depicted in Figure 5 of Reference 7. For convenience, the information presented in Figure 5 of Reference 7 is shown in Figure 57 of this report. Several difficulties were encountered in trying to duplicate the desired flow conditions. The first and probably the most severe difficulty was that the scope of the contract did not permit the construction of a propeller and drive system which would be in the proper geometric proportion to the control surfaces. Therefore, it was necessary to use an existing propeller and drive motor (borrowed from the David Taylor Model Basin) that was larger than was desired. Also, since there was no information available on the allowable speed of this propeller, a conservative rpm limit was established for the tests. In order to obtain the desired ratio of slipstream to freestream velocity with this allowable rpm, it was necessary to reduce the tunnel velocity from that used in the preceeding portion of the test. Another problem was that with the existing velocity survey equipment, it was not possible to obtain measurements at all the desired locations. The final difficulty encountered was that the hull effects are not known for the data presented in Reference 7. For the purpose of this test, the propeller slipstream is superposed upon the simulated hull flow discussed previously. This simulated hull flow may be considerably different from that existing for the reference ship.

Results of the wake velocity surveys are presented in Figures 58-60. For each aspect ratio, the propeller was positioned so that the slipstream enveloped 60 percent of the span of the control surface. In spite of the difficulties enumerated, there is good qualitative agreement in regards to flow angularity and velocity ratios between the test conditions and those presented in Reference 7. It should be noted that it is the port side of the ship that is being simulated. In this simulation positive angle of attack ($+\alpha$) corresponds to right rudder.

Data are presented in Figures 61-87 for comparison of the free stream, simulated hull, and simulated hull with slipstream conditions. In comparing the simulated hull data with the free stream characteristics, the following may be observed:

1. The lift and drag curves for the simulated hull flow exhibit an angle shift and a reduced q, dynamic pressure, effect. Observed effects are:

Aspect Ratio	Shift in α Degrees	Effective q % Freestream q
1	3.5	75
2	2.5	83
3	2.5	87

This angle shift is a result of the average simulated flow angle, whereas the reduced q effect arises from the velocity gradient in the simulated flow. These results are what would be expected from the flow that is simulated and could be predicted with reasonable accuracy from a knowledge of the flow angularity and velocity gradient in the vicinity of the control surface.

2. After eliminating the effects of the shift in α from the chordwise center of pressure curves, it may be noted that the $CP_{\bar{c}}$ moves aft with an increase in the quarter chord sweep. There is a maximum shift of approximately 2 percent of the chord for a sweep angle of 22.5 degrees. This rearward shift of $(CP)_{\bar{c}}$ with sweep is a consequence of the velocity gradient.

3. There is a slight inboard shift of the spanwise center of pressure location for the aspect ratio 2 control surfaces as a result of the simulated hull flow and a slight outboard shift for the aspect ratio 3 surfaces. The inboard $(CP)_s$ shift for the aspect ratio 2 control surface is opposite to that expected due to the increased velocity over the outboard portion of the control surface.

Slipstream effects combined with the simulated hull flow vary with aspect ratio. The probable cause of this variation is the twist in the slipstream, since this would be different for each of the aspect ratios tested (See Figures 58-60). The following slipstream effects are noted:

1. Increased slipstream velocity overcomes the reduced velocity effects of the hull simulation.

2. Slipstream twist overcomes the effects of the hull flow angularity.

3. The lift versus angle of attack curve is extended with the stall angle of attack being from 3 to 6 degrees greater in every instance.

4. Slipstream drag values are consistently higher for negative angles and slightly less or equal to free stream values for positive angles of attack.

5. Chordwise and spanwise center of pressure locations vary considerably for the different aspect ratios tested. The results differ with angle of attack.

From these results, it is seen that the propeller slipstream has significant effects upon the control surface characteristics. These effects vary with the slipstream velocity and twist experienced by the control surface, being different for each aspect ratio.

The results show large shifts in the centers of pressure which are not readily predictable. Results presented here represent one flow condition and should be construed as only a general indication of the effects of the propeller slipstream. Since the effects are significant upon the center of pressure locations, it would have been desirable to determine the cause of these shifts to see whether or not they could be predicted. This, however, was outside of the scope of this contract.

CONCLUSIONS AND RECOMMENDATIONS

From the experimental results of this investigation, free stream gap effects are presented as cross plots for faired streamwise gaps. The results indicate that the fairing pieces eliminate any gap effects in the small angle of attack region (up to about 10°). At large angles of attack, the gap effects are found to be considerably less than those anticipated from theoretical considerations. Gap effects are greatest for those control surfaces having zero quarter chord sweep angle and occur for gaps of about 10% of the control surface span. For maximum gaps tested (up to 40% span for aspect ratio 2 and 3 surfaces and 80% span for aspect ratio 1 surfaces) lift loses are small. Nowhere do they exceed 6% of the minimum gap value. Results of this investigation indicate there is a need for more information in the following areas:

1. theoretical characteristics at infinite gap for the family of control surfaces used in this investigation for comparison with the experimental results,

2. effects of boundary layer thickness upon the gap effects,

3. physical changes in the flow over the control surface as a result of streamwise gaps.

Results of the simulated hull flow investigation indicate that the hull effects are readily predictable if the flow conditions at the control surface location are known.

For the propeller slipstream investigated, drag force and center of pressure locations vary significantly in a manner that is not readily predictable. It should be pointed out that these results are for a parti-

cular hull flow simulation and propeller-control surface geometry; hence, the effect of a given hull configuration and propeller slipstream on the control surface characterisitics must be considered for each specific design. These results indicate a further need for investigation of the propeller slipstream effects to determine whether or not these effects can be predicted with reasonable accuracy or if there is an optimum position for the control surface within the slipstream.

ACKNOWLEDGEMENTS

The author wishes to express his appreciation to Mr. J. N. Fresh of the David Taylor Model Basin for his assistance in locating a propeller and drive motor for use in the slipstream investigation.

REFERENCES

1. Windsor, R. I., "Survey of Low-Aspect-Ratio Characteristics Useful in the Design of Control Surfaces", University of Maryland Wind Tunnel Engineering Report No. 62 - 1, November 1962.

2. Whicker, L. F. and Fehlner, L. F., "Free Stream Characteristics of a Family of Low-Aspect-Ratio, All-Moveable Control Surfaces for Application to Ship Design", David Taylor Model Basin, Report 933, December 1958.

3. Bleviss, Z. O. and Struble, R. A., "Some Aerodynamic Effects of Streamwise Gaps in Low Aspect Ratio Lifting Surfaces at Supersonic Speeds", Journal of the Aeronautical Sciences, Vol. 21, No. 10, October 1954.

4. Dugan, D. W. and Hikido, K., "Theoretical Investigation of the Effects Upon Lift of a Gap Between Wing and Body of a Slender Wing-Body Combination", NACA TN 3224, August 1954.

5. Windsor, R. I., "Experimental Investigation of Streamwise Gap Effects Upon the Aerodynamic Characteristics of a Low Aspect Ratio All Movable Control Surface", University of Maryland Wind Tunnel Report No. 453, 1965.

6. Cheng, H. M. and Hadler, J. B., "Wake Analysis of Ship Models Twin-Screw Military Types", David Taylor Model Basin, Hydromechanics Laboratory Research and Development Report, Report 1928, December 1964.

7. Macovsky, M. S., Duerr, R. J. and Jewell, D. A., "An Investigation of a Flow-Excited Vibration of the U. S. S. Forest Sherman (DD931)" David Taylor Model Basin Hydromechanics Laboratory Research and Development Report, Report 1188, August, 1958.

TABLE I
SIMULATED HULL FLOW
LONGITUDINAL VELOCITY COMPONENT, Vx/ V

POSITION NUMBER (SEE FIG. NO. 51)	FROM FIG. 11 REFERENCE 5	FROM TEST SECTION SURVEY
101	0.785	0.876
102	0.859	0.862
103	0.965	0.871
104	0.992	1.023
105	1.025	1.027
106	1.022	0.983
107	1.019	0.944
108	1.019	1.026
109	1.019	1.025
110	0.988	1.020
111	0.974	1.025
112	0.962	1.019
113	0.903	1.018
114	0.816	0.957
201	0.826	0.864
202	0.812	0.886
203	0.918	0.880
204	0.976	0.867
205	1.020	1.028
206	1.018	1.027
207	1.015	1.017
208	1.011	1.025
209	1.009	1.025
210	0.993	1.028
211	0.973	1.024
212	0.916	0.963
213	0.813	0.879
214	0.814	0.878
301	0.795	0.823
302	0.773	0.818
303	0.861	0.893
304	0.973	0.873
305	1.030	1.023
306	1.007	1.025
307	1.002	1.031
308	1.007	1.028
309	1.010	1.030
310	1.001	1.026
311	0.975	1.027
312	0.931	0.881
313	0.819	0.883
314	0.722	0.894

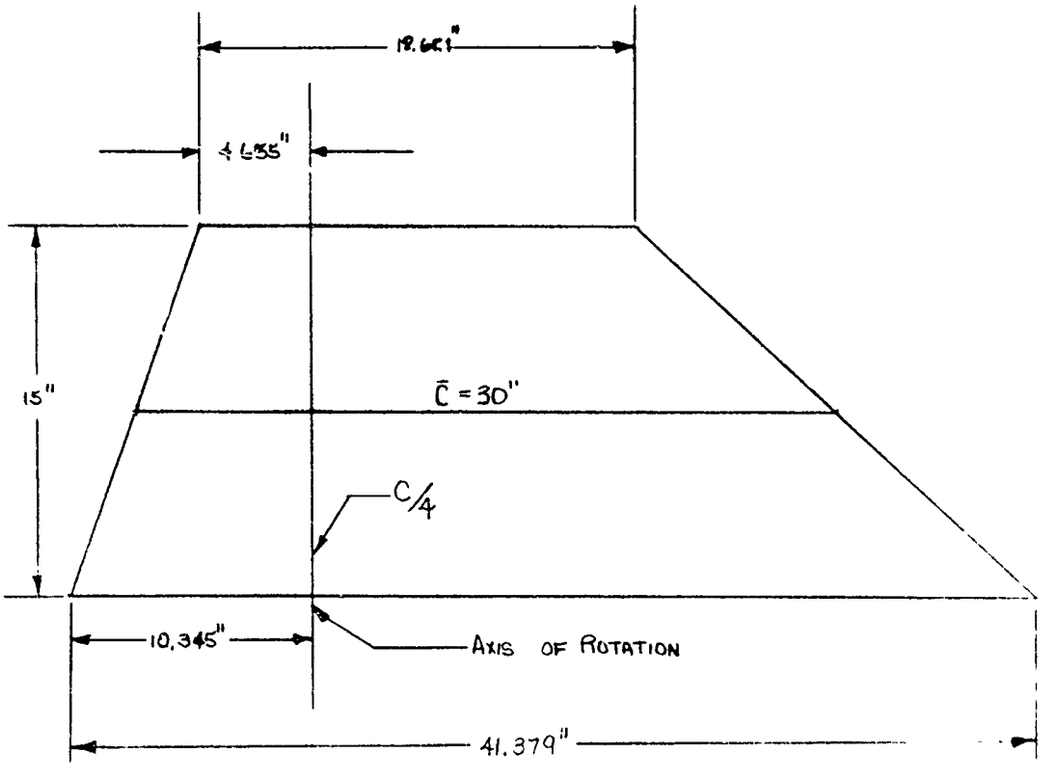

Figure No. 1
Basic Dimensions

EFFECTIVE AR = 1

$\Lambda = 0$

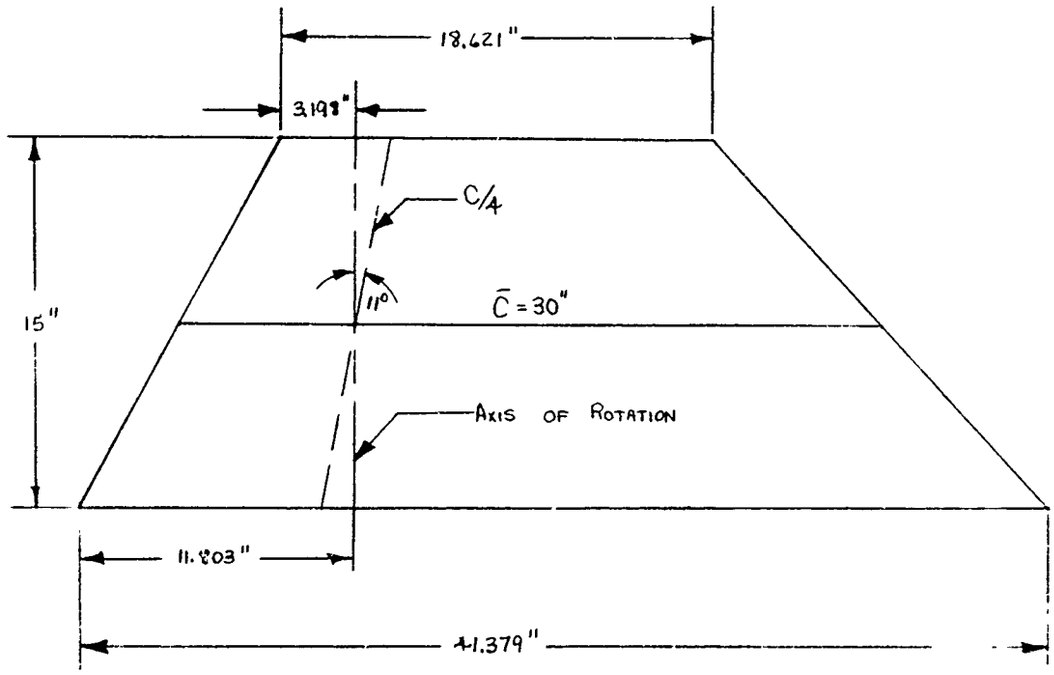

Figure No. 2
Basic Dimensions

EFFECTIVE AR = 1

Λ = 11

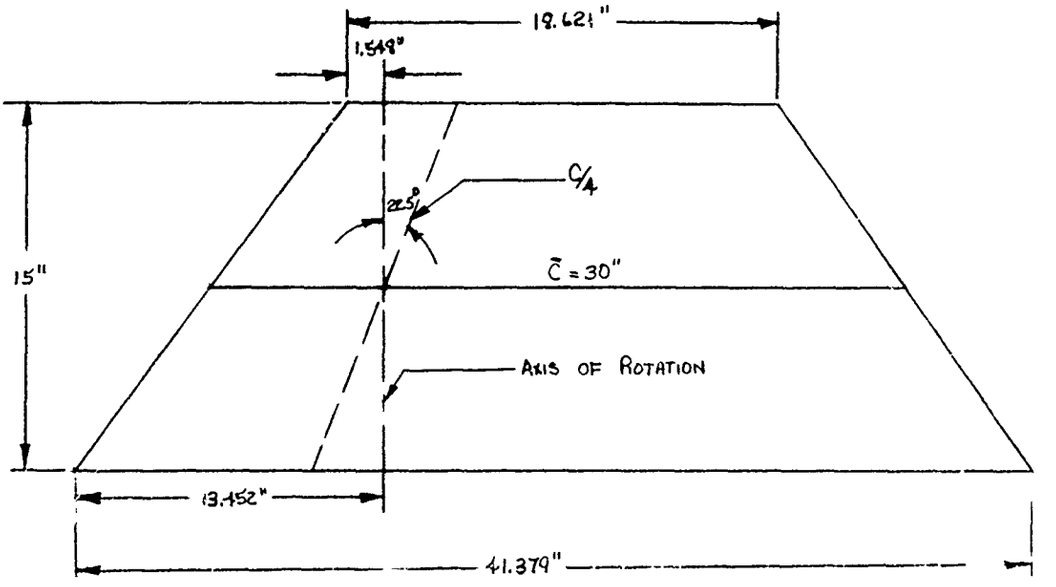

Figure No. 3
Basic Dimensions

EFFECTIVE AR = 1

Λ = 22.5

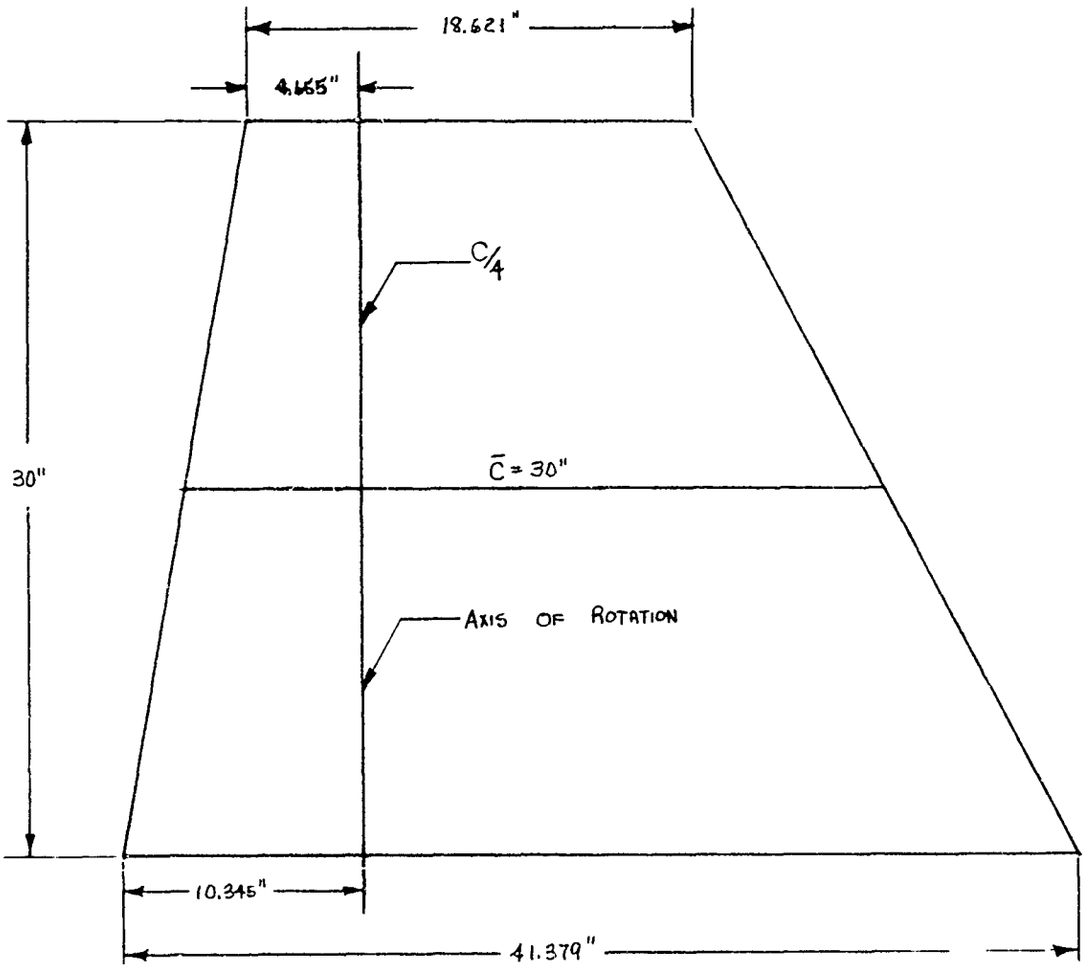

Figure No. 4
Basic Dimensions

EFFECTIVE AR = 2

$\Lambda = 0$

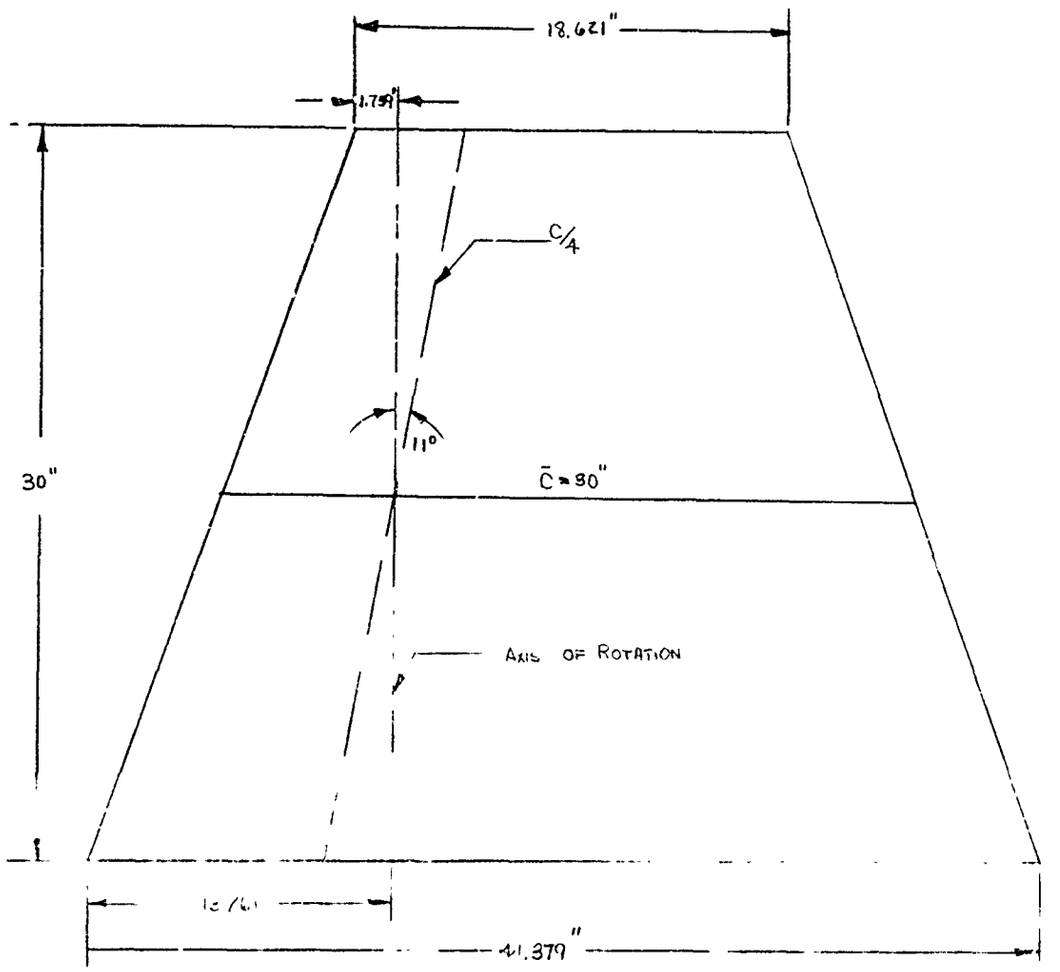

Figure No. 5
Basic Dimensions

EFFECTIVE AR = 2

$\Lambda = 11$

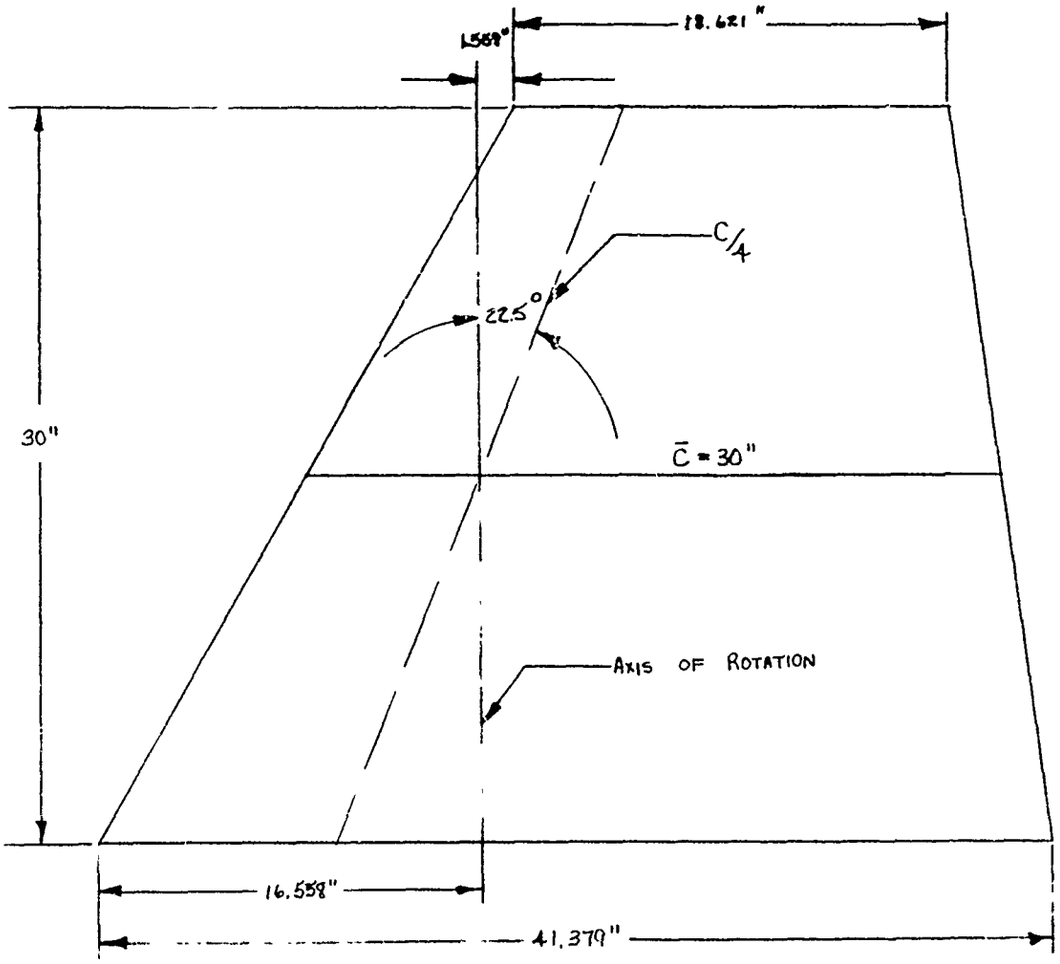

Figure No. 6
Basic Dimensions

EFFECTIVE AR = 2

$\Lambda = 22.5$

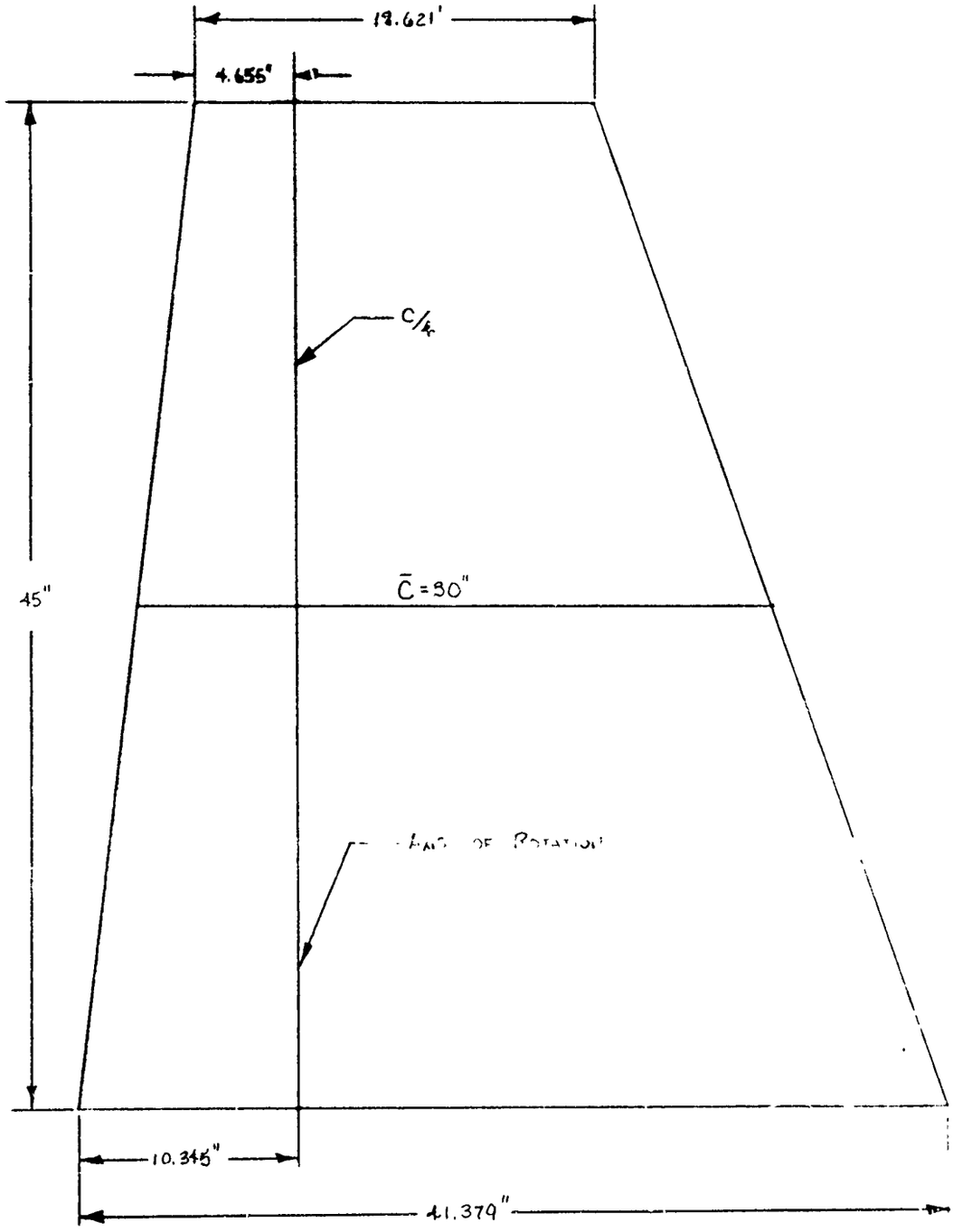

Figure No. 7
Basic Dimensions

EFFECTIVE AR = 3

$\Lambda = 0$

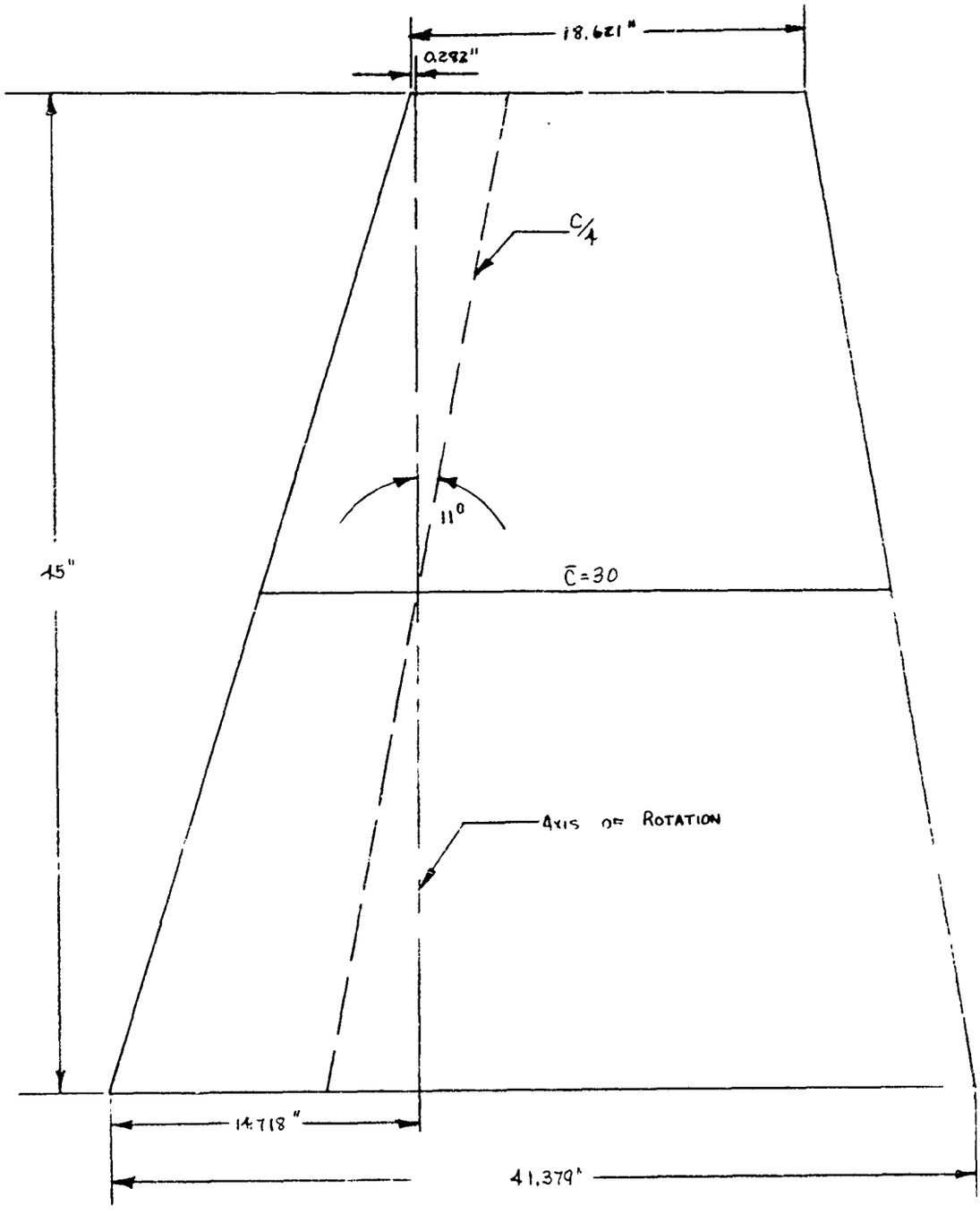

Figure No. 8
Basic Dimensions

EFFECTIVE AR = 3

Λ = 11

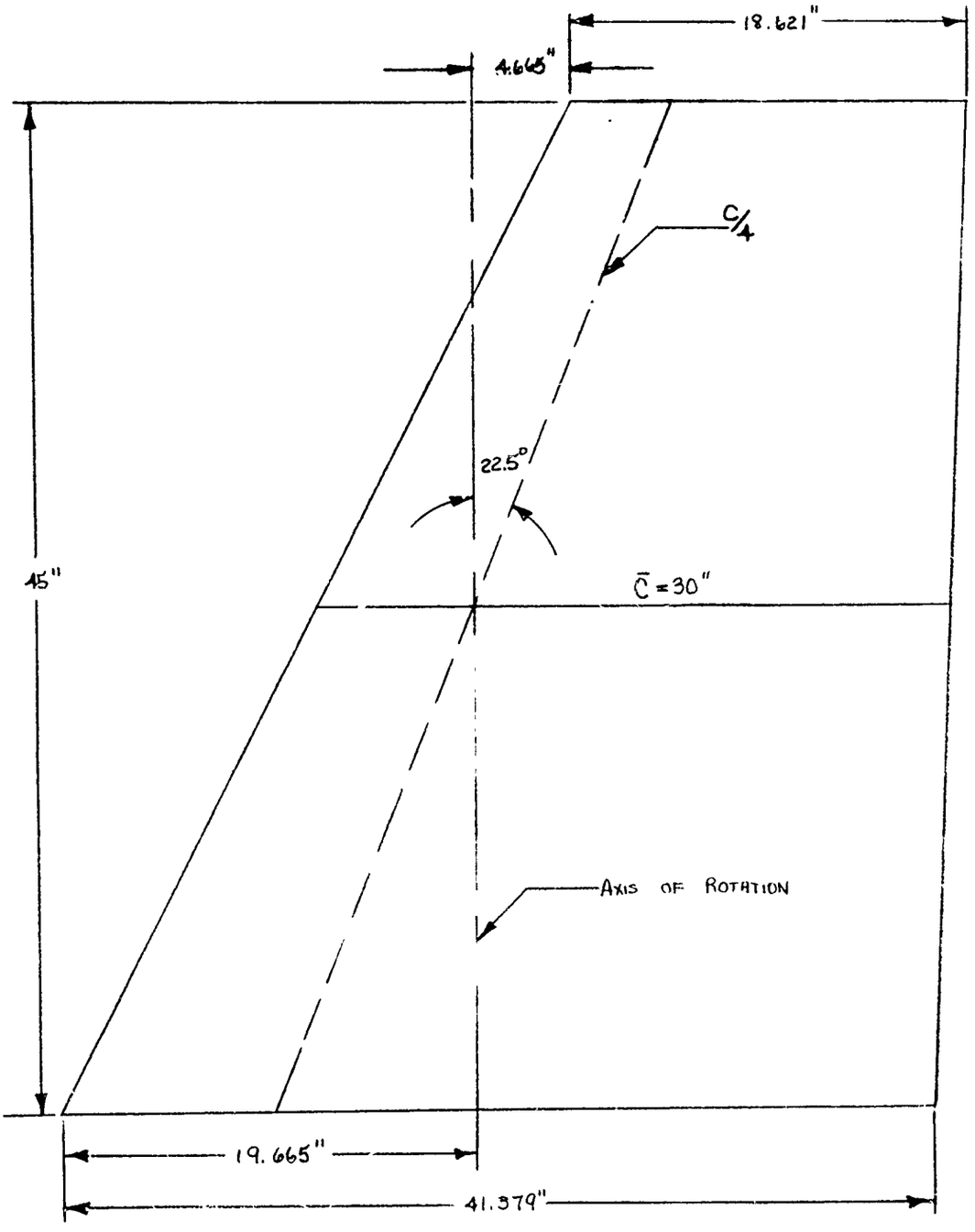

Figure No. 9
Basic Dimensions

EFFECTIVE AR = 3

$\Lambda = 22.5$

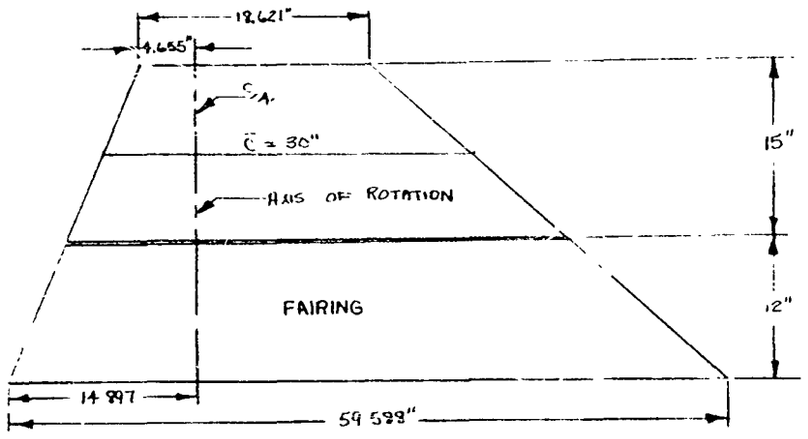

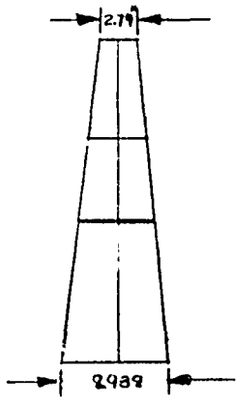

Figure No. 10
Fairing Details

EFFECTIVE AR = 1

$\Lambda = 0$

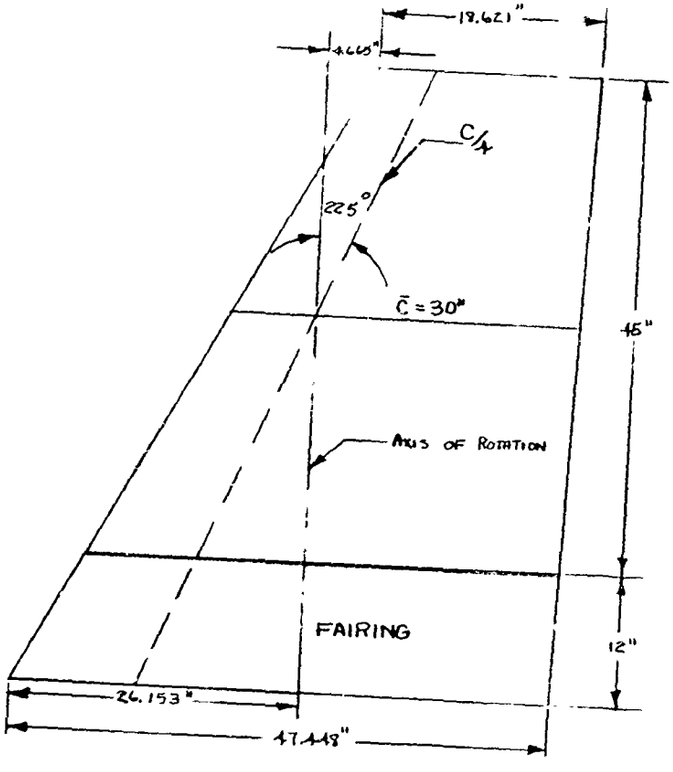

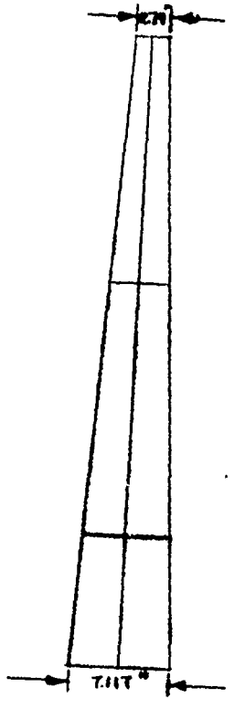

Figure No. 11
Fairing Details

EFFECTIVE AR = 3

Λ = 22.5

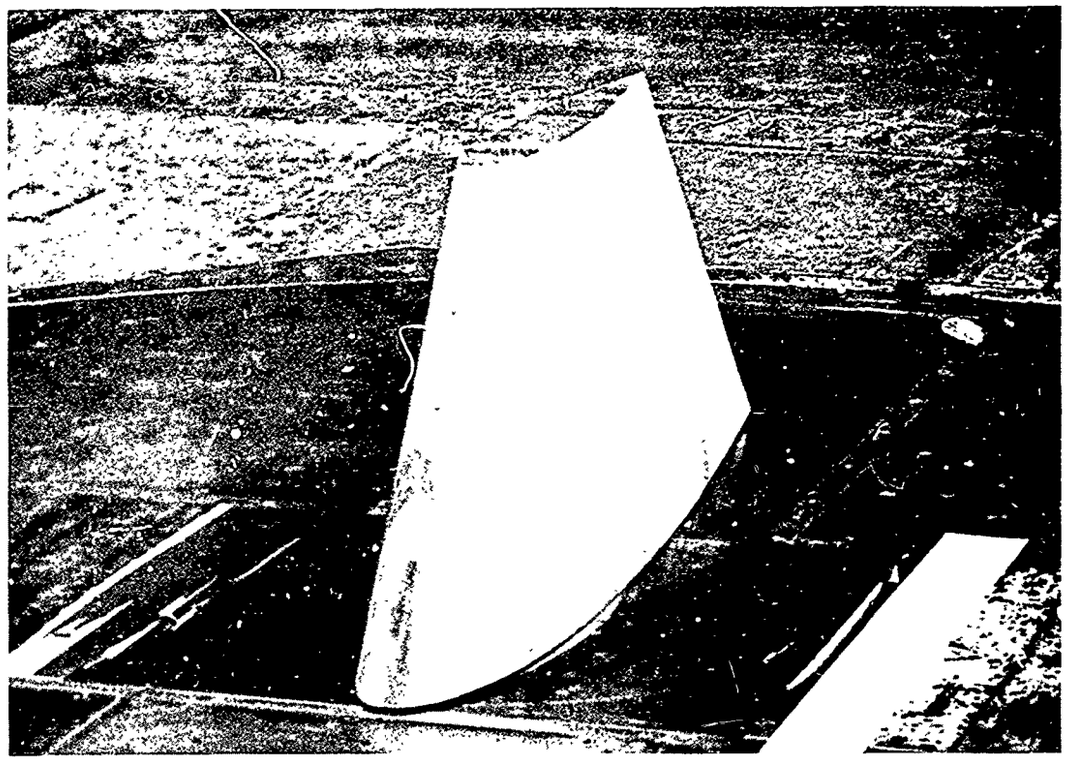

Figure No. 12. Aspect Ratio 1, Λ= 11°, Control Surface Mounted on Tunnel Floor With Minimum Gap.

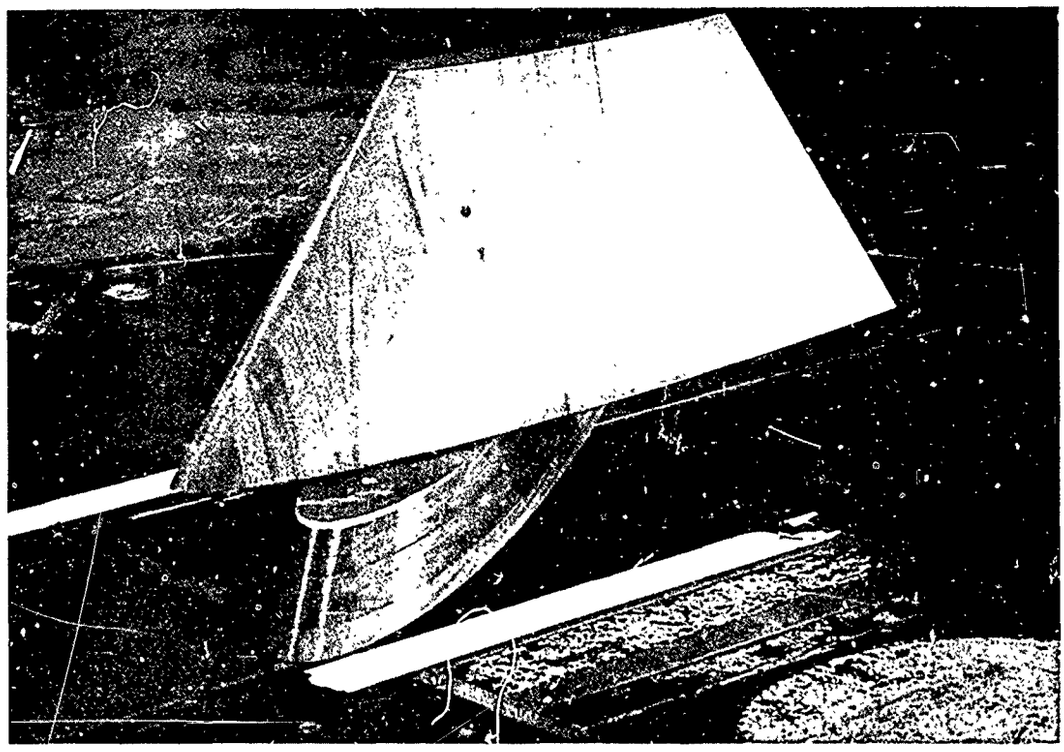

Figure No. 13. Aspect Ratio 1, Λ= 22.5°, Control Surface With 4.5 inch Gap, α = 35°.

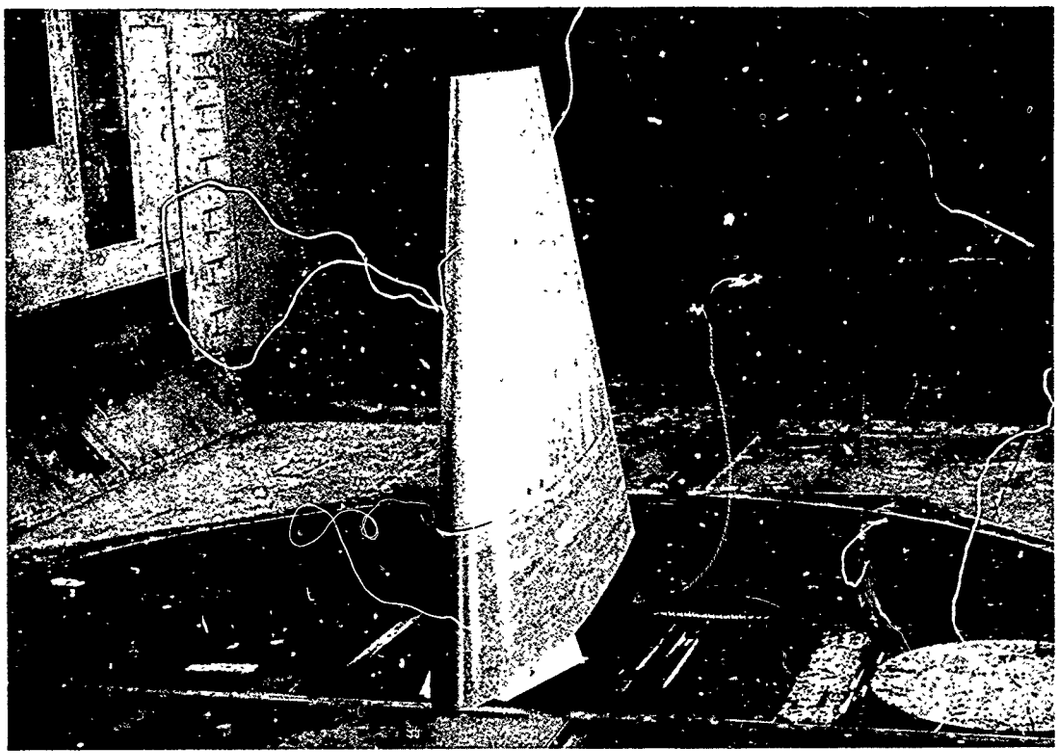

Figure No. 14. Aspect Ratio 2, $\Lambda = 0°$, Control Surface With 12 inch Gap, $\alpha = 0°$.

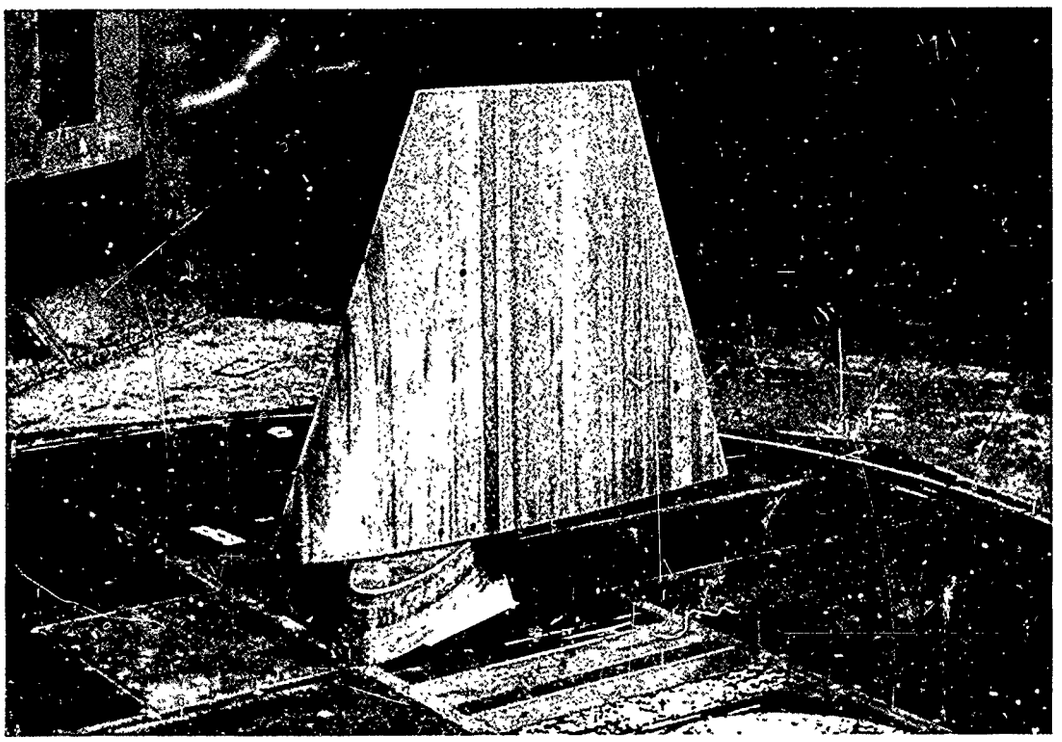

Figure No. 15. Aspect Ratio 2, $\Lambda = 11°$, Control Surface With 4.5 inch Gap, $\alpha = 30°$.

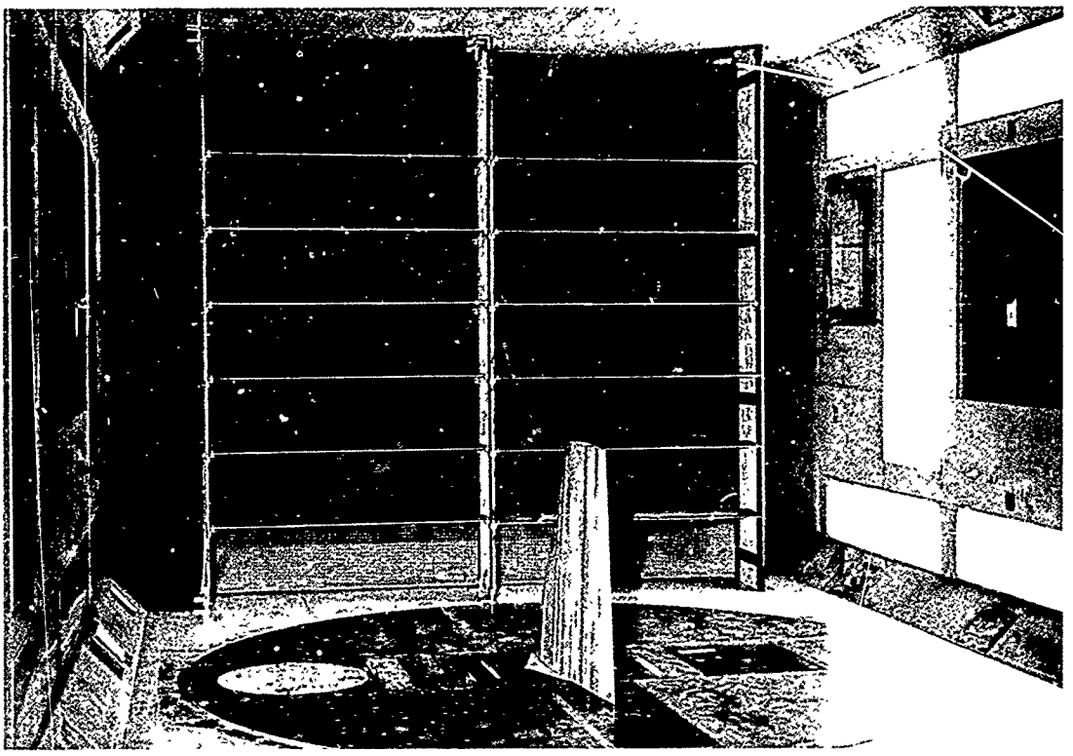

Figure No. 16. Turning Vanes and Screen Installed at Leading Edge of Test Section to Simulate Hull Flow Conditions.

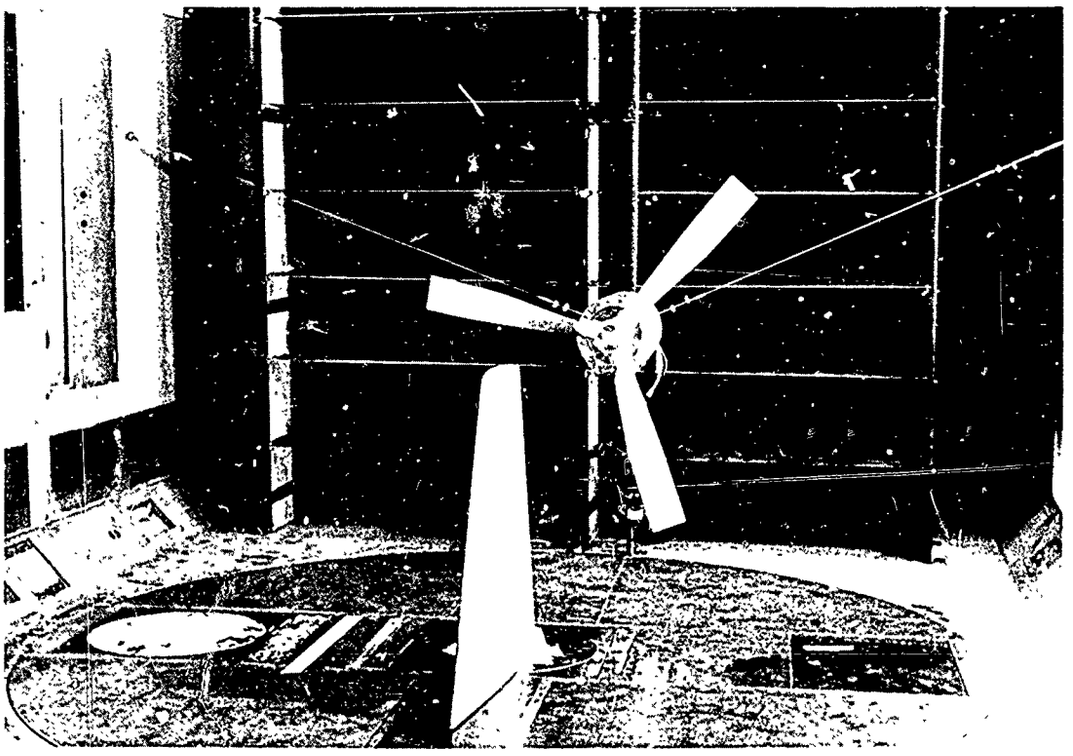

Figure No. 17. Propeller and Drive Motor Installed With Turning Vanes and Screen.

Figure No. 18

Free Stream, Faired Gap Effects on Lift Coefficient, Aspect Ratio 1, $\Lambda = 0^{\circ}$.

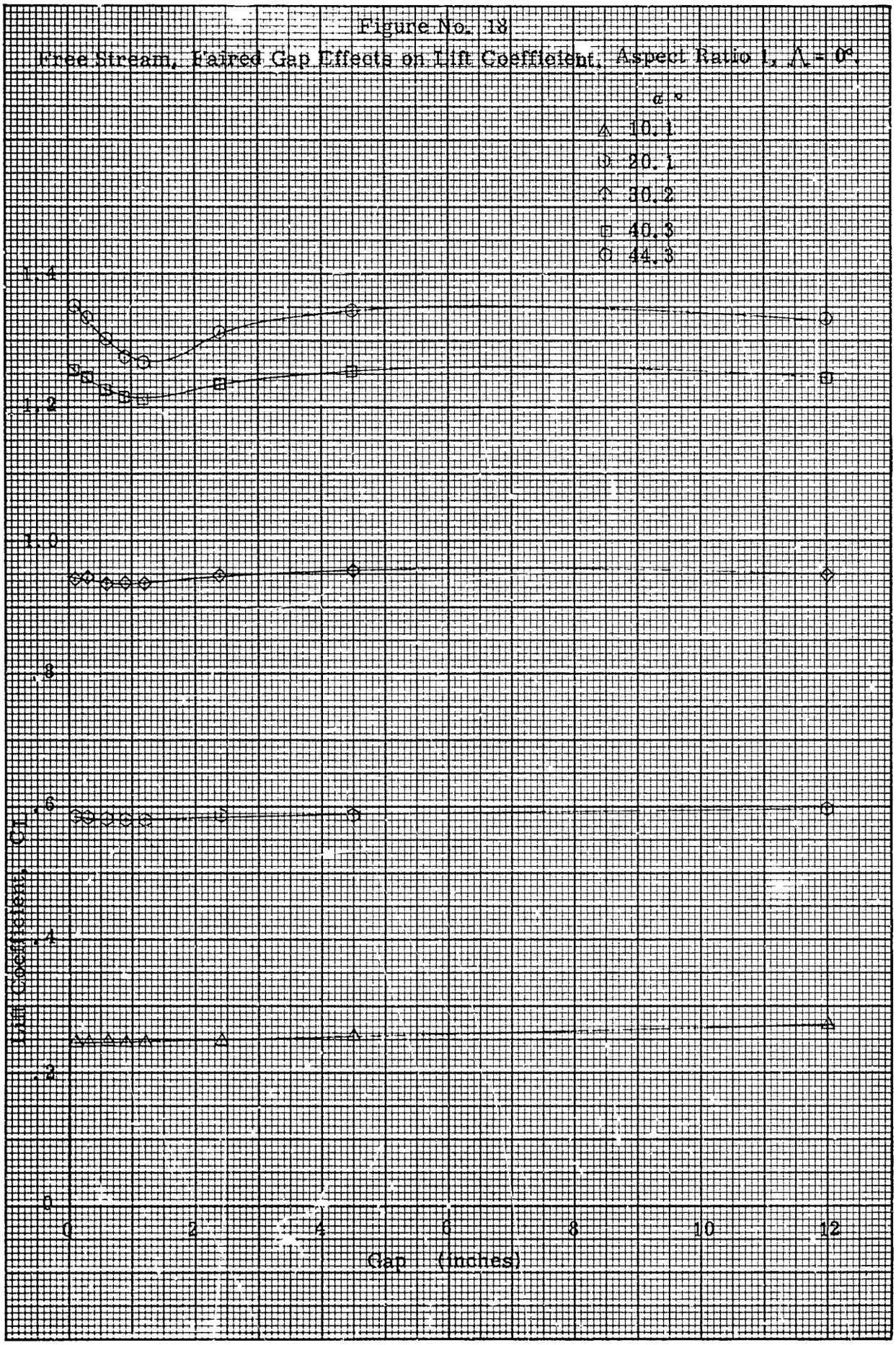

Figure No. 19

Free Stream, Faired Gap Effects on Lift Coefficient, Aspect Ratio 1, Λ=11°.

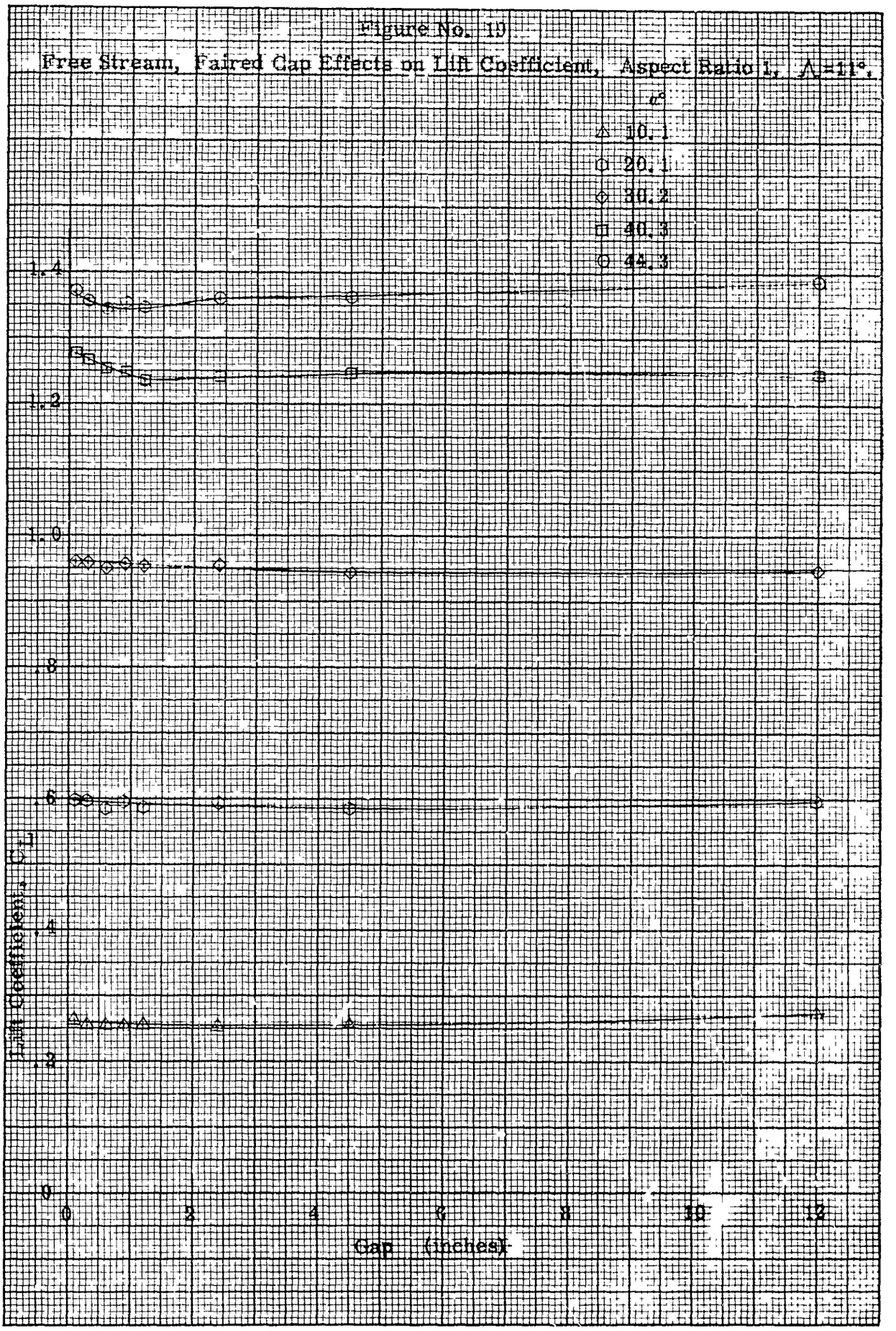

K&E 10 X 10 TO ½ INCH 46 1323
7 X 10 INCHES MADE IN U.S.A.
KEUFFEL & ESSER CO

Figure No. 20

Free Stream, Paired Gap Effects on Lift Coefficient, Aspect Ratio 1, $\Lambda = 22.5°$

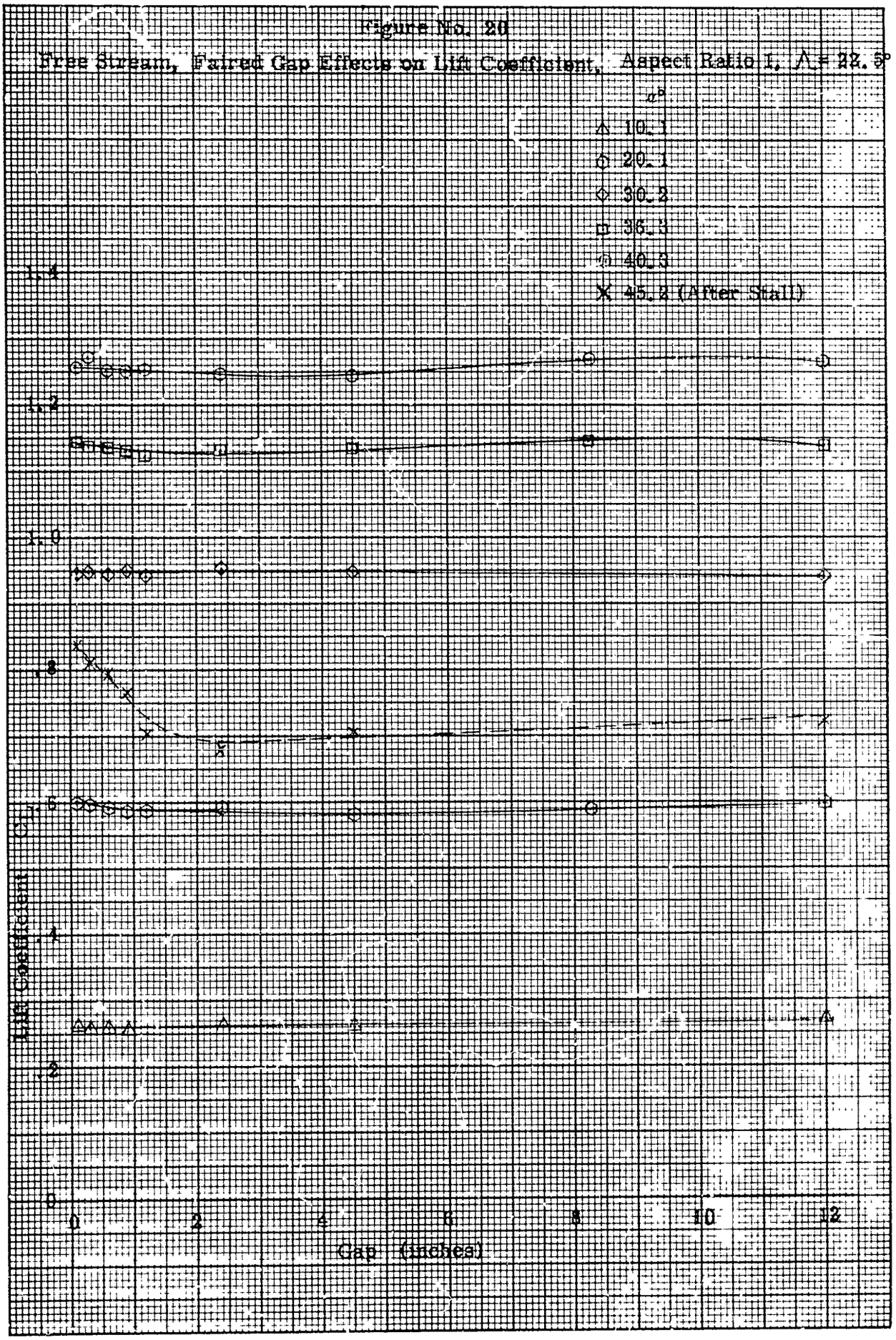

K&E 10 X 10 TO ½ INCH 46 1323
7 X 10 INCHES MADE IN U.S.A.
KEUFFEL & ESSER CO.

Figure No. 21

Free Stream, Faired Gap Effects on Lift Coefficients, Aspect Ratio 2, $\Lambda = 0^\circ$

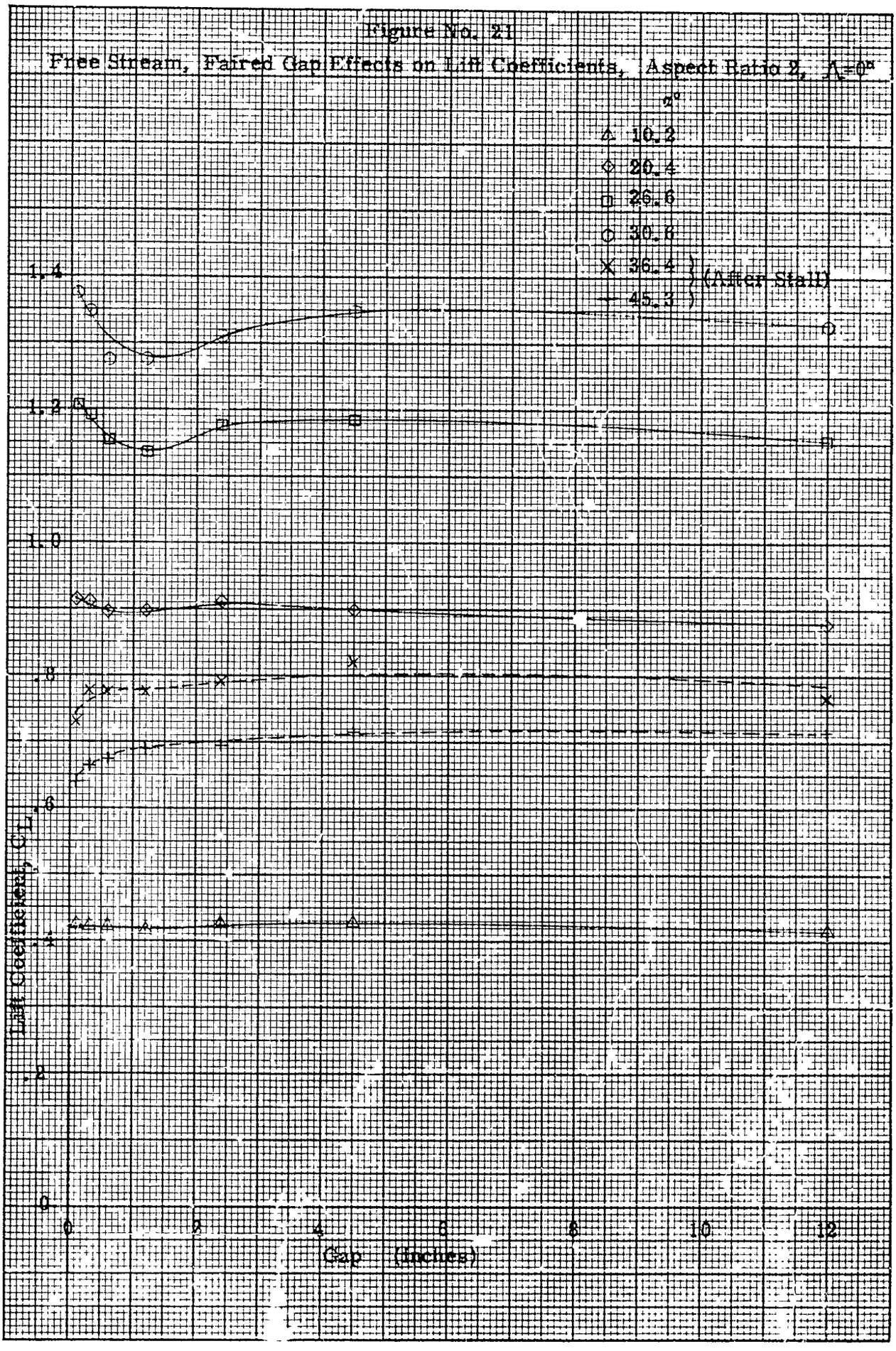

K+E 7 x 10 INCHES 10 T NCH 132
KEUFFEL & ESSER CO

Figure No. 22

Free Stream, Faired Cap Effects on Lift Coefficients, Aspect Ratio 2, Λ=11°

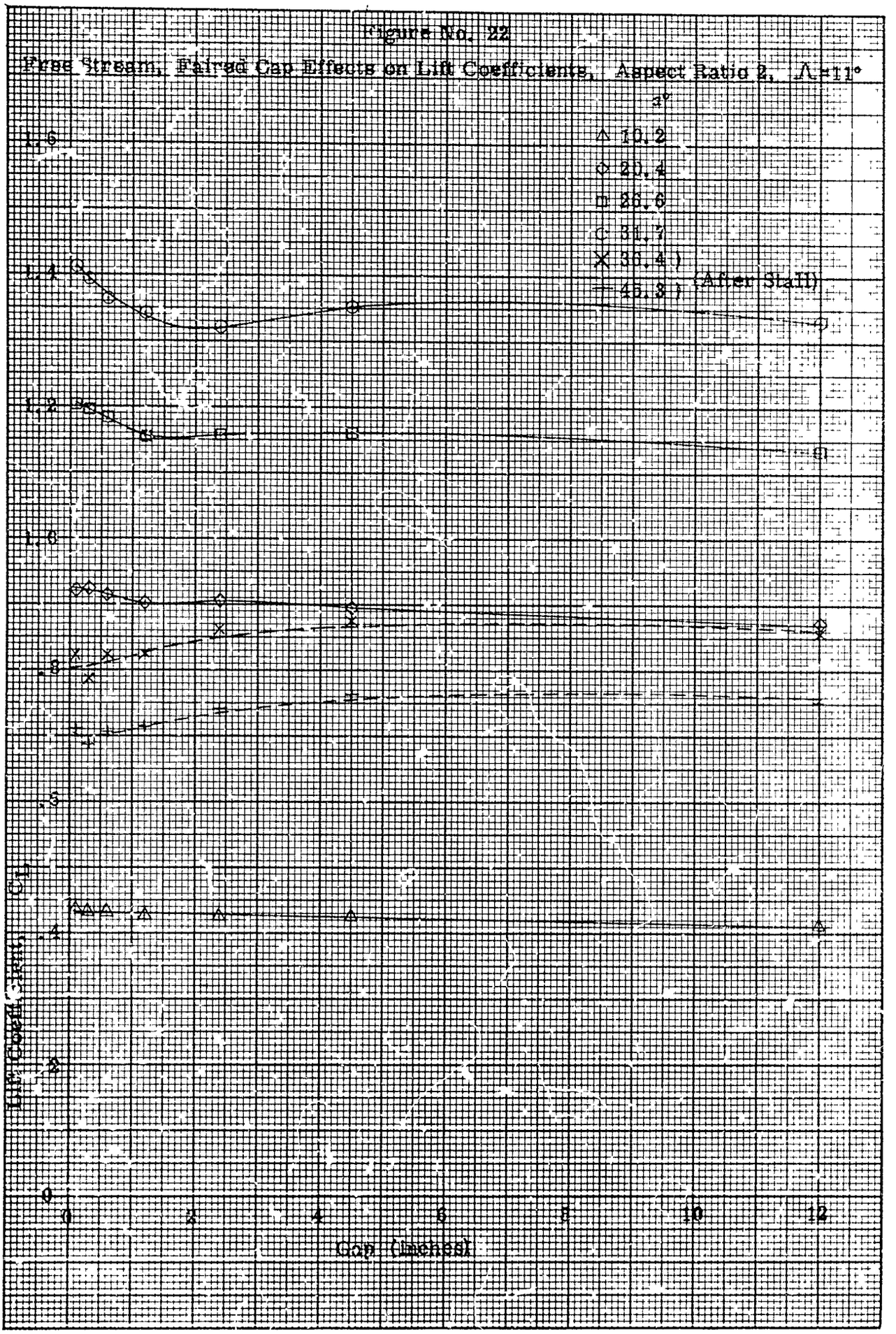

K•E 10 X 10 TO ½ INCH 46 1323
7 X 10 INCHES MADE IN U.S.A.
KEUFFEL & ESSER CO.

Figure No. 23

Free Stream, Faired Gap Effects on Lift Coefficients, Aspect Ratio 2, $\Lambda_{.}$=22.5°

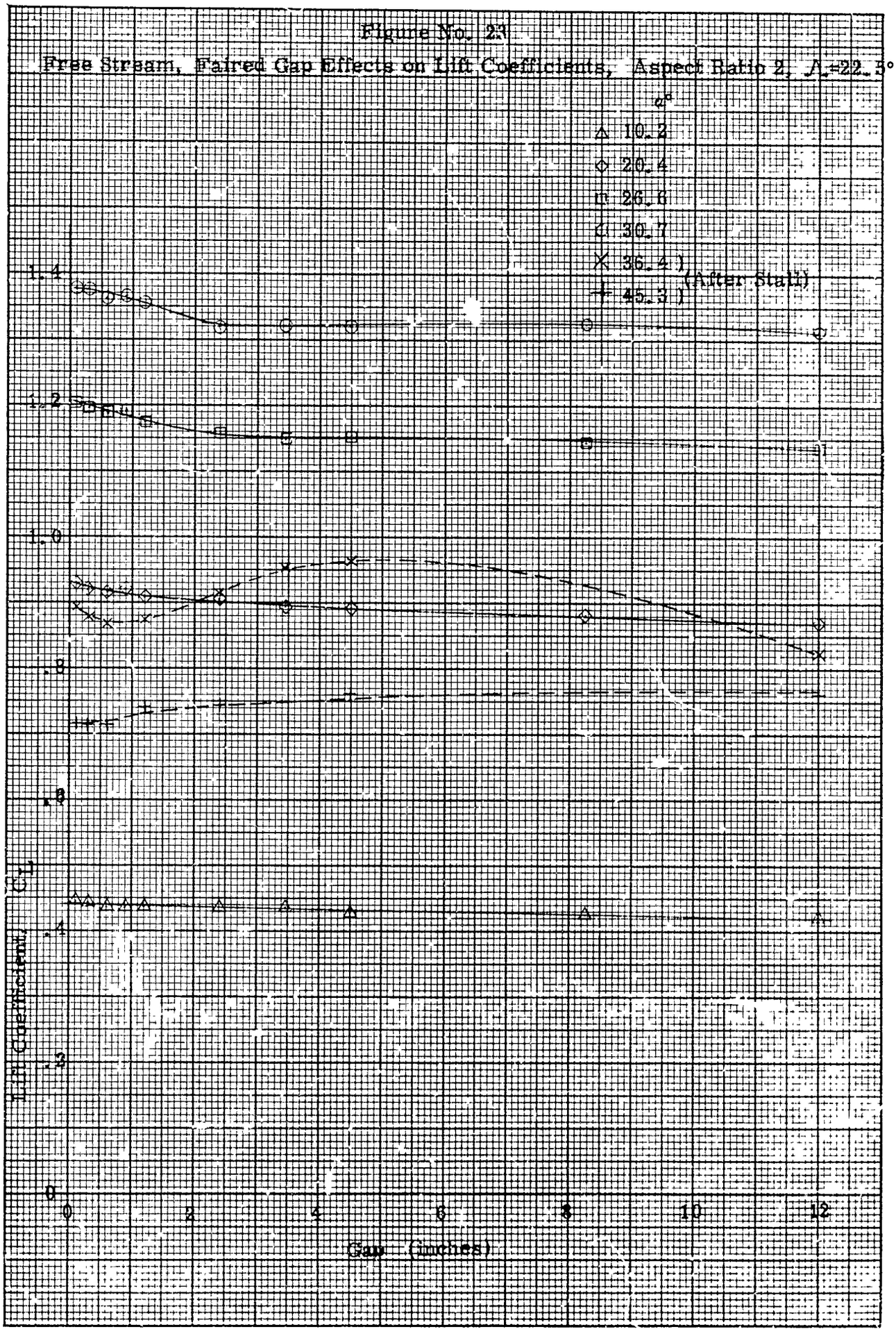

K&E 10 X 10 TO ½ INCH 46 1323
7 X 10 INCHS MADE IN U.S.A.
KEUFFEL & ESSER CO.

K+E 10 X 10 TO ½ INCH 46 1323
7 X 10 INCHES MADE IN U.S.A.
KEUFFEL & ESSER CO.

Figure No. 24

Free Stream, Paired Gap Effects on Lift Coefficients, Aspect Ratio 3, $\Lambda_{\frac{1}{4}} = 0°$

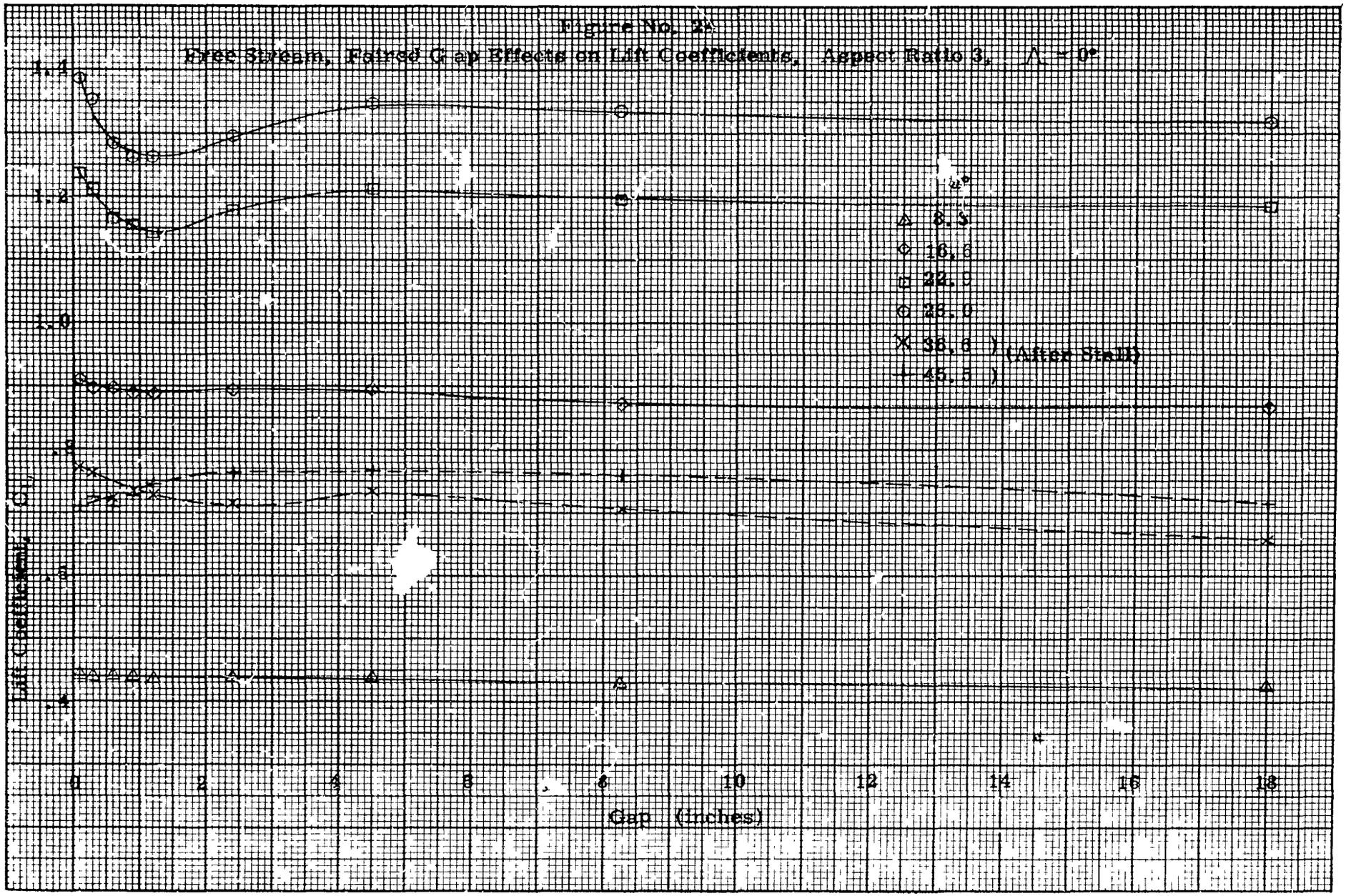

K+E 10 X 10 TO ½ INCH 46 1323
7 X 10 INCHES MADE IN U.S.A.
KEUFFEL & ESSER CO.

Figure No. 25

Free Stream, Paired Gap Effects on Lift Coefficients, Aspect Ratio 3, $\Lambda_{LE} = 11°$

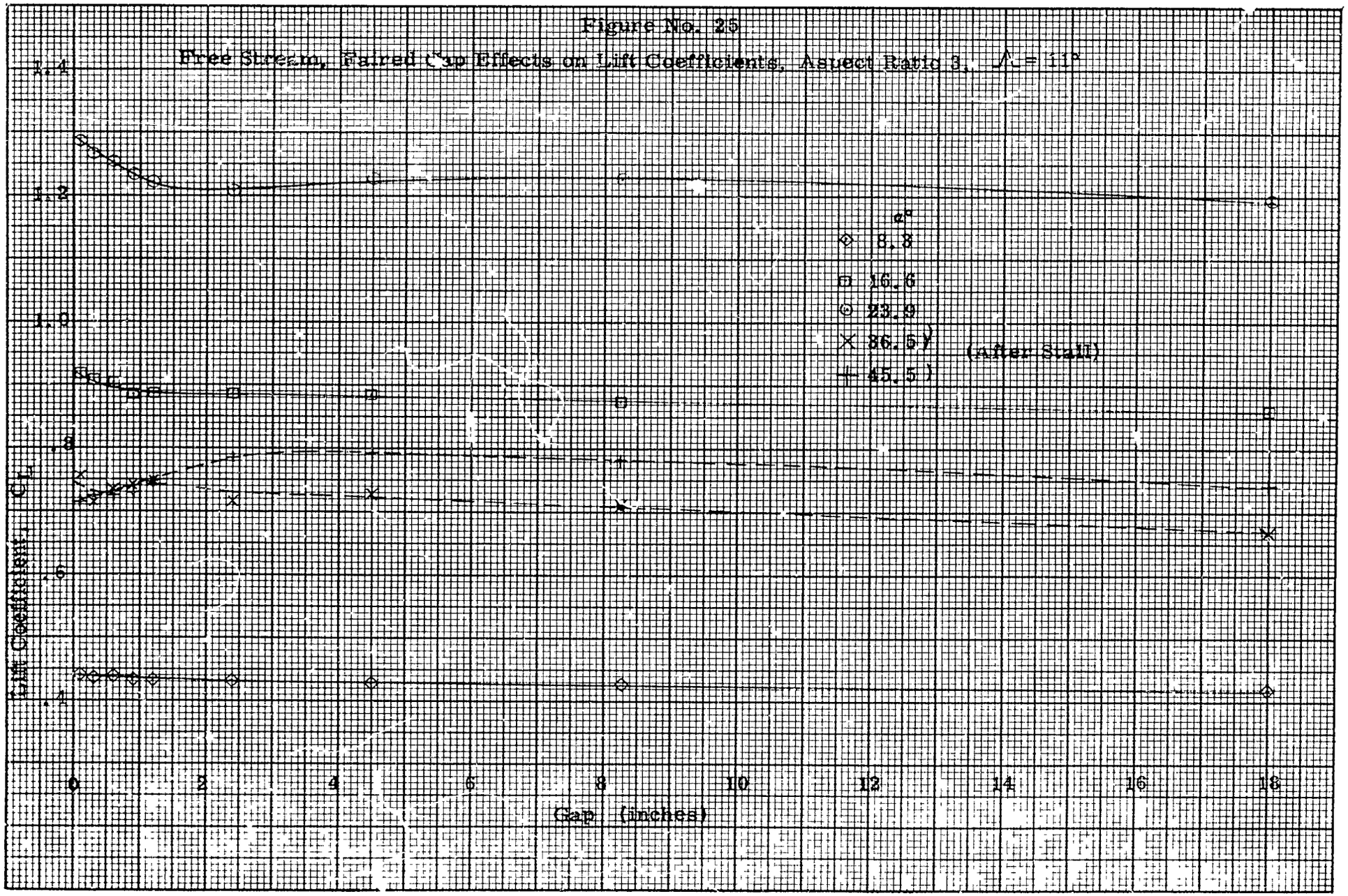

K•Σ 10 X 10 TO ½ INCH 46 1323
7 X 10 INCHES MADE IN U.S.A.
KEUFFEL & ESSER CO.

Figure No. 26

Free Stream, Fauvel Gap Effects on Lift Coefficients, Aspect Ratio 3, $\Lambda = 22.5°$

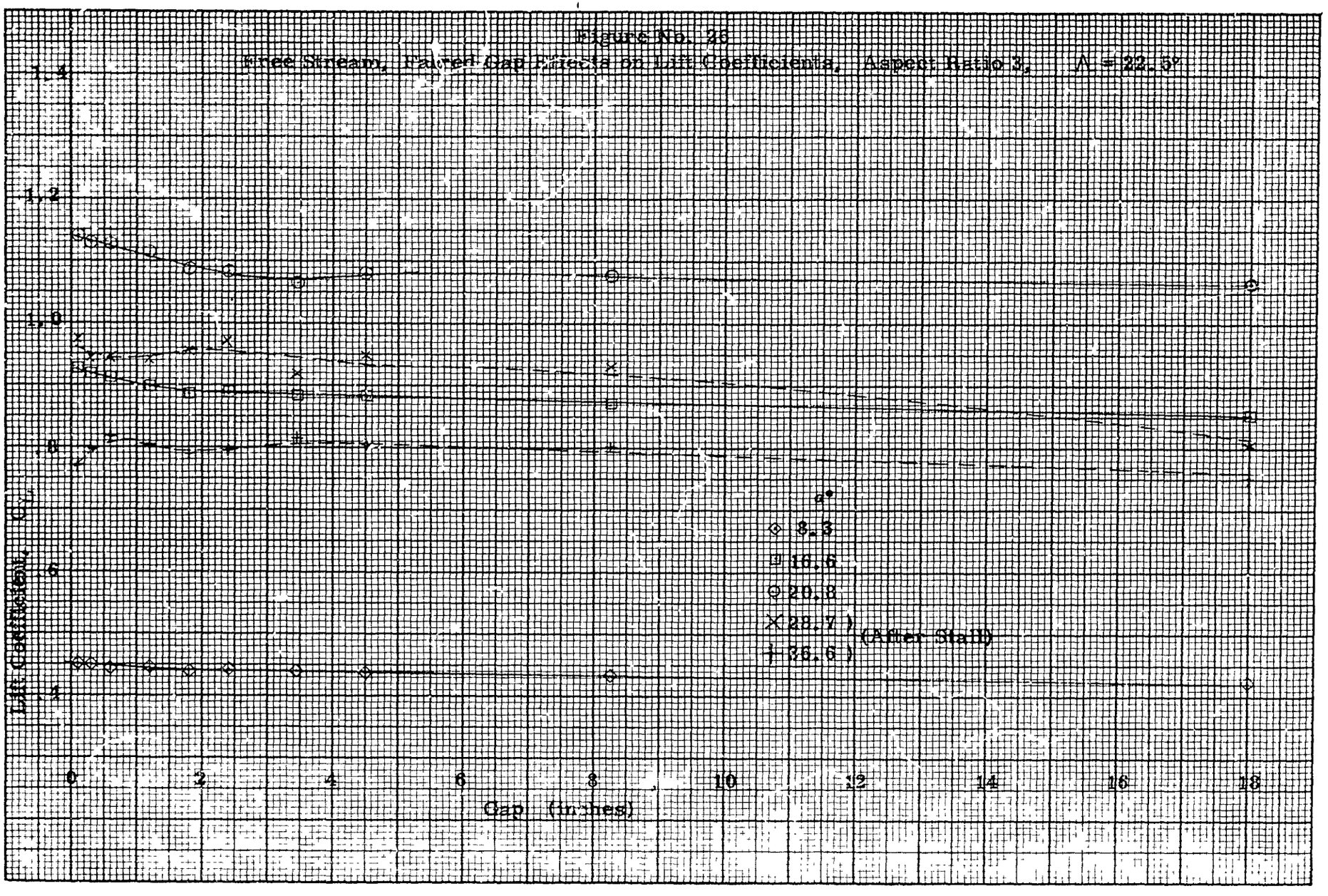

Figure No. 27

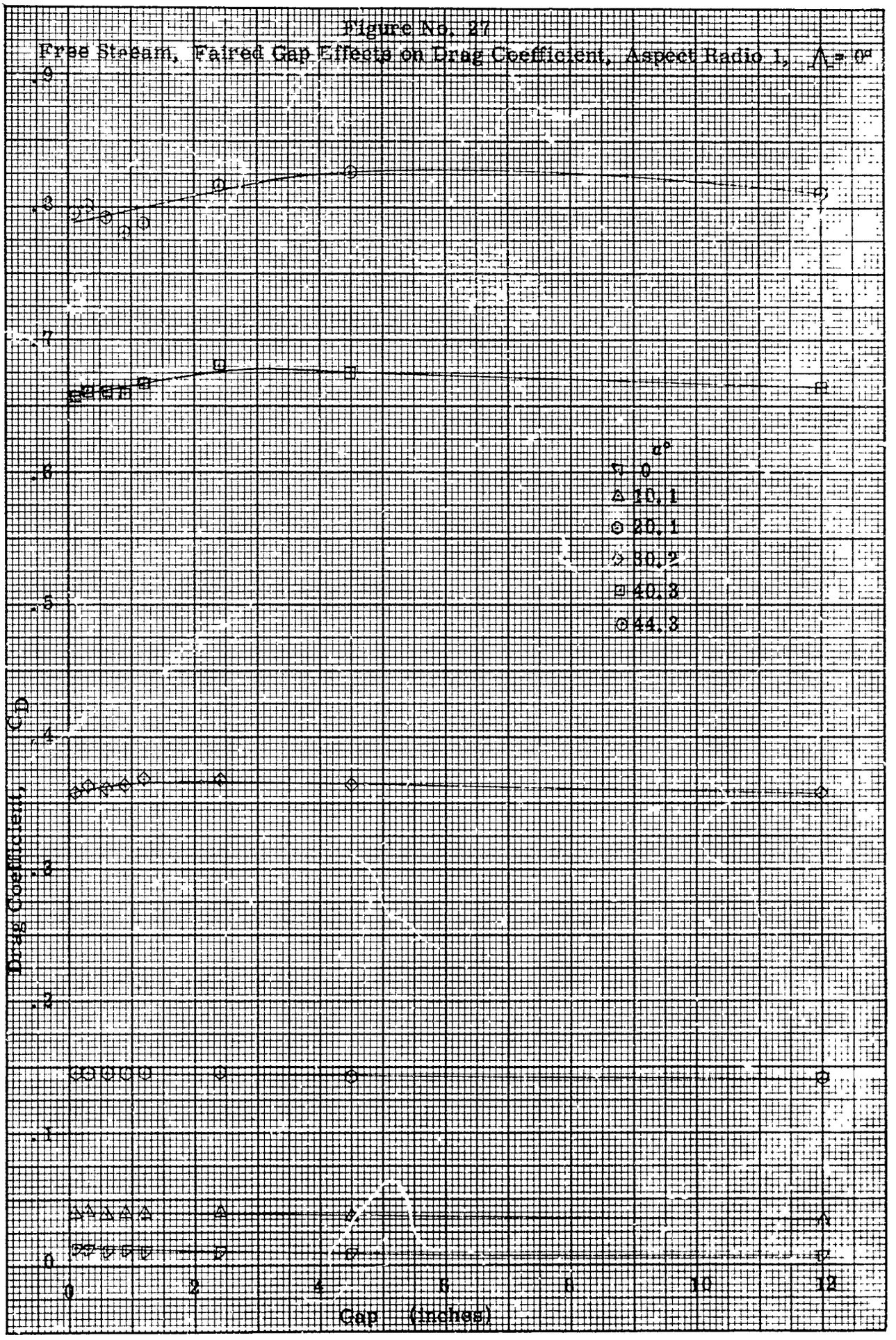

K•E 10 X 10 TO ½ INCH 46 1323
7 X 10 INCHES MADE IN U.S.A.
KEUFFEL & ESSER CO.

Figure No. 23

Free Stream, Faired Gap Effects on Drag Coefficient, Aspect Ratio 1, $\Lambda = 11^{\circ}$

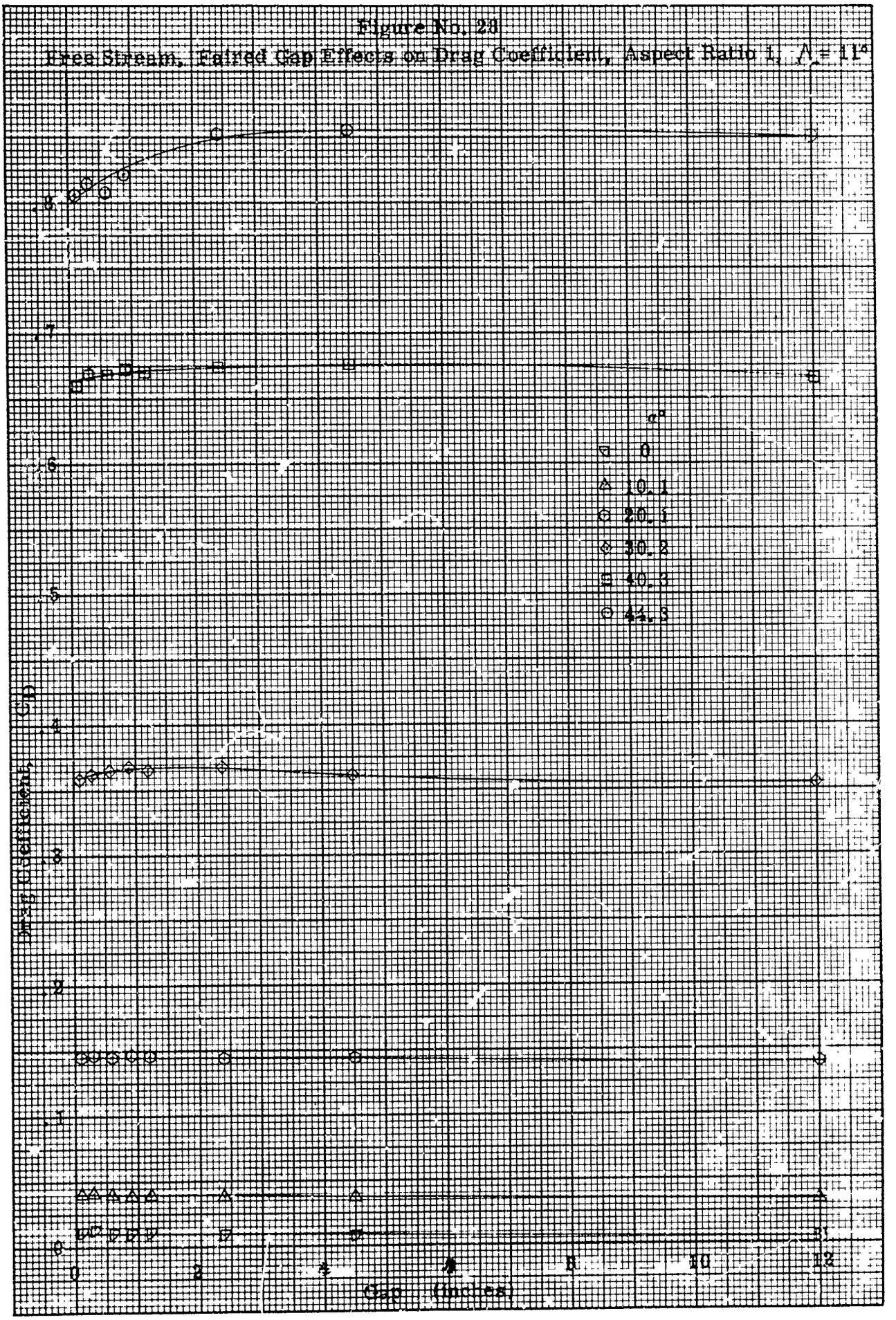

K•E 10 X 10 TO ½ INCH 46 1323
7 X 10 INCHES MADE IN U.S.A.
KEUFFEL & ESSER CO

Figure No. 29

Free Stream, Faired Gap Effects on Drag Coefficient, Aspect Radio 1, $\Lambda = 22.5°$

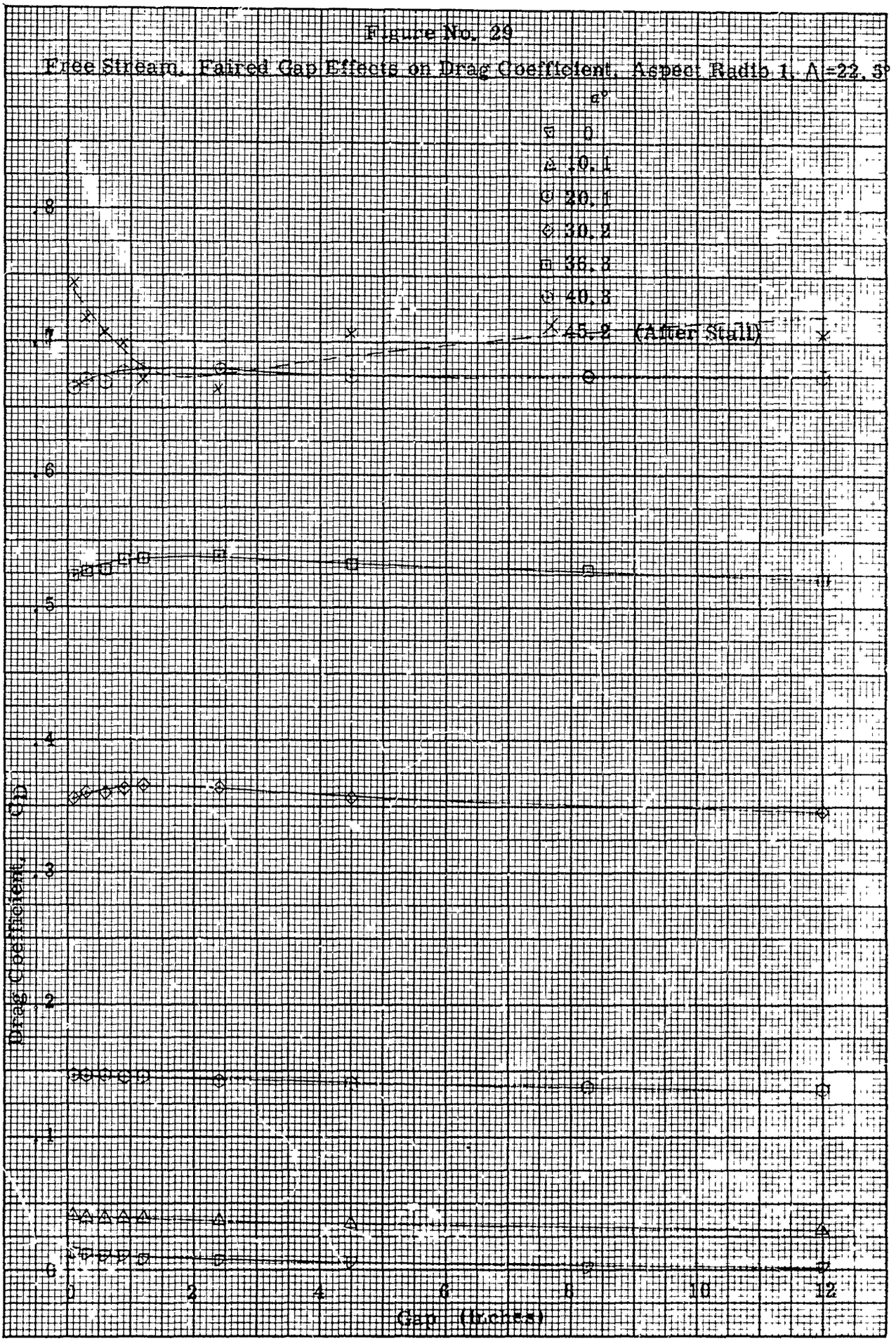

K&E 10 X 10 TO ½ INCH 46 1323
7 X 10 INCHES MADE IN U.S.A.
KEUFFEL & ESSER CO.

Figure No. 39

Free Stream, Paired Gap Effects on Drag Coefficient, Aspect Ratio 2, $\Lambda = 0^{\circ}$

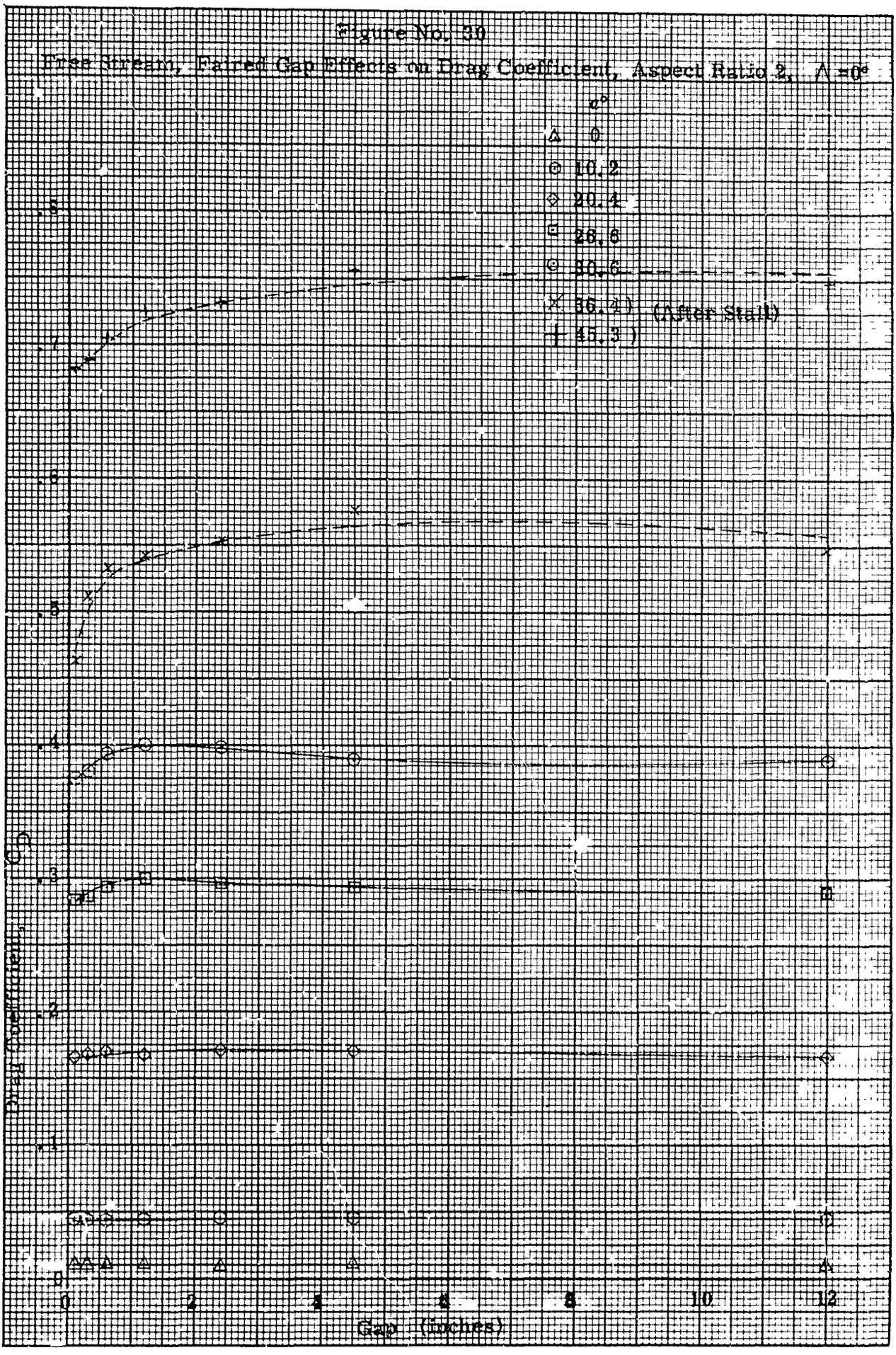

K&E 10 X 10 TO ½ INCH 46 1323
7 X 10 INCHES MADE IN U.S.A.
KEUFFEL & ESSER CO.

Figure No. 31

Free Stream, Paired Gap Effects on Drag Coefficient, Aspect Ratio 2, $\Lambda_{LE} = 1.^{\circ}$

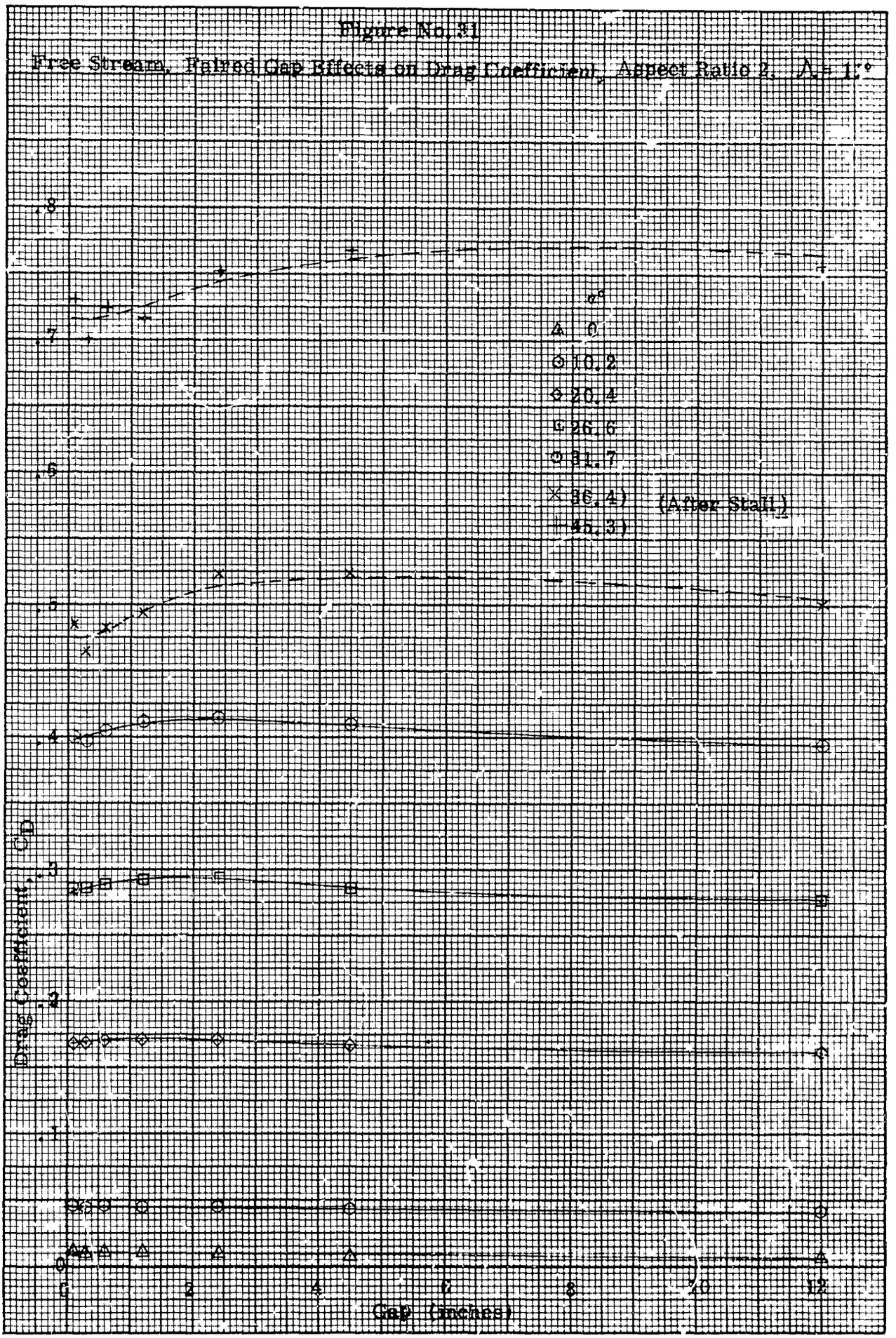

Figure No. 32

Free Stream, Faired Gap Effects on Drag Coefficient, Aspect Ratio 2, Λ=22.5°

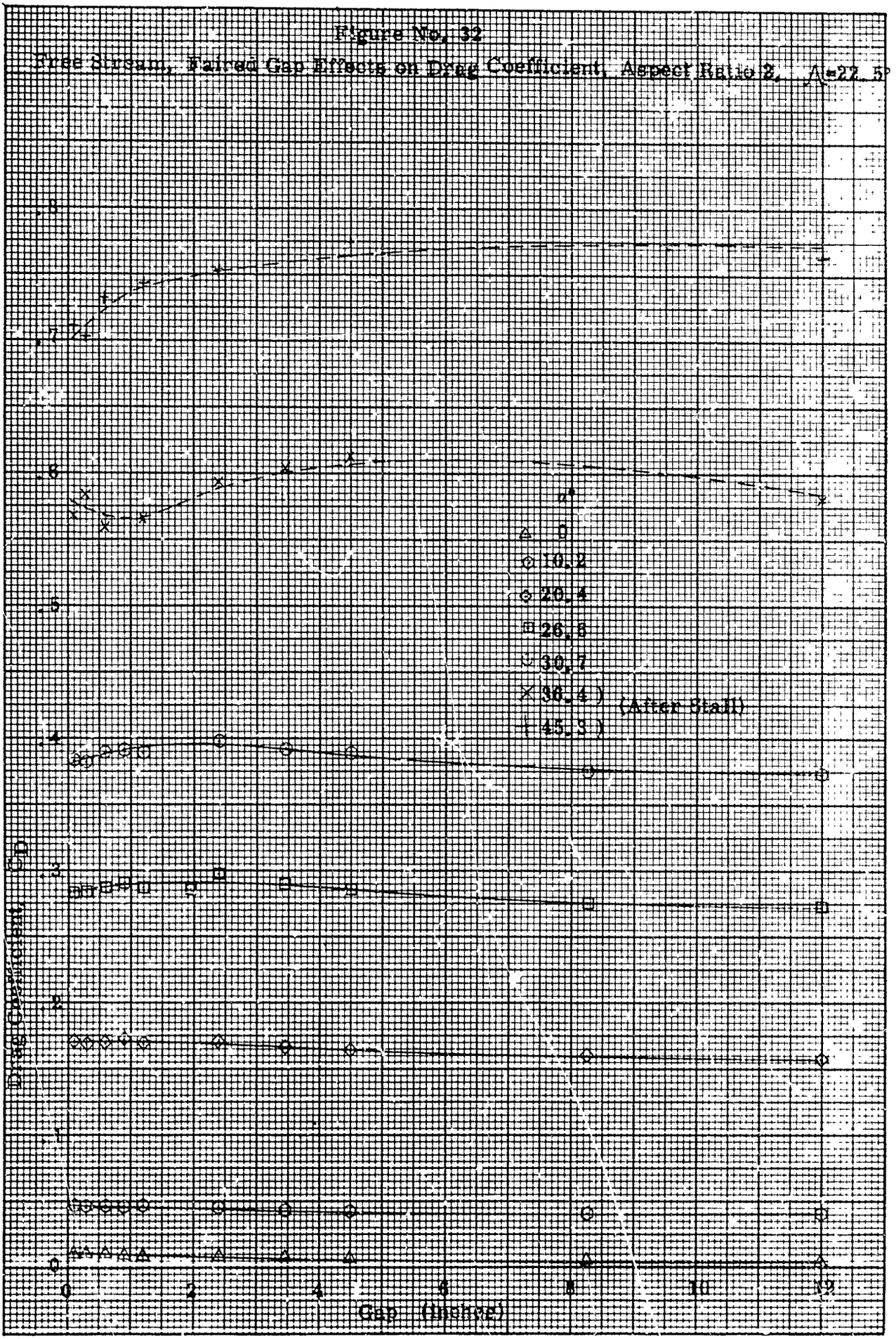

K•E 10 X 10 TO ½ INCH 46 1323
7 X 10 INCHES MADE IN U.S.A.
KEUFFEL & ESSER CO.

K&E 10 X 10 TO ½ INCH 46 1323
7 X 10 INCHES MADE IN U.S.A.
KEUFFEL & ESSER CO.

Figure No. 33

Free Stream, Faired Gap Effects on Drag Coefficient, Aspect Ratio 3, $\Lambda = 0°$

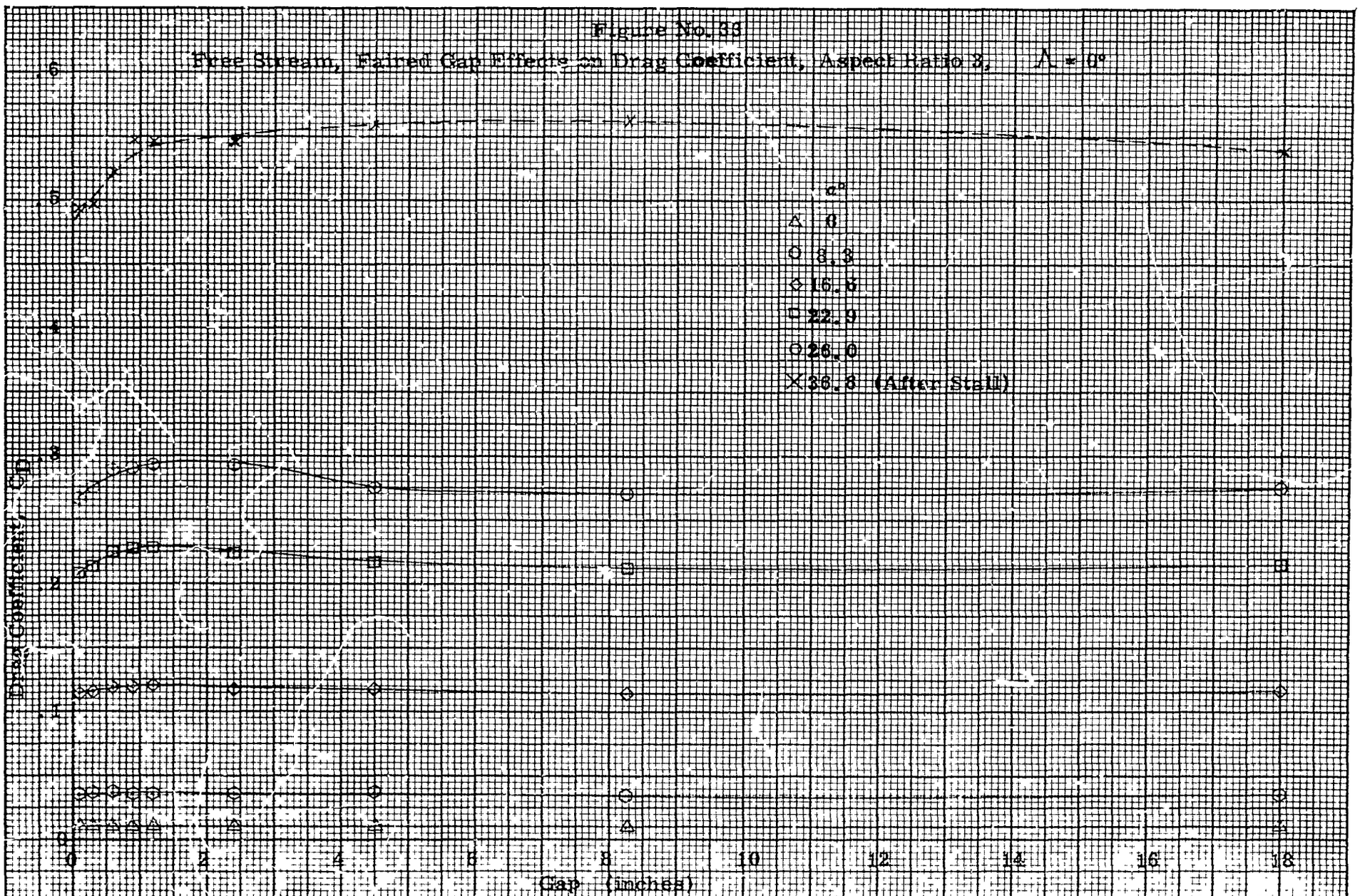

K&E 10 X 10 TO ½ INCH 46 1323
7 X 10 INCHES MADE IN U.S.A.
KEUFFEL & ESSER CO.

Figure No. 34

Free Stream, Faired Gap Effects on Drag Coefficient, Aspect Ratio 3, Λ_c = 11°

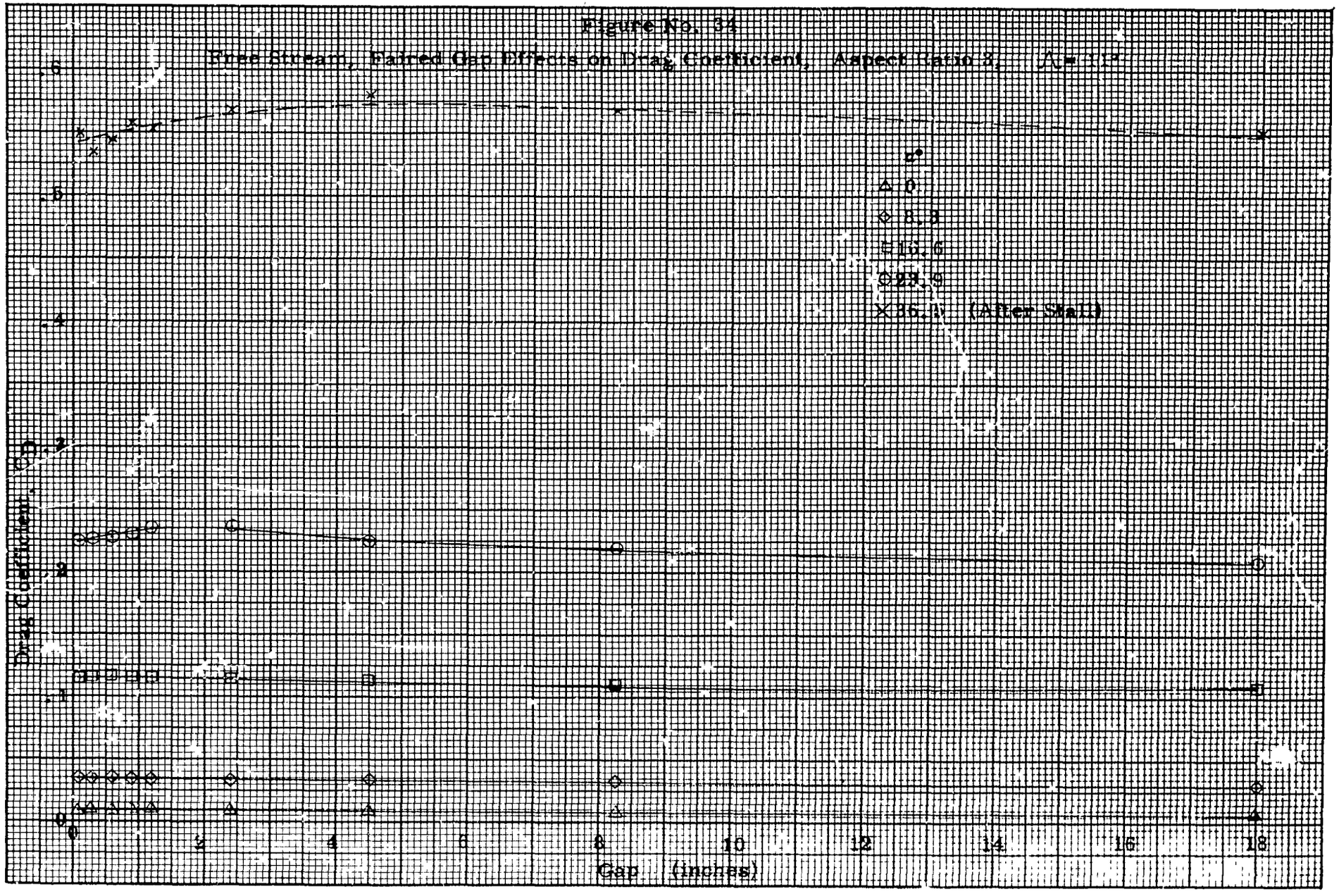

K•E 10 x 10 TO ½ INCH 46 1323
7 X 10 INCHES MADE IN U.S.A.
KEUFFEL & ESSER CO.

Figure No. 35

Free Stream, Paired Gap Effects on Drag Coefficients, Aspect Ratio 3, $\Lambda = 22.5°$

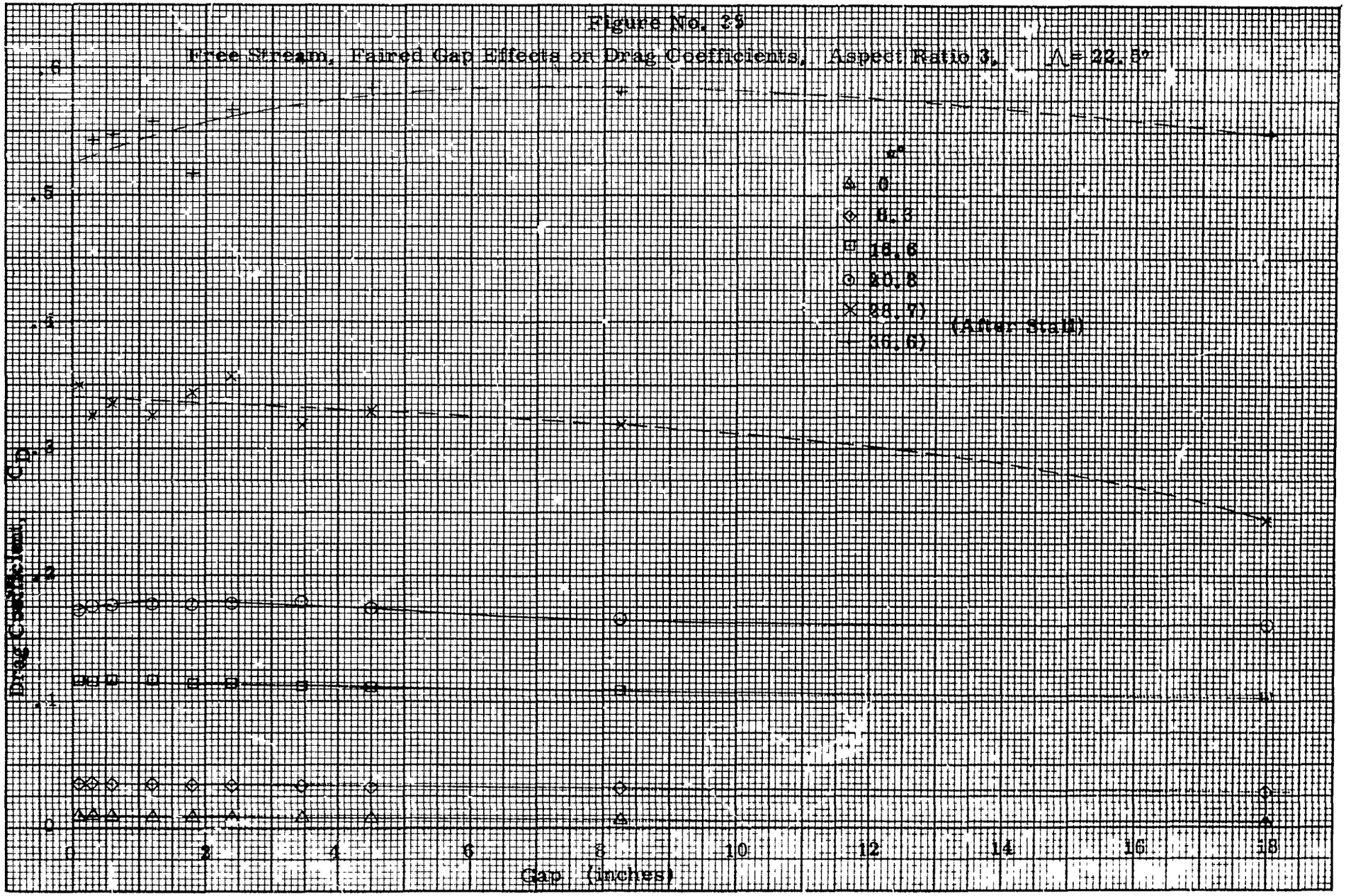

Figure No. 36

Free Stream, Faired Gap Effects on Chordwise Center of Pressure,

Aspect Ratio 1, $\Lambda = 0°$

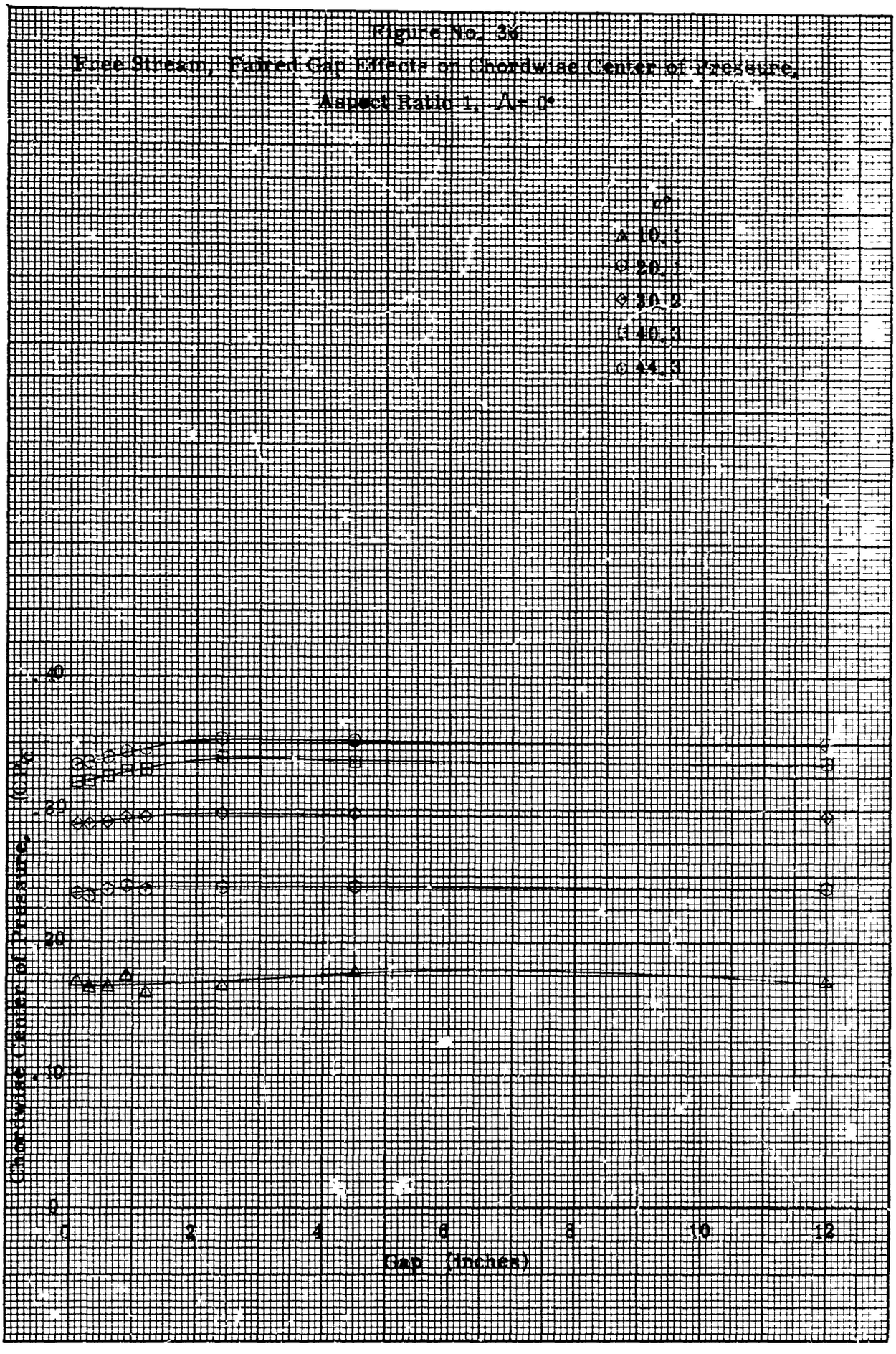

K&E 10 X 10 TO ½ INCH 46 1323
7 X 10 INCHES MADE IN U.S.A.
KEUFFEL & ESSER CO.

Figure No. 37

Free Stream, Paired Gap Effects on Chordwise Center of Pressure

Aspect Ratio 1, $\Lambda = 11^{\circ}$

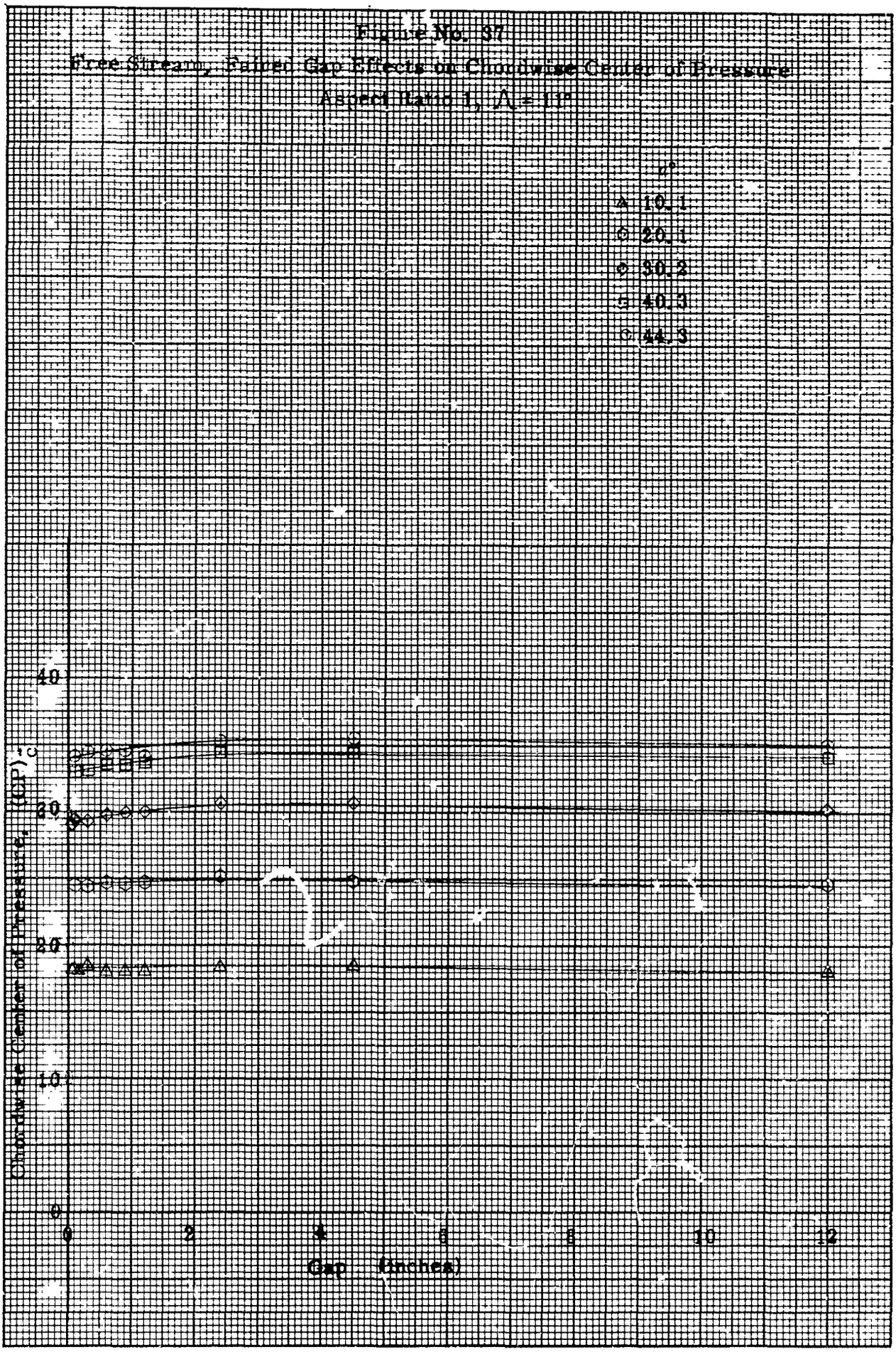

K+E 10 X 10 TO ½ INCH 46 1323
7 X 10 INCHES MADE IN U.S.A.
KEUFFEL & ESSER CO.

Figure No. 38

Free Stream, Faired Gap Effects on Chordwise Center of Pressure

Aspect Ratio 1, Λ = 22.5°

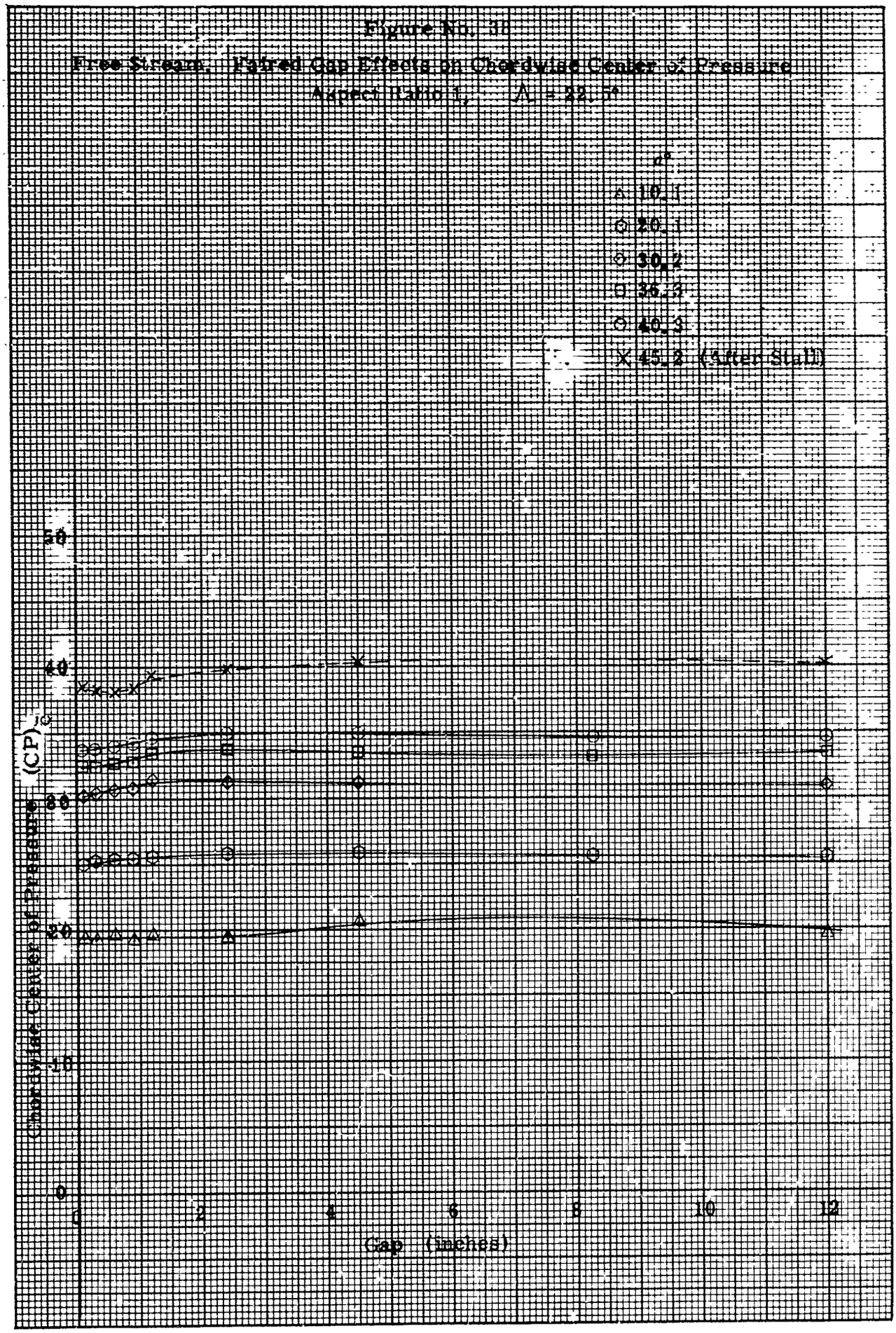

K+E 10 X 10 TO ½ INCH 46 1323
7 X 10 INCHES MADE IN U.S.A.
KEUFFEL & ESSER CO.

Figure No. 39

Free Stream, Paired Gap Effects on Chordwise Center of Pressure

Aspect Ratio 2, $\Lambda = 0°$

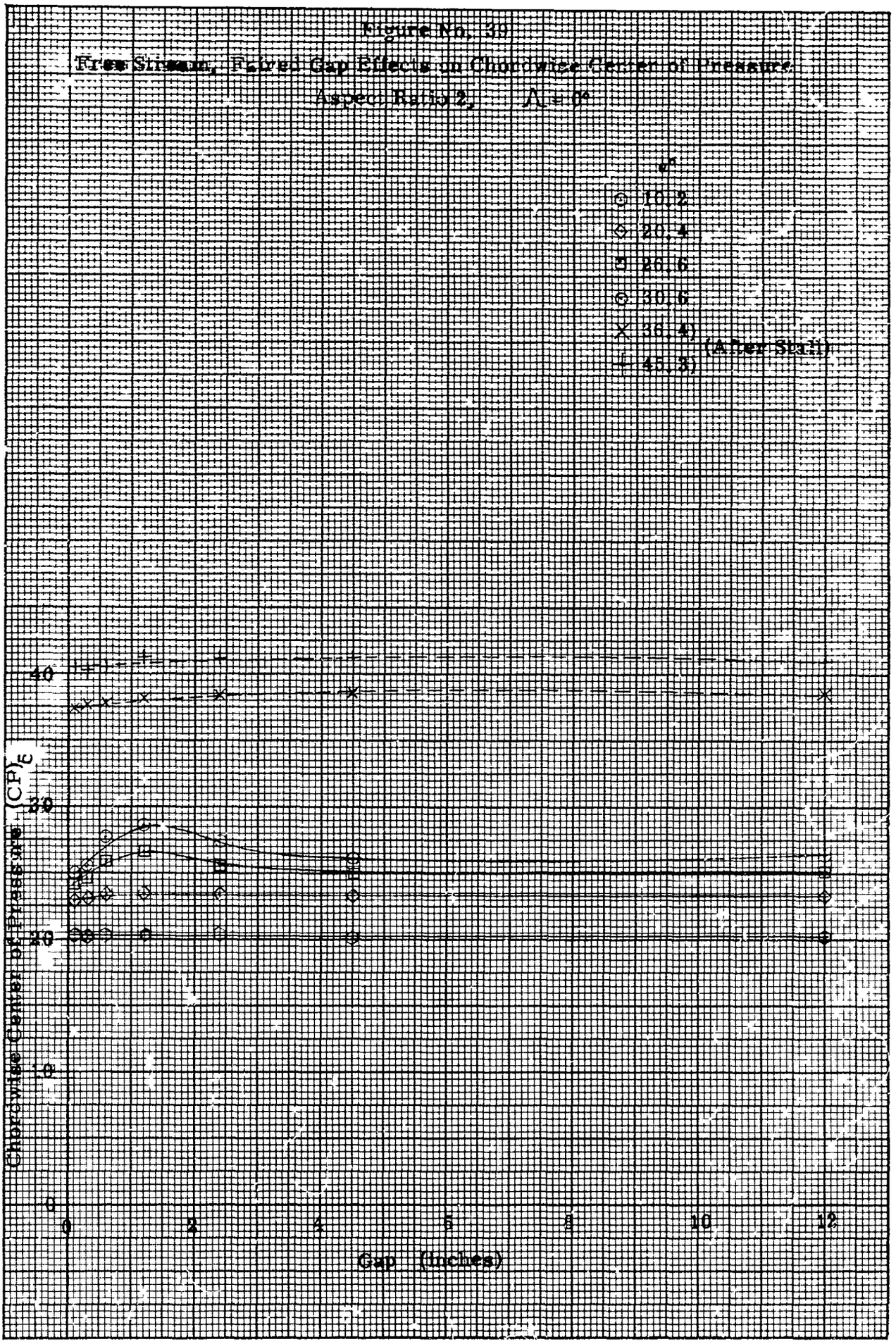

K&E 10 TC CH 1323
7 X 10 INCHES MADE IN U.S.A.
KEUFFEL & ESSER CO.

Figure No. 40

Free Stream, Paired Gap Effects on Chordwise Center of Pressure

Aspect Ratio 2, $\Lambda = 12^\circ$

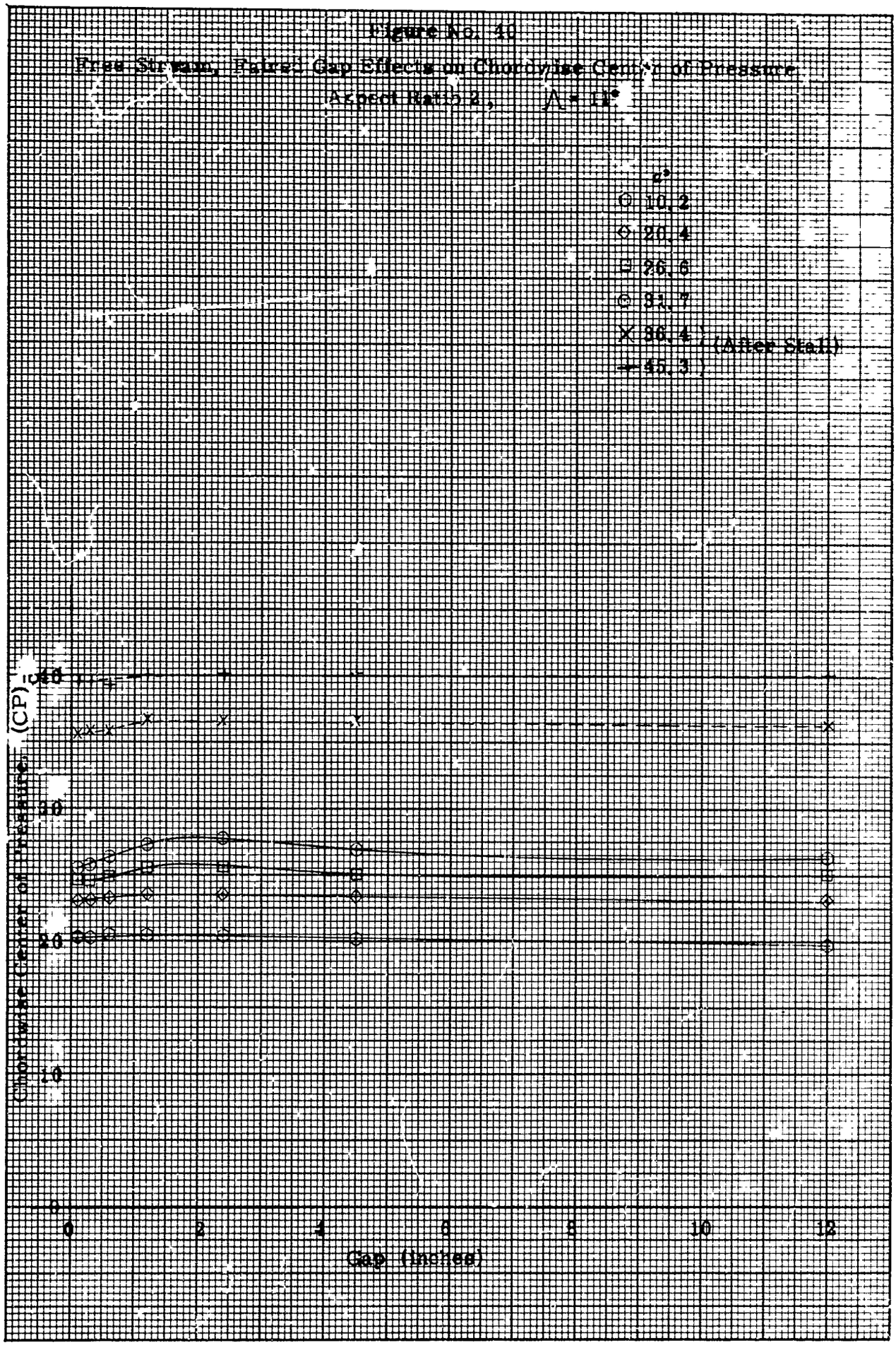

K•E 10 X 10 TO ½ INCH 46 1323
7 X 10 INCHES MADE IN U.S.A.
KEUFFEL & ESSER CO.

Figure No. 41

Free Stream, Paired Gap Effects on Chordwise Center of Pressure

Aspect Ratio 2, Λ = 42.5°

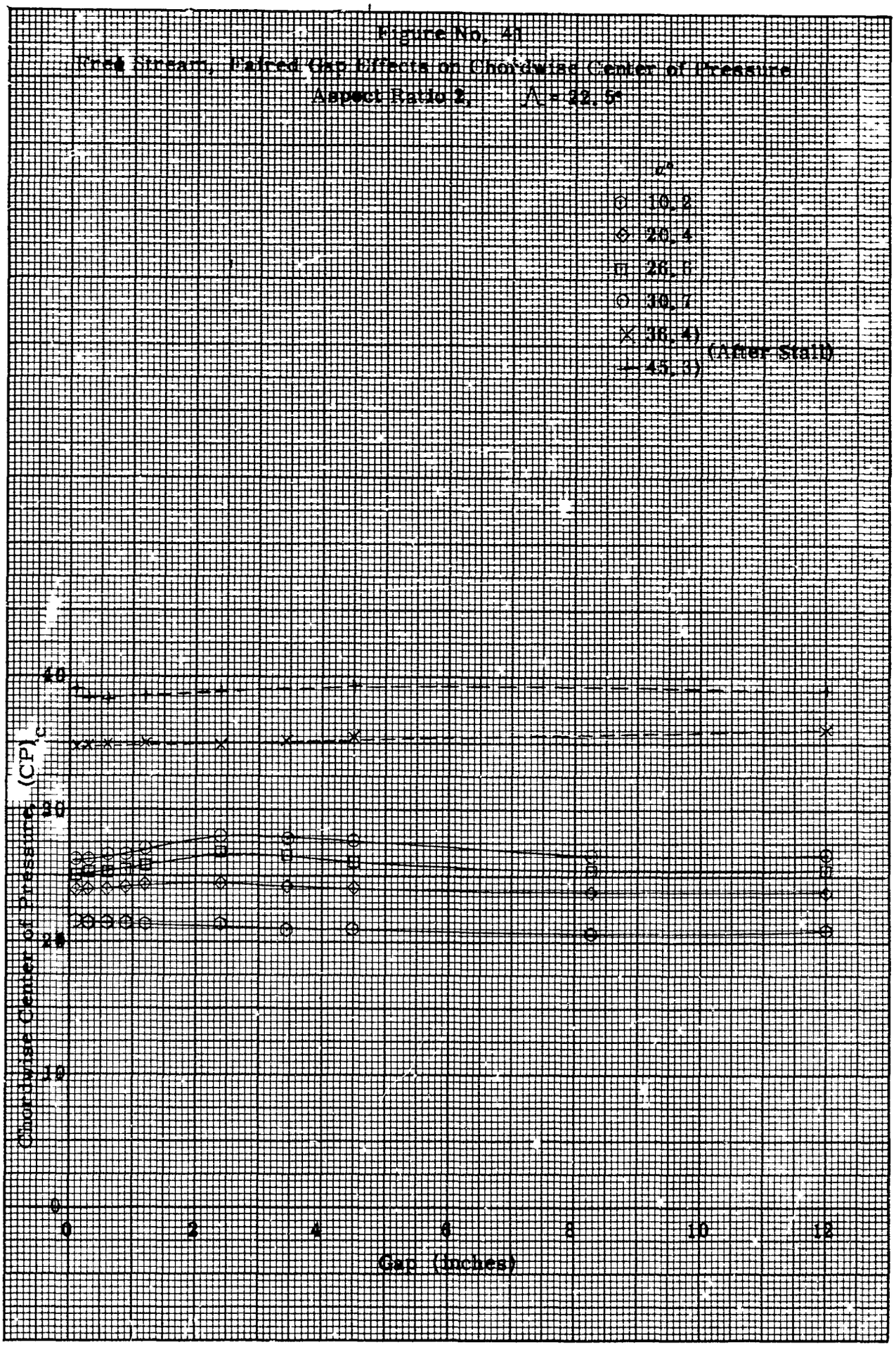

K+E 10 X 10 TO ½ INCH 46 1323
7 X 10 INCHES MADE IN U.S.A.
KEUFFEL & ESSER CO.

K+E 10 X 10 TO ½ INCH 46 1323
7 X 10 INCHES MADE IN U.S.A.
KEUFFEL & ESSER CO.

Figure No. 42

Free Stream, Faired Gap Effects on Chordwise Center of Pressure, Aspect Ratio 3, $\Lambda_c = 0°$

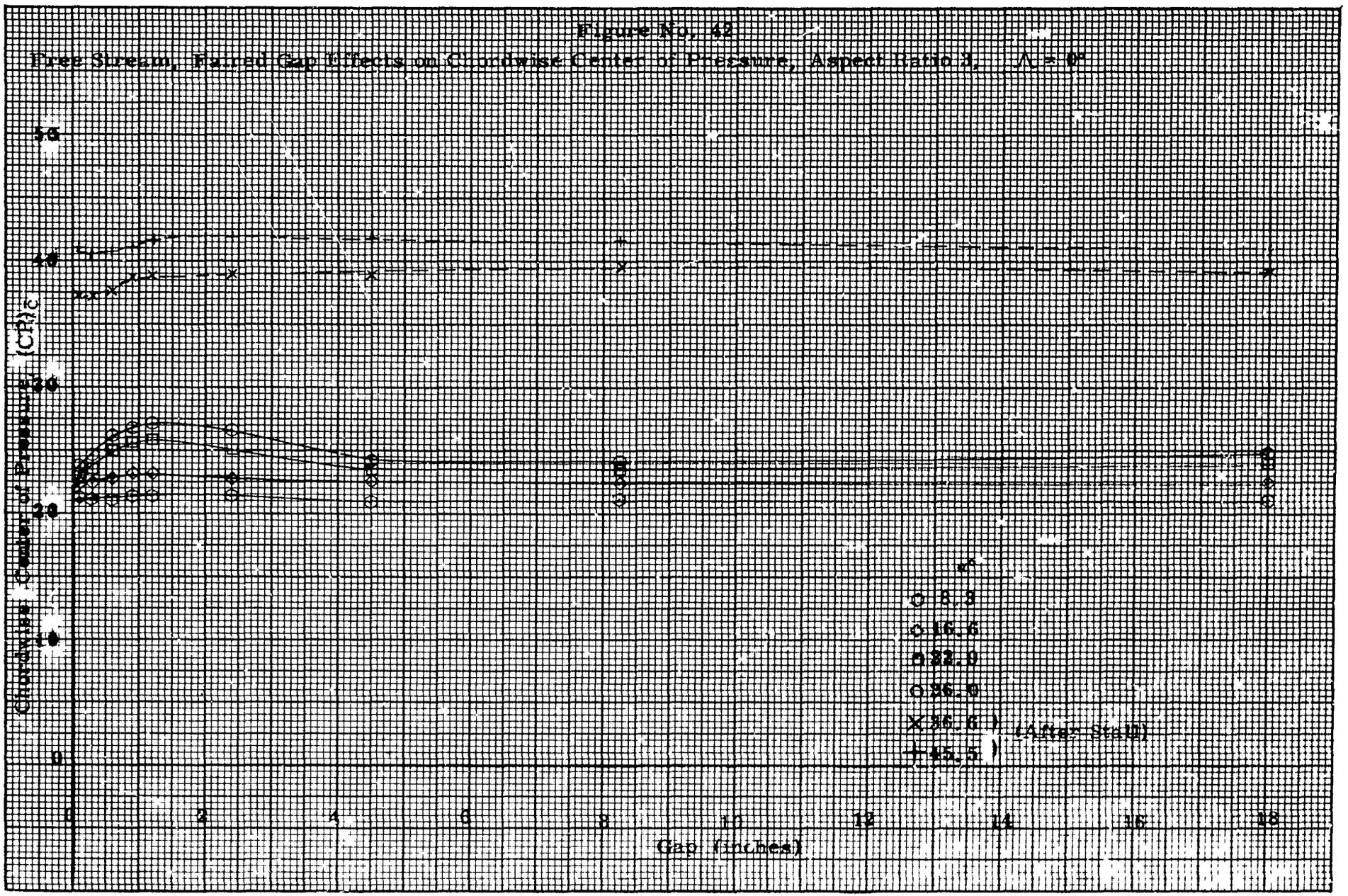

K&E 10 X 10 TO ½ INCH 46 1323
7 X 10 INCHES MADE IN U.S.A.
KEUFFEL & ESSER CO.

Figure No. 43

Free Stream, Paired Gap Effects on Chordwise Center of Pressure, Aspect Ratio 3, $\Lambda_c = 11^\circ$

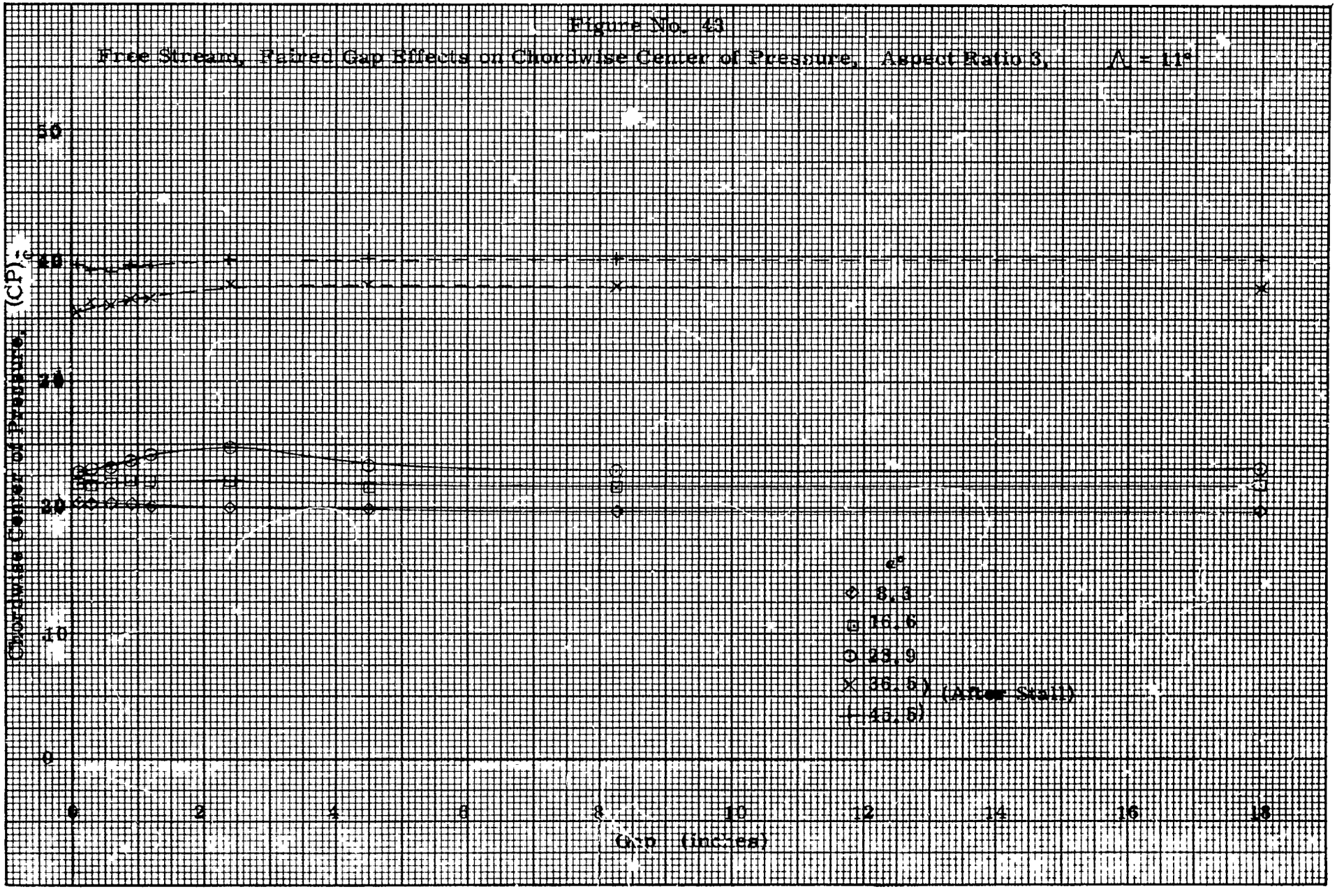

K+E 10 X 10 TO ½ INCH 46 1323
7 X 10 INCHES MADE IN U.S.A.
KEUFFEL & ESSER CO.

Figure No. 54

Free Stream, Paired Gap Effects on Chordwise Center of Pressure, Aspect Ratio 3, $\Lambda = 22.5°$

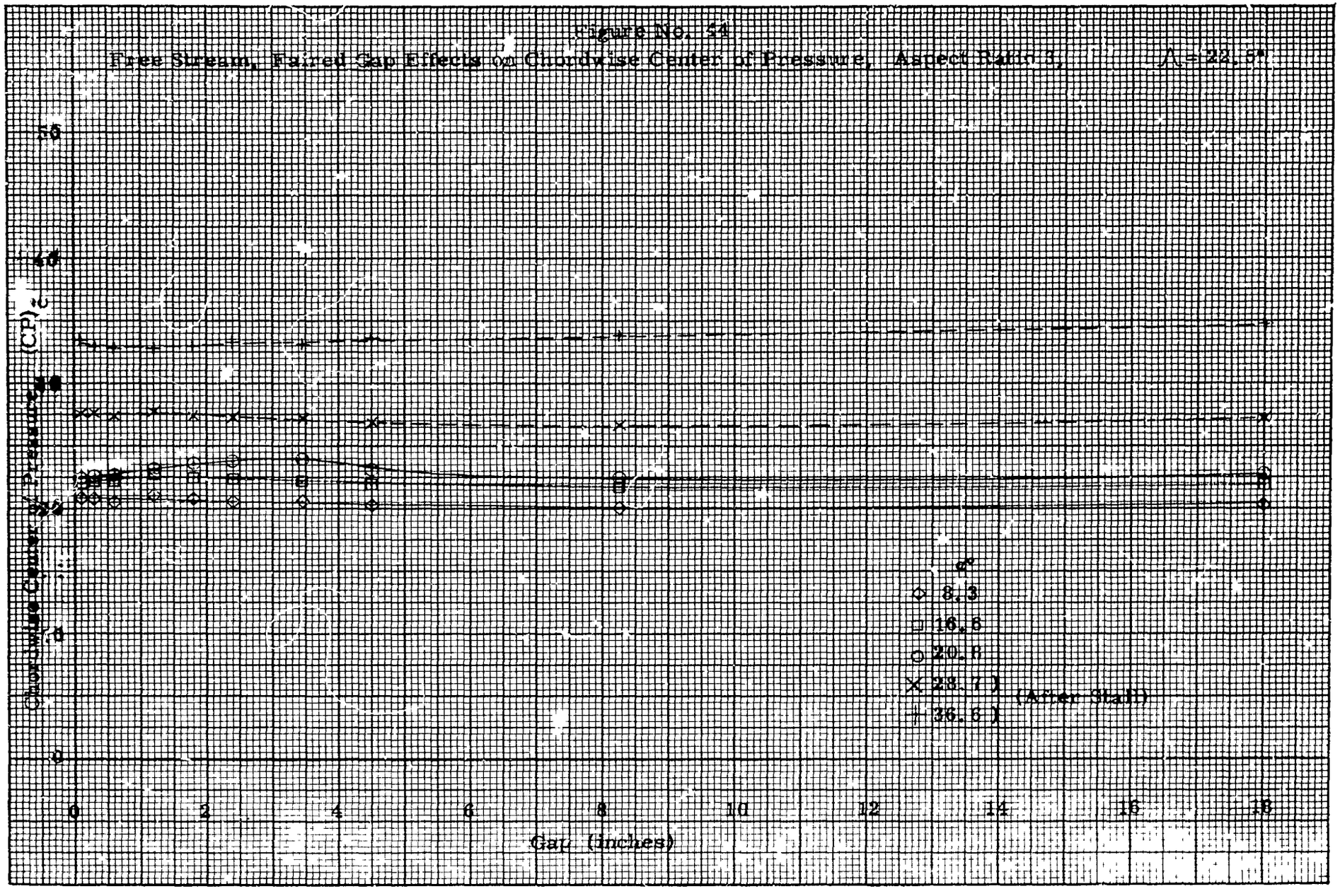

Figure No. 45

Free Stream, Paired Gap Effects on Spanwise Center of Pressure

Aspect Ratio 2, $\Lambda = 0°$

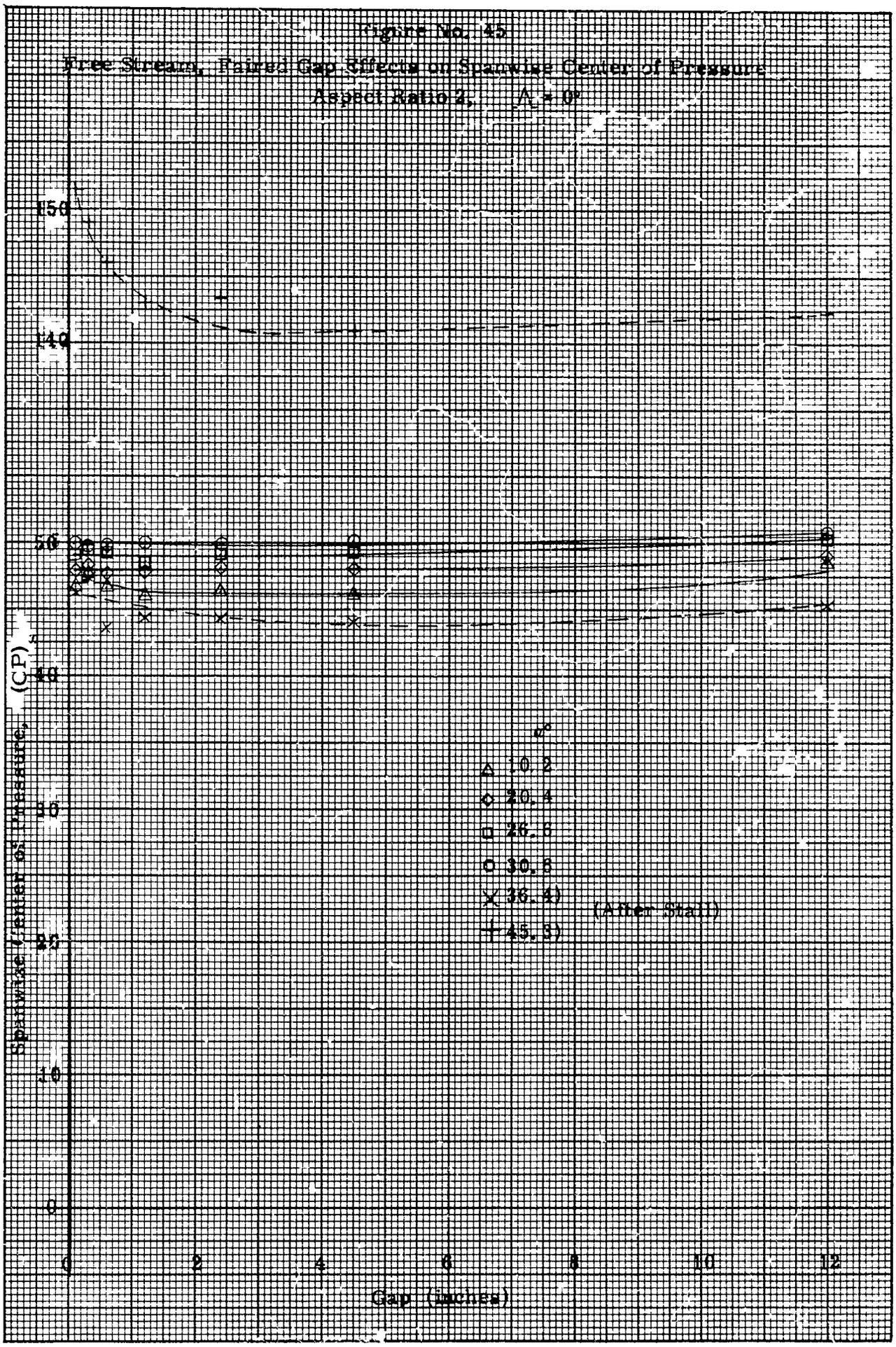

K+E 10 X 10 TO ½ INCH 46 1323
7 X 10 INCHES MADE IN U.S.A.
KEUFFEL & ESSER CO.

Figure No. 46

Free Stream, Paired Gap Effects on Spanwise Center of Pressure

Aspect Ratio 2. $\Lambda = 11°$

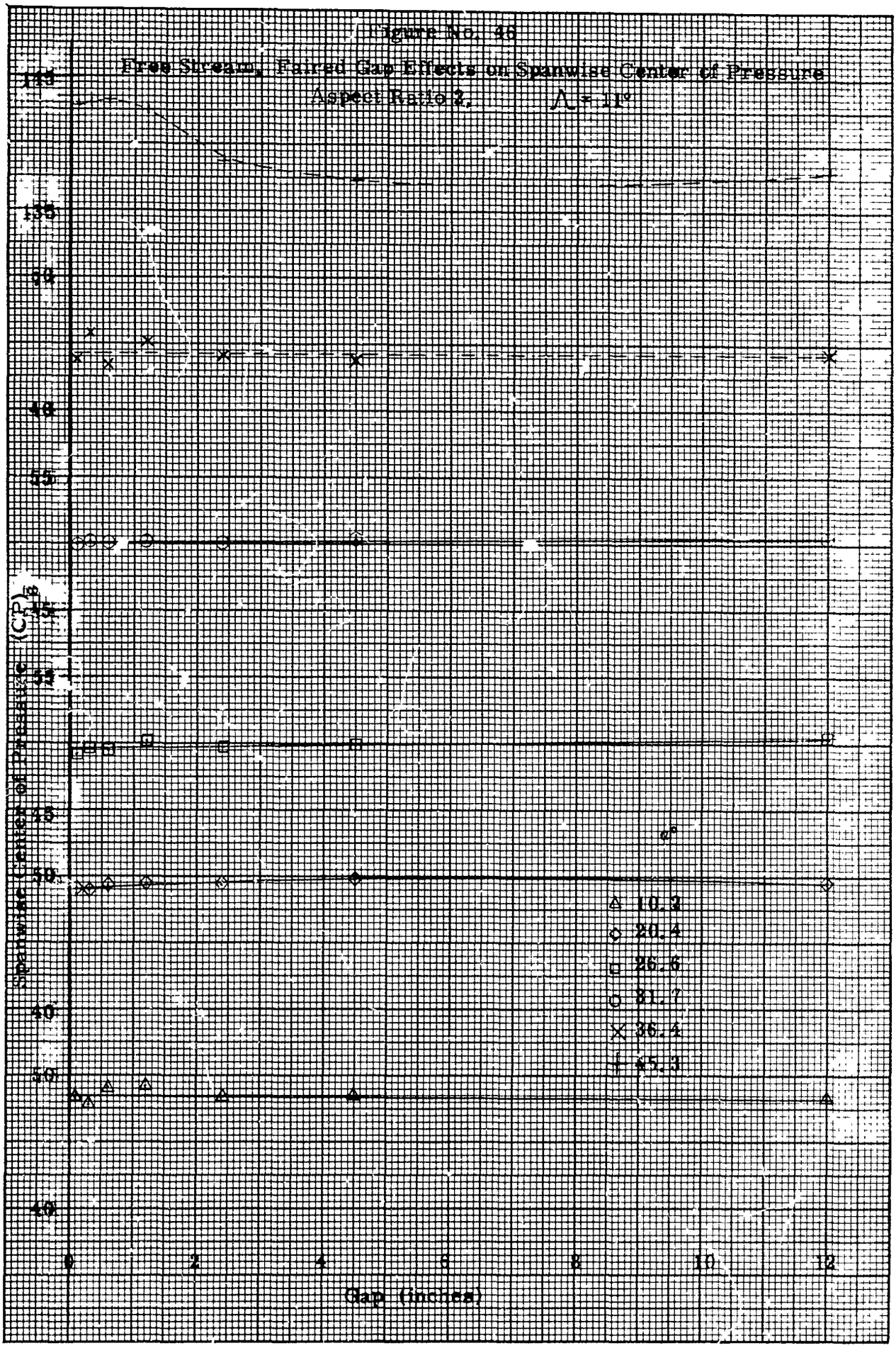

K+E 10 X 10 TO ½ INCH 46 1323
7 X 10 INCHES MADE IN U.S.A.
KEUFFEL & ESSER CO.

Figure No. 47

Free Stream, Paired Gap Effects on Spanwise Center of Pressure

Aspect Ratio 2, $\Lambda_{LE} = 22.5°$

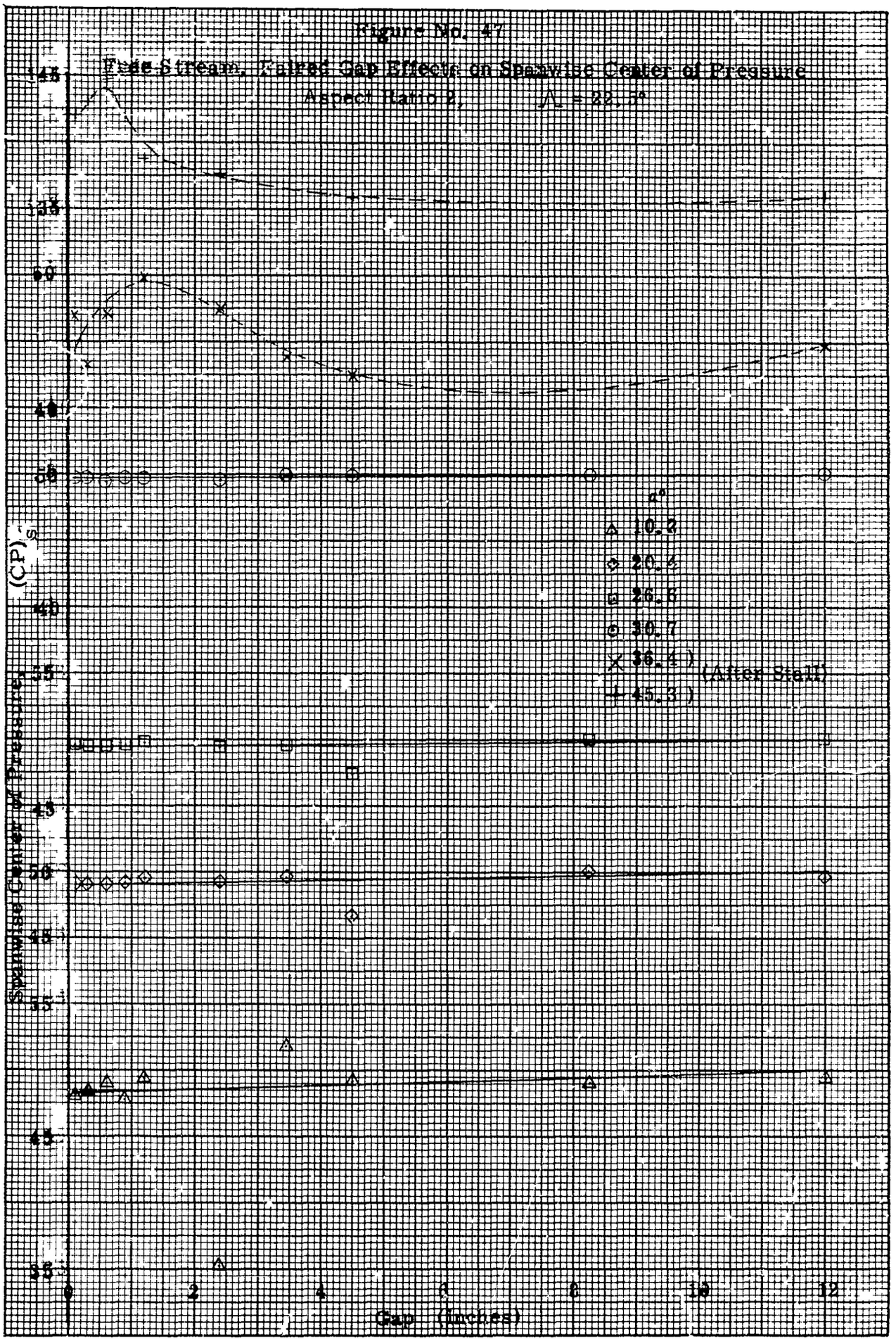

K+E 10 X 10 TO 7 X 10 INCH 359 1323 MADE IN U.S.A. KEUFFEL & ESSER CO.

K+E 10 X 10 TO ½ INCH 46 1323
7 X 10 INCHES MADE IN U.S.A.
KEUFFEL & ESSER CO.

Figure No. 48

Free Stream, Faired Gap Effects on Spanwise Center of Pressure, Aspect Ratio 3, $\Lambda = 0°$

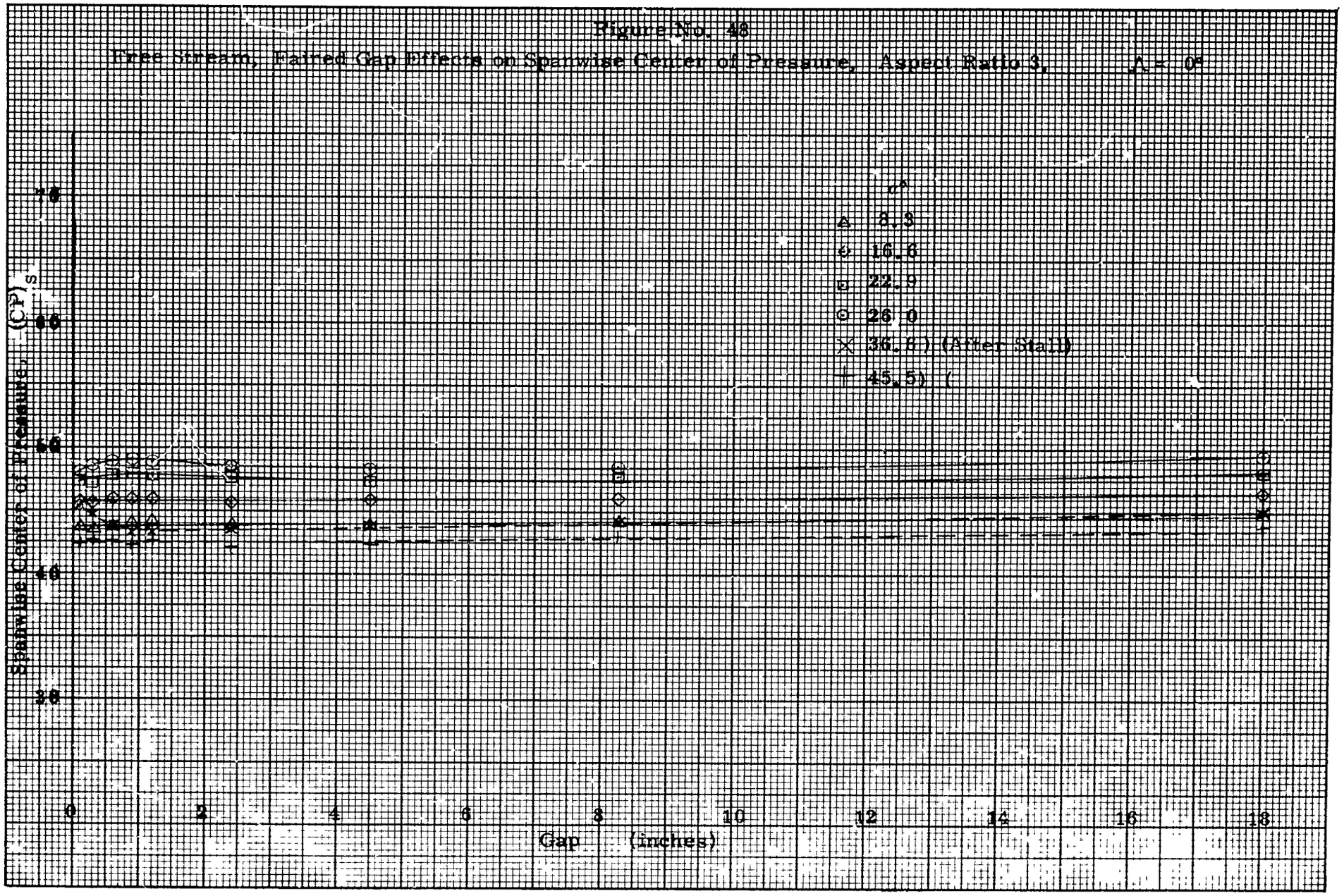

K&E 10 X 10 TO ½ INCH 46 1323
7 X 10 INCHES MADE IN U.S.A.
KEUFFEL & ESSER CO.

Figure No. 49

Free Stream, Faired Gap Effects on Spanwise Center of Pressure, Aspect Ratio 3, $\Lambda = 11°$

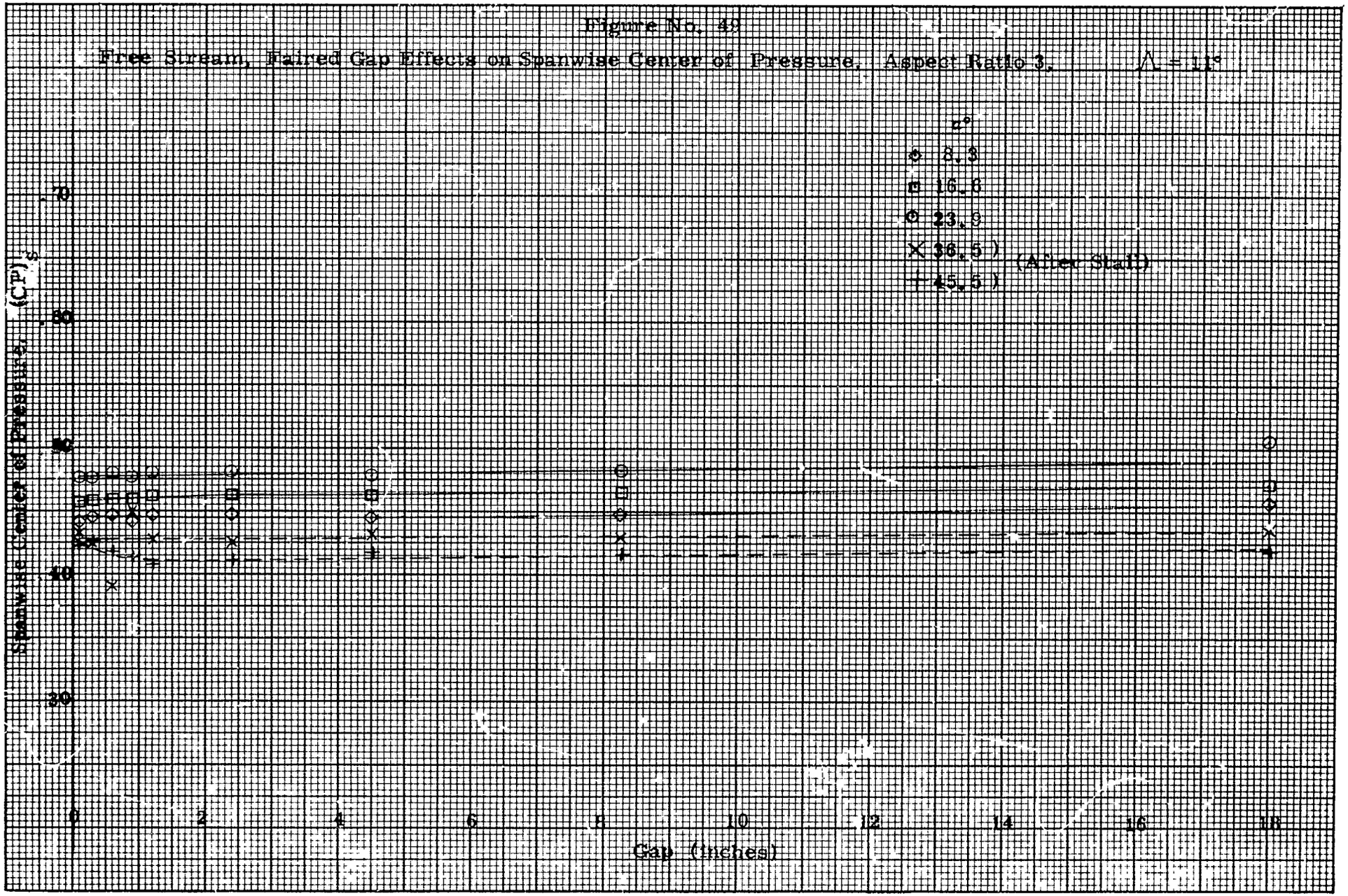

K+E 10 X 10 TO ½ INCH 46 1323
7 X 10 INCHES MADE IN U.S.A.
KEUFFEL & ESSER CO.

Figure No. 50

Free Stream, Faired Cap Effects on Spanwise Center of Pressures, Aspect Ratio 3, $\Lambda_{\frac{1}{4}}$ = 22.5°

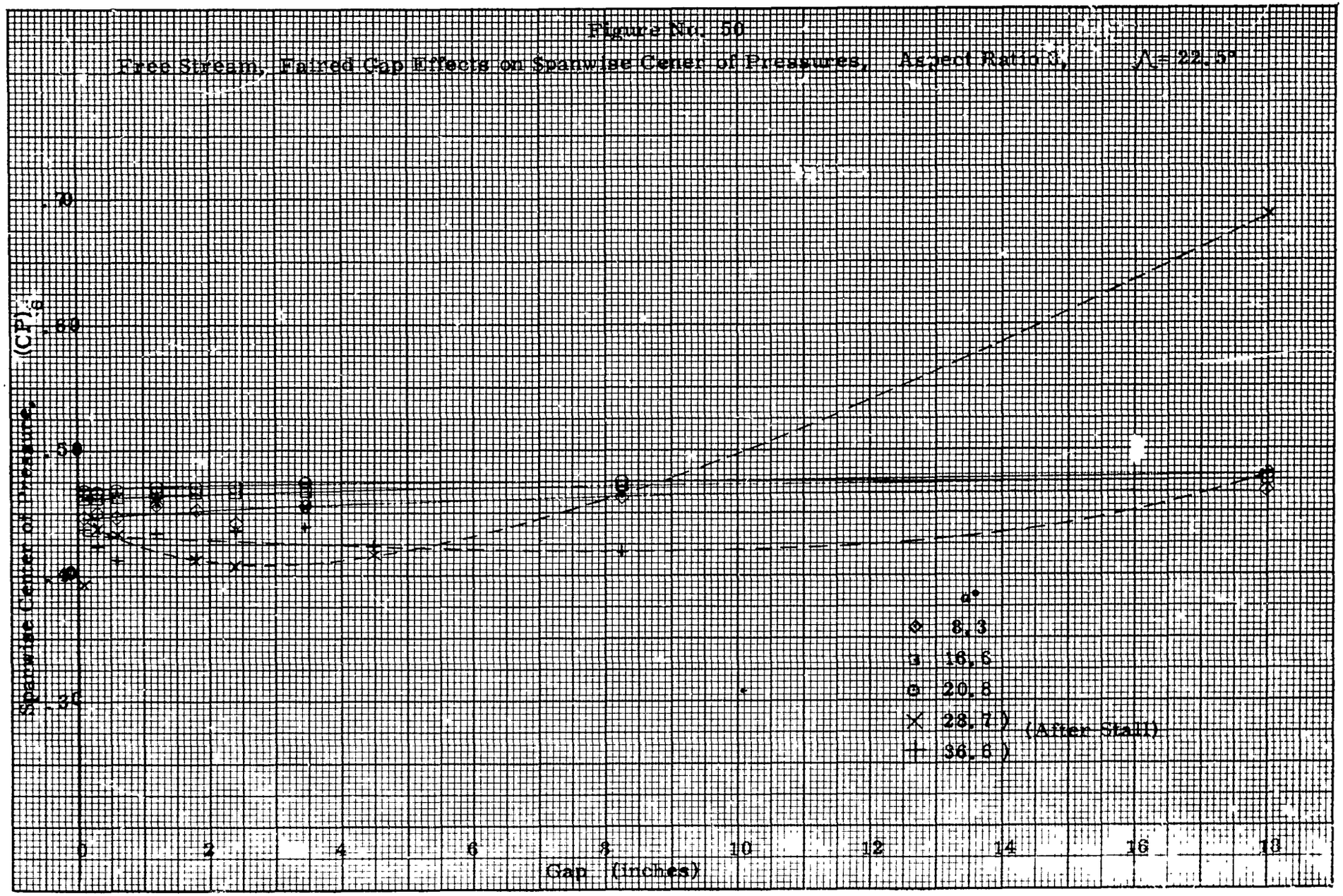

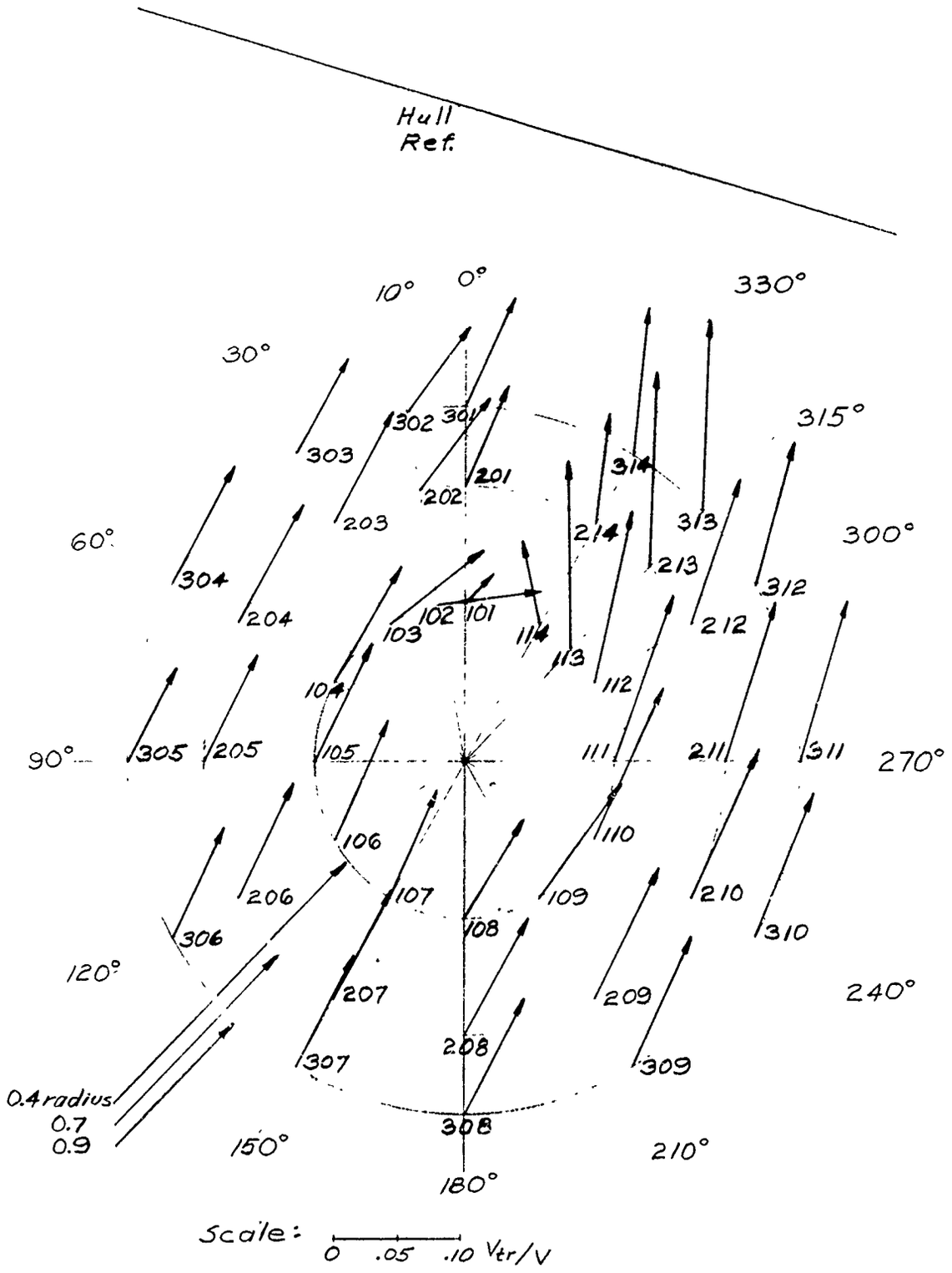

Figure No. 51. Wake Velocity Diagram
(From Figure 11 of Reference 6)

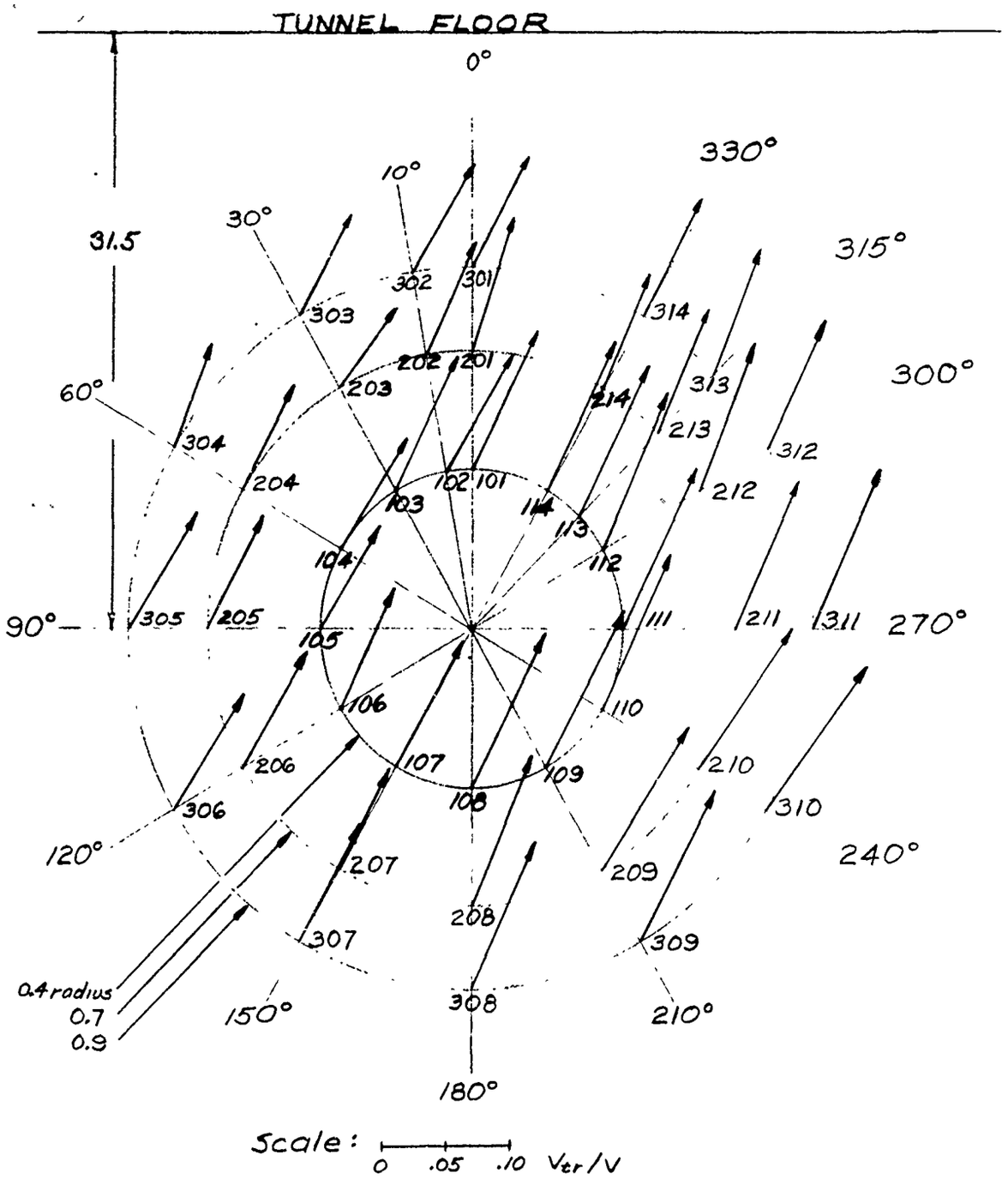

Figure No. 52. Wake Velocity Diagram For Simulated Hull Flow.

Figure No. 58

Faired Gap Effects on Lift Coefficient for Simulated Full Flow,

Aspect Ratio 2, $\Lambda = 0°$

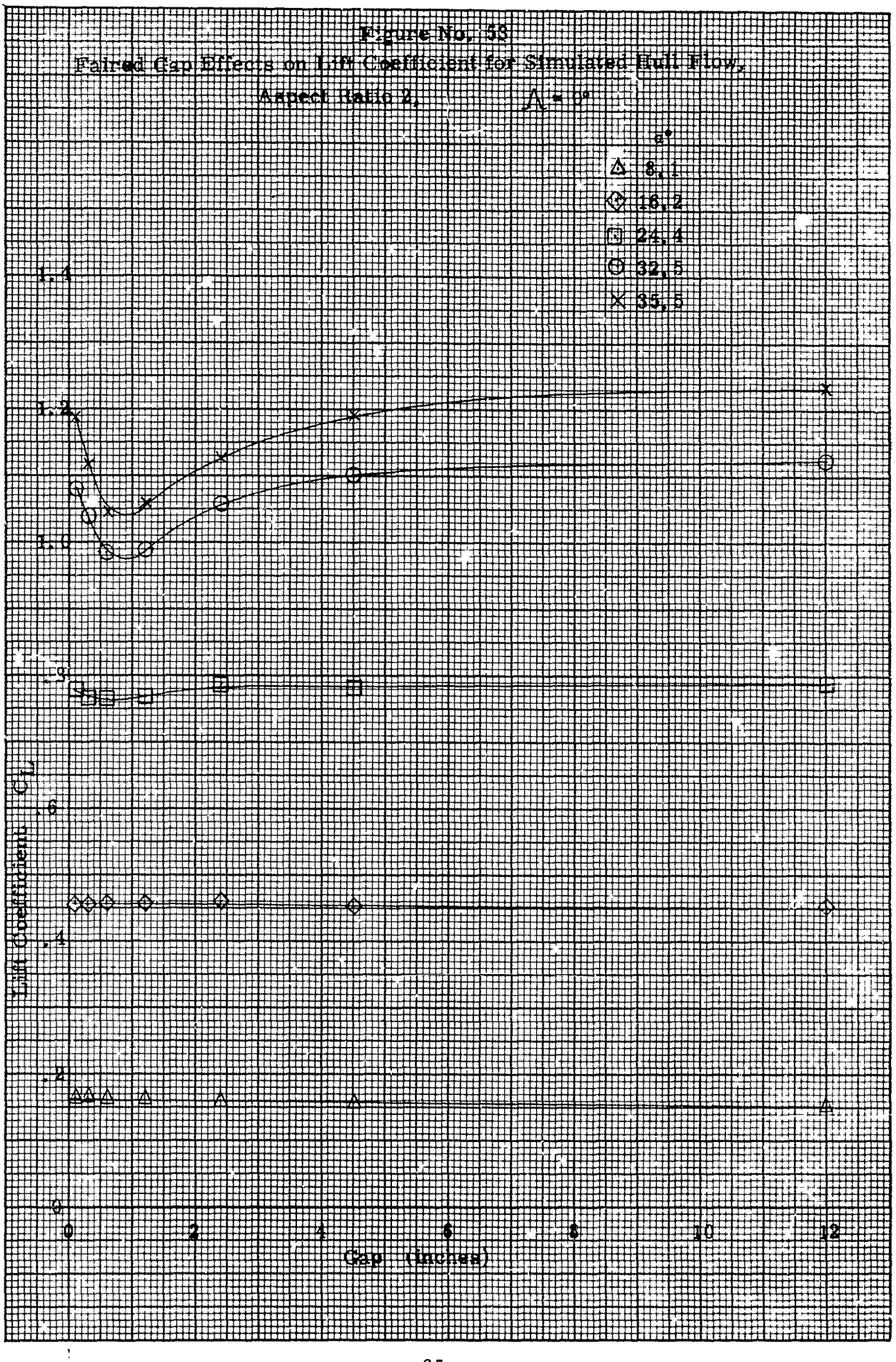

K&E 10 X 10 TO ½ INCH 359 1323
7 X 10 INCHES MADE IN U.S.A.
KEUFFEL & ESSER CO.

Figure No. 54

Tapered Gap Effects on Drag Coefficient for Simulated Hull Flow

Aspect Ratio 2, $\Lambda = 0°$

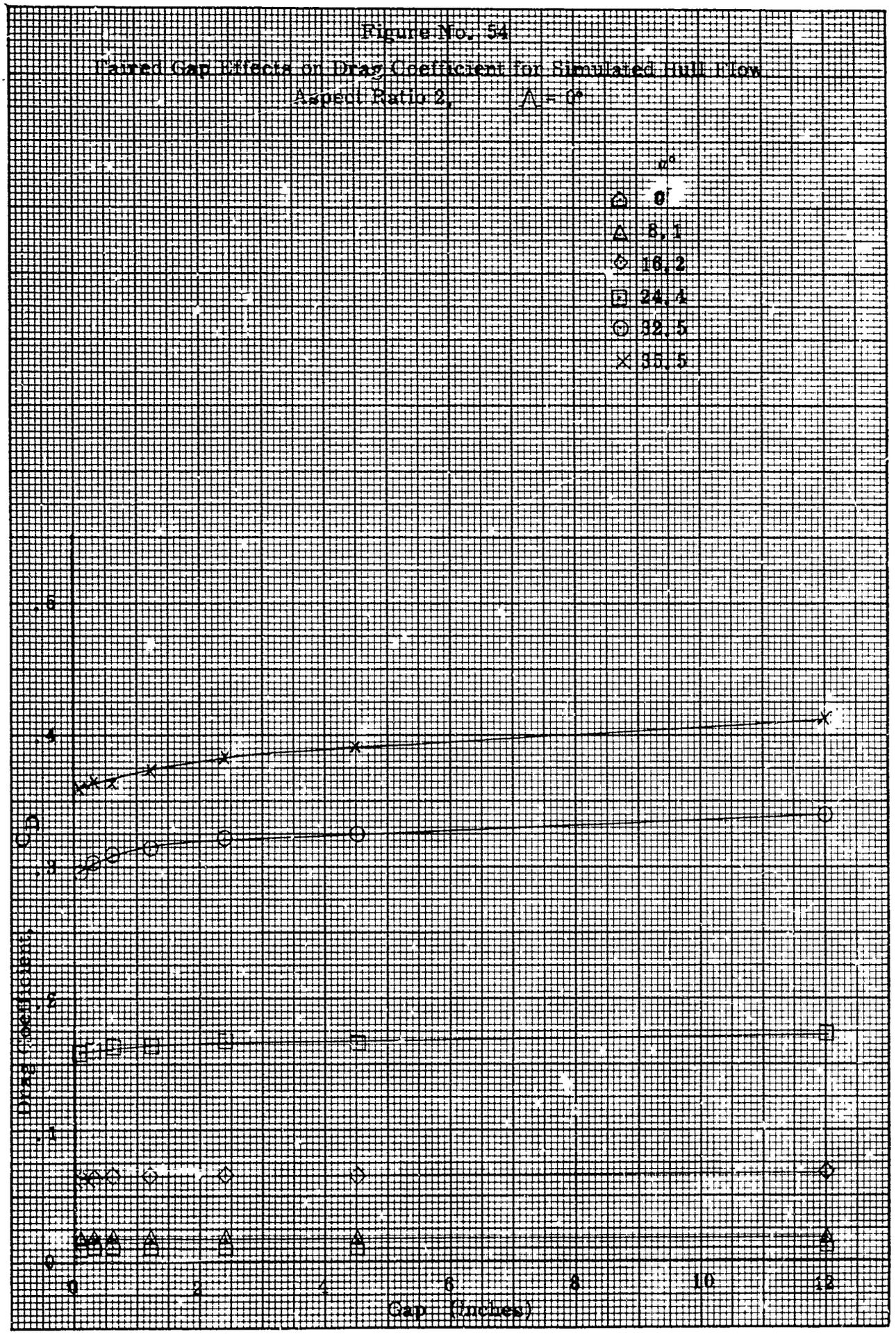

K&E 7 X 10 INCHES MADE IN U.S.A. KEUFFEL & ESSER CO.

Figure No. 55

Faired Gap Effects on Chordwise Center of Pressure for Simulated Hull Flow, Aspect Ratio 2, $A_s = 0^F$

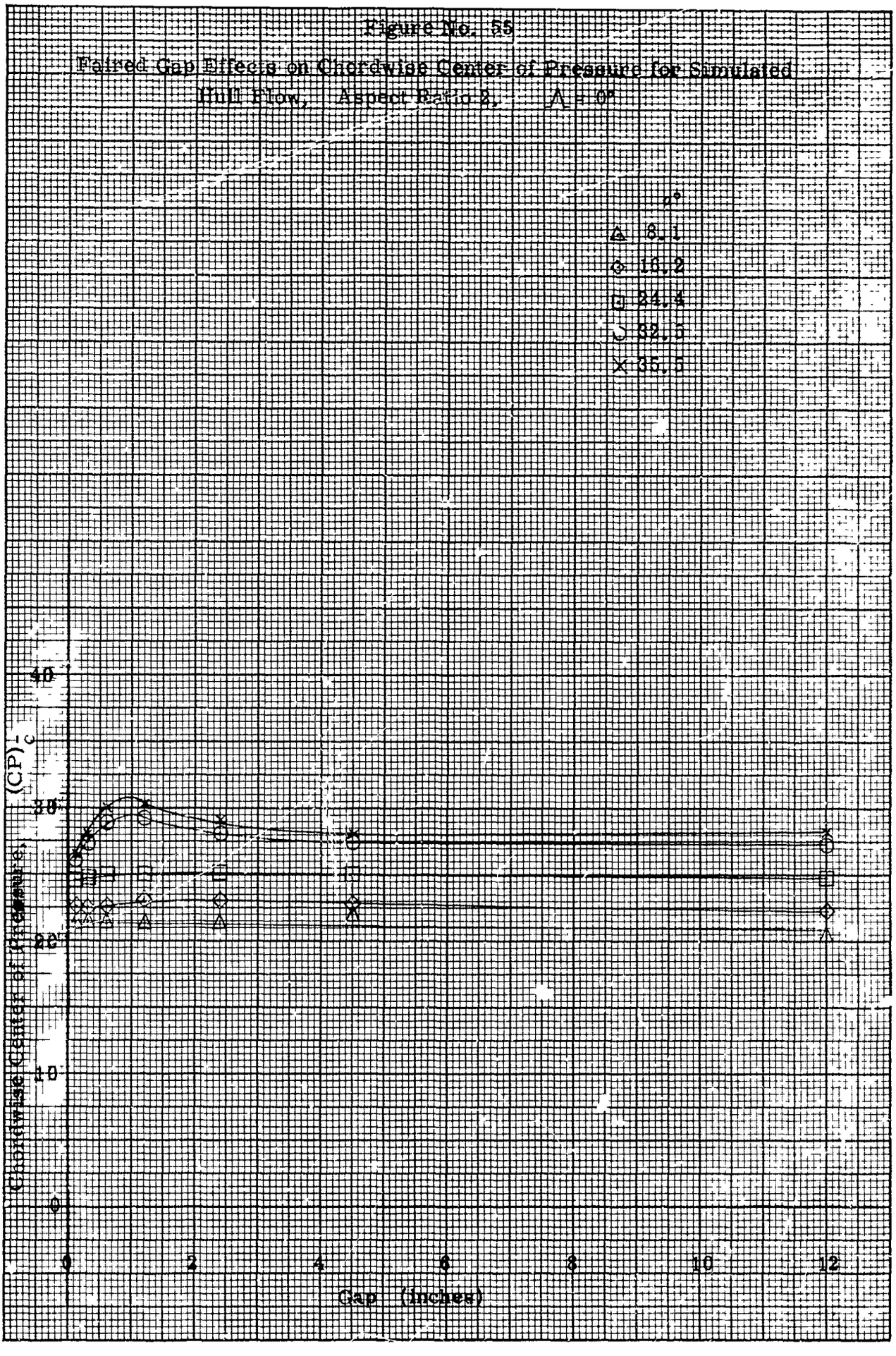

K+E 10 X 10 TO ½ INCH 46 1323
7 X 10 INCHES MADE IN U.S.A.
KEUFFEL & ESSER CO.

Figure No. 56

Faired Gap Effects on Spanwise Center of Pressure for Simulated Half Flow, Aspect Ratio 2 $\Lambda = 0°$

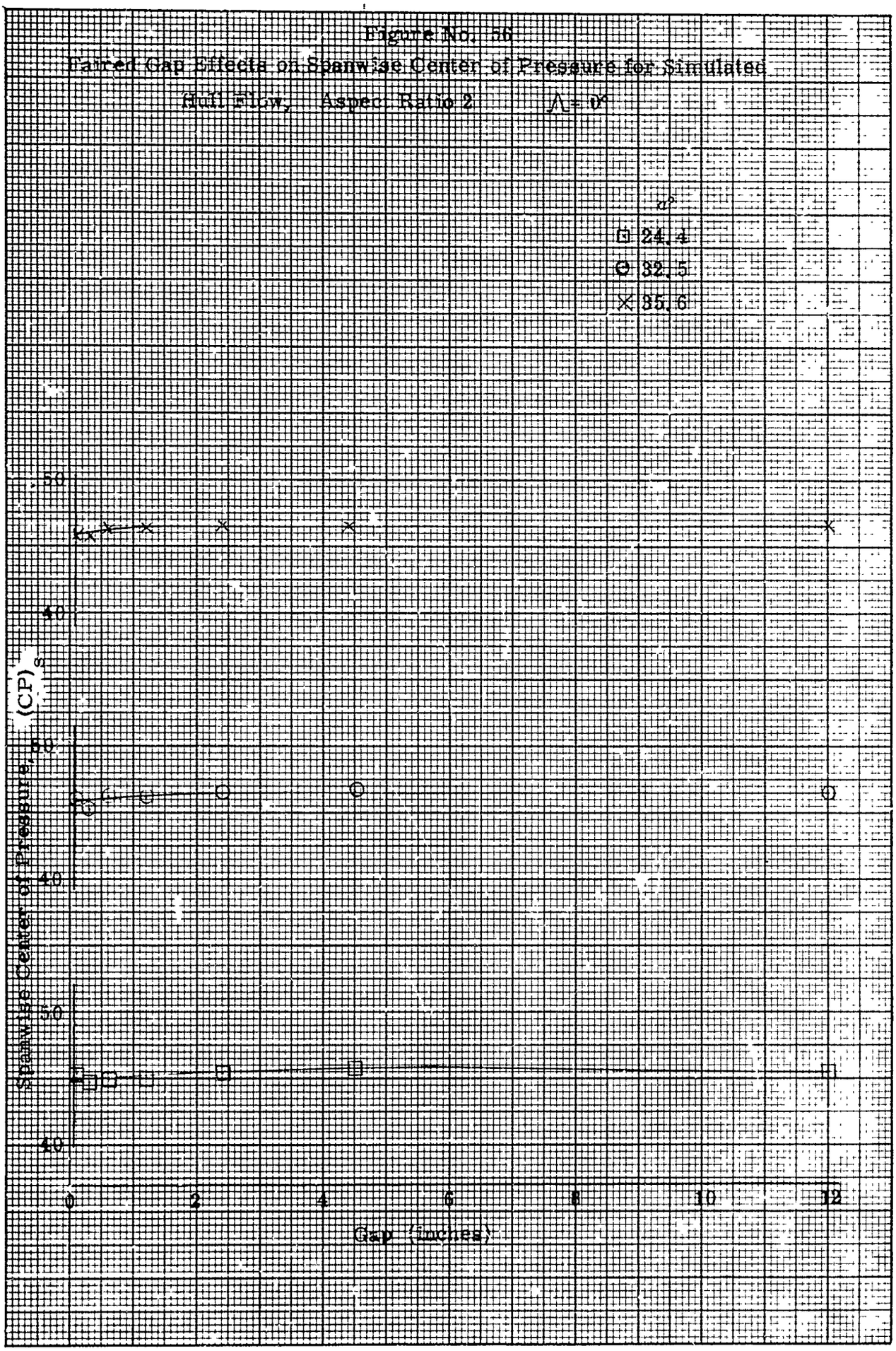

K+E 10 X 10 TO ½ INCH 46 1323
7 X 10 INCHES MADE IN U.S.A.
KEUFFEL & ESSER CO.

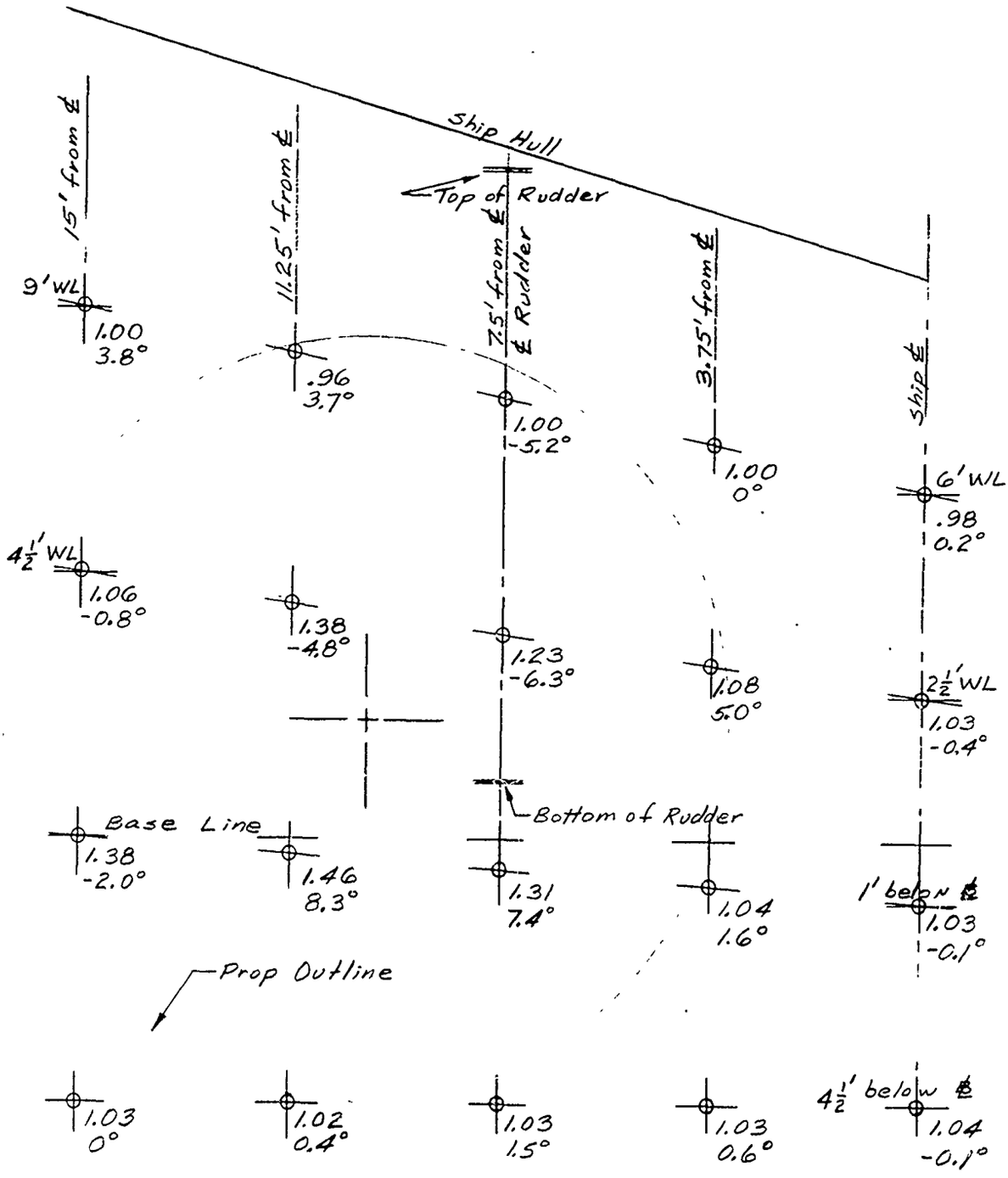

Figure No. 57. Velocity Field at Rudder Leading Edge, (From Figure 5 of Reference 7)

Note: At each location, the upper figure is the value of Vx/V, and the lower figure is the flow angle. (Positive in the direction of the ship ℄)

Note: At each location, the upper figure is the value of Vx/V, and the lower figure is the flow angle. (Positive in the direction of the ship ℄)

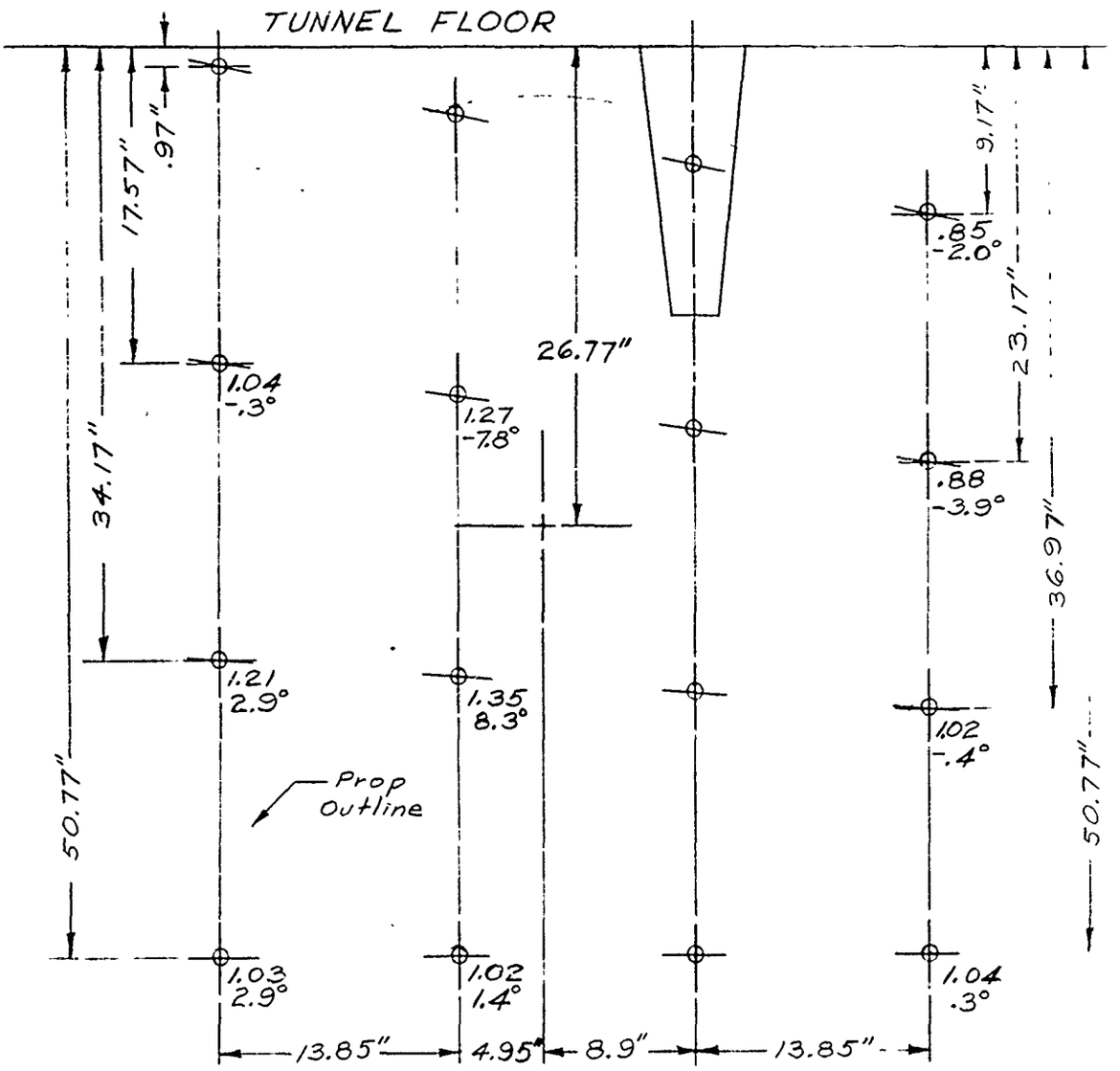

Figure No. 58. Propeller Slipstream Velocity Survey at Rudder Leading Edge, Aspect Ratio 1.

Note: At each location, the upper figure is the value of Vx/V, and the lower figure is the flow angle. (Positive in the direction of the ship $\mathbb{C}_L$)

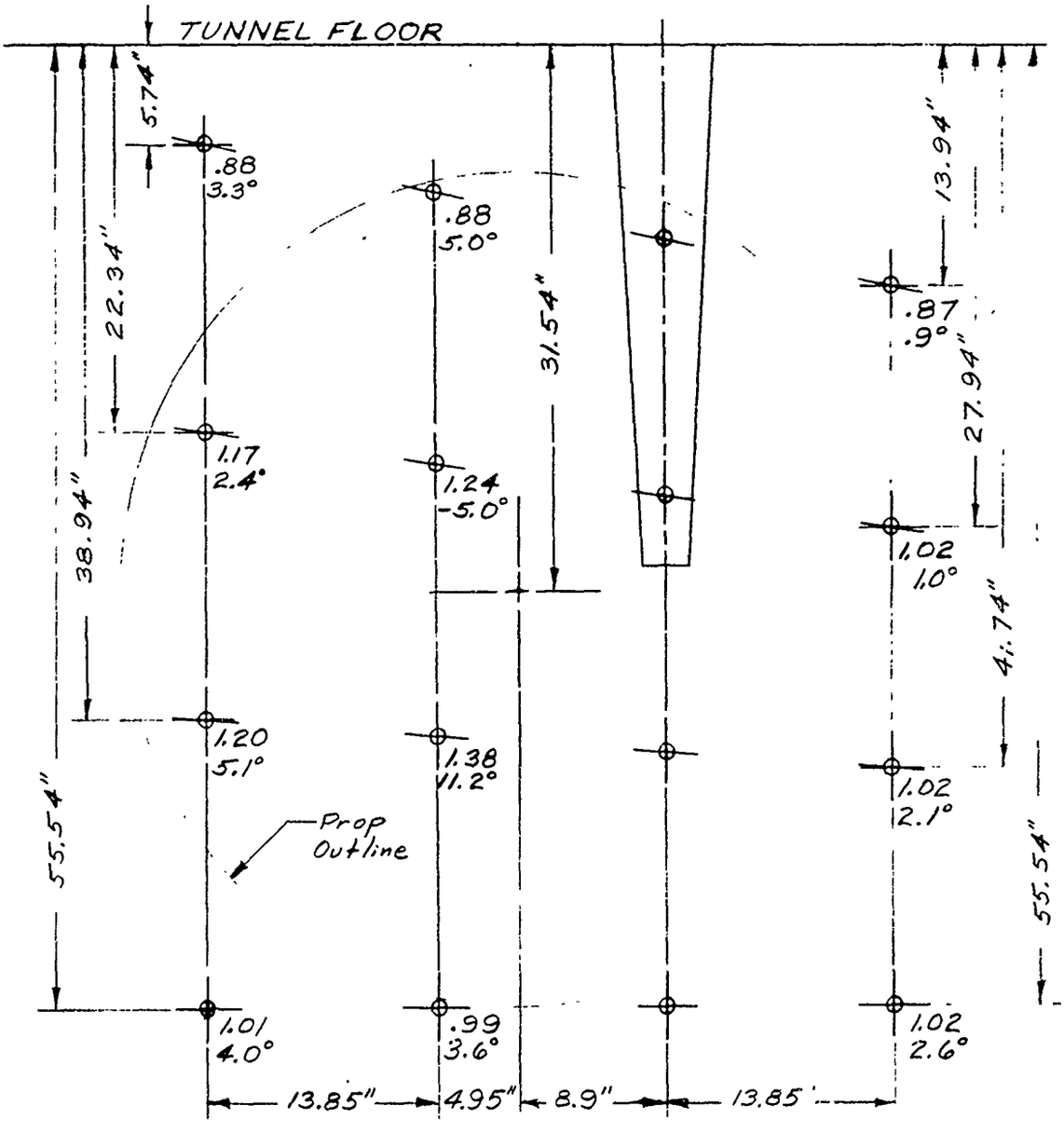

Figure No. 59. Propeller Slipstream Velocity Survey at Rudder Leading Edge, Aspect Ratio 2.

Figure No. 60. Propeller Slipstream Velocity Survey at Rudder Leading Edge, Aspect Ratio 3.

Note: At each location, the upper figure is the value of Vx/V, and the lower figure is the flow angle. (Positive in the direction of the ship $\mathbb{C}_L$)

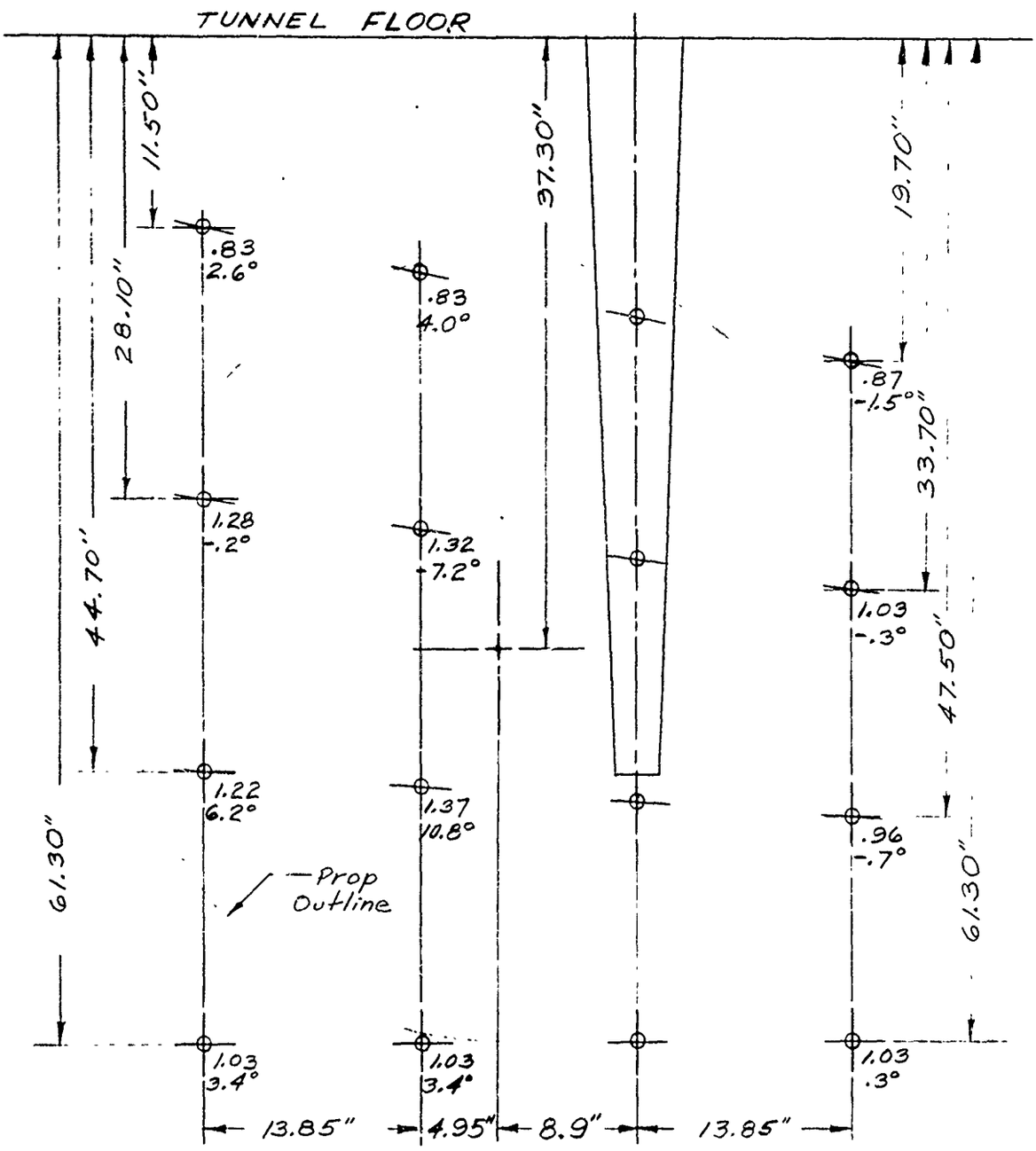

FIGURE NO 61

COMPARISON OF LIFT COEFFICIENTS FOR FREE STREAM, SIMULATED HULL FLOW AND PROPELLER SLIPSTREAM CONDITIONS, ASPECT RATIO 1, $\Lambda = 0°$

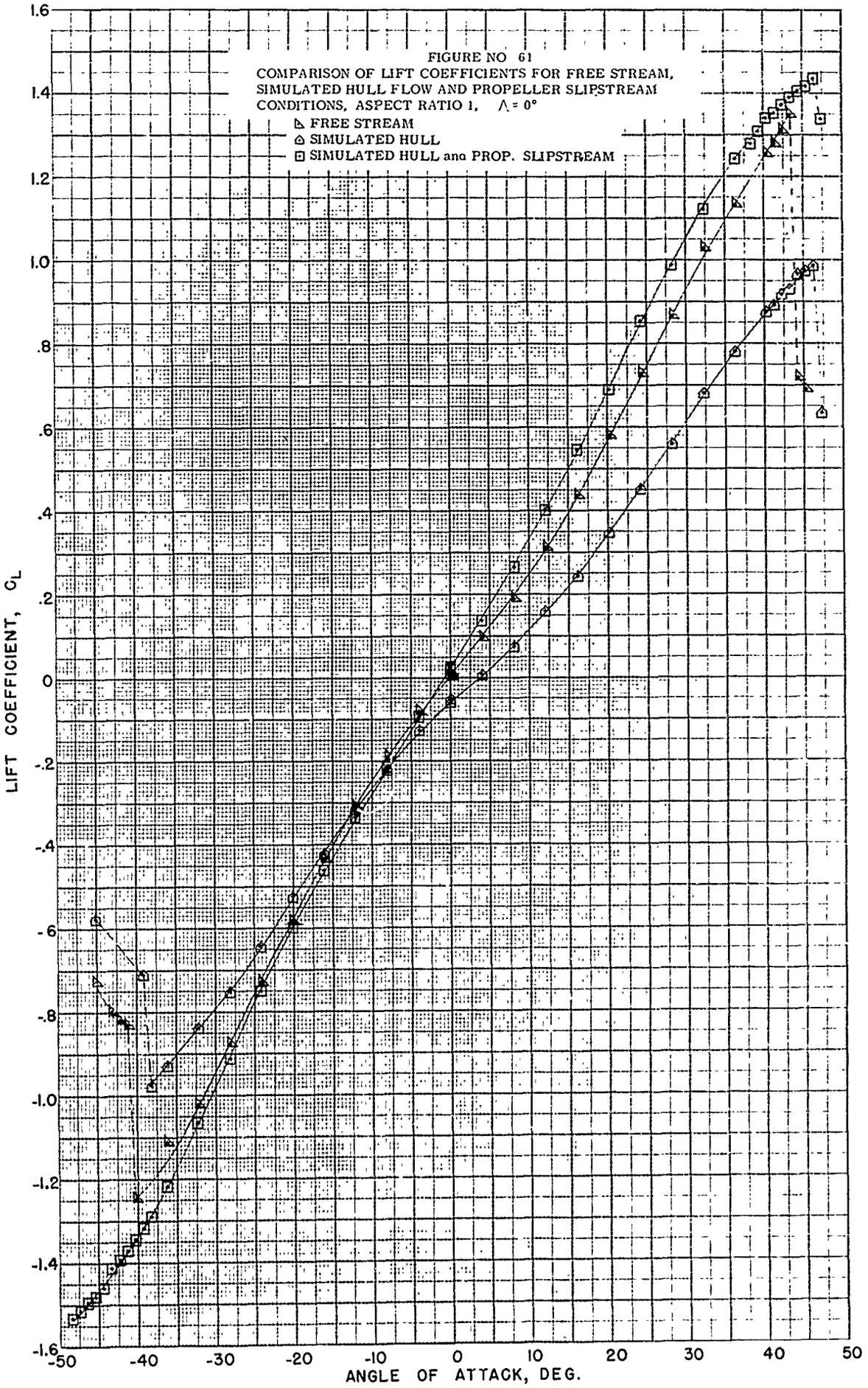

FIGURE NO 62
COMPARISON OF LIFT COEFFICIENTS FOR FREE STREAM, SIMULATED HULL FLOW AND PROPELLER SLIPSTREAM CONDITIONS, ASPECT RATIO 1, $\Lambda = 11°$

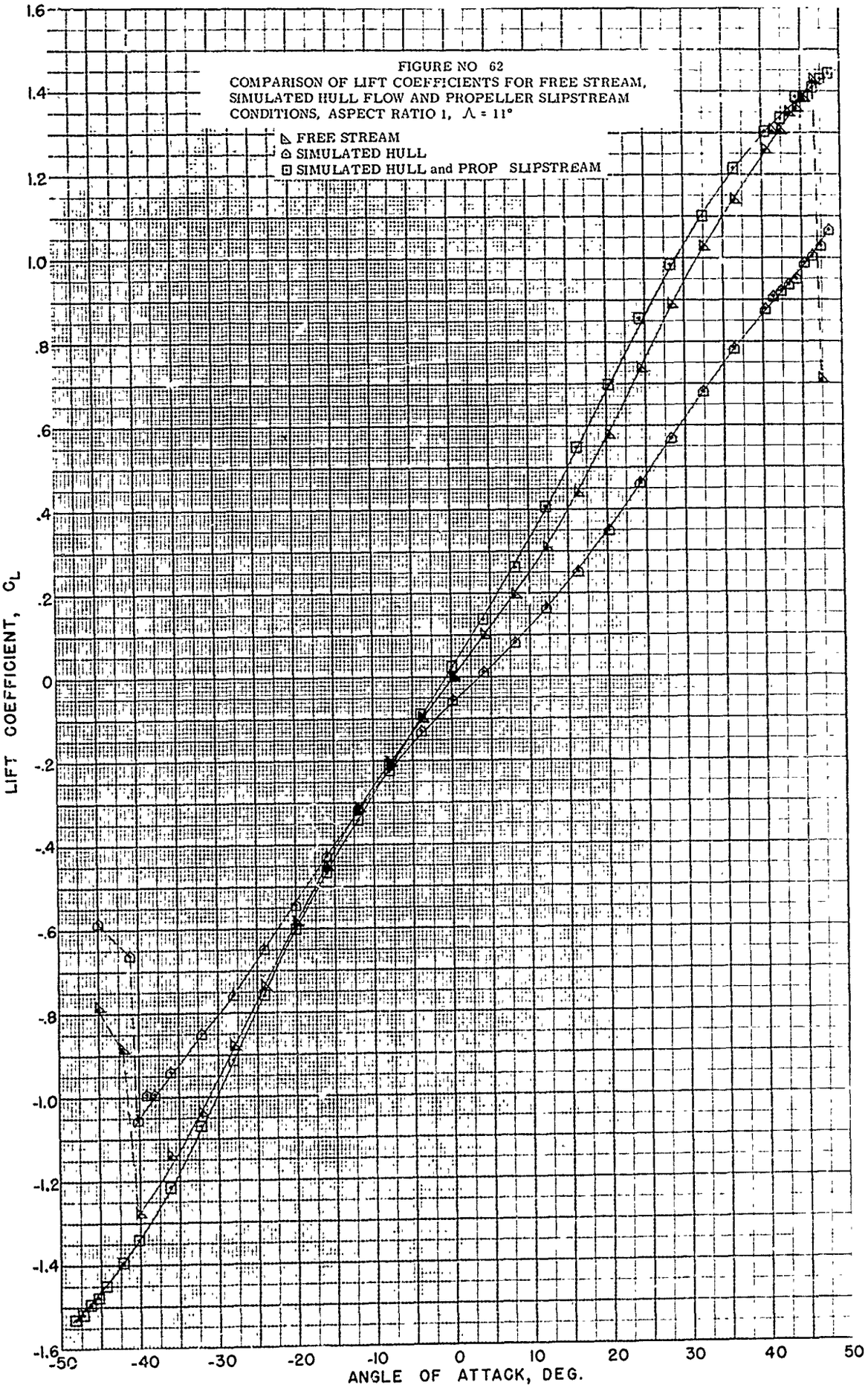

FIGURE NO 63
COMPARISON OF LIFT COEFFICIENTS FOR FREE STREAM, SIMULATED HULL FLOW AND PROPELLER SLIPSTREAM CONDITIONS, ASPECT RATIO 1, $\Lambda = 22.5°$

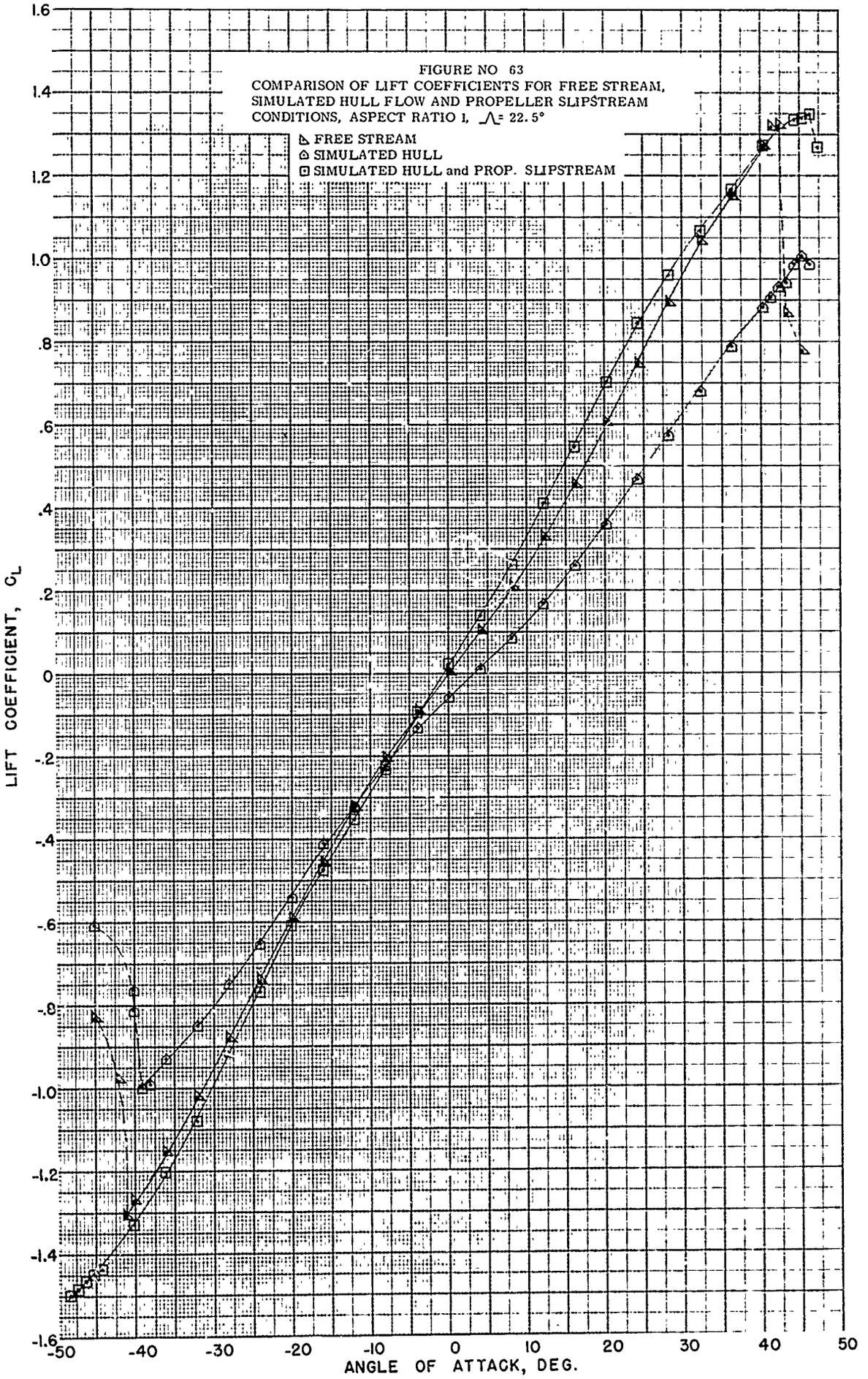

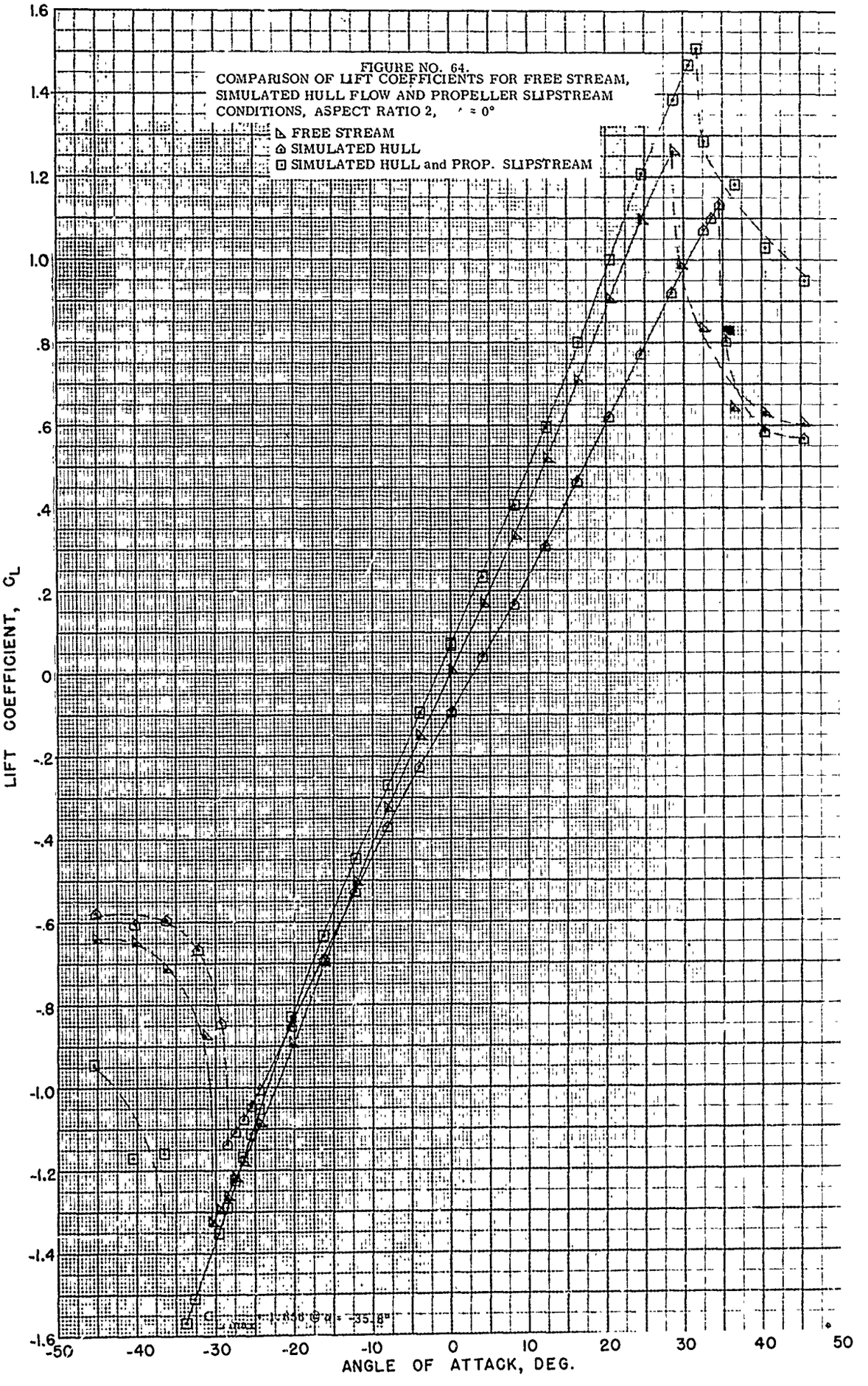
FIGURE NO. 64.
COMPARISON OF LIFT COEFFICIENTS FOR FREE STREAM, SIMULATED HULL FLOW AND PROPELLER SLIPSTREAM CONDITIONS, ASPECT RATIO 2, ' ≈ 0°
FREE STREAM
SIMULATED HULL
SIMULATED HULL and PROP. SLIPSTREAM
LIFT COEFFICIENT, C_L
ANGLE OF ATTACK, DEG.
1.6
1.4
1.2
1.0
.8
.6
.4
.2
0
-.2
-.4
-.6
-.8
-1.0
-1.2
-1.4
-1.6
-50
-40
-30
-20
-10
0
10
20
30
40
50

FIGURE NO. 65
COMPARISON OF LIFT COEFFICIENTS FOR FREE STREAM SIMULATED HULL FLOW AND PROPELLER SLIPSTREAM CONDITIONS, ASPECT RATIO 2, = 11°

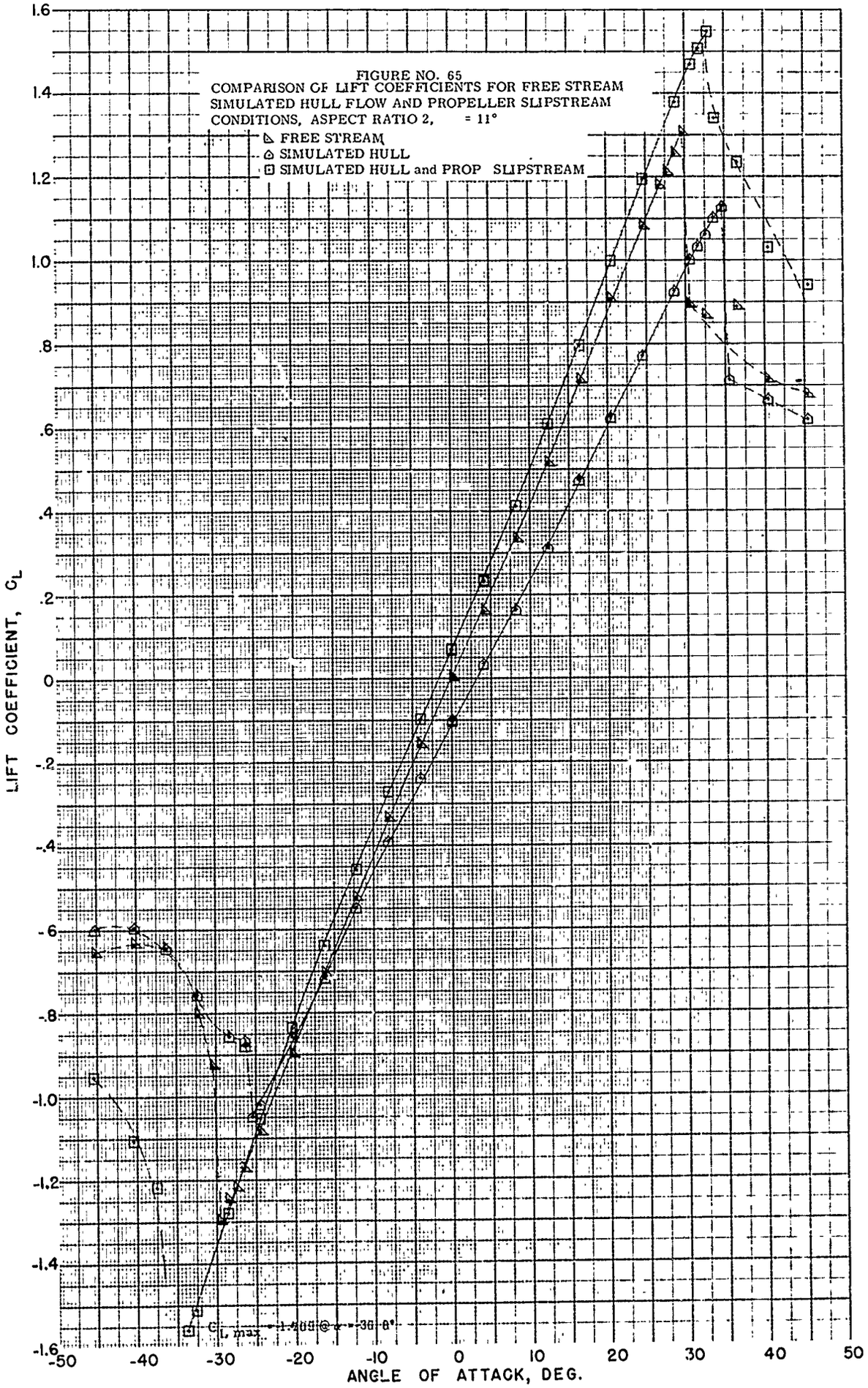

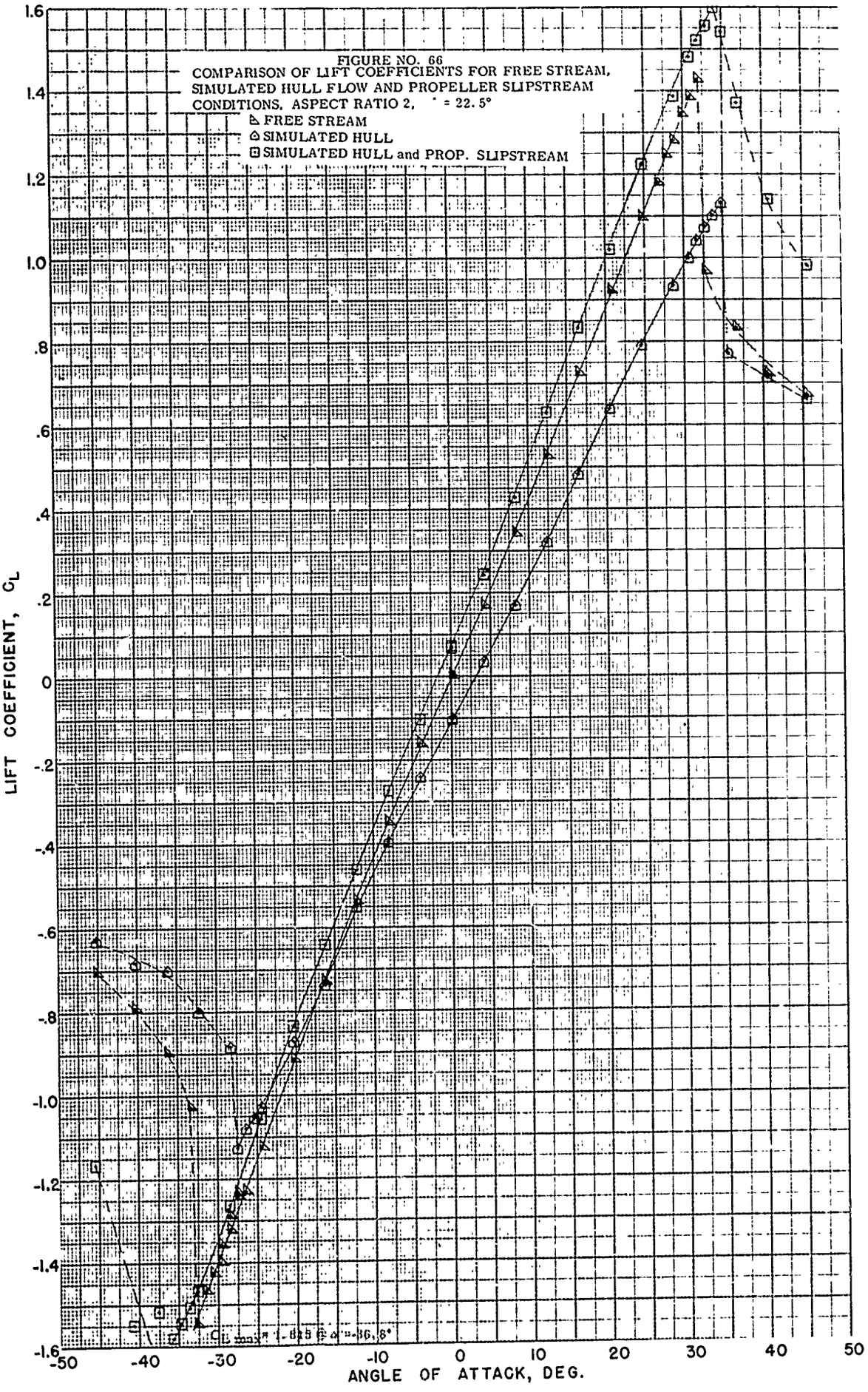
FIGURE NO. 66
COMPARISON OF LIFT COEFFICIENTS FOR FREE STREAM, SIMULATED HULL FLOW AND PROPELLER SLIPSTREAM CONDITIONS, ASPECT RATIO 2, ' = 22.5°
FREE STREAM
SIMULATED HULL
SIMULATED HULL and PROP. SLIPSTREAM
LIFT COEFFICIENT, C_L
ANGLE OF ATTACK, DEG.
1.6
1.4
1.2
1.0
.8
.6
.4
.2
0
-.2
-.4
-.6
-.8
-1.0
-1.2
-1.4
-1.6
-50
-40
-30
-20
-10
0
10
20
30
40
50

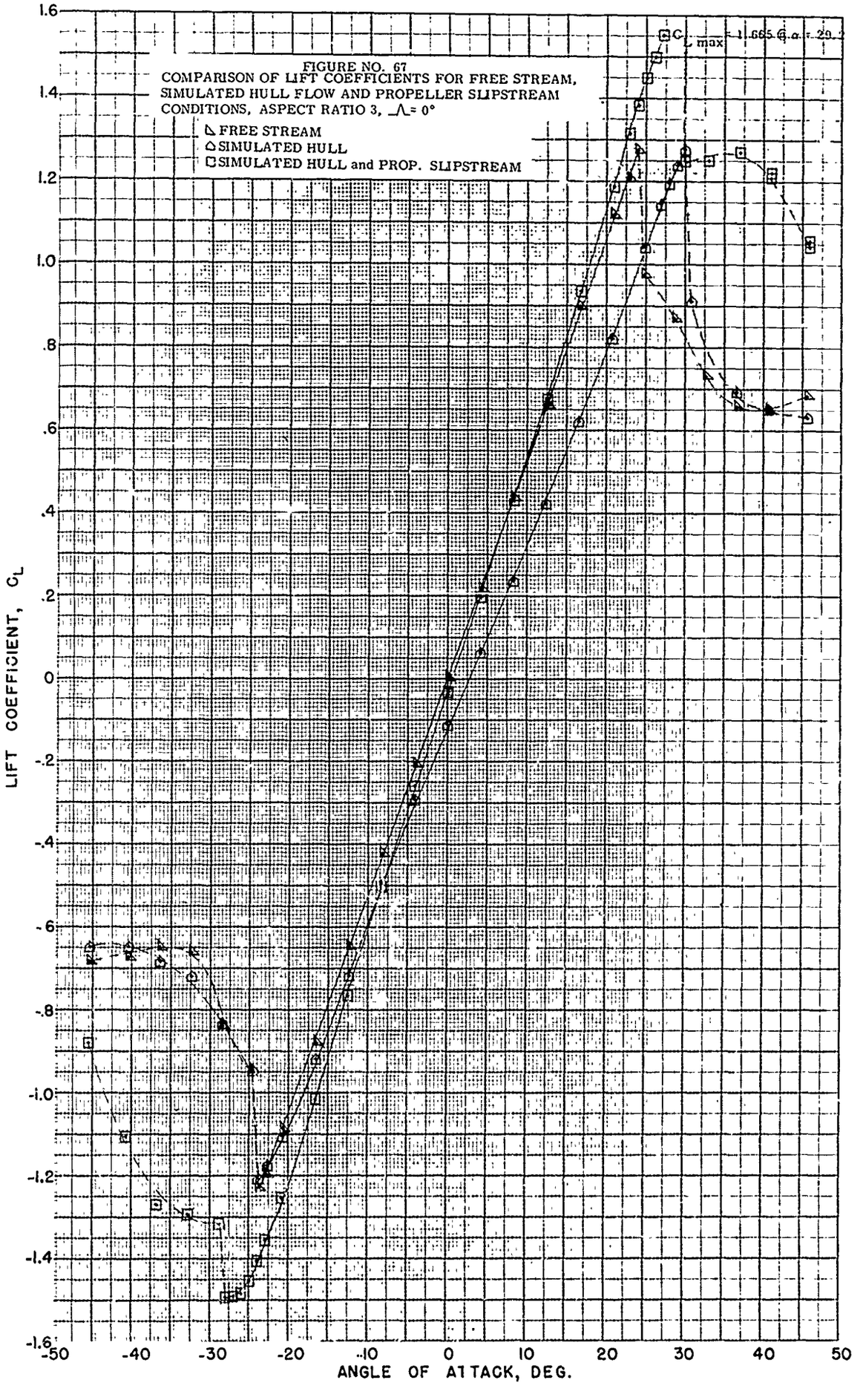
FIGURE NO. 67
COMPARISON OF LIFT COEFFICIENTS FOR FREE STREAM, SIMULATED HULL FLOW AND PROPELLER SLIPSTREAM CONDITIONS, ASPECT RATIO 3, Λ = 0°
FREE STREAM
SIMULATED HULL
SIMULATED HULL and PROP. SLIPSTREAM
C L max = 1.665 @ α = 29°
LIFT COEFFICIENT, C L
1.6
1.4
1.2
1.0
.8
.6
.4
.2
0
-.2
-.4
-.6
-.8
-1.0
-1.2
-1.4
-1.6
-50
-40
-30
-20
-10
0
10
20
30
40
50
ANGLE OF ATTACK, DEG.

FIGURE NO. 68
COMPARISON OF LIFT COEFFICIENTS FOR FREE STREAM, SIMULATED HULL FLOW AND PROPELLER SLIPSTREAM CONDITIONS. ASPECT RATIO 3. $\Lambda = 11°$

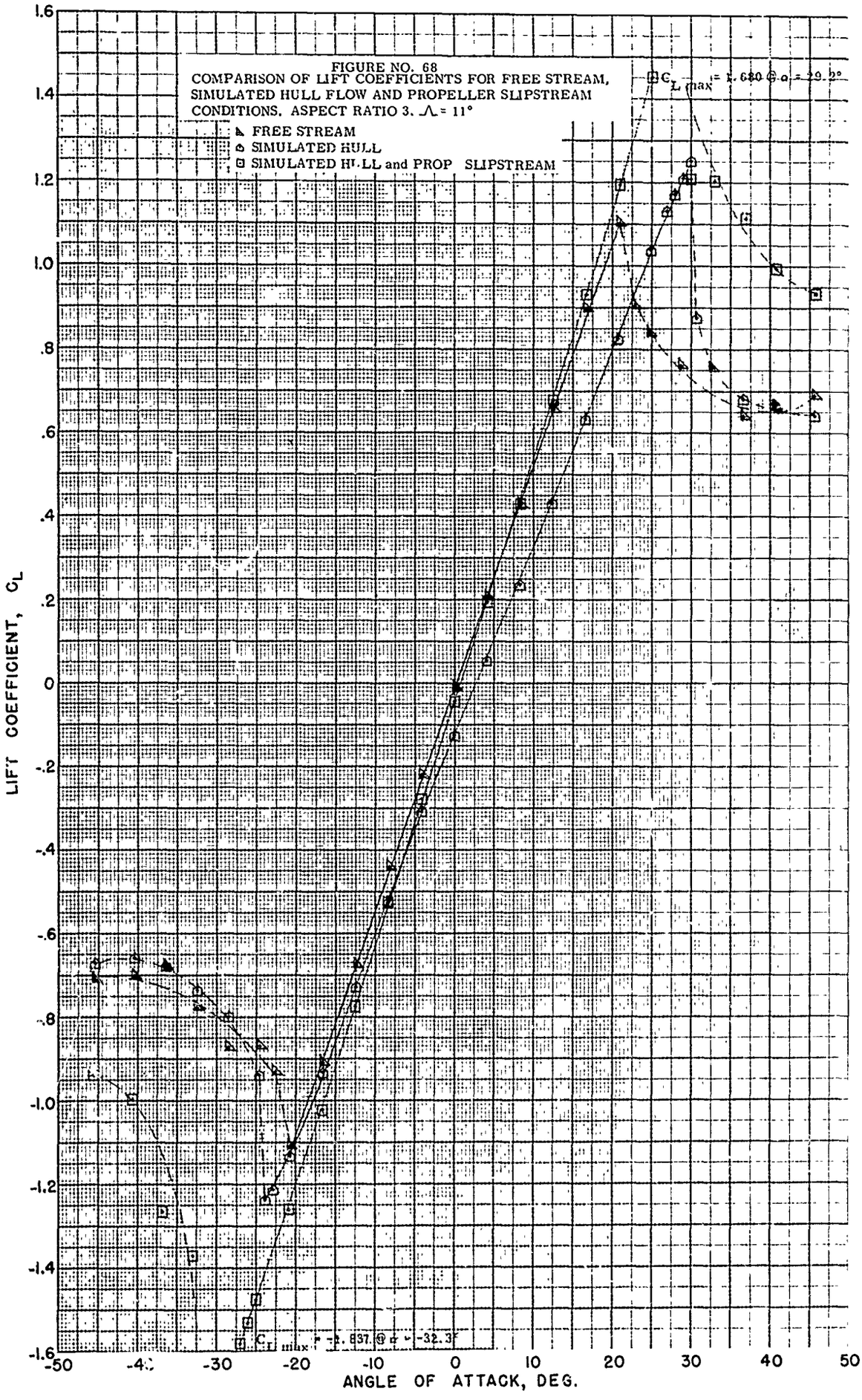

FIGURE NO. 69
COMPARISON OF LIFT COEFFICIENTS FOR FREE STREAM, SIMULATED HULL FLOW AND PROPELLER SLIPSTREAM CONDITIONS, ASPECT RATIO 3, $\Lambda = 22.5°$

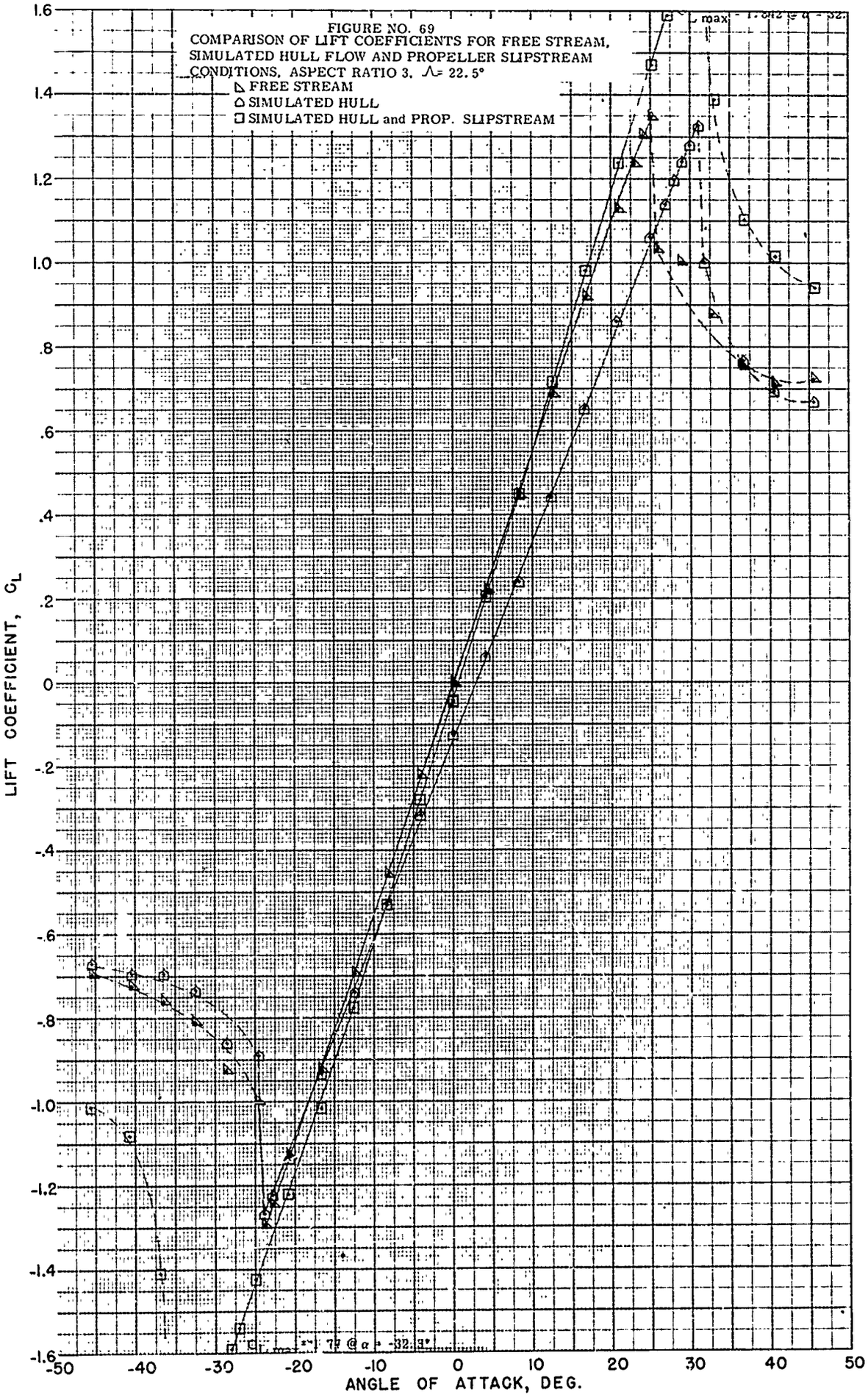

FIGURE NO. 70
COMPARISON OF DRAG COEFFICIENTS FOR FREE STREAM, SIMULATED HULL FLOW AND PROPELLER SLIPSTREAM CONDITIONS, ASPECT RATIO 1, $\Lambda = 0°$

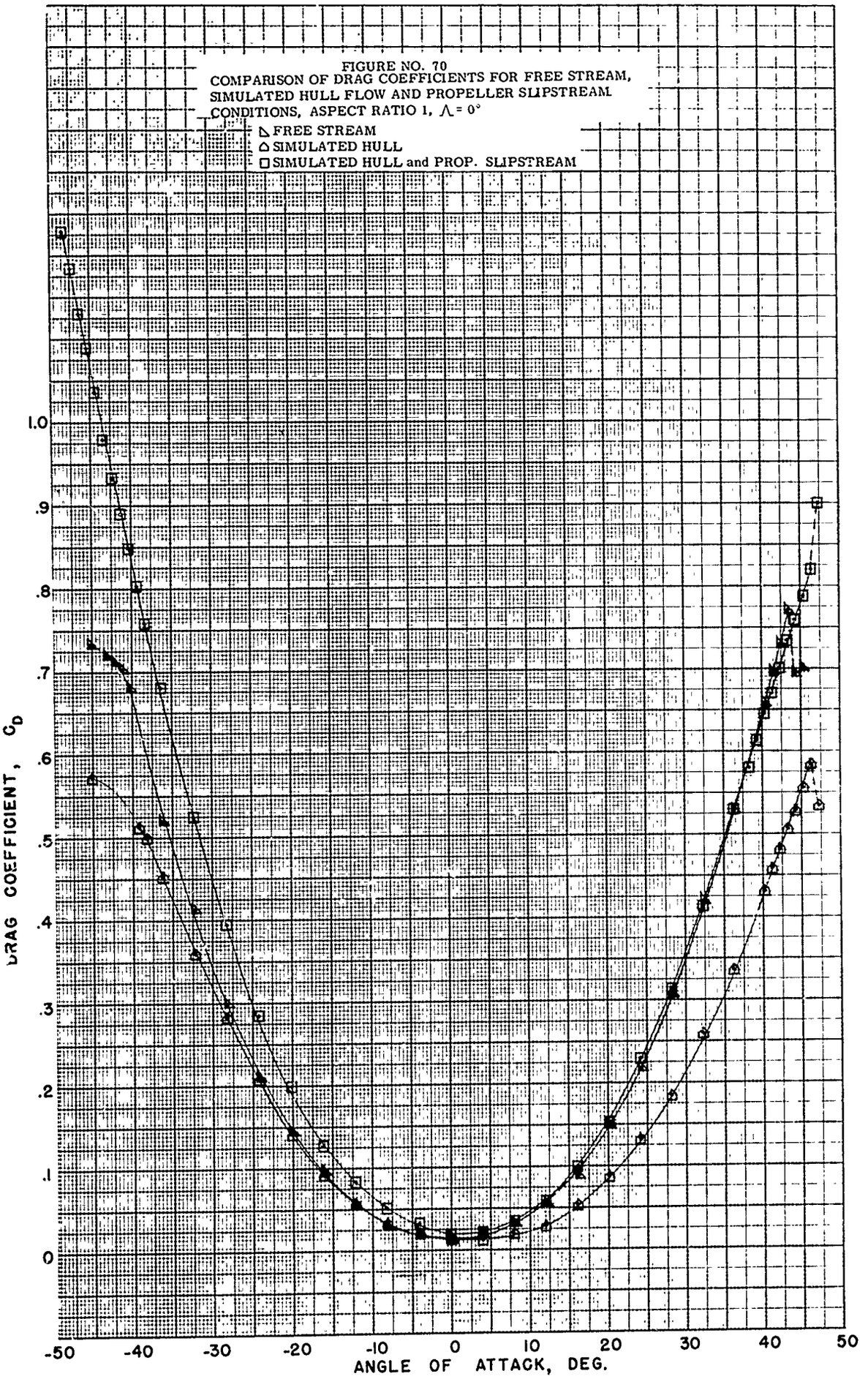

FIGURE NO. 71
COMPARISON OF DRAG COEFFICIENTS FOR FREE STREAM, SIMULATED HULL FLOW AND PROPELLER SLIPSTREAM CONDITIONS, ASPECT RATIO 1, $\Lambda = 11°$

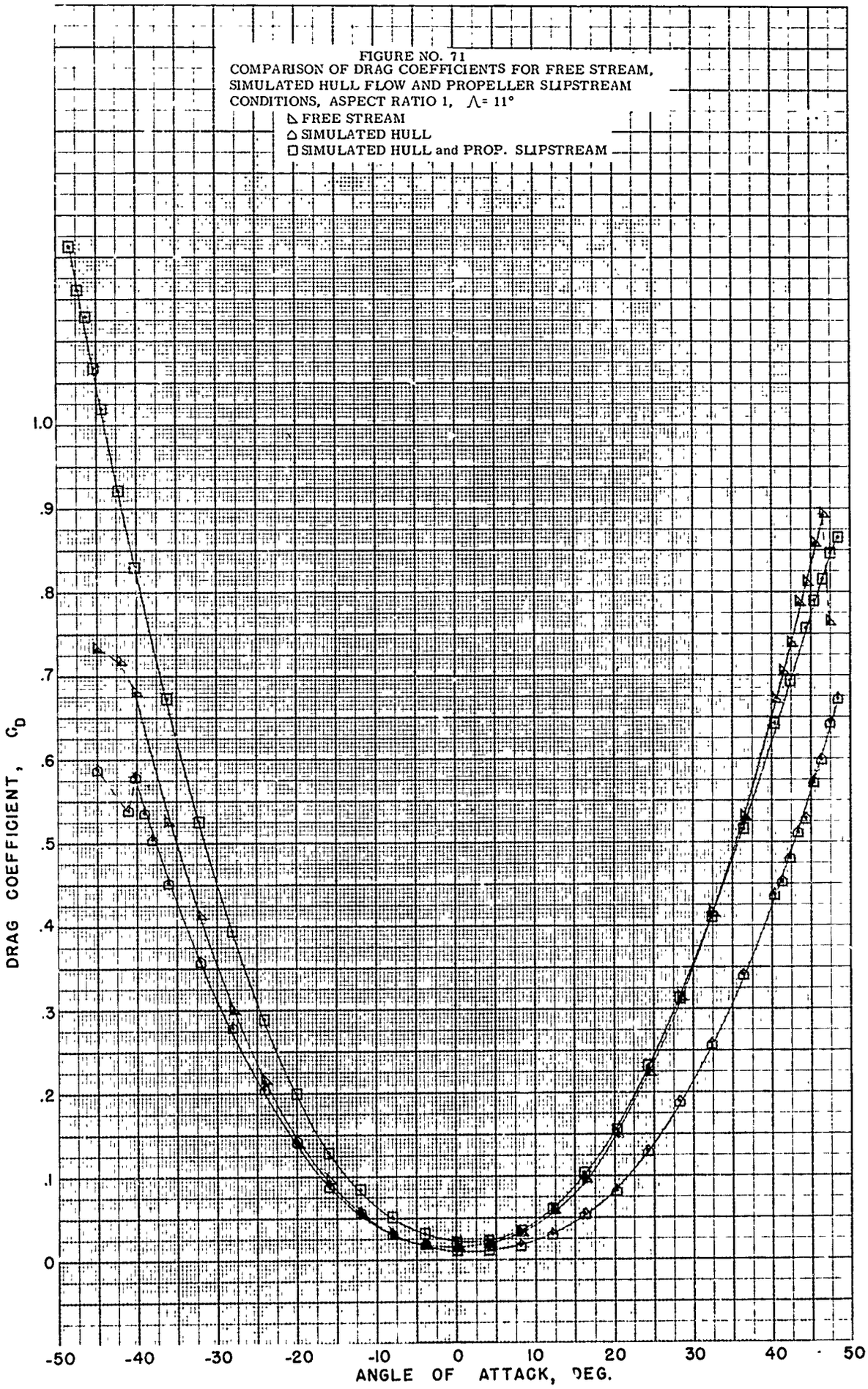

FIGURE NO. 72
COMPARISON OF DRAG COEFFICIENTS FOR FREE STREAM, SIMULATED HULL FLOW AND PROPELLER SLIPSTREAM CONDITIONS. ASPECT RATIO 1. $\Lambda = 22.5°$

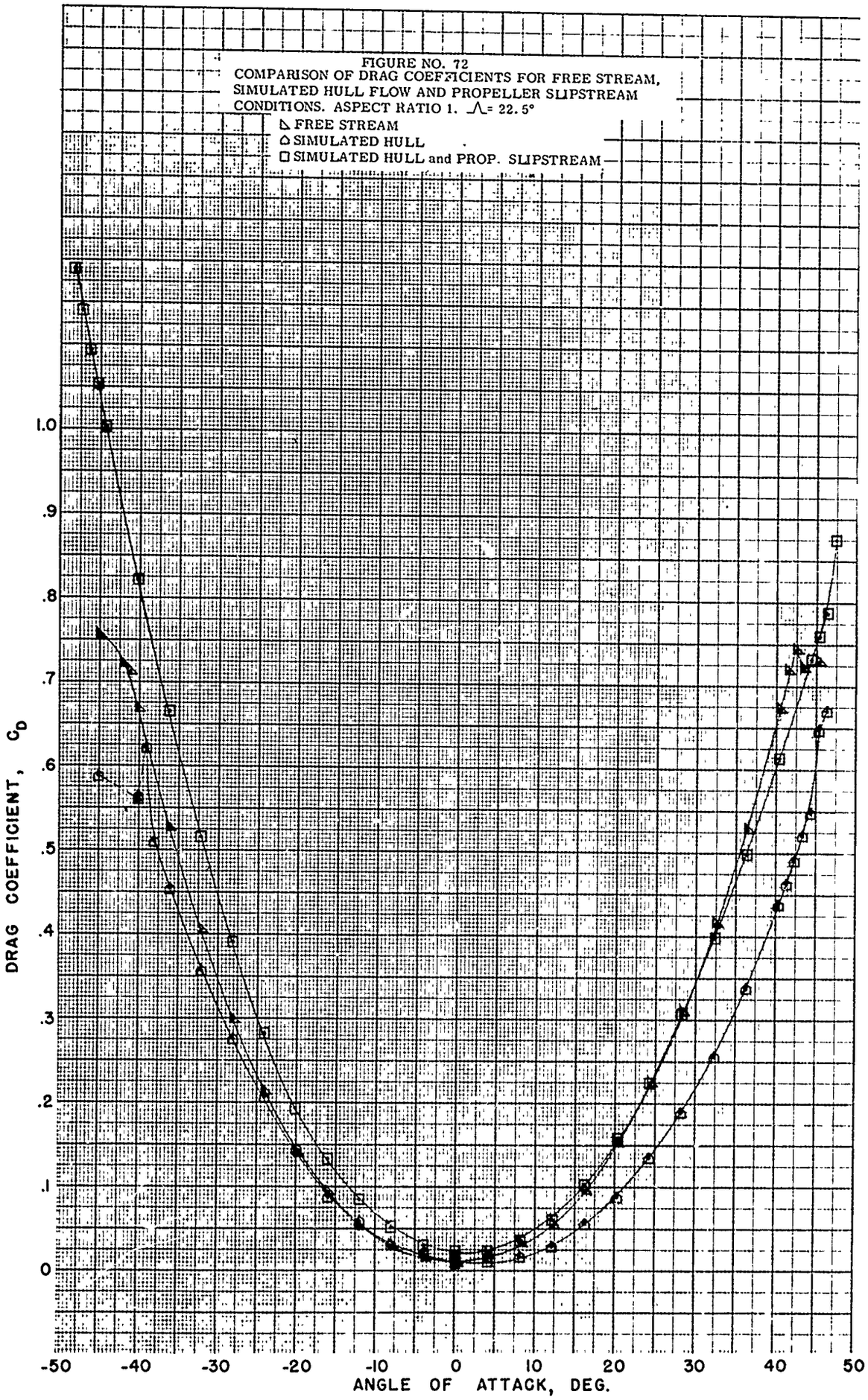

FIGURE NO. 73
COMPARISON OF DRAG COEFFICIENTS FOR FREE STREAM, SIMULATED HULL FLOW AND PROPELLER SLIPSTREAM CONDITIONS, ASPECT RATIO 2, $i_t = 0°$

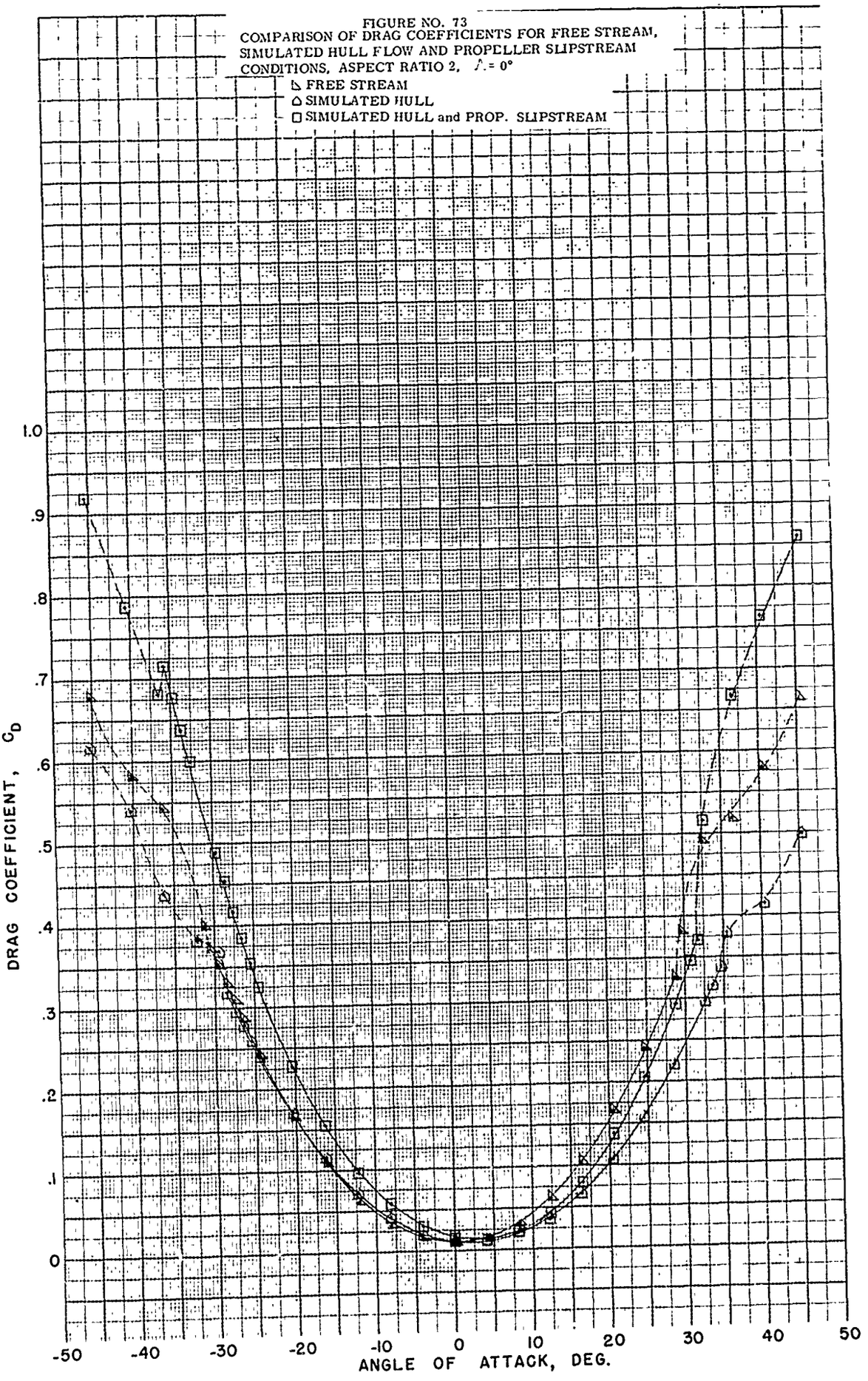

FIGURE NO. 74
COMPARISON OF DRAG COEFFICIENTS FOR FREE STREAM, SIMULATED HULL FLOW AND PROPELLER SLIPSTREAM CONDITIONS, ASPECT RATIO 2, $\Lambda = 11°$

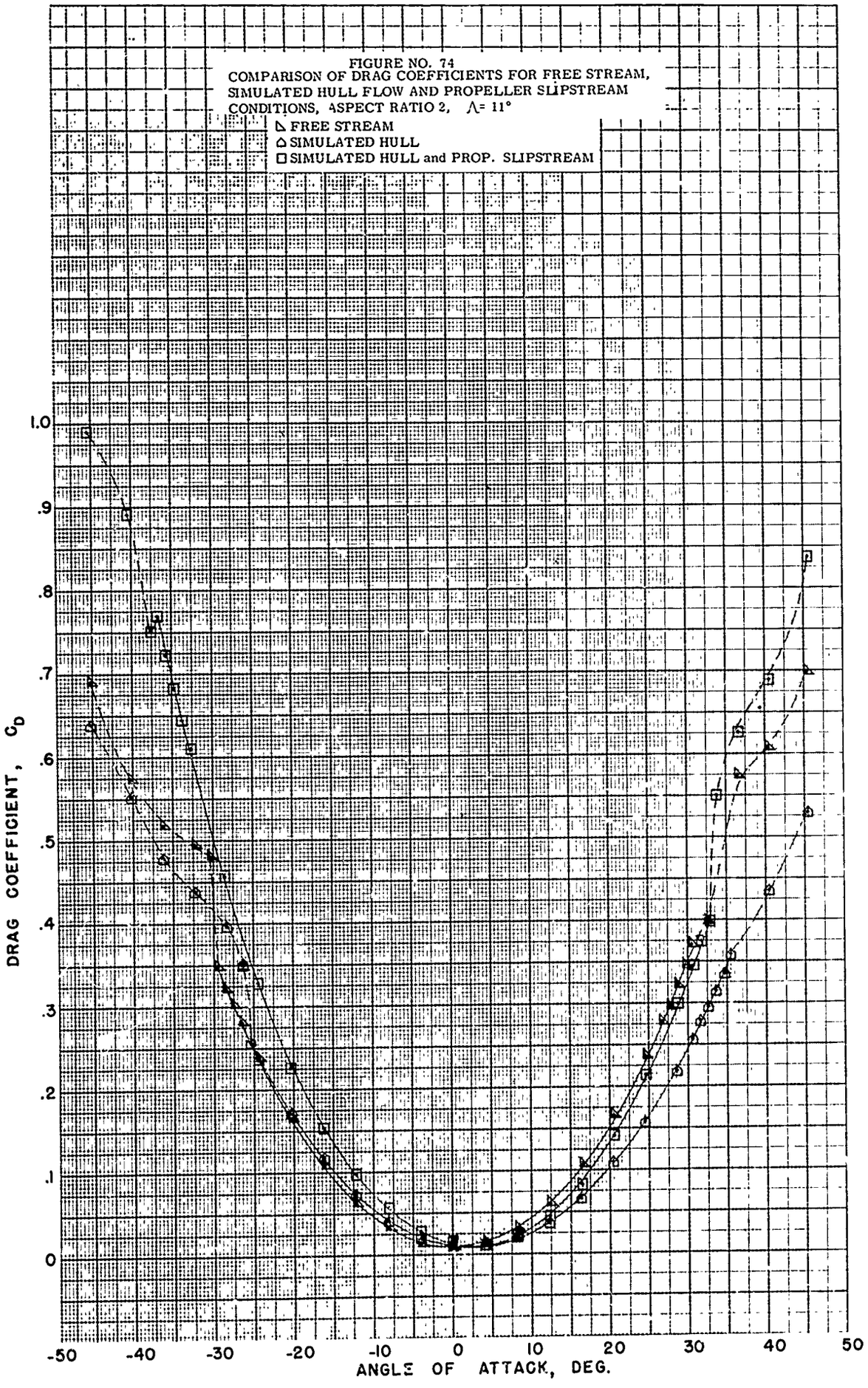

FIGURE NO. 75
COMPARISON OF DRAG COEFFICIENTS FOR FREE STREAM, SIMULATED HULL FLOW AND PROPELLER SLIPSTREAM CONDITIONS, ASPECT RATIO 2, Λ = 22.5°

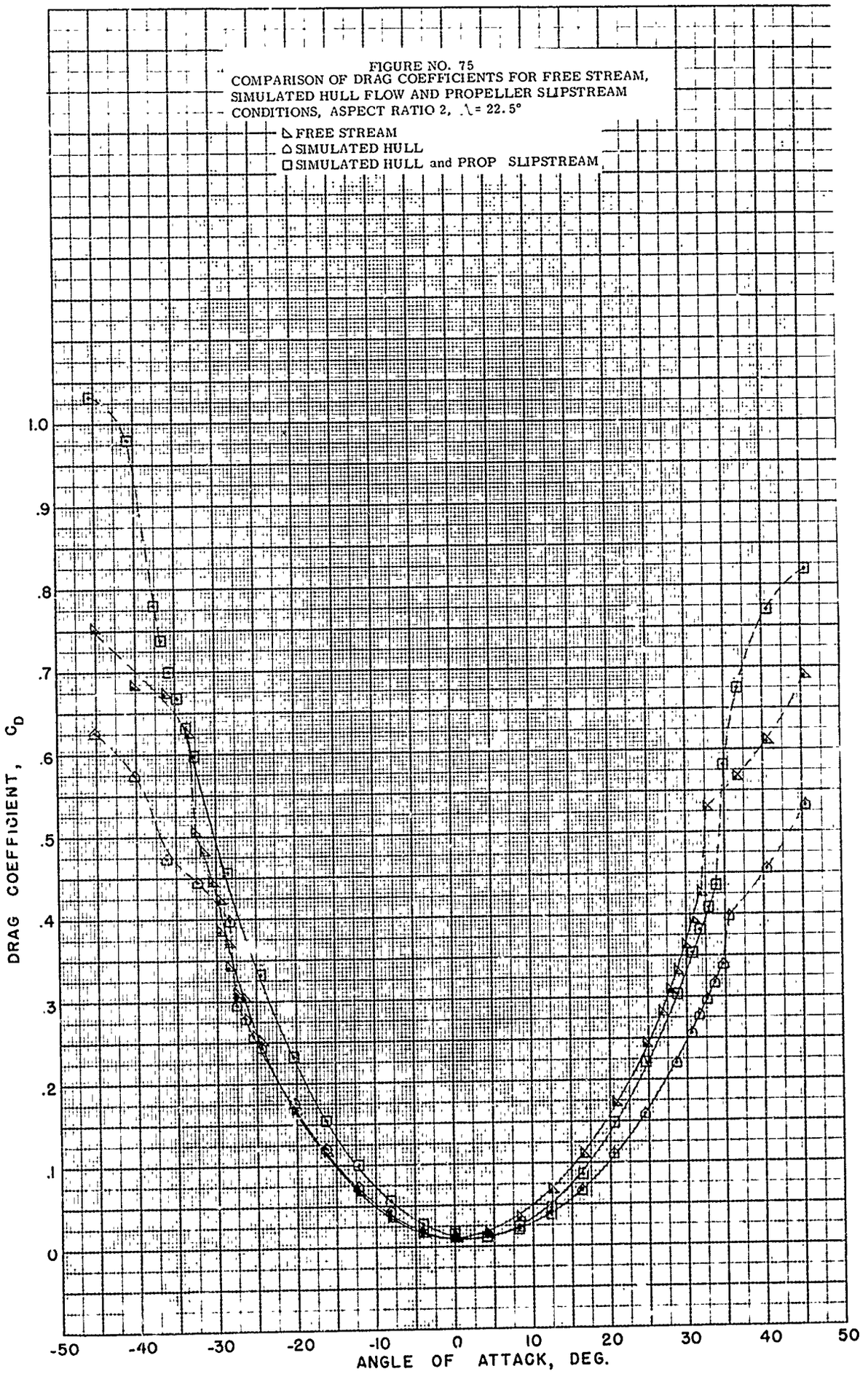

FIGURE NO. 76
COMPARISON OF DRAG COEFFICIENTS FOR FREE STREAM, SIMULATED HULL FLOW AND PROPELLER SLIPSTREAM CONDITIONS. ASPECT RATIO 3, $\Lambda = 0°$

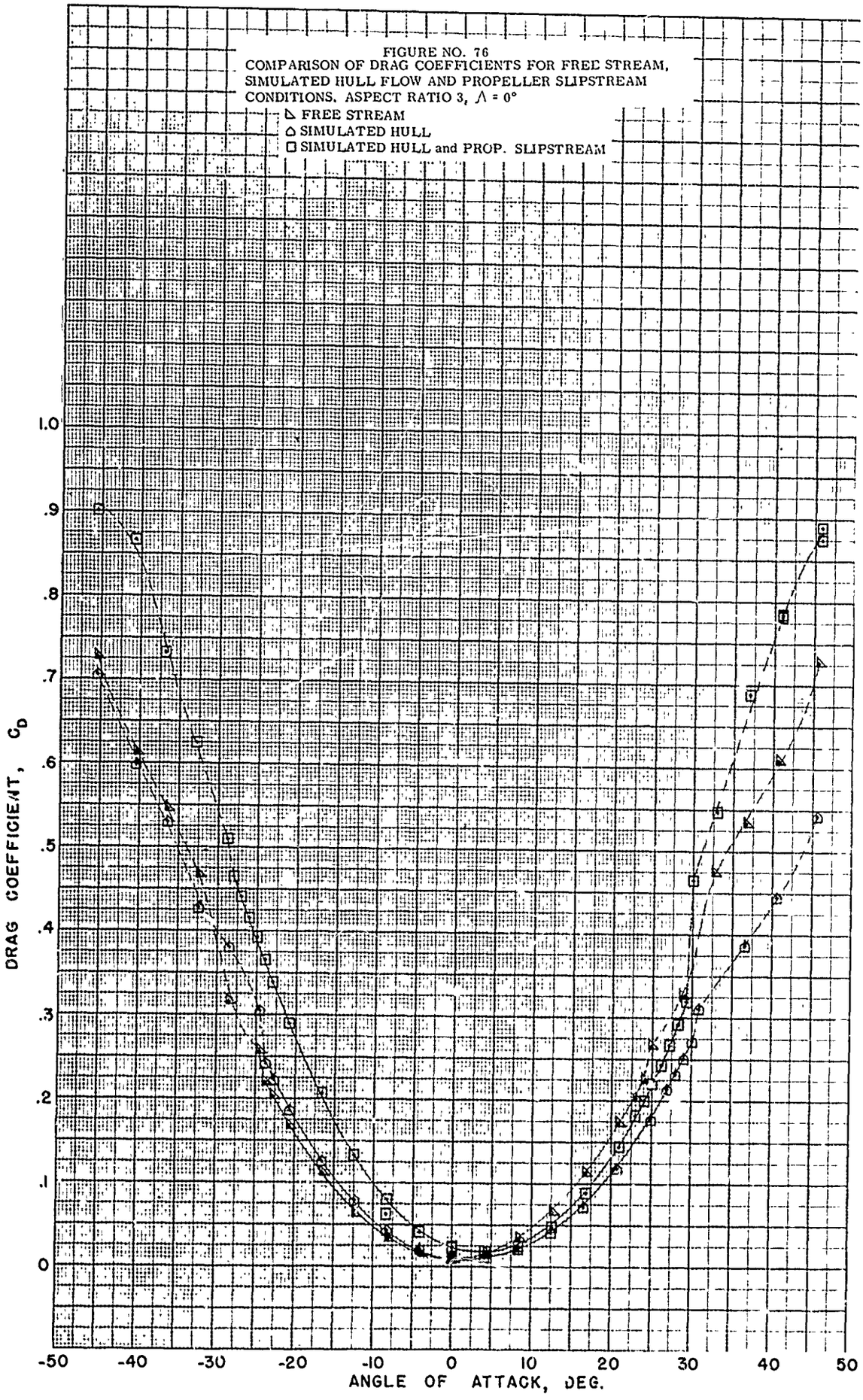

FIGURE NO. 77
COMPARISON OF DRAG COEFFICIENTS FOR FREE STREAM, SIMULATED HULL FLOW AND PROPELLER SLIPSTREAM CONDITIONS, ASPECT RATIO 3, Λ = 11°

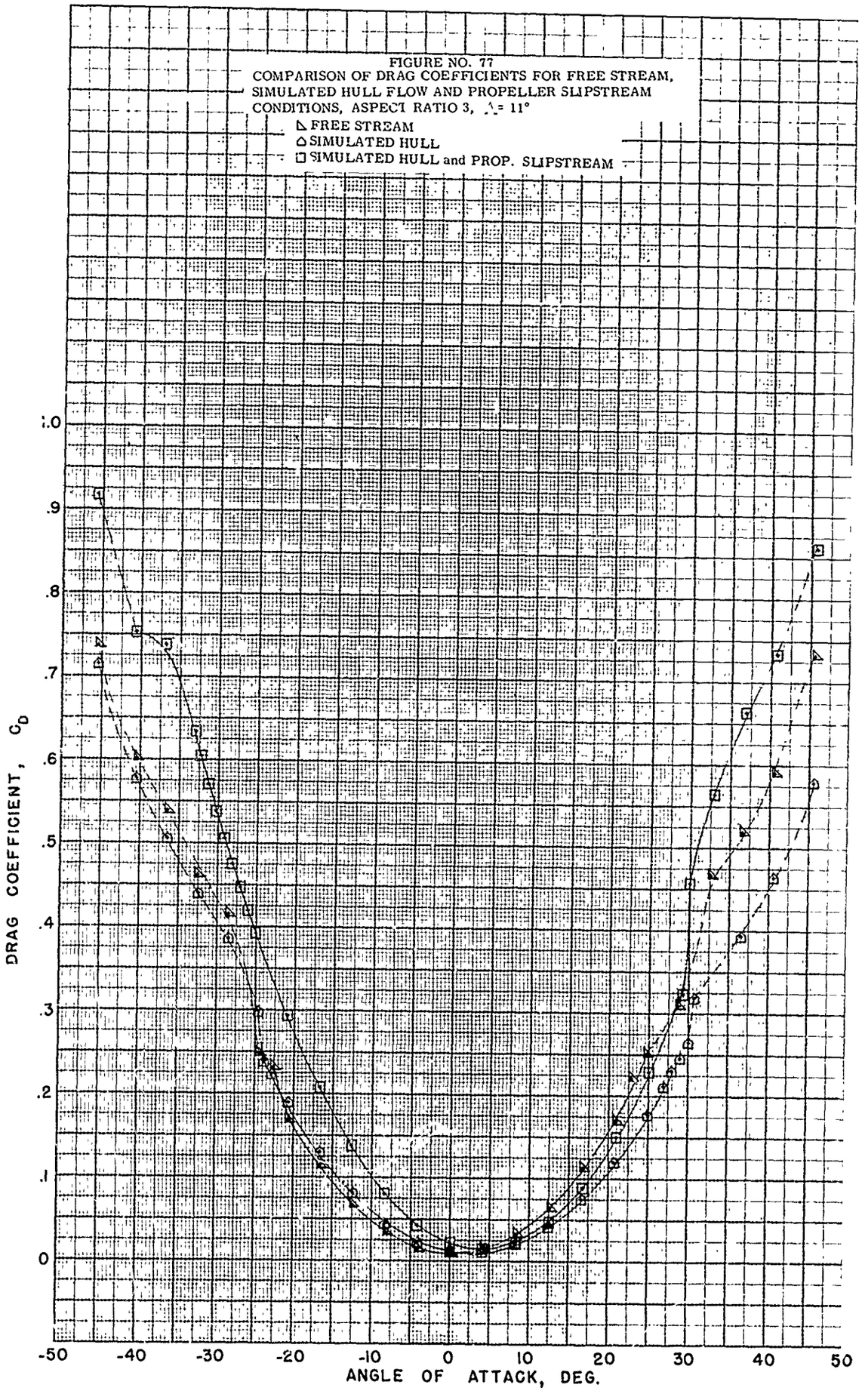

FIGURE NO. 78
COMPARISON OF DRAG COEFFICIENTS FOR FREE STREAM, SIMULATED HULL FLOW AND PROPELLER SLIPSTREAM CONDITIONS, ASPECT RATIO 3, $\Lambda = 22.5°$

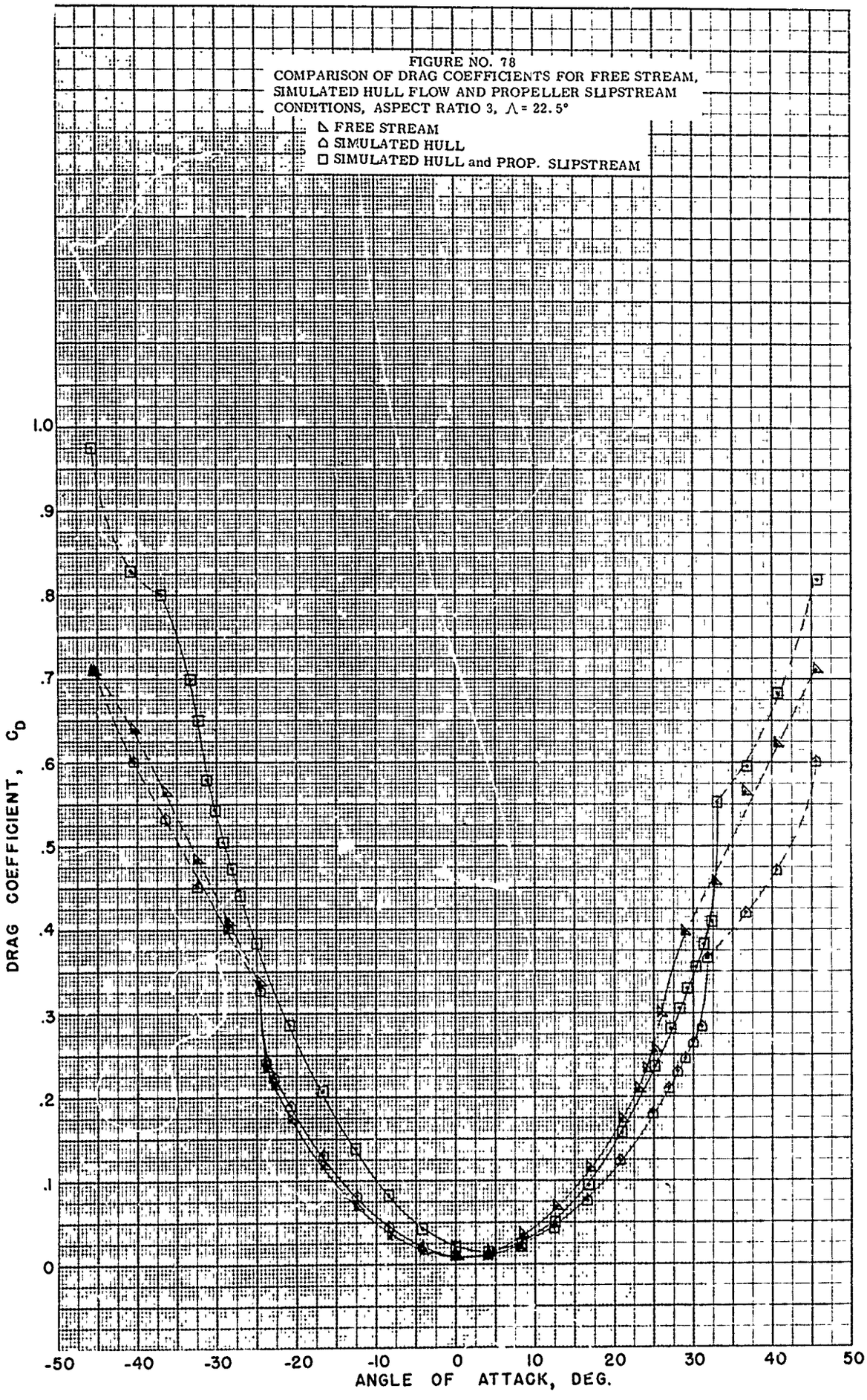

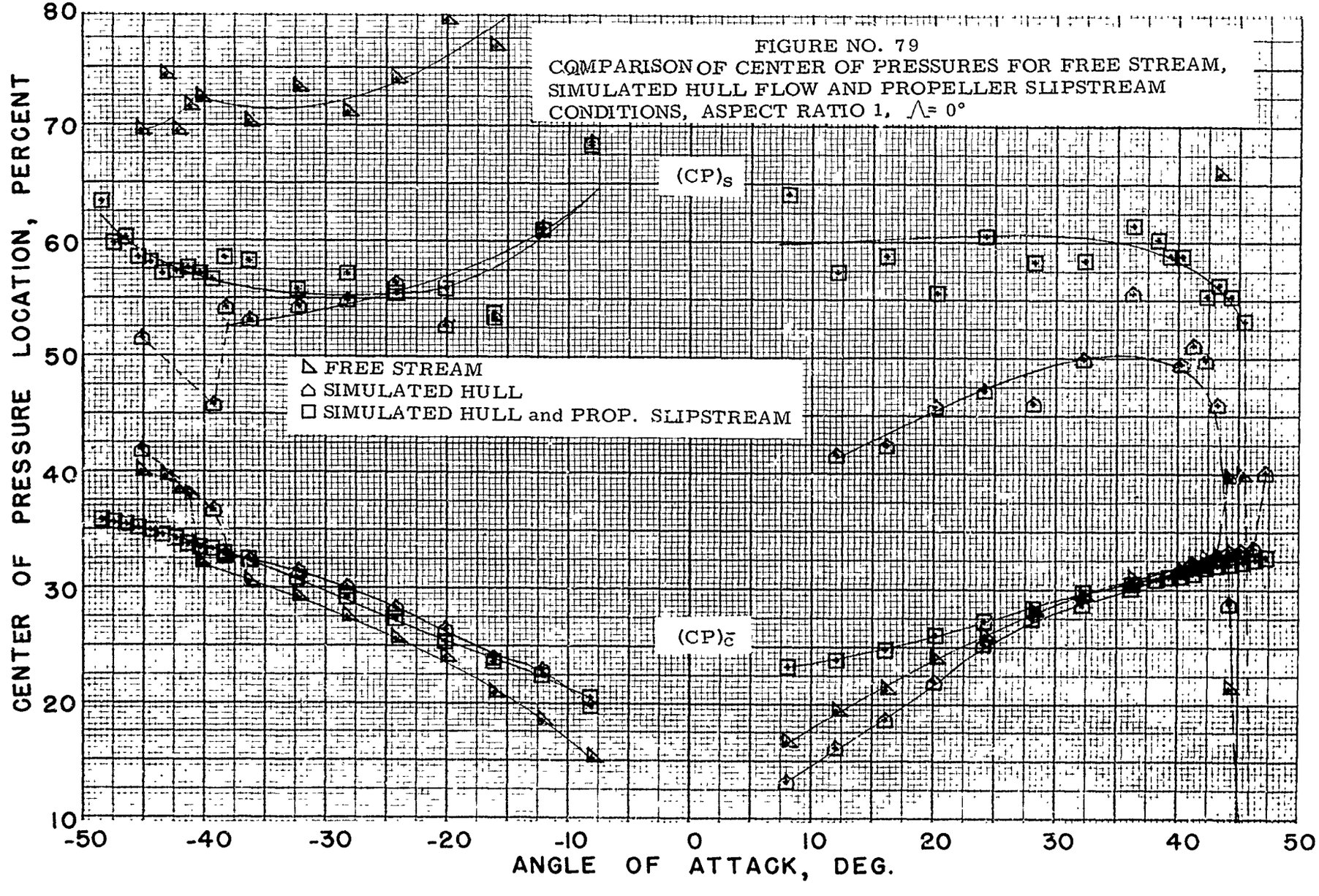
FIGURE NO. 79
COMPARISON OF CENTER OF PRESSURES FOR FREE STREAM, SIMULATED HULL FLOW AND PROPELLER SLIPSTREAM CONDITIONS, ASPECT RATIO 1, Λ= 0°
(CP)s
(CP)c̄
△ FREE STREAM
△ SIMULATED HULL
□ SIMULATED HULL and PROP. SLIPSTREAM
CENTER OF PRESSURE LOCATION, PERCENT
ANGLE OF ATTACK, DEG.
80
70
60
50
40
30
20
10
-50
-40
-30
-20
-10
0
10
20
30
40
50

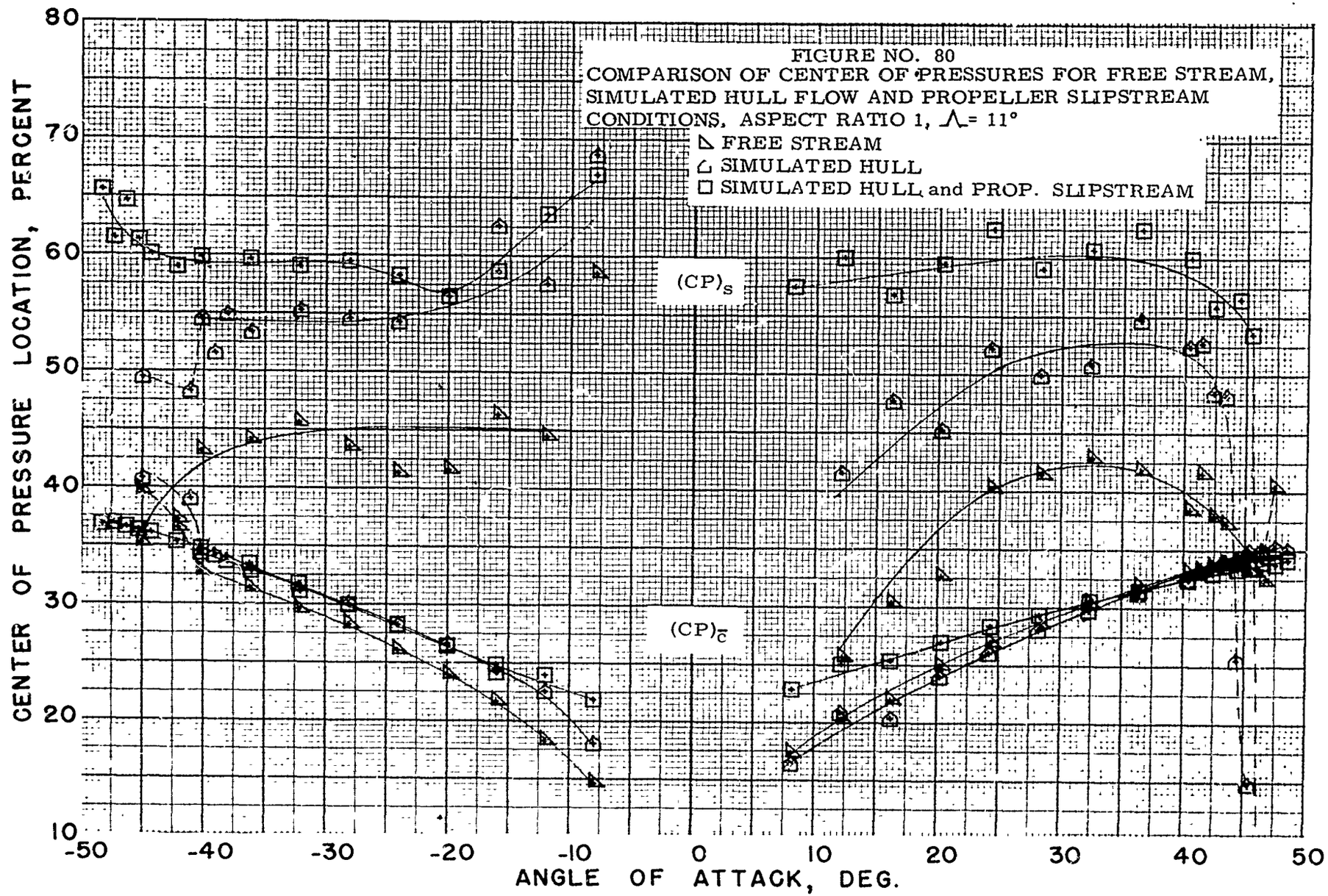
FIGURE NO. 80
COMPARISON OF CENTER OF PRESSURES FOR FREE STREAM, SIMULATED HULL FLOW AND PROPELLER SLIPSTREAM CONDITIONS, ASPECT RATIO 1, Λ= 11°
FREE STREAM
SIMULATED HULL
SIMULATED HULL and PROP. SLIPSTREAM
$(CP)_s$
$(CP)_{\bar{c}}$
CENTER OF PRESSURE LOCATION, PERCENT
ANGLE OF ATTACK, DEG.
80
70
60
50
40
30
20
10
-50
-40
-30
-20
-10
0
10
20
30
40
50

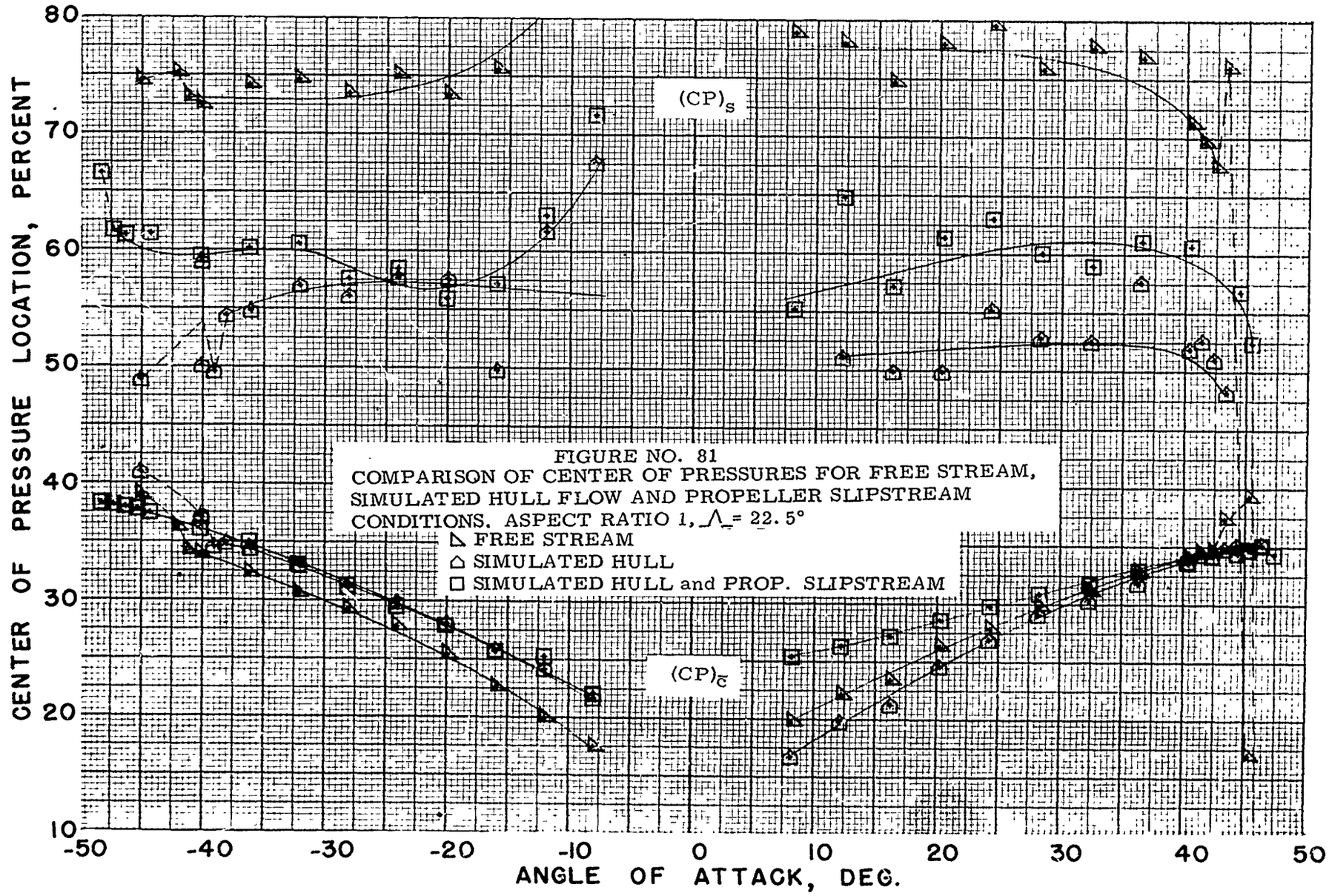
CENTER OF PRESSURE LOCATION, PERCENT
80
70
60
50
40
30
20
10
-50
-40
-30
-20
-10
0
10
20
30
40
50
ANGLE OF ATTACK, DEG.
$(CP)_s$
$(CP)_{\bar{c}}$
FIGURE NO. 81
COMPARISON OF CENTER OF PRESSURES FOR FREE STREAM, SIMULATED HULL FLOW AND PROPELLER SLIPSTREAM CONDITIONS. ASPECT RATIO 1, Λ = 22.5°
△ FREE STREAM
△ SIMULATED HULL
□ SIMULATED HULL and PROP. SLIPSTREAM

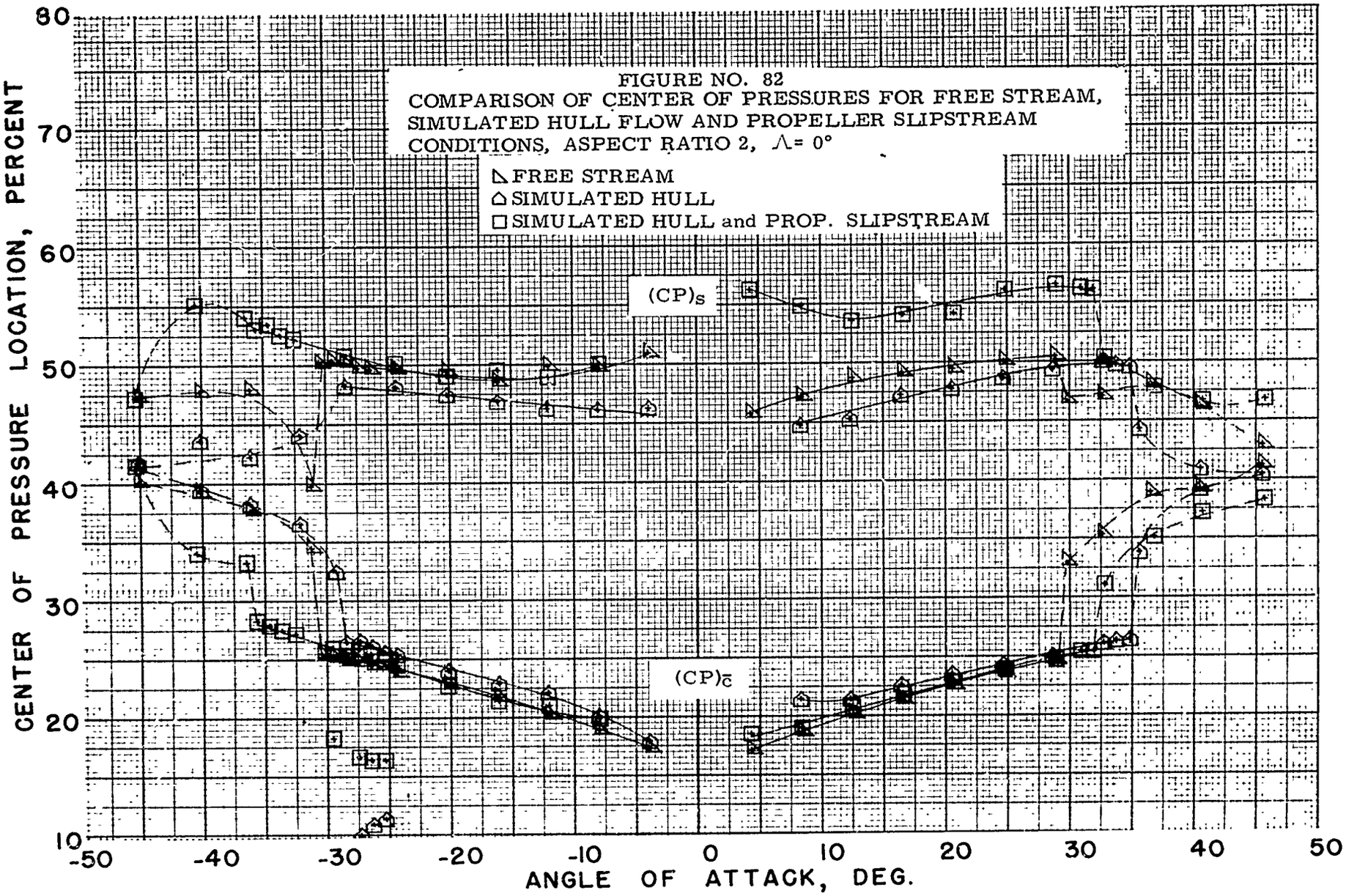
FIGURE NO. 82
COMPARISON OF CENTER OF PRESSURES FOR FREE STREAM, SIMULATED HULL FLOW AND PROPELLER SLIPSTREAM CONDITIONS, ASPECT RATIO 2, Λ= 0°
FREE STREAM
SIMULATED HULL
SIMULATED HULL and PROP. SLIPSTREAM
(CP)s
(CP)c̄
CENTER OF PRESSURE LOCATION, PERCENT
ANGLE OF ATTACK, DEG.
80
70
60
50
40
30
20
10
-50
-40
-30
-20
-10
0
10
20
30
40
50

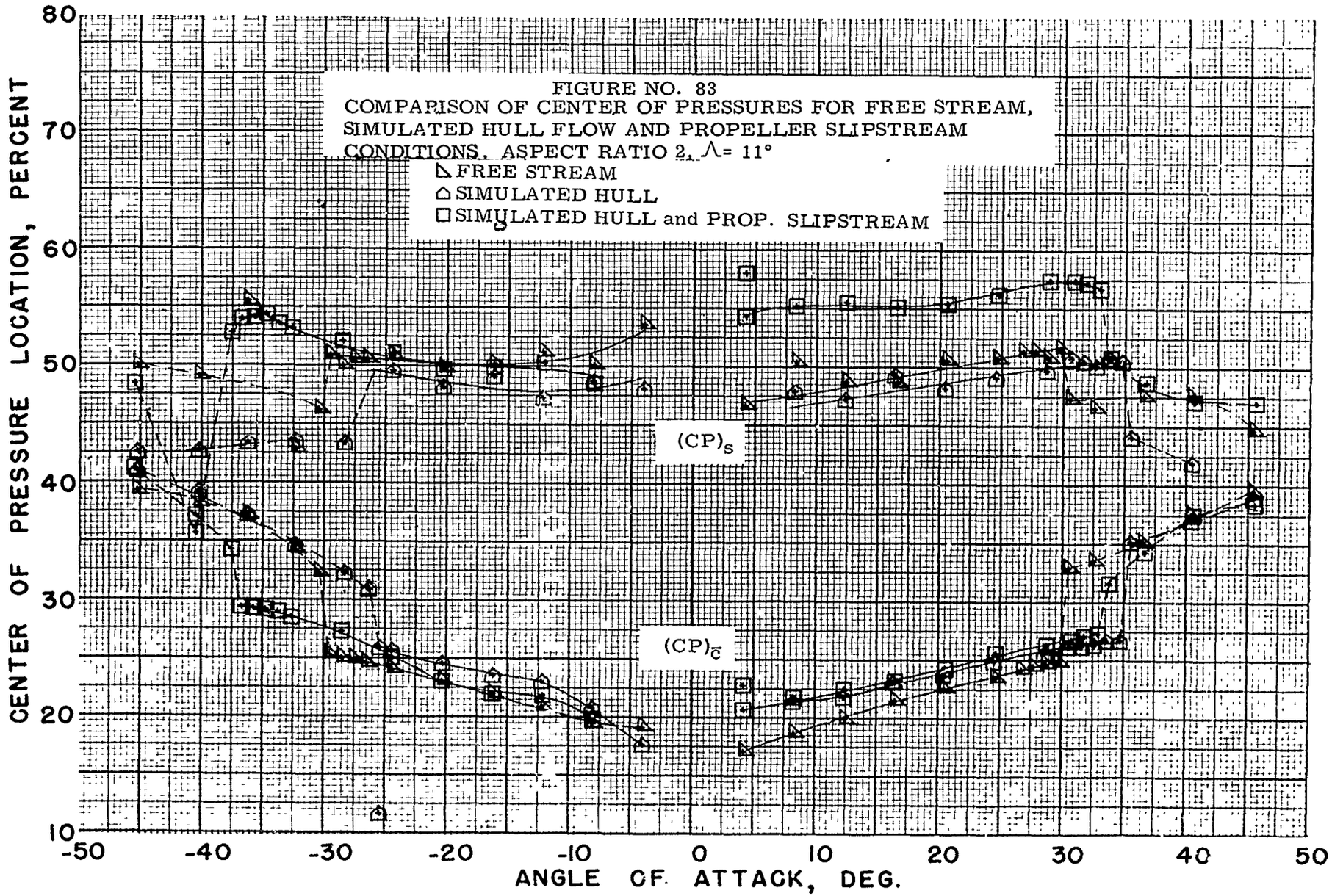
FIGURE NO. 83
COMPARISON OF CENTER OF PRESSURES FOR FREE STREAM, SIMULATED HULL FLOW AND PROPELLER SLIPSTREAM CONDITIONS. ASPECT RATIO 2, Λ= 11°
▽ FREE STREAM
△ SIMULATED HULL
□ SIMULATED HULL and PROP. SLIPSTREAM
(CP)s
(CP)c̄
CENTER OF PRESSURE LOCATION, PERCENT
80
70
60
50
40
30
20
10
-50
-40
-30
-20
-10
0
10
20
30
40
50
ANGLE OF ATTACK, DEG.

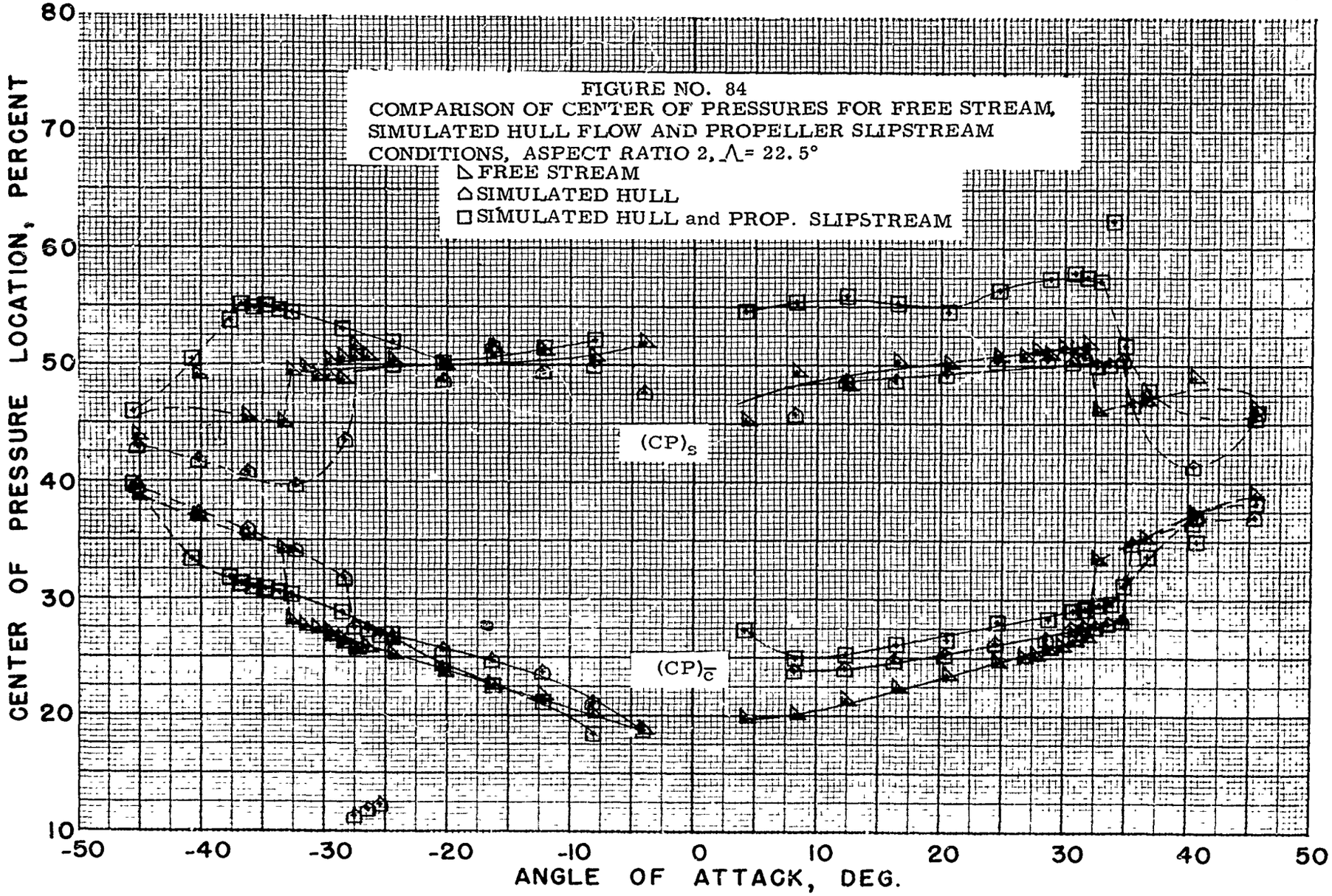
FIGURE NO. 84
COMPARISON OF CENTER OF PRESSURES FOR FREE STREAM, SIMULATED HULL FLOW AND PROPELLER SLIPSTREAM CONDITIONS, ASPECT RATIO 2, Λ = 22.5°
▷ FREE STREAM
△ SIMULATED HULL
□ SIMULATED HULL and PROP. SLIPSTREAM
(CP)s
(CP)c̄
CENTER OF PRESSURE LOCATION, PERCENT
ANGLE OF ATTACK, DEG.
80
70
60
50
40
30
20
10
-50
-40
-30
-20
-10
0
10
20
30
40
50

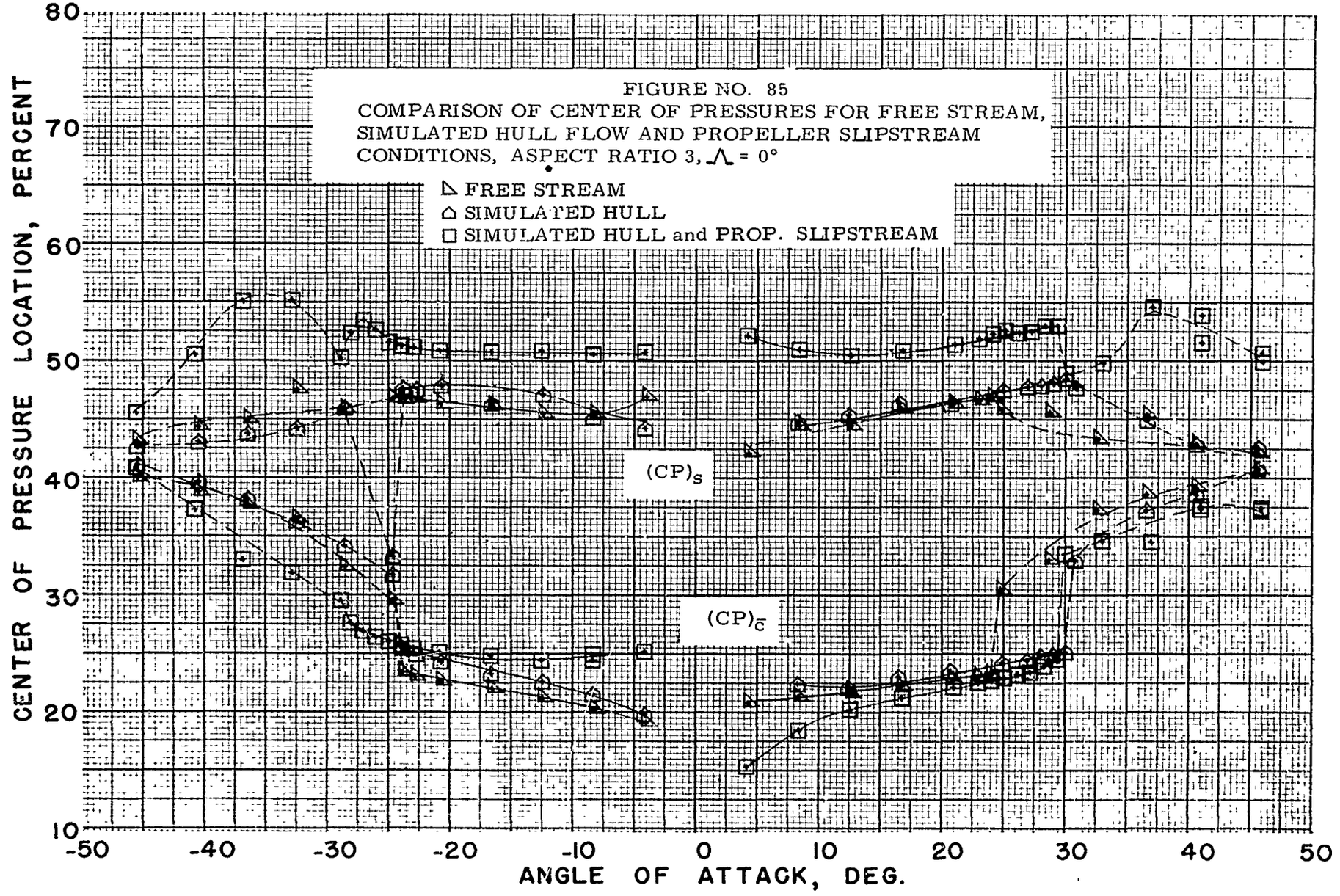
FIGURE NO. 85
COMPARISON OF CENTER OF PRESSURES FOR FREE STREAM, SIMULATED HULL FLOW AND PROPELLER SLIPSTREAM CONDITIONS, ASPECT RATIO 3, Λ = 0°
FREE STREAM
SIMULATED HULL
SIMULATED HULL and PROP. SLIPSTREAM
(CP)s
(CP)c̄
CENTER OF PRESSURE LOCATION, PERCENT
ANGLE OF ATTACK, DEG.
80
70
60
50
40
30
20
10
-50
-40
-30
-20
-10
0
10
20
30
40
50

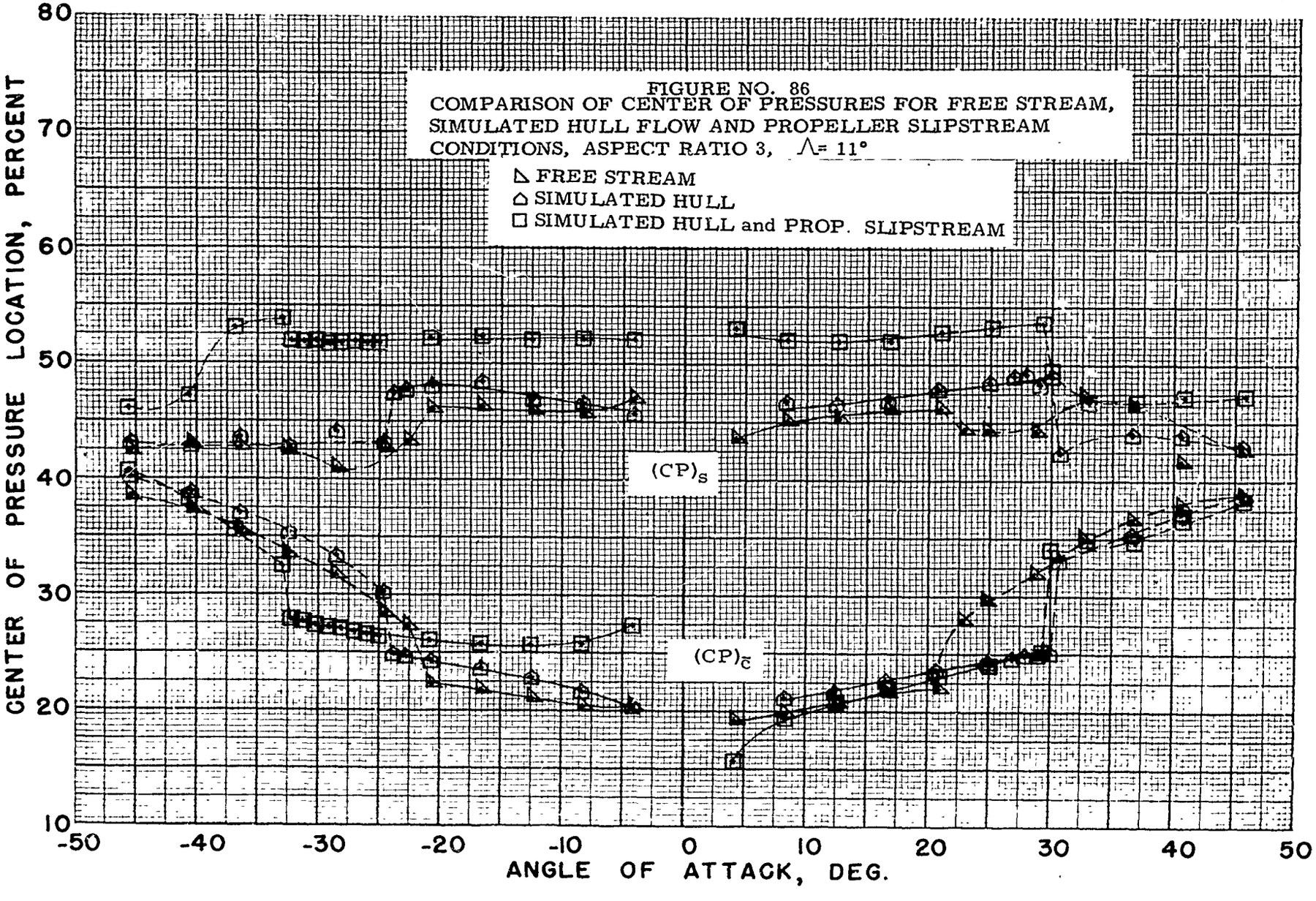
FIGURE NO. 86
COMPARISON OF CENTER OF PRESSURES FOR FREE STREAM, SIMULATED HULL FLOW AND PROPELLER SLIPSTREAM CONDITIONS, ASPECT RATIO 3, Λ= 11°
△ FREE STREAM
△ SIMULATED HULL
□ SIMULATED HULL and PROP. SLIPSTREAM
(CP)s
(CP)c̄
CENTER OF PRESSURE LOCATION, PERCENT
ANGLE OF ATTACK, DEG.
80
70
60
50
40
30
20
10
-50
-40
-30
-20
-10
0
10
20
30
40
50

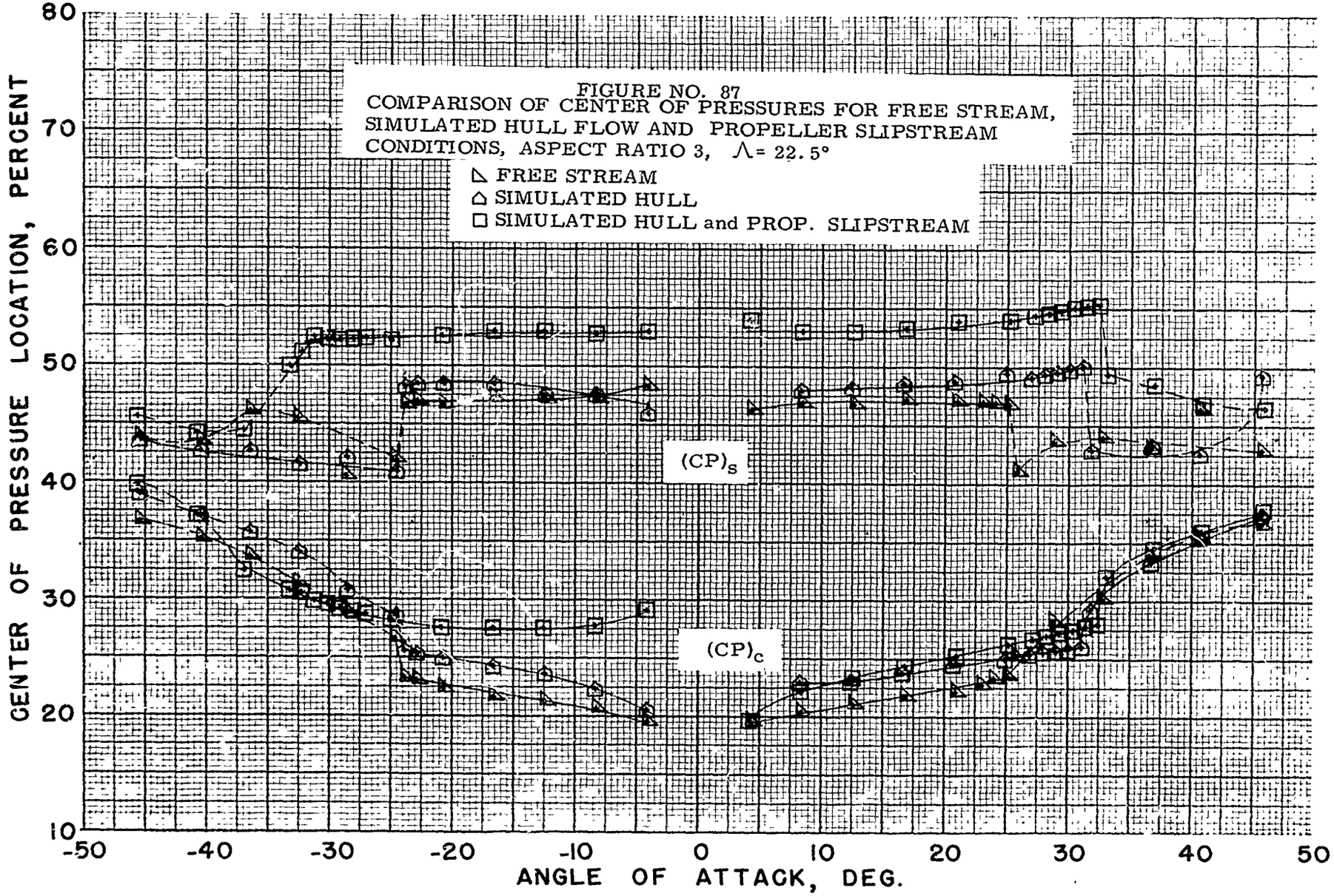
FIGURE NO. 87
COMPARISON OF CENTER OF PRESSURES FOR FREE STREAM, SIMULATED HULL FLOW AND PROPELLER SLIPSTREAM CONDITIONS, ASPECT RATIO 3, Λ= 22.5°
FREE STREAM
SIMULATED HULL
SIMULATED HULL and PROP. SLIPSTREAM
(CP)s
(CP)c
CENTER OF PRESSURE LOCATION, PERCENT
ANGLE OF ATTACK, DEG.
80
70
60
50
40
30
20
10
-50
-40
-30
-20
-10
0
10
20
30
40
50

APPENDIX A

Free Stream Characteristics For Various Gap Sizes

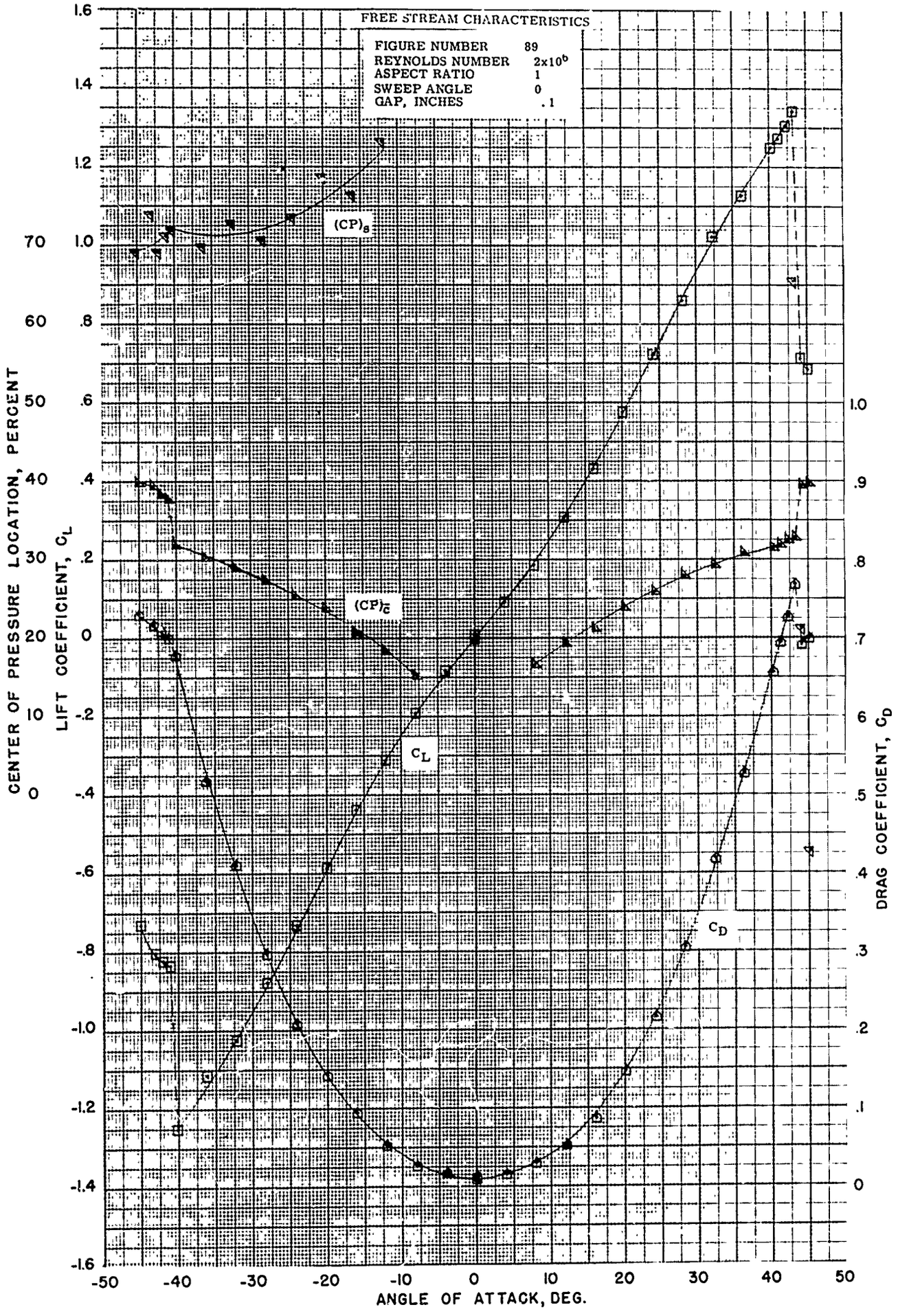
FREE STREAM CHARACTERISTICS
FIGURE NUMBER 89
REYNOLDS NUMBER 2x10^6
ASPECT RATIO 1
SWEEP ANGLE 0
GAP, INCHES .1
(CP)s
(CP)c
CL
CD
CENTER OF PRESSURE LOCATION, PERCENT
LIFT COEFFICIENT, CL
DRAG COEFFICIENT, CD
ANGLE OF ATTACK, DEG.
70
60
50
40
30
20
10
0
1.6
1.4
1.2
1.0
.8
.6
.4
.2
0
-.2
-.4
-.6
-.8
-1.0
-1.2
-1.4
-1.6
1.0
.9
.8
.7
.6
.5
.4
.3
.2
.1
0
-50
-40
-30
-20
-10
0
10
20
30
40
50

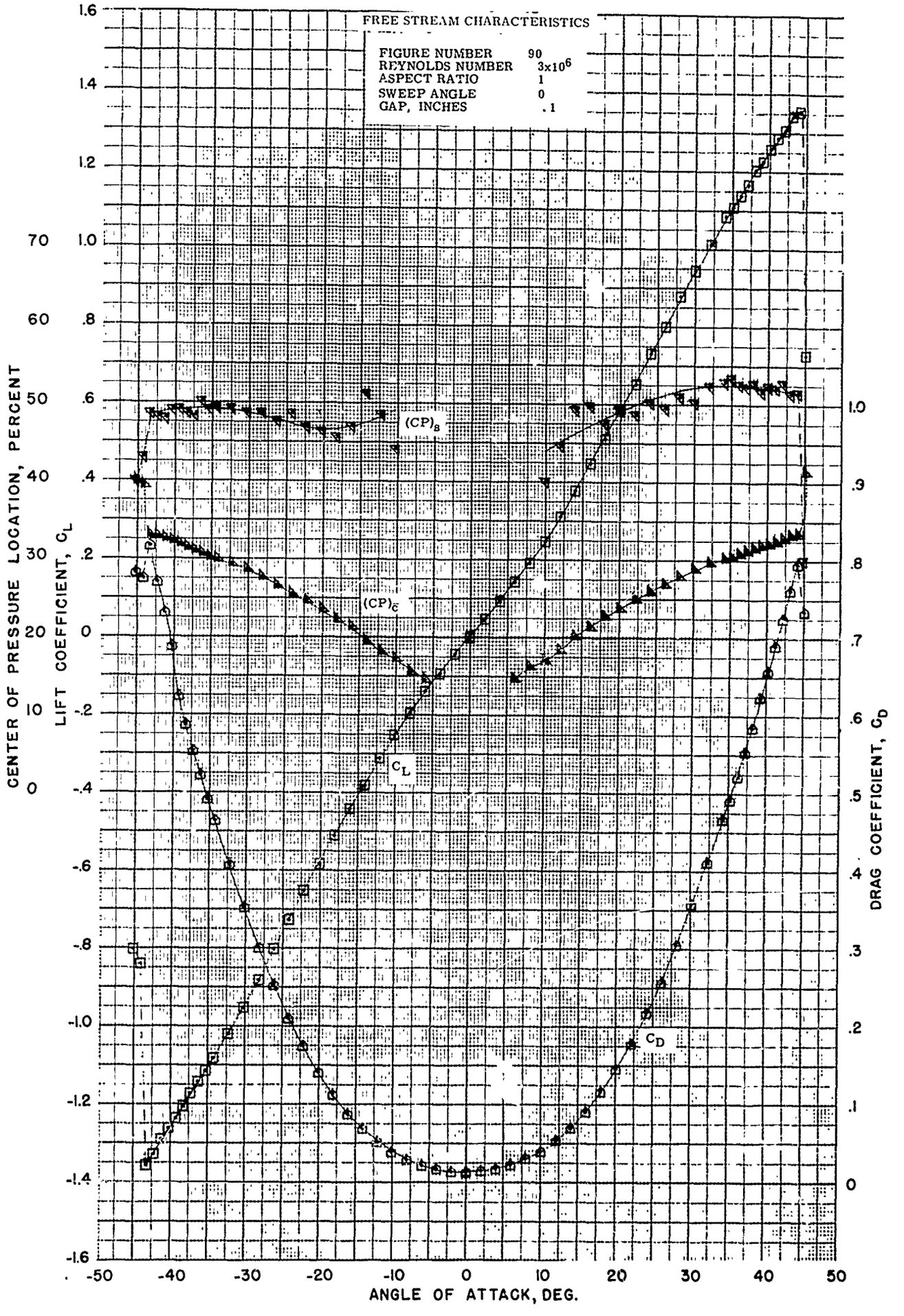
FREE STREAM CHARACTERISTICS
FIGURE NUMBER 90
REYNOLDS NUMBER 3x10^6
ASPECT RATIO 1
SWEEP ANGLE 0
GAP, INCHES .1
CENTER OF PRESSURE LOCATION, PERCENT
LIFT COEFFICIENT, C_L
DRAG COEFFICIENT, C_D
ANGLE OF ATTACK, DEG.
(CP)_B
(CP)_C
C_L
C_D
70
60
50
40
30
20
10
0
1.6
1.4
1.2
1.0
.8
.6
.4
.2
0
-.2
-.4
-.6
-.8
-1.0
-1.2
-1.4
-1.6
1.0
.9
.8
.7
.6
.5
.4
.3
.2
.1
0
-50
-40
-30
-20
-10
0
10
20
30
40
50

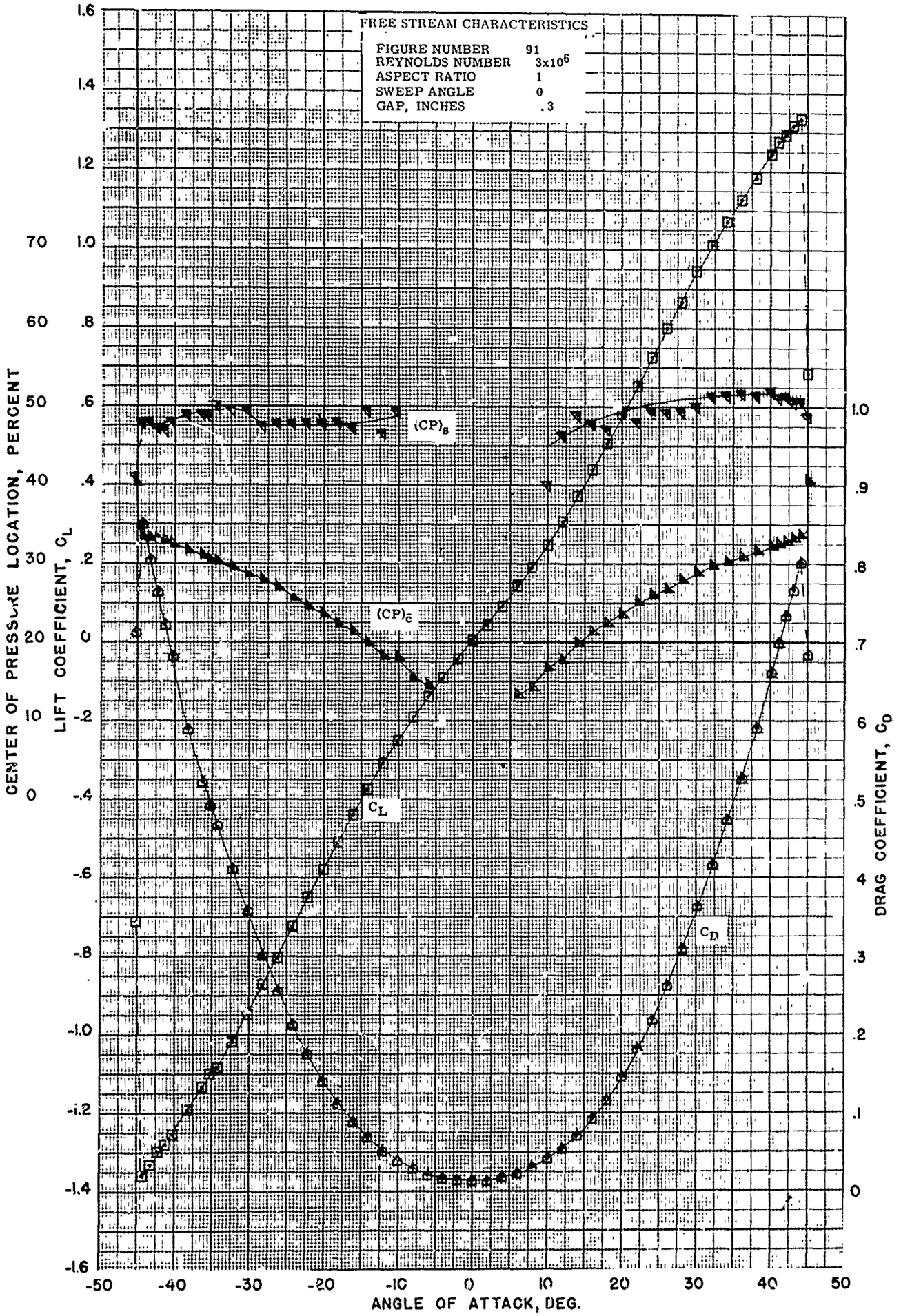
FREE STREAM CHARACTERISTICS
FIGURE NUMBER 91
REYNOLDS NUMBER 3x10^6
ASPECT RATIO 1
SWEEP ANGLE 0
GAP, INCHES .3
(CP)s
(CP)c
CL
CD
CENTER OF PRESSURE LOCATION, PERCENT
LIFT COEFFICIENT, CL
DRAG COEFFICIENT, CD
ANGLE OF ATTACK, DEG.
70
60
50
40
30
20
10
0
1.6
1.4
1.2
1.0
.8
.6
.4
.2
0
-.2
-.4
-.6
-.8
-1.0
-1.2
-1.4
-1.6
1.0
.9
.8
.7
.6
.5
.4
.3
.2
.1
0
-50
-40
-30
-20
-10
0
10
20
30
40
50

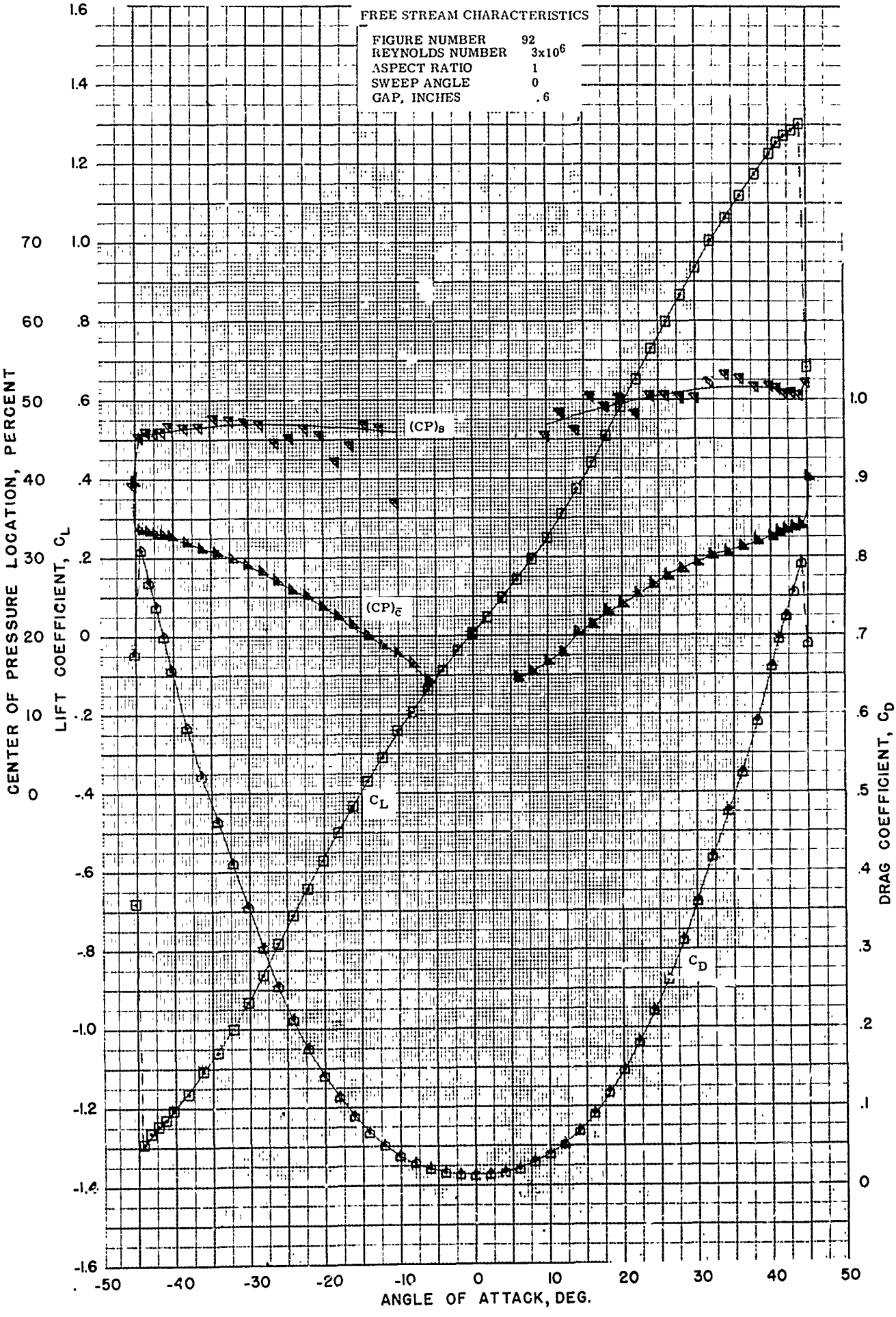
FREE STREAM CHARACTERISTICS
FIGURE NUMBER 92
REYNOLDS NUMBER 3x10^6
ASPECT RATIO 1
SWEEP ANGLE 0
GAP, INCHES .6
(CP)s
(CP)c̄
CL
CD
CENTER OF PRESSURE LOCATION, PERCENT
LIFT COEFFICIENT, CL
DRAG COEFFICIENT, CD
ANGLE OF ATTACK, DEG.
70
60
50
40
30
20
10
0
1.6
1.4
1.2
1.0
.8
.6
.4
.2
0
-.2
-.4
-.6
-.8
-1.0
-1.2
-1.4
-1.6
1.0
.9
.8
.7
.6
.5
.4
.3
.2
.1
0
-50
-40
-30
-20
-10
0
10
20
30
40
50

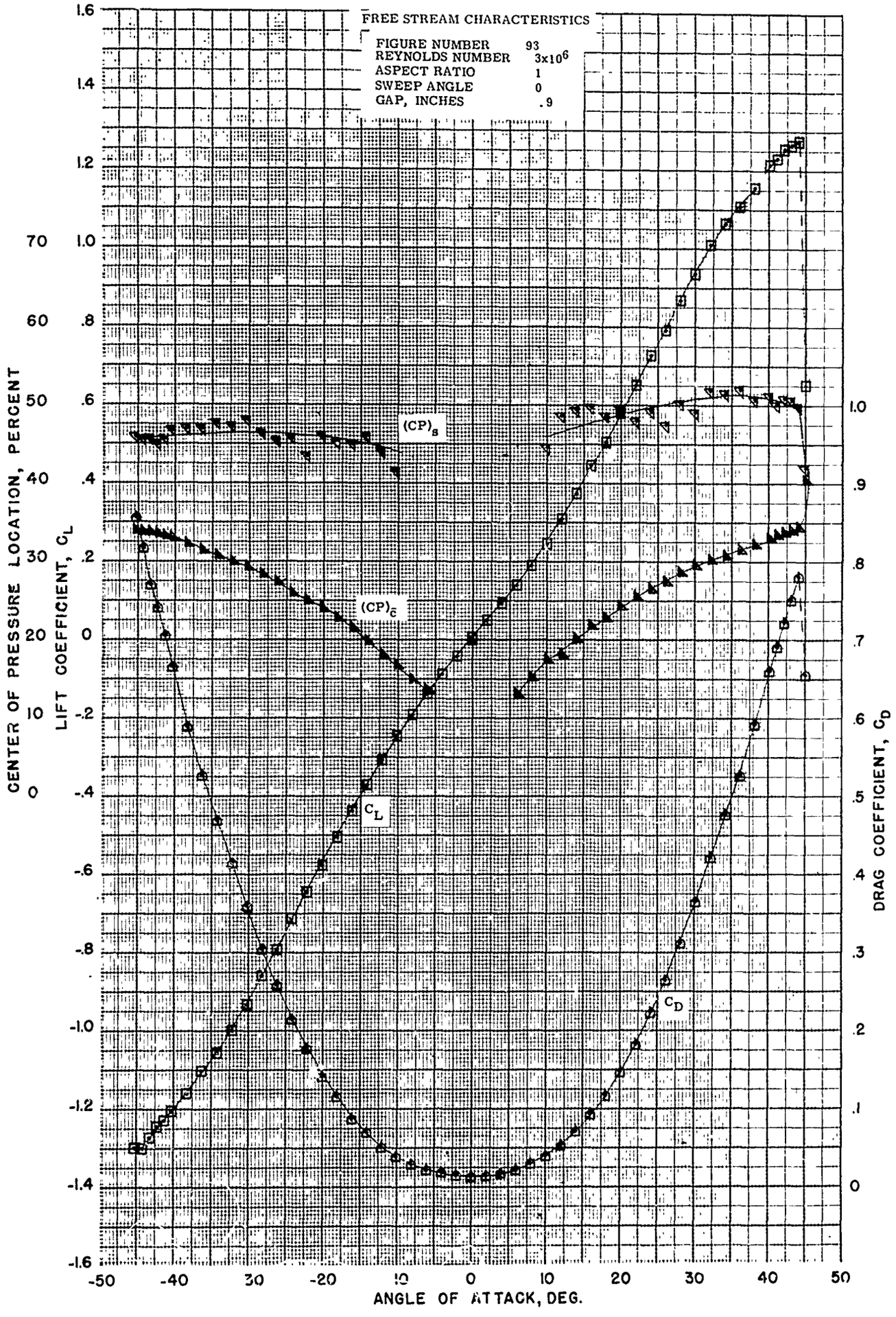
FREE STREAM CHARACTERISTICS
FIGURE NUMBER 93
REYNOLDS NUMBER 3x10^6
ASPECT RATIO 1
SWEEP ANGLE 0
GAP, INCHES .9
CENTER OF PRESSURE LOCATION, PERCENT
LIFT COEFFICIENT, C_L
DRAG COEFFICIENT, C_D
ANGLE OF ATTACK, DEG.
$(CP)_s$
$(CP)_c$
C_L
C_D
70
60
50
40
30
20
10
0
1.6
1.4
1.2
1.0
.8
.6
.4
.2
0
-.2
-.4
-.6
-.8
-1.0
-1.2
-1.4
-1.6
1.0
.9
.8
.7
.6
.5
.4
.3
.2
.1
0
-50
-40
30
-20
10
0
10
20
30
40
50

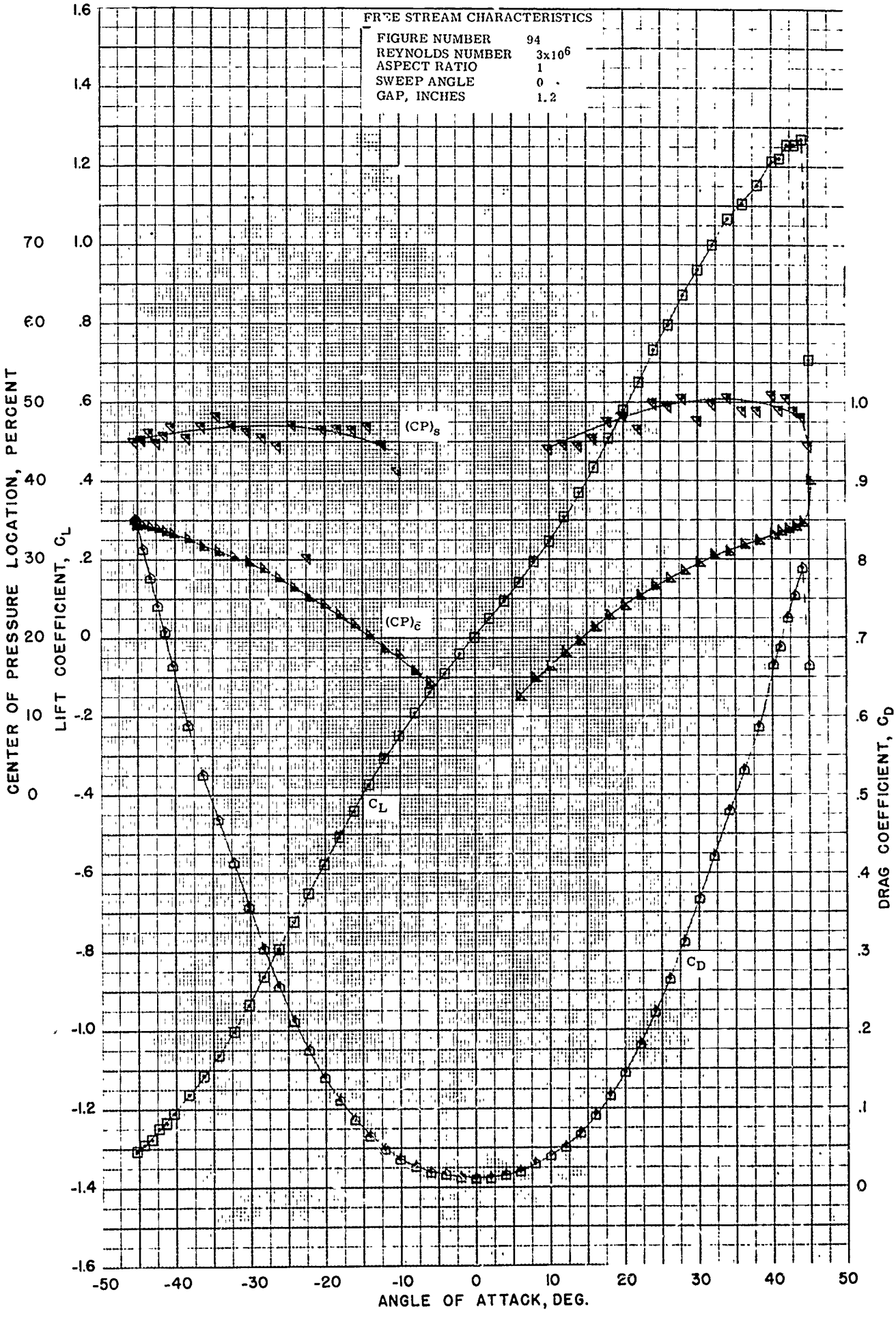
FREE STREAM CHARACTERISTICS
FIGURE NUMBER 94
REYNOLDS NUMBER 3x10^6
ASPECT RATIO 1
SWEEP ANGLE 0
GAP, INCHES 1.2
(CP)s
(CP)c
CL
CD
CENTER OF PRESSURE LOCATION, PERCENT
LIFT COEFFICIENT, CL
DRAG COEFFICIENT, CD
ANGLE OF ATTACK, DEG.
70
60
50
40
30
20
10
0
1.6
1.4
1.2
1.0
.8
.6
.4
.2
0
-.2
-.4
-.6
-.8
-1.0
-1.2
-1.4
-1.6
1.0
.9
.8
.7
.6
.5
.4
.3
.2
.1
0
-50
-40
-30
-20
-10
0
10
20
30
40
50

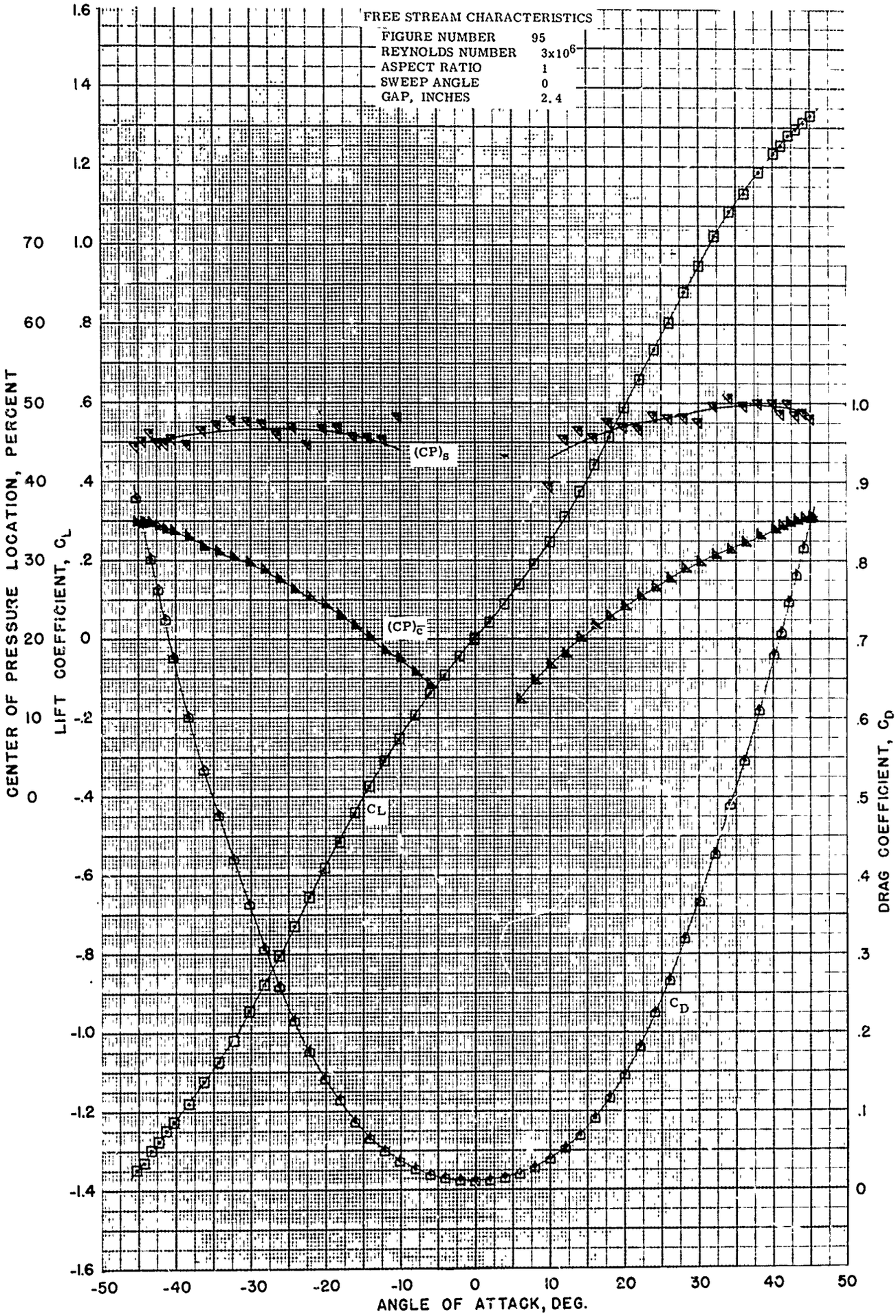
FREE STREAM CHARACTERISTICS
FIGURE NUMBER 95
REYNOLDS NUMBER 3x10^6
ASPECT RATIO 1
SWEEP ANGLE 0
GAP, INCHES 2.4
CENTER OF PRESSURE LOCATION, PERCENT
LIFT COEFFICIENT, C_L
DRAG COEFFICIENT, C_D
ANGLE OF ATTACK, DEG.
$(CP)_s$
$(CP)_{\bar{c}}$
C_L
C_D
70
60
50
40
30
20
10
0
1.6
1.4
1.2
1.0
.8
.6
.4
.2
0
-.2
-.4
-.6
-.8
-1.0
-1.2
-1.4
-1.6
1.0
.9
.8
.7
.6
.5
.4
.3
.2
.1
0
-50
-40
-30
-20
-10
0
10
20
30
40
50

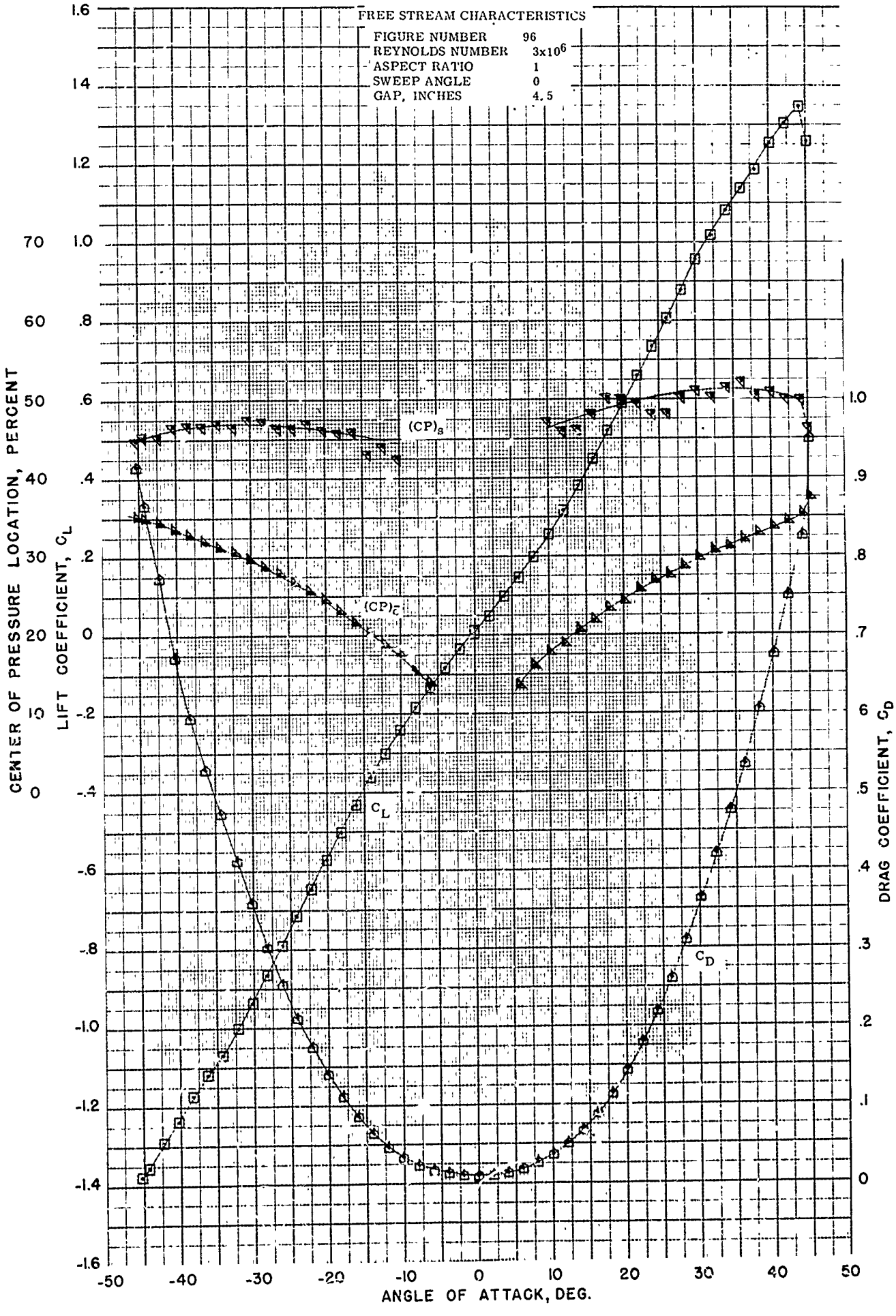
FREE STREAM CHARACTERISTICS
FIGURE NUMBER 96
REYNOLDS NUMBER 3x10^6
ASPECT RATIO 1
SWEEP ANGLE 0
GAP, INCHES 4.5
(CP)s
(CP)c
CL
CD
CENTER OF PRESSURE LOCATION, PERCENT
LIFT COEFFICIENT, CL
DRAG COEFFICIENT, CD
ANGLE OF ATTACK, DEG.
70
60
50
40
30
20
10
0
1.6
1.4
1.2
1.0
.8
.6
.4
.2
0
-.2
-.4
-.6
-.8
-1.0
-1.2
-1.4
-1.6
1.0
.9
.8
.7
.6
.5
.4
.3
.2
.1
0
-50
-40
-30
-20
-10
0
10
20
30
40
50

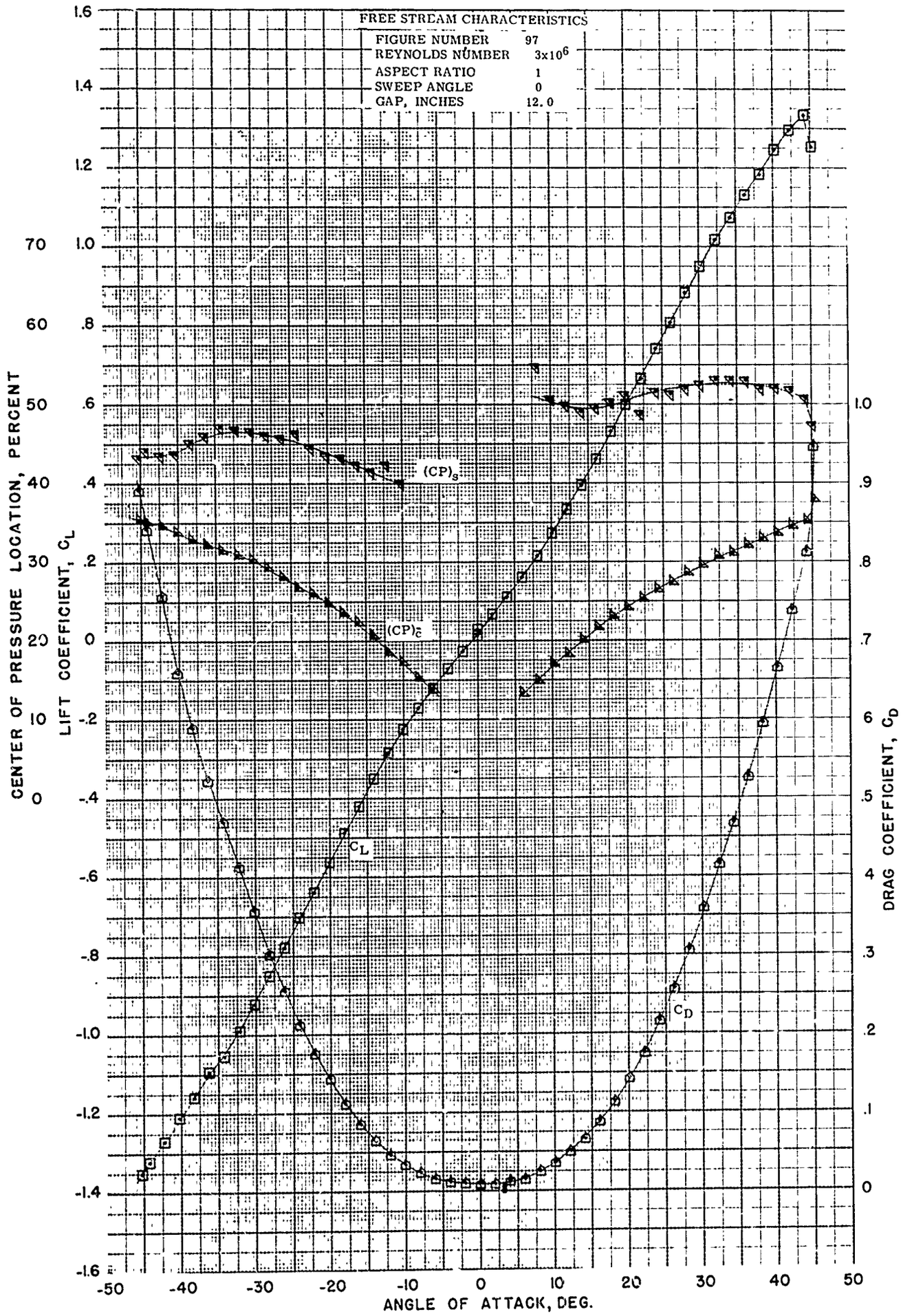
FREE STREAM CHARACTERISTICS
FIGURE NUMBER 97
REYNOLDS NUMBER 3x10^6
ASPECT RATIO 1
SWEEP ANGLE 0
GAP, INCHES 12.0
CENTER OF PRESSURE LOCATION, PERCENT
LIFT COEFFICIENT, C_L
DRAG COEFFICIENT, C_D
ANGLE OF ATTACK, DEG.
$(CP)_s$
$(CP)_c$
C_L
C_D
70
60
50
40
30
20
10
0
1.6
1.4
1.2
1.0
.8
.6
.4
.2
0
-.2
-.4
-.6
-.8
-1.0
-1.2
-1.4
-1.6
1.0
.9
.8
.7
.6
.5
.4
.3
.2
.1
0
-50
-40
-30
-20
-10
0
10
20
30
40
50

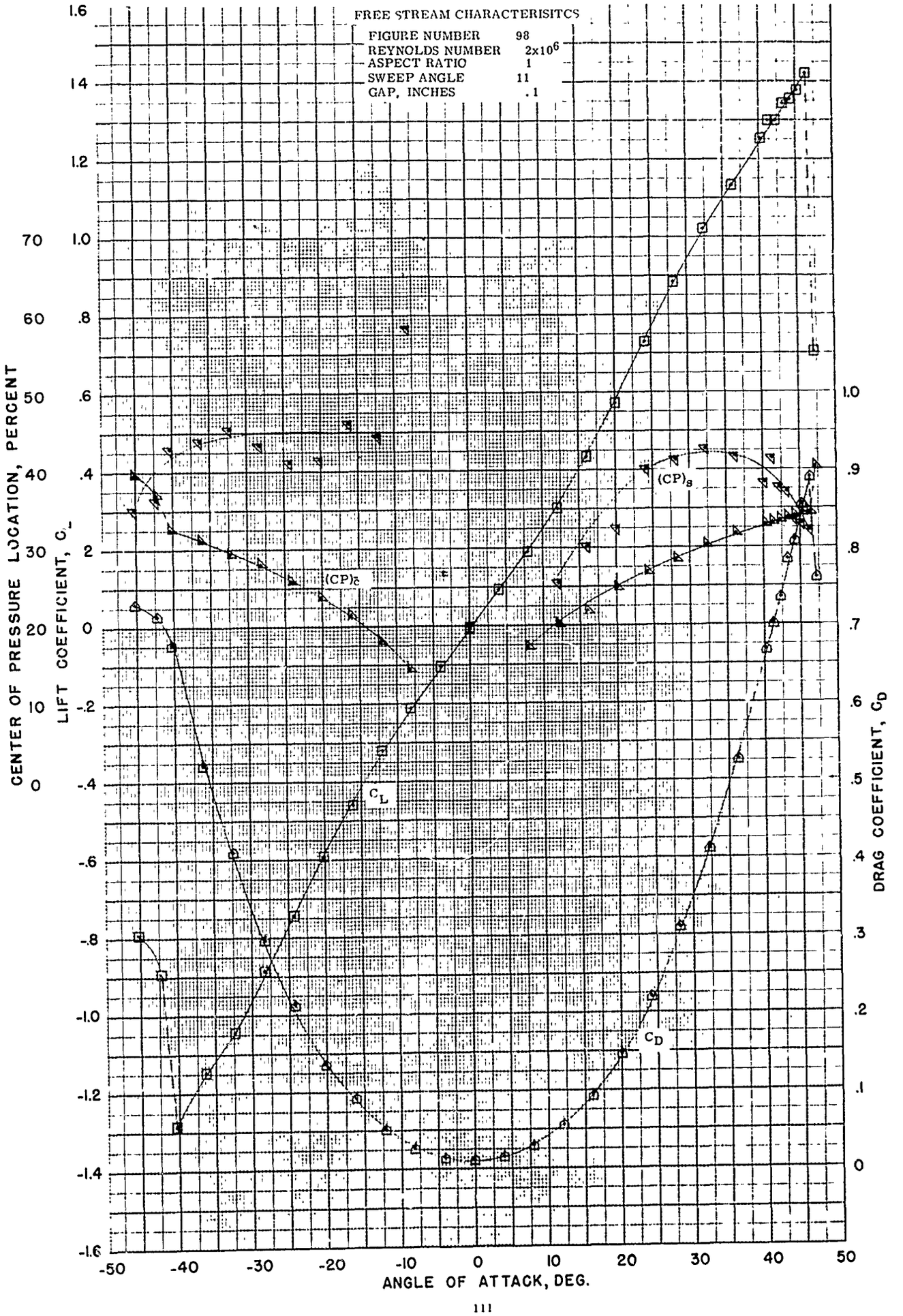
FREE STREAM CHARACTERISITCS
FIGURE NUMBER 98
REYNOLDS NUMBER 2x10^6
ASPECT RATIO 1
SWEEP ANGLE 11
GAP, INCHES .1
CENTER OF PRESSURE LOCATION, PERCENT
LIFT COEFFICIENT, C_L
DRAG COEFFICIENT, C_D
ANGLE OF ATTACK, DEG.
$(CP)_c$
$(CP)_s$
C_L
C_D
70
60
50
40
30
20
10
0
1.6
1.4
1.2
1.0
.8
.6
.4
.2
0
-.2
-.4
-.6
-.8
-1.0
-1.2
-1.4
-1.6
1.0
.9
.8
.7
.6
.5
.4
.3
.2
.1
0
-50
-40
-30
-20
-10
0
10
20
30
40
50

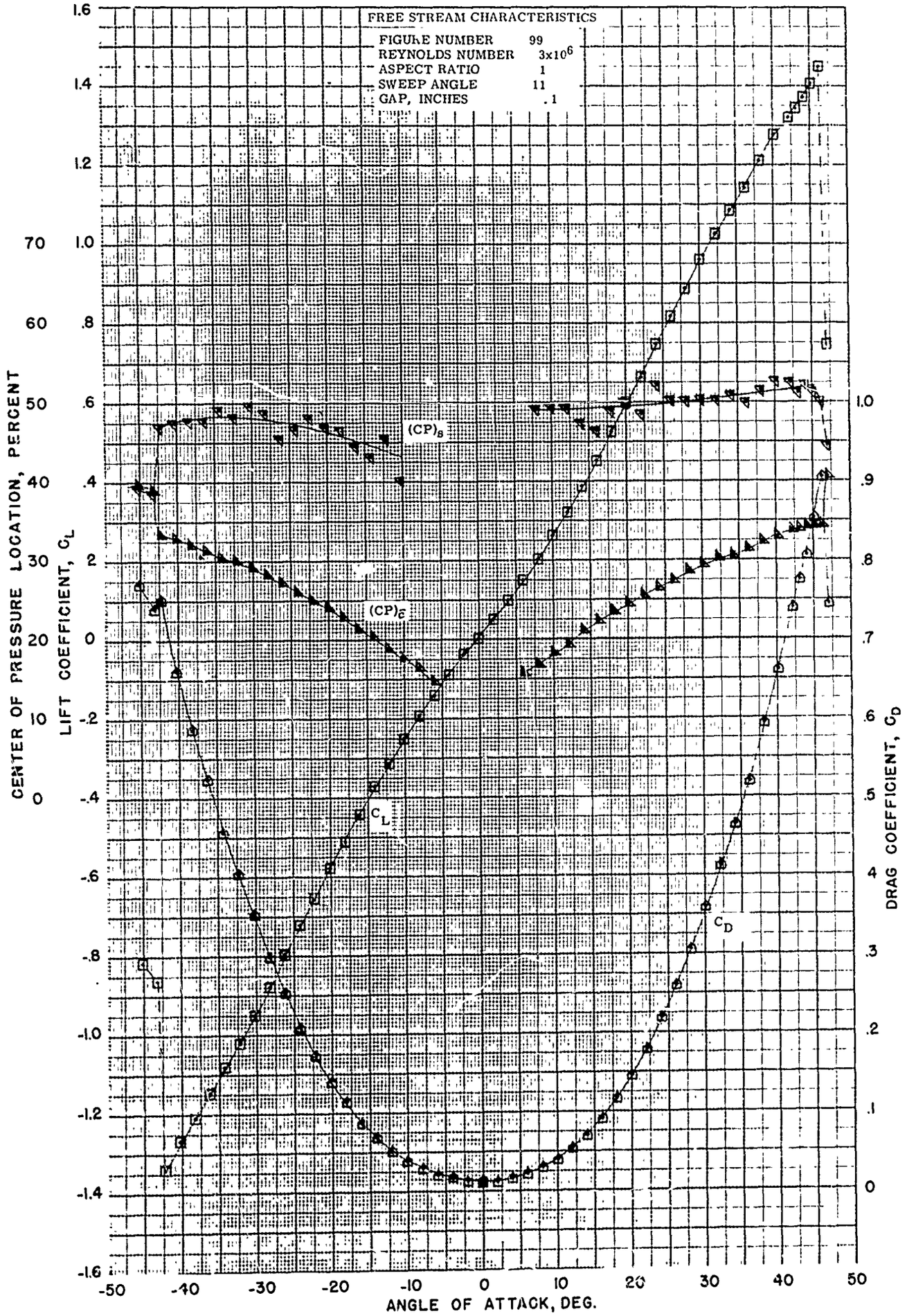
FREE STREAM CHARACTERISTICS
FIGURE NUMBER 99
REYNOLDS NUMBER 3x10^6
ASPECT RATIO 1
SWEEP ANGLE 11
GAP, INCHES .1
CENTER OF PRESSURE LOCATION, PERCENT
LIFT COEFFICIENT, C_L
DRAG COEFFICIENT, C_D
ANGLE OF ATTACK, DEG.
$(CP)_B$
$(CP)_E$
C_L
C_D
70
60
50
40
30
20
10
0
1.6
1.4
1.2
1.0
.8
.6
.4
.2
0
-.2
-.4
-.6
-.8
-1.0
-1.2
-1.4
-1.6
1.0
.9
.8
.7
.6
.5
.4
.3
.2
.1
0
-50
-40
-30
-20
-10
0
10
20
30
40
50

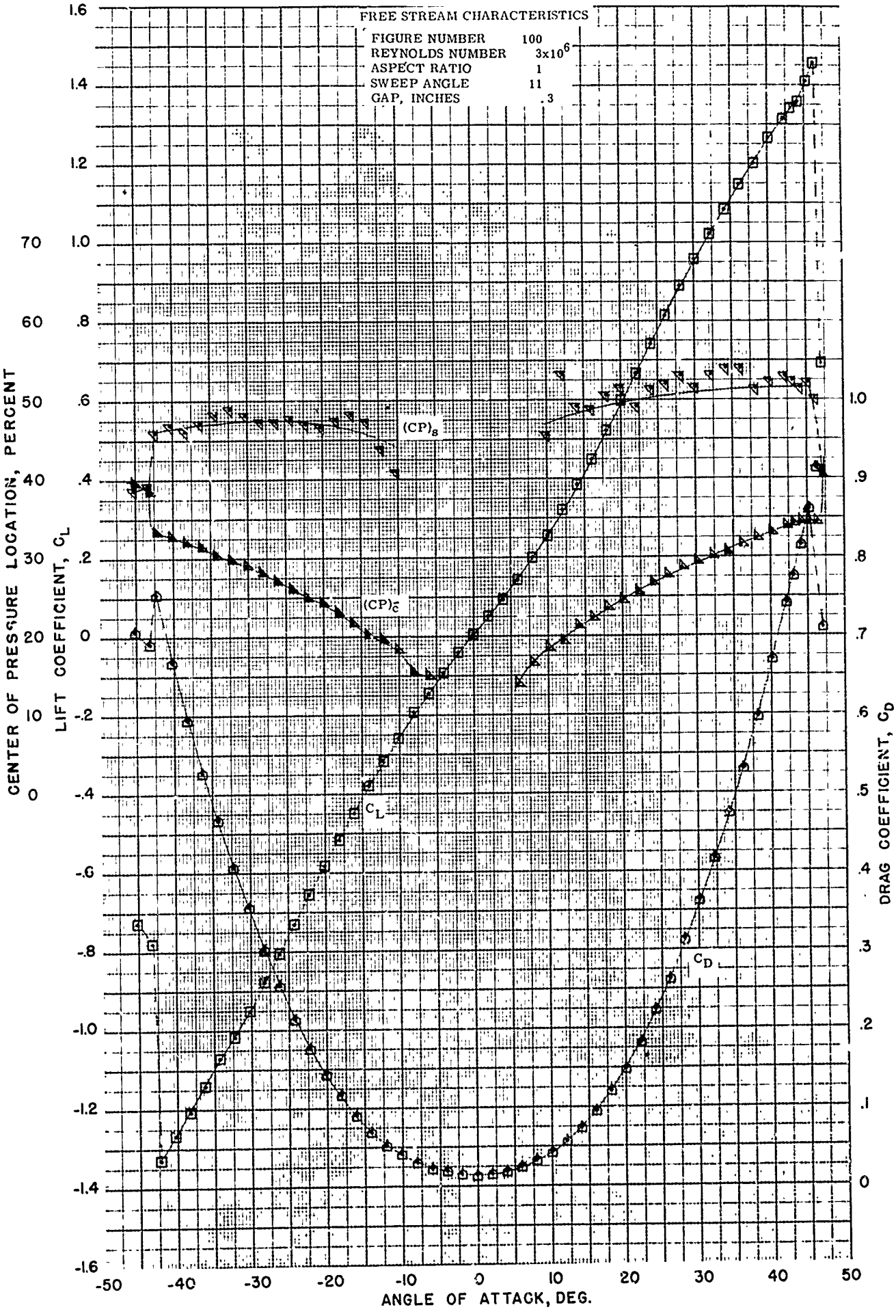
FREE STREAM CHARACTERISTICS
FIGURE NUMBER 100
REYNOLDS NUMBER 3x10^6
ASPECT RATIO 1
SWEEP ANGLE 11
GAP, INCHES .3
CENTER OF PRESSURE LOCATION, PERCENT
LIFT COEFFICIENT, C_L
DRAG COEFFICIENT, C_D
ANGLE OF ATTACK, DEG.
$(CP)_B$
$(CP)_{\bar{c}}$
C_L
C_D
70
60
50
40
30
20
10
0
1.6
1.4
1.2
1.0
.8
.6
.4
.2
0
-.2
-.4
-.6
-.8
-1.0
-1.2
-1.4
-1.6
1.0
.9
.8
.7
.6
.5
.4
.3
.2
.1
0
-50
-40
-30
-20
-10
0
10
20
30
40
50

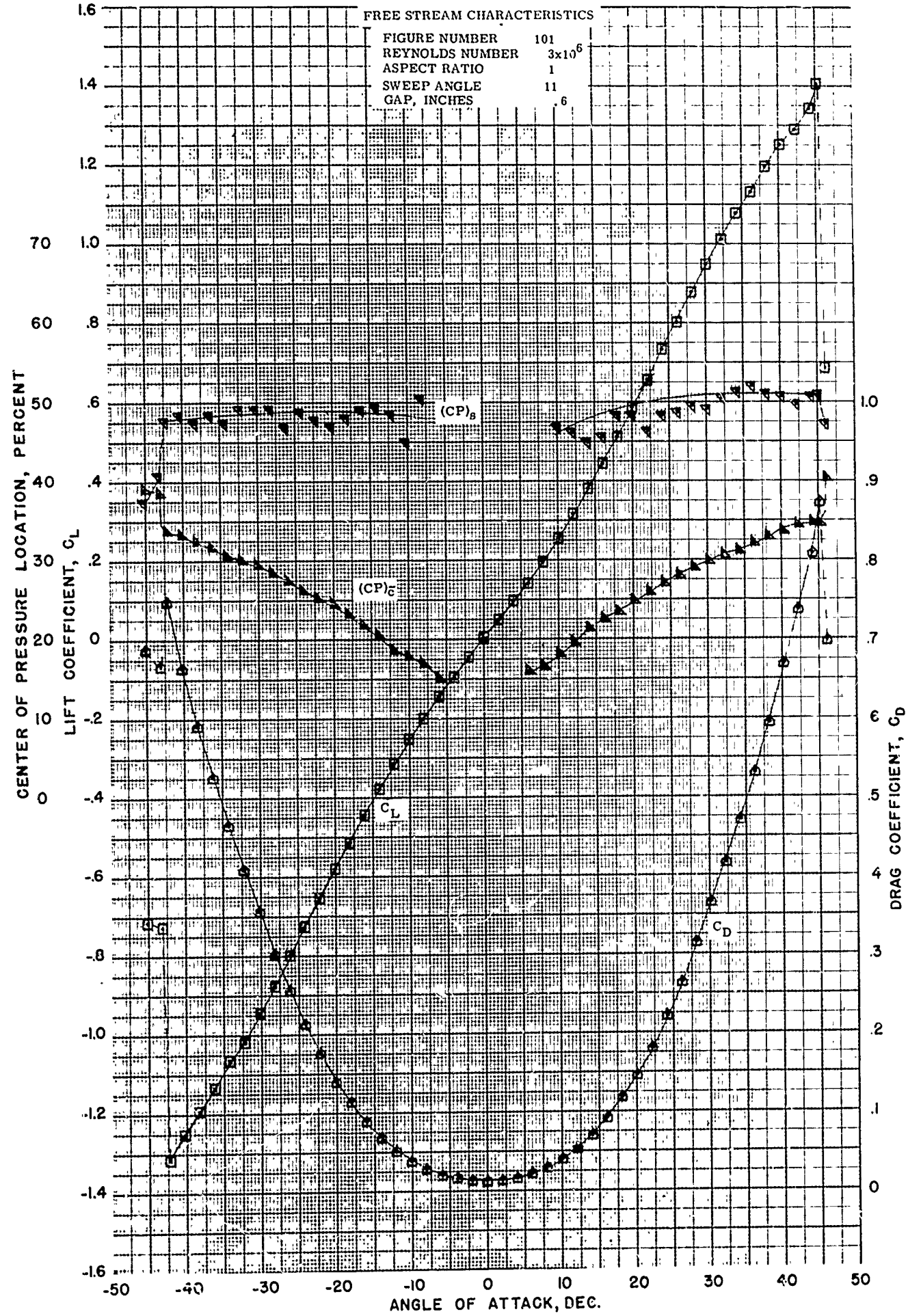
FREE STREAM CHARACTERISTICS
FIGURE NUMBER 101
REYNOLDS NUMBER 3x10^6
ASPECT RATIO 1
SWEEP ANGLE 11
GAP, INCHES .6
CENTER OF PRESSURE LOCATION, PERCENT
LIFT COEFFICIENT, C_L
DRAG COEFFICIENT, C_D
ANGLE OF ATTACK, DEC.
$(CP)_B$
$(CP)_{\bar{c}}$
C_L
C_D
70
60
50
40
30
20
10
0
1.6
1.4
1.2
1.0
.8
.6
.4
.2
0
-.2
-.4
-.6
-.8
-1.0
-1.2
-1.4
-1.6
1.0
.9
.8
.7
.6
.5
.4
.3
.2
.1
0
-50
-40
-30
-20
-10
0
10
20
30
40
50

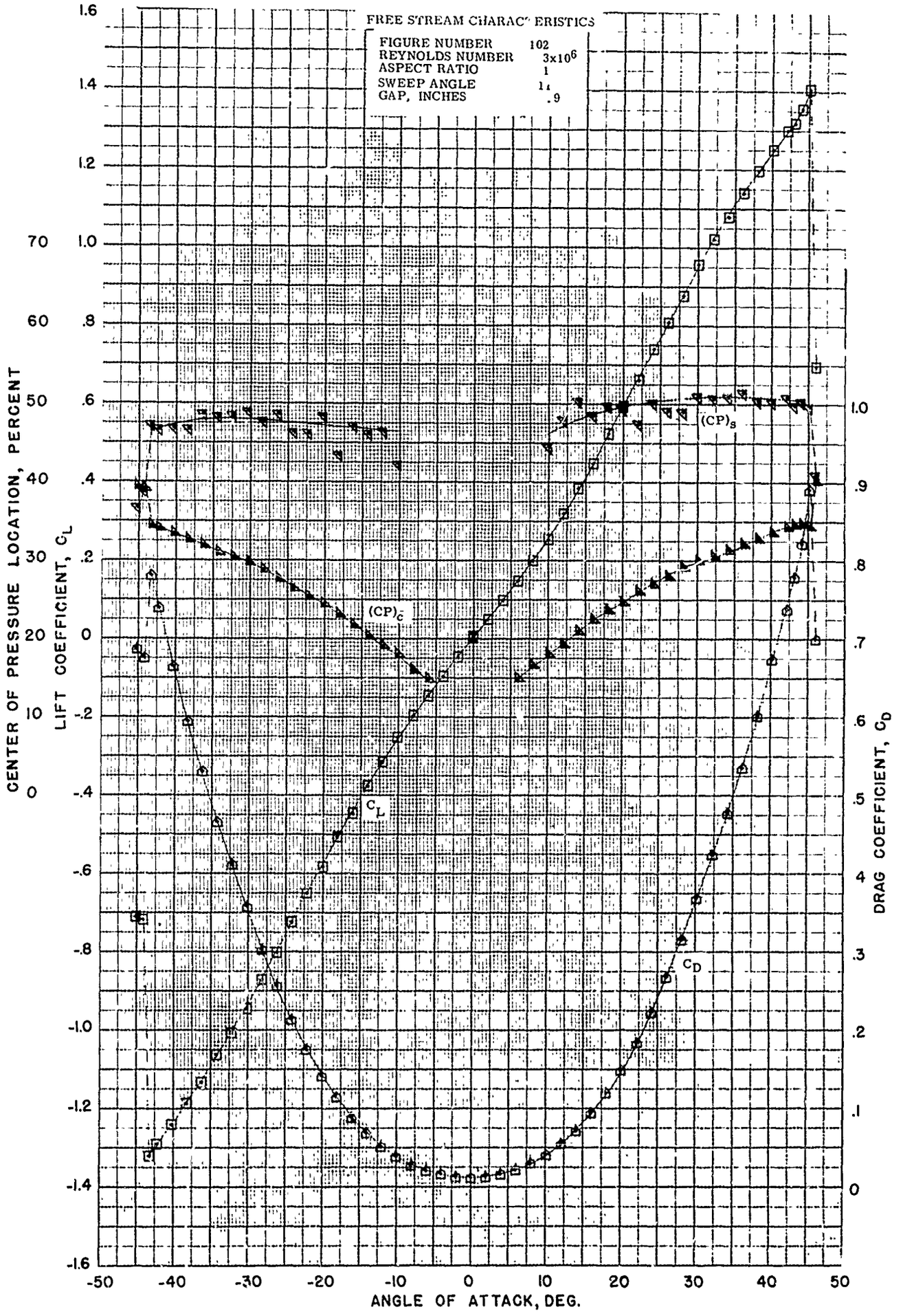
FREE STREAM CHARACTERISTICS
FIGURE NUMBER 102
REYNOLDS NUMBER 3x10^6
ASPECT RATIO 1
SWEEP ANGLE 14
GAP, INCHES .9
CENTER OF PRESSURE LOCATION, PERCENT
LIFT COEFFICIENT, C_L
DRAG COEFFICIENT, C_D
ANGLE OF ATTACK, DEG.
$(CP)_s$
$(CP)_c$
C_L
C_D
70
60
50
40
30
20
10
0
1.6
1.4
1.2
1.0
.8
.6
.4
.2
0
-.2
-.4
-.6
-.8
-1.0
-1.2
-1.4
-1.6
1.0
.9
.8
.7
.6
.5
.4
.3
.2
.1
0
-50
-40
-30
-20
-10
0
10
20
30
40
50

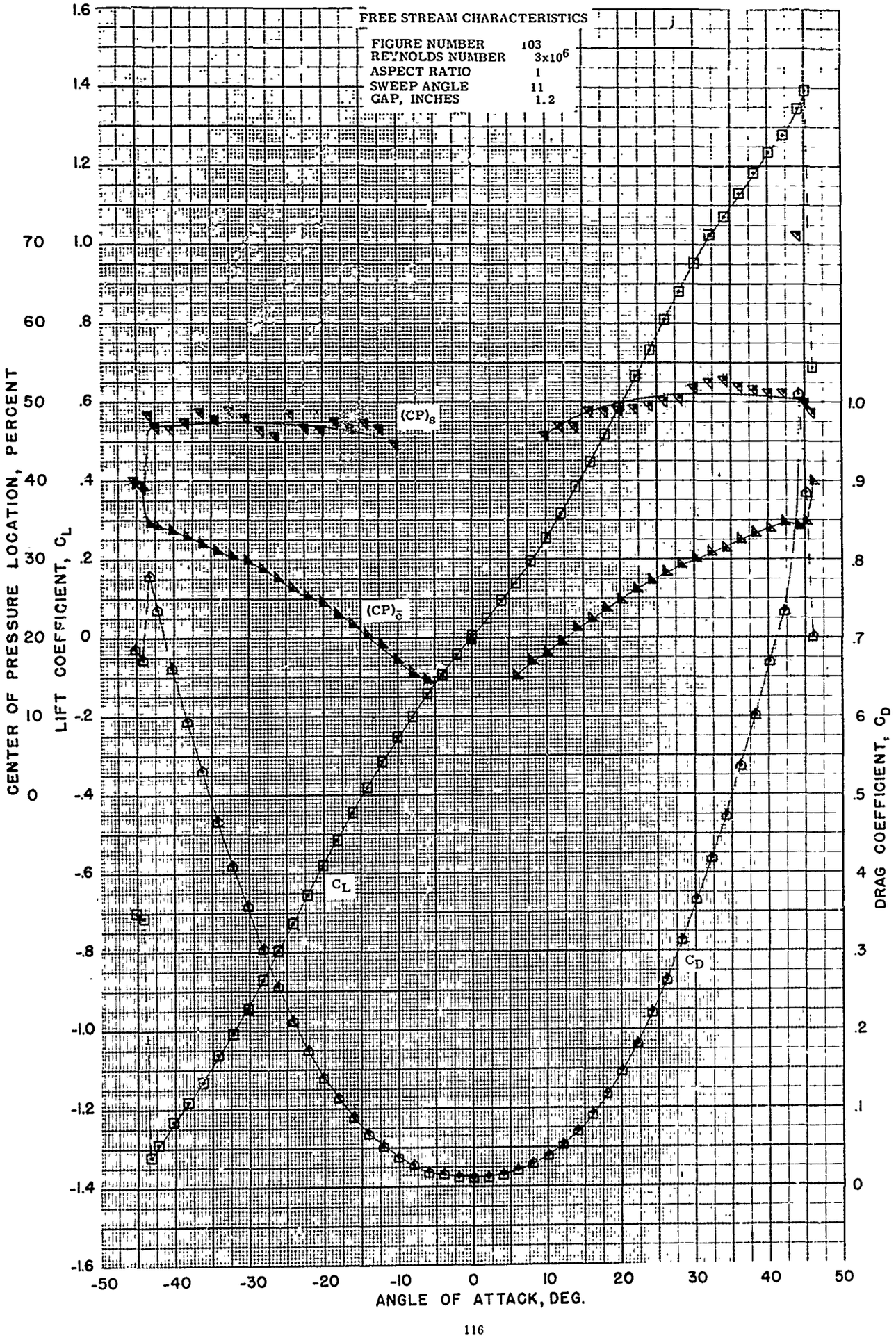
FREE STREAM CHARACTERISTICS
FIGURE NUMBER 103
REYNOLDS NUMBER 3x10^6
ASPECT RATIO 1
SWEEP ANGLE 11
GAP, INCHES 1.2
CENTER OF PRESSURE LOCATION, PERCENT
LIFT COEFFICIENT, C_L
DRAG COEFFICIENT, C_D
ANGLE OF ATTACK, DEG.
$(CP)_s$
$(CP)_{\bar{c}}$
C_L
C_D
70 60 50 40 30 20 10 0
1.6 1.4 1.2 1.0 .8 .6 .4 .2 0 -.2 -.4 -.6 -.8 -1.0 -1.2 -1.4 -1.6
1.0 .9 .8 .7 6 .5 4 .3 .2 .1 0
-50 -40 -30 -20 -10 0 10 20 30 40 50

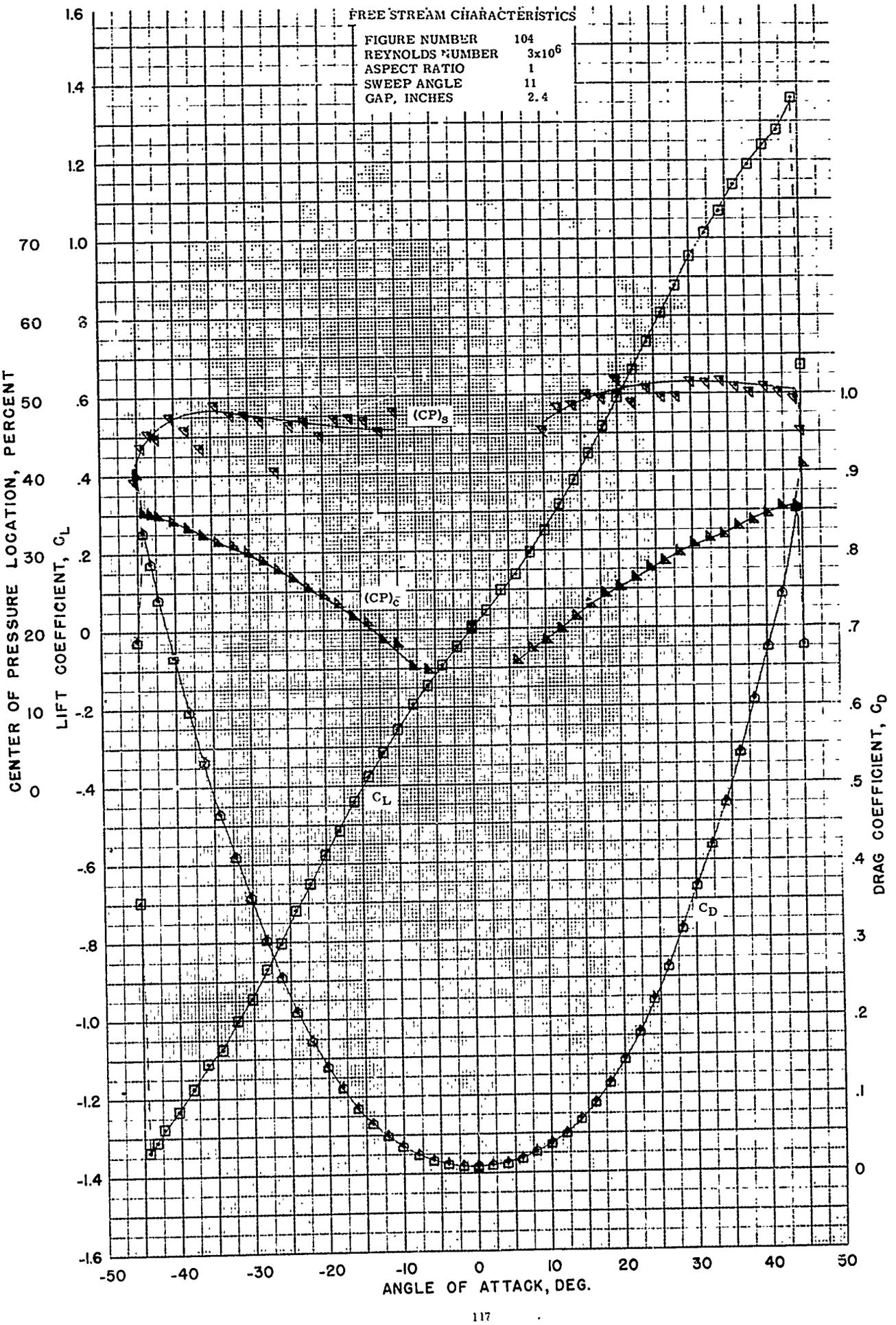
FREE STREAM CHARACTERISTICS
FIGURE NUMBER 104
REYNOLDS NUMBER 3x10^6
ASPECT RATIO 1
SWEEP ANGLE 11
GAP, INCHES 2.4
(CP)s
(CP)c̄
CL
CD
CENTER OF PRESSURE LOCATION, PERCENT
LIFT COEFFICIENT, CL
DRAG COEFFICIENT, CD
ANGLE OF ATTACK, DEG.
70
60
50
40
30
20
10
0
1.6
1.4
1.2
1.0
.8
.6
.4
.2
0
-.2
-.4
-.6
-.8
-1.0
-1.2
-1.4
-1.6
1.0
.9
.8
.7
.6
.5
.4
.3
.2
.1
0
-50
-40
-30
-20
-10
0
10
20
30
40
50

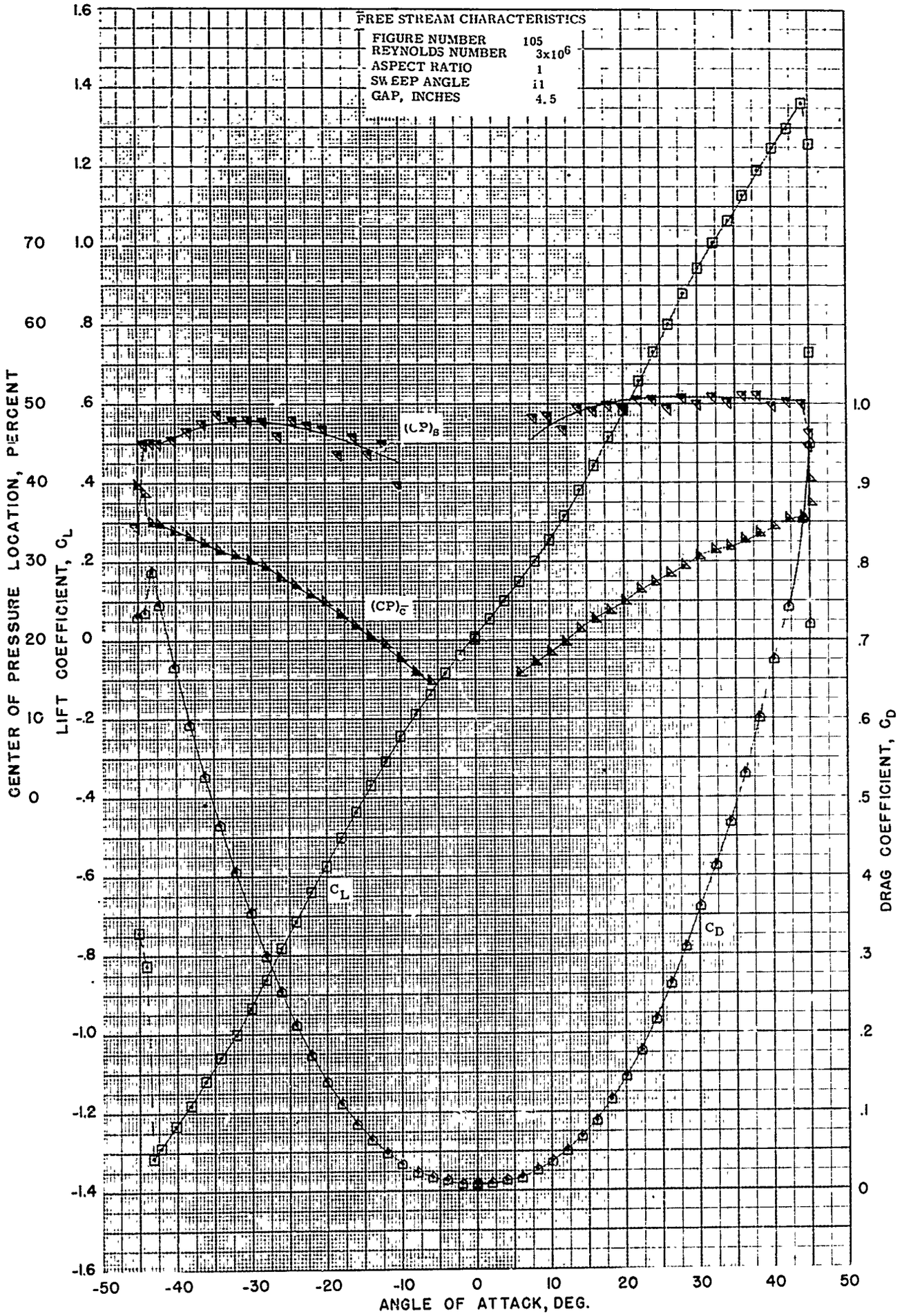
FREE STREAM CHARACTERISTICS
FIGURE NUMBER 105
REYNOLDS NUMBER 3x10^6
ASPECT RATIO 1
SWEEP ANGLE 11
GAP, INCHES 4.5
(CP)B
(CP)C
CL
CD
CENTER OF PRESSURE LOCATION, PERCENT
LIFT COEFFICIENT, CL
DRAG COEFFICIENT, CD
ANGLE OF ATTACK, DEG.
70
60
50
40
30
20
10
0
1.6
1.4
1.2
1.0
.8
.6
.4
.2
0
-.2
-.4
-.6
-.8
-1.0
-1.2
-1.4
-1.6
1.0
.9
.8
.7
.6
.5
.4
.3
.2
.1
0
-50
-40
-30
-20
-10
0
10
20
30
40
50

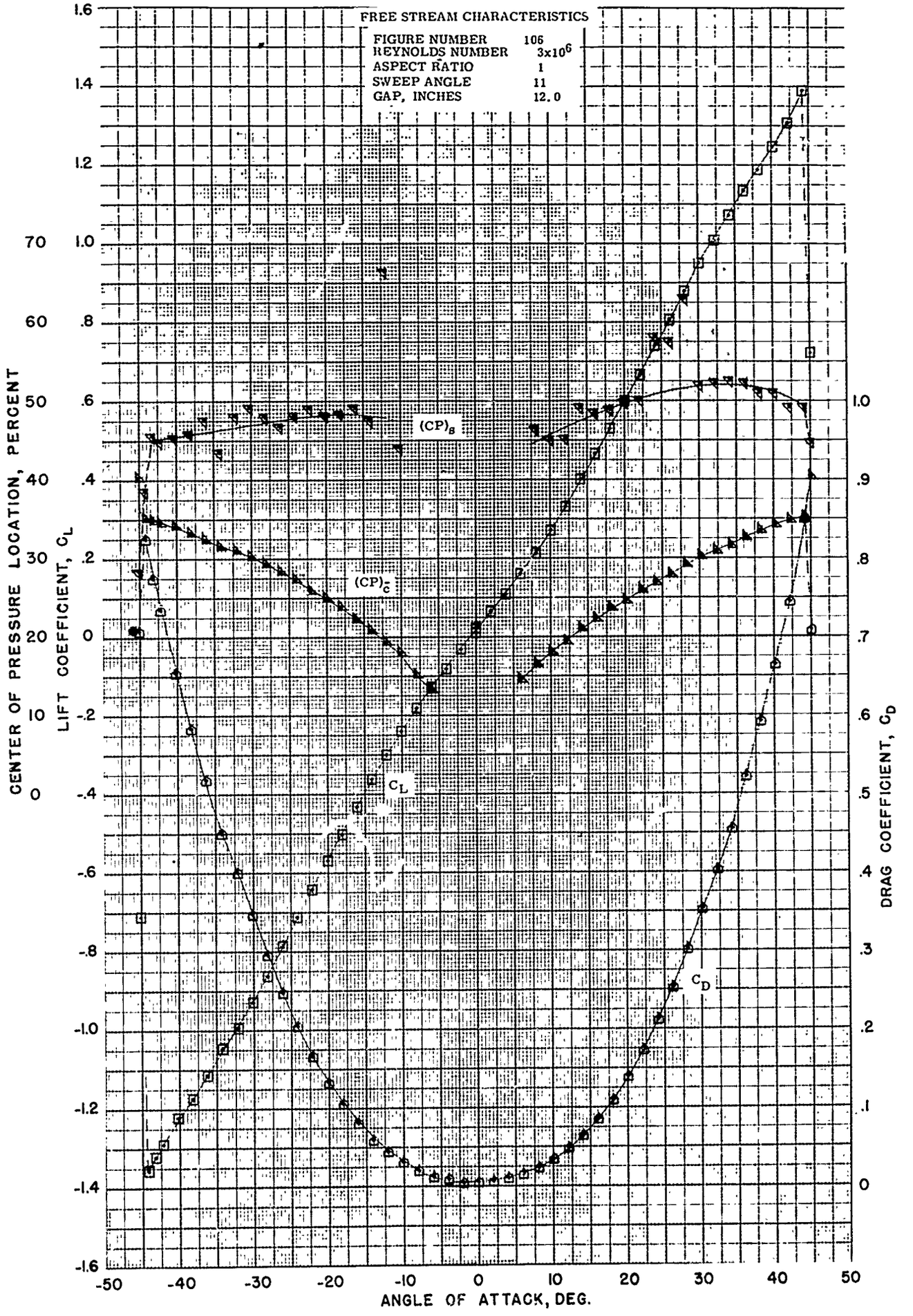
FREE STREAM CHARACTERISTICS
FIGURE NUMBER 106
REYNOLDS NUMBER 3x10^6
ASPECT RATIO 1
SWEEP ANGLE 11
GAP, INCHES 12.0
CENTER OF PRESSURE LOCATION, PERCENT
LIFT COEFFICIENT, C_L
DRAG COEFFICIENT, C_D
ANGLE OF ATTACK, DEG.
$(CP)_s$
$(CP)_c$
C_L
C_D
70
60
50
40
30
20
10
0
1.6
1.4
1.2
1.0
.8
.6
.4
.2
0
-.2
-.4
-.6
-.8
-1.0
-1.2
-1.4
-1.6
1.0
.9
.8
.7
.6
.5
.4
.3
.2
.1
0
-50
-40
-30
-20
-10
0
10
20
30
40
50

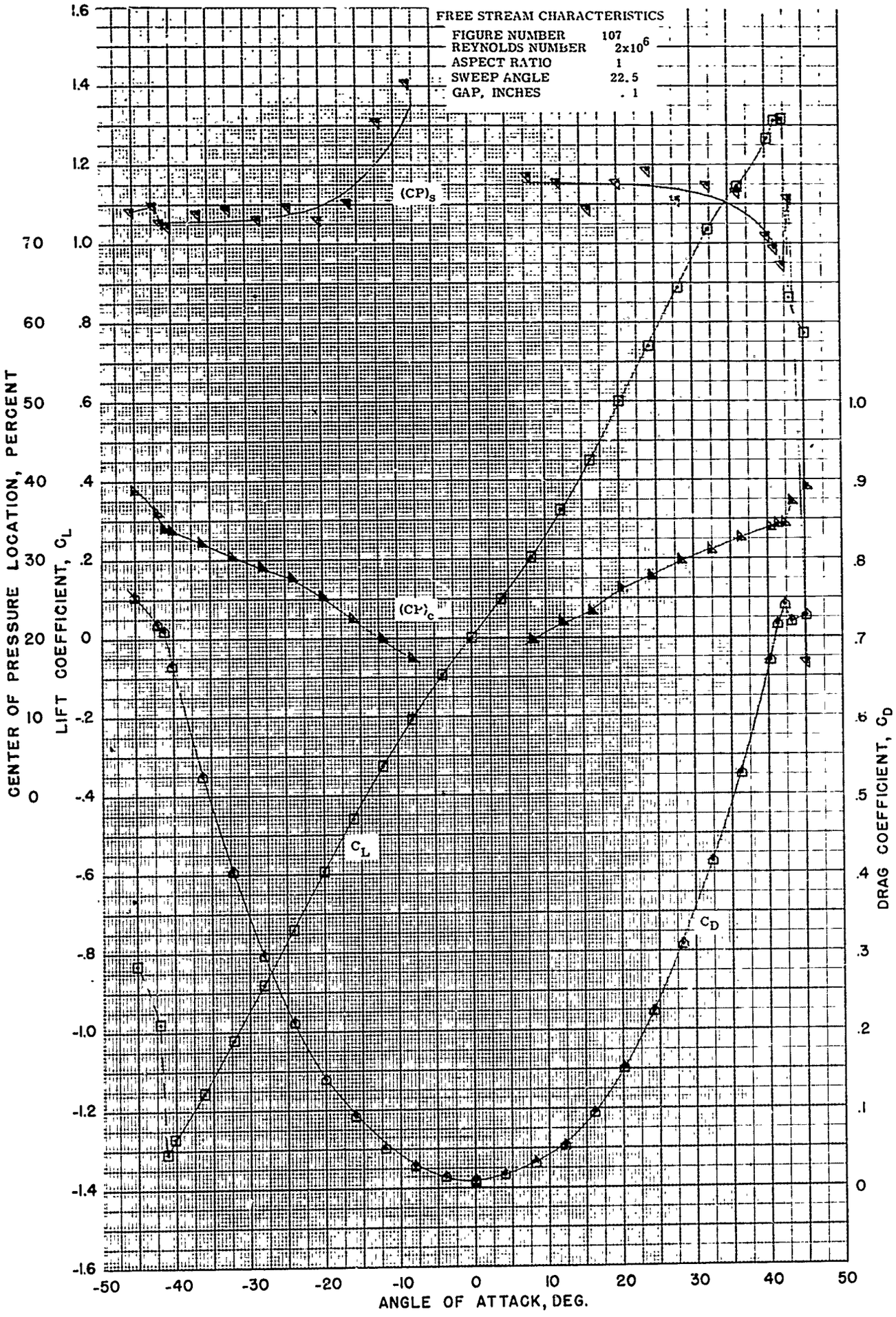
FREE STREAM CHARACTERISTICS
FIGURE NUMBER 107
REYNOLDS NUMBER 2x10^6
ASPECT RATIO 1
SWEEP ANGLE 22.5
GAP, INCHES .1
(CP)s
(CP)c
CL
CD
CENTER OF PRESSURE LOCATION, PERCENT
LIFT COEFFICIENT, CL
DRAG COEFFICIENT, CD
ANGLE OF ATTACK, DEG.
70
60
50
40
30
20
10
0
1.6
1.4
1.2
1.0
.8
.6
.4
.2
0
-.2
-.4
-.6
-.8
-1.0
-1.2
-1.4
-1.6
1.0
.9
.8
.7
.6
.5
.4
.3
.2
.1
0
-50
-40
-30
-20
-10
0
10
20
30
40
50

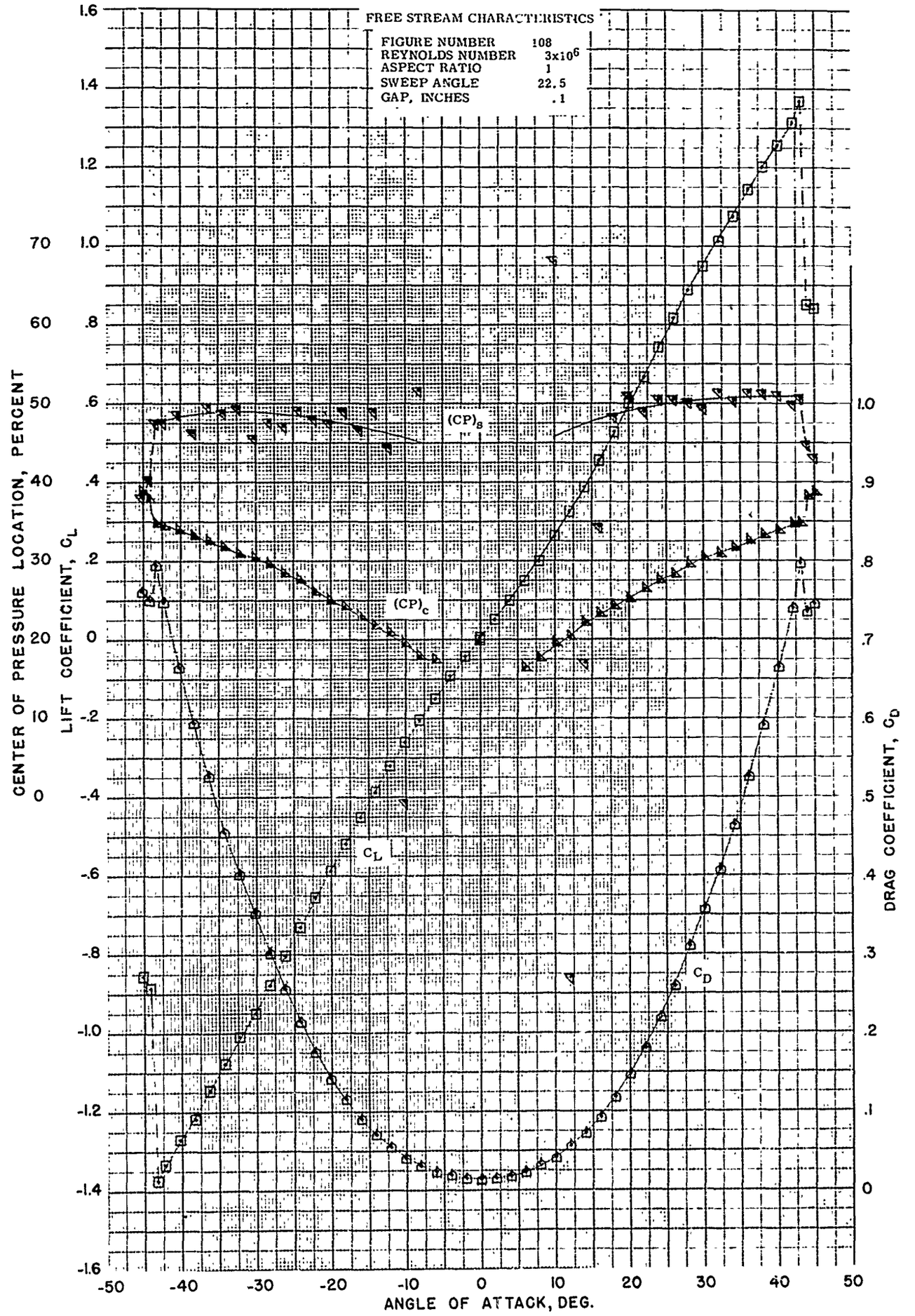
FREE STREAM CHARACTERISTICS
FIGURE NUMBER 108
REYNOLDS NUMBER 3x10^6
ASPECT RATIO 1
SWEEP ANGLE 22.5
GAP, INCHES .1
(CP)s
(CP)c
CL
CD
CENTER OF PRESSURE LOCATION, PERCENT
LIFT COEFFICIENT, CL
DRAG COEFFICIENT, CD
ANGLE OF ATTACK, DEG.
70
60
50
40
30
20
10
0
1.6
1.4
1.2
1.0
.8
.6
.4
.2
0
-.2
-.4
-.6
-.8
-1.0
-1.2
-1.4
-1.6
1.0
.9
.8
.7
.6
.5
.4
.3
.2
.1
0
-50
-40
-30
-20
-10
0
10
20
30
40
50

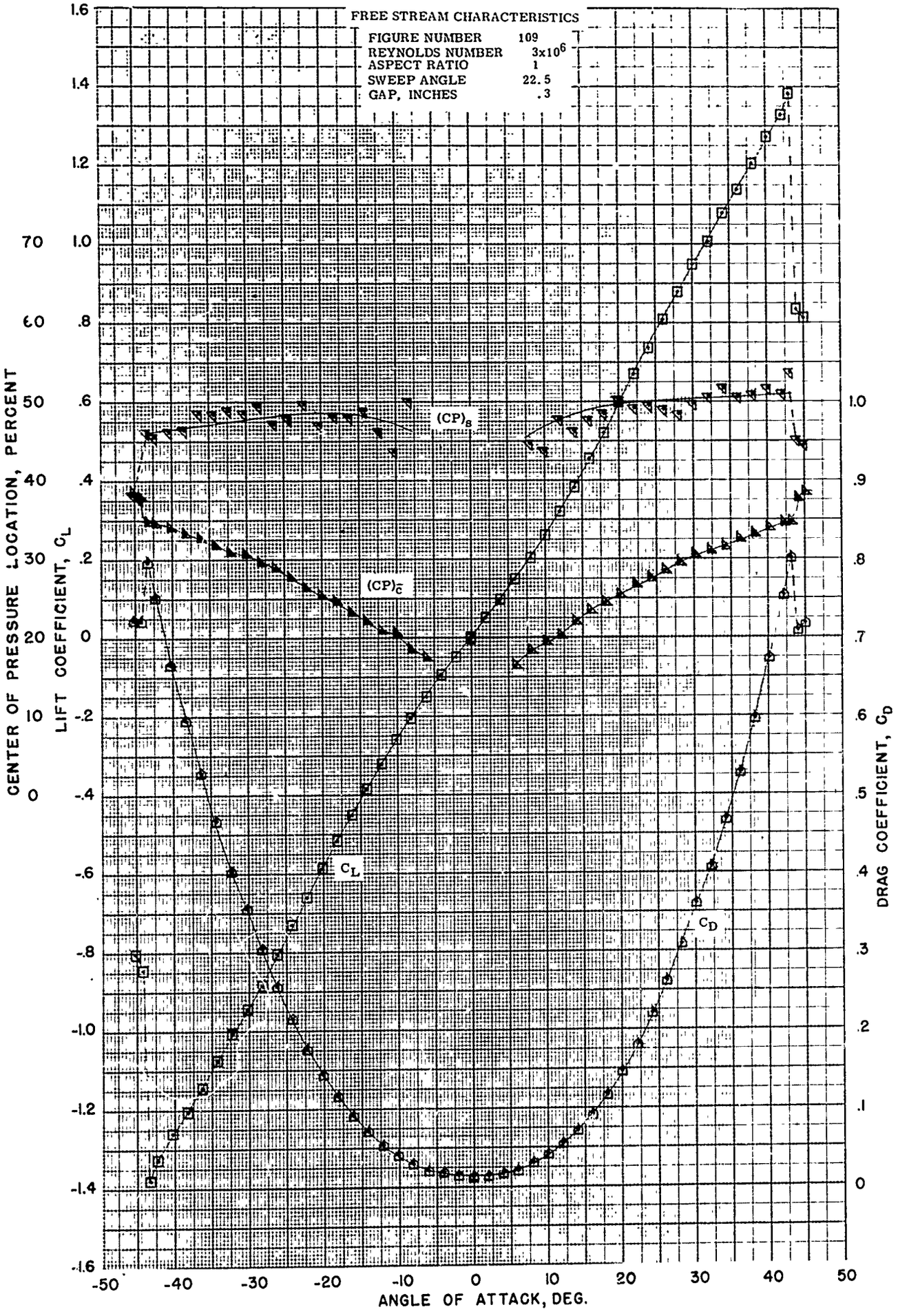
FREE STREAM CHARACTERISTICS
FIGURE NUMBER 109
REYNOLDS NUMBER 3x10^6
ASPECT RATIO 1
SWEEP ANGLE 22.5
GAP, INCHES .3
CENTER OF PRESSURE LOCATION, PERCENT
LIFT COEFFICIENT, C_L
DRAG COEFFICIENT, C_D
ANGLE OF ATTACK, DEG.
$(CP)_B$
$(CP)_{\bar{c}}$
C_L
C_D
70
60
50
40
30
20
10
0
1.6
1.4
1.2
1.0
.8
.6
.4
.2
0
-.2
-.4
-.6
-.8
-1.0
-1.2
-1.4
-1.6
1.0
.9
.8
.7
.6
.5
.4
.3
.2
.1
0
-50
-40
-30
-20
-10
0
10
20
30
40
50

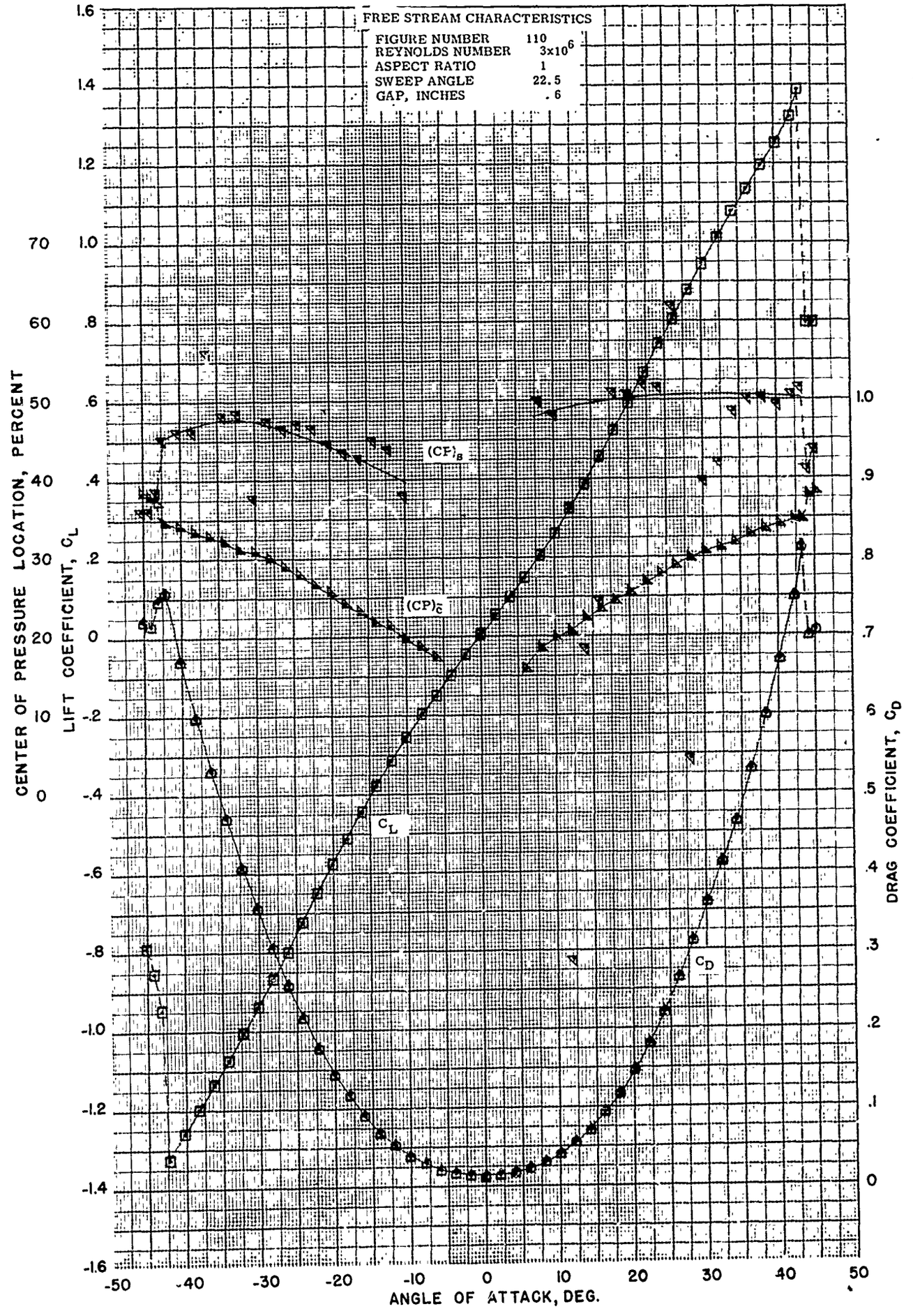
FREE STREAM CHARACTERISTICS
FIGURE NUMBER 110
REYNOLDS NUMBER 3x10^6
ASPECT RATIO 1
SWEEP ANGLE 22.5
GAP, INCHES .6
CENTER OF PRESSURE LOCATION, PERCENT
LIFT COEFFICIENT, C_L
DRAG COEFFICIENT, C_D
ANGLE OF ATTACK, DEG.
$(CP)_s$
$(CP)_c$
C_L
C_D
70
60
50
40
30
20
10
0
1.6
1.4
1.2
1.0
.8
.6
.4
.2
0
-.2
-.4
-.6
-.8
-1.0
-1.2
-1.4
-1.6
1.0
.9
.8
.7
.6
.5
.4
.3
.2
.1
0
-50
-40
-30
-20
-10
0
10
20
30
40
50

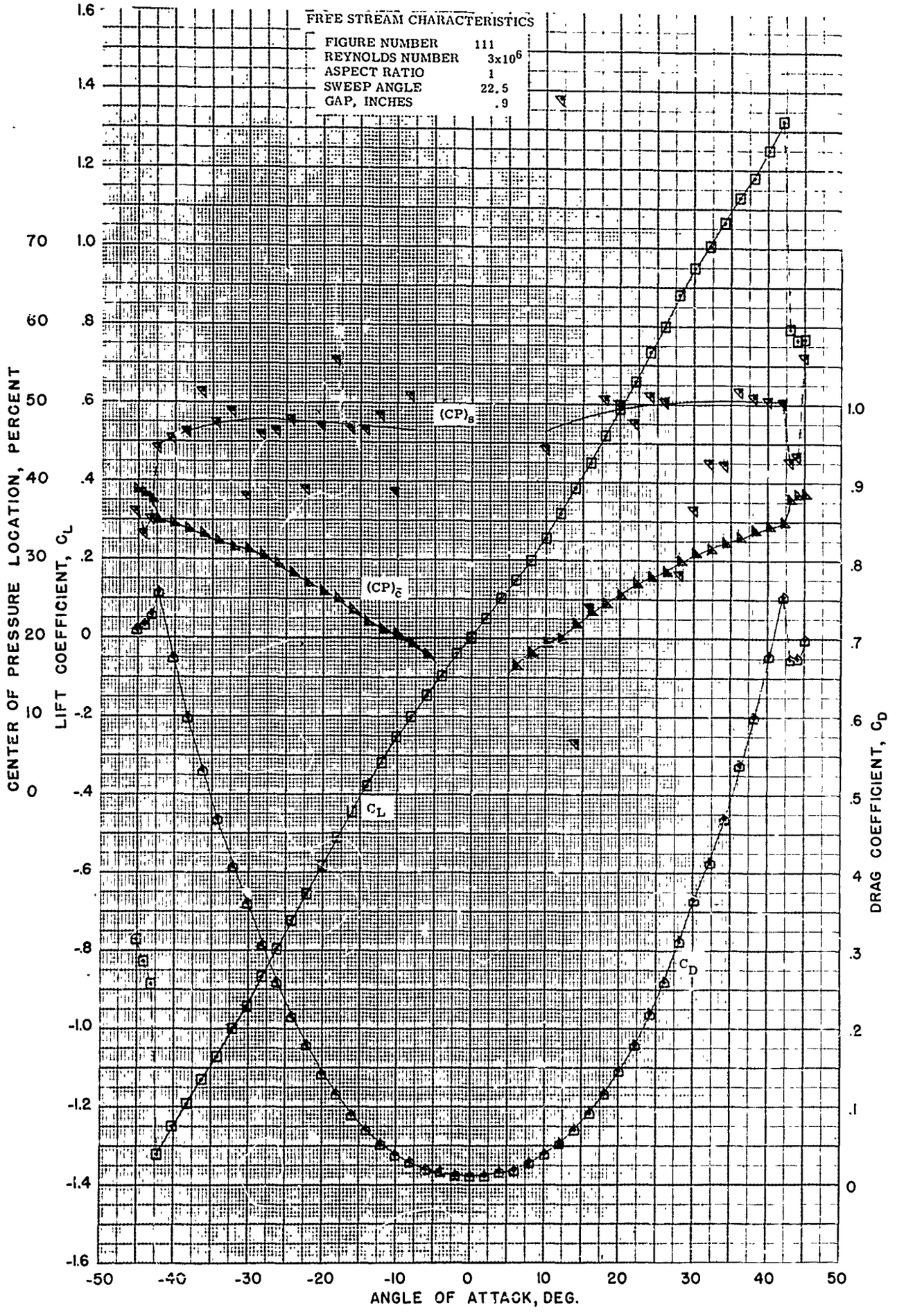
FREE STREAM CHARACTERISTICS
FIGURE NUMBER 111
REYNOLDS NUMBER 3x10^6
ASPECT RATIO 1
SWEEP ANGLE 22.5
GAP, INCHES .9
(CP)s
(CP)c̄
CL
CD
CENTER OF PRESSURE LOCATION, PERCENT
LIFT COEFFICIENT, CL
DRAG COEFFICIENT, CD
ANGLE OF ATTACK, DEG.
70
60
50
40
30
20
10
0
1.6
1.4
1.2
1.0
.8
.6
.4
.2
0
-.2
-.4
-.6
-.8
-1.0
-1.2
-1.4
-1.6
1.0
.9
.8
.7
.6
.5
.4
.3
.2
.1
0
-50
-40
-30
-20
-10
0
10
20
30
40
50

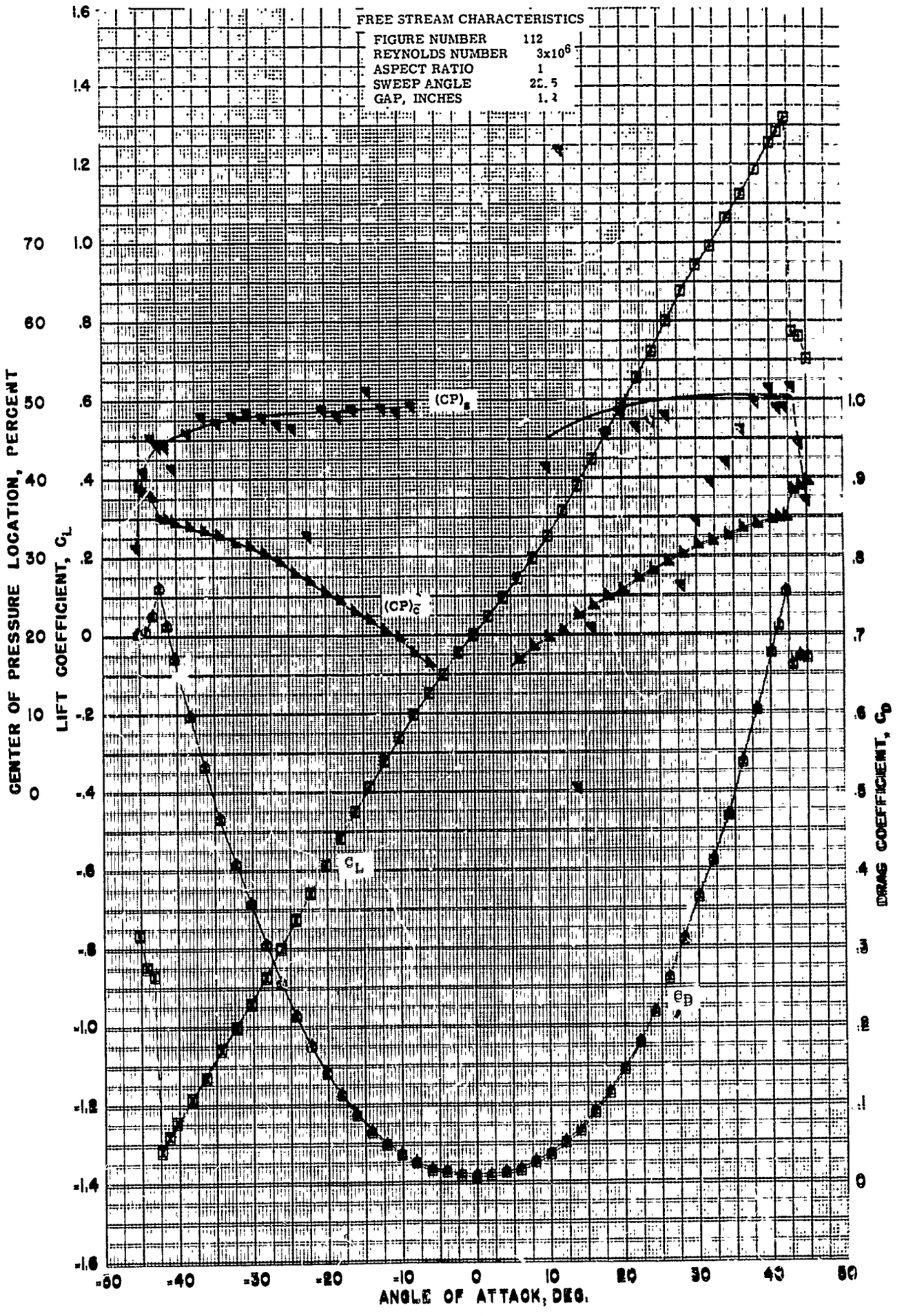
FREE STREAM CHARACTERISTICS
FIGURE NUMBER 112
REYNOLDS NUMBER 3x10^6
ASPECT RATIO 1
SWEEP ANGLE 22.5
GAP, INCHES 1.2
CENTER OF PRESSURE LOCATION, PERCENT
LIFT COEFFICIENT, C_L
DRAG COEFFICIENT, C_D
ANGLE OF ATTACK, DEG.
$(CP)_s$
$(CP)_{\bar{c}}$
C_L
θ_B
70
60
50
40
30
20
10
0
1.6
1.4
1.2
1.0
.8
.6
.4
.2
0
-.2
-.4
-.6
-.8
-1.0
-1.2
-1.4
-1.6
1.0
.9
.8
.7
.6
.5
.4
.3
.2
.1
0
-50
-40
-30
-20
-10
0
10
20
30
40
50

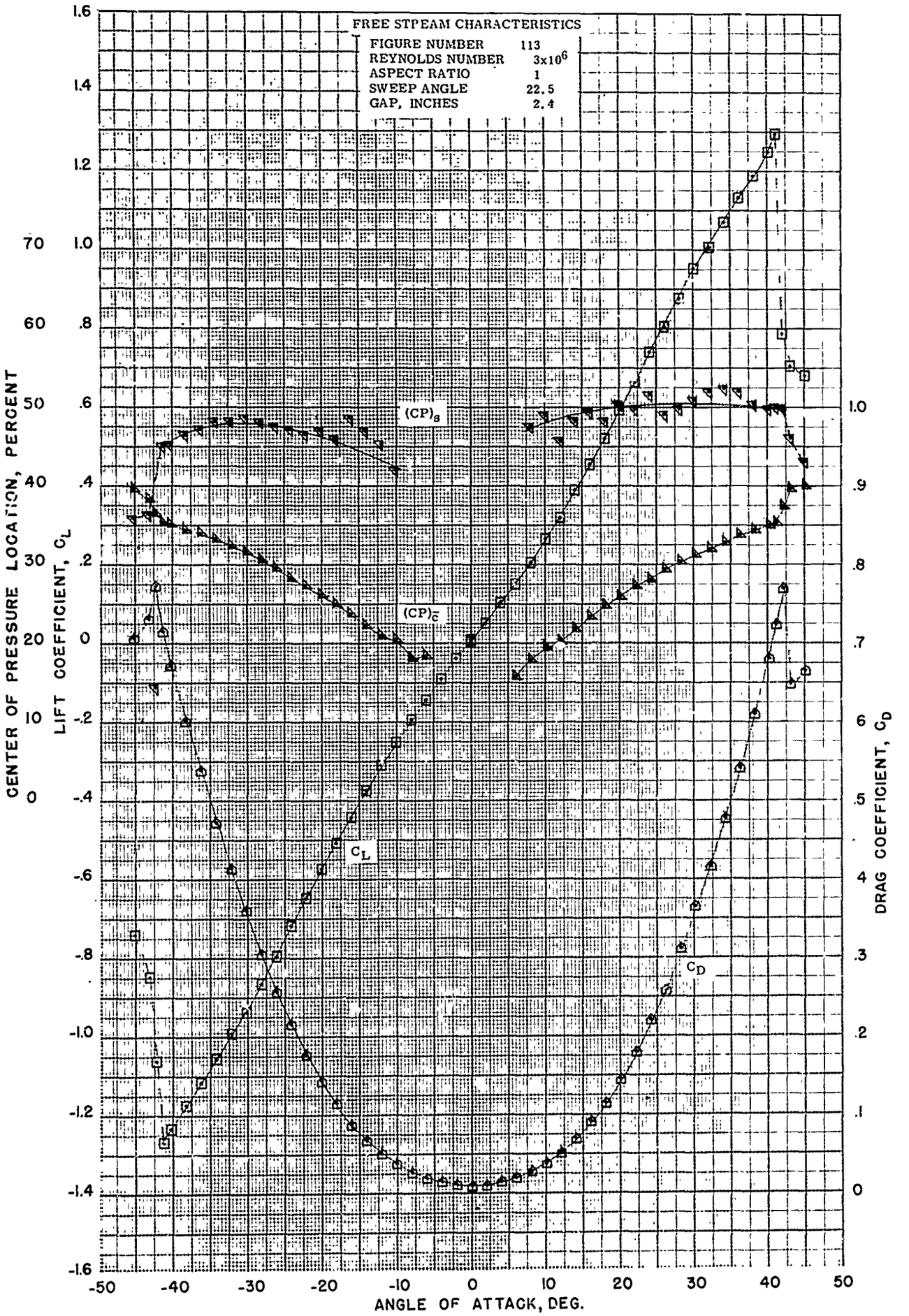
FREE STREAM CHARACTERISTICS
FIGURE NUMBER 113
REYNOLDS NUMBER 3x10^6
ASPECT RATIO 1
SWEEP ANGLE 22.5
GAP, INCHES 2.4
(CP)s
(CP)c
CL
CD
CENTER OF PRESSURE LOCATION, PERCENT
LIFT COEFFICIENT, CL
DRAG COEFFICIENT, CD
ANGLE OF ATTACK, DEG.
70
60
50
40
30
20
10
0
1.6
1.4
1.2
1.0
.8
.6
.4
.2
0
-.2
-.4
-.6
-.8
-1.0
-1.2
-1.4
-1.6
1.0
.9
.8
.7
.6
.5
.4
.3
.2
.1
0
-50
-40
-30
-20
-10
0
10
20
30
40
50

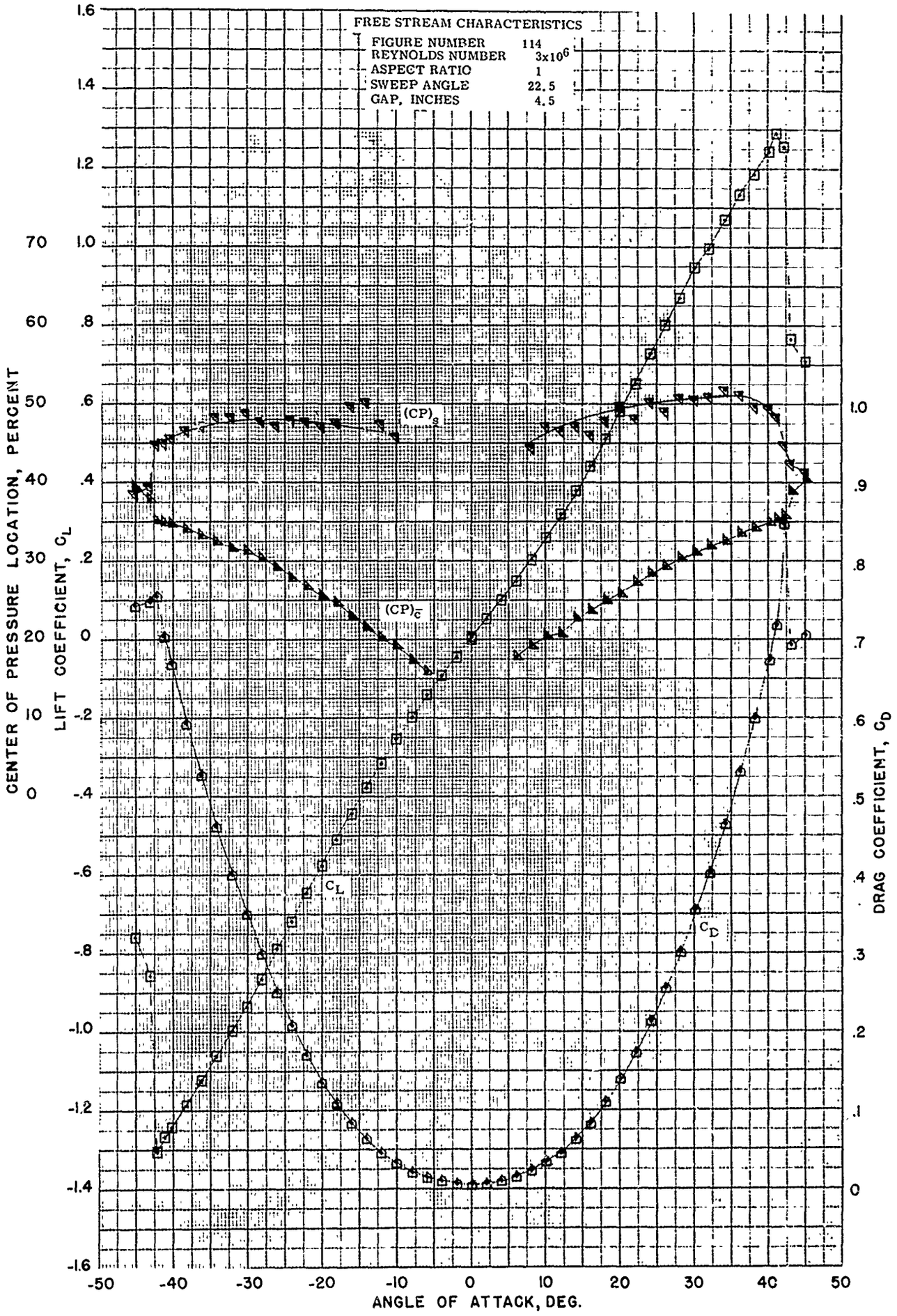
FREE STREAM CHARACTERISTICS
FIGURE NUMBER 114
REYNOLDS NUMBER 3x10^6
ASPECT RATIO 1
SWEEP ANGLE 22.5
GAP, INCHES 4.5
(CP)_s
(CP)_c
C_L
C_D
CENTER OF PRESSURE LOCATION, PERCENT
LIFT COEFFICIENT, C_L
DRAG COEFFICIENT, C_D
ANGLE OF ATTACK, DEG.
70
60
50
40
30
20
10
0
1.6
1.4
1.2
1.0
.8
.6
.4
.2
0
-.2
-.4
-.6
-.8
-1.0
-1.2
-1.4
-1.6
1.0
.9
.8
.7
.6
.5
.4
.3
.2
.1
0
-50
-40
-30
-20
-10
0
10
20
30
40
50

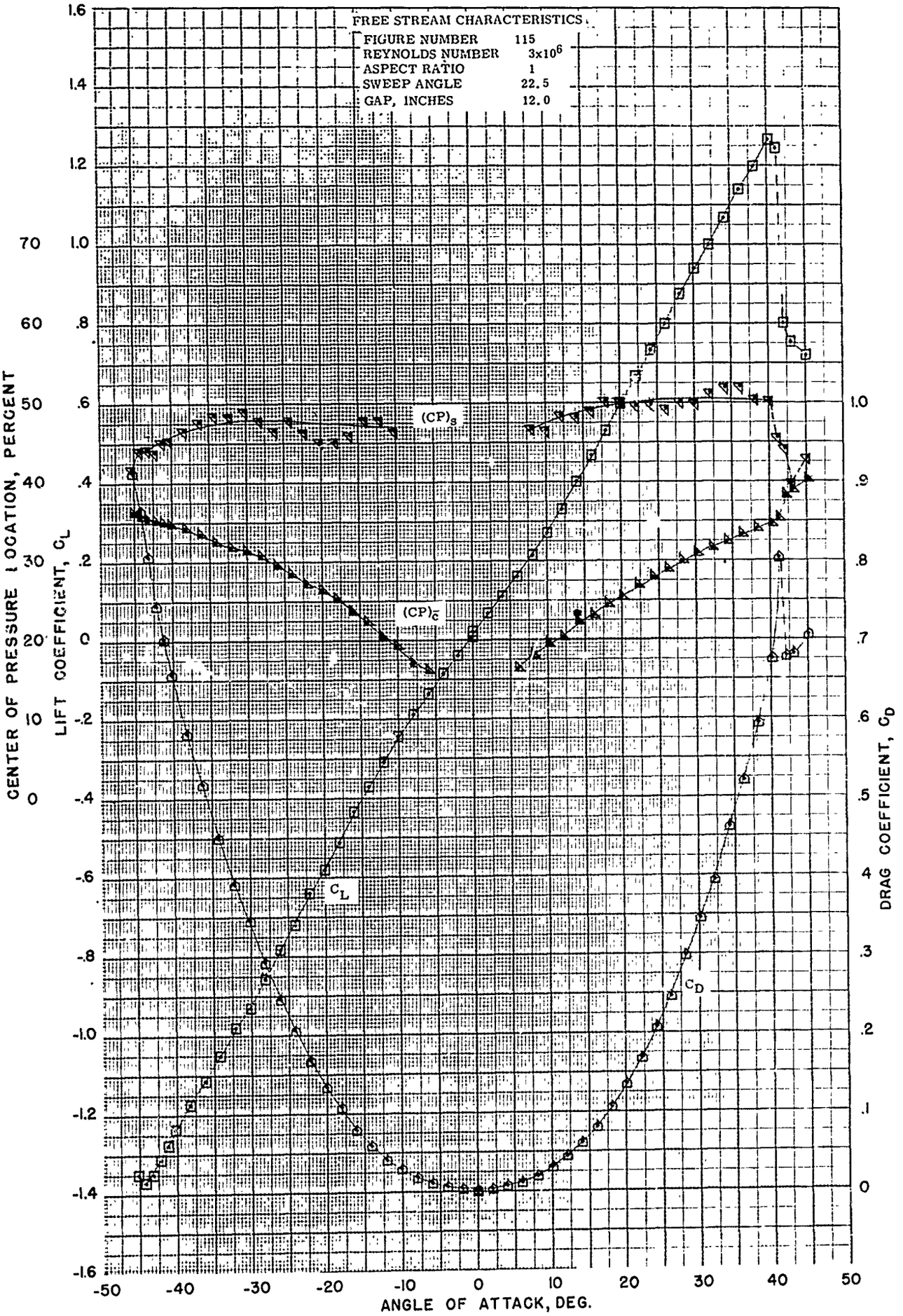
FREE STREAM CHARACTERISTICS
FIGURE NUMBER 115
REYNOLDS NUMBER 3x10^6
ASPECT RATIO 1
SWEEP ANGLE 22.5
GAP, INCHES 12.0
CENTER OF PRESSURE LOCATION, PERCENT
LIFT COEFFICIENT, C_L
DRAG COEFFICIENT, C_D
ANGLE OF ATTACK, DEG.
$(CP)_s$
$(CP)_{\bar{c}}$
C_L
C_D
70
60
50
40
30
20
10
0
1.6
1.4
1.2
1.0
.8
.6
.4
.2
0
-.2
-.4
-.6
-.8
-1.0
-1.2
-1.4
-1.6
1.0
.9
.8
.7
.6
.5
.4
.3
.2
.1
0
-50
-40
-30
-20
-10
0
10
20
30
40
50

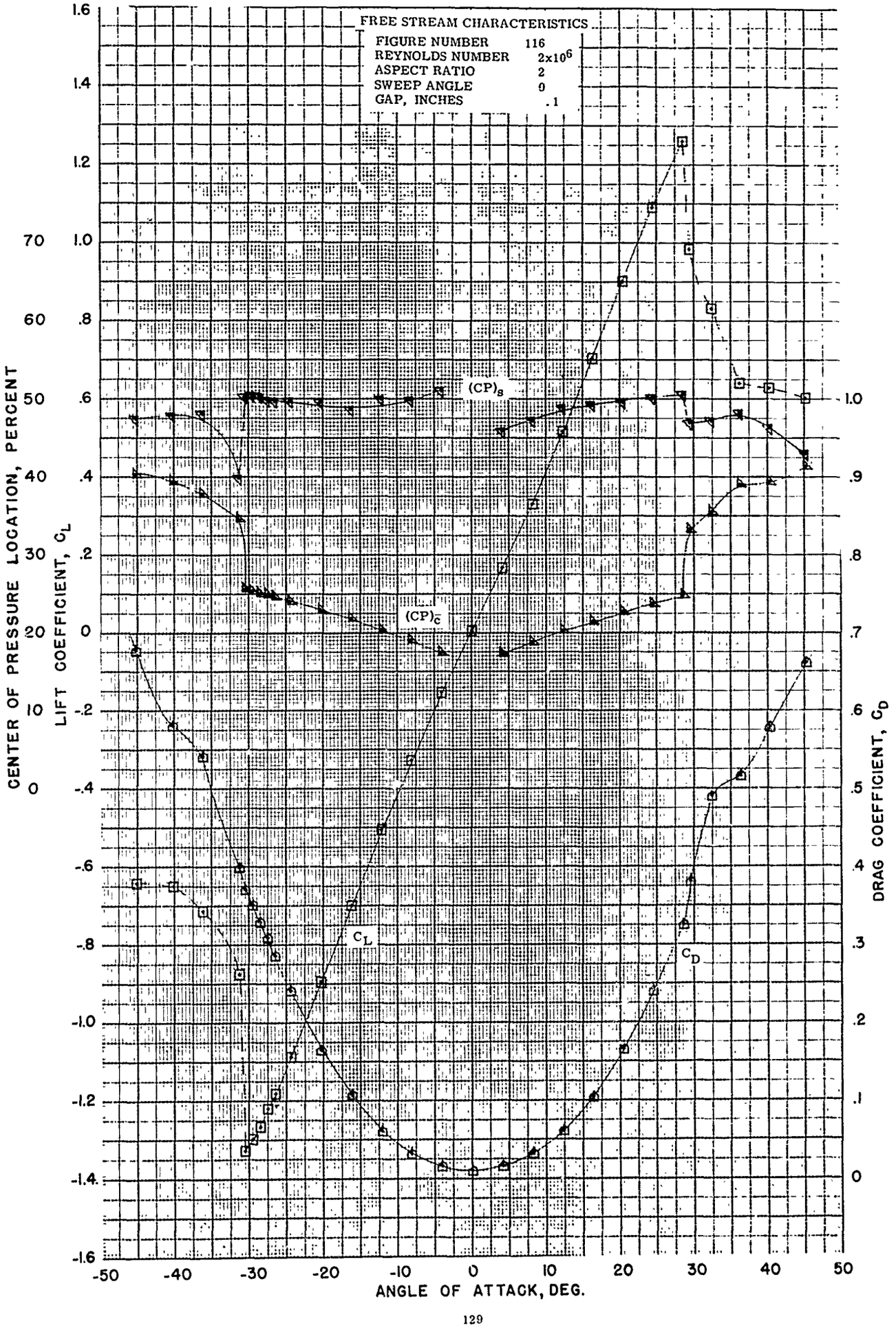
FREE STREAM CHARACTERISTICS
FIGURE NUMBER 116
REYNOLDS NUMBER 2x10^6
ASPECT RATIO 2
SWEEP ANGLE 0
GAP, INCHES .1
CENTER OF PRESSURE LOCATION, PERCENT
LIFT COEFFICIENT, C_L
DRAG COEFFICIENT, C_D
ANGLE OF ATTACK, DEG.
$(CP)_s$
$(CP)_{\bar{c}}$
C_L
C_D
70
60
50
40
30
20
10
0
1.6
1.4
1.2
1.0
.8
.6
.4
.2
0
-.2
-.4
-.6
-.8
-1.0
-1.2
-1.4
-1.6
1.0
.9
.8
.7
.6
.5
.4
.3
.2
.1
0
-50
-40
-30
-20
-10
0
10
20
30
40
50

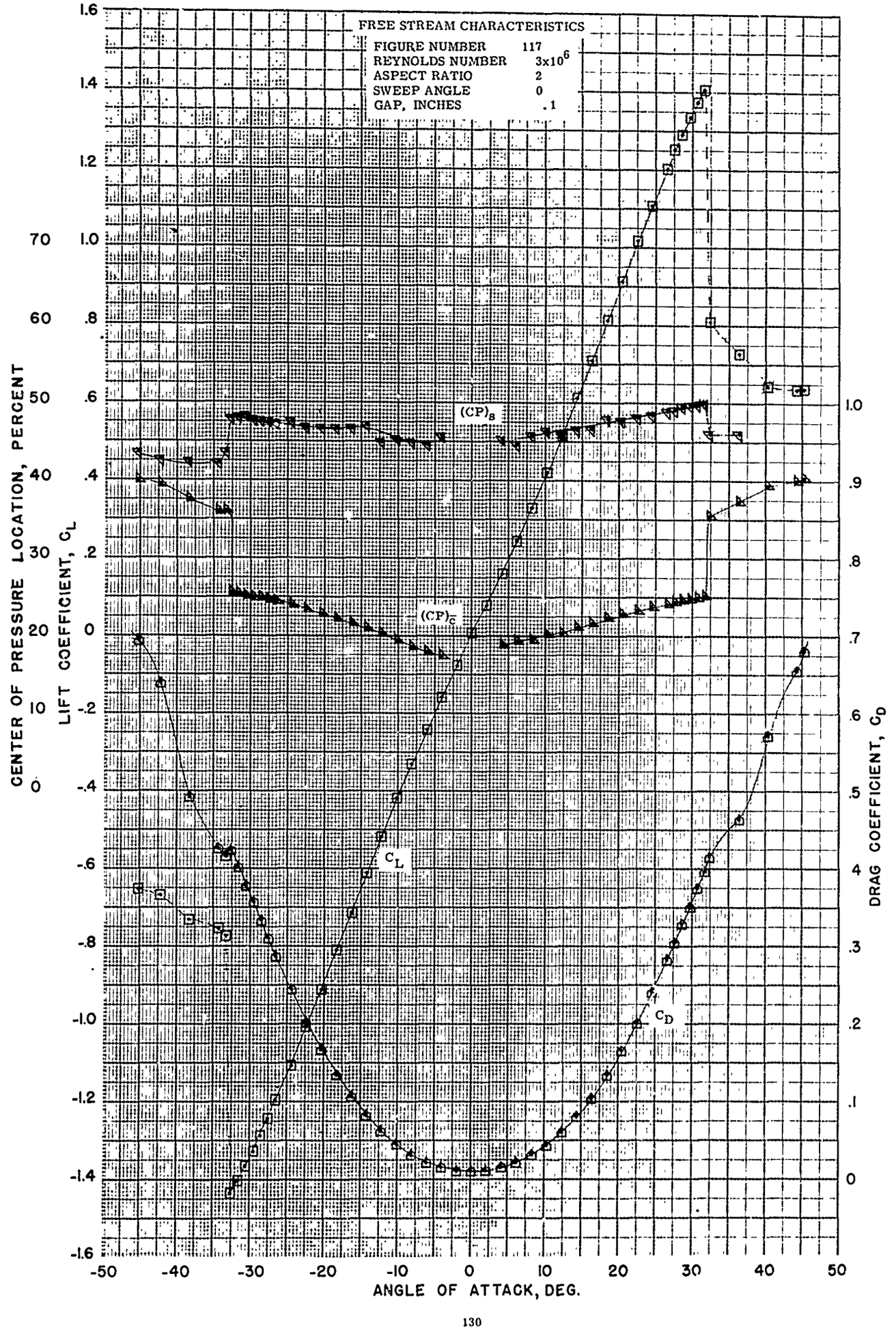
FREE STREAM CHARACTERISTICS
FIGURE NUMBER 117
REYNOLDS NUMBER 3x10^6
ASPECT RATIO 2
SWEEP ANGLE 0
GAP, INCHES .1
(CP)_S
(CP)_C
C_L
C_D
CENTER OF PRESSURE LOCATION, PERCENT
LIFT COEFFICIENT, C_L
DRAG COEFFICIENT, C_D
ANGLE OF ATTACK, DEG.
70
60
50
40
30
20
10
0
1.6
1.4
1.2
1.0
.8
.6
.4
.2
0
-.2
-.4
-.6
-.8
-1.0
-1.2
-1.4
-1.6
1.0
.9
.8
.7
.6
.5
.4
.3
.2
.1
0
-50
-40
-30
-20
-10
0
10
20
30
40
50

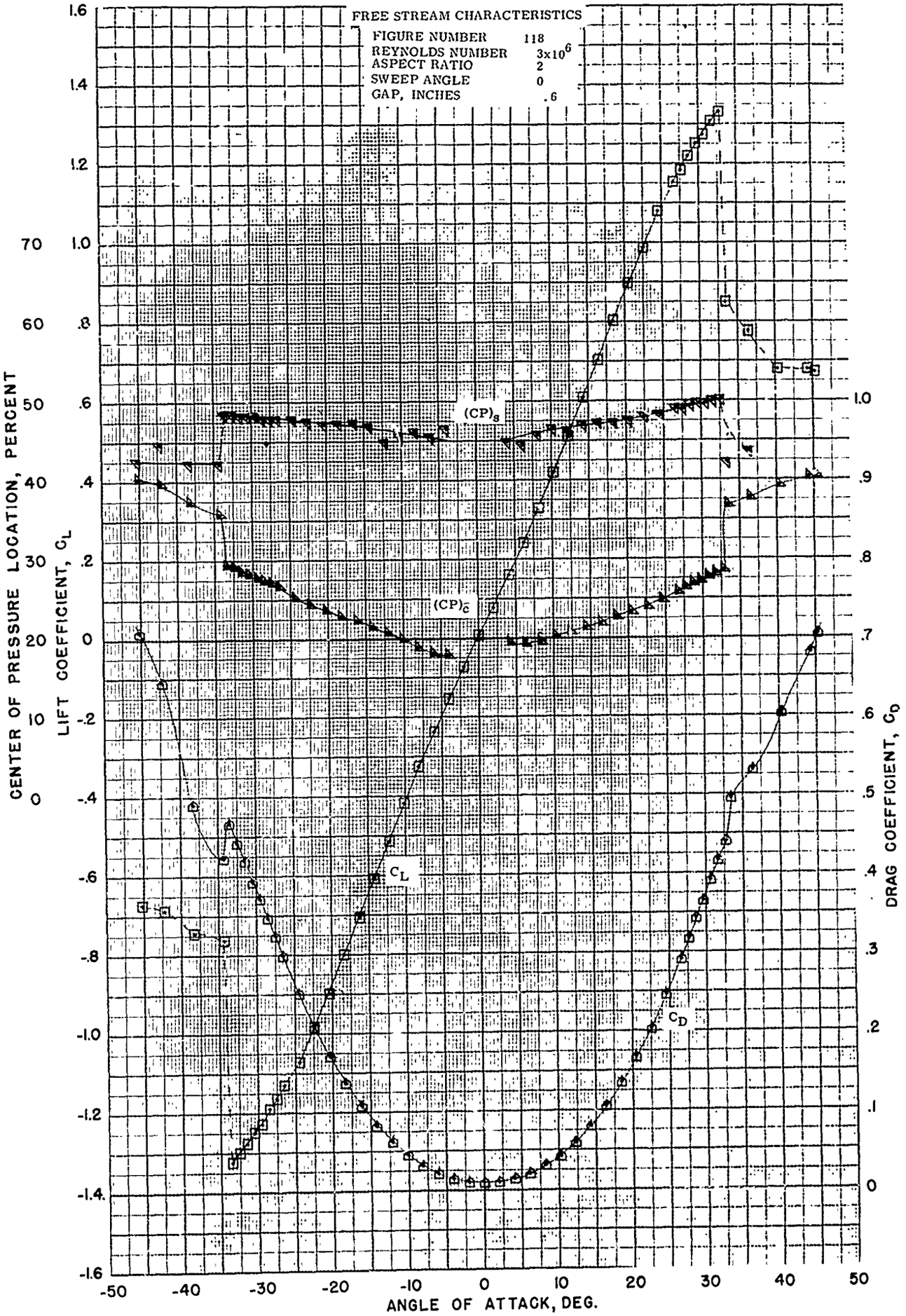
FREE STREAM CHARACTERISTICS
FIGURE NUMBER 118
REYNOLDS NUMBER 3x10^6
ASPECT RATIO 2
SWEEP ANGLE 0
GAP, INCHES .6
CENTER OF PRESSURE LOCATION, PERCENT
LIFT COEFFICIENT, C_L
DRAG COEFFICIENT, C_D
ANGLE OF ATTACK, DEG.
$(CP)_s$
$(CP)_c$
C_L
C_D
70
60
50
40
30
20
10
0
1.6
1.4
1.2
1.0
.8
.6
.4
.2
0
-.2
-.4
-.6
-.8
-1.0
-1.2
-1.4
-1.6
1.0
.9
.8
.7
.6
.5
.4
.3
.2
.1
0
-50
-40
-30
-20
-10
0
10
20
30
40
50

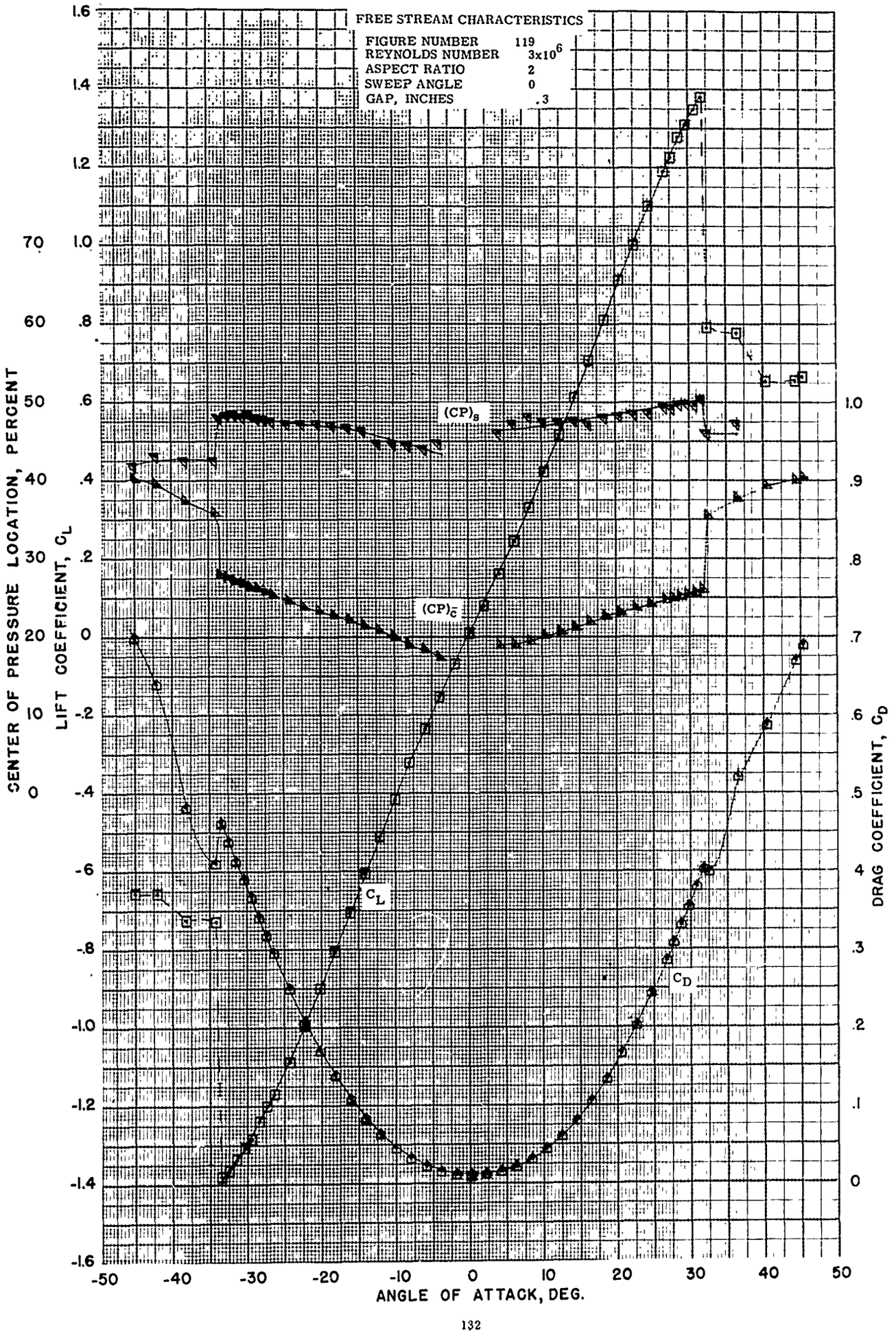
FREE STREAM CHARACTERISTICS
FIGURE NUMBER 119
REYNOLDS NUMBER 3x10^6
ASPECT RATIO 2
SWEEP ANGLE 0
GAP, INCHES .3
CENTER OF PRESSURE LOCATION, PERCENT
LIFT COEFFICIENT, C_L
DRAG COEFFICIENT, C_D
ANGLE OF ATTACK, DEG.
$(CP)_s$
$(CP)_c$
C_L
C_D
70
60
50
40
30
20
10
0
1.6
1.4
1.2
1.0
.8
.6
.4
.2
0
-.2
-.4
-.6
-.8
-1.0
-1.2
-1.4
-1.6
1.0
.9
.8
.7
.6
.5
.4
.3
.2
.1
0
-50
-40
-30
-20
-10
0
10
20
30
40
50

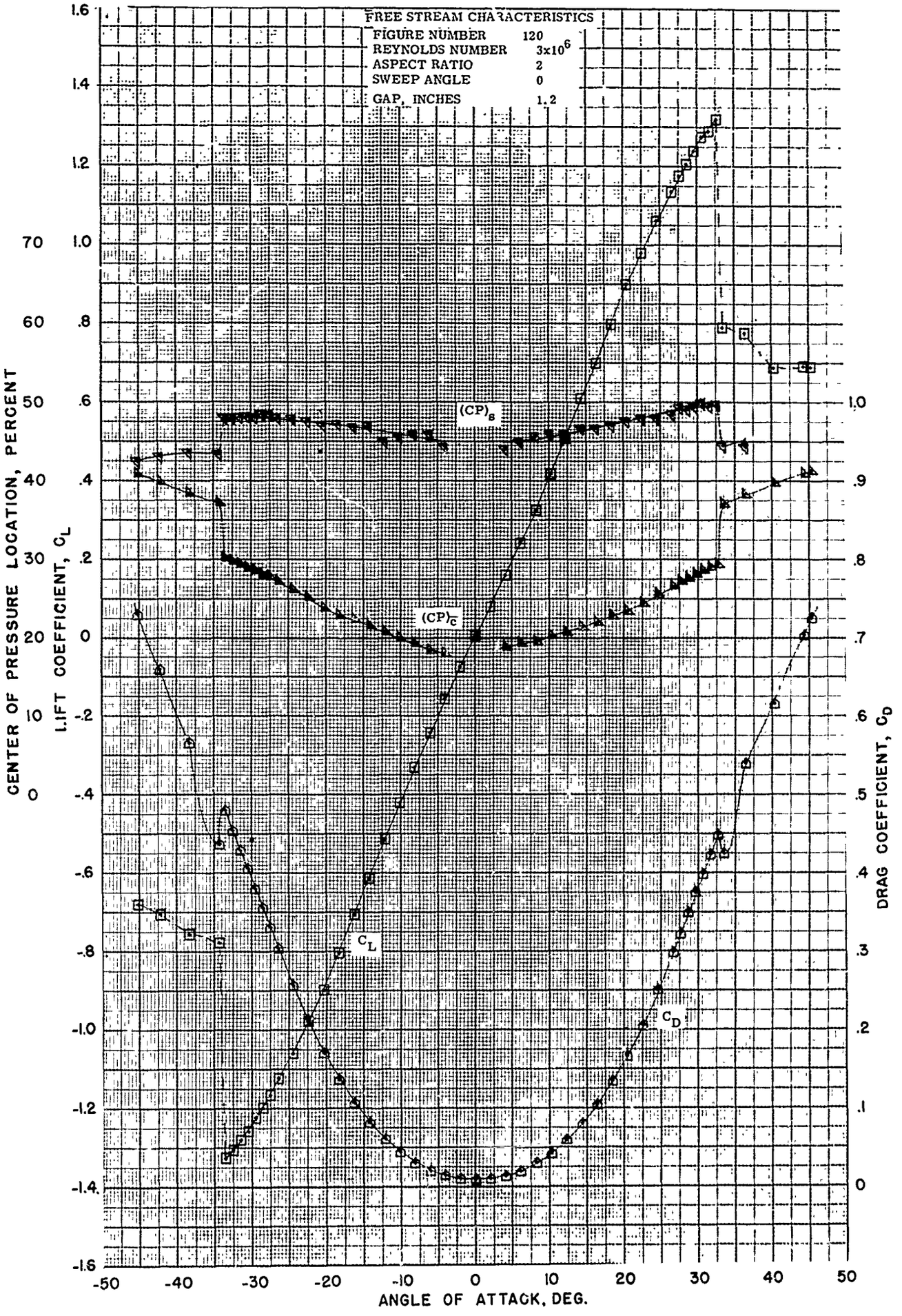
FREE STREAM CHARACTERISTICS
FIGURE NUMBER 120
REYNOLDS NUMBER 3x10^6
ASPECT RATIO 2
SWEEP ANGLE 0
GAP, INCHES 1.2
(CP)s
(CP)c
CL
CD
CENTER OF PRESSURE LOCATION, PERCENT
LIFT COEFFICIENT, CL
DRAG COEFFICIENT, CD
ANGLE OF ATTACK, DEG.
70
60
50
40
30
20
10
0
1.6
1.4
1.2
1.0
.8
.6
.4
.2
0
-.2
-.4
-.6
-.8
-1.0
-1.2
-1.4
-1.6
1.0
.9
.8
.7
.6
.5
.4
.3
.2
.1
0
-50
-40
-30
-20
-10
0
10
20
30
40
50

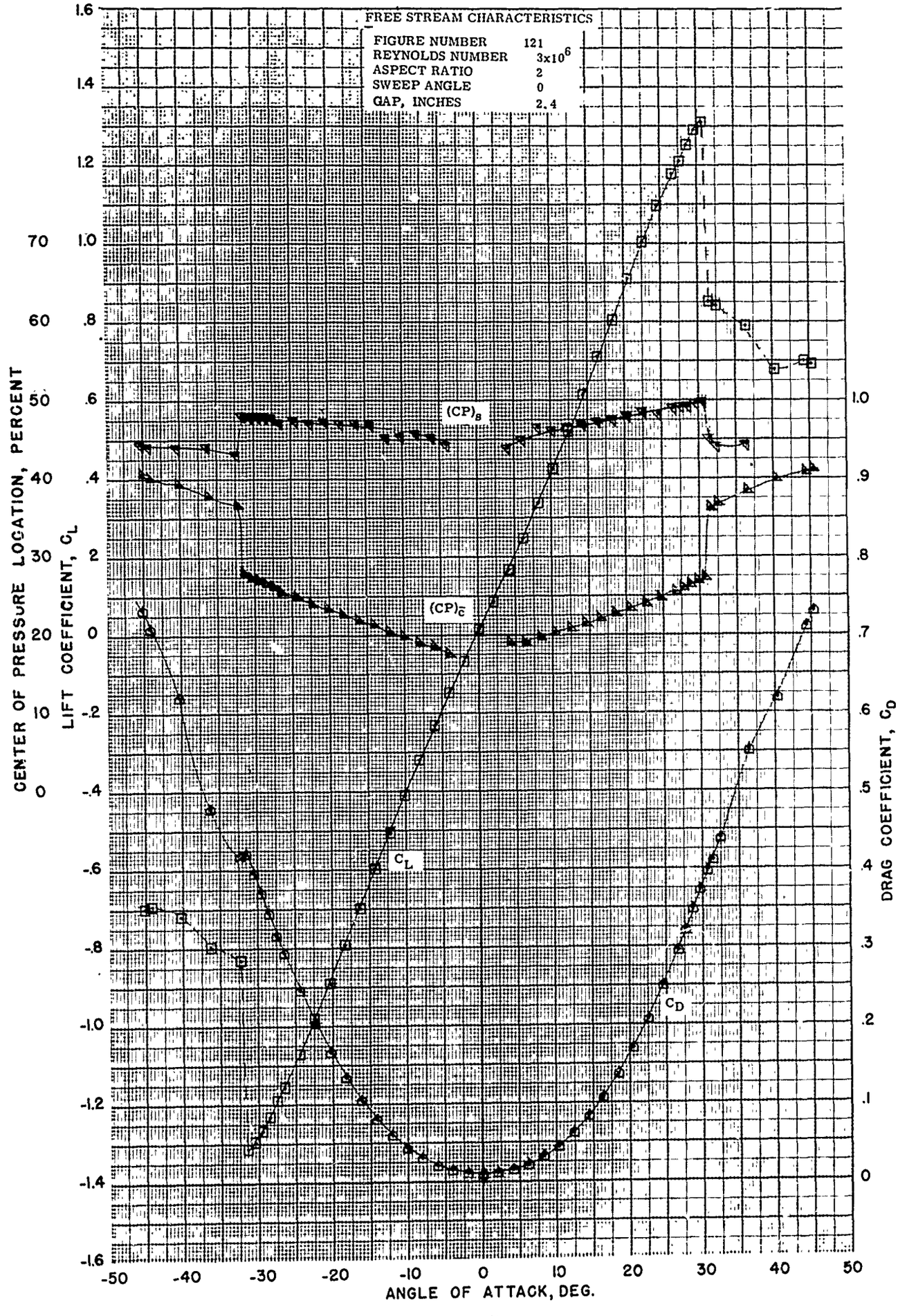
FREE STREAM CHARACTERISTICS
FIGURE NUMBER 121
REYNOLDS NUMBER 3x10^6
ASPECT RATIO 2
SWEEP ANGLE 0
GAP, INCHES 2.4
(CP)s
(CP)c
CL
CD
CENTER OF PRESSURE LOCATION, PERCENT
LIFT COEFFICIENT, CL
DRAG COEFFICIENT, CD
ANGLE OF ATTACK, DEG.
70
60
50
40
30
20
10
0
1.6
1.4
1.2
1.0
.8
.6
.4
2
0
-.2
-.4
-.6
-.8
-1.0
-1.2
-1.4
-1.6
1.0
.9
.8
.7
.6
.5
.4
.3
.2
.1
0
-50
-40
-30
-20
-10
0
10
20
30
40
50

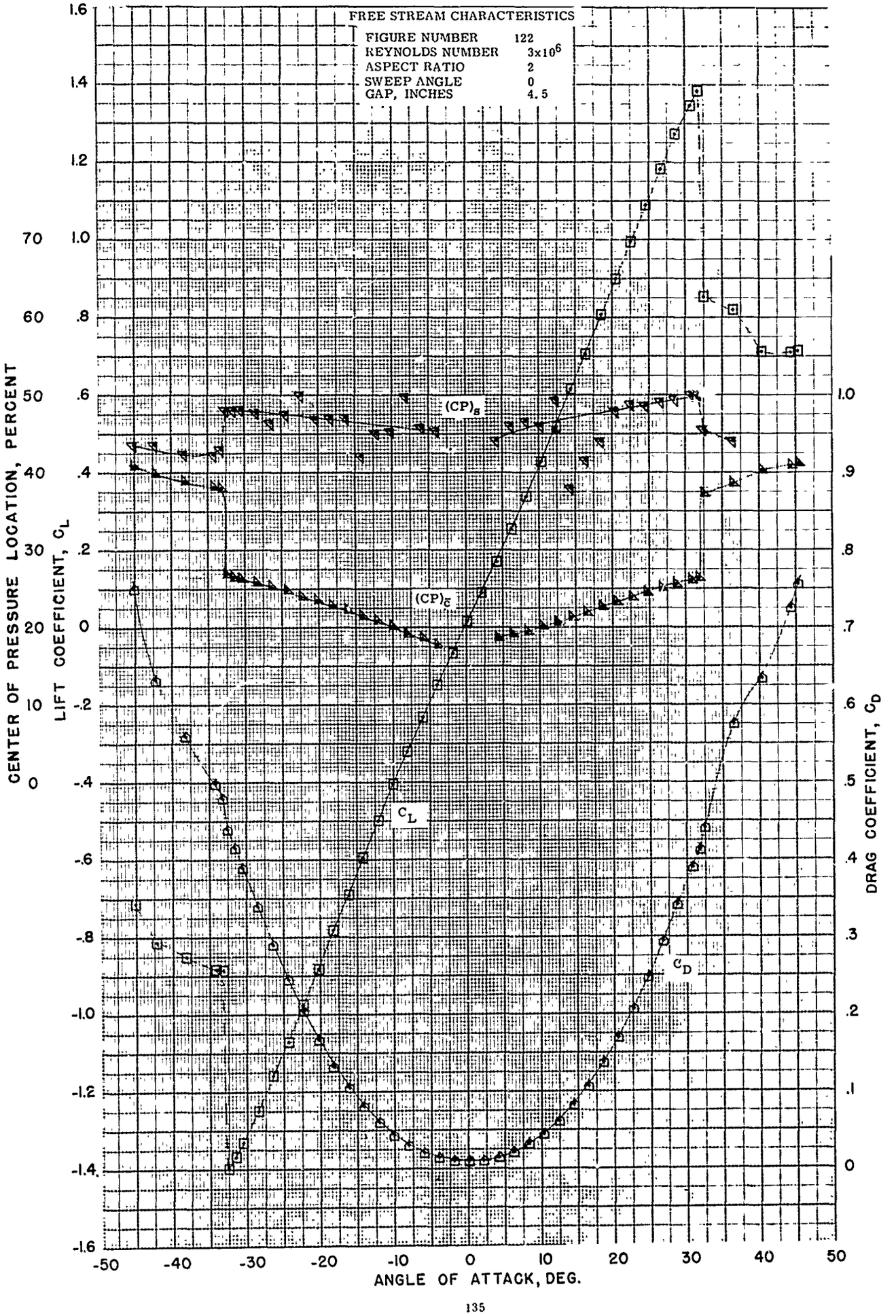
FREE STREAM CHARACTERISTICS
FIGURE NUMBER 122
REYNOLDS NUMBER 3x10^6
ASPECT RATIO 2
SWEEP ANGLE 0
GAP, INCHES 4.5
CENTER OF PRESSURE LOCATION, PERCENT
LIFT COEFFICIENT, C_L
DRAG COEFFICIENT, C_D
ANGLE OF ATTACK, DEG.
$(CP)_s$
$(CP)_{\bar{c}}$
C_L
C_D
70
60
50
40
30
20
10
0
1.6
1.4
1.2
1.0
.8
.6
.4
.2
0
-.2
-.4
-.6
-.8
-1.0
-1.2
-1.4
-1.6
1.0
.9
.8
.7
.6
.5
.4
.3
.2
.1
0
-50
-40
-30
-20
-10
0
10
20
30
40
50

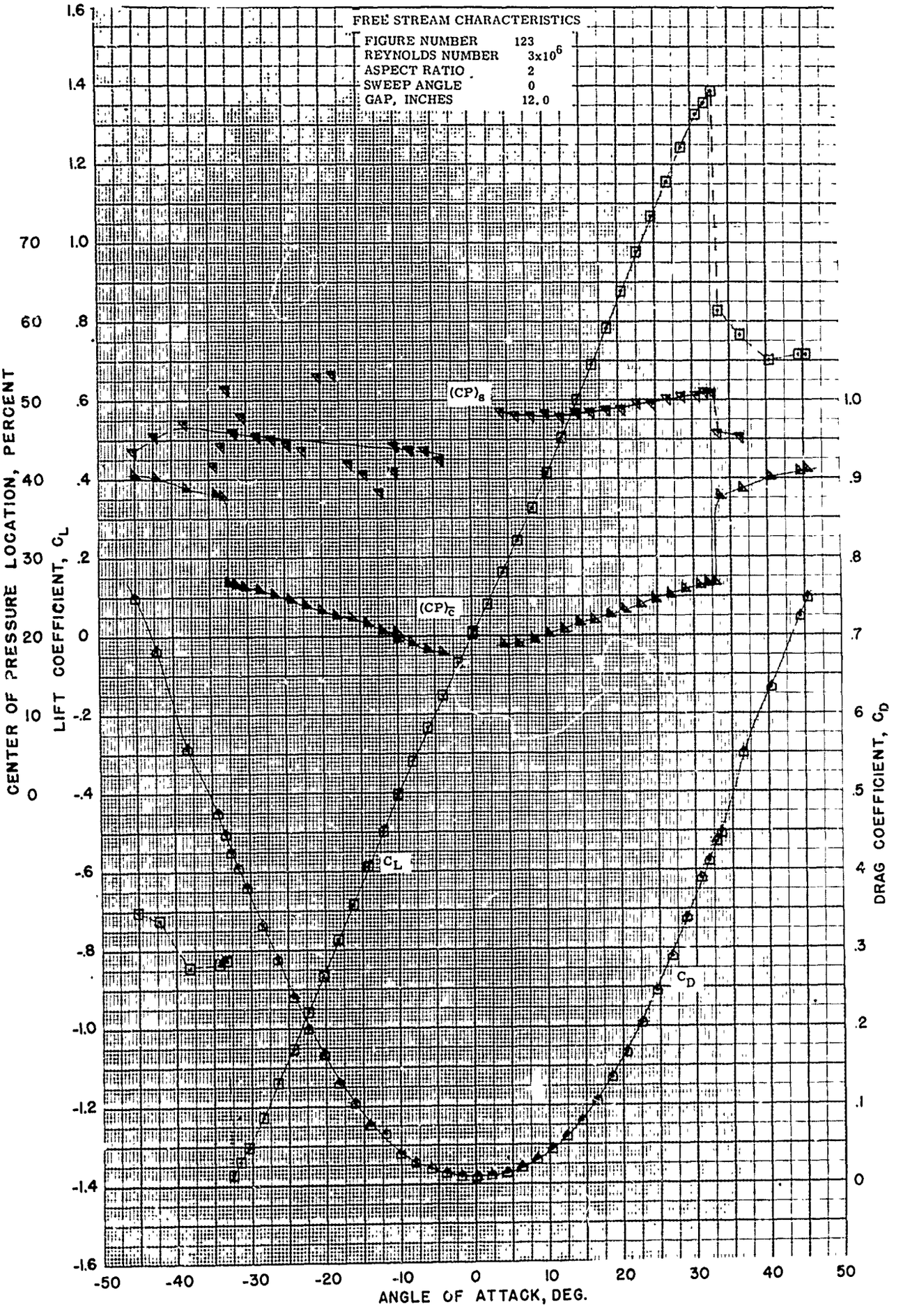
FREE STREAM CHARACTERISTICS
FIGURE NUMBER 123
REYNOLDS NUMBER 3x10^6
ASPECT RATIO 2
SWEEP ANGLE 0
GAP, INCHES 12.0
(CP)s
(CP)c
CL
CD
CENTER OF PRESSURE LOCATION, PERCENT
LIFT COEFFICIENT, CL
DRAG COEFFICIENT, CD
ANGLE OF ATTACK, DEG.
70
60
50
40
30
20
10
0
1.6
1.4
1.2
1.0
.8
.6
.4
.2
0
-.2
-.4
-.6
-.8
-1.0
-1.2
-1.4
-1.6
1.0
.9
.8
.7
.6
.5
.4
.3
.2
.1
0
-50
-40
-30
-20
-10
0
10
20
30
40
50

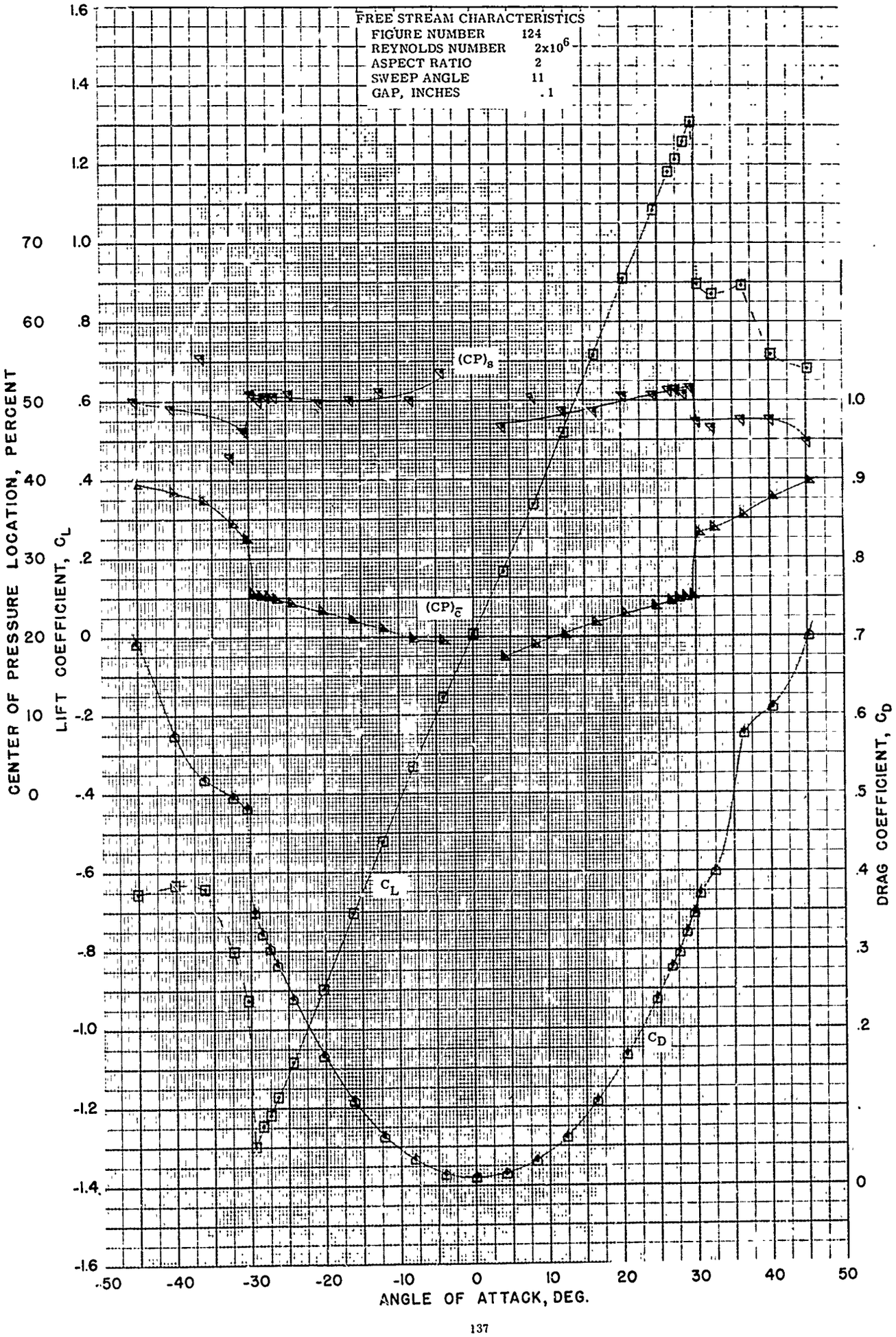
FREE STREAM CHARACTERISTICS
FIGURE NUMBER 124
REYNOLDS NUMBER 2x10^6
ASPECT RATIO 2
SWEEP ANGLE 11
GAP, INCHES .1
(CP)s
(CP)c̄
CL
CD
CENTER OF PRESSURE LOCATION, PERCENT
LIFT COEFFICIENT, CL
DRAG COEFFICIENT, CD
ANGLE OF ATTACK, DEG.
70
60
50
40
30
20
10
0
1.6
1.4
1.2
1.0
.8
.6
.4
.2
0
-.2
-.4
-.6
-.8
-1.0
-1.2
-1.4
-1.6
1.0
.9
.8
.7
.6
.5
.4
.3
.2
0
-50
-40
-30
-20
-10
0
10
20
30
40
50

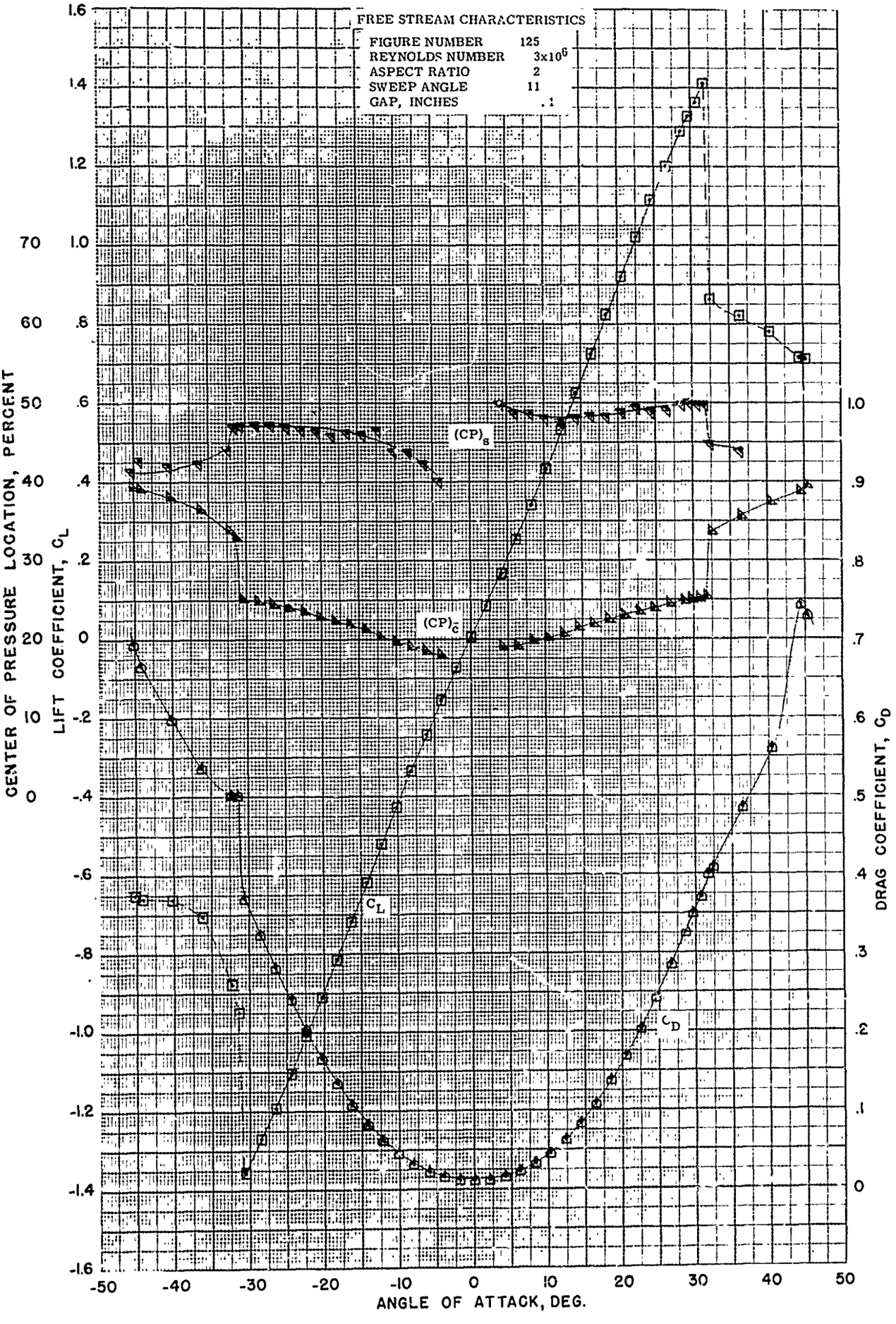
FREE STREAM CHARACTERISTICS
FIGURE NUMBER 125
REYNOLDS NUMBER 3x10^6
ASPECT RATIO 2
SWEEP ANGLE 11
GAP, INCHES .1
CENTER OF PRESSURE LOCATION, PERCENT
LIFT COEFFICIENT, C_L
DRAG COEFFICIENT, C_D
ANGLE OF ATTACK, DEG.
$(CP)_s$
$(CP)_c$
C_L
C_D
70
60
50
40
30
20
10
0
1.6
1.4
1.2
1.0
.8
.6
.4
.2
0
-.2
-.4
-.6
-.8
-1.0
-1.2
-1.4
-1.6
1.0
.9
.8
.7
.6
.5
.4
.3
.2
.1
0
-50
-40
-30
-20
-10
0
10
20
30
40
50

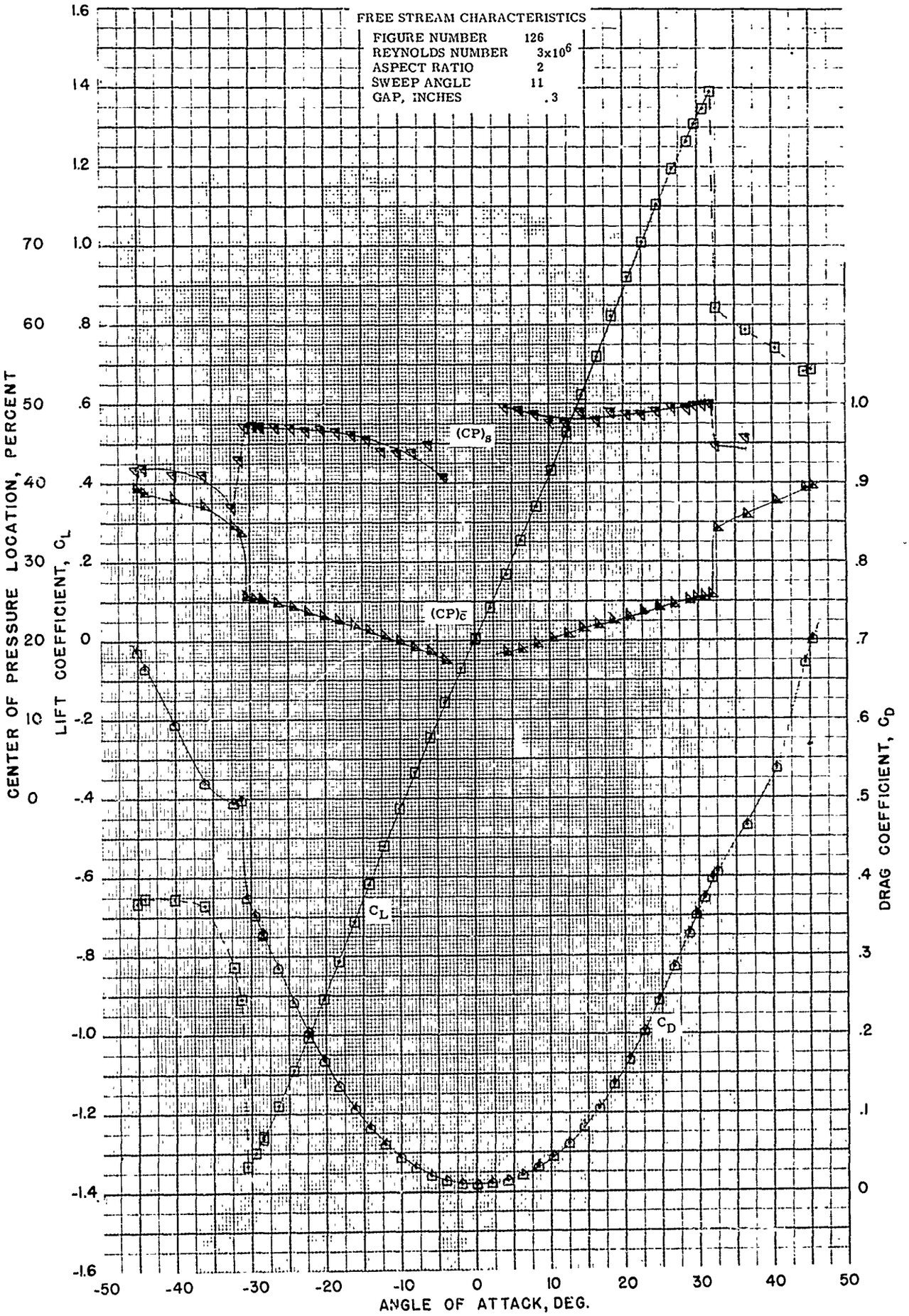
FREE STREAM CHARACTERISTICS
FIGURE NUMBER 126
REYNOLDS NUMBER 3x10^6
ASPECT RATIO 2
SWEEP ANGLE 11
GAP, INCHES .3
CENTER OF PRESSURE LOCATION, PERCENT
LIFT COEFFICIENT, C_L
DRAG COEFFICIENT, C_D
ANGLE OF ATTACK, DEG.
$(CP)_s$
$(CP)_{\bar{c}}$
C_L
C_D
70
60
50
40
30
20
10
0
1.6
1.4
1.2
1.0
.8
.6
.4
.2
0
-.2
-.4
-.6
-.8
-1.0
-1.2
-1.4
-1.6
1.0
.9
.8
.7
.6
.5
.4
.3
.2
.1
0
-50
-40
-30
-20
-10
0
10
20
30
40
50

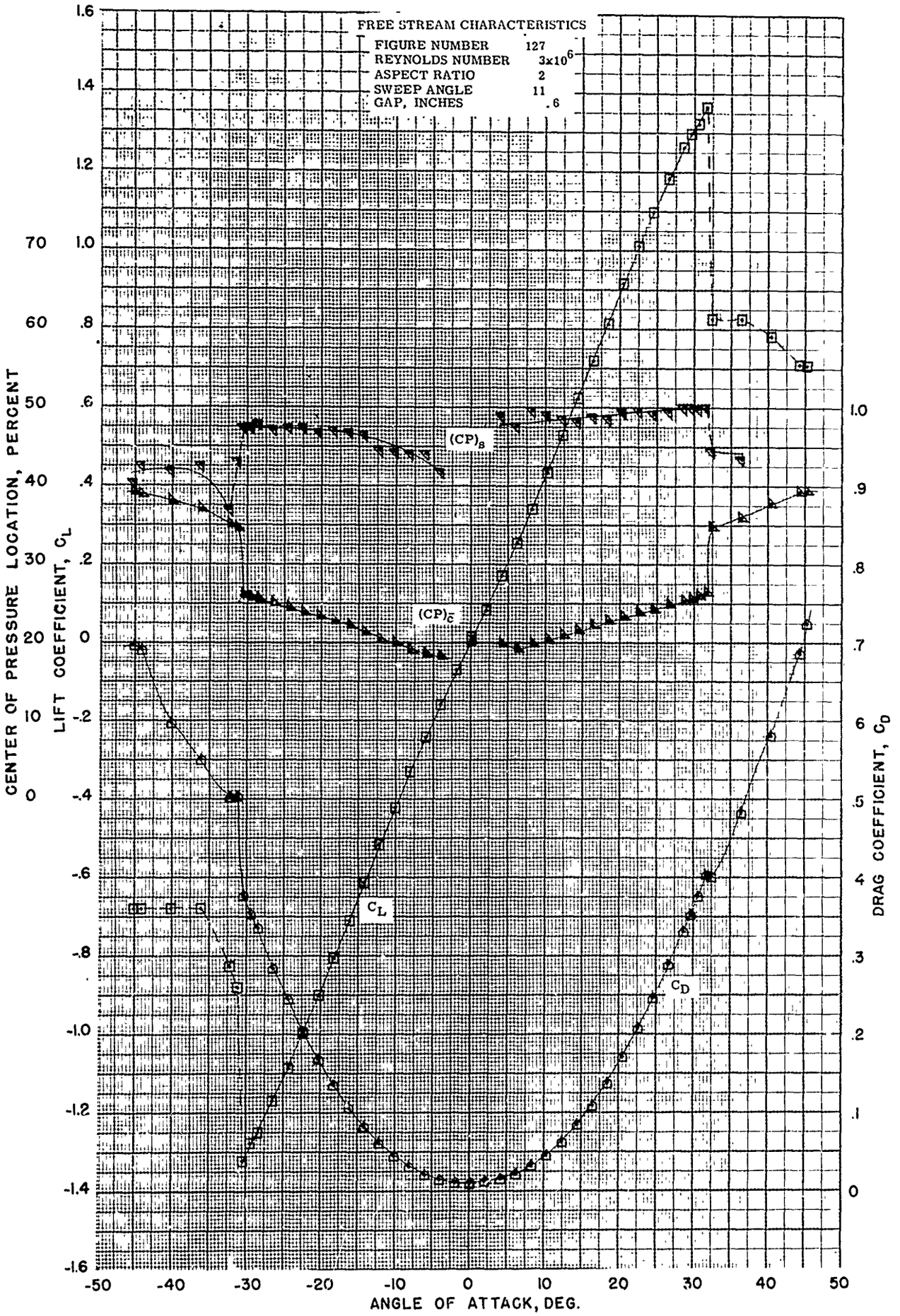
FREE STREAM CHARACTERISTICS
FIGURE NUMBER 127
REYNOLDS NUMBER 3x10^6
ASPECT RATIO 2
SWEEP ANGLE 11
GAP, INCHES .6
CENTER OF PRESSURE LOCATION, PERCENT
LIFT COEFFICIENT, C_L
DRAG COEFFICIENT, C_D
ANGLE OF ATTACK, DEG.
$(CP)_s$
$(CP)_{\bar{c}}$
C_L
C_D
70
60
50
40
30
20
10
0
1.6
1.4
1.2
1.0
.8
.6
.4
.2
0
-.2
-.4
-.6
-.8
-1.0
-1.2
-1.4
-1.6
1.0
.9
.8
.7
.6
.5
.4
.3
.2
.1
0
-50
-40
-30
-20
-10
0
10
20
30
40
50

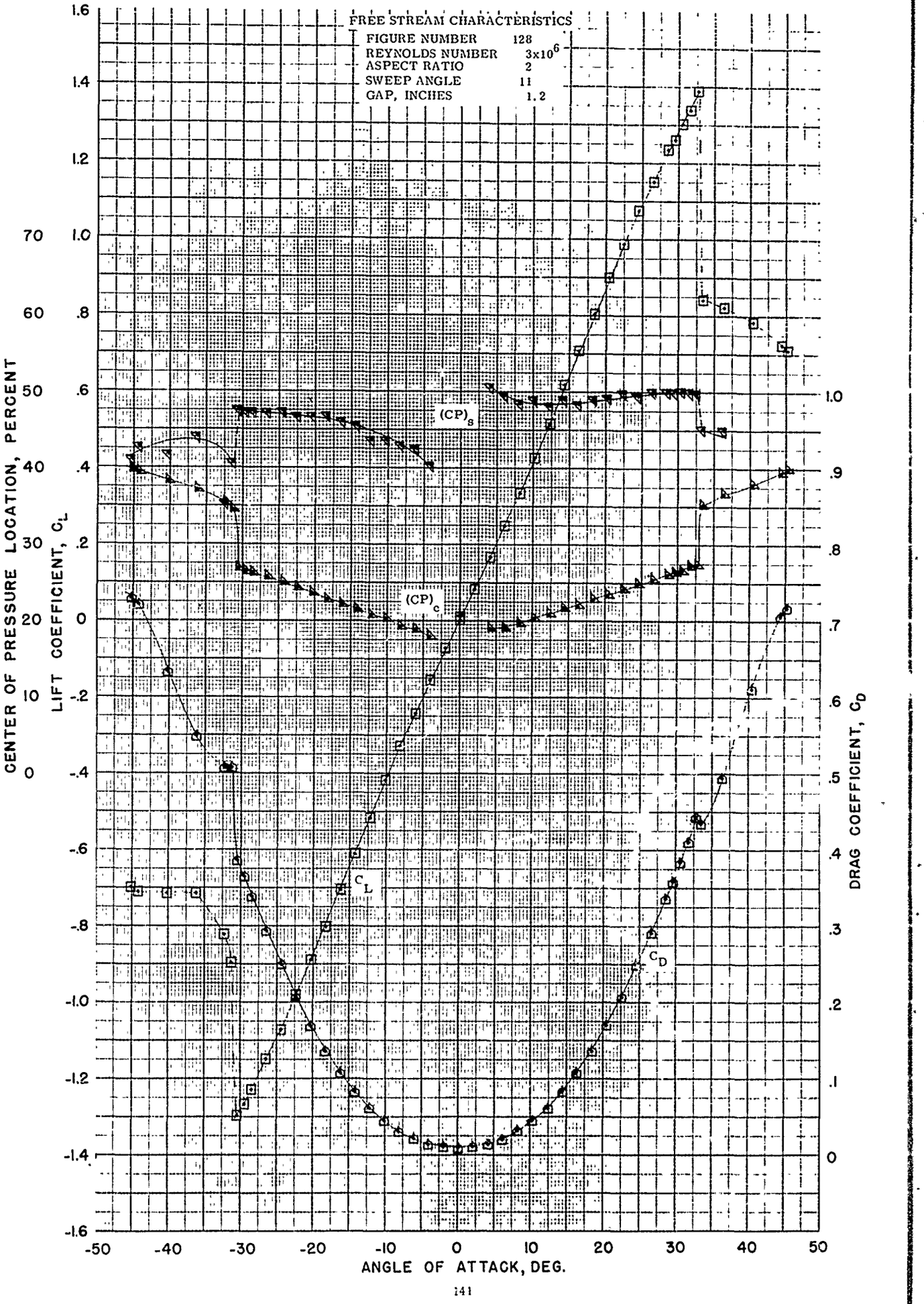
FREE STREAM CHARACTERISTICS
FIGURE NUMBER 128
REYNOLDS NUMBER 3x10^6
ASPECT RATIO 2
SWEEP ANGLE 11
GAP, INCHES 1.2
CENTER OF PRESSURE LOCATION, PERCENT
LIFT COEFFICIENT, C_L
DRAG COEFFICIENT, C_D
ANGLE OF ATTACK, DEG.
(CP)_s
(CP)_c
C_L
C_D
70
60
50
40
30
20
10
0
1.6
1.4
1.2
1.0
.8
.6
.4
.2
0
-.2
-.4
-.6
-.8
-1.0
-1.2
-1.4
-1.6
1.0
.9
.8
.7
.6
.5
.4
.3
.2
.1
0
-50
-40
-30
-20
-10
0
10
20
30
40
50

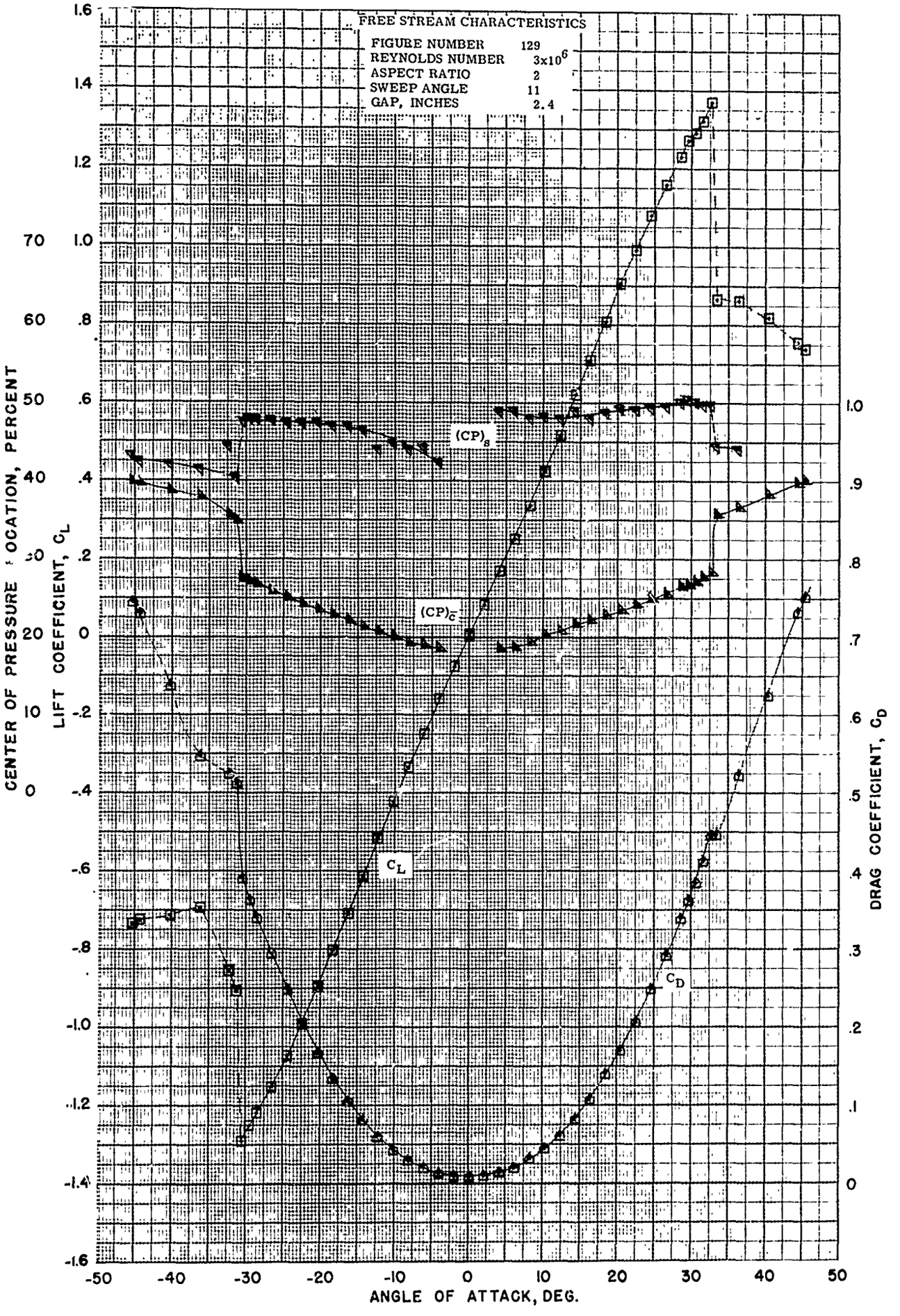
FREE STREAM CHARACTERISTICS
FIGURE NUMBER 129
REYNOLDS NUMBER 3x10^6
ASPECT RATIO 2
SWEEP ANGLE 11
GAP, INCHES 2.4
(CP)s
(CP)c̄
CL
CD
CENTER OF PRESSURE LOCATION, PERCENT
LIFT COEFFICIENT, CL
DRAG COEFFICIENT, CD
ANGLE OF ATTACK, DEG.
70
60
50
40
30
20
10
0
1.6
1.4
1.2
1.0
.8
.6
.4
.2
0
-.2
-.4
-.6
-.8
-1.0
-1.2
-1.4
-1.6
1.0
.9
.8
.7
.6
.5
.4
.3
.2
.1
0
-50
-40
-30
-20
-10
0
10
20
30
40
50

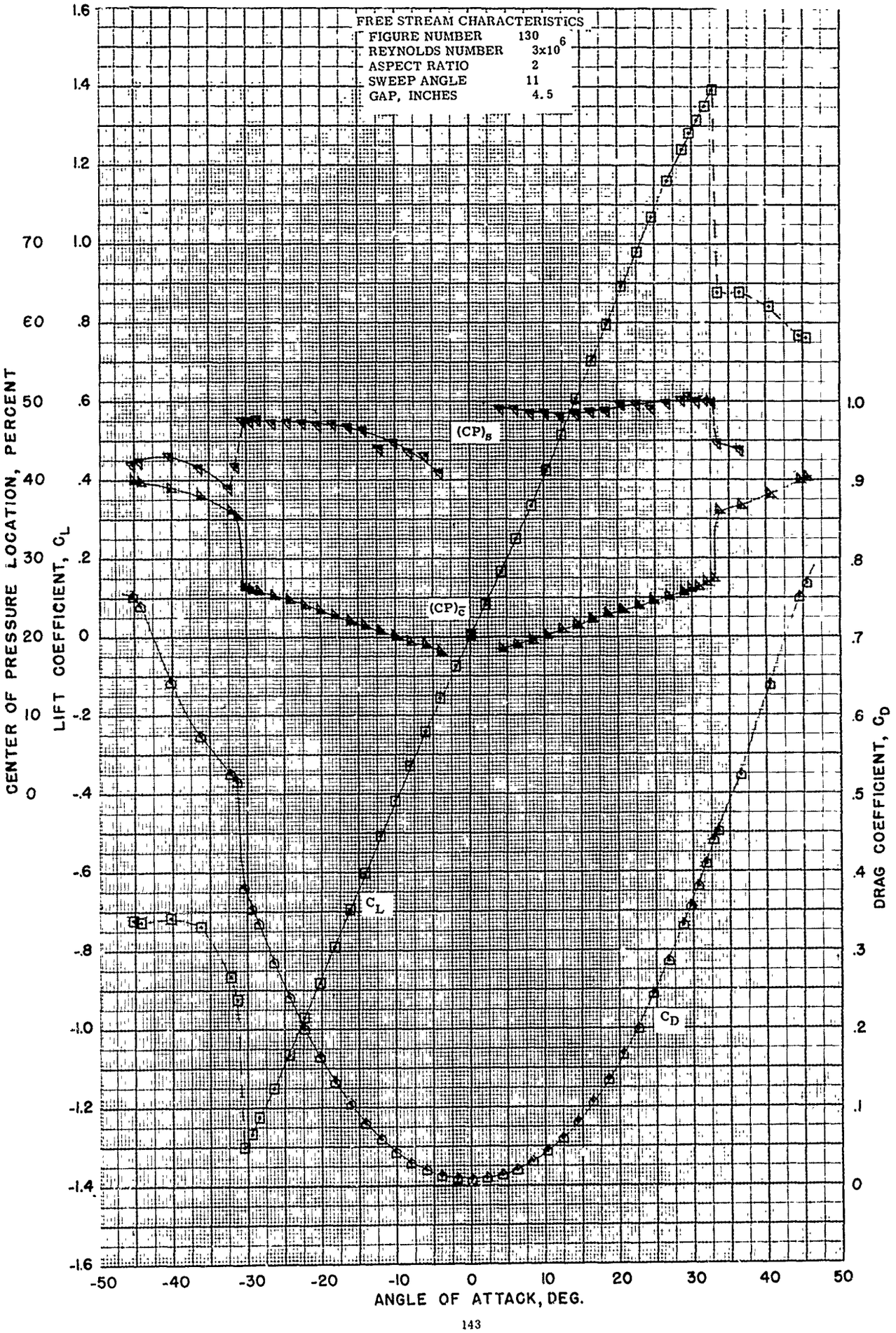
FREE STREAM CHARACTERISTICS
FIGURE NUMBER 130
REYNOLDS NUMBER 3×10^6
ASPECT RATIO 2
SWEEP ANGLE 11
GAP, INCHES 4.5
$(CP)_s$
$(CP)_c$
C_L
C_D
CENTER OF PRESSURE LOCATION, PERCENT
LIFT COEFFICIENT, C_L
DRAG COEFFICIENT, C_D
ANGLE OF ATTACK, DEG.
70
60
50
40
30
20
10
0
1.6
1.4
1.2
1.0
.8
.6
.4
.2
0
-.2
-.4
-.6
-.8
-1.0
-1.2
-1.4
-1.6
1.0
.9
.8
.7
.6
.5
.4
.3
.2
.1
0
-50
-40
-30
-20
-10
0
10
20
30
40
50

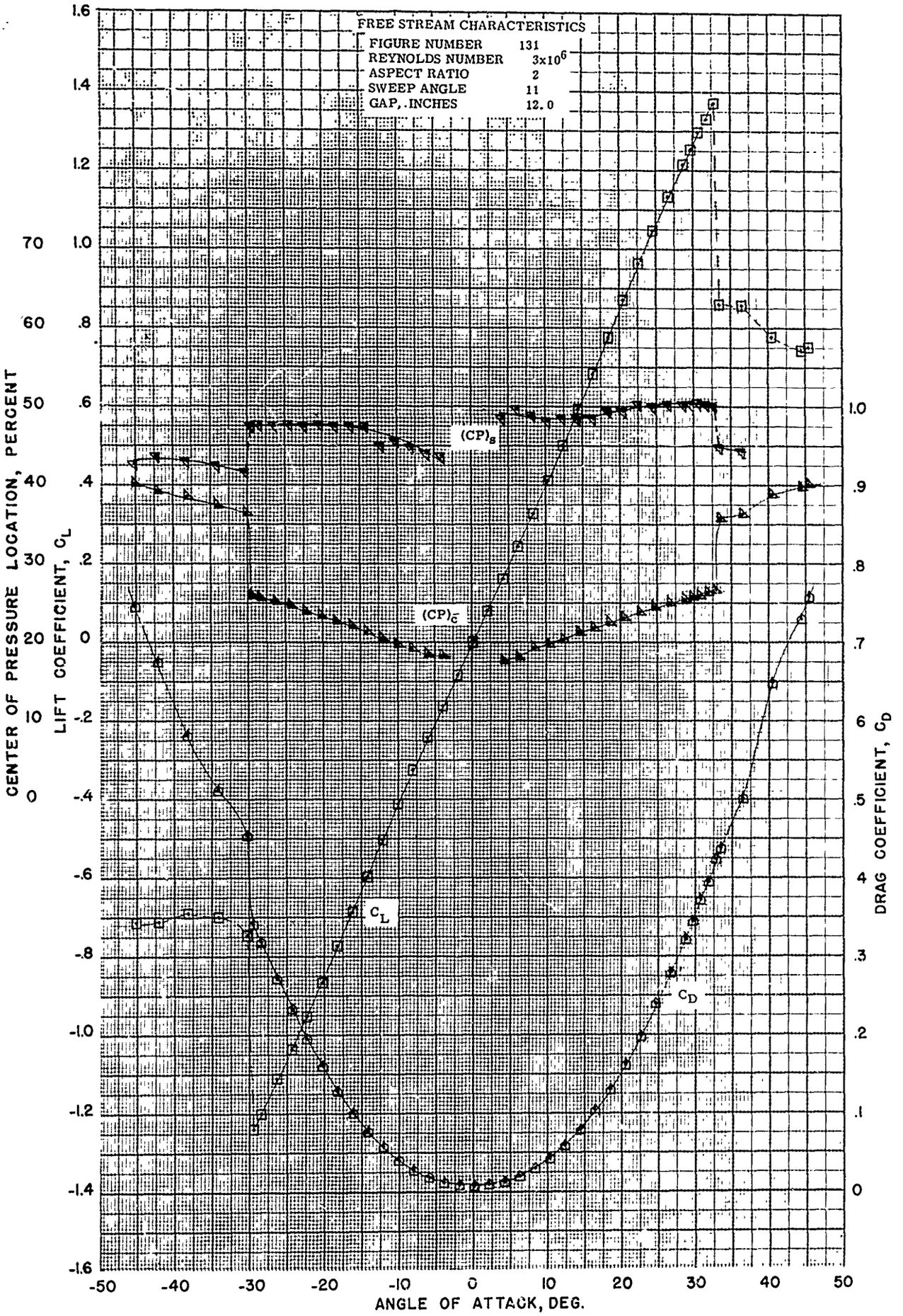
FREE STREAM CHARACTERISTICS
FIGURE NUMBER 131
REYNOLDS NUMBER 3x10^6
ASPECT RATIO 2
SWEEP ANGLE 11
GAP, INCHES 12.0
(CP)s
(CP)c
CL
CD
CENTER OF PRESSURE LOCATION, PERCENT
LIFT COEFFICIENT, CL
DRAG COEFFICIENT, CD
ANGLE OF ATTACK, DEG.
70
60
50
40
30
20
10
0
1.6
1.4
1.2
1.0
.8
.6
.4
.2
0
-.2
-.4
-.6
-.8
-1.0
-1.2
-1.4
-1.6
1.0
.9
.8
.7
6
.5
4
.3
.2
.1
0
-50
-40
-30
-20
-10
0
10
20
30
40
50

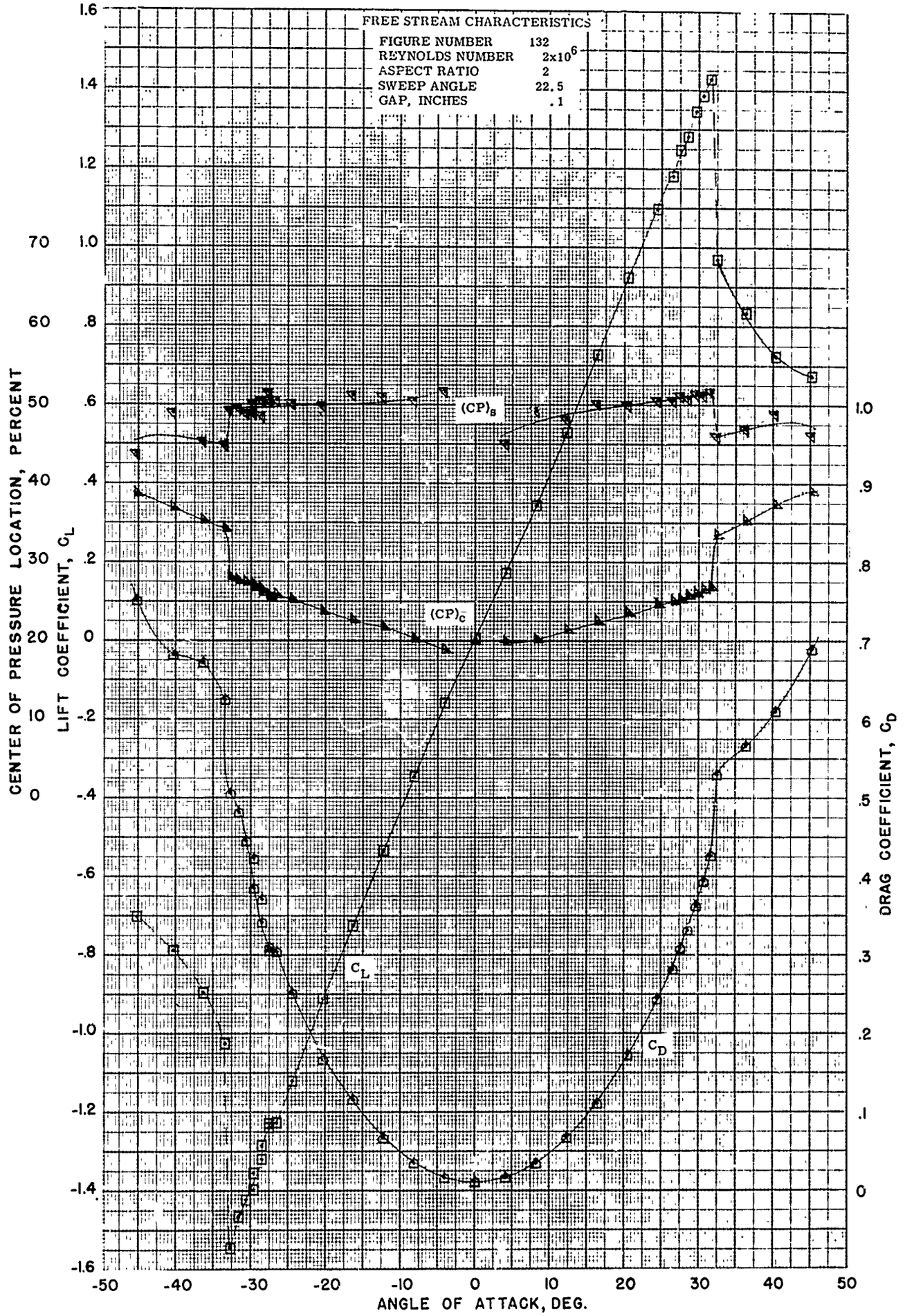
FREE STREAM CHARACTERISTICS
FIGURE NUMBER 132
REYNOLDS NUMBER 2x10^6
ASPECT RATIO 2
SWEEP ANGLE 22.5
GAP, INCHES .1
CENTER OF PRESSURE LOCATION, PERCENT
LIFT COEFFICIENT, C_L
DRAG COEFFICIENT, C_D
ANGLE OF ATTACK, DEG.
$(CP)_B$
$(CP)_C$
C_L
C_D
70
60
50
40
30
20
10
0
1.6
1.4
1.2
1.0
.8
.6
.4
.2
0
-.2
-.4
-.6
-.8
-1.0
-1.2
-1.4
-1.6
1.0
.9
.8
.7
.6
.5
.4
.3
.2
.1
0
-50
-40
-30
-20
-10
0
10
20
30
40
50

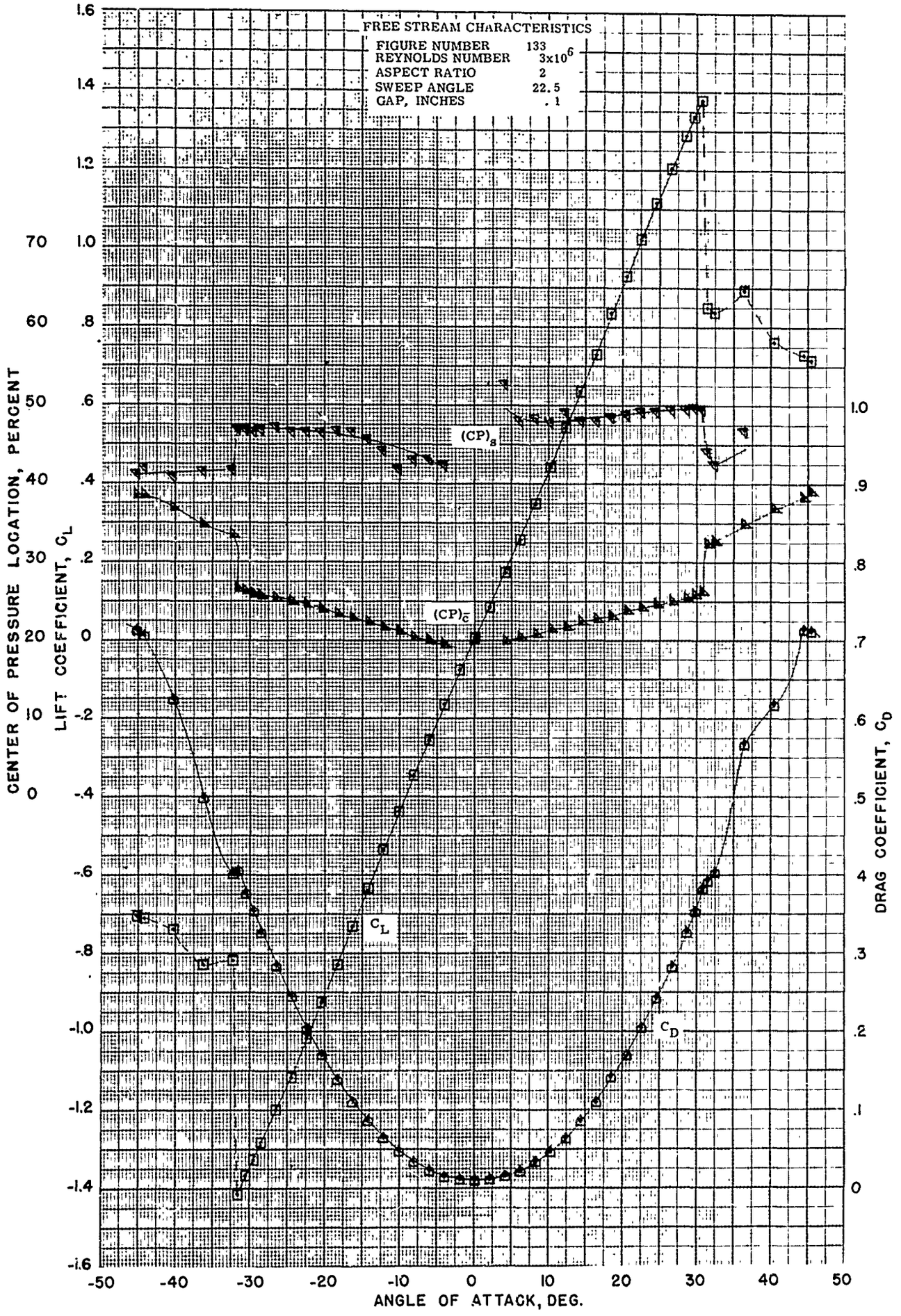
FREE STREAM CHARACTERISTICS
FIGURE NUMBER 133
REYNOLDS NUMBER 3x10^6
ASPECT RATIO 2
SWEEP ANGLE 22.5
GAP, INCHES .1
(CP)s
(CP)c
CL
CD
CENTER OF PRESSURE LOCATION, PERCENT
LIFT COEFFICIENT, CL
DRAG COEFFICIENT, CD
ANGLE OF ATTACK, DEG.
70
60
50
40
30
20
10
0
1.6
1.4
1.2
1.0
.8
.6
.4
.2
0
-.2
-.4
-.6
-.8
-1.0
-1.2
-1.4
-1.6
1.0
.9
.8
.7
.6
.5
.4
.3
.2
.1
0
-50
-40
-30
-20
-10
0
10
20
30
40
50

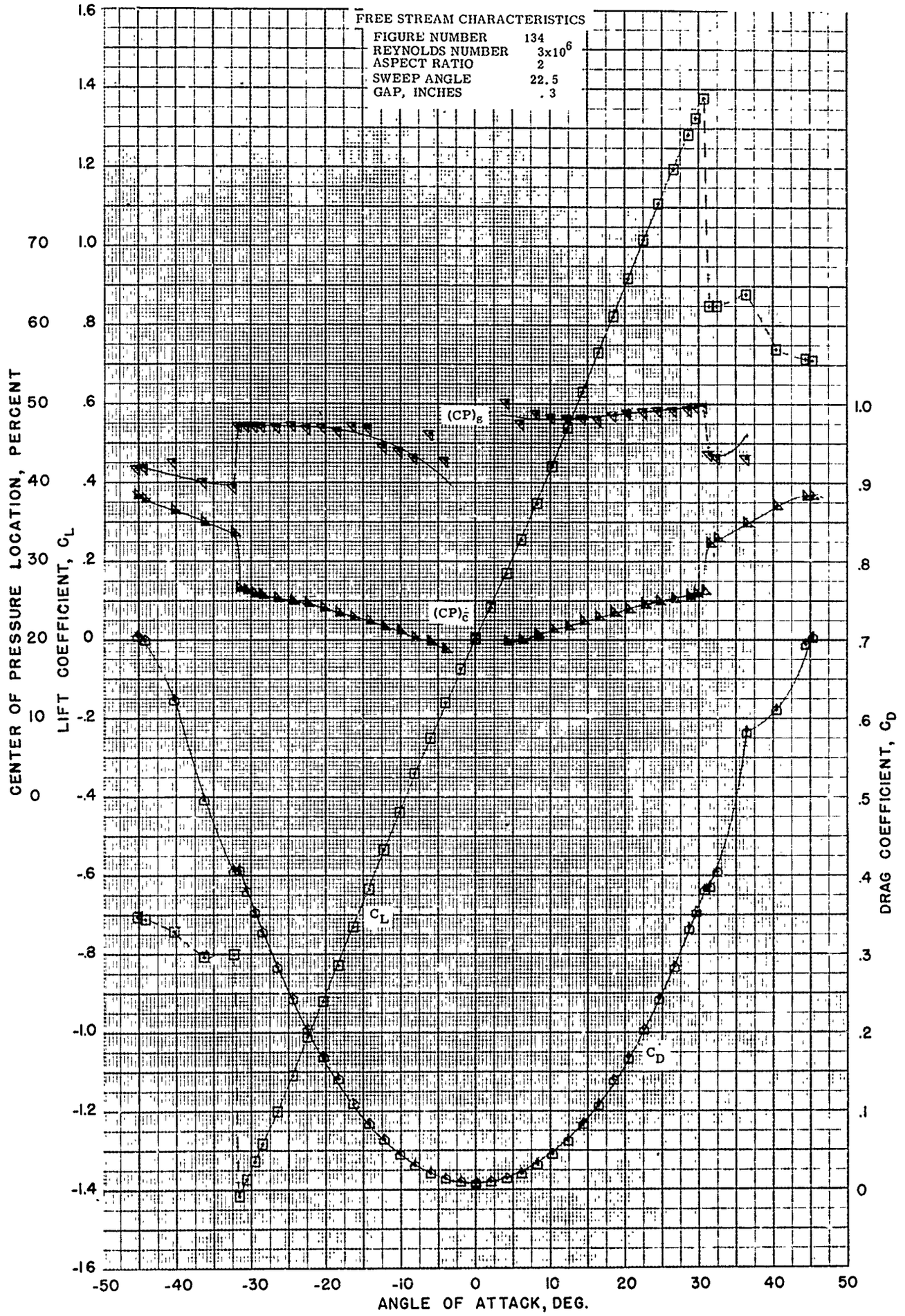
FREE STREAM CHARACTERISTICS
FIGURE NUMBER 134
REYNOLDS NUMBER 3x10^6
ASPECT RATIO 2
SWEEP ANGLE 22.5
GAP, INCHES .3
CENTER OF PRESSURE LOCATION, PERCENT
LIFT COEFFICIENT, C_L
DRAG COEFFICIENT, C_D
ANGLE OF ATTACK, DEG.
$(CP)_g$
$(CP)_{\bar{c}}$
C_L
C_D
70
60
50
40
30
20
10
0
1.6
1.4
1.2
1.0
.8
.6
.4
.2
0
-.2
-.4
-.6
-.8
-1.0
-1.2
-1.4
-1.6
1.0
.9
.8
.7
.6
.5
.4
.3
.2
.1
0
-50
-40
-30
-20
-10
0
10
20
30
40
50

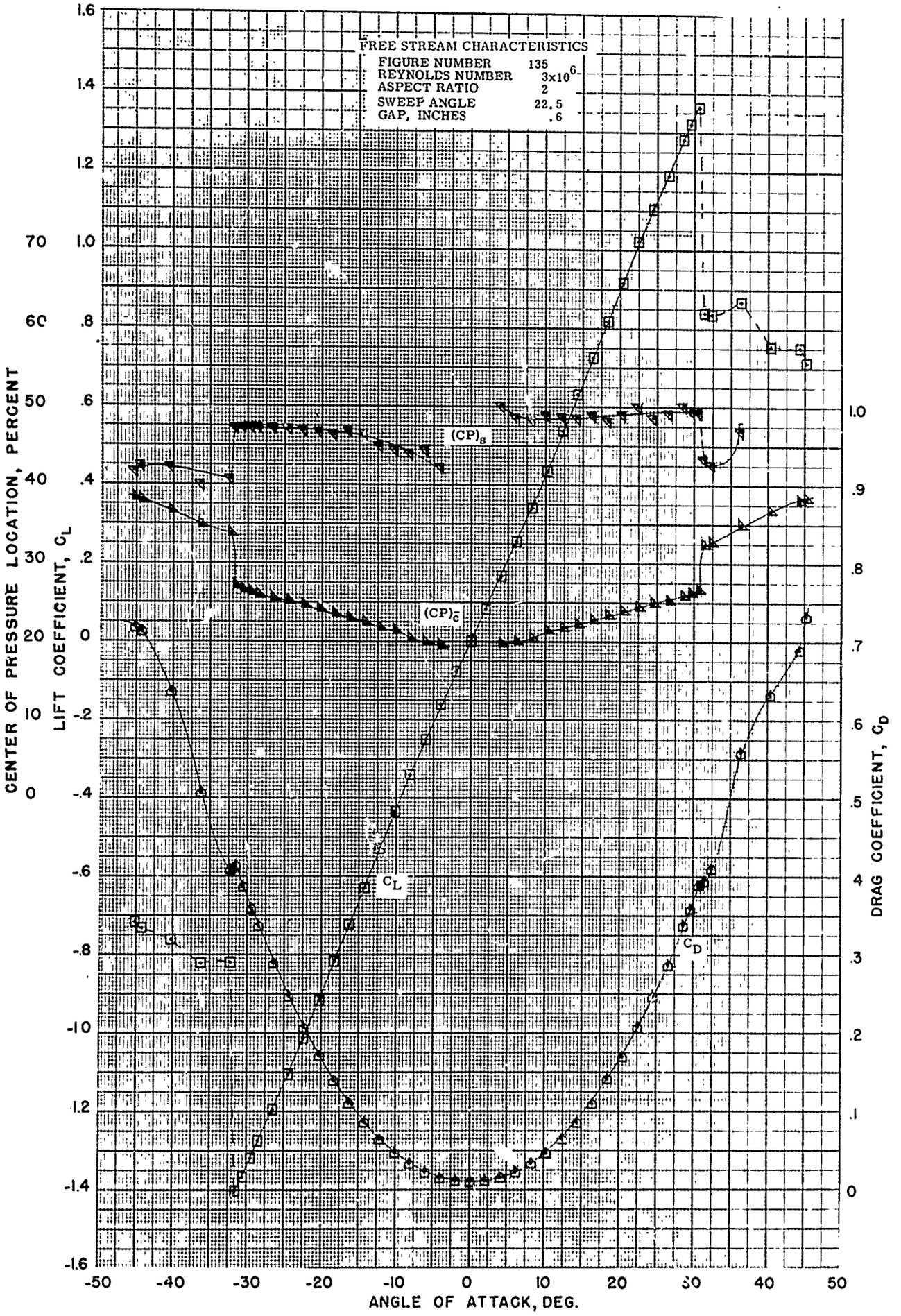
FREE STREAM CHARACTERISTICS
FIGURE NUMBER 135
REYNOLDS NUMBER 3x10^6
ASPECT RATIO 2
SWEEP ANGLE 22.5
GAP, INCHES .6
CENTER OF PRESSURE LOCATION, PERCENT
LIFT COEFFICIENT, C_L
DRAG COEFFICIENT, C_D
ANGLE OF ATTACK, DEG.
$(CP)_s$
$(CP)_{\bar{c}}$
C_L
C_D
70
60
50
40
30
20
10
0
1.6
1.4
1.2
1.0
.8
.6
.4
.2
0
-.2
-.4
-.6
-.8
-1.0
-1.2
-1.4
-1.6
1.0
.9
.8
.7
.6
.5
.4
.3
.2
.1
0
-50
-40
-30
-20
-10
0
10
20
30
40
50

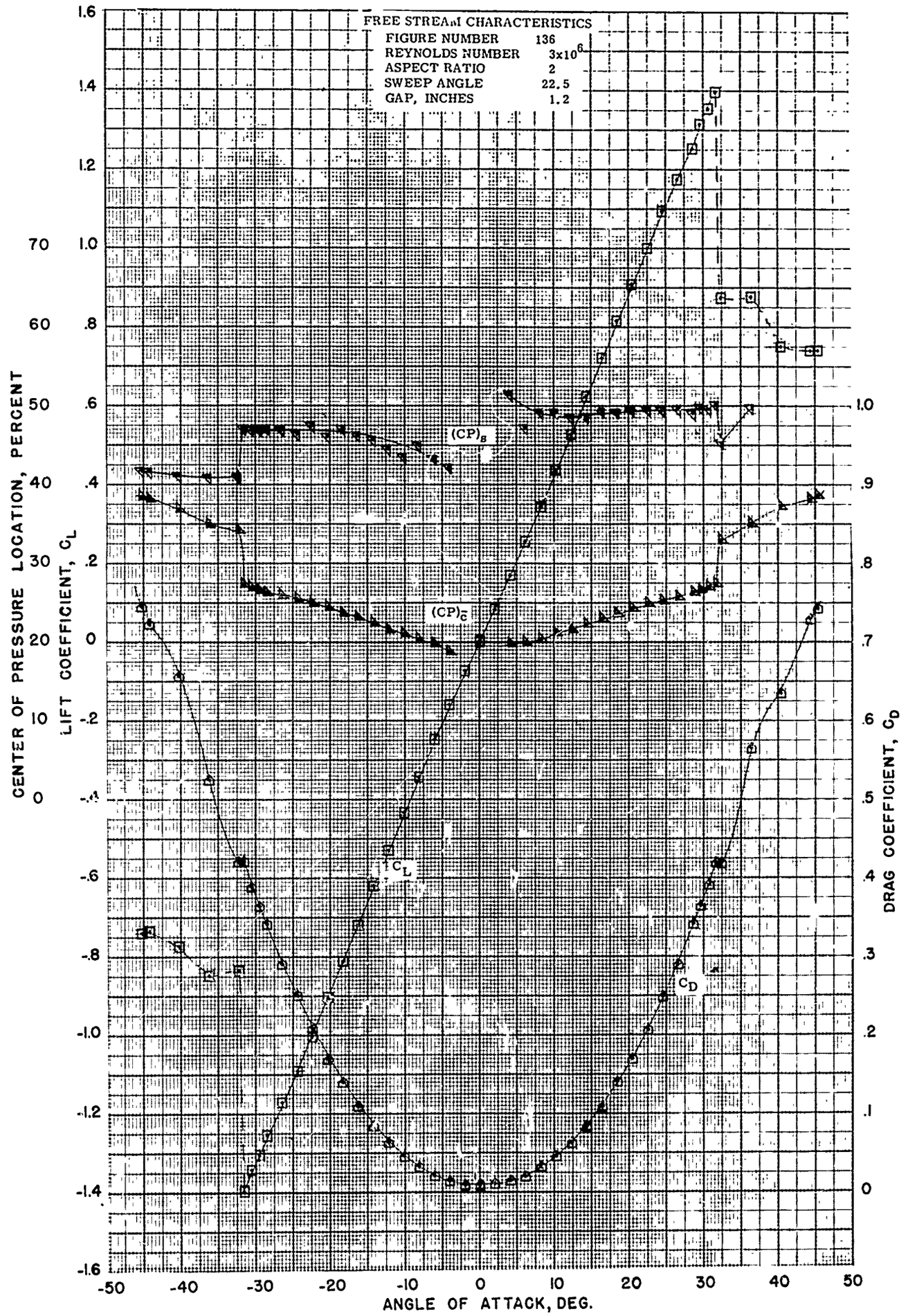
FREE STREAM CHARACTERISTICS
FIGURE NUMBER 136
REYNOLDS NUMBER 3x10^6
ASPECT RATIO 2
SWEEP ANGLE 22.5
GAP, INCHES 1.2
CENTER OF PRESSURE LOCATION, PERCENT
LIFT COEFFICIENT, C_L
DRAG COEFFICIENT, C_D
ANGLE OF ATTACK, DEG.
$(CP)_B$
$(CP)_{\bar{c}}$
C_L
C_D
70
60
50
40
30
20
10
0
1.6
1.4
1.2
1.0
.8
.6
.4
.2
0
-.2
-.4
-.6
-.8
-1.0
-1.2
-1.4
-1.6
1.0
.9
.8
.7
.6
.5
.4
.3
.2
.1
0
-50
-40
-30
-20
-10
0
10
20
30
40
50

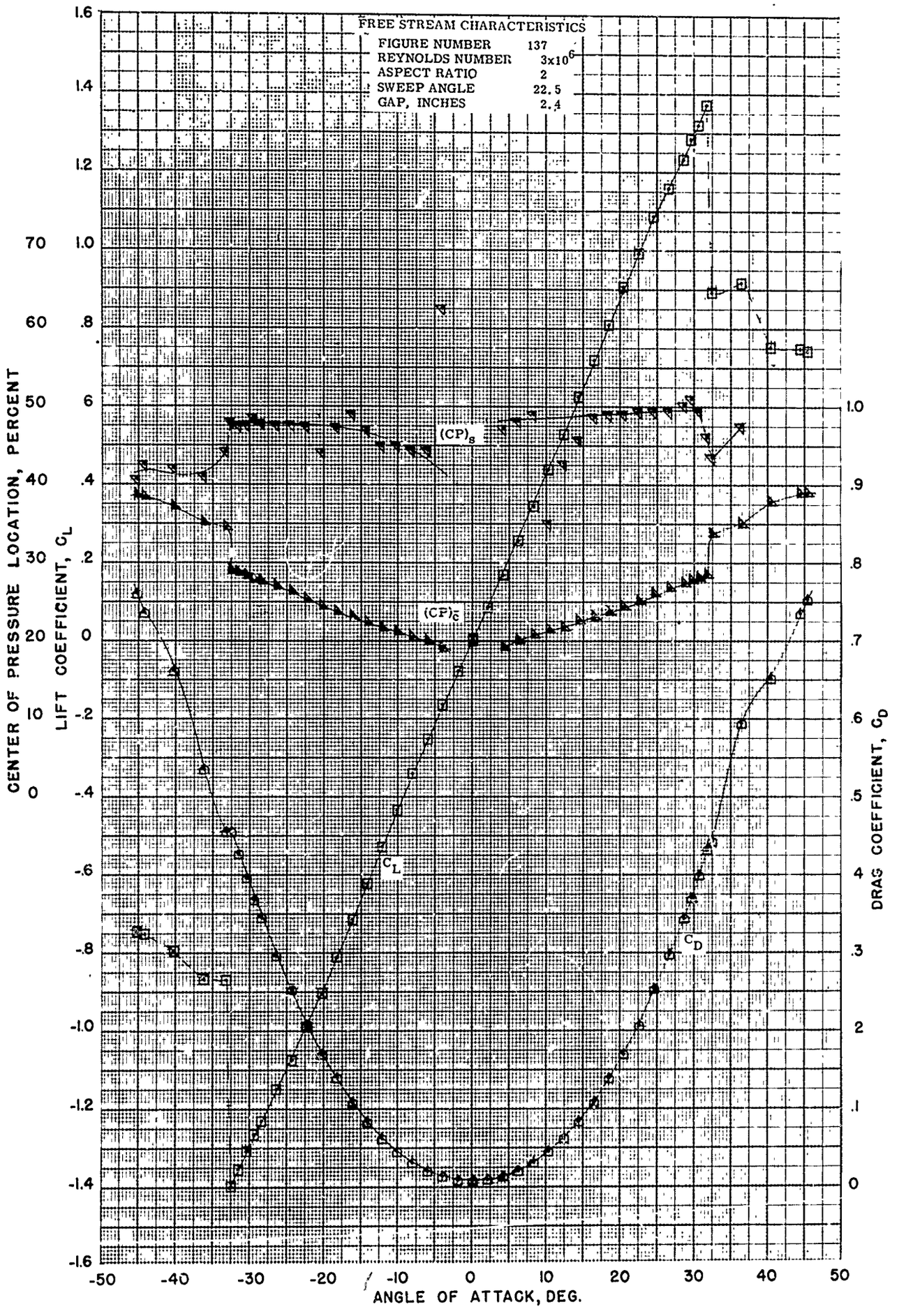
FREE STREAM CHARACTERISTICS
FIGURE NUMBER 137
REYNOLDS NUMBER 3x10^6
ASPECT RATIO 2
SWEEP ANGLE 22.5
GAP, INCHES 2.4
(CP)s
(CP)c
CL
CD
CENTER OF PRESSURE LOCATION, PERCENT
LIFT COEFFICIENT, CL
DRAG COEFFICIENT, CD
ANGLE OF ATTACK, DEG.
70
60
50
40
30
20
10
0
1.6
1.4
1.2
1.0
.8
.6
.4
.2
0
-.2
-.4
-.6
-.8
-1.0
-1.2
-1.4
-1.6
1.0
.9
.8
.7
.6
.5
.4
.3
2
.1
0
-50
-40
-30
-20
-10
0
10
20
30
40
50

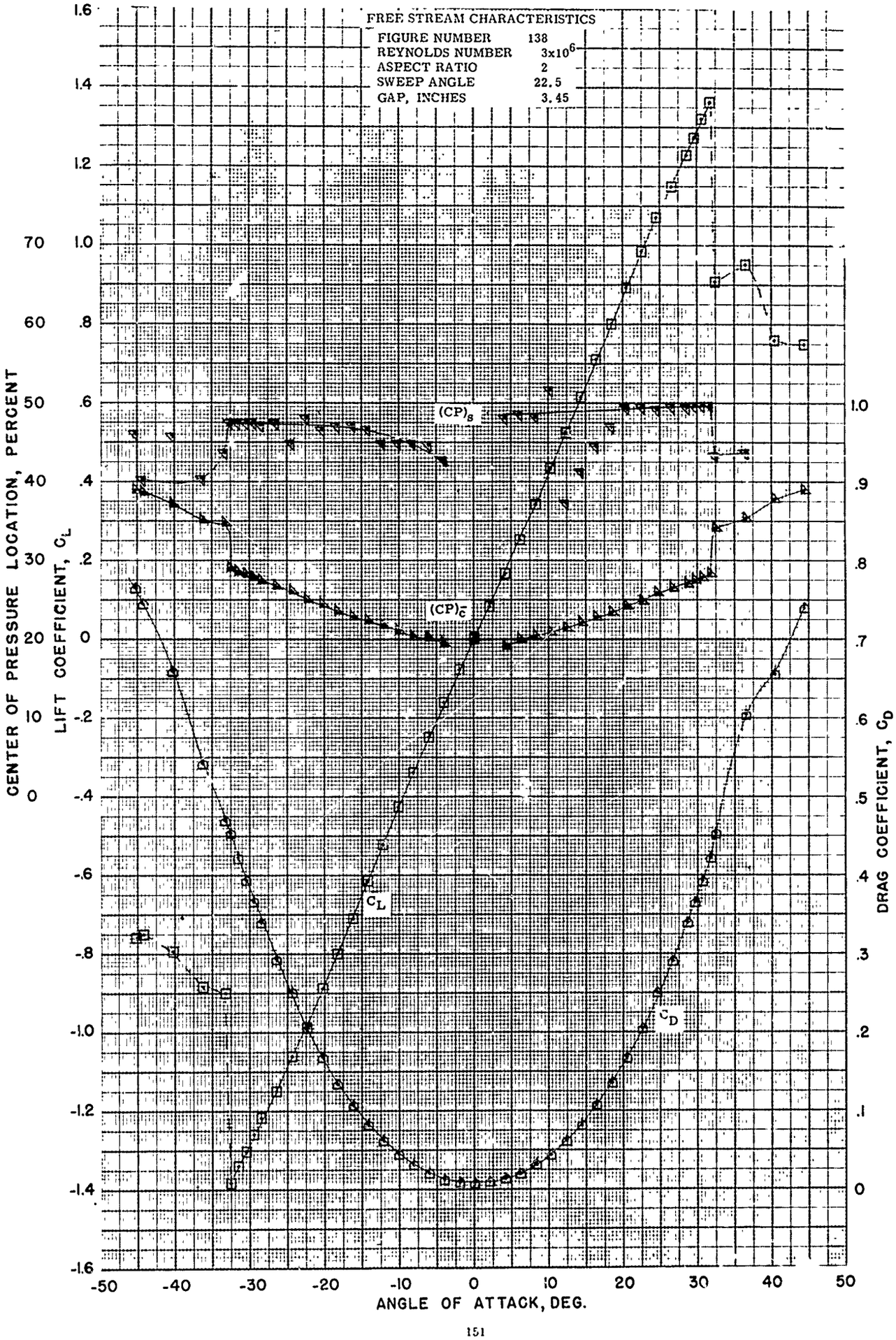
FREE STREAM CHARACTERISTICS
FIGURE NUMBER 138
REYNOLDS NUMBER 3x10^6
ASPECT RATIO 2
SWEEP ANGLE 22.5
GAP, INCHES 3.45
(CP)s
(CP)c̄
CL
CD
CENTER OF PRESSURE LOCATION, PERCENT
LIFT COEFFICIENT, CL
DRAG COEFFICIENT, CD
ANGLE OF ATTACK, DEG.
70
60
50
40
30
20
10
0
1.6
1.4
1.2
1.0
.8
.6
.4
.2
0
-.2
-.4
-.6
-.8
-1.0
-1.2
-1.4
-1.6
1.0
.9
.8
.7
.6
.5
.4
.3
.2
.1
0
-50
-40
-30
-20
-10
0
10
20
30
40
50

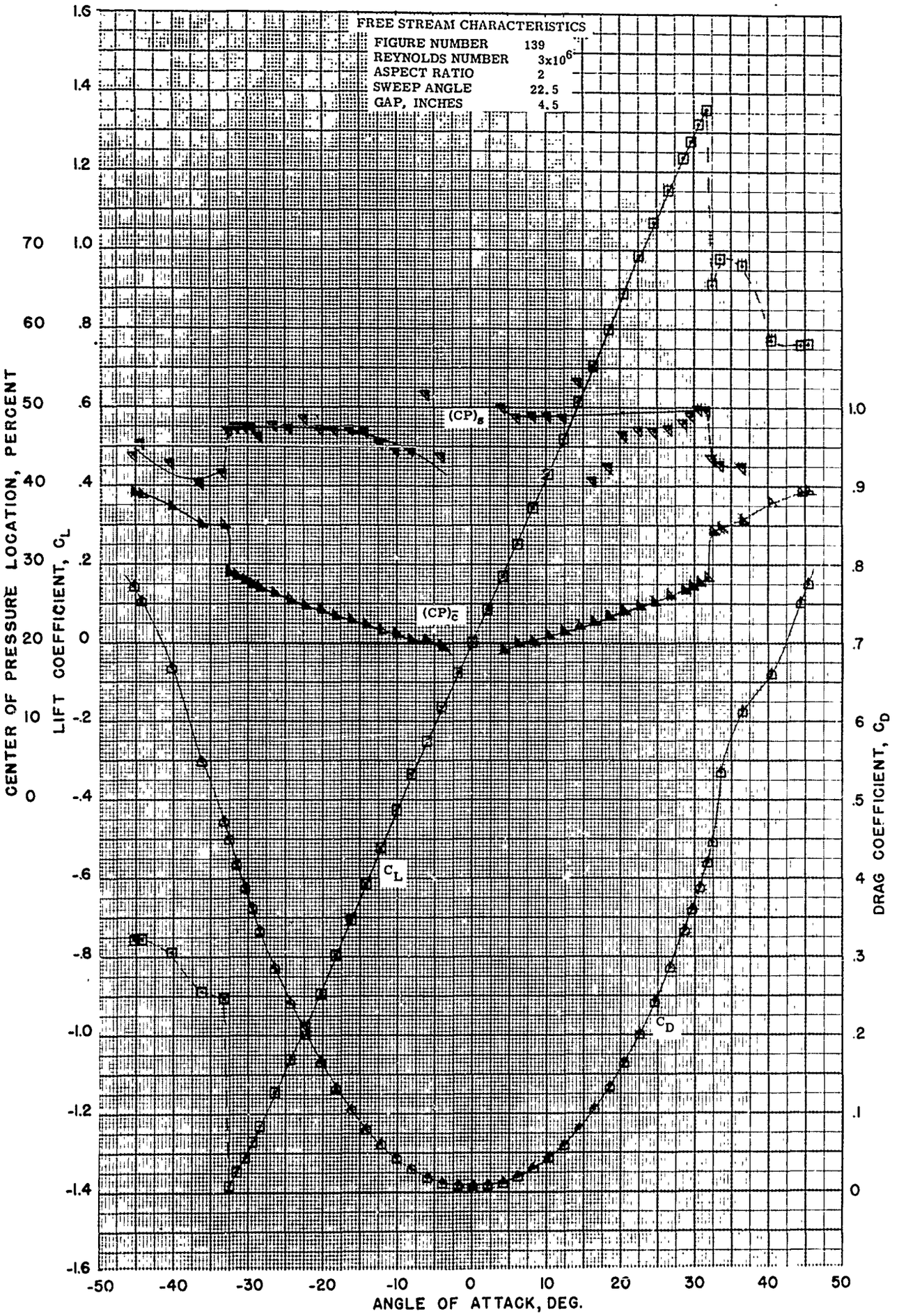
FREE STREAM CHARACTERISTICS
FIGURE NUMBER 139
REYNOLDS NUMBER 3x10^6
ASPECT RATIO 2
SWEEP ANGLE 22.5
GAP, INCHES 4.5
CENTER OF PRESSURE LOCATION, PERCENT
LIFT COEFFICIENT, C_L
DRAG COEFFICIENT, C_D
ANGLE OF ATTACK, DEG.
$(CP)_s$
$(CP)_{\bar{c}}$
C_L
C_D
70
60
50
40
30
20
10
0
1.6
1.4
1.2
1.0
.8
.6
.4
.2
0
-.2
-.4
-.6
-.8
-1.0
-1.2
-1.4
-1.6
1.0
.9
.8
.7
.6
.5
.4
.3
.2
.1
0
-50
-40
-30
-20
-10
0
10
20
30
40
50

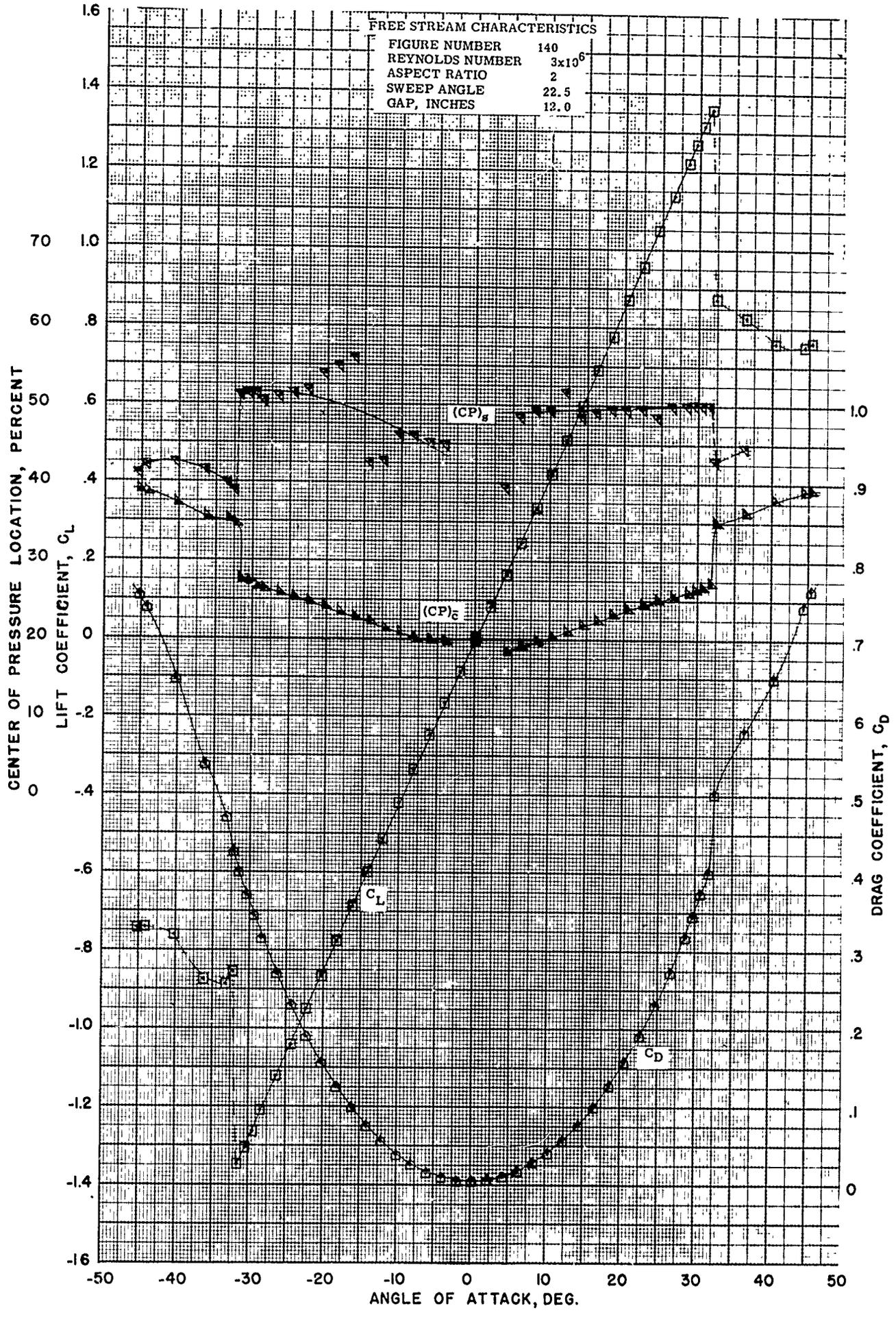
FREE STREAM CHARACTERISTICS
FIGURE NUMBER 140
REYNOLDS NUMBER 3x10^6
ASPECT RATIO 2
SWEEP ANGLE 22.5
GAP, INCHES 12.0
(CP)_s
(CP)_c̄
C_L
C_D
CENTER OF PRESSURE LOCATION, PERCENT
LIFT COEFFICIENT, C_L
DRAG COEFFICIENT, C_D
ANGLE OF ATTACK, DEG.
70
60
50
40
30
20
10
0
1.6
1.4
1.2
1.0
.8
.6
.4
.2
0
-.2
-.4
-.6
-.8
-1.0
-1.2
-1.4
-1.6
1.0
.9
.8
.7
.6
.5
.4
.3
.2
.1
0
-50
-40
-30
-20
-10
0
10
20
30
40
50

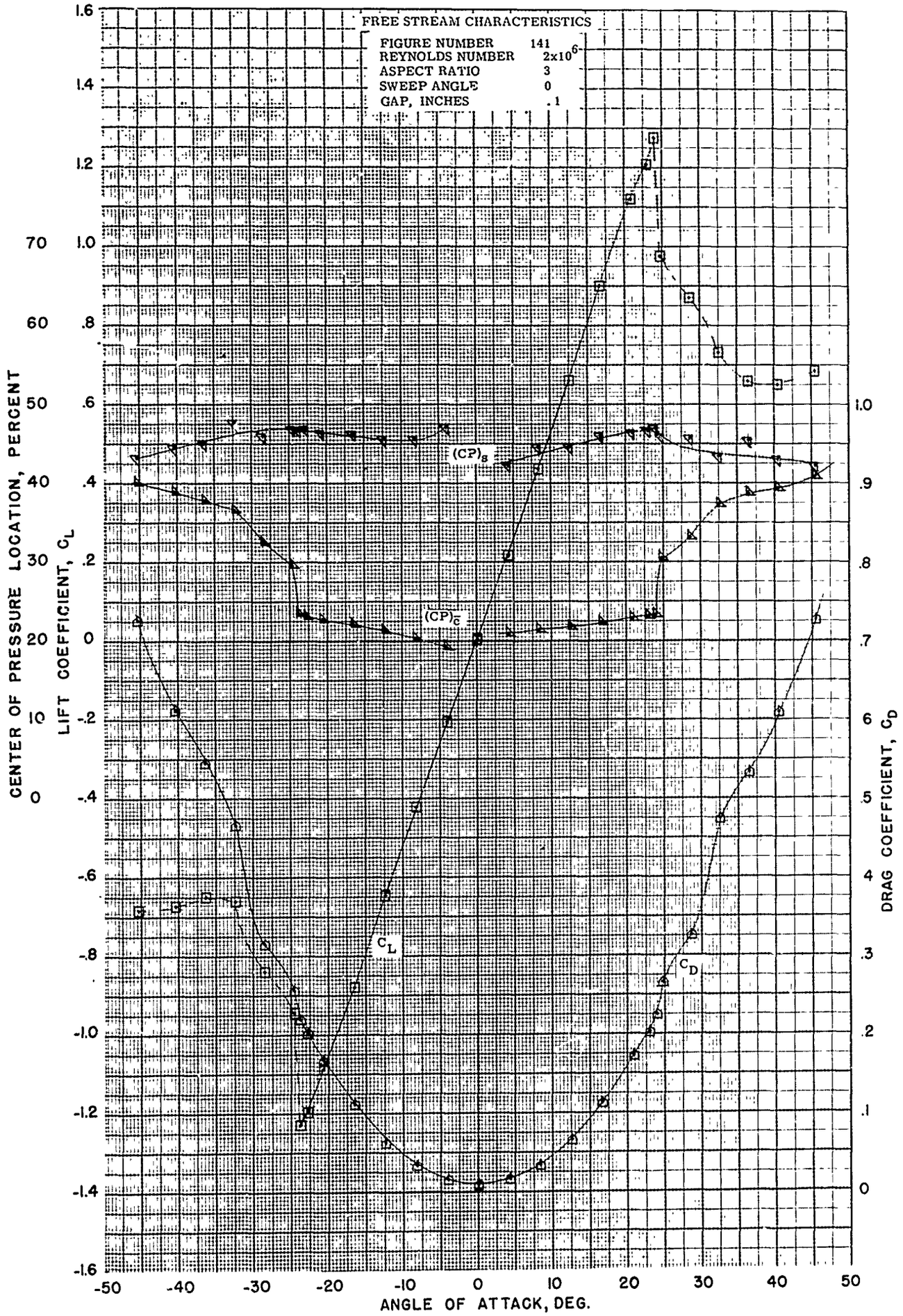
FREE STREAM CHARACTERISTICS
FIGURE NUMBER 141
REYNOLDS NUMBER 2x10^6
ASPECT RATIO 3
SWEEP ANGLE 0
GAP, INCHES .1
CENTER OF PRESSURE LOCATION, PERCENT
LIFT COEFFICIENT, C_L
DRAG COEFFICIENT, C_D
ANGLE OF ATTACK, DEG.
$(CP)_s$
$(CP)_c$
C_L
C_D
70 60 50 40 30 20 10 0
1.6 1.4 1.2 1.0 .8 .6 .4 .2 0 -.2 -.4 -.6 -.8 -1.0 -1.2 -1.4 -1.6
1.0 .9 .8 .7 6 5 4 .3 .2 .1 0
-50 -40 -30 -20 -10 0 10 20 30 40 50

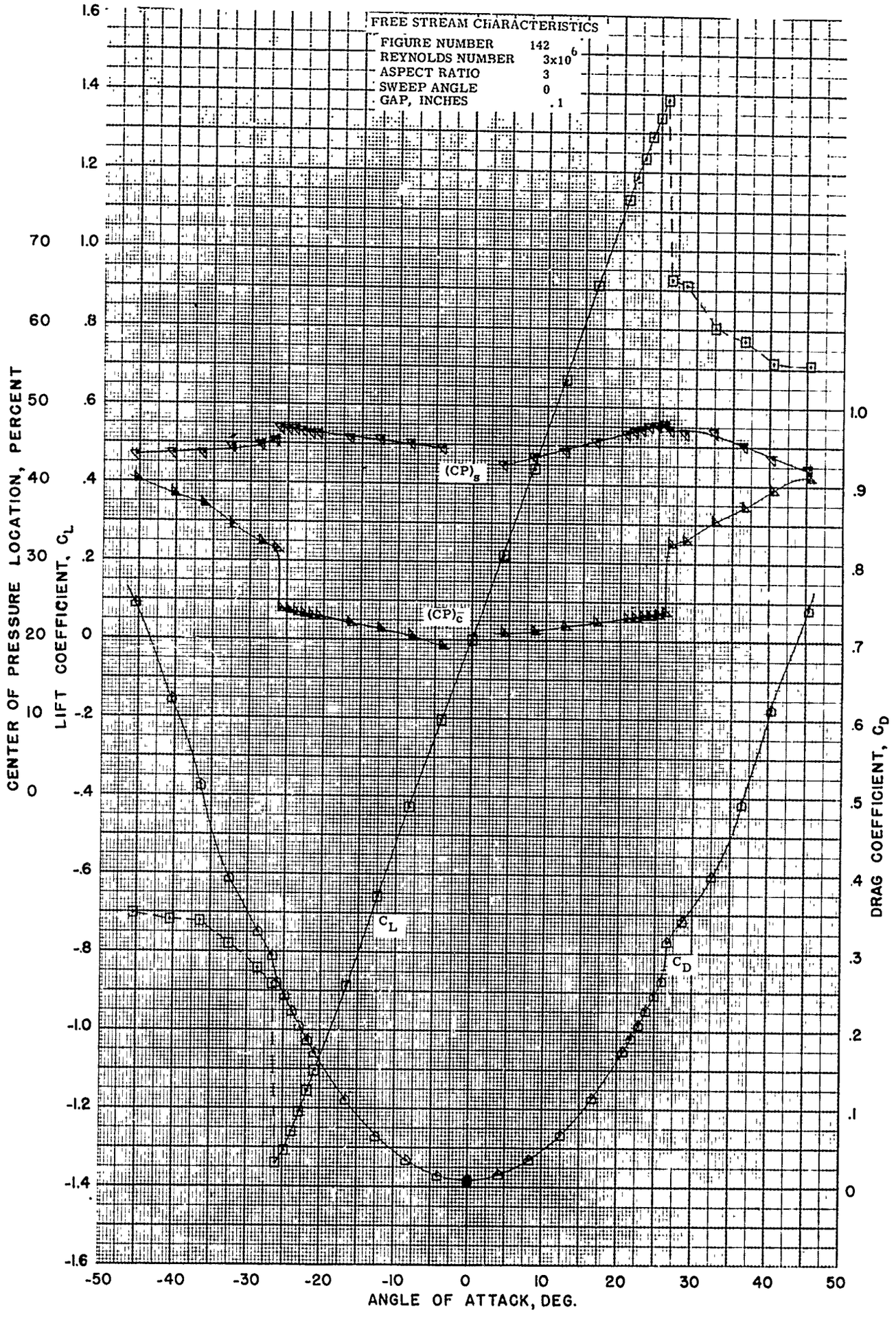
FREE STREAM CHARACTERISTICS
FIGURE NUMBER 142
REYNOLDS NUMBER 3x10^6
ASPECT RATIO 3
SWEEP ANGLE 0
GAP, INCHES .1
CENTER OF PRESSURE LOCATION, PERCENT
LIFT COEFFICIENT, C_L
DRAG COEFFICIENT, C_D
ANGLE OF ATTACK, DEG.
$(CP)_s$
$(CP)_c$
C_L
C_D
70
60
50
40
30
20
10
0
1.6
1.4
1.2
1.0
.8
.6
.4
.2
0
-.2
-.4
-.6
-.8
-1.0
-1.2
-1.4
-1.6
1.0
.9
.8
.7
.6
.5
.4
.3
.2
.1
0
-50
-40
-30
-20
-10
0
10
20
30
40
50

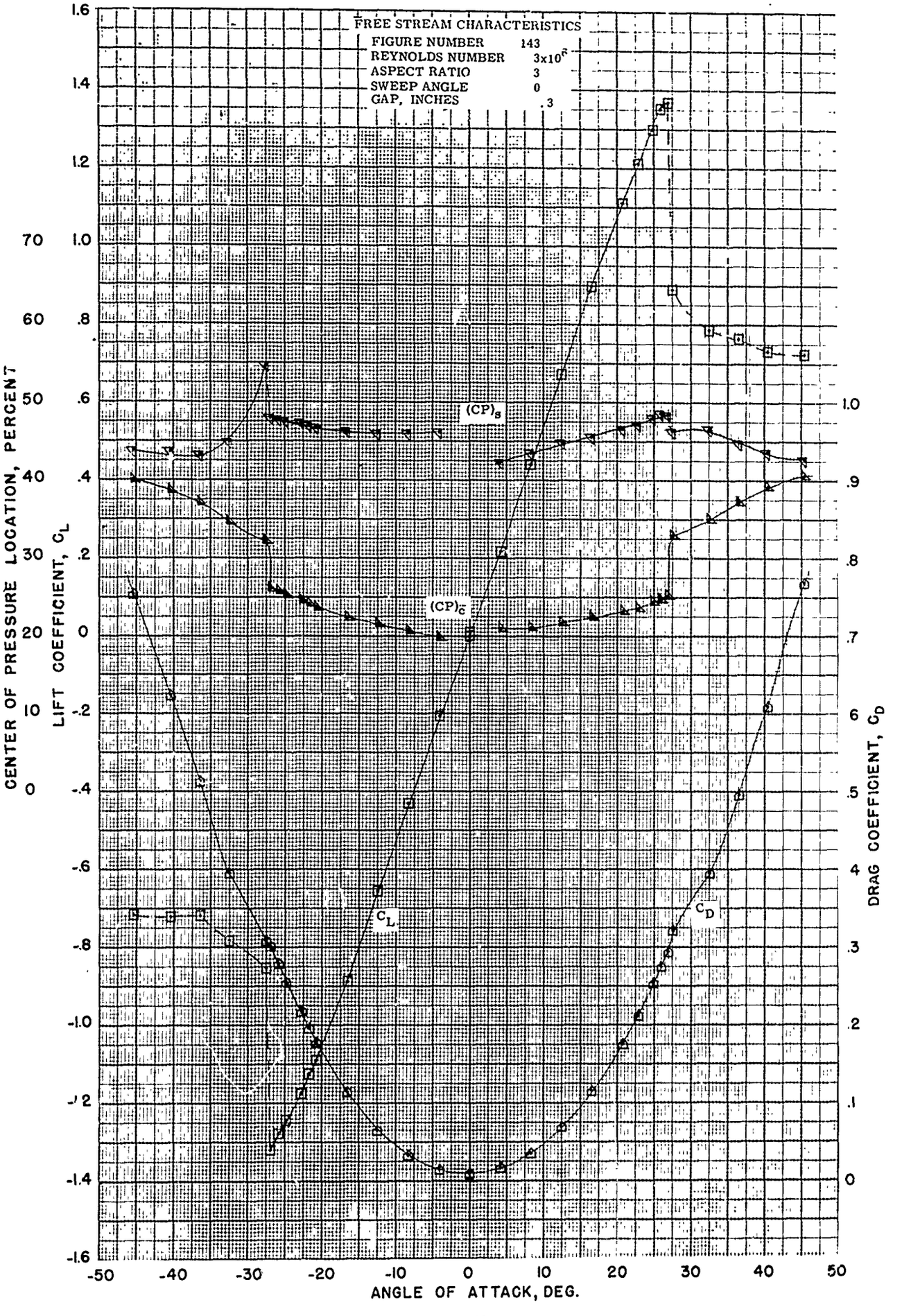
FREE STREAM CHARACTERISTICS
FIGURE NUMBER 143
REYNOLDS NUMBER 3x10^6
ASPECT RATIO 3
SWEEP ANGLE 0
GAP, INCHES .3
CENTER OF PRESSURE LOCATION, PERCENT
LIFT COEFFICIENT, C_L
DRAG COEFFICIENT, C_D
ANGLE OF ATTACK, DEG.
$(CP)_s$
$(CP)_c$
C_L
C_D
70
60
50
40
30
20
10
0
1.6
1.4
1.2
1.0
.8
.6
.4
.2
0
-.2
-.4
-.6
-.8
-1.0
-1.2
-1.4
-1.6
1.0
.9
.8
.7
.6
.5
.4
.3
.2
.1
0
-50
-40
-30
-20
-10
0
10
20
30
40
50

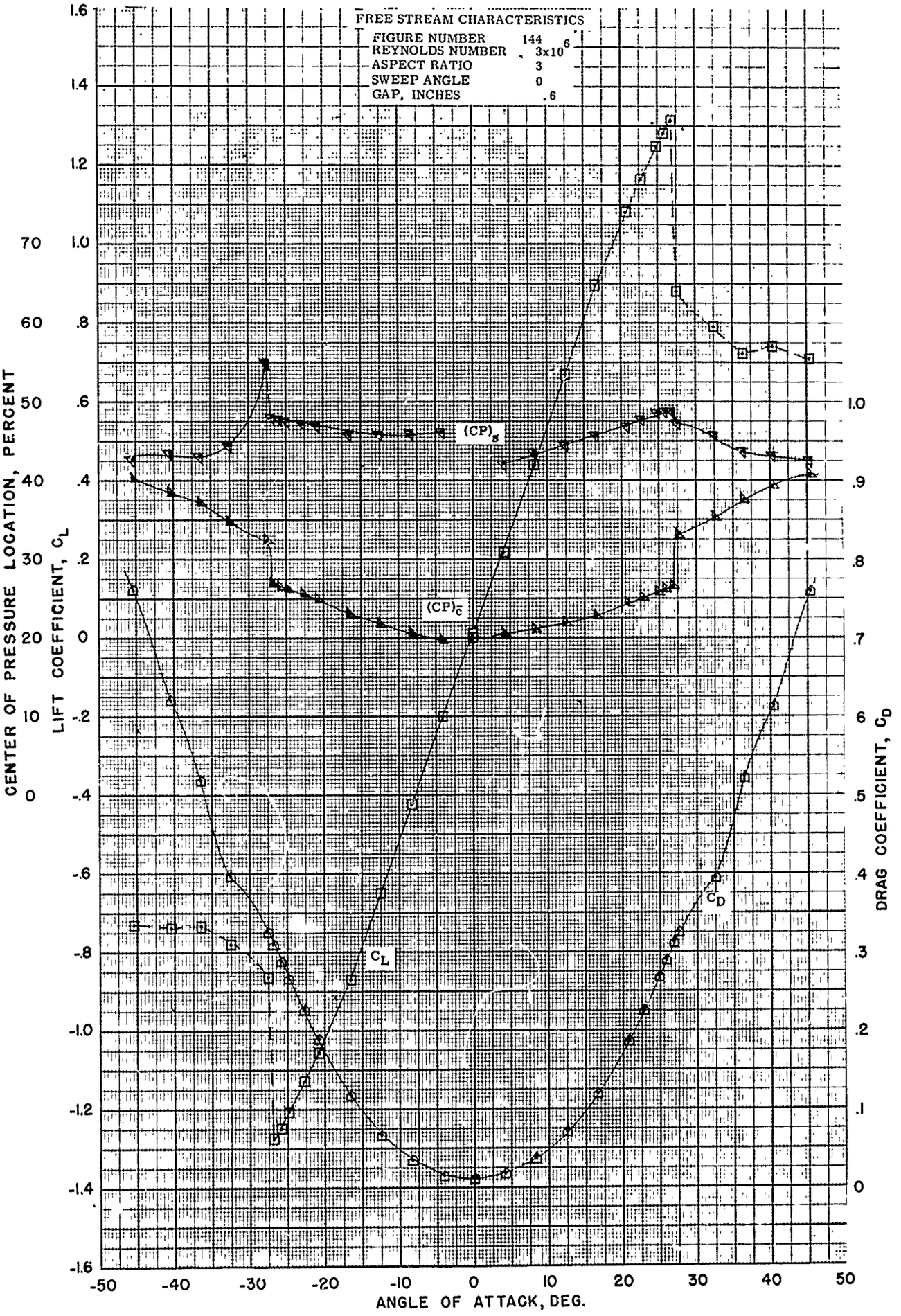
FREE STREAM CHARACTERISTICS
FIGURE NUMBER 144
REYNOLDS NUMBER 3x10^6
ASPECT RATIO 3
SWEEP ANGLE 0
GAP, INCHES .6
CENTER OF PRESSURE LOCATION, PERCENT
LIFT COEFFICIENT, C_L
DRAG COEFFICIENT, C_D
ANGLE OF ATTACK, DEG.
$(CP)_s$
$(CP)_c$
C_L
C_D
70
60
50
40
30
20
10
0
1.6
1.4
1.2
1.0
.8
.6
.4
.2
0
-.2
-.4
-.6
-.8
-1.0
-1.2
-1.4
-1.6
1.0
.9
.8
.7
.6
.5
.4
.3
.2
.1
0
-50
-40
-30
-20
-10
0
10
20
30
40
50

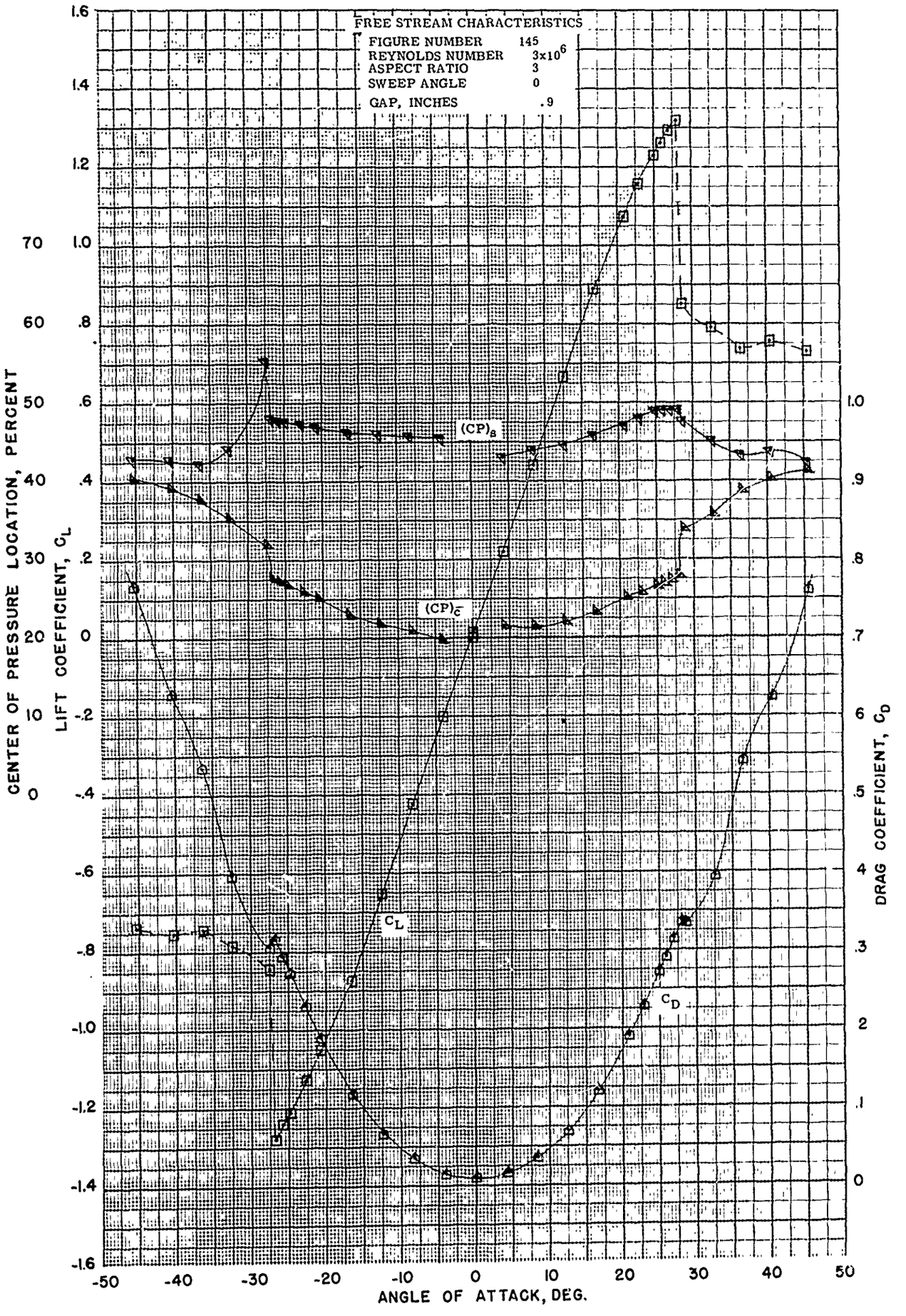
FREE STREAM CHARACTERISTICS
FIGURE NUMBER 145
REYNOLDS NUMBER 3x10^6
ASPECT RATIO 3
SWEEP ANGLE 0
GAP, INCHES .9
CENTER OF PRESSURE LOCATION, PERCENT
LIFT COEFFICIENT, C_L
DRAG COEFFICIENT, C_D
ANGLE OF ATTACK, DEG.
$(CP)_B$
$(CP)_{\bar{c}}$
C_L
C_D
70
60
50
40
30
20
10
0
1.6
1.4
1.2
1.0
.8
.6
.4
.2
0
-.2
-.4
-.6
-.8
-1.0
-1.2
-1.4
-1.6
1.0
.9
.8
.7
.6
.5
.4
.3
.2
.1
0
-50
-40
-30
-20
-10
0
10
20
30
40
50

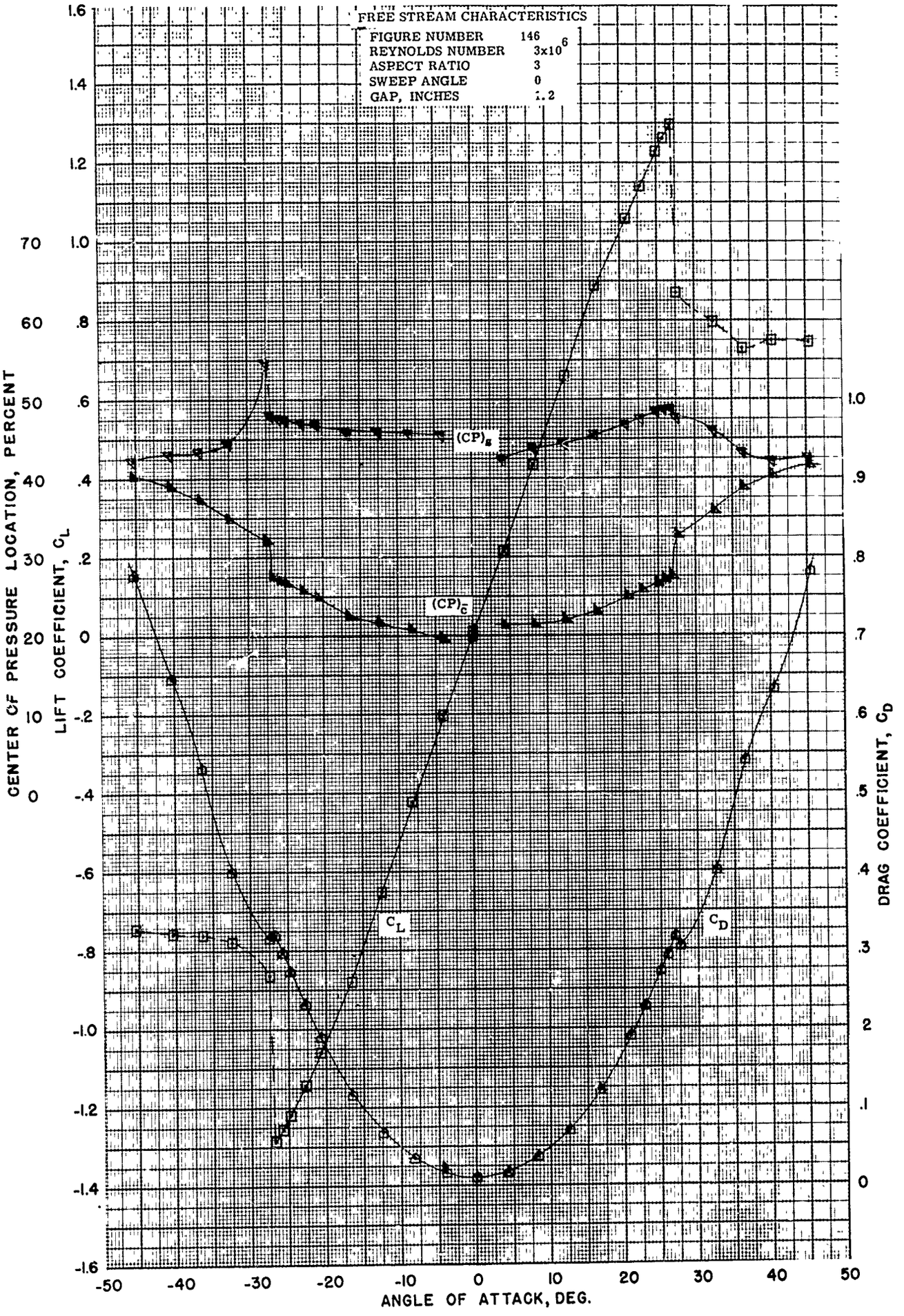
FREE STREAM CHARACTERISTICS
FIGURE NUMBER 146
REYNOLDS NUMBER 3x10^6
ASPECT RATIO 3
SWEEP ANGLE 0
GAP, INCHES 1.2
CENTER OF PRESSURE LOCATION, PERCENT
LIFT COEFFICIENT, C_L
DRAG COEFFICIENT, C_D
ANGLE OF ATTACK, DEG.
$(CP)_{\bar{c}}$
C_L
C_D

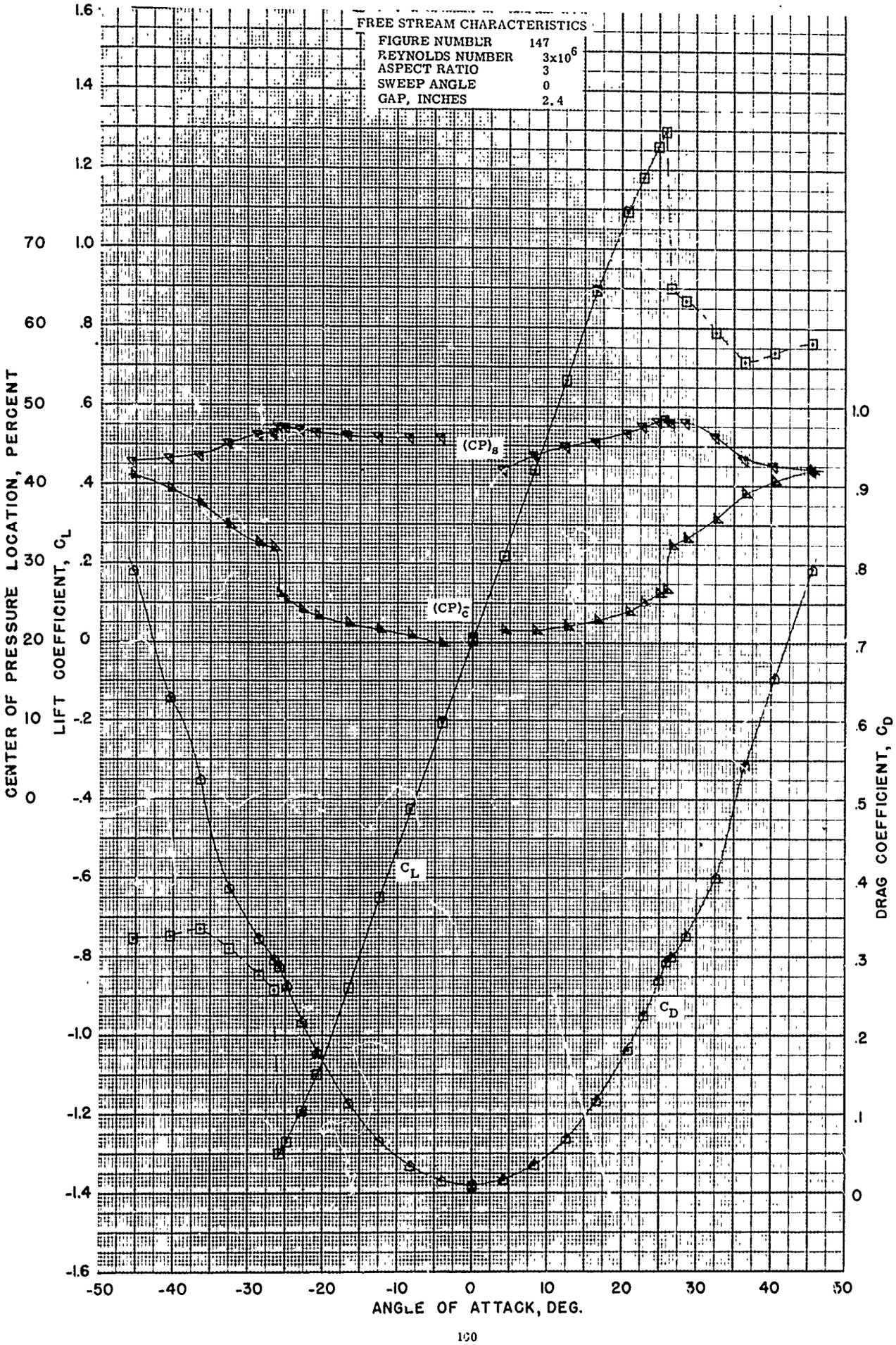
FREE STREAM CHARACTERISTICS
FIGURE NUMBER 147
REYNOLDS NUMBER 3x10^6
ASPECT RATIO 3
SWEEP ANGLE 0
GAP, INCHES 2.4
CENTER OF PRESSURE LOCATION, PERCENT
LIFT COEFFICIENT, C_L
DRAG COEFFICIENT, C_D
ANGLE OF ATTACK, DEG.
$(CP)_B$
$(CP)_C$
C_L
C_D
70
60
50
40
30
20
10
0
1.6
1.4
1.2
1.0
.8
.6
.4
.2
0
-.2
-.4
-.6
-.8
-1.0
-1.2
-1.4
-1.6
1.0
.9
.8
.7
.6
.5
.4
.3
.2
.1
0
-50
-40
-30
-20
-10
0
10
20
30
40
50

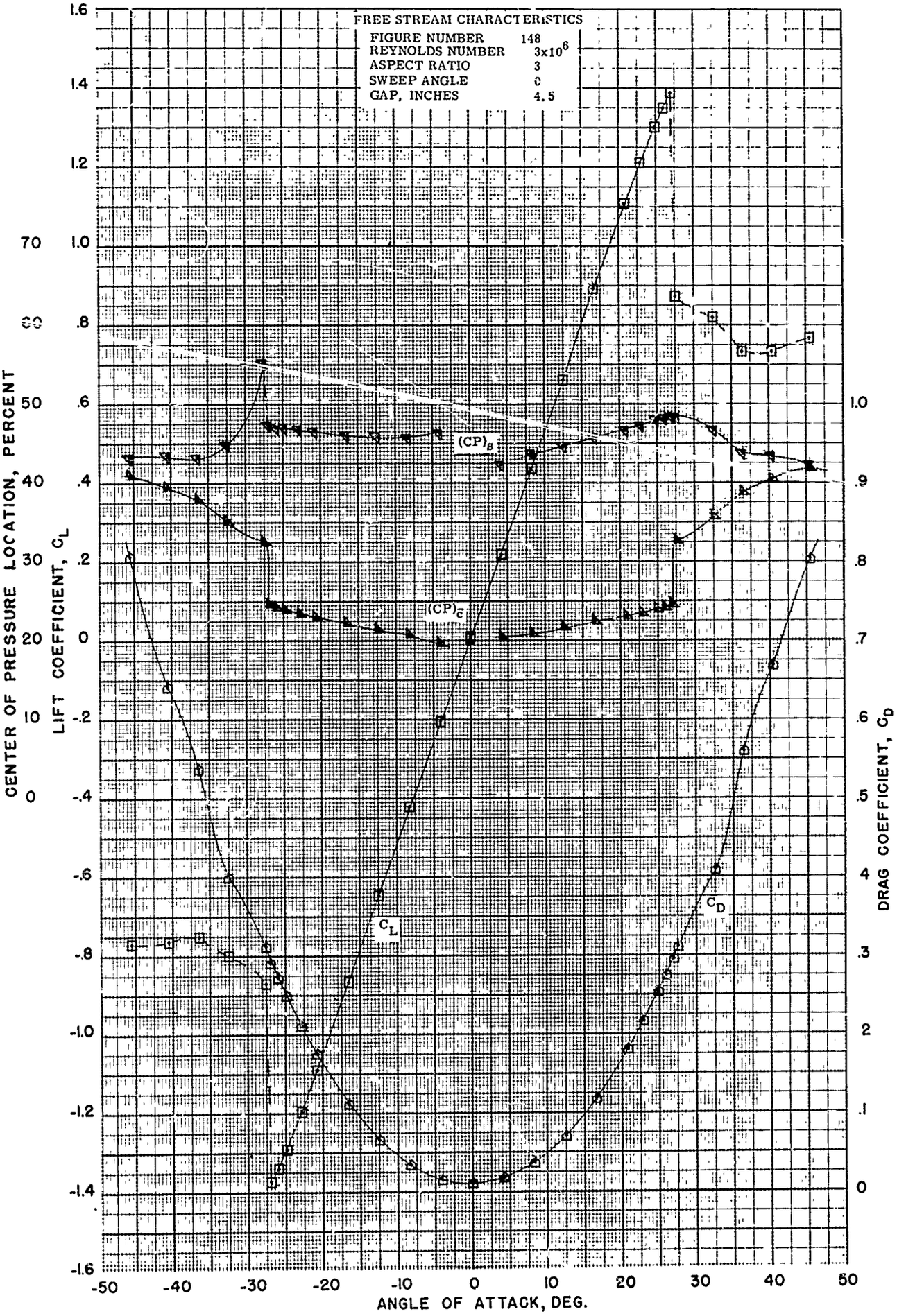
FREE STREAM CHARACTERISTICS
FIGURE NUMBER 148
REYNOLDS NUMBER 3x10^6
ASPECT RATIO 3
SWEEP ANGLE 0
GAP, INCHES 4.5
CENTER OF PRESSURE LOCATION, PERCENT
LIFT COEFFICIENT, C_L
DRAG COEFFICIENT, C_D
ANGLE OF ATTACK, DEG.
$(CP)_B$
$(CP)_C$
C_L
C_D
70
60
50
40
30
20
10
0
1.6
1.4
1.2
1.0
.8
.6
.4
.2
0
-.2
-.4
-.6
-.8
-1.0
-1.2
-1.4
-1.6
1.0
.9
.8
.7
.6
.5
.4
.3
.2
.1
0
-50
-40
-30
-20
-10
0
10
20
30
40
50

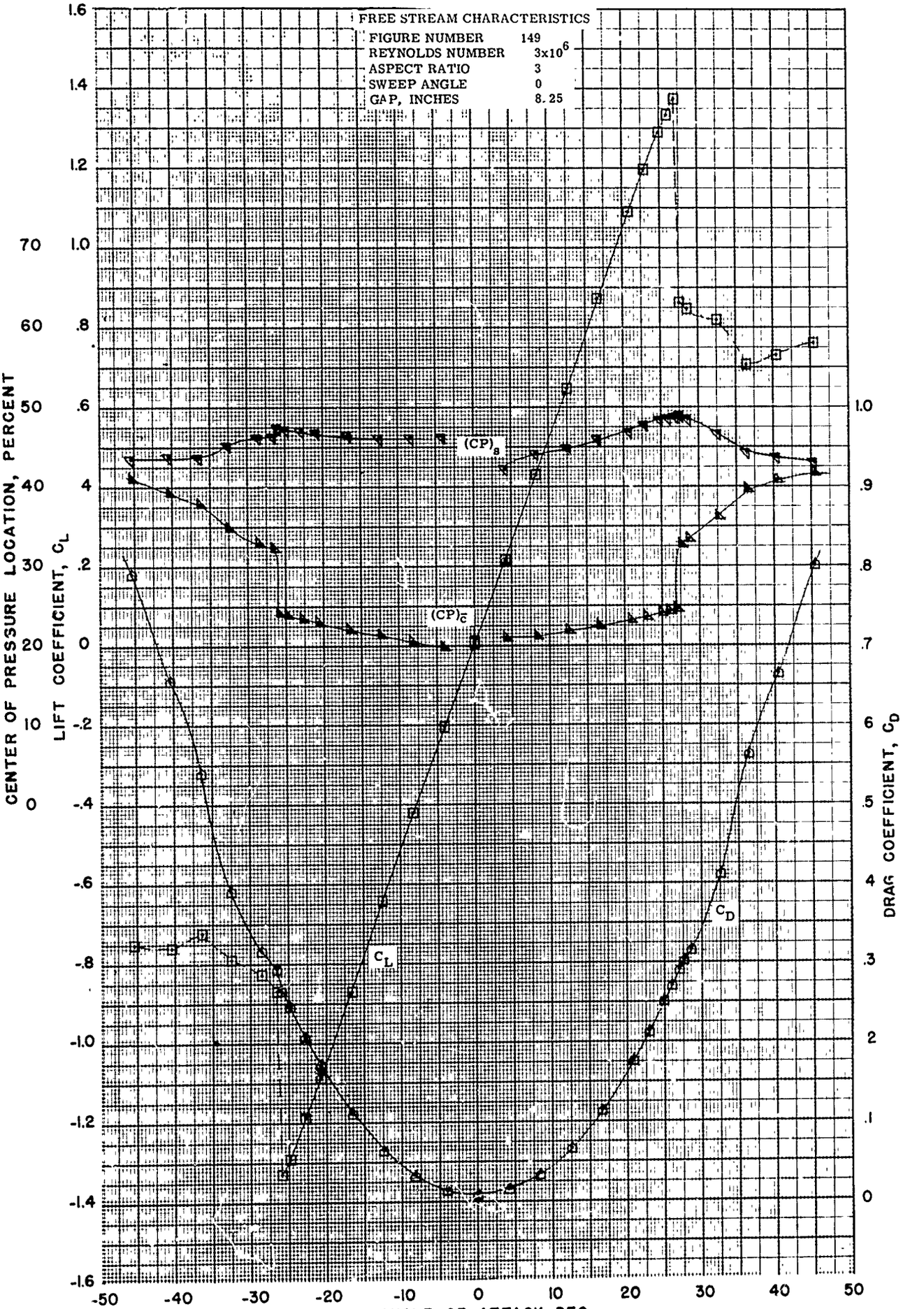
FREE STREAM CHARACTERISTICS
FIGURE NUMBER 149
REYNOLDS NUMBER 3x10^6
ASPECT RATIO 3
SWEEP ANGLE 0
GAP, INCHES 8.25
CENTER OF PRESSURE LOCATION, PERCENT
LIFT COEFFICIENT, C_L
DRAG COEFFICIENT, C_D
ANGLE OF ATTACK, DEG.
$(CP)_s$
$(CP)_{\bar{c}}$
C_L
C_D
70
60
50
40
30
20
10
0
1.6
1.4
1.2
1.0
.8
.6
.4
.2
0
-.2
-.4
-.6
-.8
-1.0
-1.2
-1.4
-1.6
1.0
.9
.8
.7
6
.5
4
.3
2
.1
0
-50
-40
-30
-20
-10
0
10
20
30
40
50

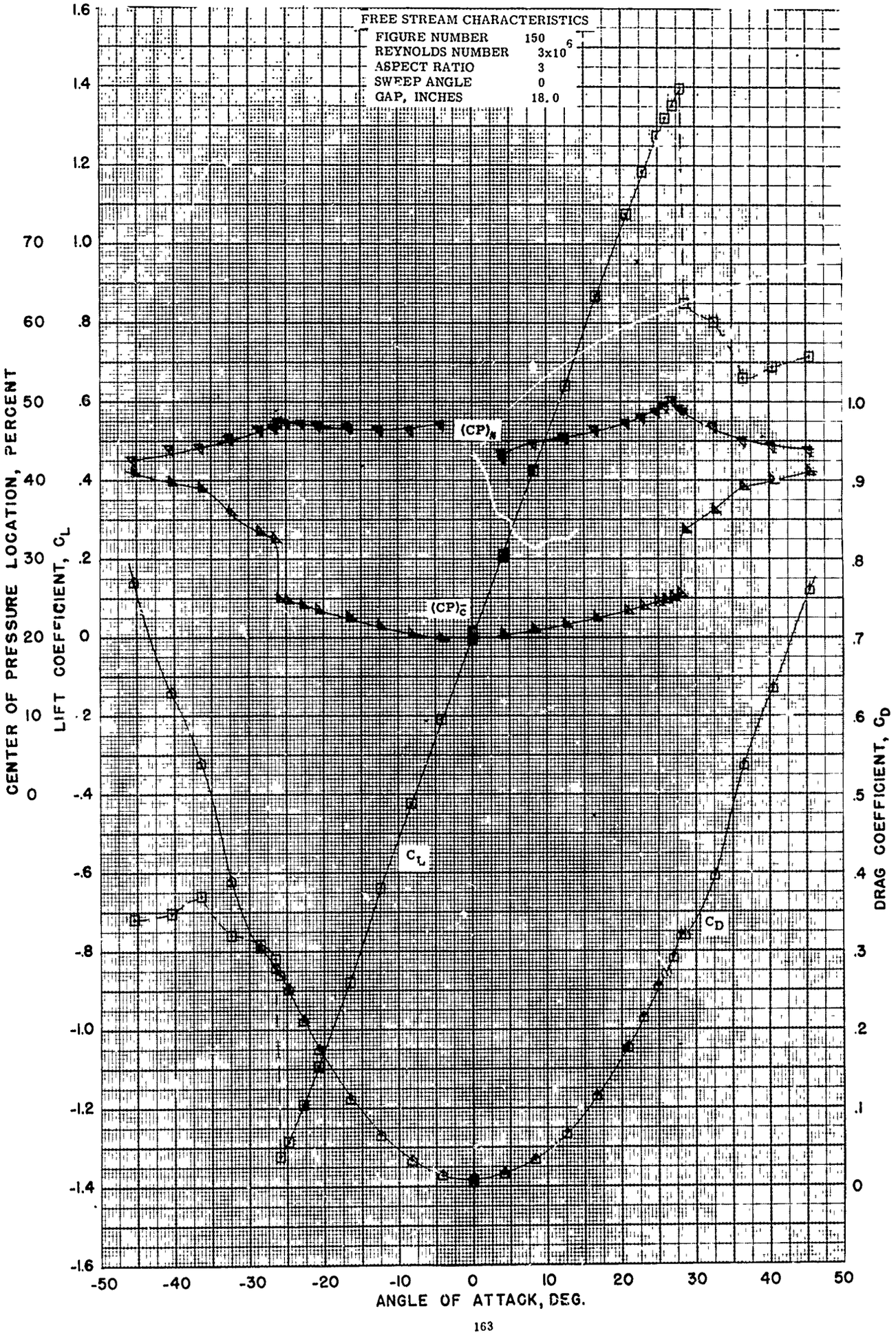
FREE STREAM CHARACTERISTICS
FIGURE NUMBER 150
REYNOLDS NUMBER 3x10^6
ASPECT RATIO 3
SWEEP ANGLE 0
GAP, INCHES 18.0
(CP)N
(CP)c
CL
CD
CENTER OF PRESSURE LOCATION, PERCENT
LIFT COEFFICIENT, CL
DRAG COEFFICIENT, CD
ANGLE OF ATTACK, DEG.
70
60
50
40
30
20
10
0
1.6
1.4
1.2
1.0
.8
.6
.4
.2
0
-.2
-.4
-.6
-.8
-1.0
-1.2
-1.4
-1.6
1.0
.9
.8
.7
.6
.5
.4
.3
.2
.1
0
-50
-40
-30
-20
-10
0
10
20
30
40
50

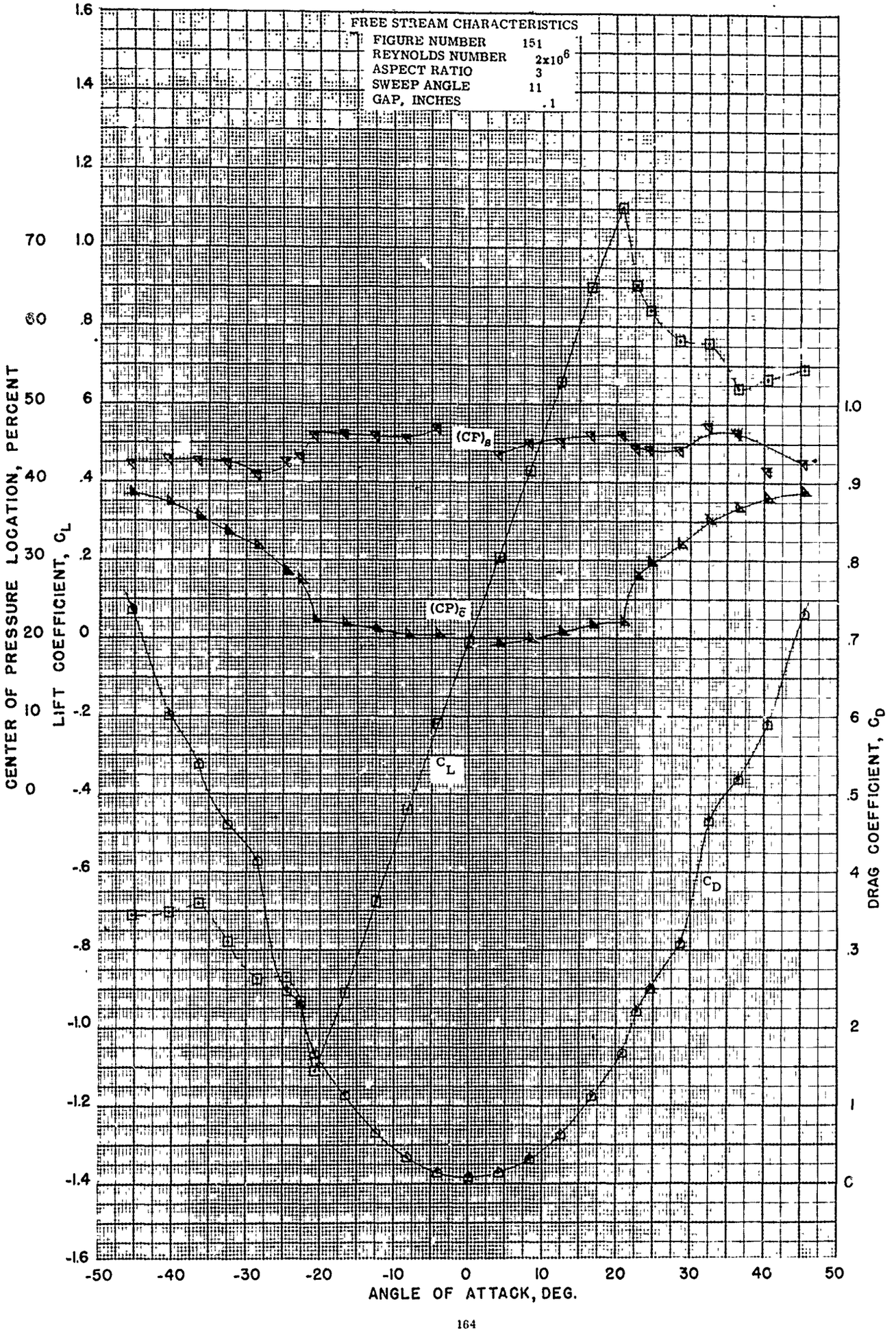
FREE STREAM CHARACTERISTICS
FIGURE NUMBER 151
REYNOLDS NUMBER 2x10^6
ASPECT RATIO 3
SWEEP ANGLE 11
GAP, INCHES .1
(CF)B
(CP)c̄
CL
CD
CENTER OF PRESSURE LOCATION, PERCENT
LIFT COEFFICIENT, CL
DRAG COEFFICIENT, CD
ANGLE OF ATTACK, DEG.
70
60
50
40
30
20
10
0
1.6
1.4
1.2
1.0
.8
.6
.4
.2
0
-.2
-.4
-.6
-.8
-1.0
-1.2
-1.4
-1.6
1.0
.9
.8
.7
.6
.5
.4
.3
.2
.1
0
-50
-40
-30
-20
-10
0
10
20
30
40
50

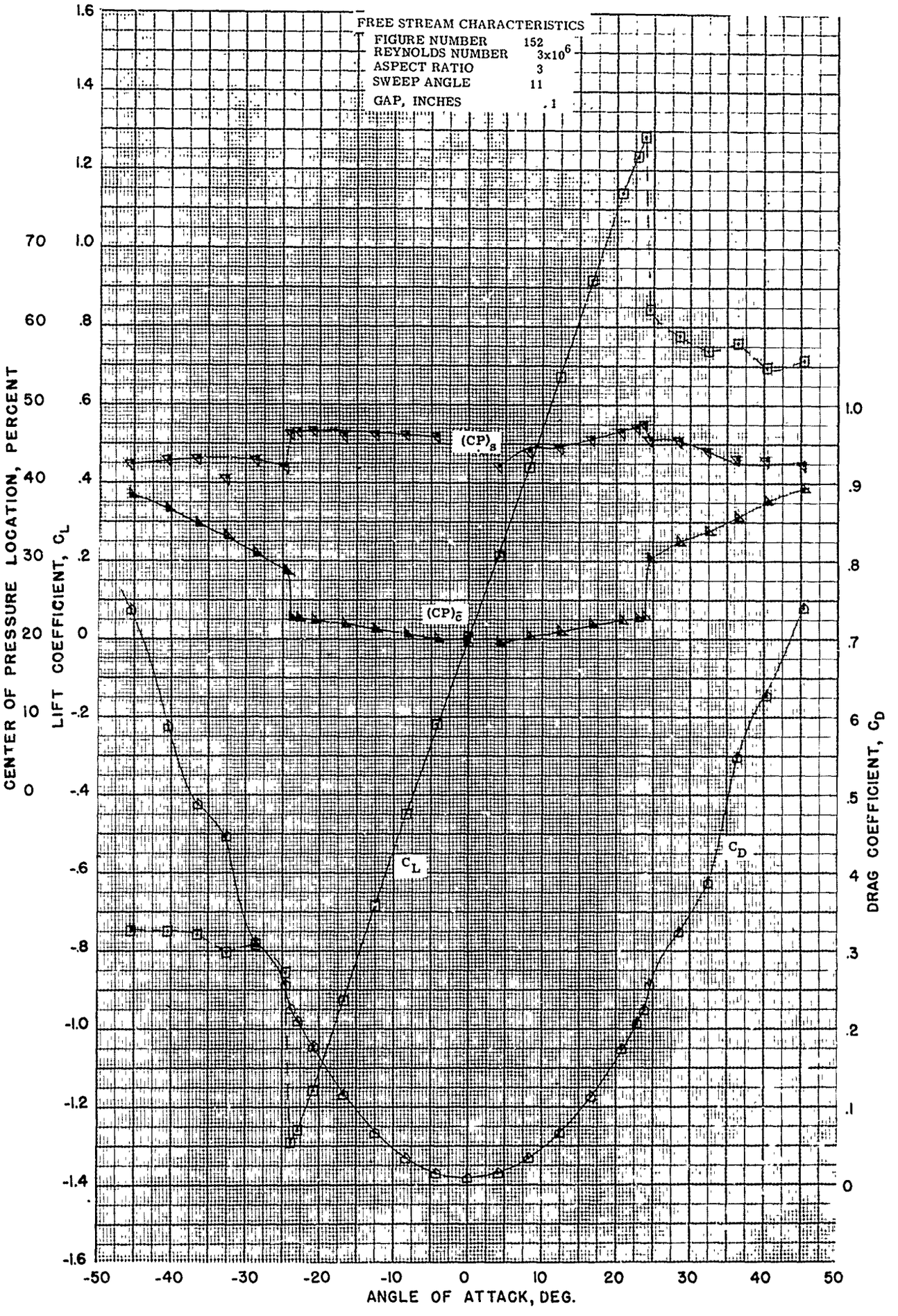
FREE STREAM CHARACTERISTICS
FIGURE NUMBER 152
REYNOLDS NUMBER 3x10^6
ASPECT RATIO 3
SWEEP ANGLE 11
GAP, INCHES .1
CENTER OF PRESSURE LOCATION, PERCENT
LIFT COEFFICIENT, C_L
DRAG COEFFICIENT, C_D
ANGLE OF ATTACK, DEG.
$(CP)_s$
$(CP)_c$
C_L
C_D
70
60
50
40
30
20
10
0
1.6
1.4
1.2
1.0
.8
.6
.4
.2
0
-.2
-.4
-.6
-.8
-1.0
-1.2
-1.4
-1.6
1.0
.9
.8
.7
.6
.5
.4
.3
.2
.1
0
-50
-40
-30
-20
-10
0
10
20
30
40
50

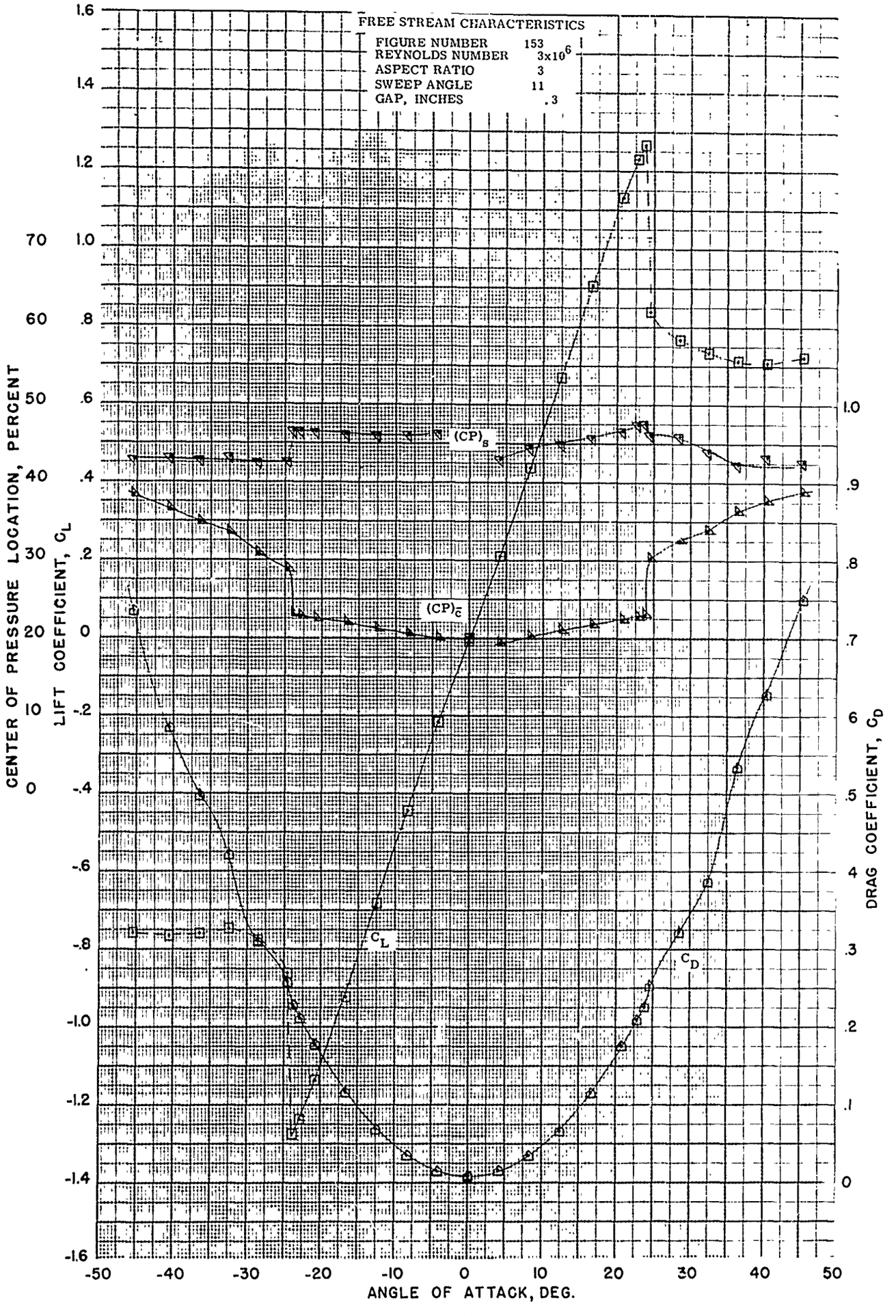
FREE STREAM CHARACTERISTICS
FIGURE NUMBER 153
REYNOLDS NUMBER 3x10^6
ASPECT RATIO 3
SWEEP ANGLE 11
GAP, INCHES .3
CENTER OF PRESSURE LOCATION, PERCENT
LIFT COEFFICIENT, C_L
DRAG COEFFICIENT, C_D
ANGLE OF ATTACK, DEG.
$(CP)_s$
$(CP)_c$
C_L
C_D
70
60
50
40
30
20
10
0
1.6
1.4
1.2
1.0
.8
.6
.4
.2
0
-.2
-.4
-.6
-.8
-1.0
-1.2
-1.4
-1.6
1.0
.9
.8
.7
.6
.5
.4
.3
.2
.1
0
-50
-40
-30
-20
-10
0
10
20
30
40
50

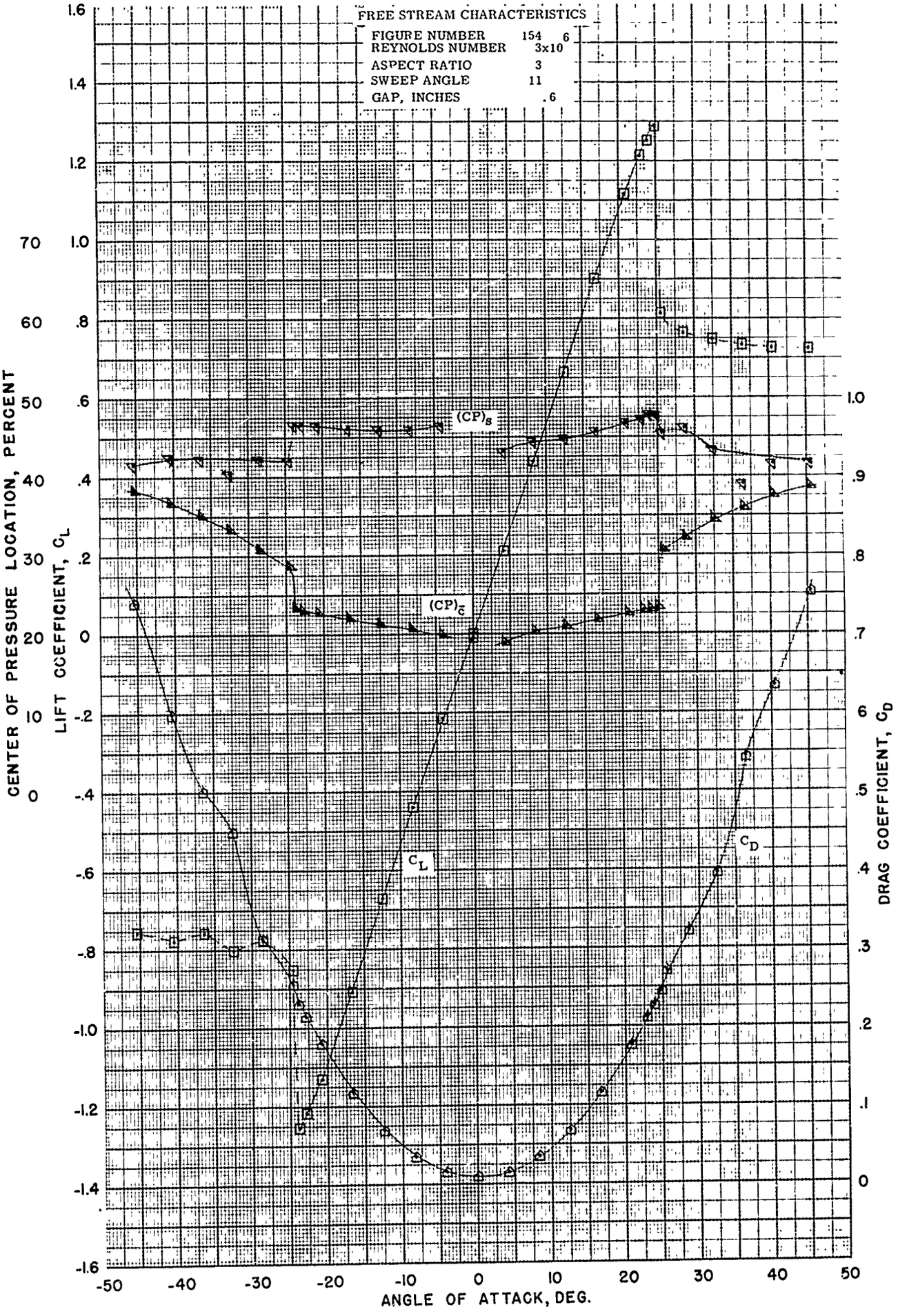
FREE STREAM CHARACTERISTICS
FIGURE NUMBER 154 6
REYNOLDS NUMBER 3x10
ASPECT RATIO 3
SWEEP ANGLE 11
GAP, INCHES .6
CENTER OF PRESSURE LOCATION, PERCENT
LIFT COEFFICIENT, C_L
DRAG COEFFICIENT, C_D
ANGLE OF ATTACK, DEG.
$(CP)_s$
$(CP)_{\bar{c}}$
C_L
C_D
70
60
50
40
30
20
10
0
1.6
1.4
1.2
1.0
.8
.6
.4
.2
0
-.2
-.4
-.6
-.8
-1.0
-1.2
-1.4
-1.6
1.0
.9
.8
.7
.6
.5
.4
.3
.2
.1
0
-50
-40
-30
-20
-10
0
10
20
30
40
50

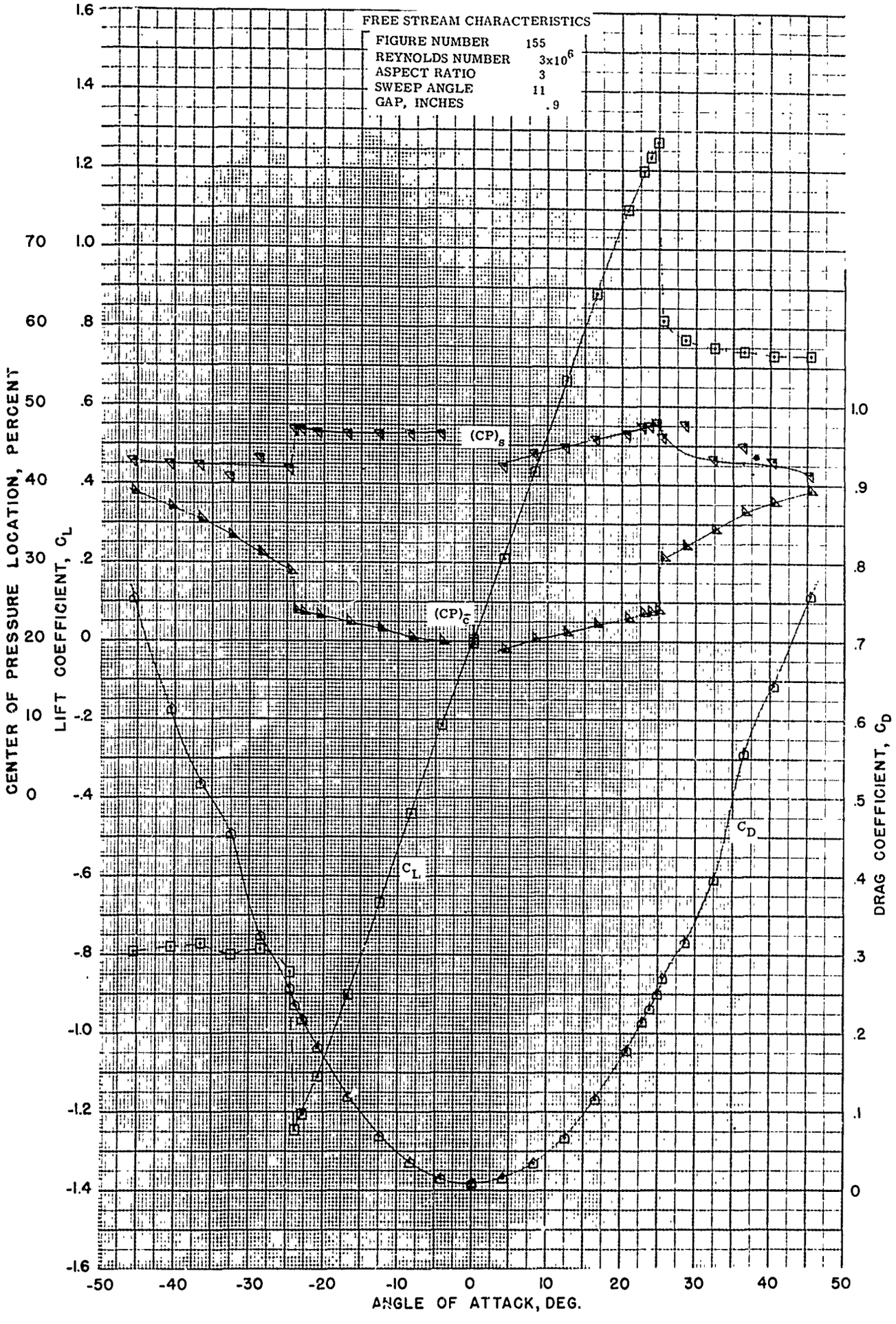
FREE STREAM CHARACTERISTICS
FIGURE NUMBER 155
REYNOLDS NUMBER 3x10^6
ASPECT RATIO 3
SWEEP ANGLE 11
GAP, INCHES .9
CENTER OF PRESSURE LOCATION, PERCENT
LIFT COEFFICIENT, C_L
DRAG COEFFICIENT, C_D
ANGLE OF ATTACK, DEG.
$(CP)_s$
$(CP)_c$
C_L
C_D
70
60
50
40
30
20
10
0
1.6
1.4
1.2
1.0
.8
.6
.4
.2
0
-.2
-.4
-.6
-.8
-1.0
-1.2
-1.4
-1.6
1.0
.9
.8
.7
.6
.5
.4
.3
.2
.1
0
-50
-40
-30
-20
-10
0
10
20
30
40
50

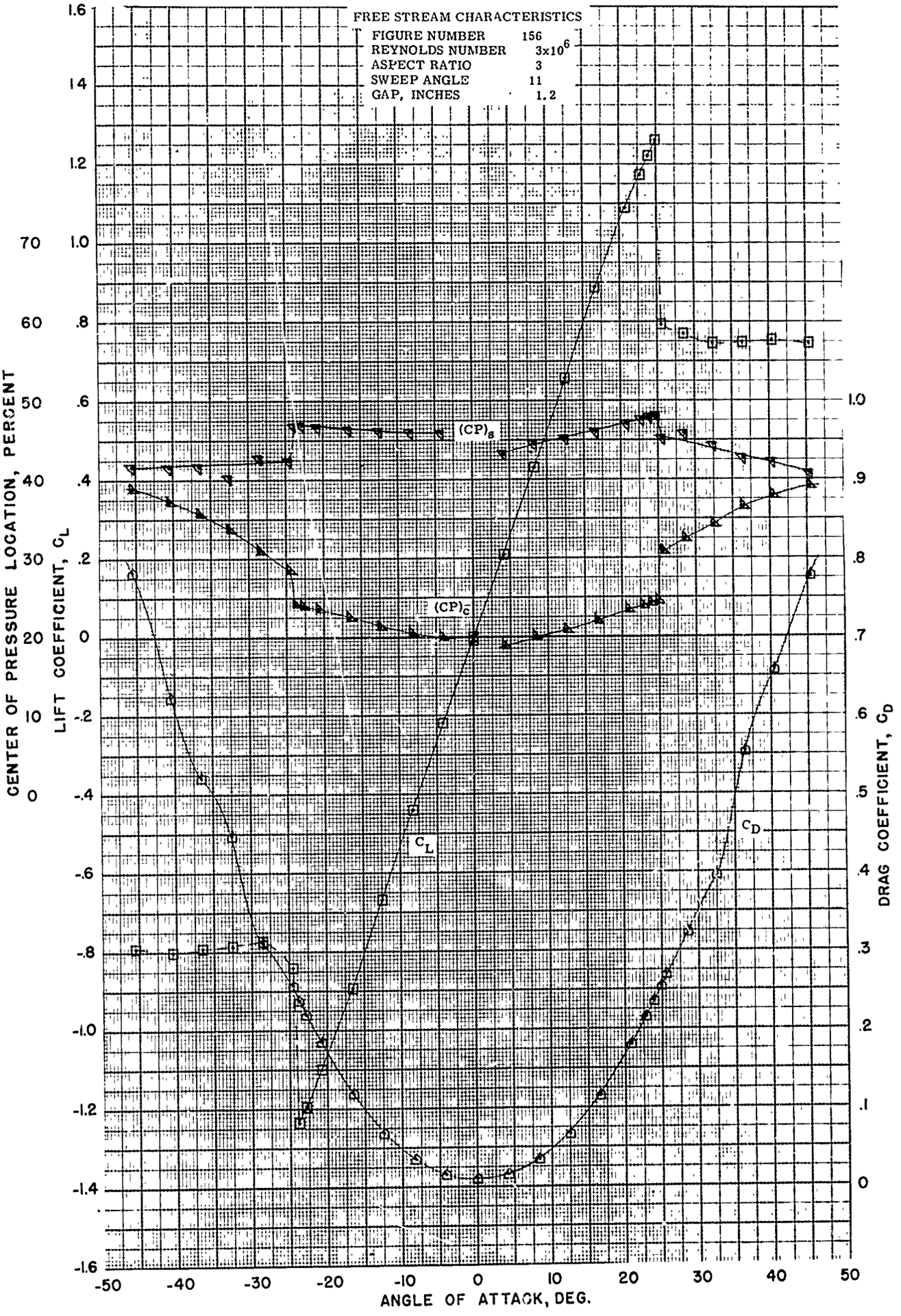
FREE STREAM CHARACTERISTICS
FIGURE NUMBER 156
REYNOLDS NUMBER 3x10^6
ASPECT RATIO 3
SWEEP ANGLE 11
GAP, INCHES 1.2
CENTER OF PRESSURE LOCATION, PERCENT
LIFT COEFFICIENT, C_L
DRAG COEFFICIENT, C_D
ANGLE OF ATTACK, DEG.
(CP)_s
(CP)_c
C_L
C_D
70
60
50
40
30
20
10
0
1.6
1.4
1.2
1.0
.8
.6
.4
.2
0
-.2
-.4
-.6
-.8
-1.0
-1.2
-1.4
-1.6
1.0
.9
.8
.7
.6
.5
.4
.3
.2
.1
0
-50
-40
-30
-20
-10
0
10
20
30
40
50

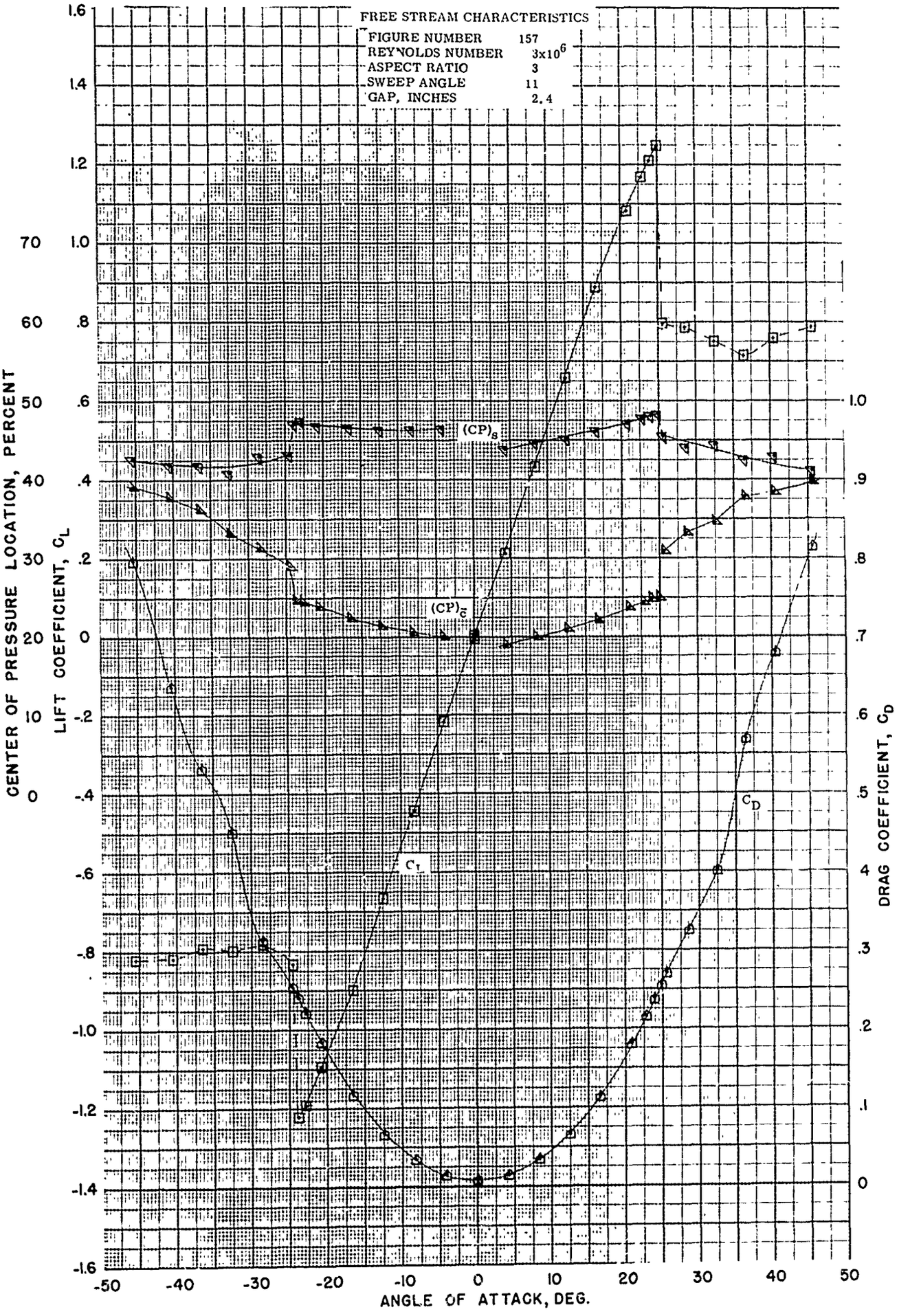
FREE STREAM CHARACTERISTICS
FIGURE NUMBER 157
REYNOLDS NUMBER 3x10^6
ASPECT RATIO 3
SWEEP ANGLE 11
GAP, INCHES 2.4
CENTER OF PRESSURE LOCATION, PERCENT
LIFT COEFFICIENT, C_L
DRAG COEFFICIENT, C_D
ANGLE OF ATTACK, DEG.
$(CP)_s$
$(CP)_{\bar{c}}$
C_L
C_D
70
60
50
40
30
20
10
0
1.6
1.4
1.2
1.0
.8
.6
.4
.2
0
-.2
-.4
-.6
-.8
-1.0
-1.2
-1.4
-1.6
1.0
.9
.8
.7
.6
.5
.4
.3
.2
.1
0
-50
-40
-30
-20
-10
0
10
20
30
40
50

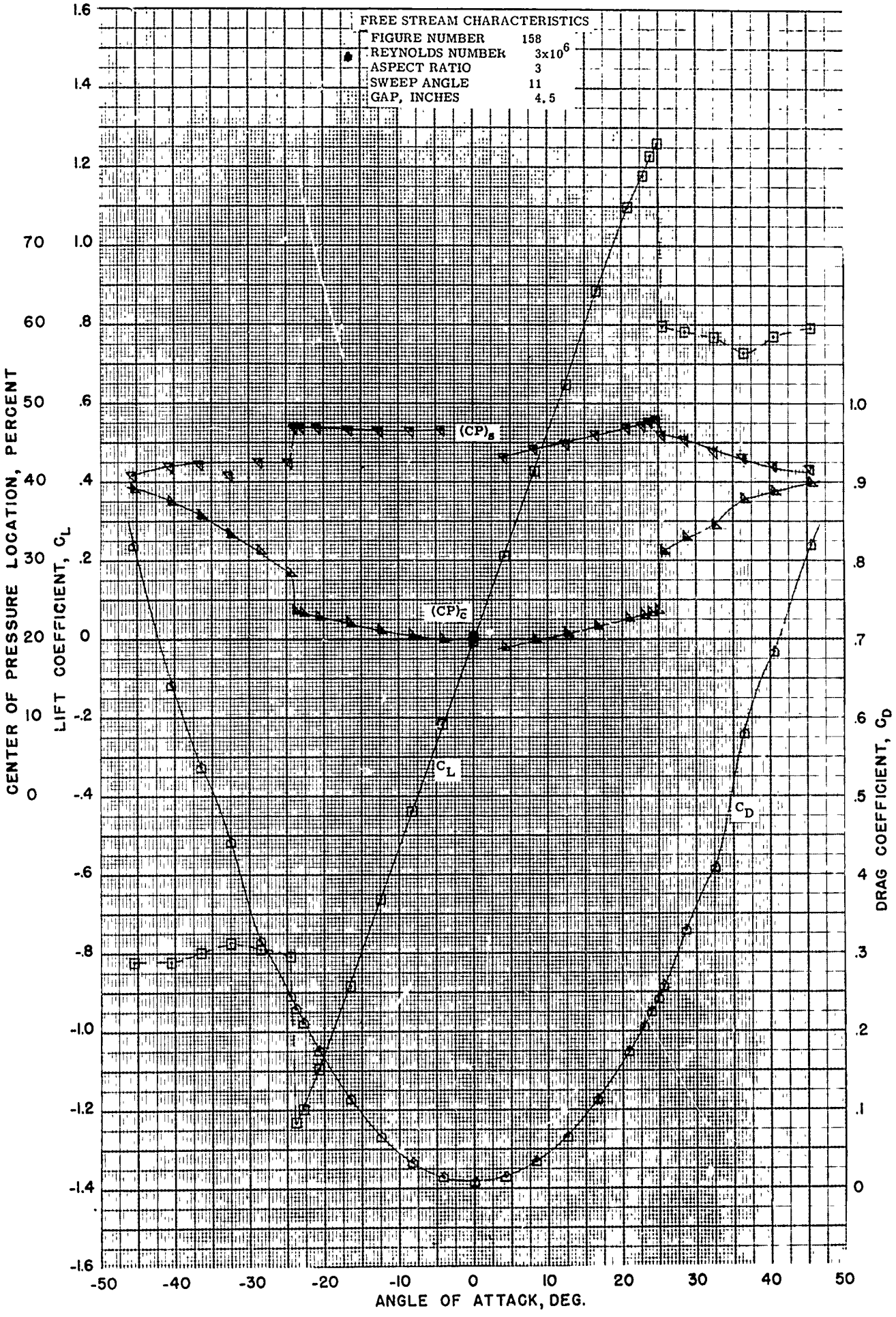
FREE STREAM CHARACTERISTICS
FIGURE NUMBER 158
REYNOLDS NUMBER 3x10^6
ASPECT RATIO 3
SWEEP ANGLE 11
GAP, INCHES 4.5
(CP)s
(CP)c
CL
CD
CENTER OF PRESSURE LOCATION, PERCENT
LIFT COEFFICIENT, CL
DRAG COEFFICIENT, CD
ANGLE OF ATTACK, DEG.
70
60
50
40
30
20
10
0
1.6
1.4
1.2
1.0
.8
.6
.4
.2
0
-.2
-.4
-.6
-.8
-1.0
-1.2
-1.4
-1.6
1.0
.9
.8
.7
.6
.5
.4
.3
.2
.1
0
-50
-40
-30
-20
-10
0
10
20
30
40
50

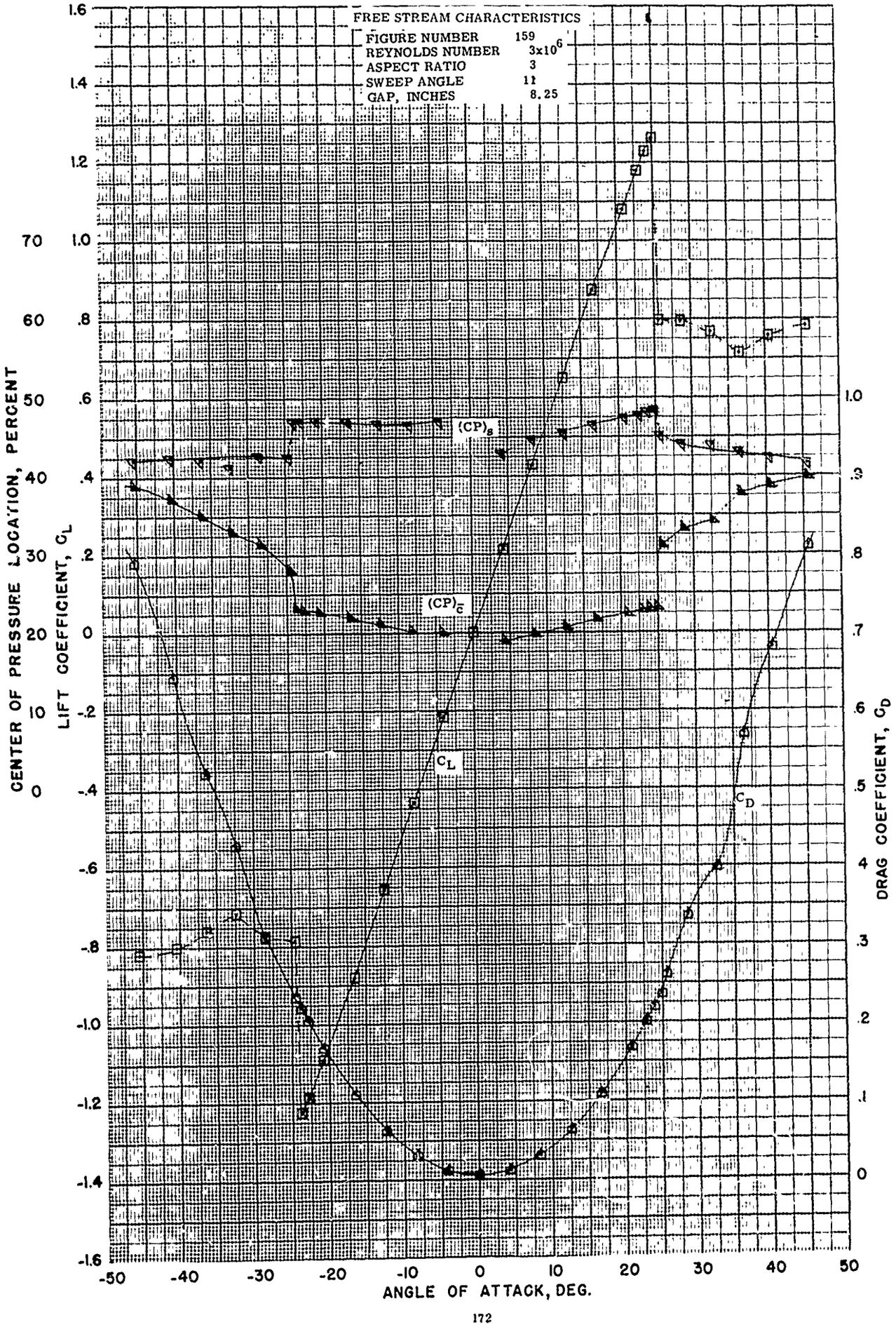
FREE STREAM CHARACTERISTICS
FIGURE NUMBER 159
REYNOLDS NUMBER 3x10^6
ASPECT RATIO 3
SWEEP ANGLE 11
GAP, INCHES 8.25
CENTER OF PRESSURE LOCATION, PERCENT
LIFT COEFFICIENT, C_L
DRAG COEFFICIENT, C_D
ANGLE OF ATTACK, DEG.
$(CP)_s$
$(CP)_{\bar{c}}$
C_L
C_D
70
60
50
40
30
20
10
0
1.6
1.4
1.2
1.0
.8
.6
.4
.2
0
-.2
-.4
-.6
-.8
-1.0
-1.2
-1.4
-1.6
1.0
.9
.8
.7
.6
.5
.4
.3
.2
.1
0
-50
-40
-30
-20
-10
0
10
20
30
40
50

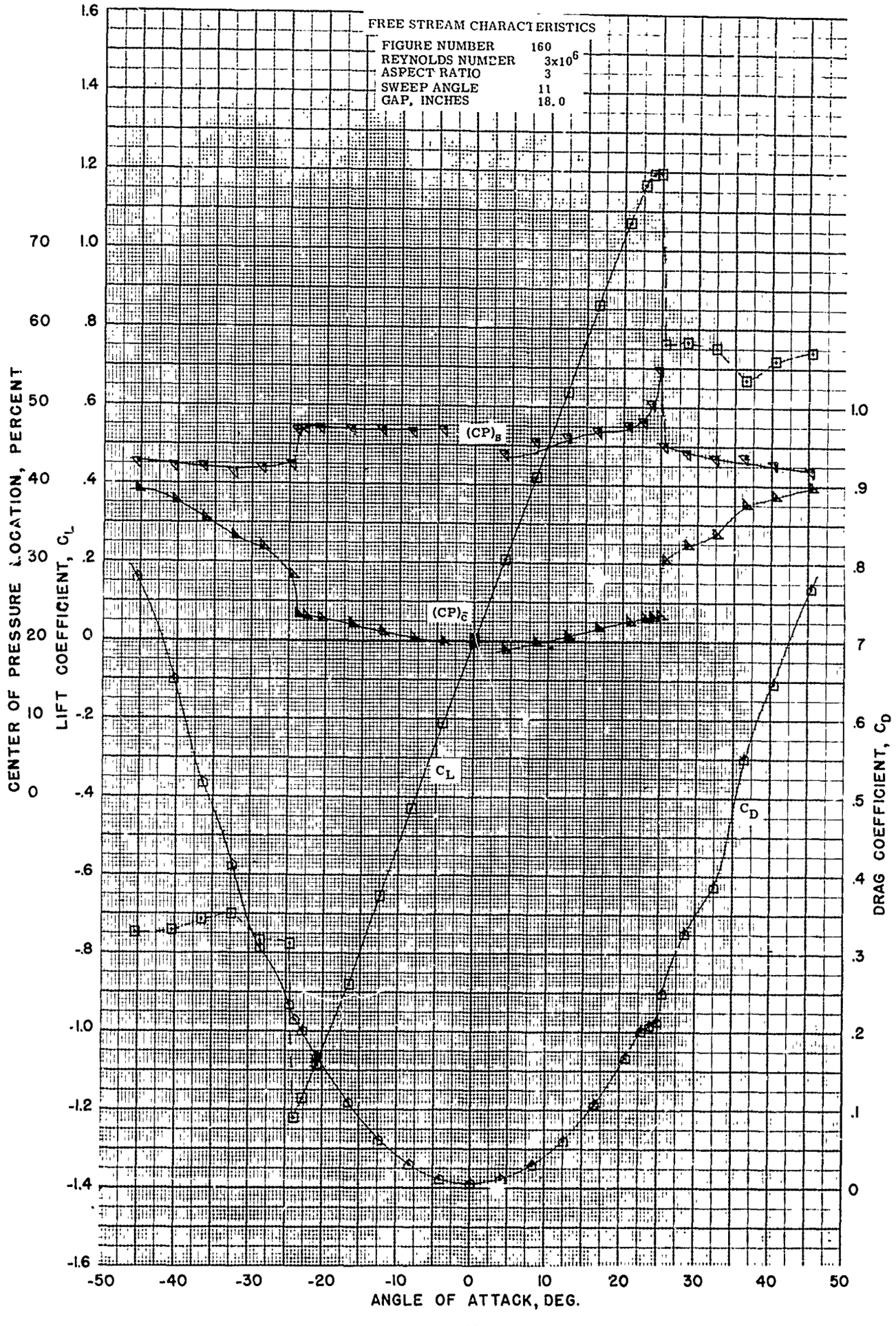
FREE STREAM CHARACTERISTICS
FIGURE NUMBER 160
REYNOLDS NUMBER 3x10^6
ASPECT RATIO 3
SWEEP ANGLE 11
GAP, INCHES 18.0
CENTER OF PRESSURE LOCATION, PERCENT
LIFT COEFFICIENT, C_L
DRAG COEFFICIENT, C_D
ANGLE OF ATTACK, DEG.
$(CP)_s$
$(CP)_c$
C_L
C_D
70
60
50
40
30
20
10
0
1.6
1.4
1.2
1.0
.8
.6
.4
.2
0
-.2
-.4
-.6
-.8
-1.0
-1.2
-1.4
-1.6
1.0
.9
.8
.7
.6
.5
.4
.3
.2
.1
0
-50
-40
-30
-20
-10
0
10
20
30
40
50

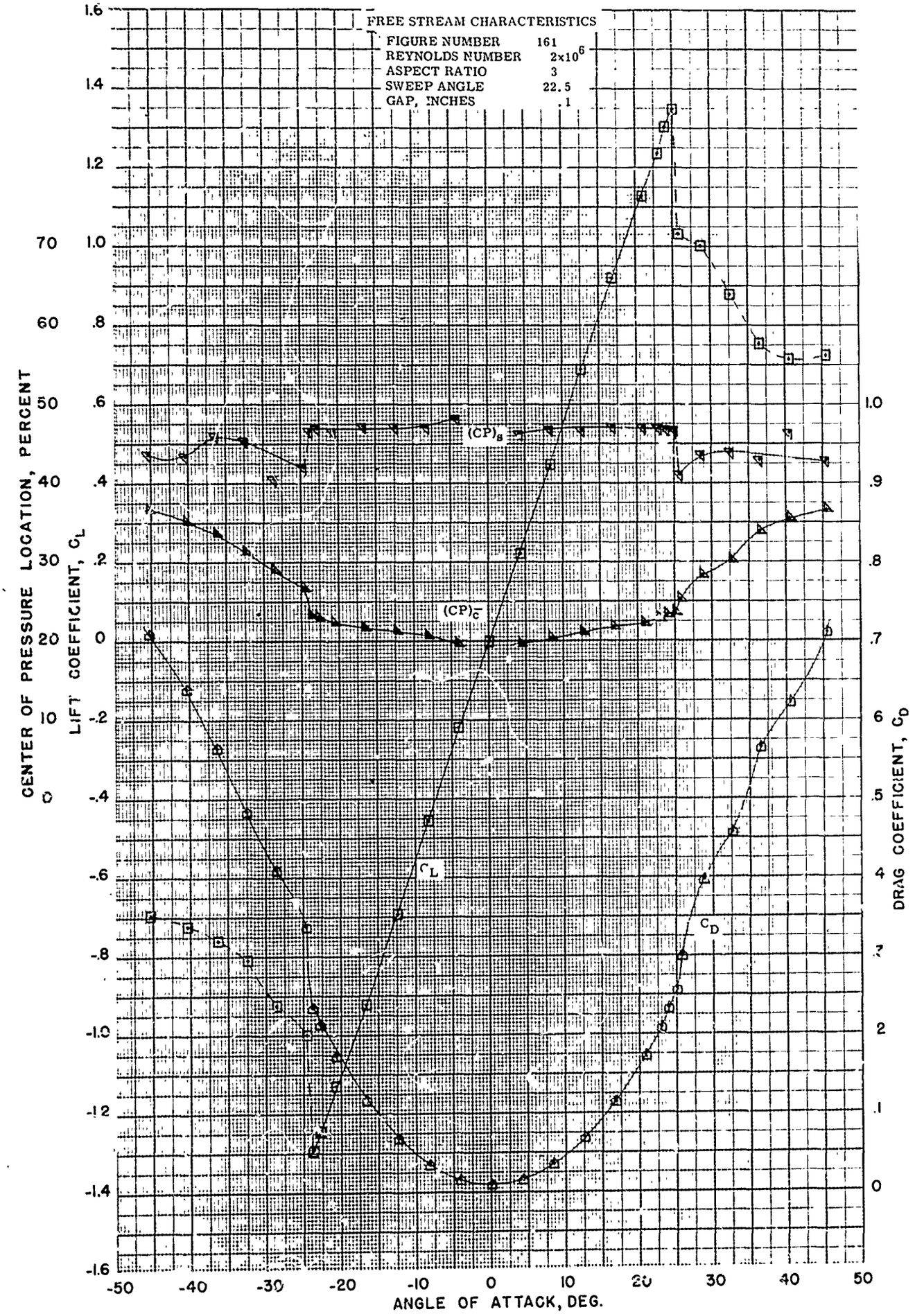
FREE STREAM CHARACTERISTICS
FIGURE NUMBER 161
REYNOLDS NUMBER 2x10^6
ASPECT RATIO 3
SWEEP ANGLE 22.5
GAP, INCHES .1
CENTER OF PRESSURE LOCATION, PERCENT
LIFT COEFFICIENT, C_L
DRAG COEFFICIENT, C_D
ANGLE OF ATTACK, DEG.
$(CP)_s$
$(CP)_{\bar{c}}$
C_L
C_D
70
60
50
40
30
20
10
0
1.6
1.4
1.2
1.0
.8
.6
.4
.2
0
-.2
-.4
-.6
-.8
-1.0
-1.2
-1.4
-1.6
1.0
.9
.8
.7
6
.5
4
2
0
-50
-40
-30
-20
-10
0
10
20
30
40
50

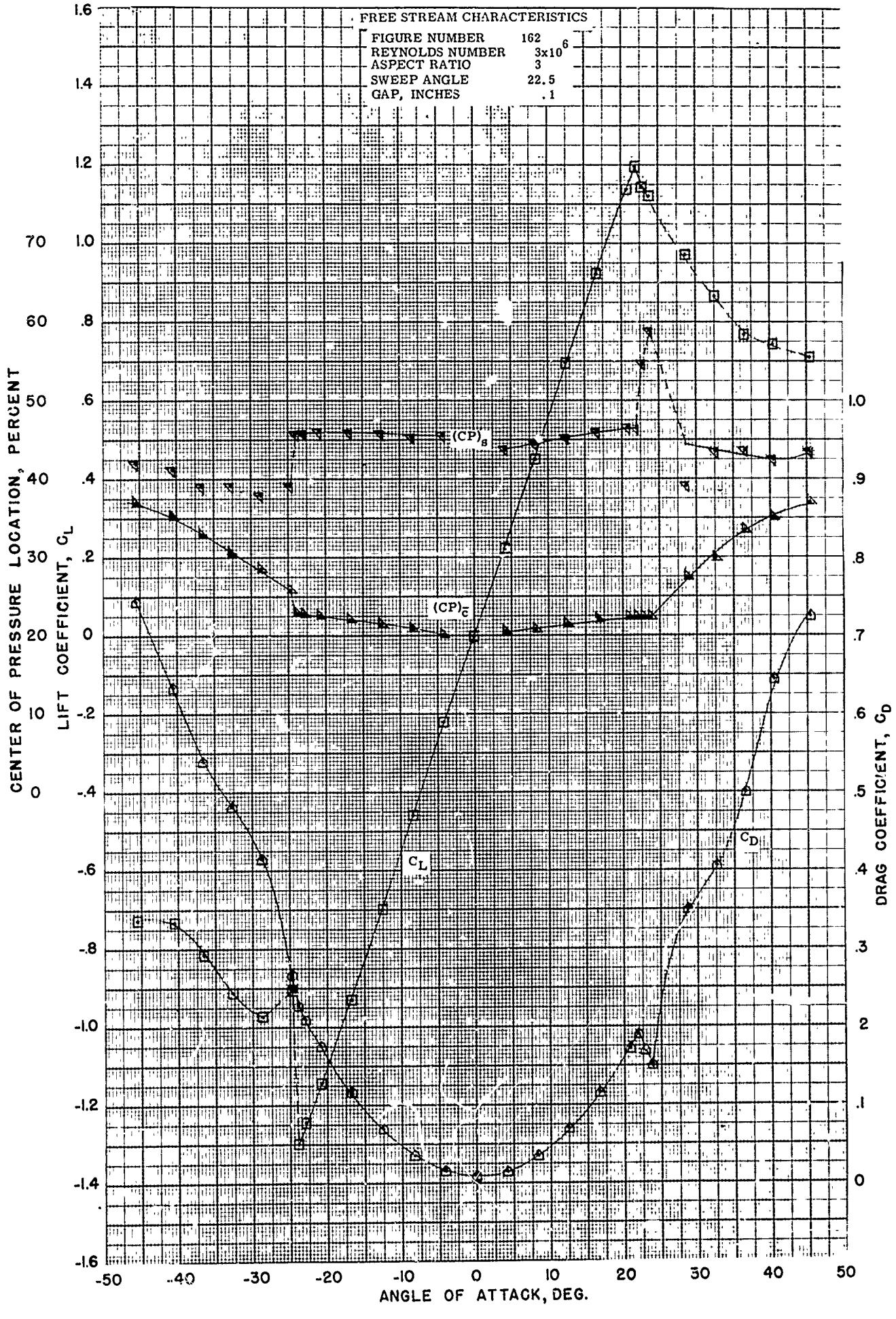
FREE STREAM CHARACTERISTICS
FIGURE NUMBER 162
REYNOLDS NUMBER 3x10^6
ASPECT RATIO 3
SWEEP ANGLE 22.5
GAP, INCHES .1
CENTER OF PRESSURE LOCATION, PERCENT
LIFT COEFFICIENT, C_L
DRAG COEFFICIENT, C_D
ANGLE OF ATTACK, DEG.
$(CP)_s$
$(CP)_{\bar{c}}$
C_L
C_D
70
60
50
40
30
20
10
0
1.6
1.4
1.2
1.0
.8
.6
.4
.2
0
-.2
-.4
-.6
-.8
-1.0
-1.2
-1.4
-1.6
1.0
.9
.8
.7
.6
.5
.4
.3
2
.1
0
-50
-40
-30
-20
-10
0
10
20
30
40
50

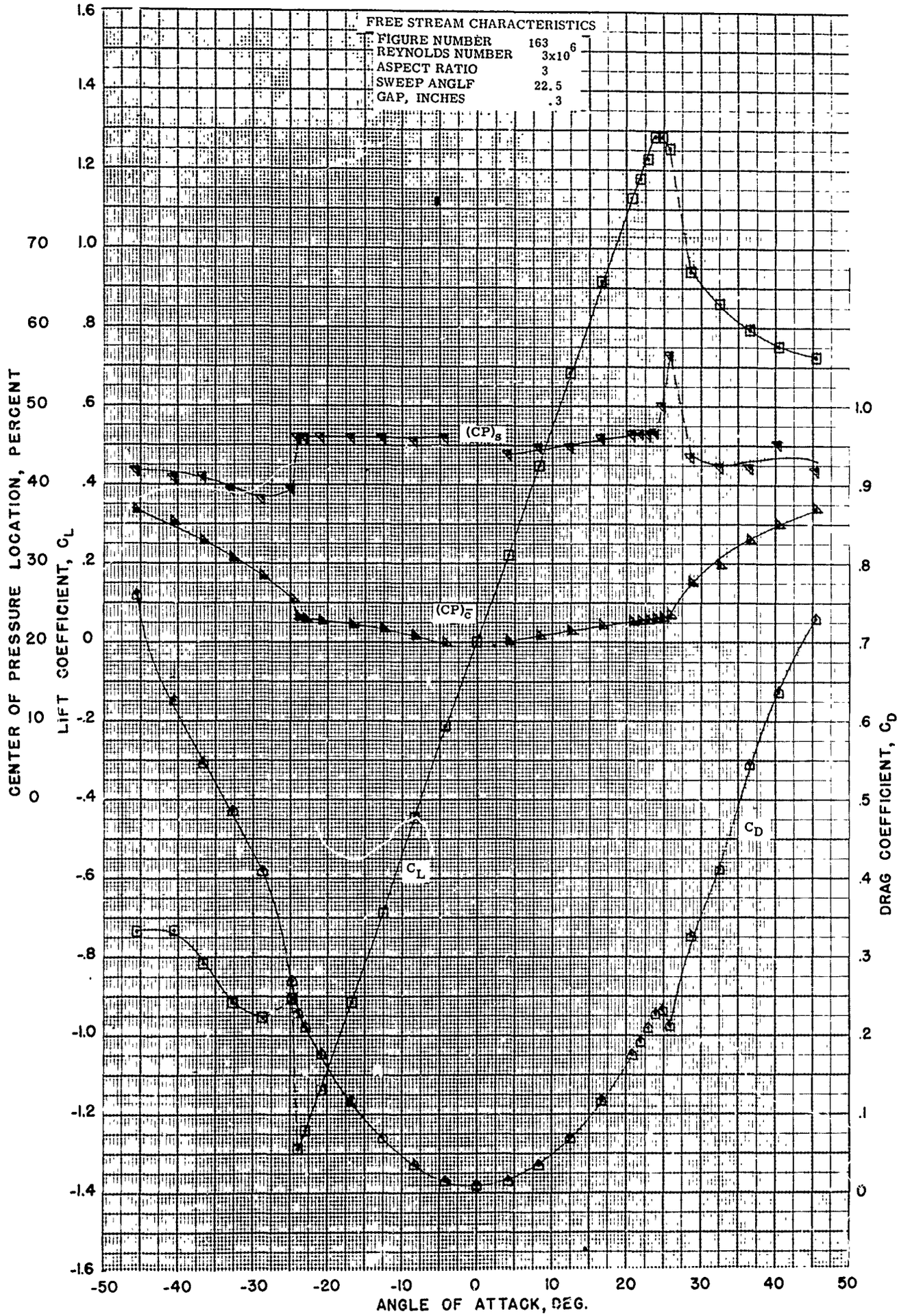
FREE STREAM CHARACTERISTICS
FIGURE NUMBER 163
REYNOLDS NUMBER 3x10^6
ASPECT RATIO 3
SWEEP ANGLE 22.5
GAP, INCHES .3
CENTER OF PRESSURE LOCATION, PERCENT
LIFT COEFFICIENT, C_L
DRAG COEFFICIENT, C_D
ANGLE OF ATTACK, DEG.
$(CP)_s$
$(CP)_{\bar{c}}$
C_L
C_D
70
60
50
40
30
20
10
0
1.6
1.4
1.2
1.0
.8
.6
.4
.2
0
-.2
-.4
-.6
-.8
-1.0
-1.2
-1.4
-1.6
1.0
.9
.8
.7
.6
.5
.4
.3
.2
.1
0
-50
-40
-30
-20
-10
0
10
20
30
40
50

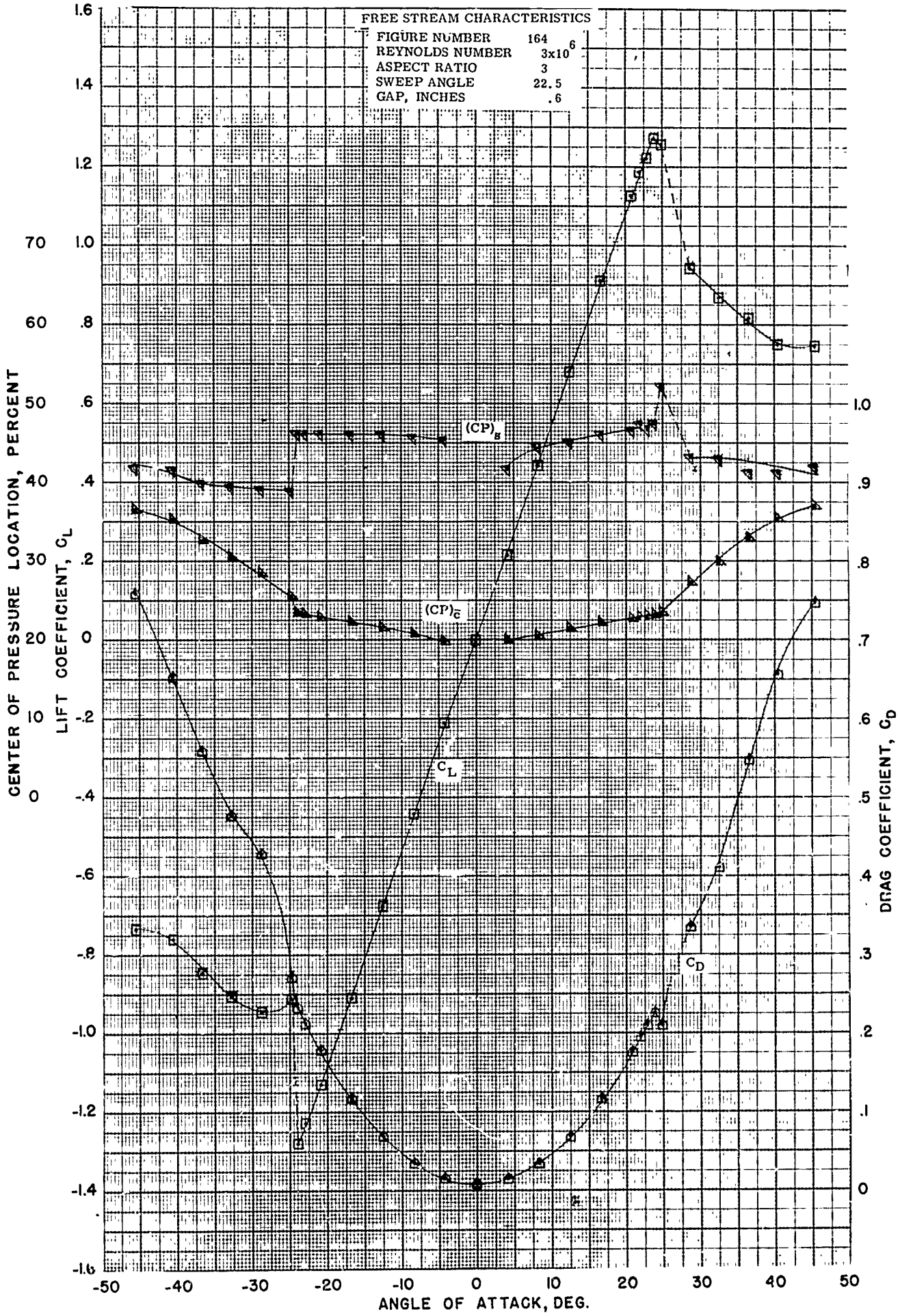
FREE STREAM CHARACTERISTICS
FIGURE NUMBER 164
REYNOLDS NUMBER 3x10^6
ASPECT RATIO 3
SWEEP ANGLE 22.5
GAP, INCHES .6
CENTER OF PRESSURE LOCATION, PERCENT
LIFT COEFFICIENT, C_L
DRAG COEFFICIENT, C_D
ANGLE OF ATTACK, DEG.
$(CP)_g$
$(CP)_{\bar{c}}$
C_L
C_D
70
60
50
40
30
20
10
0
1.6
1.4
1.2
1.0
.8
.6
.4
.2
0
-.2
-.4
-.6
-.8
-1.0
-1.2
-1.4
-1.6
1.0
.9
.8
.7
.6
.5
.4
.3
.2
.1
0
-50
-40
-30
-20
-10
0
10
20
30
40
50

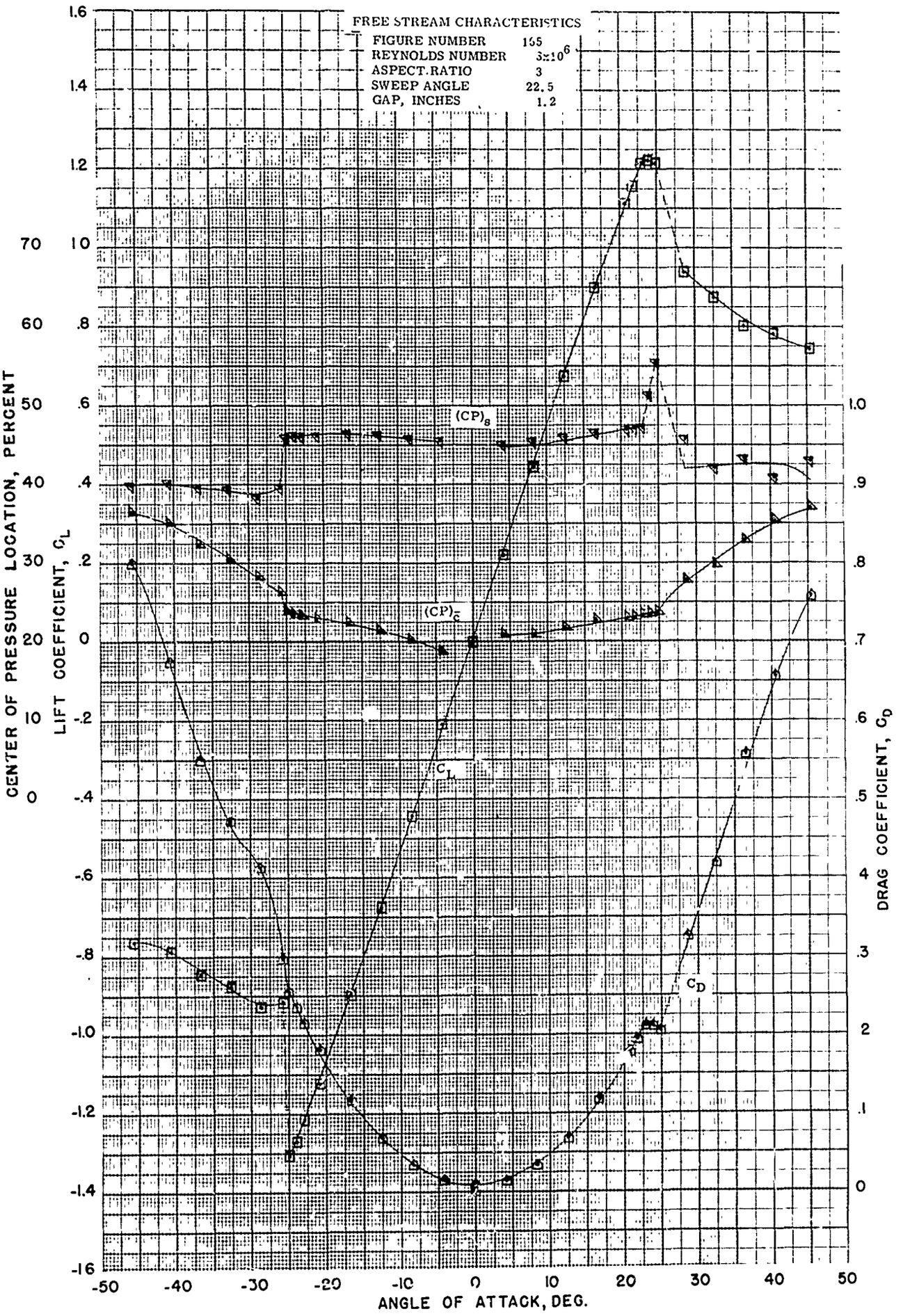
FREE STREAM CHARACTERISTICS
FIGURE NUMBER 165
REYNOLDS NUMBER 3×10^6
ASPECT RATIO 3
SWEEP ANGLE 22.5
GAP, INCHES 1.2
$(CP)_s$
$(CP)_{\bar{c}}$
C_L
C_D
CENTER OF PRESSURE LOCATION, PERCENT
LIFT COEFFICIENT, C_L
DRAG COEFFICIENT, C_D
ANGLE OF ATTACK, DEG.
70 60 50 40 30 20 10 0
1.6 1.4 1.2 1.0 .8 .6 .4 .2 0 -.2 -.4 -.6 -.8 -1.0 -1.2 -1.4 -1.6
1.0 .9 .8 .7 .6 .5 .4 .3 .2 .1 0
-50 -40 -30 -20 -10 0 10 20 30 40 50

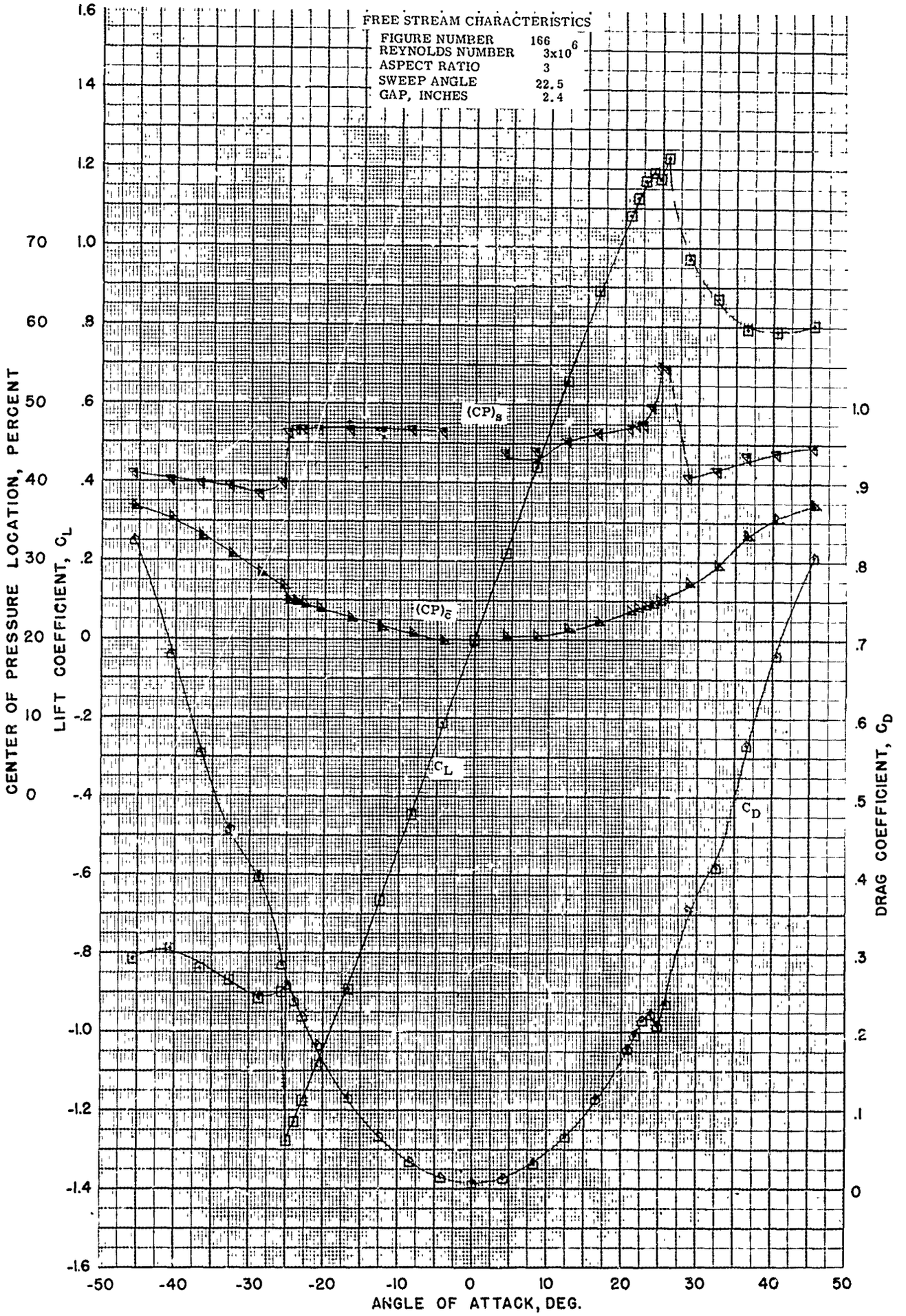
FREE STREAM CHARACTERISTICS
FIGURE NUMBER 166
REYNOLDS NUMBER 3x10^6
ASPECT RATIO 3
SWEEP ANGLE 22.5
GAP, INCHES 2.4
CENTER OF PRESSURE LOCATION, PERCENT
LIFT COEFFICIENT, C_L
DRAG COEFFICIENT, C_D
ANGLE OF ATTACK, DEG.
$(CP)_s$
$(CP)_c$
C_L
C_D
70
60
50
40
30
20
10
0
1.6
1.4
1.2
1.0
.8
.6
.4
.2
0
-.2
-.4
-.6
-.8
-1.0
-1.2
-1.4
-1.6
1.0
.9
.8
.7
.6
.5
.4
.3
.2
.1
0
-50
-40
-30
-20
-10
0
10
20
30
40
50

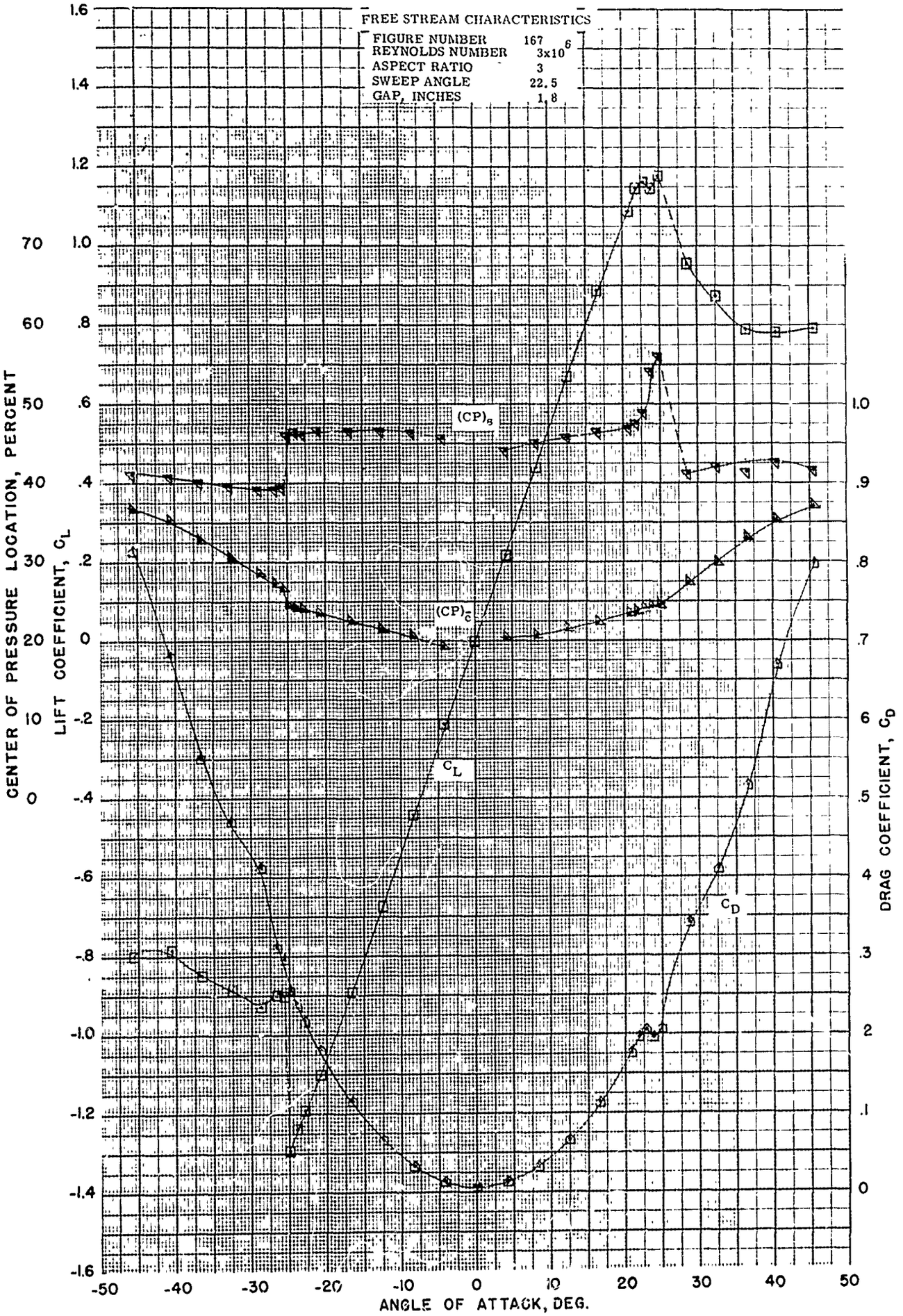
FREE STREAM CHARACTERISTICS
FIGURE NUMBER 167
REYNOLDS NUMBER 3x10^6
ASPECT RATIO 3
SWEEP ANGLE 22.5
GAP, INCHES 1.8
CENTER OF PRESSURE LOCATION, PERCENT
LIFT COEFFICIENT, C_L
DRAG COEFFICIENT, C_D
ANGLE OF ATTACK, DEG.
$(CP)_s$
$(CP)_{\bar{c}}$
C_L
C_D
70
60
50
40
30
20
10
0
1.6
1.4
1.2
1.0
.8
.6
.4
.2
0
-.2
-.4
-.6
-.8
-1.0
-1.2
-1.4
-1.6
1.0
.9
.8
.7
6
.5
4
.3
2
.1
0
-50
-40
-30
-20
-10
0
10
20
30
40
50

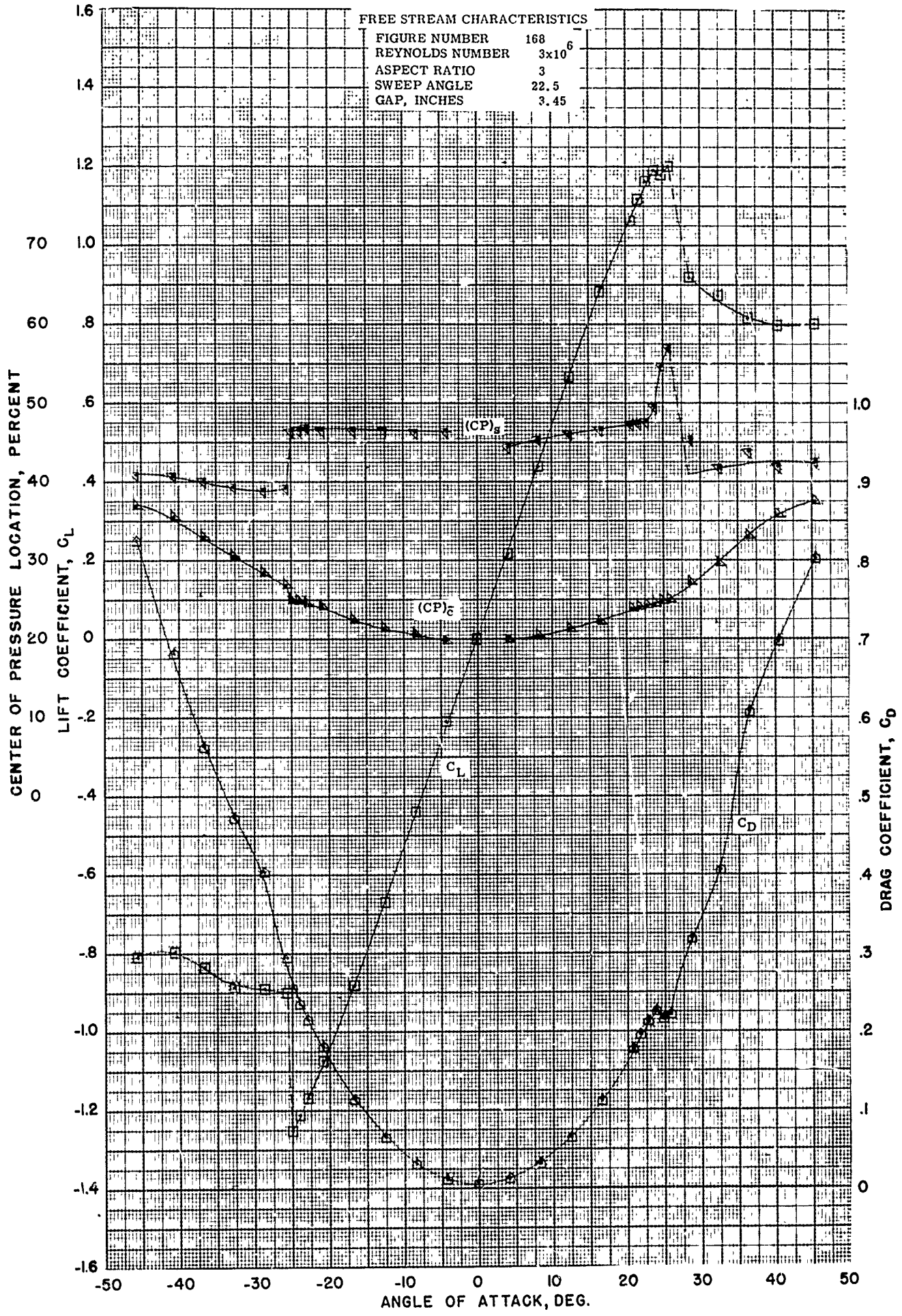
FREE STREAM CHARACTERISTICS
FIGURE NUMBER 168
REYNOLDS NUMBER 3x10^6
ASPECT RATIO 3
SWEEP ANGLE 22.5
GAP, INCHES 3.45
CENTER OF PRESSURE LOCATION, PERCENT
LIFT COEFFICIENT, C_L
DRAG COEFFICIENT, C_D
ANGLE OF ATTACK, DEG.
$(CP)_s$
$(CP)_c$
C_L
C_D
70
60
50
40
30
20
10
0
1.6
1.4
1.2
1.0
.8
.6
.4
.2
0
-.2
-.4
-.6
-.8
-1.0
-1.2
-1.4
-1.6
1.0
.9
.8
.7
.6
.5
.4
.3
.2
.1
0
-50
-40
-30
-20
-10
0
10
20
30
40
50

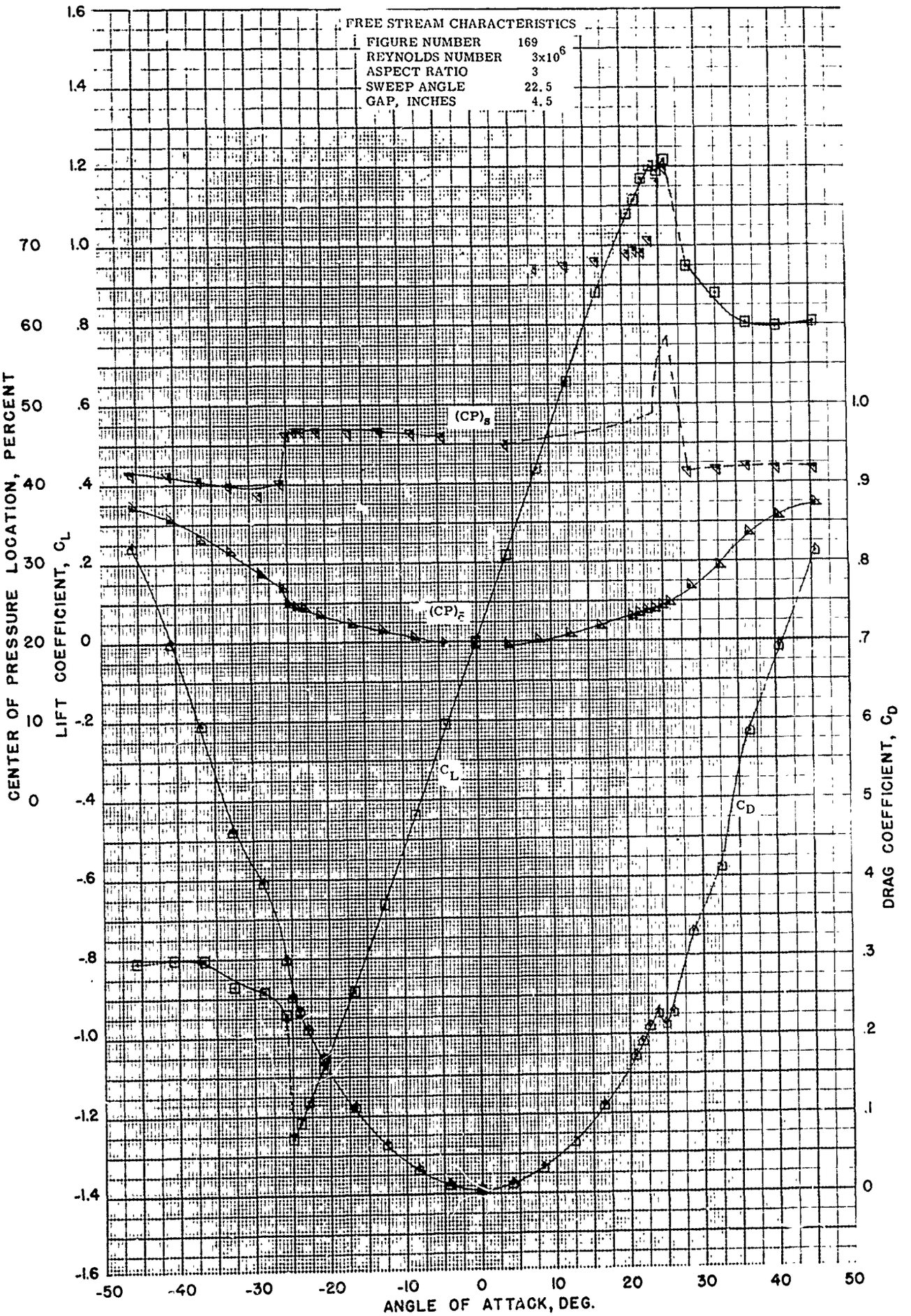
FREE STREAM CHARACTERISTICS
FIGURE NUMBER 169
REYNOLDS NUMBER 3x10^6
ASPECT RATIO 3
SWEEP ANGLE 22.5
GAP, INCHES 4.5
CENTER OF PRESSURE LOCATION, PERCENT
LIFT COEFFICIENT, C_L
DRAG COEFFICIENT, C_D
ANGLE OF ATTACK, DEG.
$(CP)_S$
$(CP)_F$
C_L
C_D
70
60
50
40
30
20
10
0
1.6
1.4
1.2
1.0
.8
.6
.4
.2
0
-.2
-.4
-.6
-.8
-1.0
-1.2
-1.4
-1.6
1.0
.9
.8
.7
6
5
4
.3
.2
.1
0
-50
-40
-30
-20
-10
0
10
20
30
40
50

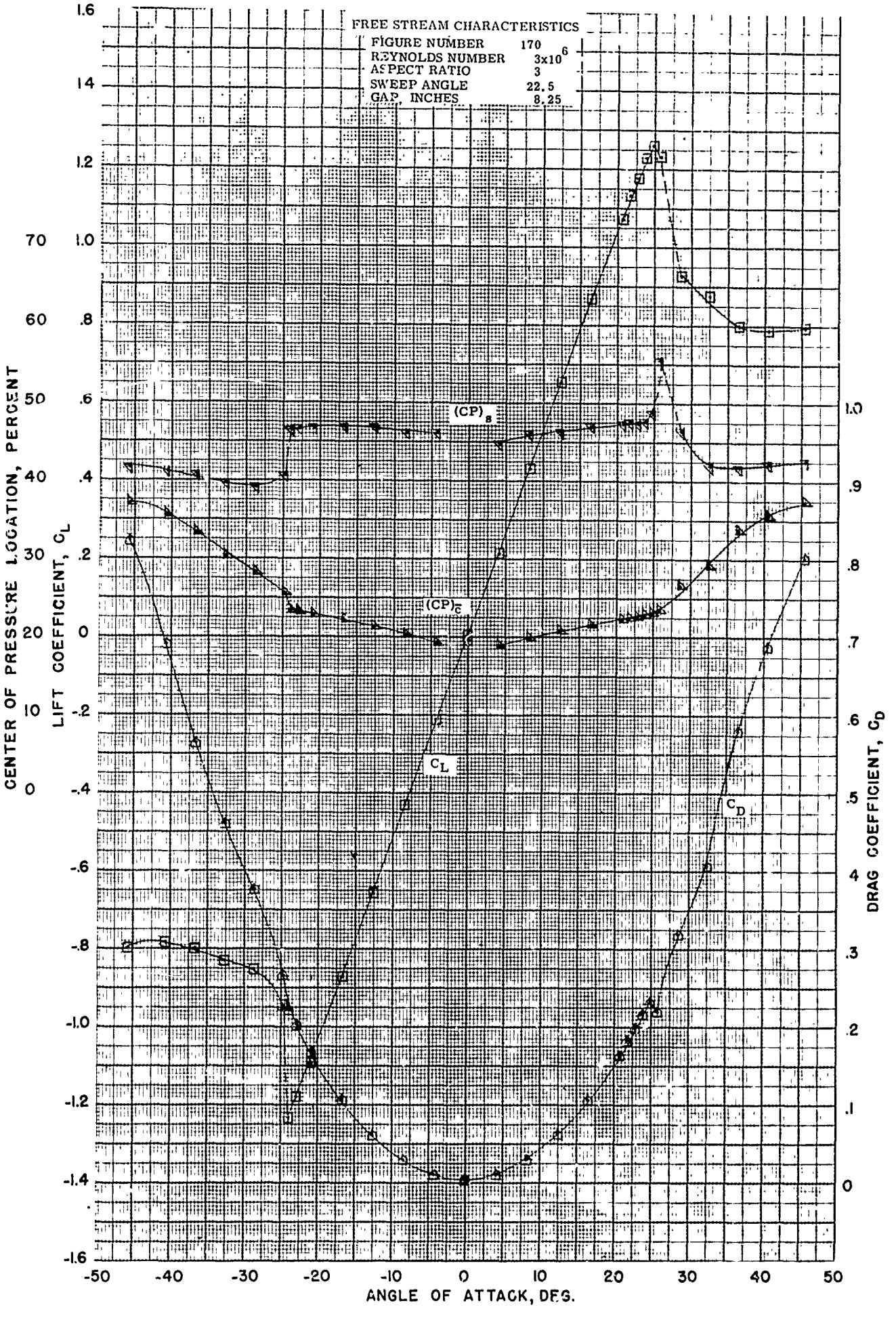
FREE STREAM CHARACTERISTICS
FIGURE NUMBER 170
REYNOLDS NUMBER 3x10^6
ASPECT RATIO 3
SWEEP ANGLE 22.5
GAP, INCHES 8.25
(CP)α
(CP)ε
CL
CD
CENTER OF PRESSURE LOCATION, PERCENT
LIFT COEFFICIENT, CL
DRAG COEFFICIENT, CD
ANGLE OF ATTACK, DEG.
70
60
50
40
30
20
10
0
1.6
1.4
1.2
1.0
.8
.6
.4
.2
0
-.2
-.4
-.6
-.8
-1.0
-1.2
-1.4
-1.6
1.0
.9
.8
.7
.6
.5
.4
.3
.2
.1
0
-50
-40
-30
-20
-10
0
10
20
30
40
50

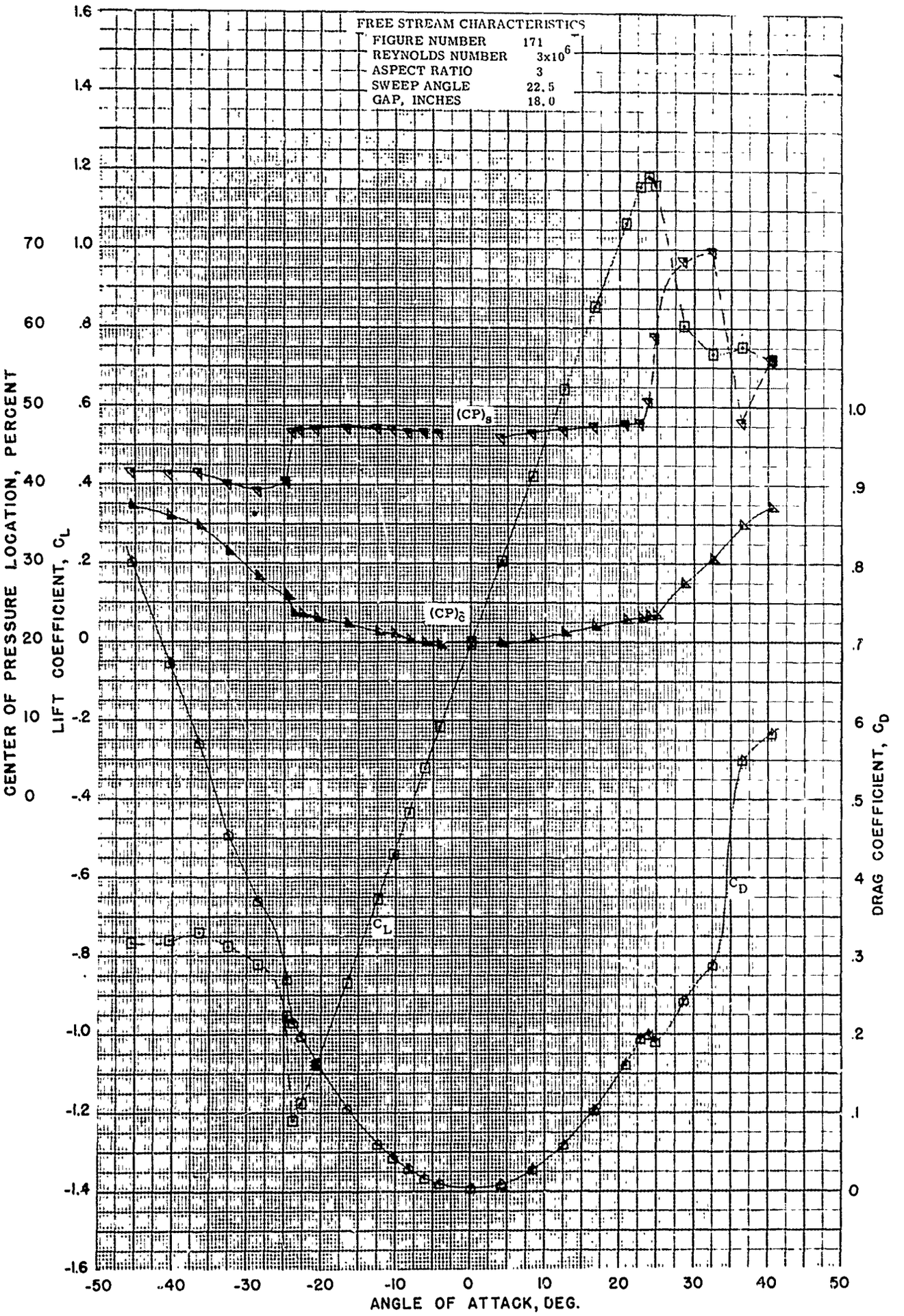
FREE STREAM CHARACTERISTICS
FIGURE NUMBER 171
REYNOLDS NUMBER 3x10^6
ASPECT RATIO 3
SWEEP ANGLE 22.5
GAP, INCHES 18.0
CENTER OF PRESSURE LOCATION, PERCENT
LIFT COEFFICIENT, C_L
DRAG COEFFICIENT, C_D
ANGLE OF ATTACK, DEG.
$(CP)_s$
$(CP)_c$
C_L
C_D
70
60
50
40
30
20
10
0
1.6
1.4
1.2
1.0
.8
.6
.4
.2
0
-.2
-.4
-.6
-.8
-1.0
-1.2
-1.4
-1.6
1.0
.9
.8
.7
.6
.5
.4
.3
.2
.1
0
-50
-40
-30
-20
-10
0
10
20
30
40
50

APPENDIX B

Simulated Hull Flow Characteristics For Various Gap Sizes

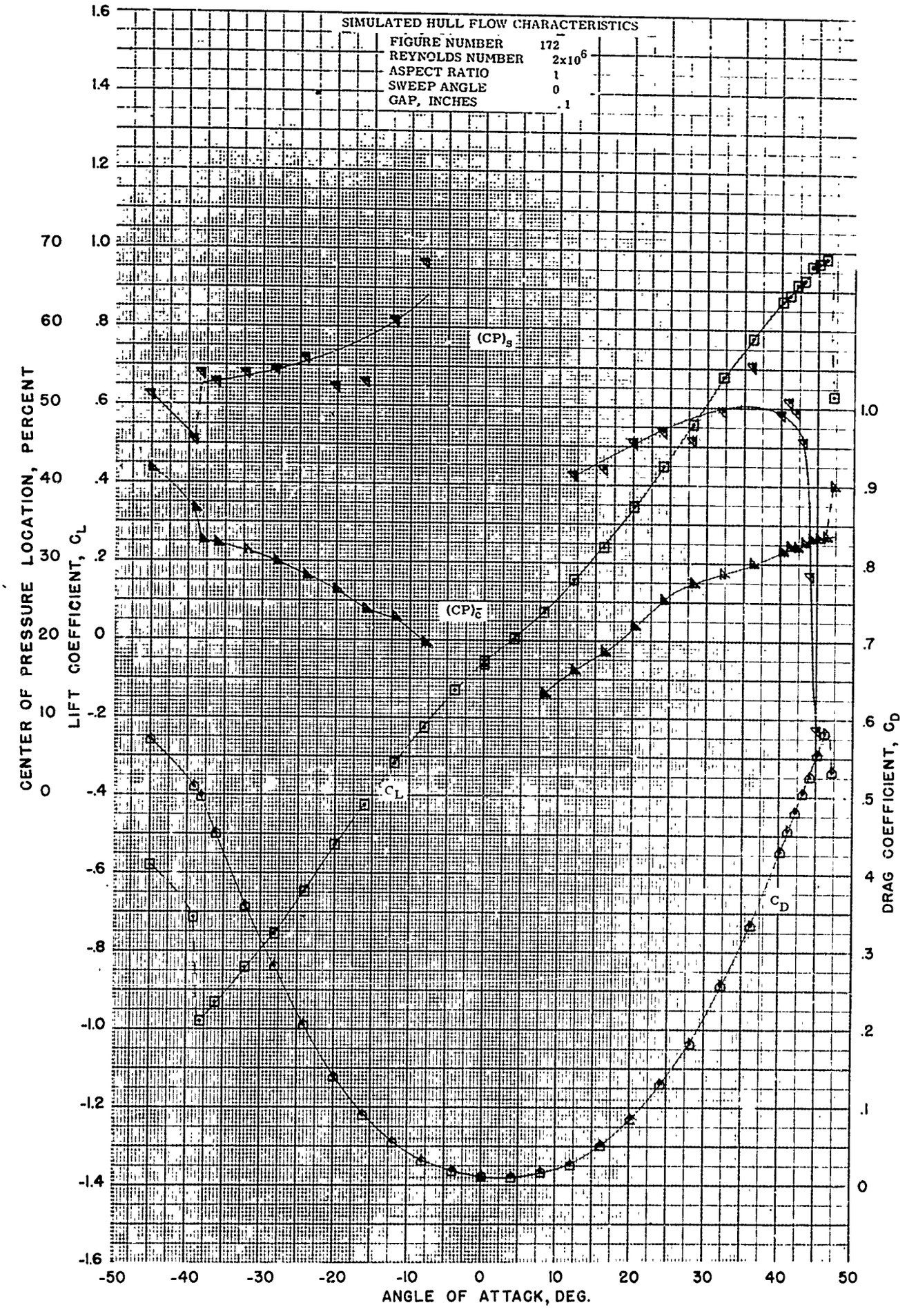
SIMULATED HULL FLOW CHARACTERISTICS
FIGURE NUMBER 172
REYNOLDS NUMBER 2x10^6
ASPECT RATIO 1
SWEEP ANGLE 0
GAP, INCHES .1
CENTER OF PRESSURE LOCATION, PERCENT
LIFT COEFFICIENT, C_L
DRAG COEFFICIENT, C_D
ANGLE OF ATTACK, DEG.
$(CP)_s$
$(CP)_c$
C_L
C_D
70
60
50
40
30
20
10
0
1.6
1.4
1.2
1.0
.8
.6
.4
.2
0
-.2
-.4
-.6
-.8
-1.0
-1.2
-1.4
-1.6
1.0
.9
.8
.7
.6
.5
.4
.3
.2
.1
0
-50
-40
-30
-20
-10
0
10
20
30
40
50

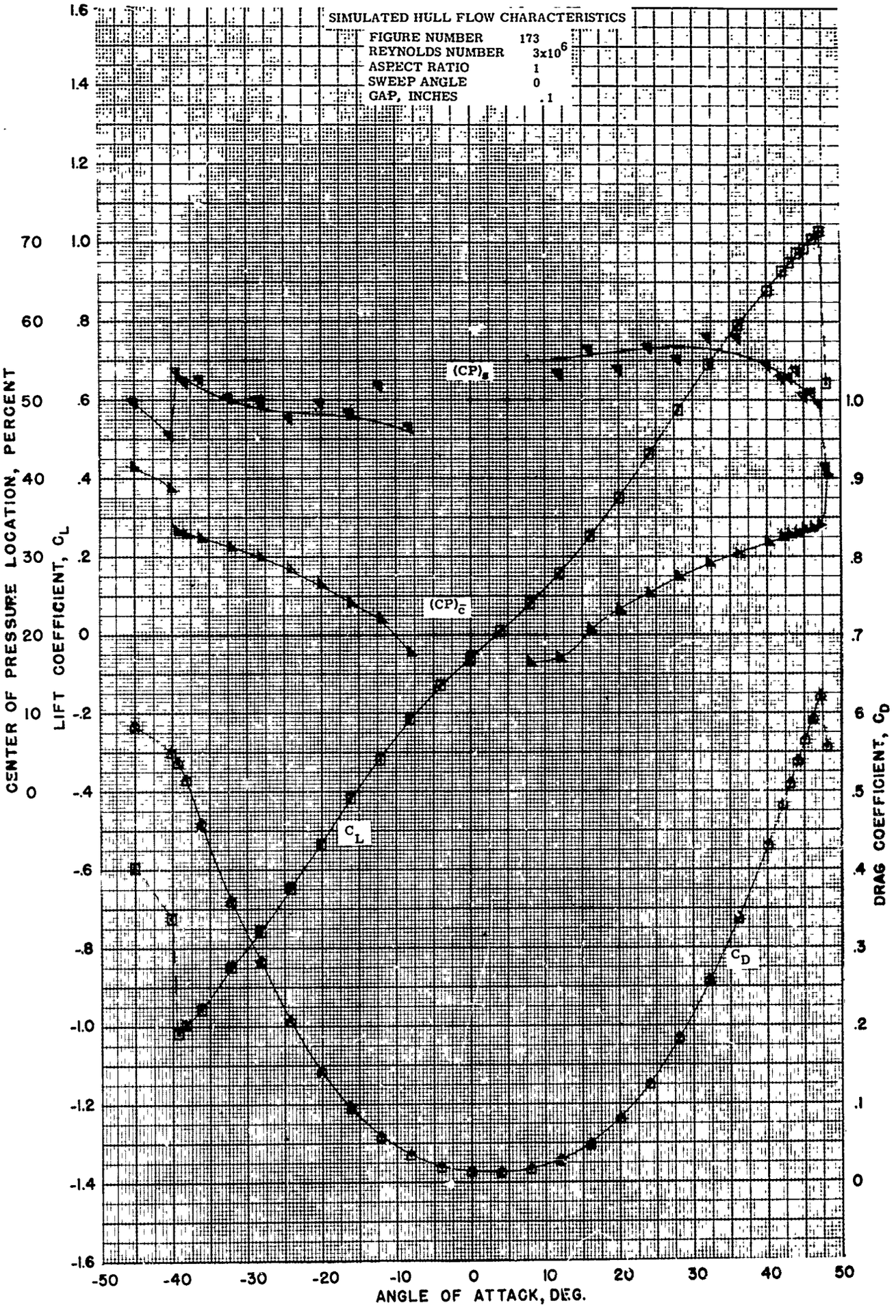
SIMULATED HULL FLOW CHARACTERISTICS
FIGURE NUMBER 173
REYNOLDS NUMBER 3x10^6
ASPECT RATIO 1
SWEEP ANGLE 0
GAP, INCHES .1
CENTER OF PRESSURE LOCATION, PERCENT
LIFT COEFFICIENT, C_L
DRAG COEFFICIENT, C_D
ANGLE OF ATTACK, DEG.
$(CP)_s$
$(CP)_{\bar{c}}$
C_L
C_D
70
60
50
40
30
20
10
0
1.6
1.4
1.2
1.0
.8
.6
.4
.2
0
-.2
-.4
-.6
-.8
-1.0
-1.2
-1.4
-1.6
1.0
.9
.8
.7
.6
.5
.4
.3
.2
.1
0
-50
-40
-30
-20
-10
0
10
20
30
40
50

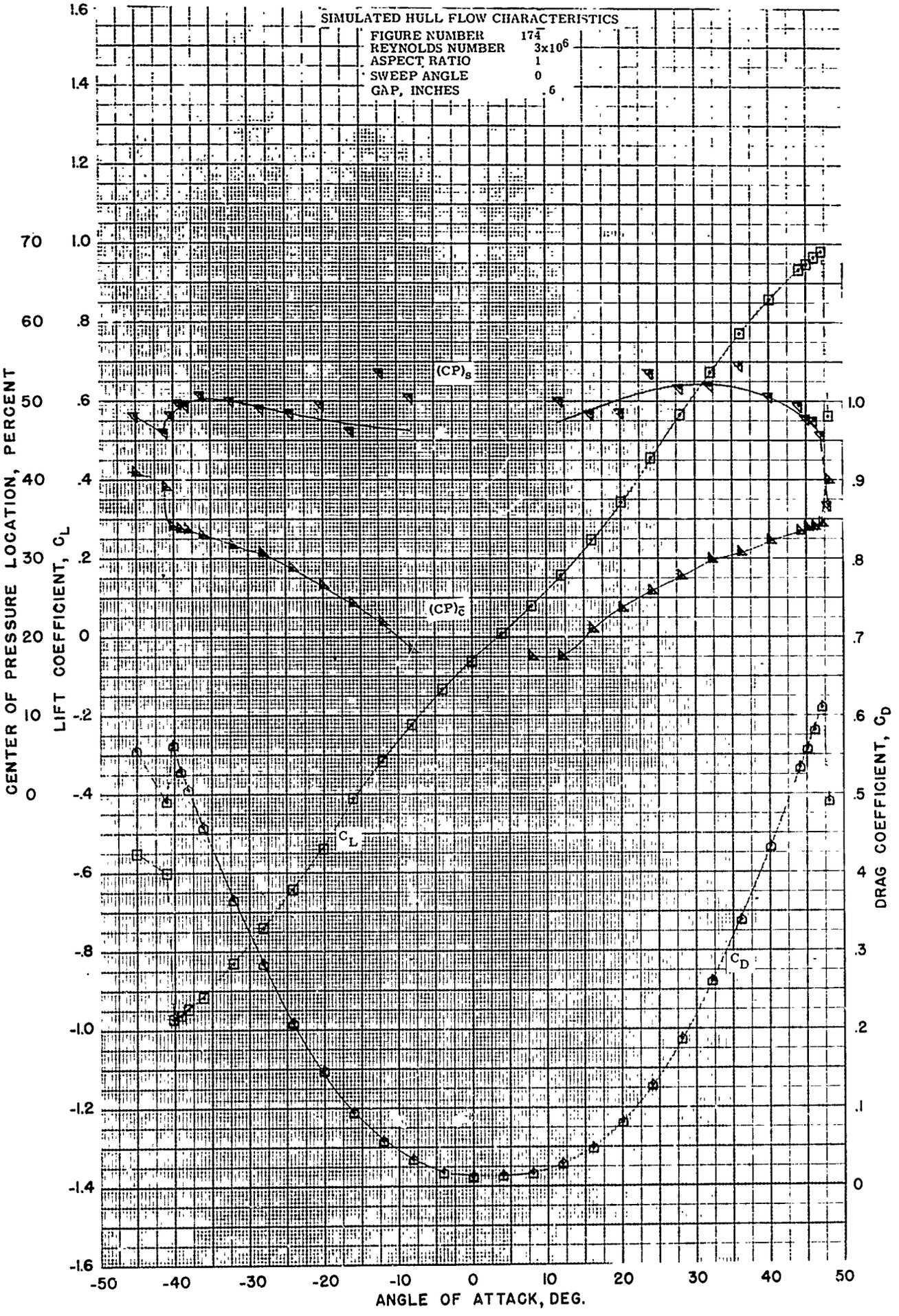
SIMULATED HULL FLOW CHARACTERISTICS
FIGURE NUMBER 174
REYNOLDS NUMBER 3x10^6
ASPECT RATIO 1
SWEEP ANGLE 0
GAP, INCHES .6
CENTER OF PRESSURE LOCATION, PERCENT
LIFT COEFFICIENT, C_L
DRAG COEFFICIENT, C_D
ANGLE OF ATTACK, DEG.
$(CP)_s$
$(CP)_{\bar{c}}$
C_L
C_D
70
60
50
40
30
20
10
0
1.6
1.4
1.2
1.0
.8
.6
.4
.2
0
-.2
-.4
-.6
-.8
-1.0
-1.2
-1.4
-1.6
1.0
.9
.8
.7
.6
.5
.4
.3
.2
.1
0
-50
-40
-30
-20
-10
0
10
20
30
40
50

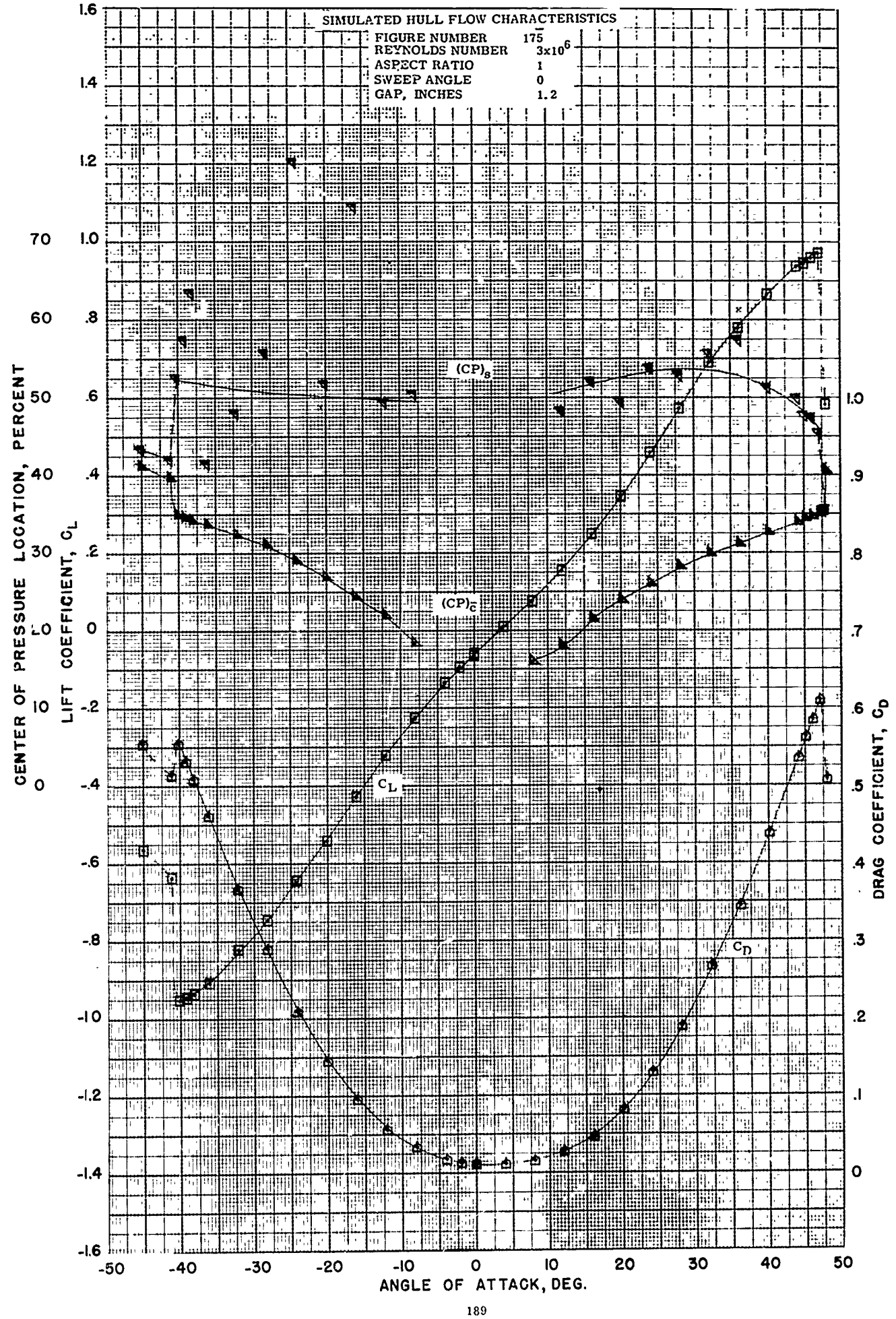
SIMULATED HULL FLOW CHARACTERISTICS
FIGURE NUMBER 175
REYNOLDS NUMBER 3x10^6
ASPECT RATIO 1
SWEEP ANGLE 0
GAP, INCHES 1.2
(CP)s
(CP)c
CL
CD
CENTER OF PRESSURE LOCATION, PERCENT
LIFT COEFFICIENT, CL
DRAG COEFFICIENT, CD
ANGLE OF ATTACK, DEG.
70
60
50
40
30
20
10
0
1.6
1.4
1.2
1.0
.8
.6
.4
.2
0
-.2
-.4
-.6
-.8
-1.0
-1.2
-1.4
-1.6
1.0
.9
.8
.7
.6
.5
.4
.3
.2
.1
0
-50
-40
-30
-20
-10
0
10
20
30
40
50

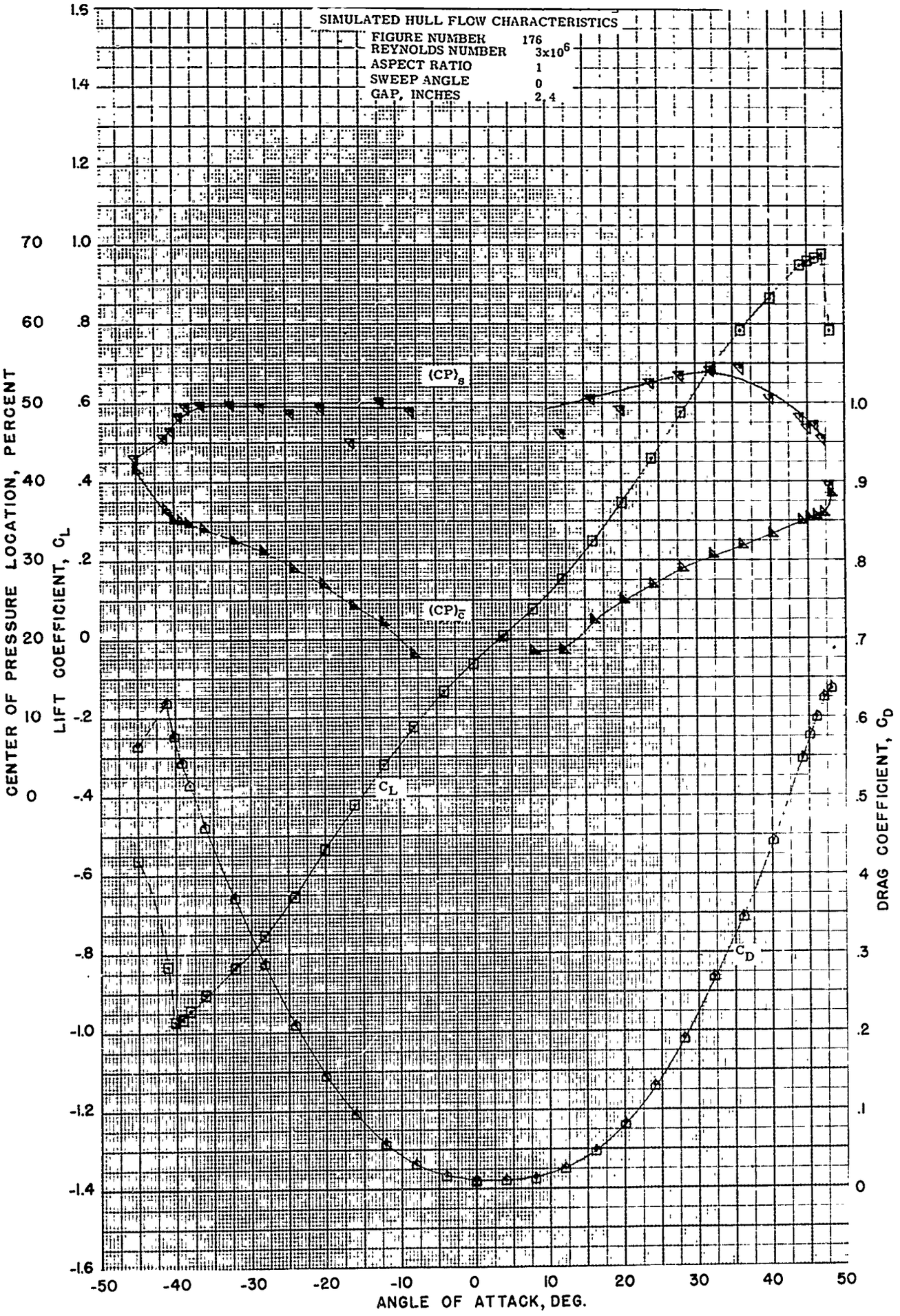
SIMULATED HULL FLOW CHARACTERISTICS
FIGURE NUMBER 176
REYNOLDS NUMBER 3x10^6
ASPECT RATIO 1
SWEEP ANGLE 0
GAP, INCHES 2, 4
CENTER OF PRESSURE LOCATION, PERCENT
LIFT COEFFICIENT, C_L
DRAG COEFFICIENT, C_D
ANGLE OF ATTACK, DEG.
$(CP)_s$
$(CP)_{\bar{c}}$
C_L
C_D
70
60
50
40
30
20
10
0
1.5
1.4
1.2
1.0
.8
.6
.4
.2
0
-.2
-.4
-.6
-.8
-1.0
-1.2
-1.4
-1.6
1.0
.9
.8
.7
.6
.5
.4
.3
.2
.1
0
-50
-40
-30
-20
-10
0
10
20
30
40
50

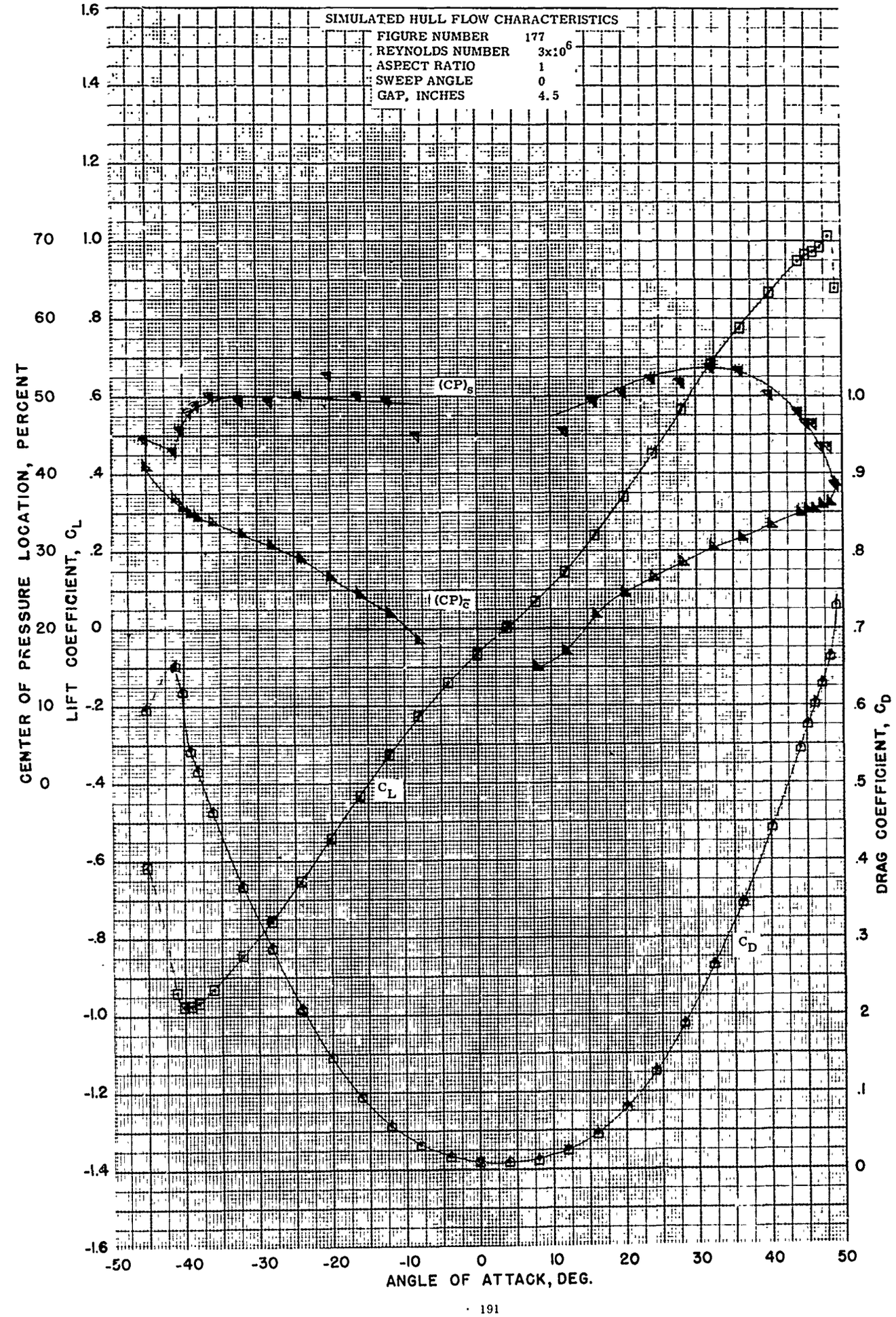
SIMULATED HULL FLOW CHARACTERISTICS
FIGURE NUMBER 177
REYNOLDS NUMBER 3x10^6
ASPECT RATIO 1
SWEEP ANGLE 0
GAP, INCHES 4.5
CENTER OF PRESSURE LOCATION, PERCENT
LIFT COEFFICIENT, C_L
DRAG COEFFICIENT, C_D
ANGLE OF ATTACK, DEG.
$(CP)_S$
$(CP)_C$
C_L
C_D
70
60
50
40
30
20
10
0
1.6
1.4
1.2
1.0
.8
.6
.4
.2
0
-.2
-.4
-.6
-.8
-1.0
-1.2
-1.4
-1.6
1.0
.9
.8
.7
.6
.5
.4
.3
2
.1
0
-50
-40
-30
-20
-10
0
10
20
30
40
50

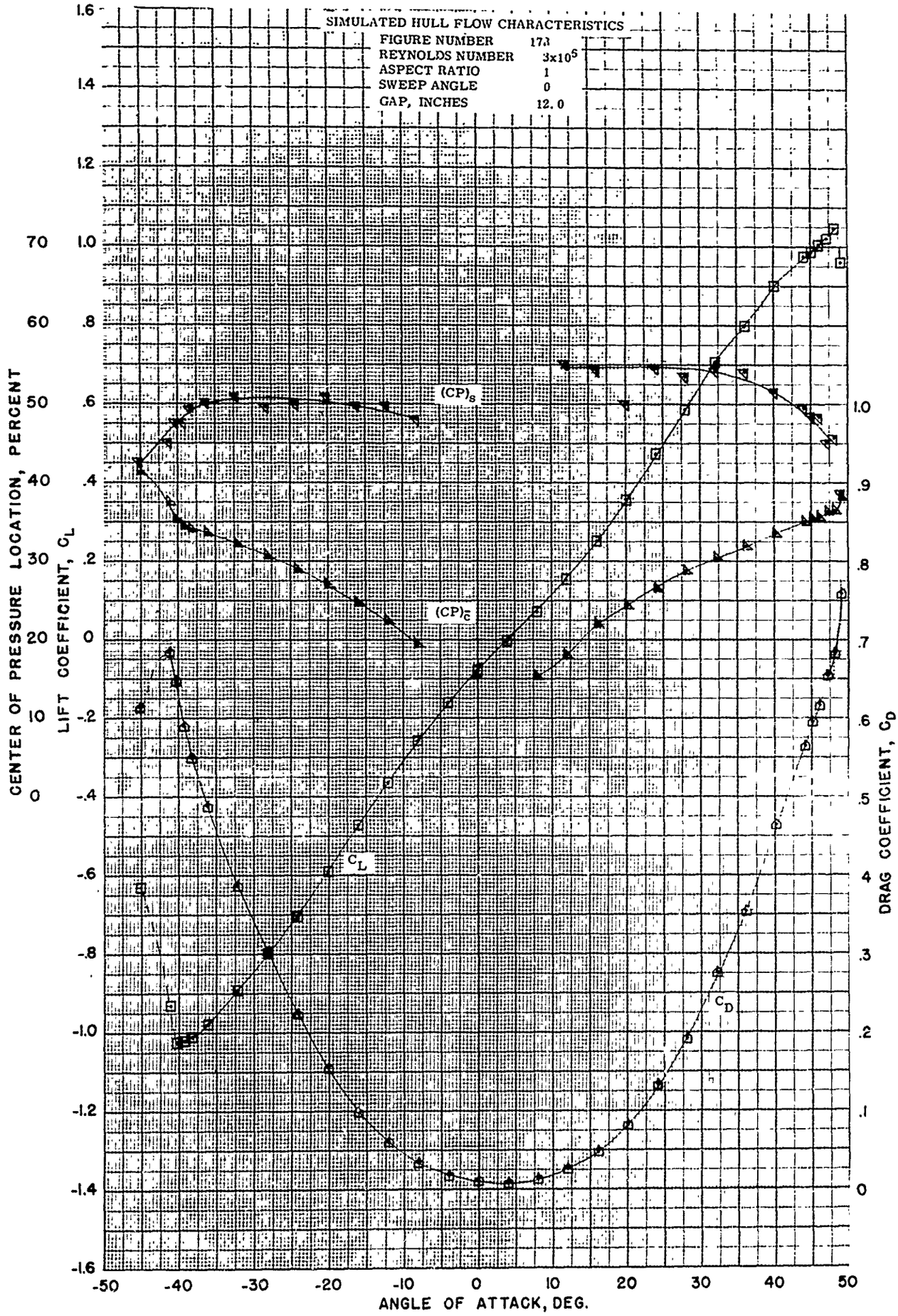
SIMULATED HULL FLOW CHARACTERISTICS
FIGURE NUMBER 17.3
REYNOLDS NUMBER 3x10^6
ASPECT RATIO 1
SWEEP ANGLE 0
GAP, INCHES 12.0
CENTER OF PRESSURE LOCATION, PERCENT
LIFT COEFFICIENT, C_L
DRAG COEFFICIENT, C_D
ANGLE OF ATTACK, DEG.
$(CP)_s$
$(CP)_c$
C_L
C_D
70
60
50
40
30
20
10
0
1.6
1.4
1.2
1.0
.8
.6
.4
.2
0
-.2
-.4
-.6
-.8
-1.0
-1.2
-1.4
-1.6
1.0
.9
.8
.7
.6
.5
.4
.3
.2
.1
0
-50
-40
-30
-20
-10
0
10
20
30
40
50

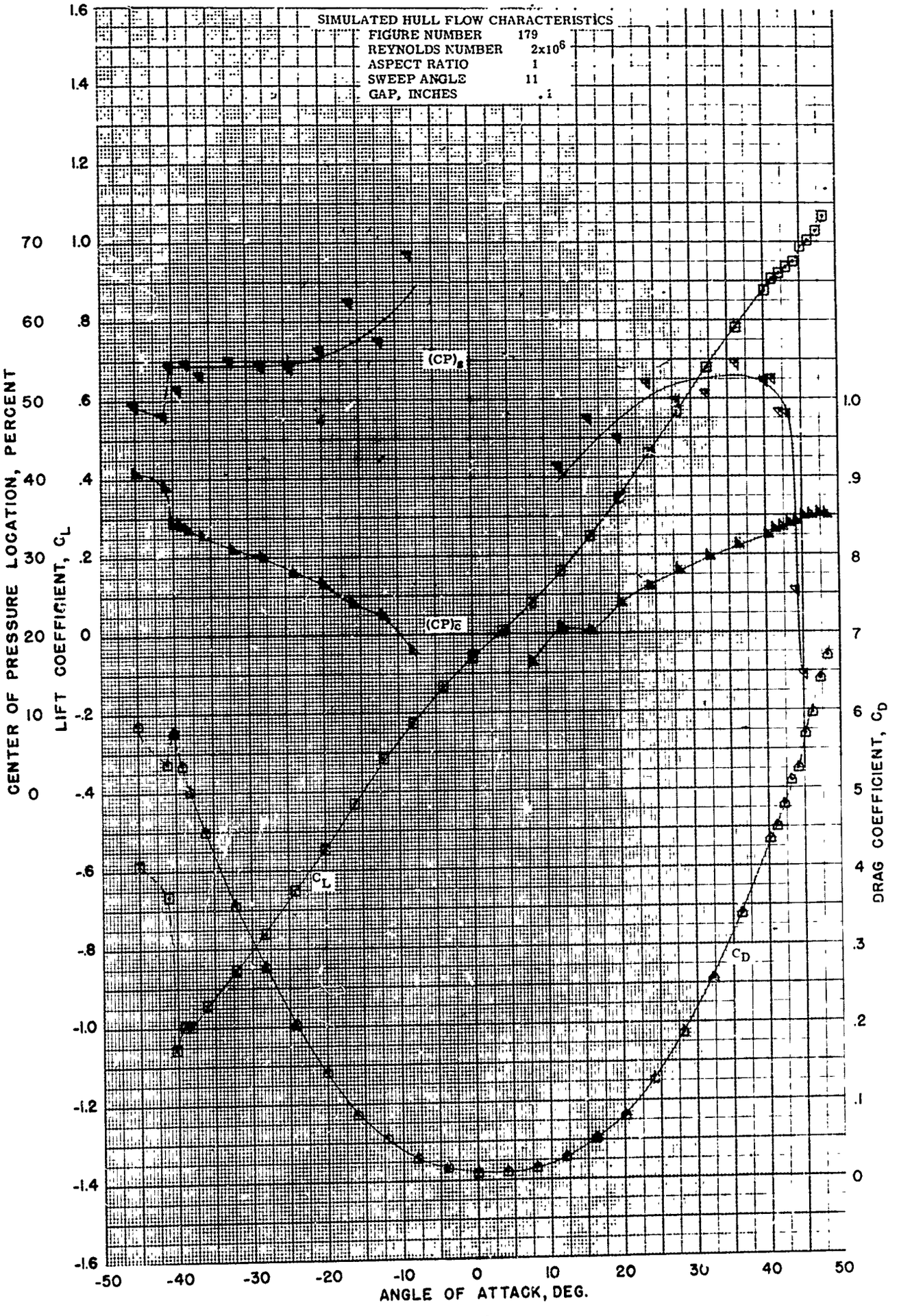
SIMULATED HULL FLOW CHARACTERISTICS
FIGURE NUMBER 179
REYNOLDS NUMBER 2x10^6
ASPECT RATIO 1
SWEEP ANGLE 11
GAP, INCHES .1
CENTER OF PRESSURE LOCATION, PERCENT
LIFT COEFFICIENT, C_L
DRAG COEFFICIENT, C_D
ANGLE OF ATTACK, DEG.
$(CP)_\alpha$
$(CP)_\varepsilon$
C_L
C_D
70
60
50
40
30
20
10
0
1.6
1.4
1.2
1.0
.8
.6
.4
.2
0
-.2
-.4
-.6
-.8
-1.0
-1.2
-1.4
-1.6
1.0
.9
.8
.7
.6
.5
.4
.3
.2
.1
0
-50
-40
-30
-20
-10
0
10
20
30
40
50

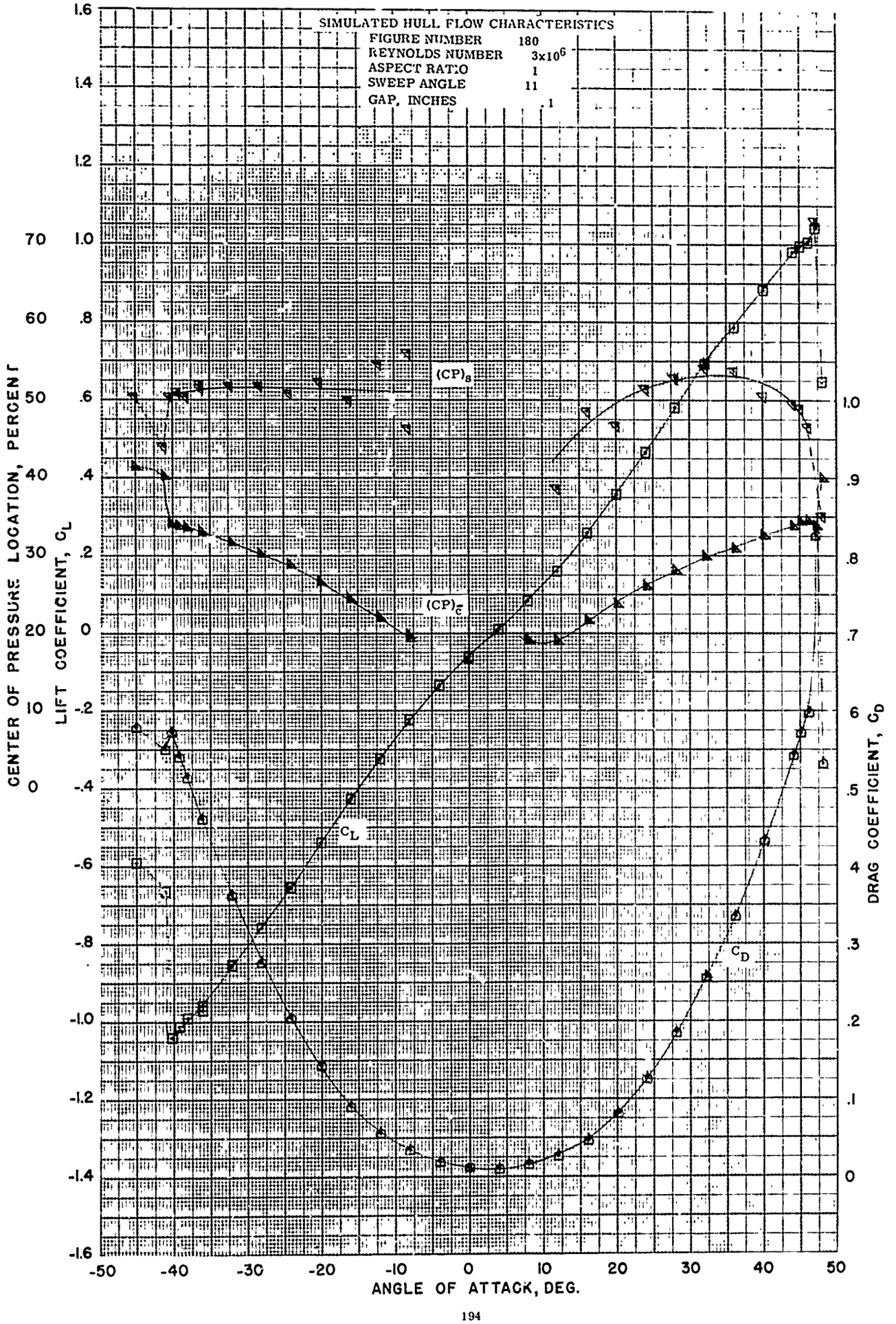
SIMULATED HULL FLOW CHARACTERISTICS
FIGURE NUMBER 180
REYNOLDS NUMBER 3x10^6
ASPECT RATIO 1
SWEEP ANGLE 11
GAP, INCHES .1
CENTER OF PRESSURE LOCATION, PERCENT
LIFT COEFFICIENT, C_L
DRAG COEFFICIENT, C_D
ANGLE OF ATTACK, DEG.
$(CP)_s$
$(CP)_c$
C_L
C_D
70
60
50
40
30
20
10
0
1.6
1.4
1.2
1.0
.8
.6
.4
.2
0
-.2
-.4
-.6
-.8
-1.0
-1.2
-1.4
-1.6
1.0
.9
.8
.7
.6
.5
.4
.3
.2
.1
0
-50
-40
-30
-20
-10
0
10
20
30
40
50

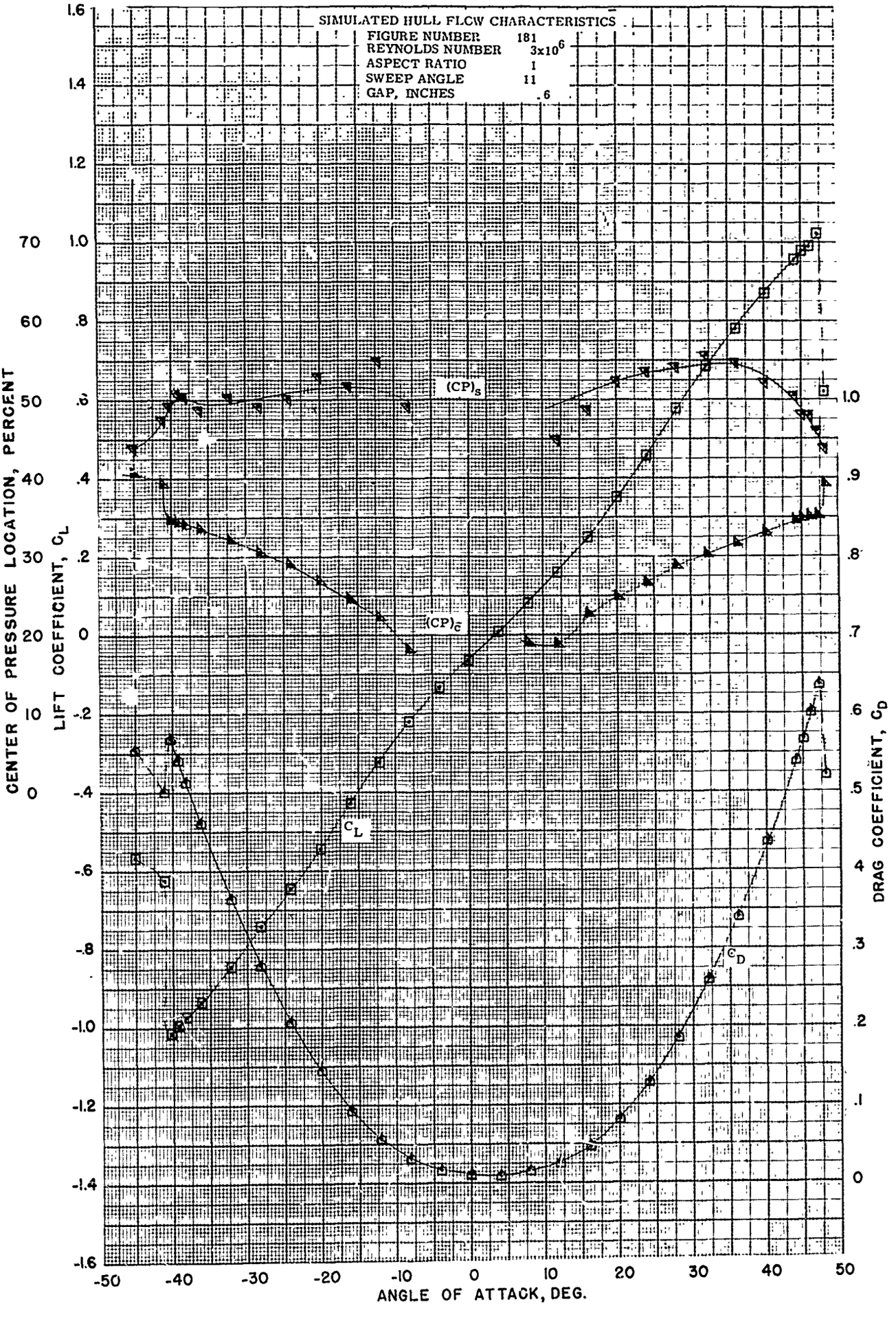
SIMULATED HULL FLOW CHARACTERISTICS
FIGURE NUMBER 181
REYNOLDS NUMBER 3×10^6
ASPECT RATIO 1
SWEEP ANGLE 11
GAP, INCHES .6
CENTER OF PRESSURE LOCATION, PERCENT
LIFT COEFFICIENT, C_L
DRAG COEFFICIENT, C_D
ANGLE OF ATTACK, DEG.
$(CP)_s$
$(CP)_c$
C_L
C_D
70
60
50
40
30
20
10
0
1.6
1.4
1.2
1.0
.8
.6
.4
.2
0
-.2
-.4
-.6
-.8
-1.0
-1.2
-1.4
-1.6
1.0
.9
.8
.7
.6
.5
.4
.3
.2
.1
0
-50
-40
-30
-20
-10
0
10
20
30
40
50

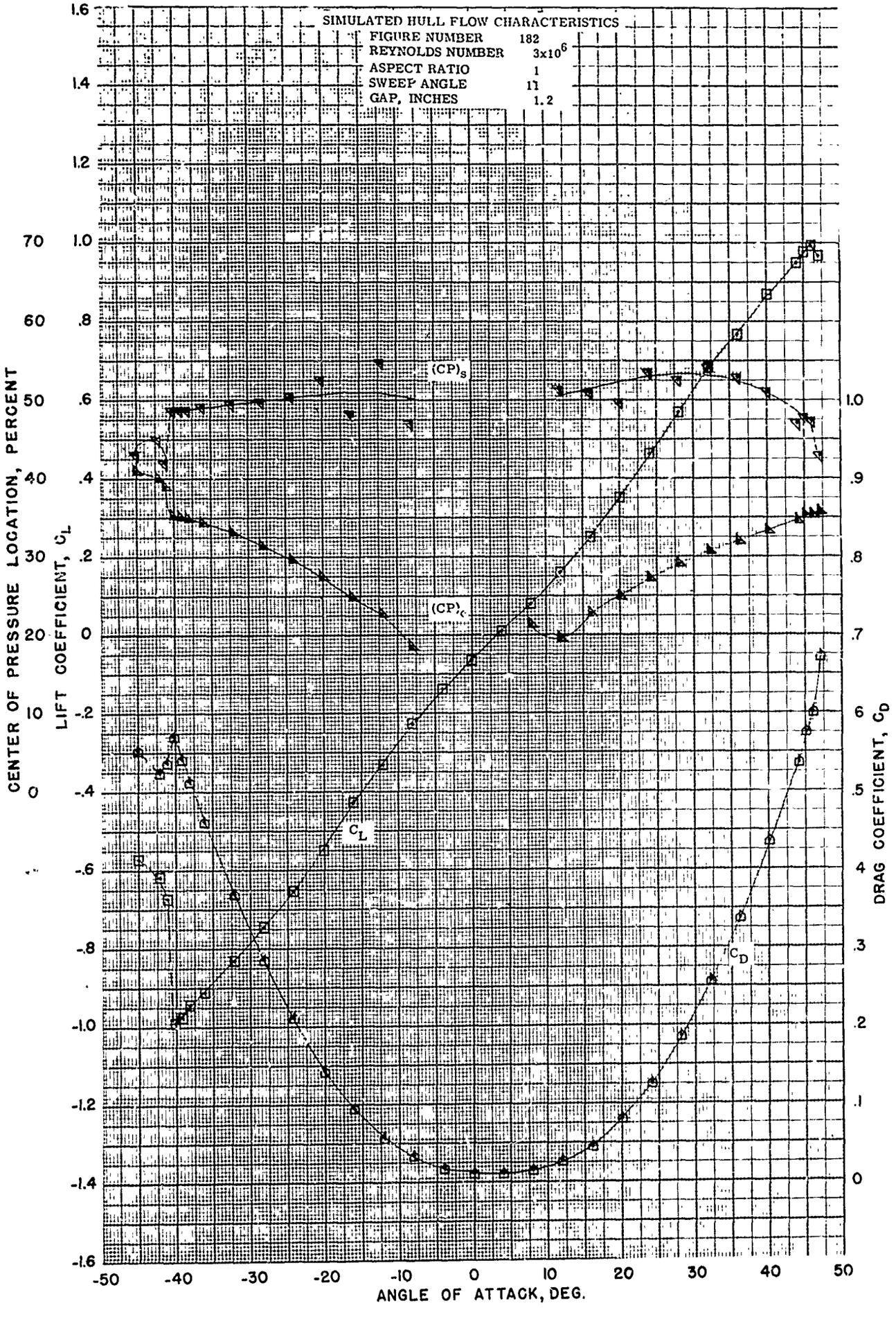
SIMULATED HULL FLOW CHARACTERISTICS
FIGURE NUMBER 182
REYNOLDS NUMBER 3×10^6
ASPECT RATIO 1
SWEEP ANGLE 11
GAP, INCHES 1.2
CENTER OF PRESSURE LOCATION, PERCENT
LIFT COEFFICIENT, C_L
DRAG COEFFICIENT, C_D
$(CP)_S$
$(CP)_C$
C_L
C_D
ANGLE OF ATTACK, DEG.
70
60
50
40
30
20
10
0
1.6
1.4
1.2
1.0
.8
.6
.4
.2
0
-.2
-.4
-.6
-.8
-1.0
-1.2
-1.4
-1.6
1.0
.9
.8
.7
.6
.5
.4
.3
.2
.1
0
-50
-40
-30
-20
-10
0
10
20
30
40
50

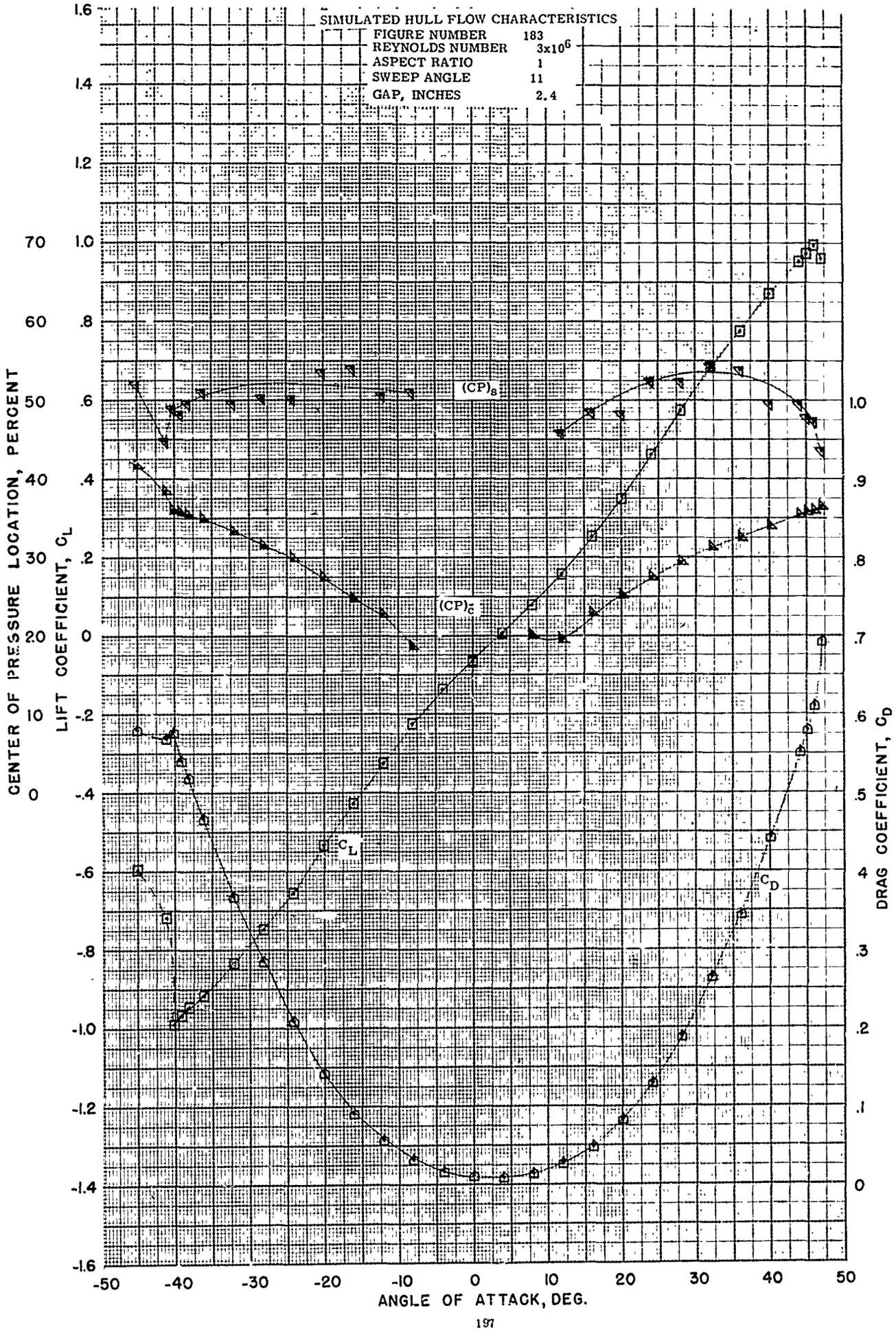
SIMULATED HULL FLOW CHARACTERISTICS
FIGURE NUMBER 183
REYNOLDS NUMBER 3×10^6
ASPECT RATIO 1
SWEEP ANGLE 11
GAP, INCHES 2.4
CENTER OF PRESSURE LOCATION, PERCENT
LIFT COEFFICIENT, C_L
DRAG COEFFICIENT, C_D
ANGLE OF ATTACK, DEG.
$(CP)_s$
$(CP)_c$
C_L
C_D
70
60
50
40
30
20
10
0
1.6
1.4
1.2
1.0
.8
.6
.4
.2
0
-.2
-.4
-.6
-.8
-1.0
-1.2
-1.4
-1.6
1.0
.9
.8
.7
.6
.5
.4
.3
.2
.1
0
-50
-40
-30
-20
-10
0
10
20
30
40
50

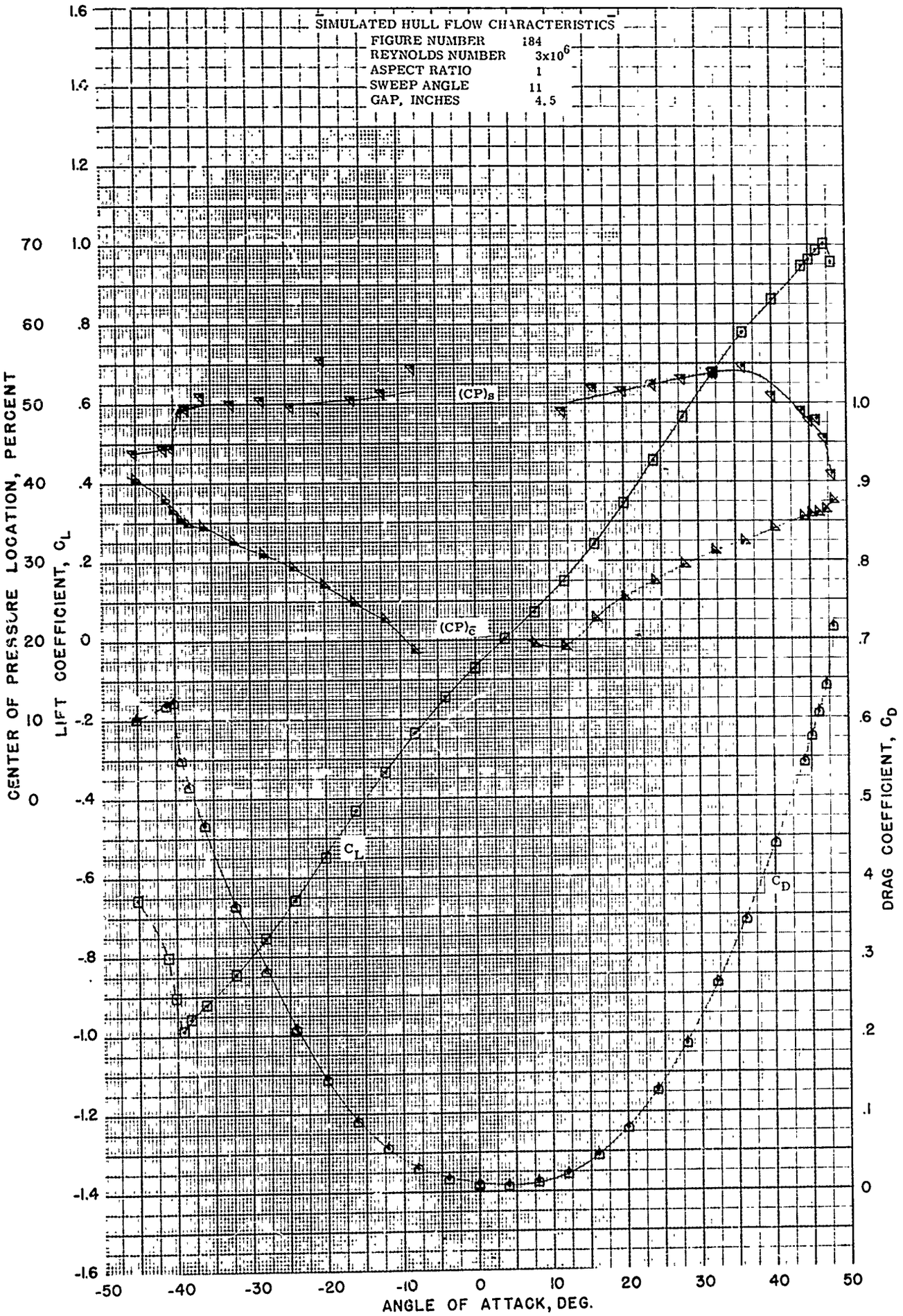
SIMULATED HULL FLOW CHARACTERISTICS
FIGURE NUMBER 184
REYNOLDS NUMBER 3x10^6
ASPECT RATIO 1
SWEEP ANGLE 11
GAP, INCHES 4.5
CENTER OF PRESSURE LOCATION, PERCENT
LIFT COEFFICIENT, C_L
DRAG COEFFICIENT, C_D
ANGLE OF ATTACK, DEG.
$(CP)_S$
$(CP)_C$
C_L
C_D
70
60
50
40
30
20
10
0
1.6
1.4
1.2
1.0
.8
.6
.4
.2
0
-.2
-.4
-.6
-.8
-1.0
-1.2
-1.4
-1.6
1.0
.9
.8
.7
.6
.5
.4
.3
.2
.1
0
-50
-40
-30
-20
-10
0
10
20
30
40
50

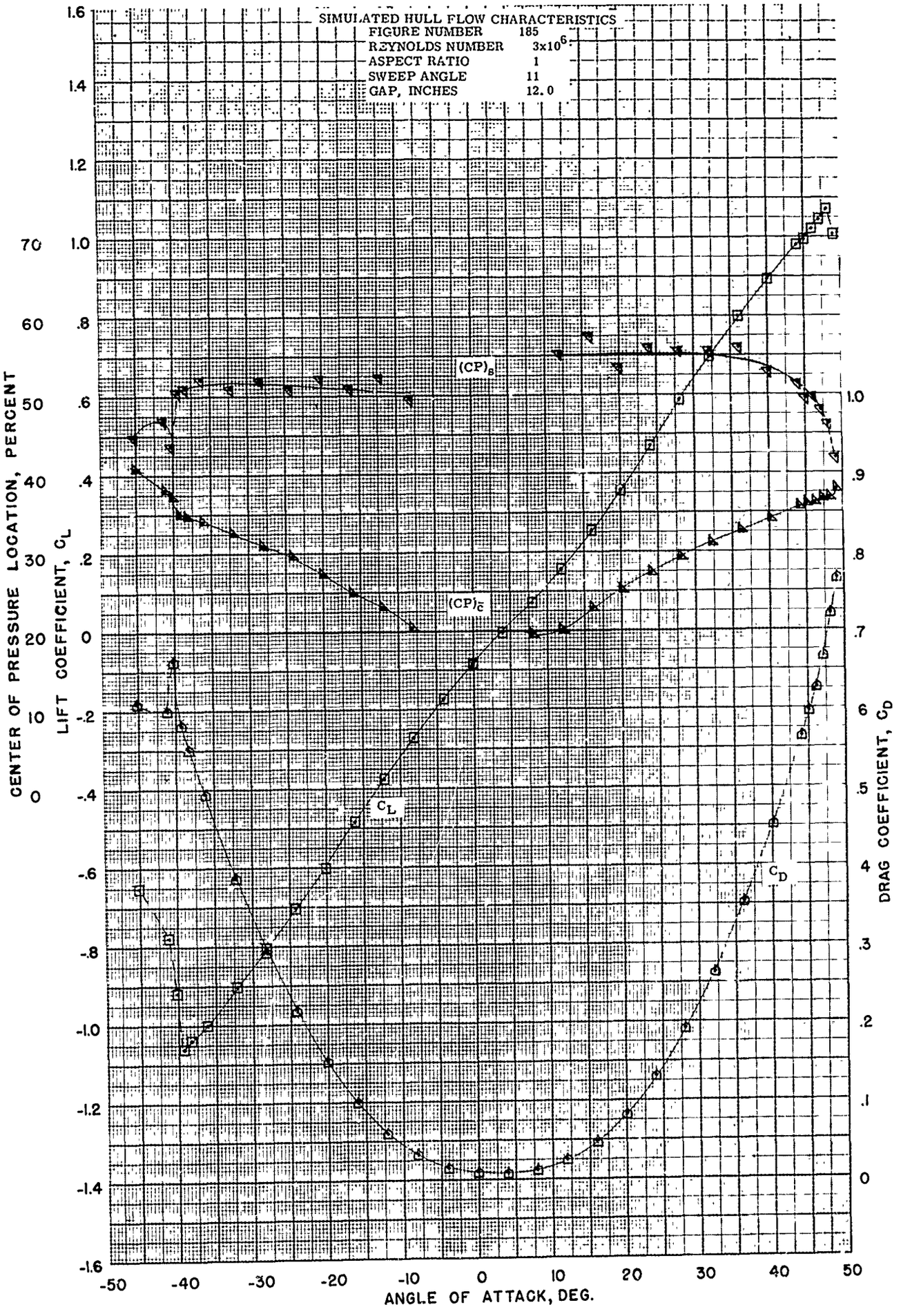
SIMULATED HULL FLOW CHARACTERISTICS
FIGURE NUMBER 185
REYNOLDS NUMBER 3x10^6
ASPECT RATIO 1
SWEEP ANGLE 11
GAP, INCHES 12.0
CENTER OF PRESSURE LOCATION, PERCENT
LIFT COEFFICIENT, C_L
DRAG COEFFICIENT, C_D
ANGLE OF ATTACK, DEG.
$(CP)_s$
$(CP)_{\bar{c}}$
C_L
C_D
70
60
50
40
30
20
10
0
1.6
1.4
1.2
1.0
.8
.6
.4
.2
0
-.2
-.4
-.6
-.8
-1.0
-1.2
-1.4
-1.6
1.0
.9
.8
.7
.6
.5
.4
.3
.2
.1
0
-50
-40
-30
-20
-10
0
10
20
30
40
50

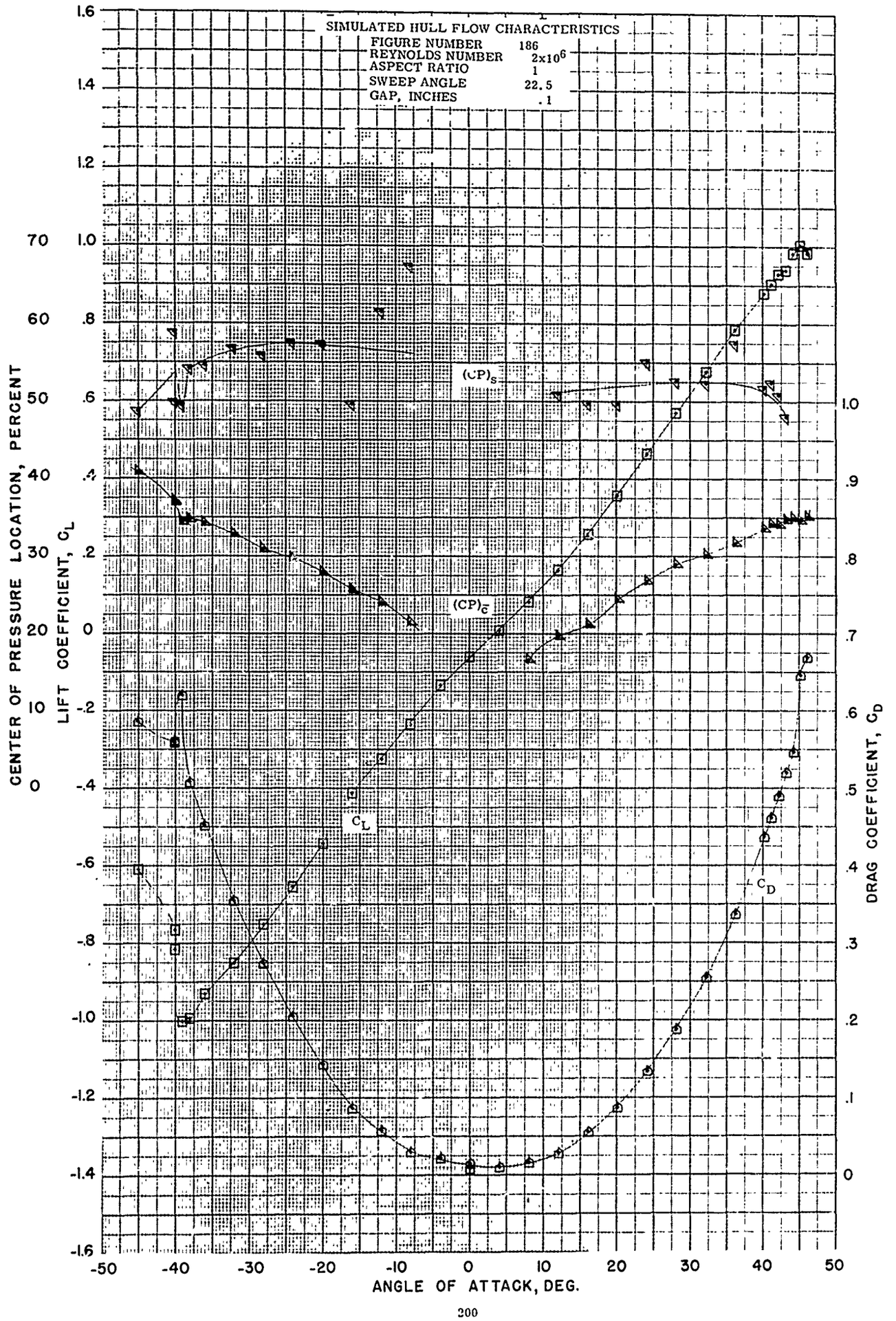
SIMULATED HULL FLOW CHARACTERISTICS
FIGURE NUMBER 186
REYNOLDS NUMBER 2x10^6
ASPECT RATIO 1
SWEEP ANGLE 22.5
GAP, INCHES .1
CENTER OF PRESSURE LOCATION, PERCENT
LIFT COEFFICIENT, C_L
DRAG COEFFICIENT, C_D
ANGLE OF ATTACK, DEG.
$(CP)_s$
$(CP)_{\bar{c}}$
C_L
C_D
70
60
50
40
30
20
10
0
1.6
1.4
1.2
1.0
.8
.6
.4
.2
0
-.2
-.4
-.6
-.8
-1.0
-1.2
-1.4
-1.6
1.0
.9
.8
.7
.6
.5
.4
.3
.2
.1
0
-50
-40
-30
-20
-10
0
10
20
30
40
50

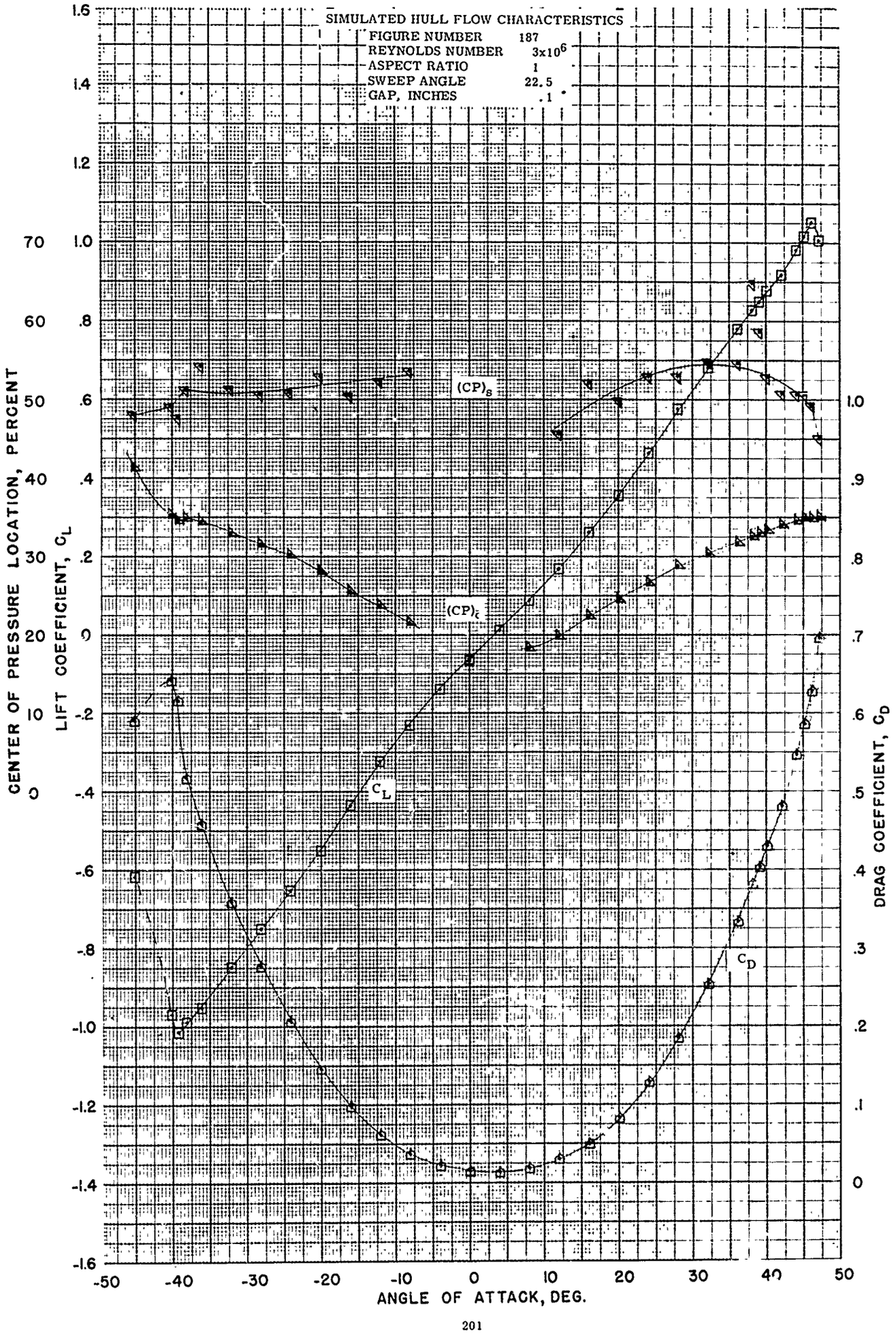
SIMULATED HULL FLOW CHARACTERISTICS
FIGURE NUMBER 187
REYNOLDS NUMBER 3x10^6
ASPECT RATIO 1
SWEEP ANGLE 22.5
GAP, INCHES .1
CENTER OF PRESSURE LOCATION, PERCENT
LIFT COEFFICIENT, C_L
DRAG COEFFICIENT, C_D
ANGLE OF ATTACK, DEG.
$(CP)_s$
$(CP)_c$
C_L
C_D
70
60
50
40
30
20
10
0
1.6
1.4
1.2
1.0
.8
.6
.4
.2
0
-.2
-.4
-.6
-.8
-1.0
-1.2
-1.4
-1.6
1.0
.9
.8
.7
.6
.5
.4
.3
.2
.1
0
-50
-40
-30
-20
-10
0
10
20
30
40
50

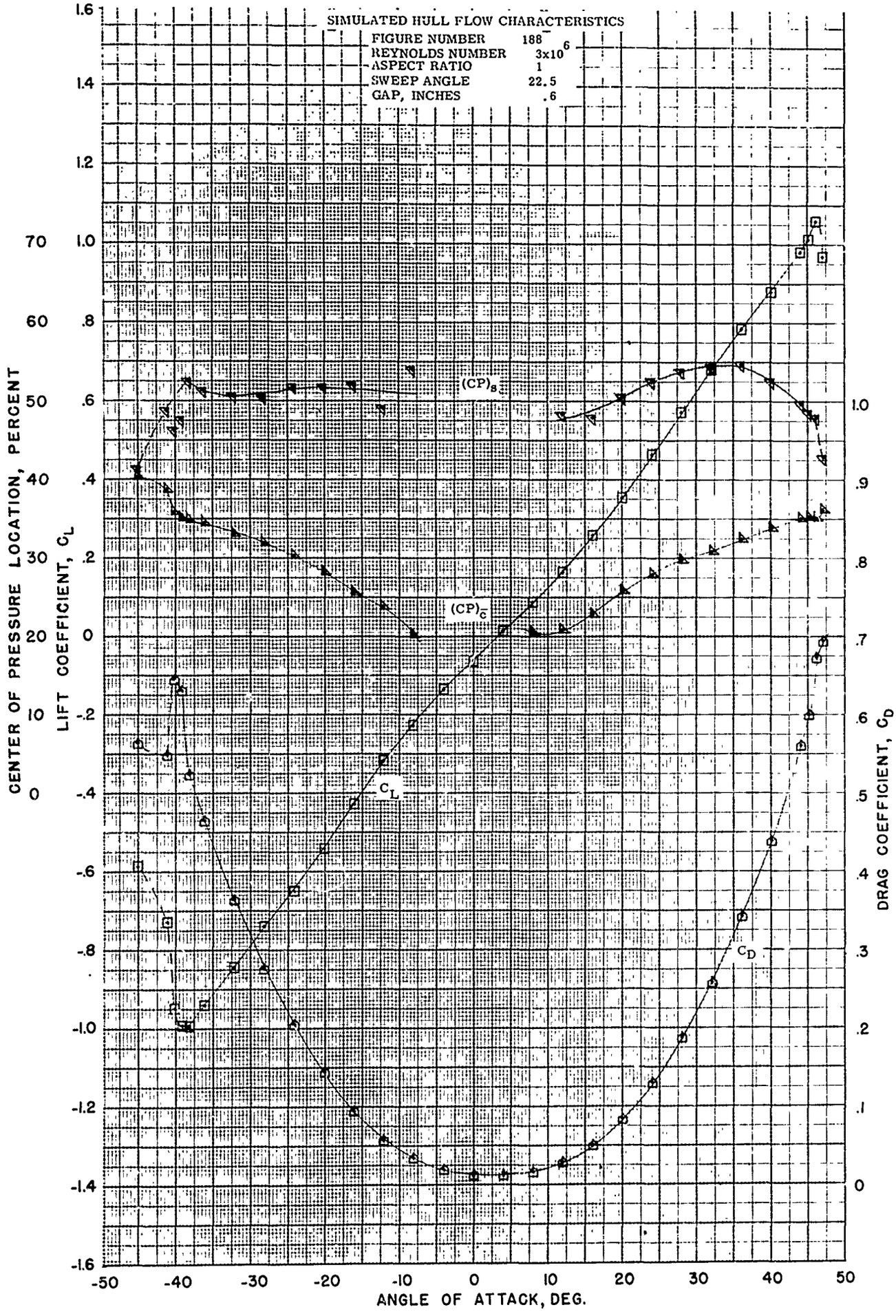
SIMULATED HULL FLOW CHARACTERISTICS
FIGURE NUMBER 188
REYNOLDS NUMBER 3x10^6
ASPECT RATIO 1
SWEEP ANGLE 22.5
GAP, INCHES .6
CENTER OF PRESSURE LOCATION, PERCENT
LIFT COEFFICIENT, C_L
DRAG COEFFICIENT, C_D
ANGLE OF ATTACK, DEG.
$(CP)_s$
$(CP)_c$
C_L
C_D
70
60
50
40
30
20
10
0
1.6
1.4
1.2
1.0
.8
.6
.4
.2
0
-.2
-.4
-.6
-.8
-1.0
-1.2
-1.4
-1.6
1.0
.9
.8
.7
.6
.5
.4
.3
.2
.1
0
-50
-40
-30
-20
-10
0
10
20
30
40
50

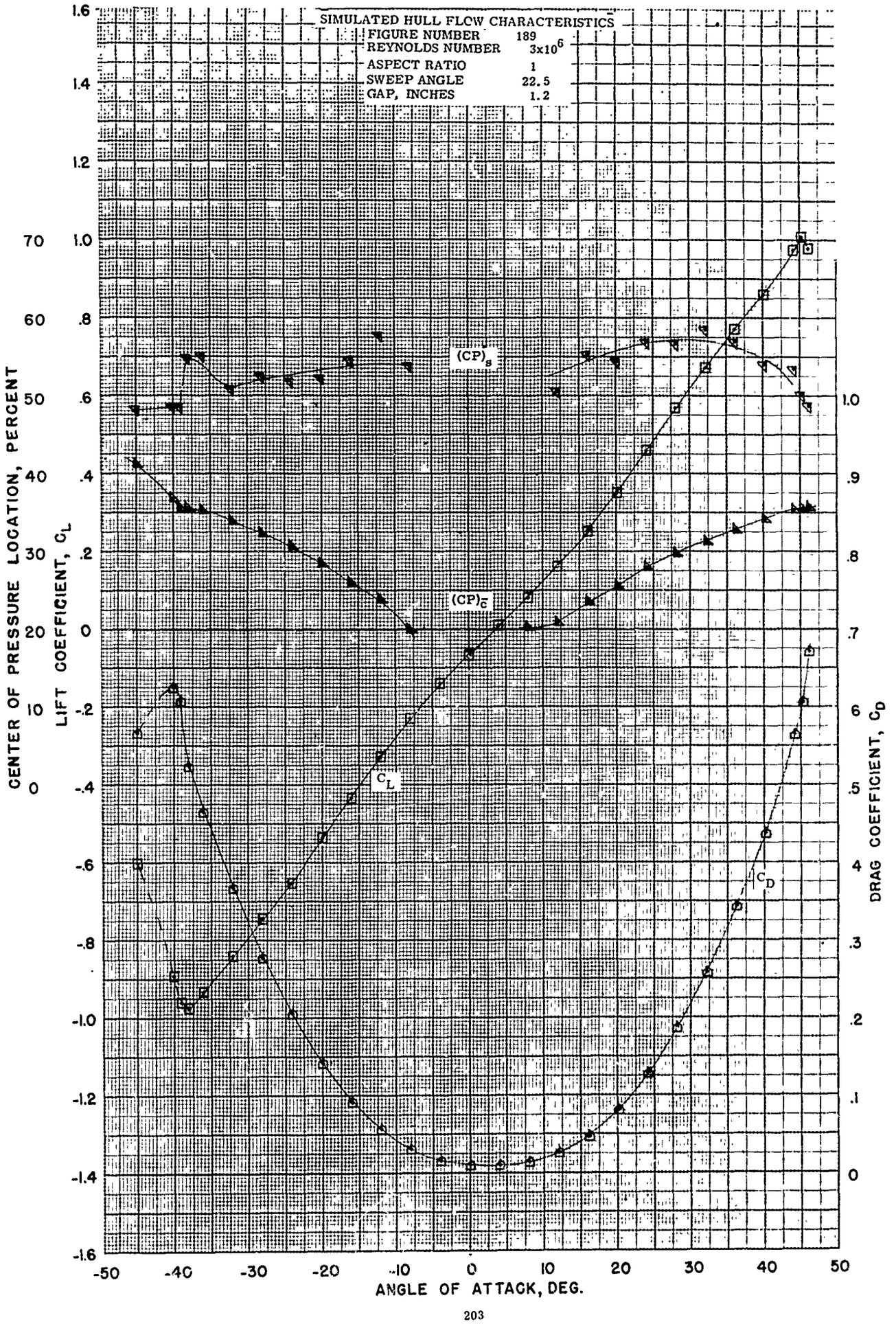
SIMULATED HULL FLOW CHARACTERISTICS
FIGURE NUMBER 189
REYNOLDS NUMBER 3x10^6
ASPECT RATIO 1
SWEEP ANGLE 22.5
GAP, INCHES 1.2
(CP)s
(CP)c
CL
CD
CENTER OF PRESSURE LOCATION, PERCENT
LIFT COEFFICIENT, CL
DRAG COEFFICIENT, CD
ANGLE OF ATTACK, DEG.
70
60
50
40
30
20
10
0
1.6
1.4
1.2
1.0
.8
.6
.4
.2
0
-.2
-.4
-.6
-.8
-1.0
-1.2
-1.4
-1.6
1.0
.9
.8
.7
.6
.5
.4
.3
.2
.1
0
-50
-40
-30
-20
-10
0
10
20
30
40
50

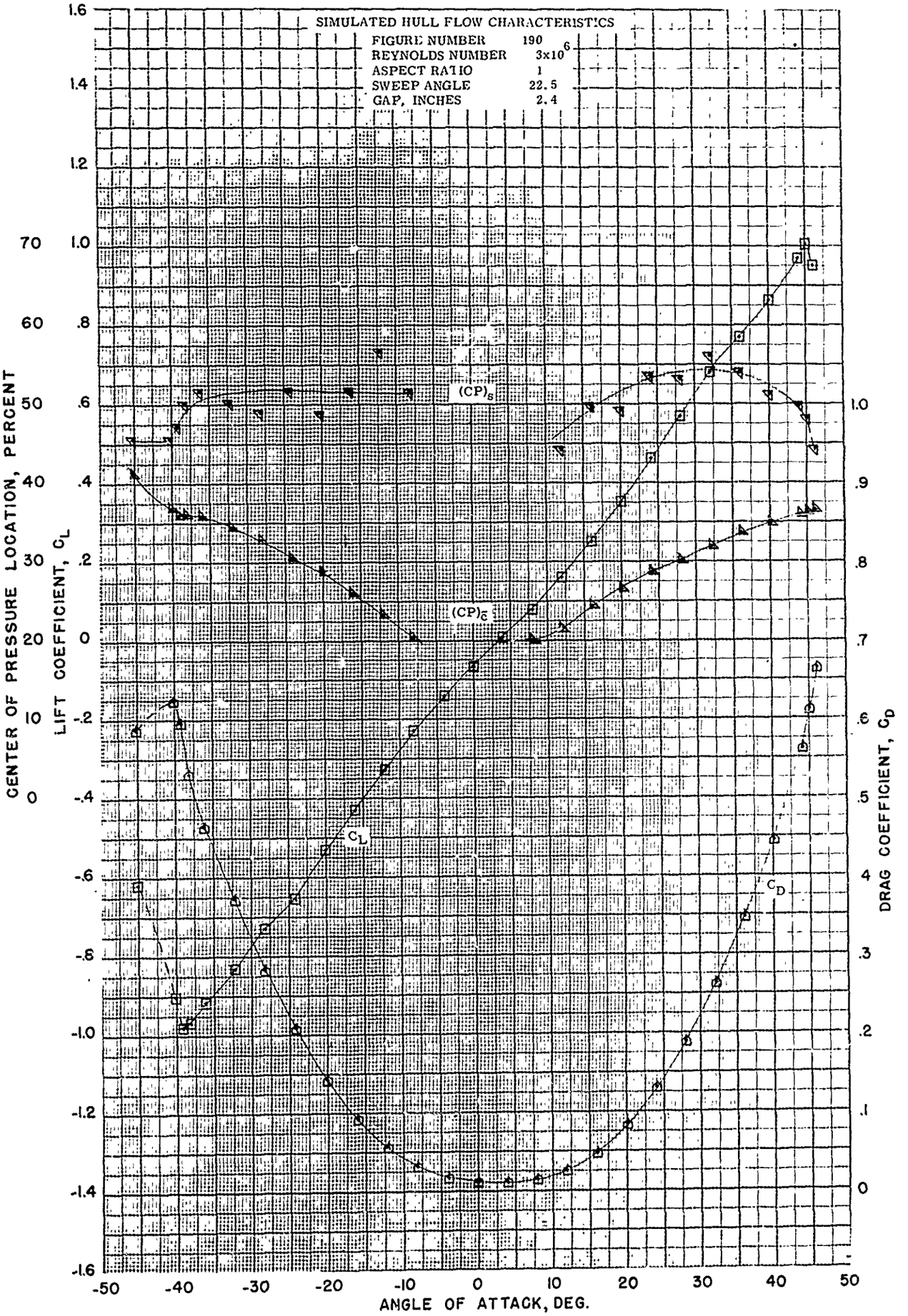
SIMULATED HULL FLOW CHARACTERISTICS
FIGURE NUMBER 190
REYNOLDS NUMBER 3x10^6
ASPECT RATIO 1
SWEEP ANGLE 22.5
GAP, INCHES 2.4
CENTER OF PRESSURE LOCATION, PERCENT
LIFT COEFFICIENT, C_L
DRAG COEFFICIENT, C_D
ANGLE OF ATTACK, DEG.
$(CP)_s$
$(CP)_{\bar{c}}$
C_L
C_D
70
60
50
40
30
20
10
0
1.6
1.4
1.2
1.0
.8
.6
.4
.2
0
-.2
-.4
-.6
-.8
-1.0
-1.2
-1.4
-1.6
1.0
.9
.8
.7
.6
.5
.4
.3
.2
.1
0
-50
-40
-30
-20
-10
0
10
20
30
40
50

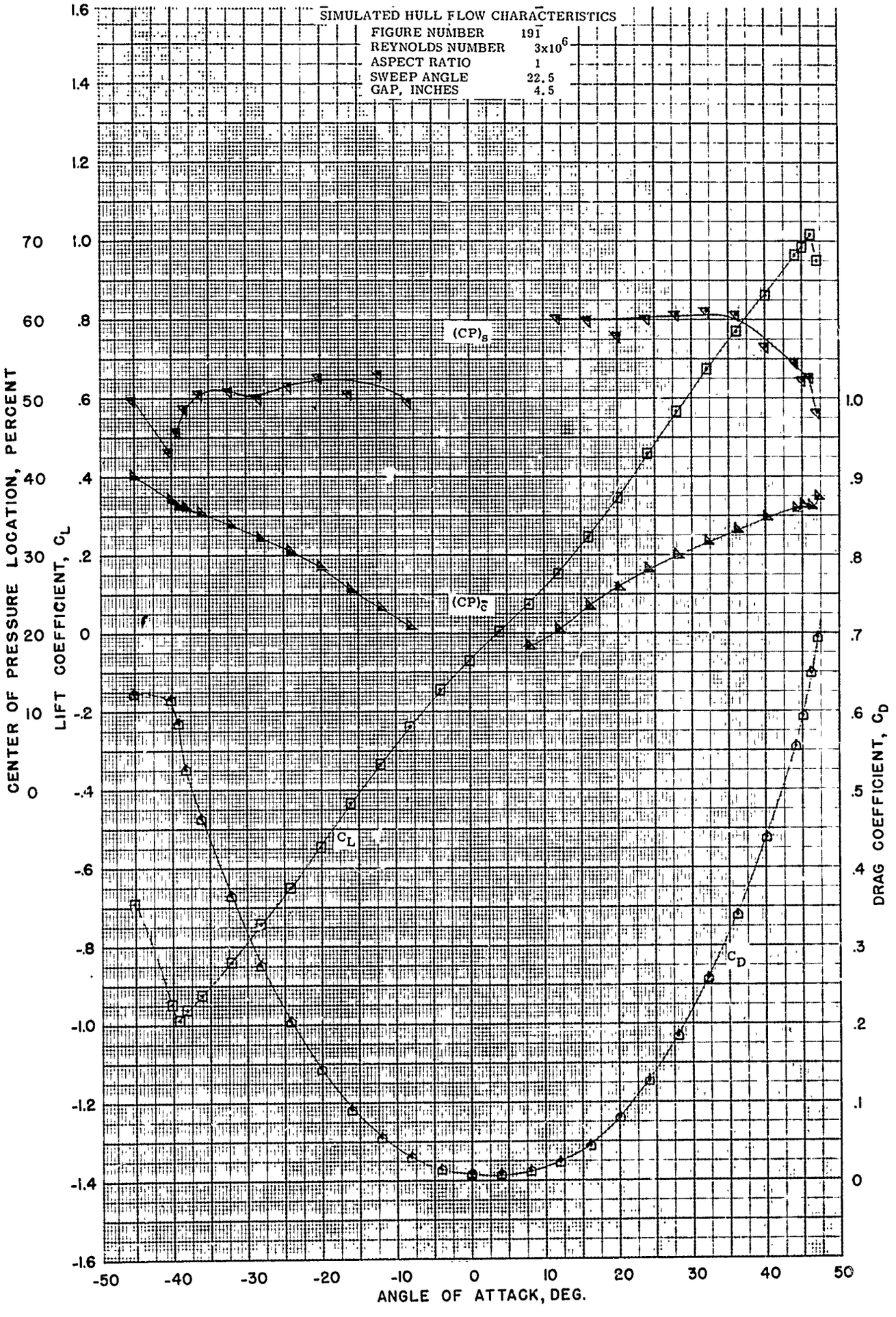
SIMULATED HULL FLOW CHARACTERISTICS
FIGURE NUMBER 191
REYNOLDS NUMBER 3x10^6
ASPECT RATIO 1
SWEEP ANGLE 22.5
GAP, INCHES 4.5
(CP)s
(CP)c
CL
CD
CENTER OF PRESSURE LOCATION, PERCENT
LIFT COEFFICIENT, CL
DRAG COEFFICIENT, CD
ANGLE OF ATTACK, DEG.
70
60
50
40
30
20
10
0
1.6
1.4
1.2
1.0
.8
.6
.4
.2
0
-.2
-.4
-.6
-.8
-1.0
-1.2
-1.4
-1.6
1.0
.9
.8
.7
.6
.5
.4
.3
.2
.1
0
-50
-40
-30
-20
-10
0
10
20
30
40
50

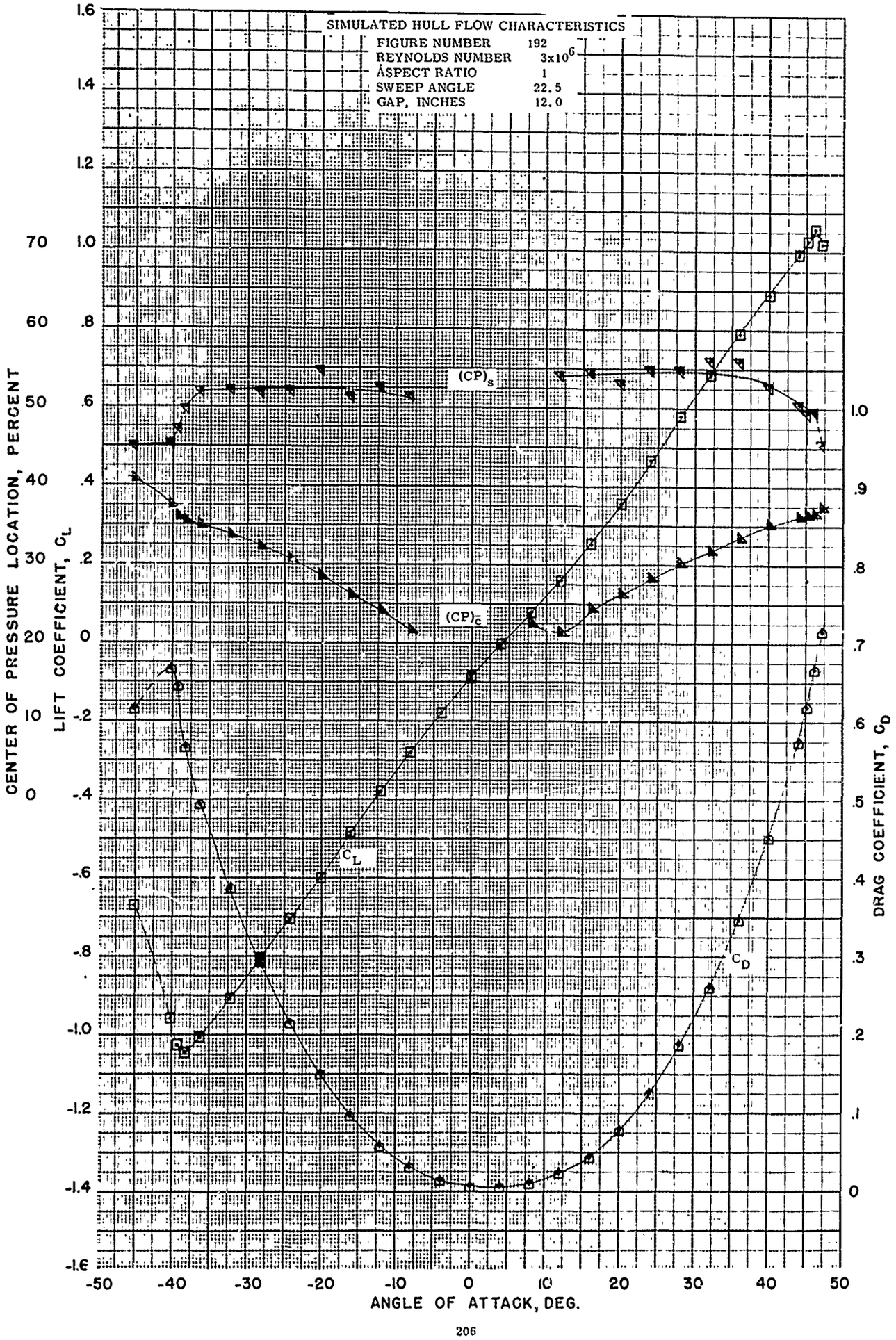
SIMULATED HULL FLOW CHARACTERISTICS
FIGURE NUMBER 192
REYNOLDS NUMBER 3x10^6
ASPECT RATIO 1
SWEEP ANGLE 22.5
GAP, INCHES 12.0
CENTER OF PRESSURE LOCATION, PERCENT
LIFT COEFFICIENT, C_L
DRAG COEFFICIENT, C_D
ANGLE OF ATTACK, DEG.
$(CP)_s$
$(CP)_c$
C_L
C_D
70
60
50
40
30
20
10
0
1.6
1.4
1.2
1.0
.8
.6
.4
.2
0
-.2
-.4
-.6
-.8
-1.0
-1.2
-1.4
-1.6
1.0
.9
.8
.7
.6
.5
.4
.3
.2
.1
0
-50
-40
-30
-20
-10
0
10
20
30
40
50

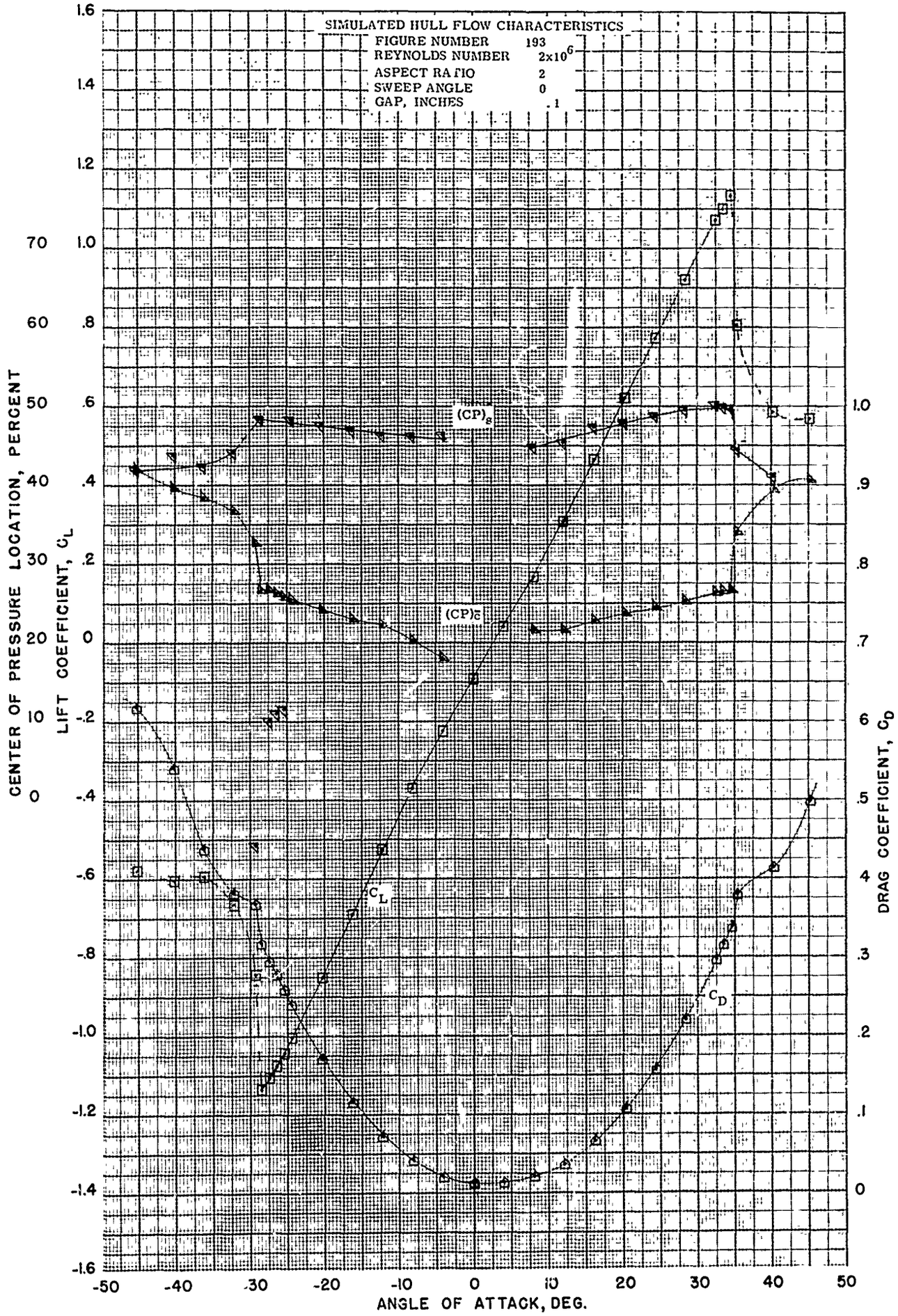
SIMULATED HULL FLOW CHARACTERISTICS
FIGURE NUMBER 193
REYNOLDS NUMBER 2×10^6
ASPECT RATIO 2
SWEEP ANGLE 0
GAP, INCHES .1
$(CP)_g$
$(CP)_{\bar{c}}$
C_L
C_D
CENTER OF PRESSURE LOCATION, PERCENT
LIFT COEFFICIENT, C_L
DRAG COEFFICIENT, C_D
ANGLE OF ATTACK, DEG.
70
60
50
40
30
20
10
0
1.6
1.4
1.2
1.0
.8
.6
.4
.2
0
-.2
-.4
-.6
-.8
-1.0
-1.2
-1.4
-1.6
1.0
.9
.8
.7
.6
.5
.4
.3
.2
.1
0
-50
-40
-30
-20
-10
0
10
20
30
40
50

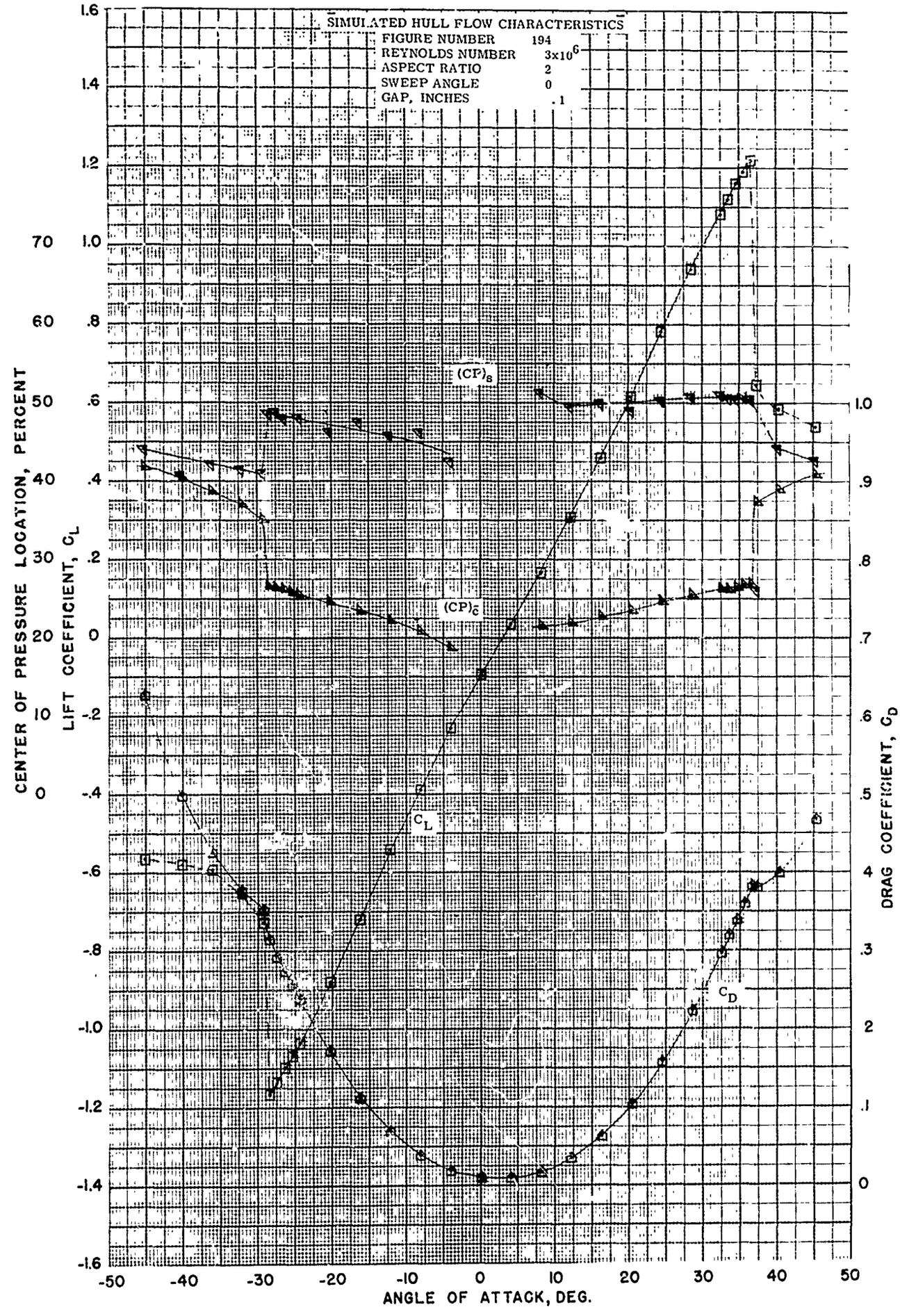
SIMULATED HULL FLOW CHARACTERISTICS
FIGURE NUMBER 194
REYNOLDS NUMBER 3x10^6
ASPECT RATIO 2
SWEEP ANGLE 0
GAP, INCHES .1
CENTER OF PRESSURE LOCATION, PERCENT
LIFT COEFFICIENT, C_L
DRAG COEFFICIENT, C_D
ANGLE OF ATTACK, DEG.
$(CP)_s$
$(CP)_{\bar{c}}$
C_L
C_D
70
60
50
40
30
20
10
0
1.6
1.4
1.2
1.0
.8
.6
.4
.2
0
-.2
-.4
-.6
-.8
-1.0
-1.2
-1.4
-1.6
1.0
.9
.8
.7
.6
.5
.4
.3
.2
.1
0
-50
-40
-30
-20
-10
0
10
20
30
40
50

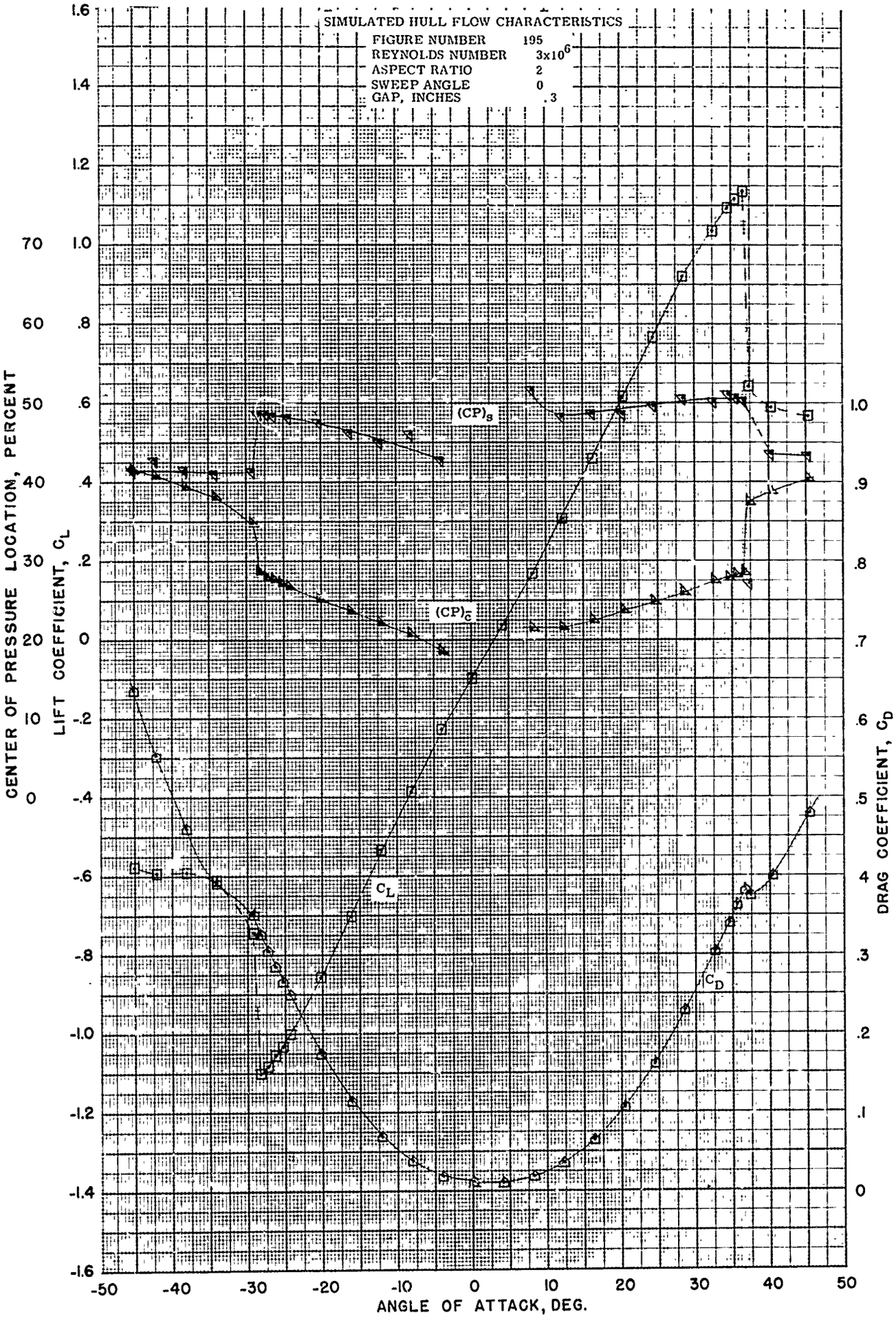
SIMULATED HULL FLOW CHARACTERISTICS
FIGURE NUMBER 195
REYNOLDS NUMBER 3x10^6
ASPECT RATIO 2
SWEEP ANGLE 0
GAP, INCHES .3
CENTER OF PRESSURE LOCATION, PERCENT
LIFT COEFFICIENT, C_L
DRAG COEFFICIENT, C_D
ANGLE OF ATTACK, DEG.
$(CP)_s$
$(CP)_c$
C_L
C_D
70
60
50
40
30
20
10
0
1.6
1.4
1.2
1.0
.8
.6
.4
.2
0
-.2
-.4
-.6
-.8
-1.0
-1.2
-1.4
-1.6
1.0
.9
.8
.7
.6
.5
.4
.3
.2
.1
0
-50
-40
-30
-20
-10
0
10
20
30
40
50

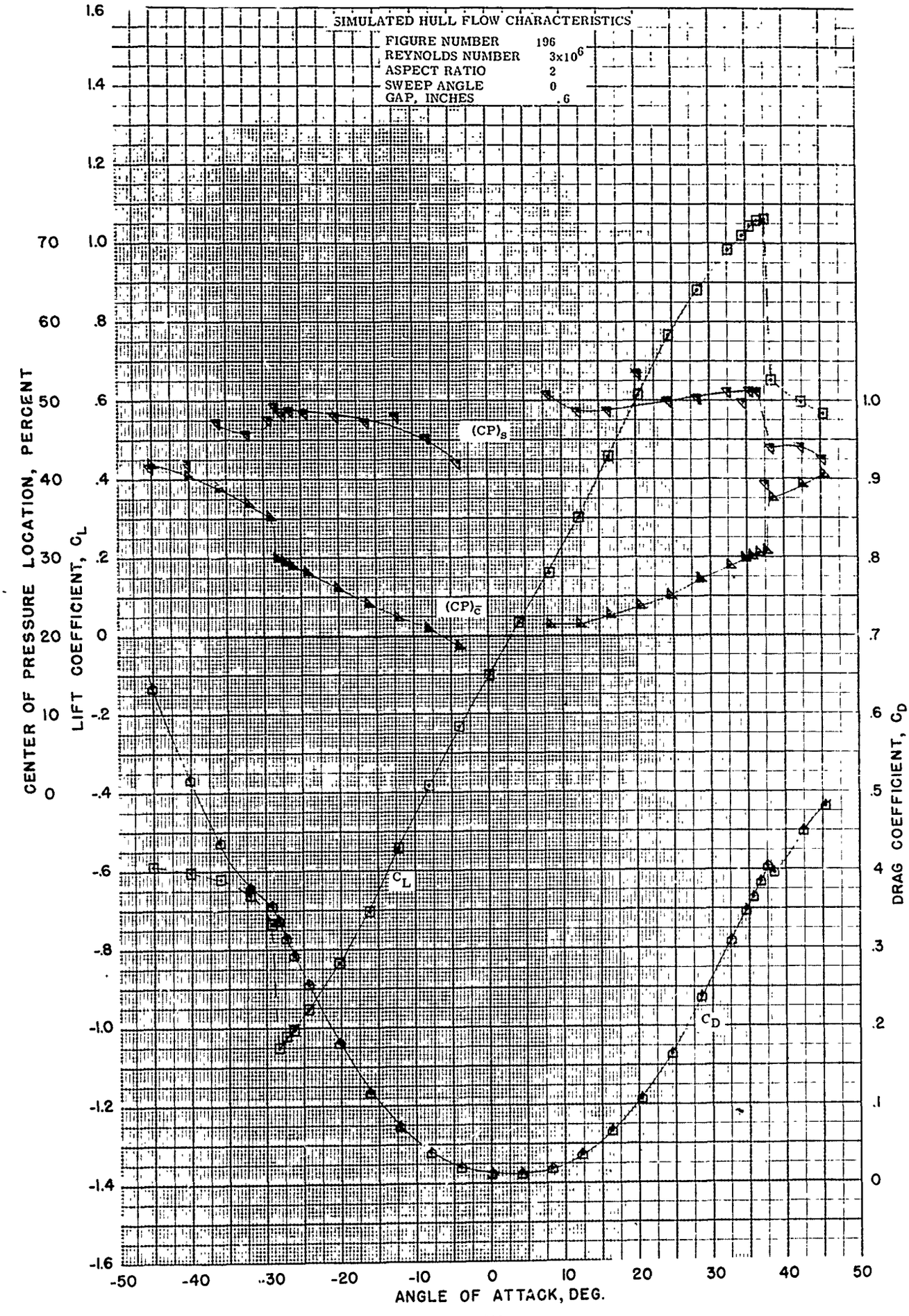
SIMULATED HULL FLOW CHARACTERISTICS
FIGURE NUMBER 196
REYNOLDS NUMBER 3x10^6
ASPECT RATIO 2
SWEEP ANGLE 0
GAP, INCHES .6
CENTER OF PRESSURE LOCATION, PERCENT
LIFT COEFFICIENT, C_L
DRAG COEFFICIENT, C_D
ANGLE OF ATTACK, DEG.
$(CP)_s$
$(CP)_{\bar{c}}$
C_L
C_D
70
60
50
40
30
20
10
0
1.6
1.4
1.2
1.0
.8
.6
.4
.2
0
-.2
-.4
-.6
-.8
-1.0
-1.2
-1.4
-1.6
1.0
.9
.8
.7
.6
.5
.4
.3
.2
.1
0
-50
-40
-30
-20
-10
0
10
20
30
40
50

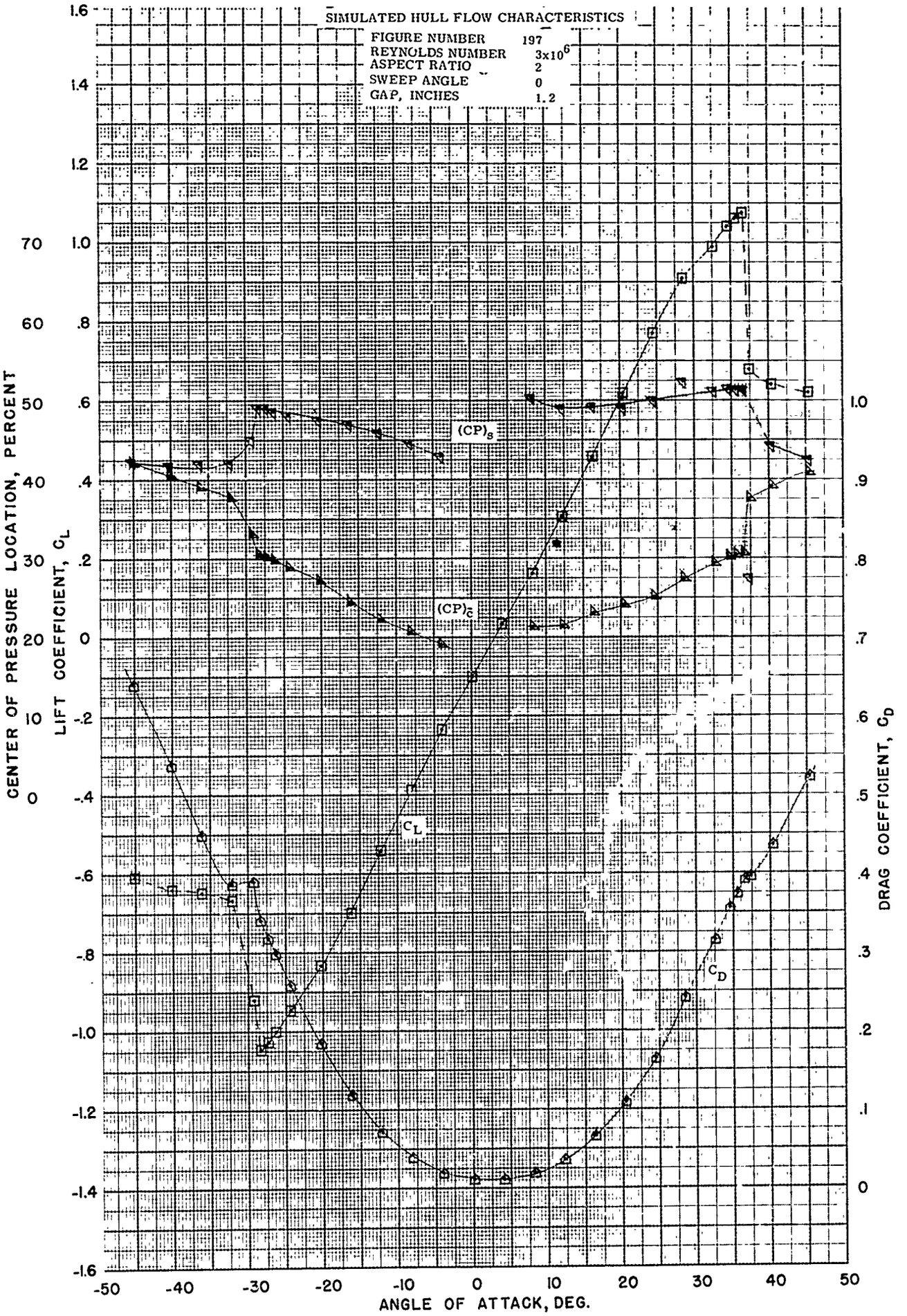
SIMULATED HULL FLOW CHARACTERISTICS
FIGURE NUMBER 197
REYNOLDS NUMBER 3x10^6
ASPECT RATIO 2
SWEEP ANGLE 0
GAP, INCHES 1.2
(CP)s
(CP)c
CL
CD
CENTER OF PRESSURE LOCATION, PERCENT
LIFT COEFFICIENT, CL
DRAG COEFFICIENT, CD
ANGLE OF ATTACK, DEG.
70
60
50
40
30
20
10
0
1.6
1.4
1.2
1.0
.8
.6
.4
.2
0
-.2
-.4
-.6
-.8
-1.0
-1.2
-1.4
-1.6
1.0
.9
.8
.7
.6
.5
.4
.3
.2
.1
0
-50
-40
-30
-20
-10
0
10
20
30
40
50

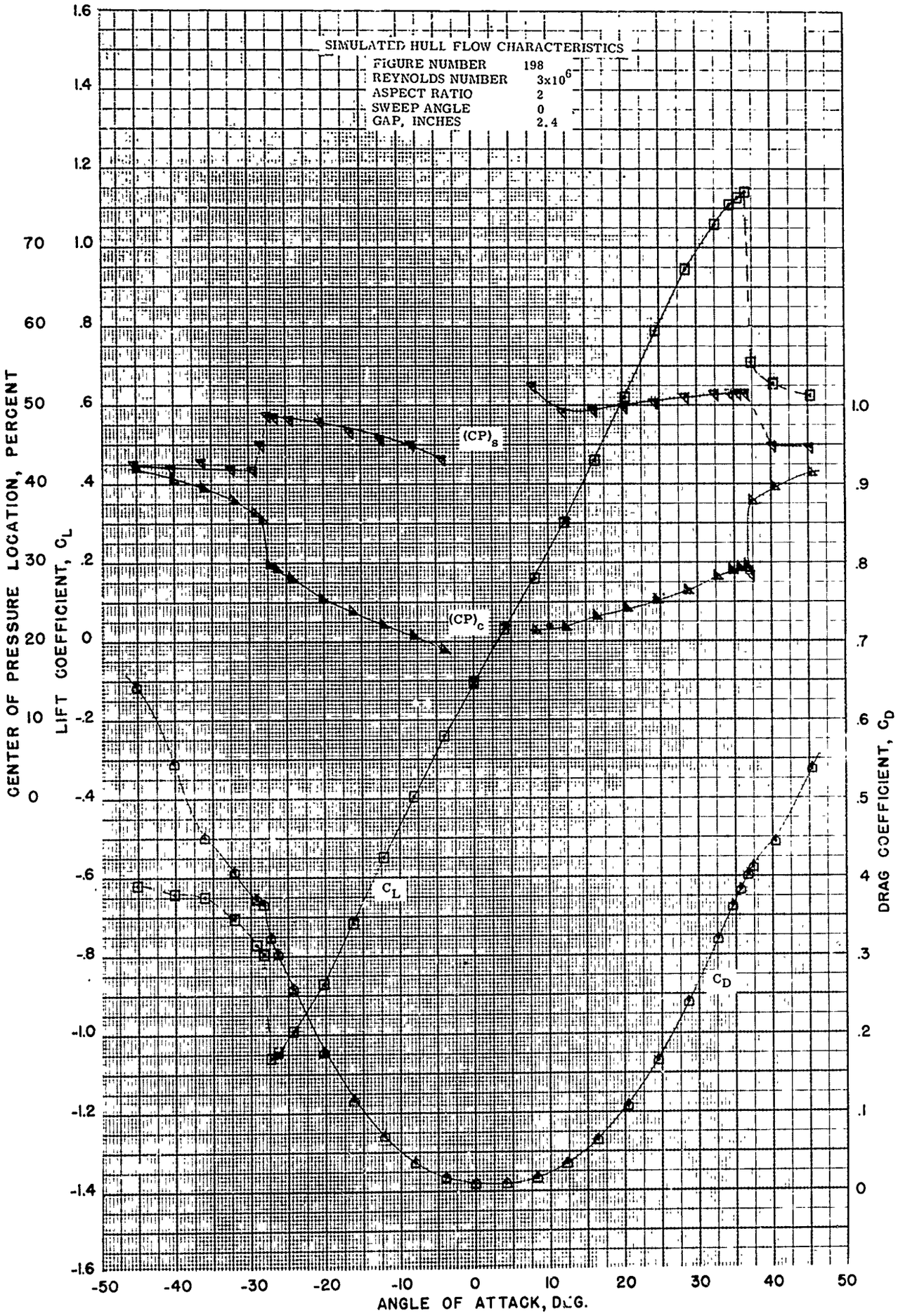
SIMULATED HULL FLOW CHARACTERISTICS
FIGURE NUMBER 198
REYNOLDS NUMBER 3x10^6
ASPECT RATIO 2
SWEEP ANGLE 0
GAP, INCHES 2.4
CENTER OF PRESSURE LOCATION, PERCENT
LIFT COEFFICIENT, C_L
DRAG COEFFICIENT, C_D
ANGLE OF ATTACK, DEG.
$(CP)_s$
$(CP)_c$
C_L
C_D
70
60
50
40
30
20
10
0
1.6
1.4
1.2
1.0
.8
.6
.4
.2
0
-.2
-.4
-.6
-.8
-1.0
-1.2
-1.4
-1.6
1.0
.9
.8
.7
.6
.5
.4
.3
.2
.1
0
-50
-40
-30
-20
-10
0
10
20
30
40
50

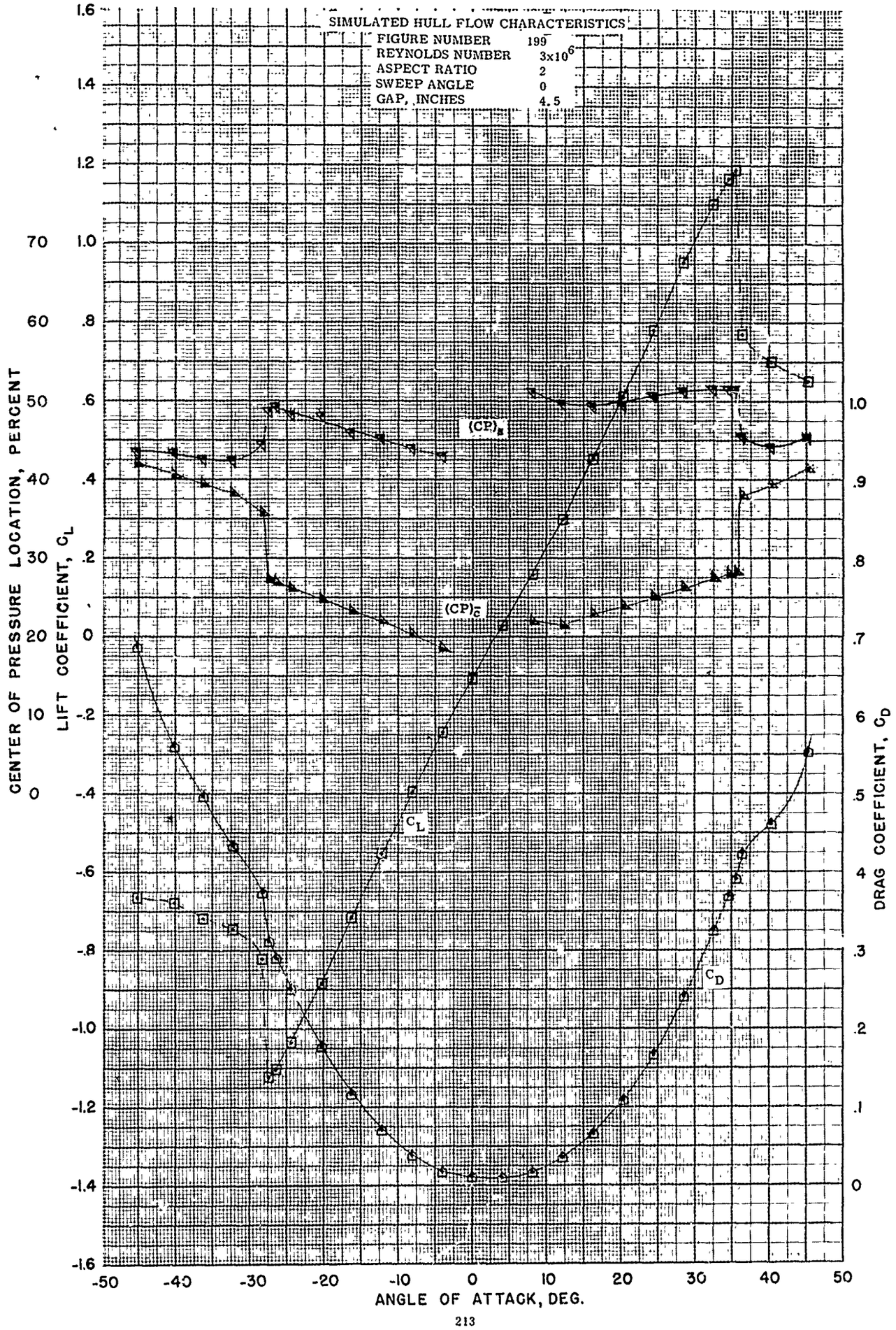
SIMULATED HULL FLOW CHARACTERISTICS
FIGURE NUMBER 199
REYNOLDS NUMBER 3×10^6
ASPECT RATIO 2
SWEEP ANGLE 0
GAP, INCHES 4.5
CENTER OF PRESSURE LOCATION, PERCENT
LIFT COEFFICIENT, C_L
DRAG COEFFICIENT, C_D
ANGLE OF ATTACK, DEG.
$(CP)_B$
$(CP)_C$
C_L
C_D
70
60
50
40
30
20
10
0
1.6
1.4
1.2
1.0
.8
.6
.4
.2
0
-.2
-.4
-.6
-.8
-1.0
-1.2
-1.4
-1.6
1.0
.9
.8
.7
6
.5
4
.3
.2
.1
0
-50
-40
-30
-20
-10
0
10
20
30
40
50

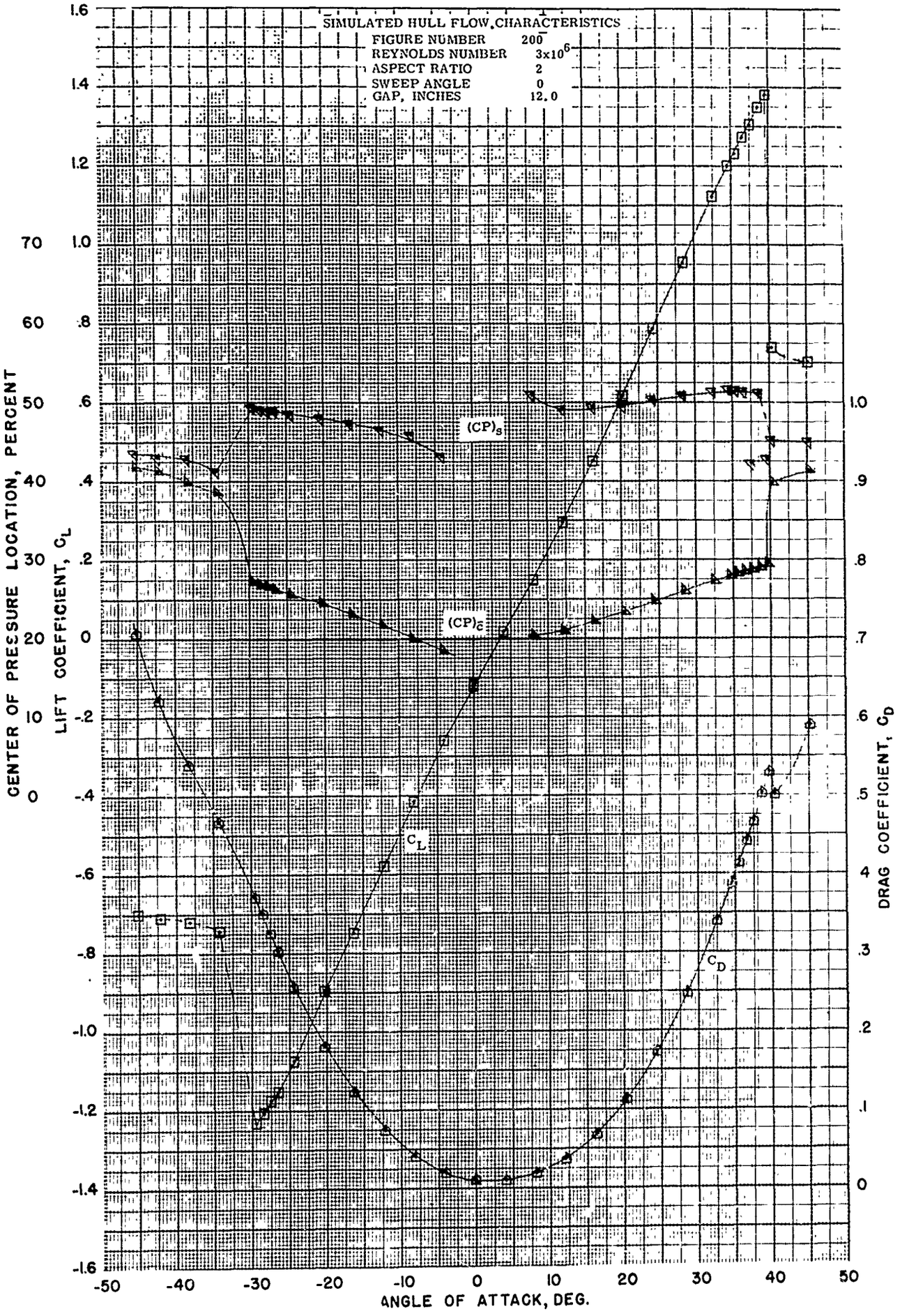
SIMULATED HULL FLOW CHARACTERISTICS
FIGURE NUMBER 200
REYNOLDS NUMBER 3x10^6
ASPECT RATIO 2
SWEEP ANGLE 0
GAP, INCHES 12.0
CENTER OF PRESSURE LOCATION, PERCENT
LIFT COEFFICIENT, C_L
DRAG COEFFICIENT, C_D
ANGLE OF ATTACK, DEG.
$(CP)_s$
$(CP)_{\bar{c}}$
C_L
C_D
70
60
50
40
30
20
10
0
1.6
1.4
1.2
1.0
.8
.6
.4
.2
0
-.2
-.4
-.6
-.8
-1.0
-1.2
-1.4
-1.6
1.0
.9
.8
.7
.6
.5
.4
.3
.2
.1
0
-50
-40
-30
-20
-10
0
10
20
30
40
50

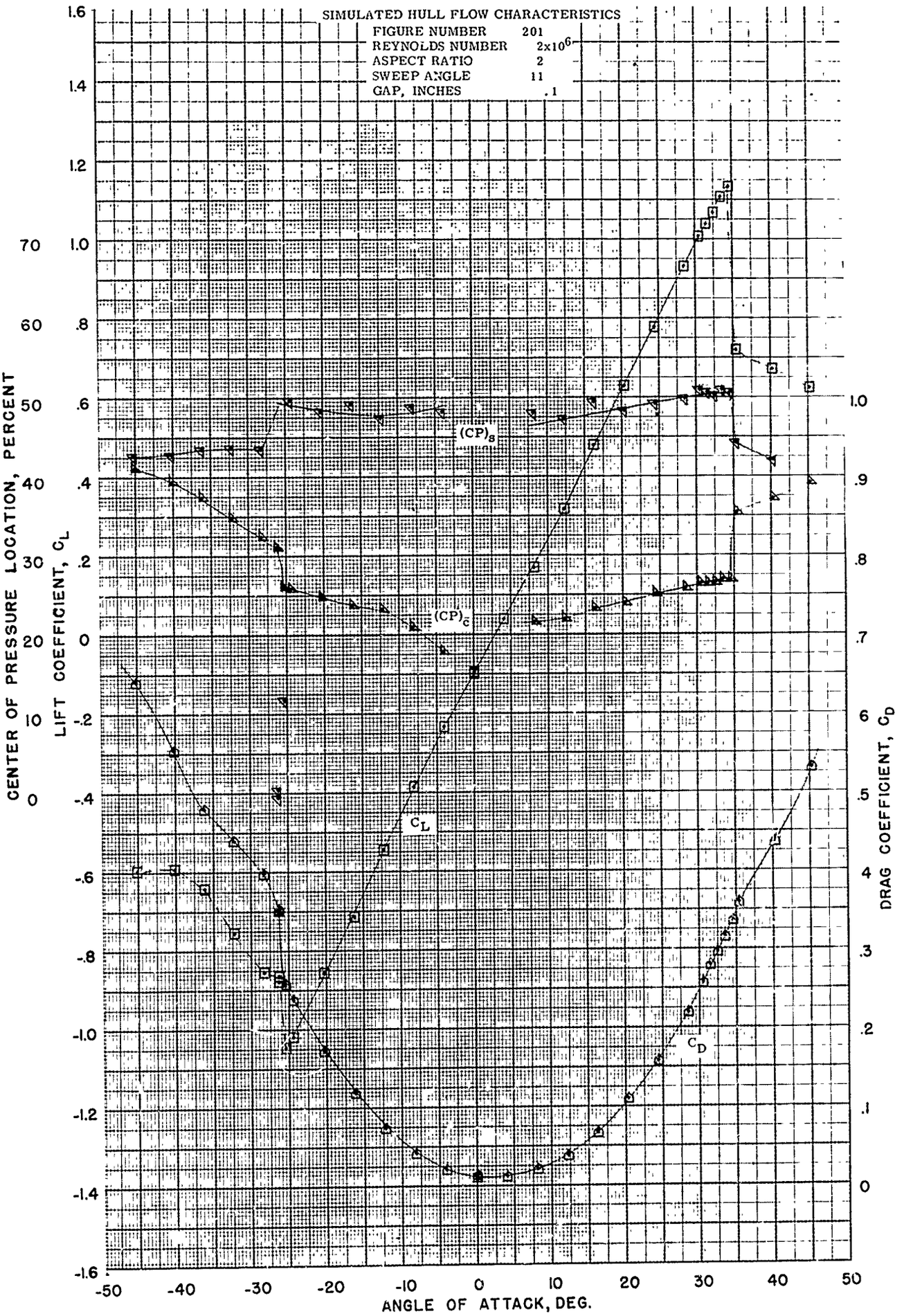
SIMULATED HULL FLOW CHARACTERISTICS
FIGURE NUMBER 201
REYNOLDS NUMBER 2x10^6
ASPECT RATIO 2
SWEEP ANGLE 11
GAP, INCHES .1
CENTER OF PRESSURE LOCATION, PERCENT
LIFT COEFFICIENT, C_L
DRAG COEFFICIENT, C_D
ANGLE OF ATTACK, DEG.
$(CP)_s$
$(CP)_{\bar{c}}$
C_L
C_D
70
60
50
40
30
20
10
0
1.6
1.4
1.2
1.0
.8
.6
.4
.2
0
-.2
-.4
-.6
-.8
-1.0
-1.2
-1.4
-1.6
1.0
.9
.8
.7
.6
.5
.4
.3
.2
.1
0
-50
-40
-30
-20
-10
0
10
20
30
40
50

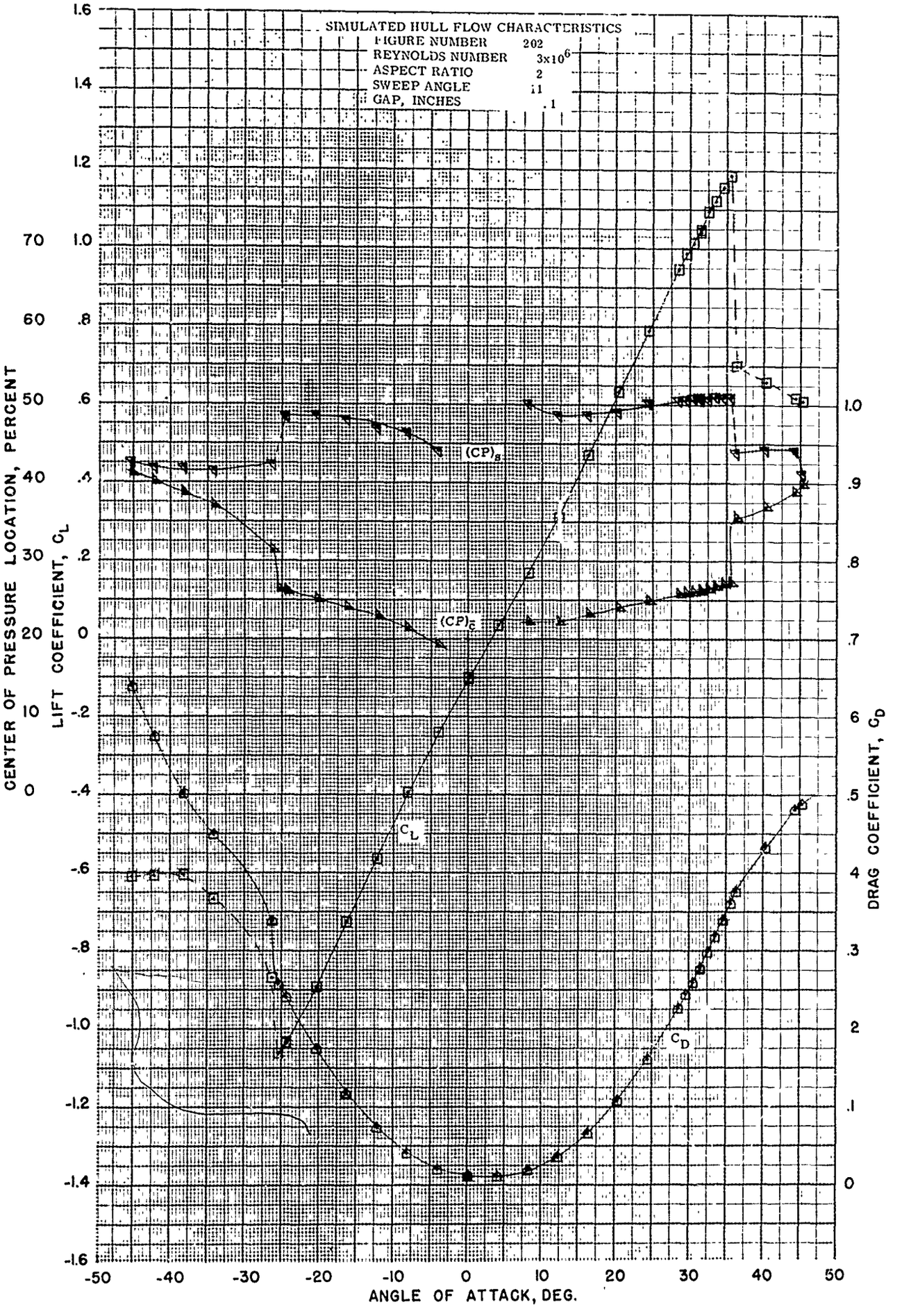
SIMULATED HULL FLOW CHARACTERISTICS
FIGURE NUMBER 202
REYNOLDS NUMBER 3×10^6
ASPECT RATIO 2
SWEEP ANGLE 11
GAP, INCHES .1
CENTER OF PRESSURE LOCATION, PERCENT
LIFT COEFFICIENT, C_L
DRAG COEFFICIENT, C_D
ANGLE OF ATTACK, DEG.
$(CP)_s$
$(CP)_c$
C_L
C_D
70
60
50
40
30
20
10
0
1.6
1.4
1.2
1.0
.8
.6
.4
.2
0
-.2
-.4
-.6
-.8
-1.0
-1.2
-1.4
-1.6
1.0
.9
.8
.7
6
.5
4
.3
2
.1
0
-50
-40
-30
-20
-10
0
10
20
30
40
50

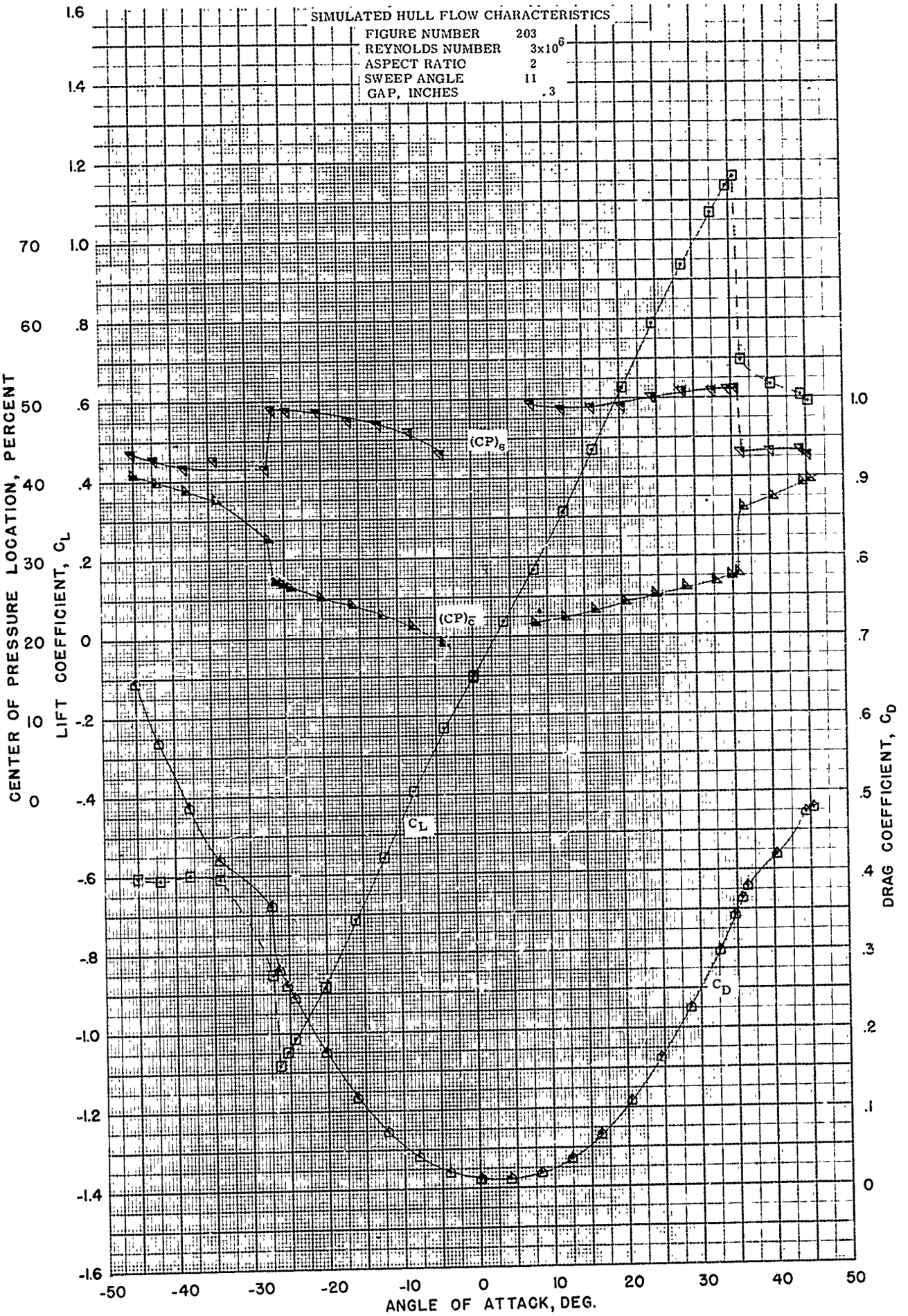
SIMULATED HULL FLOW CHARACTERISTICS
FIGURE NUMBER 203
REYNOLDS NUMBER 3x10^6
ASPECT RATIO 2
SWEEP ANGLE 11
GAP, INCHES .3
CENTER OF PRESSURE LOCATION, PERCENT
LIFT COEFFICIENT, C_L
DRAG COEFFICIENT, C_D
ANGLE OF ATTACK, DEG.
$(CP)_s$
$(CP)_{\bar{c}}$
C_L
C_D
70
60
50
40
30
20
10
0
1.6
1.4
1.2
1.0
.8
.6
.4
.2
0
-.2
-.4
-.6
-.8
-1.0
-1.2
-1.4
-1.6
1.0
.9
.8
.7
.6
.5
.4
.3
.2
.1
0
-50
-40
-30
-20
-10
0
10
20
30
40
50

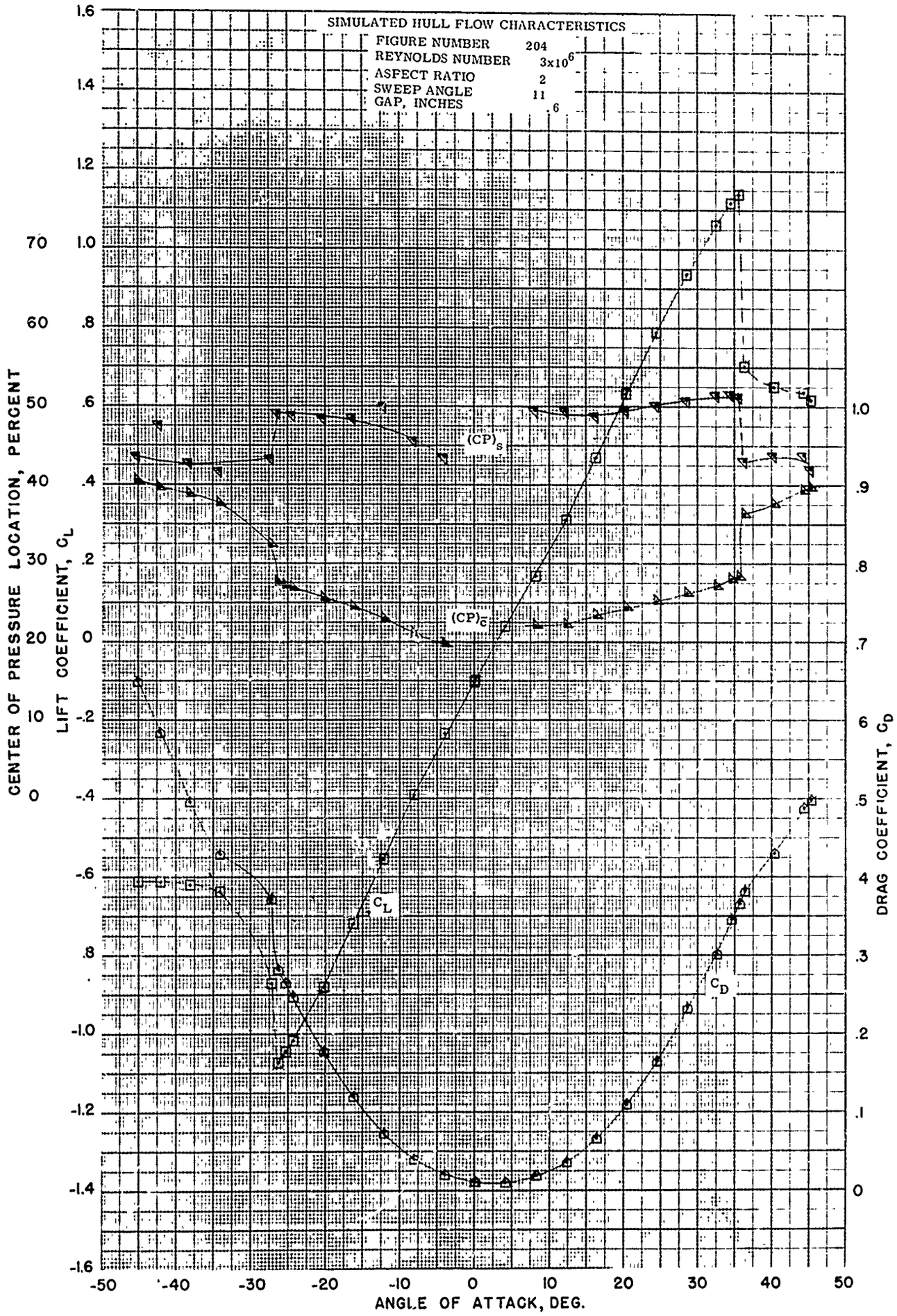
SIMULATED HULL FLOW CHARACTERISTICS
FIGURE NUMBER 204
REYNOLDS NUMBER 3x10^6
ASPECT RATIO 2
SWEEP ANGLE 11
GAP, INCHES .6
CENTER OF PRESSURE LOCATION, PERCENT
LIFT COEFFICIENT, C_L
DRAG COEFFICIENT, C_D
ANGLE OF ATTACK, DEG.
$(CP)_S$
$(CP)_{\bar{c}}$
C_L
C_D
70
60
50
40
30
20
10
0
1.6
1.4
1.2
1.0
.8
.6
.4
.2
0
-.2
-.4
-.6
-.8
-1.0
-1.2
-1.4
-1.6
1.0
.9
.8
.7
.6
.5
.4
.3
.2
.1
0
-50
-40
-30
-20
-10
0
10
20
30
40
50

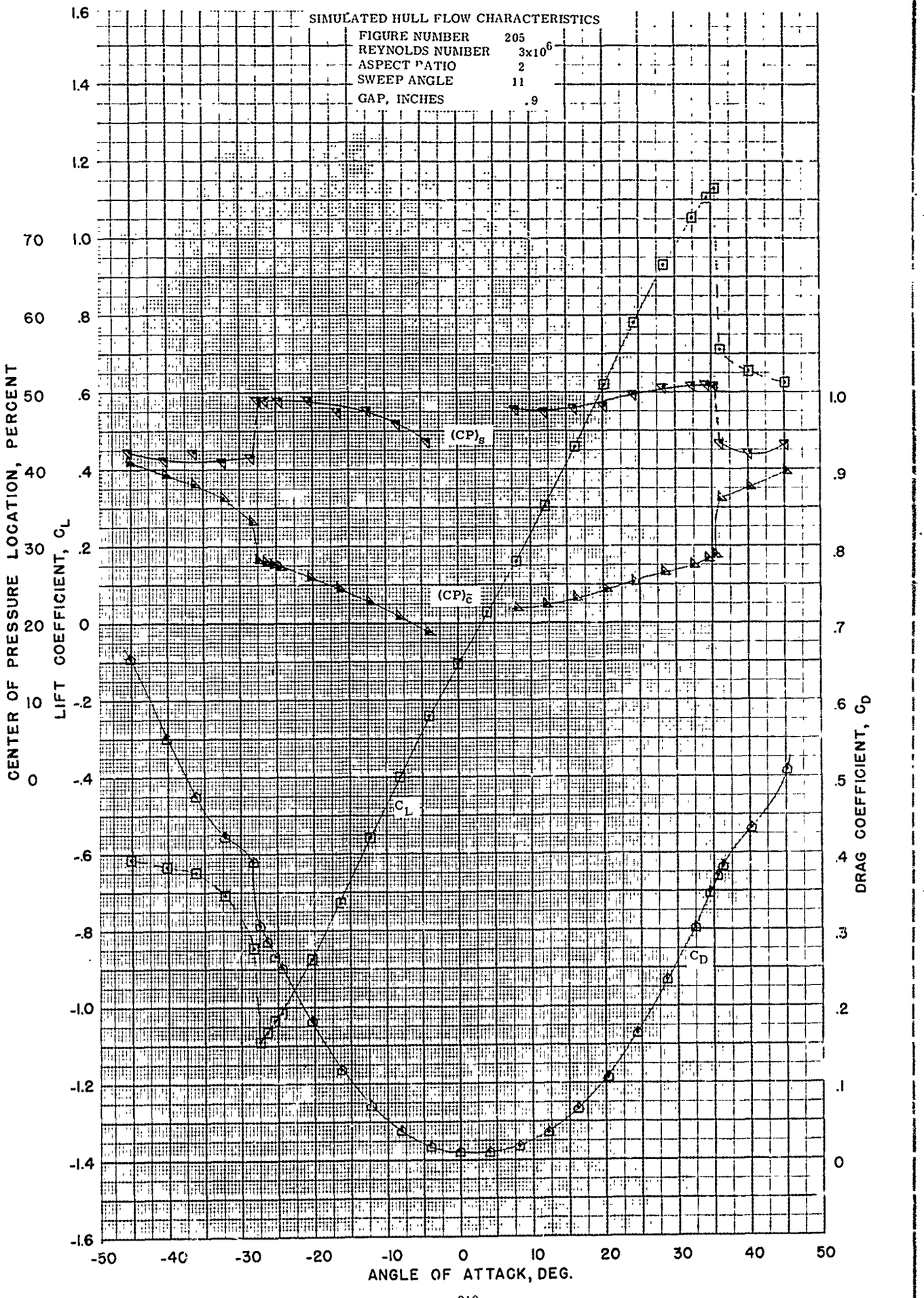
SIMULATED HULL FLOW CHARACTERISTICS
FIGURE NUMBER 205
REYNOLDS NUMBER 3x10^6
ASPECT RATIO 2
SWEEP ANGLE 11
GAP, INCHES .9
CENTER OF PRESSURE LOCATION, PERCENT
LIFT COEFFICIENT, C_L
DRAG COEFFICIENT, C_D
ANGLE OF ATTACK, DEG.
$(CP)_s$
$(CP)_{\bar{c}}$
C_L
C_D
70
60
50
40
30
20
10
0
1.6
1.4
1.2
1.0
.8
.6
.4
.2
0
-.2
-.4
-.6
-.8
-1.0
-1.2
-1.4
-1.6
1.0
.9
.8
.7
.6
.5
.4
.3
.2
.1
0
-50
-40
-30
-20
-10
0
10
20
30
40
50

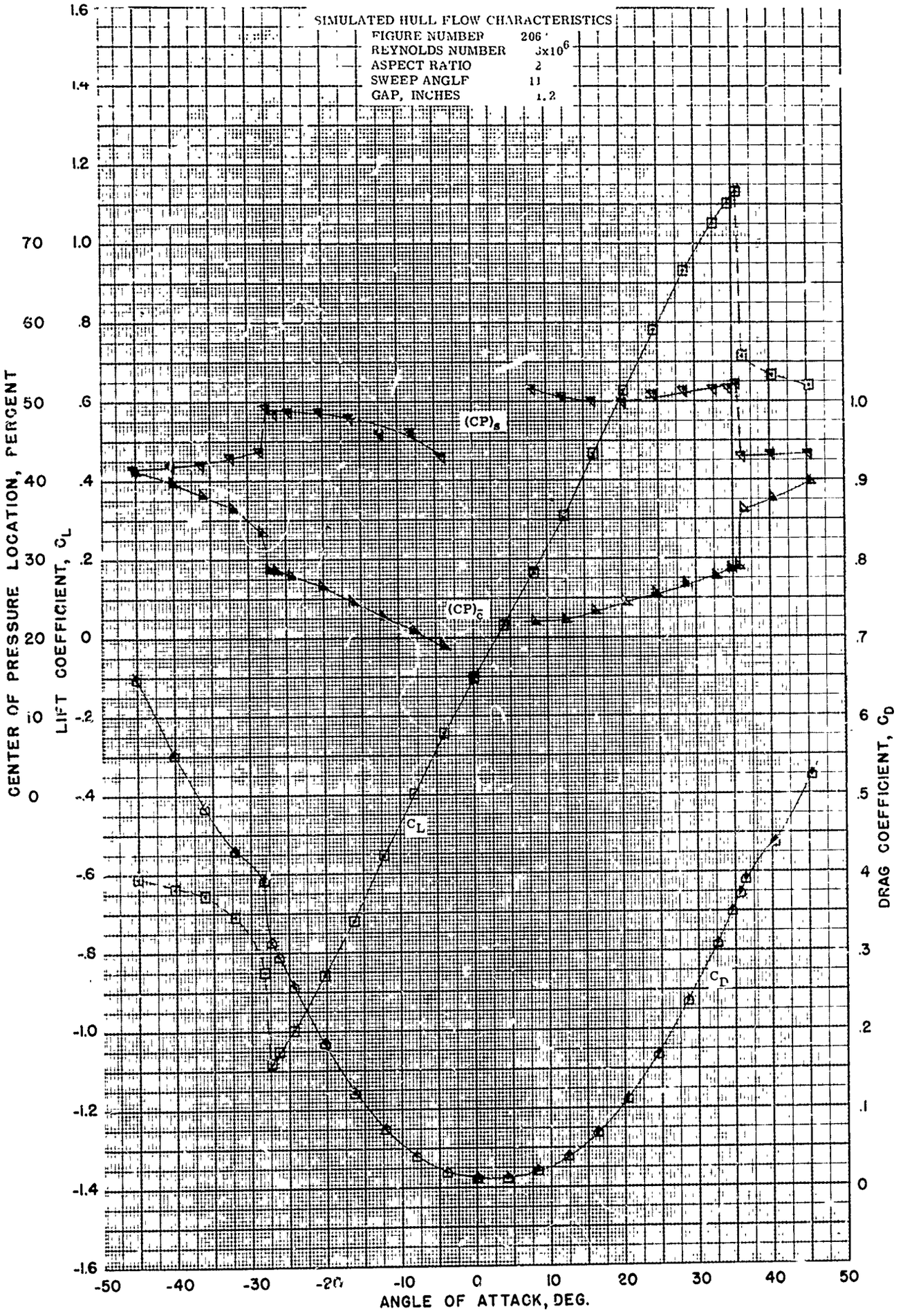
SIMULATED HULL FLOW CHARACTERISTICS
FIGURE NUMBER 206
REYNOLDS NUMBER 3x10^6
ASPECT RATIO 2
SWEEP ANGLE 11
GAP, INCHES 1.2
CENTER OF PRESSURE LOCATION, PERCENT
LIFT COEFFICIENT, C_L
DRAG COEFFICIENT, C_D
ANGLE OF ATTACK, DEG.
$(CP)_s$
$(CP)_c$
C_L
C_D
70
60
50
40
30
20
10
0
1.6
1.4
1.2
1.0
.8
.6
.4
.2
0
-.2
-.4
-.6
-.8
-1.0
-1.2
-1.4
-1.6
1.0
.9
.8
.7
.6
.5
.4
.3
.2
.1
0
-50
-40
-30
-20
-10
0
10
20
30
40
50

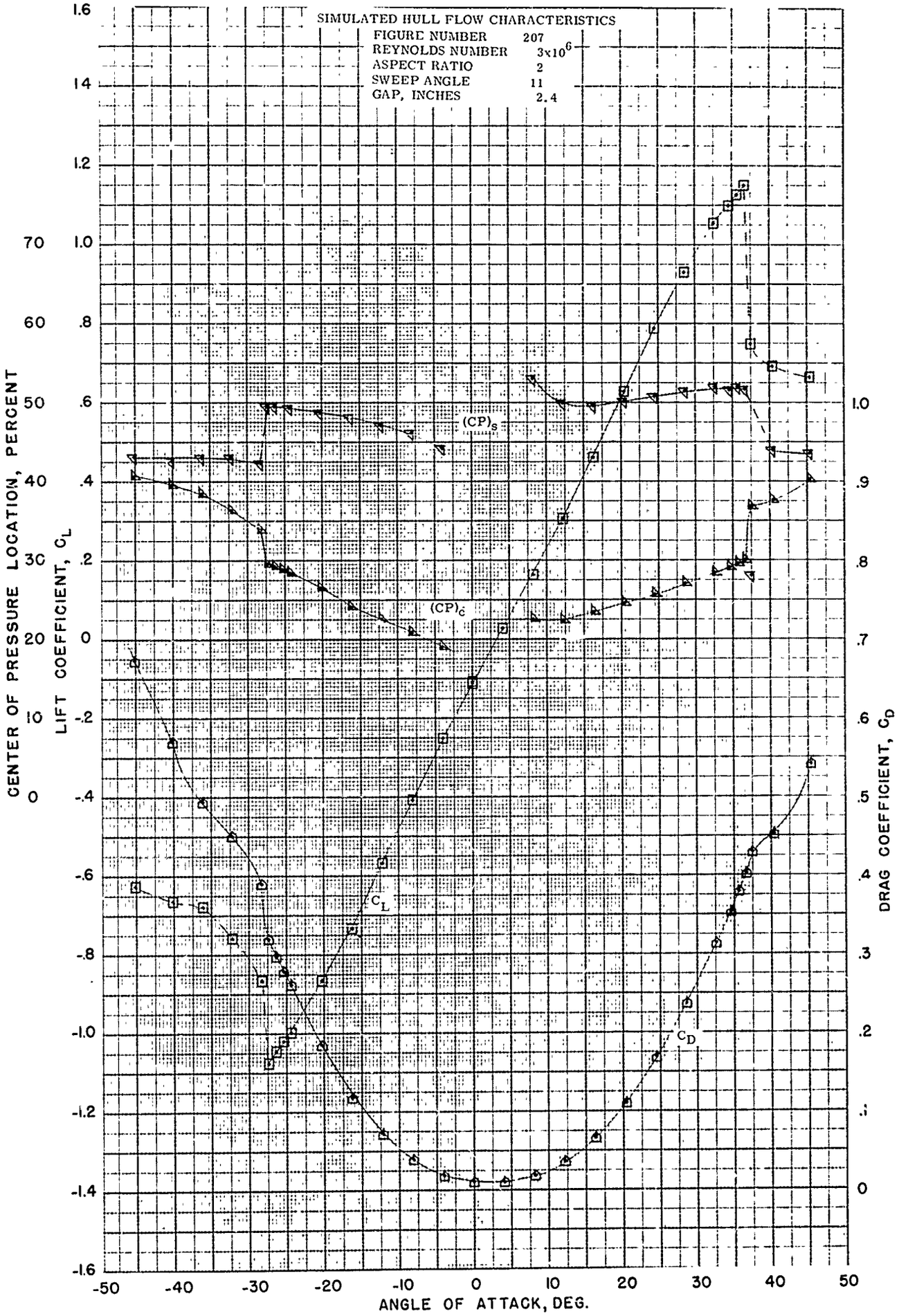
SIMULATED HULL FLOW CHARACTERISTICS
FIGURE NUMBER 207
REYNOLDS NUMBER 3×10^6
ASPECT RATIO 2
SWEEP ANGLE 11
GAP, INCHES 2.4
CENTER OF PRESSURE LOCATION, PERCENT
LIFT COEFFICIENT, C_L
DRAG COEFFICIENT, C_D
ANGLE OF ATTACK, DEG.
$(CP)_s$
$(CP)_c$
C_L
C_D
70
60
50
40
30
20
10
0
1.6
1.4
1.2
1.0
.8
.6
.4
.2
0
-.2
-.4
-.6
-.8
-1.0
-1.2
-1.4
-1.6
1.0
.9
.8
.7
.6
.5
.4
.3
.2
.1
0
-50
-40
-30
-20
-10
0
10
20
30
40
50

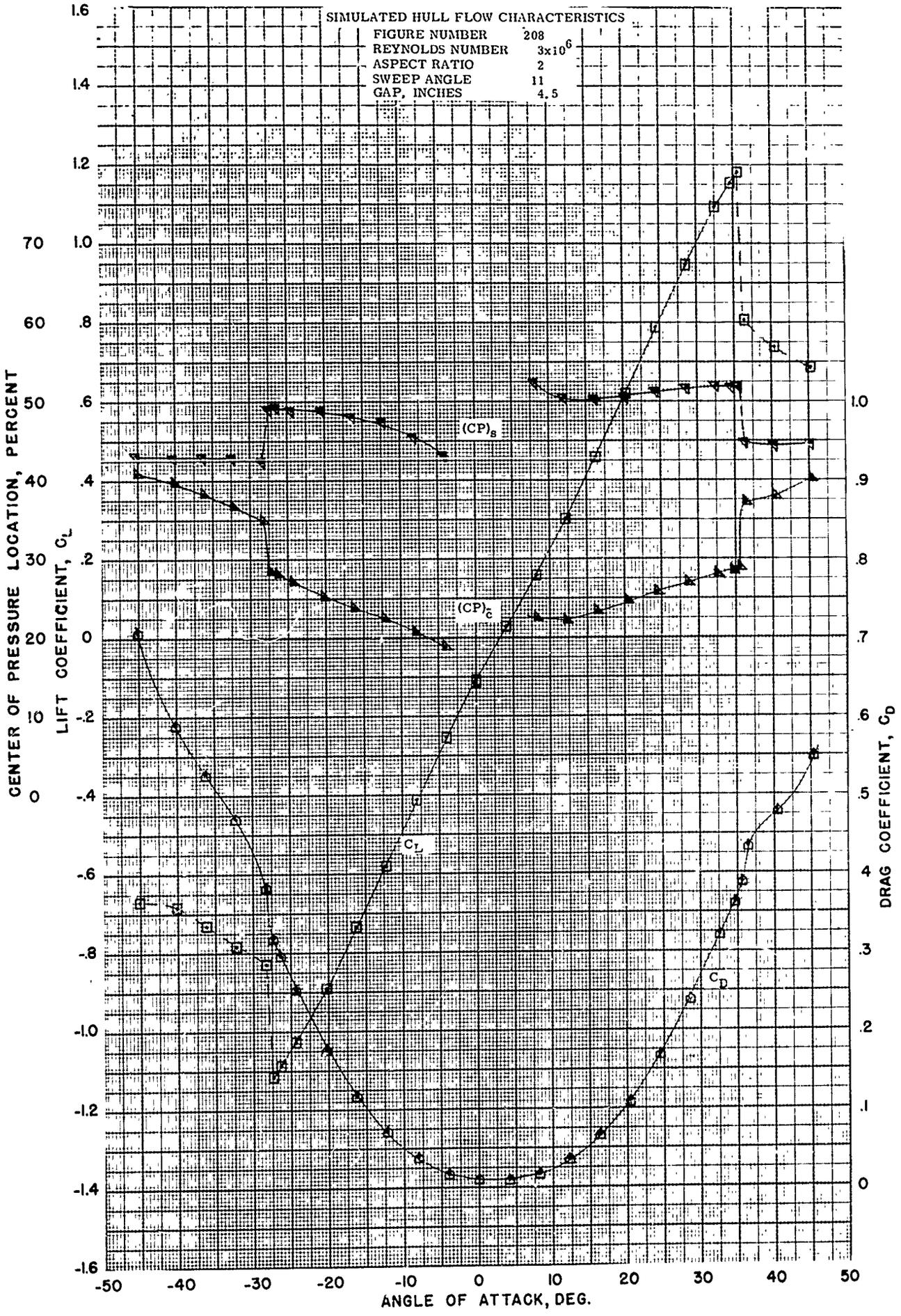
SIMULATED HULL FLOW CHARACTERISTICS
FIGURE NUMBER 208
REYNOLDS NUMBER 3x10^6
ASPECT RATIO 2
SWEEP ANGLE 11
GAP, INCHES 4.5
CENTER OF PRESSURE LOCATION, PERCENT
LIFT COEFFICIENT, C_L
DRAG COEFFICIENT, C_D
ANGLE OF ATTACK, DEG.
$(CP)_s$
$(CP)_c$
C_L
C_D
70
60
50
40
30
20
10
0
1.6
1.4
1.2
1.0
.8
.6
.4
.2
0
-.2
-.4
-.6
-.8
-1.0
-1.2
-1.4
-1.6
1.0
.9
.8
.7
.6
.5
.4
.3
.2
.1
0
-50
-40
-30
-20
-10
0
10
20
30
40
50

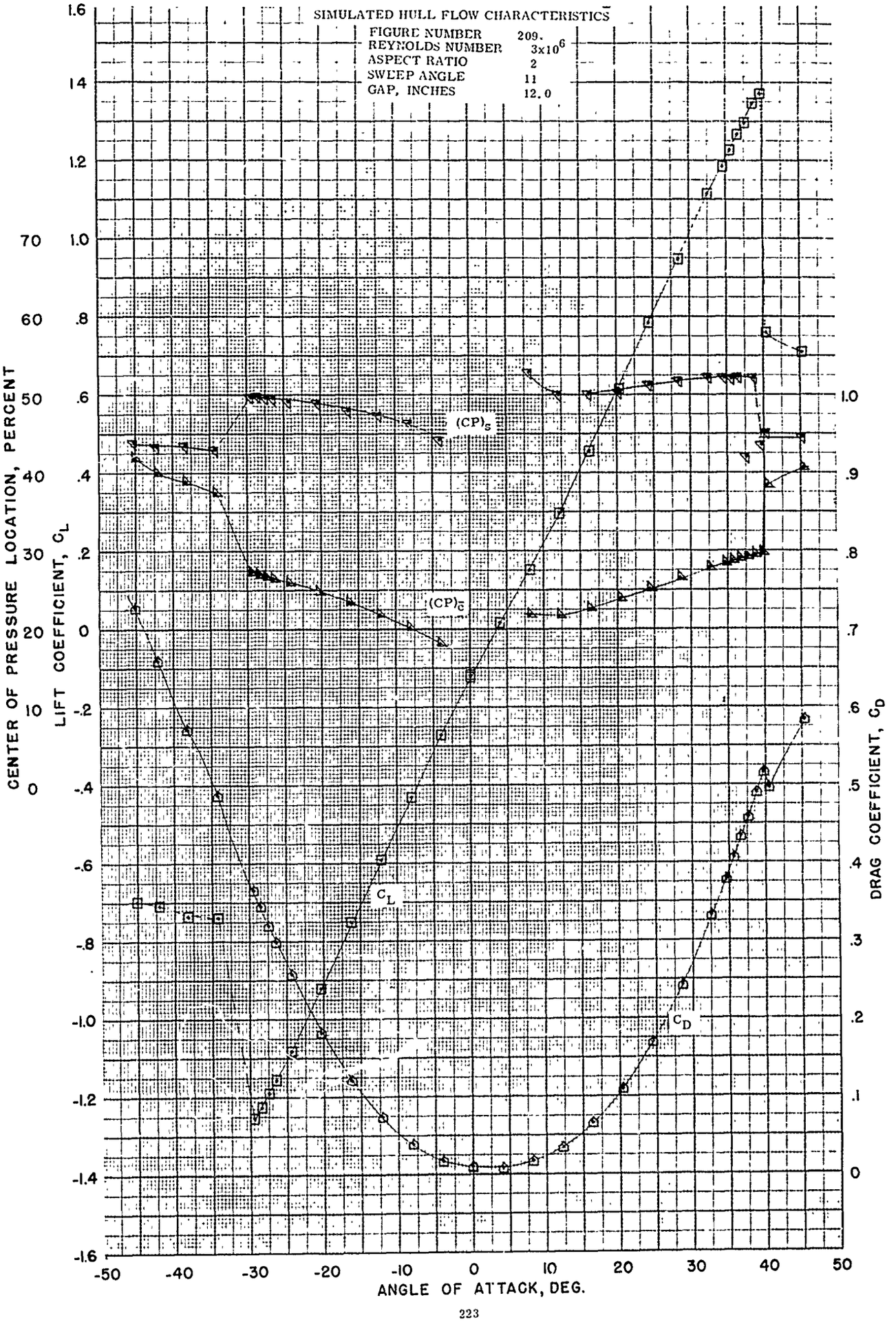
SIMULATED HULL FLOW CHARACTERISTICS
FIGURE NUMBER 209.
REYNOLDS NUMBER 3x10^6
ASPECT RATIO 2
SWEEP ANGLE 11
GAP, INCHES 12.0
CENTER OF PRESSURE LOCATION, PERCENT
LIFT COEFFICIENT, C_L
DRAG COEFFICIENT, C_D
ANGLE OF ATTACK, DEG.
$(CP)_s$
$(CP)_{\bar{c}}$
C_L
C_D
70
60
50
40
30
20
10
0
1.6
1.4
1.2
1.0
.8
.6
.4
.2
0
-.2
-.4
-.6
-.8
-1.0
-1.2
-1.4
-1.6
1.0
.9
.8
.7
.6
.5
.4
.3
.2
.1
0
-50
-40
-30
-20
-10
0
10
20
30
40
50

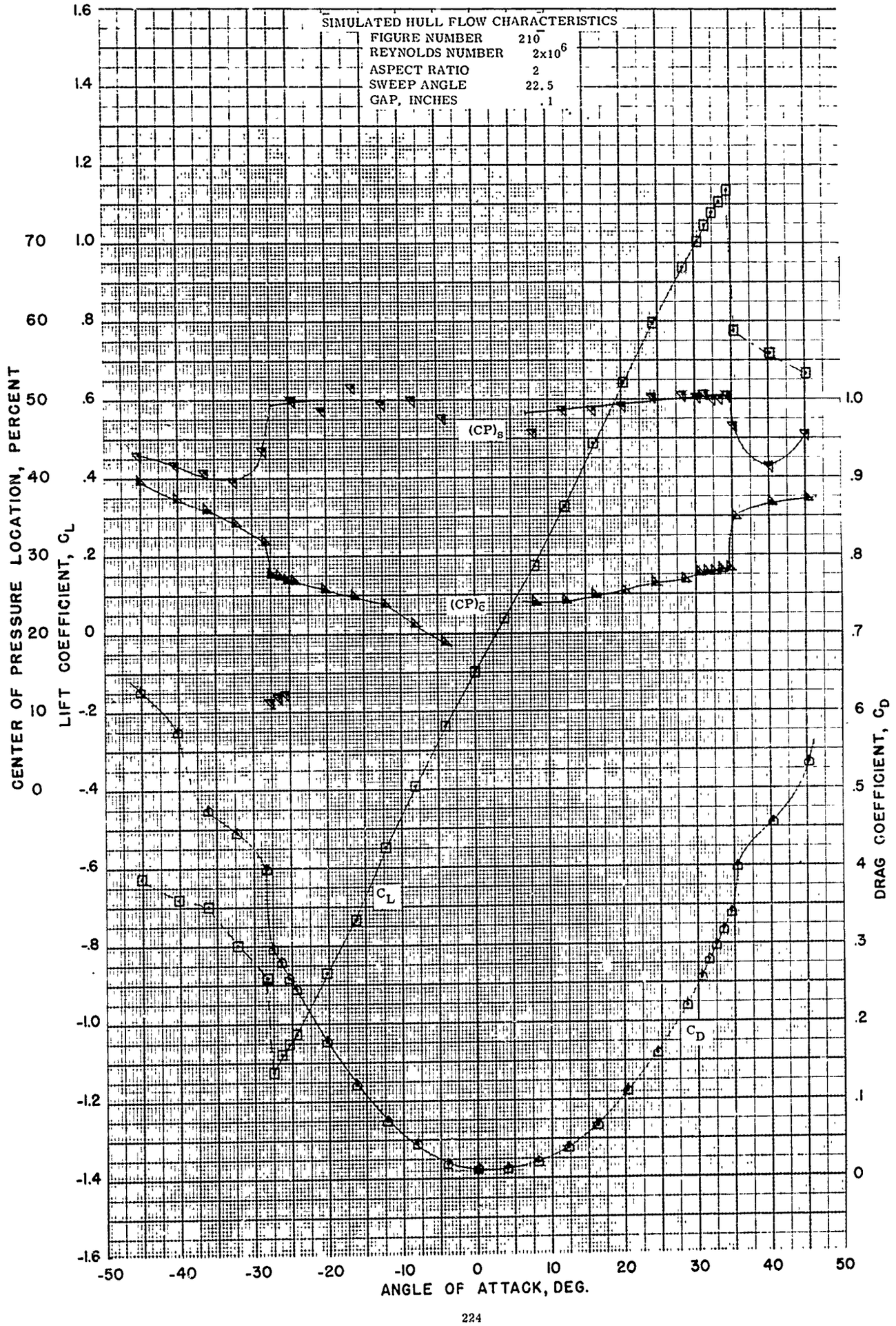
SIMULATED HULL FLOW CHARACTERISTICS
FIGURE NUMBER 210
REYNOLDS NUMBER 2x10^6
ASPECT RATIO 2
SWEEP ANGLE 22.5
GAP, INCHES .1
CENTER OF PRESSURE LOCATION, PERCENT
LIFT COEFFICIENT, C_L
DRAG COEFFICIENT, C_D
ANGLE OF ATTACK, DEG.
$(CP)_s$
$(CP)_c$
C_L
C_D
70
60
50
40
30
20
10
0
1.6
1.4
1.2
1.0
.8
.6
.4
.2
0
-.2
-.4
-.6
-.8
-1.0
-1.2
-1.4
-1.6
1.0
.9
.8
.7
.6
.5
.4
.3
.2
.1
0
-50
-40
-30
-20
-10
0
10
20
30
40
50

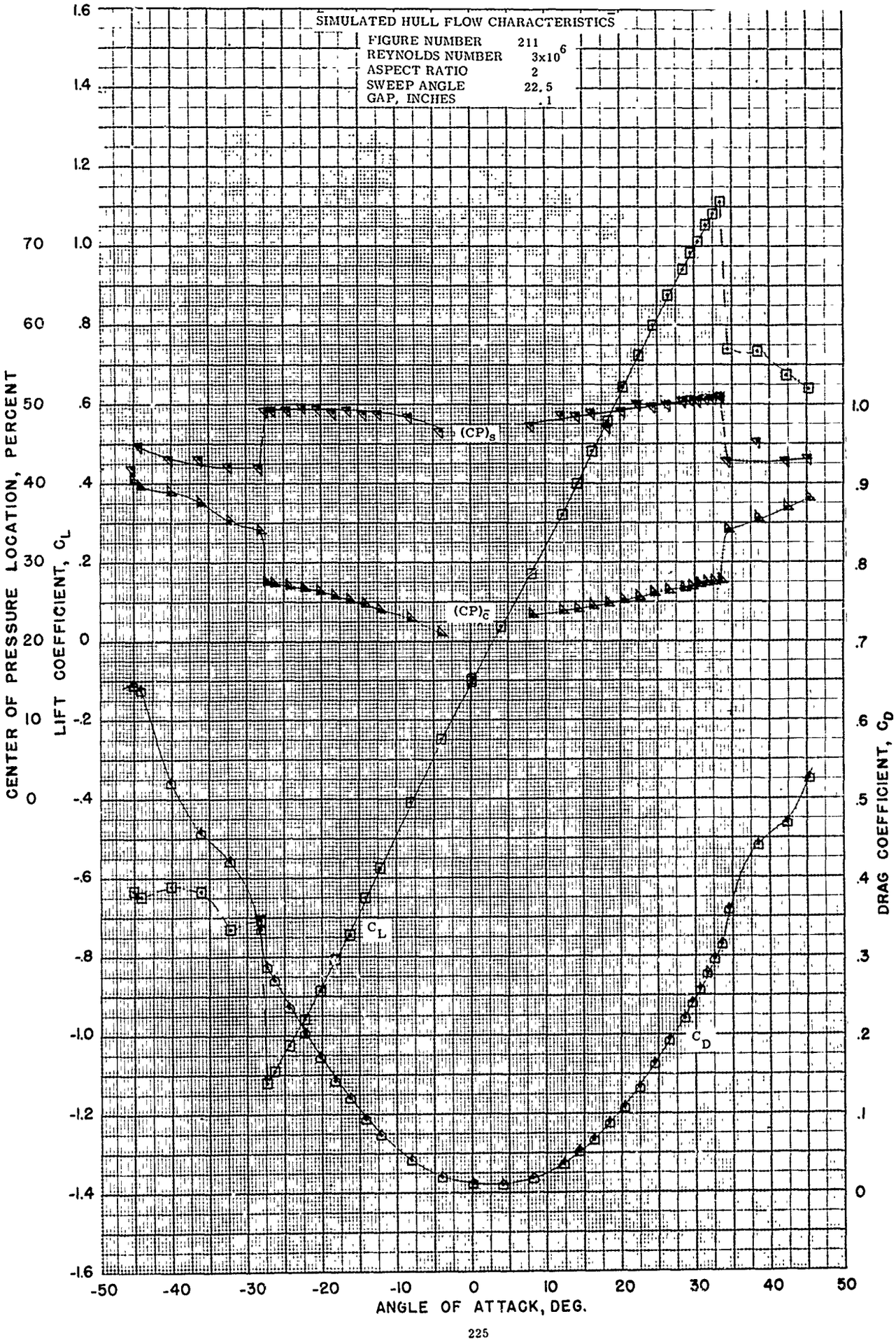
SIMULATED HULL FLOW CHARACTERISTICS
FIGURE NUMBER 211
REYNOLDS NUMBER 3x10^6
ASPECT RATIO 2
SWEEP ANGLE 22.5
GAP, INCHES .1
CENTER OF PRESSURE LOCATION, PERCENT
LIFT COEFFICIENT, C_L
DRAG COEFFICIENT, C_D
ANGLE OF ATTACK, DEG.
$(CP)_s$
$(CP)_c$
C_L
C_D
70
60
50
40
30
20
10
0
1.6
1.4
1.2
1.0
.8
.6
.4
.2
0
-.2
-.4
-.6
-.8
-1.0
-1.2
-1.4
-1.6
1.0
.9
.8
.7
.6
.5
.4
.3
.2
.1
0
-50
-40
-30
-20
-10
0
10
20
30
40
50

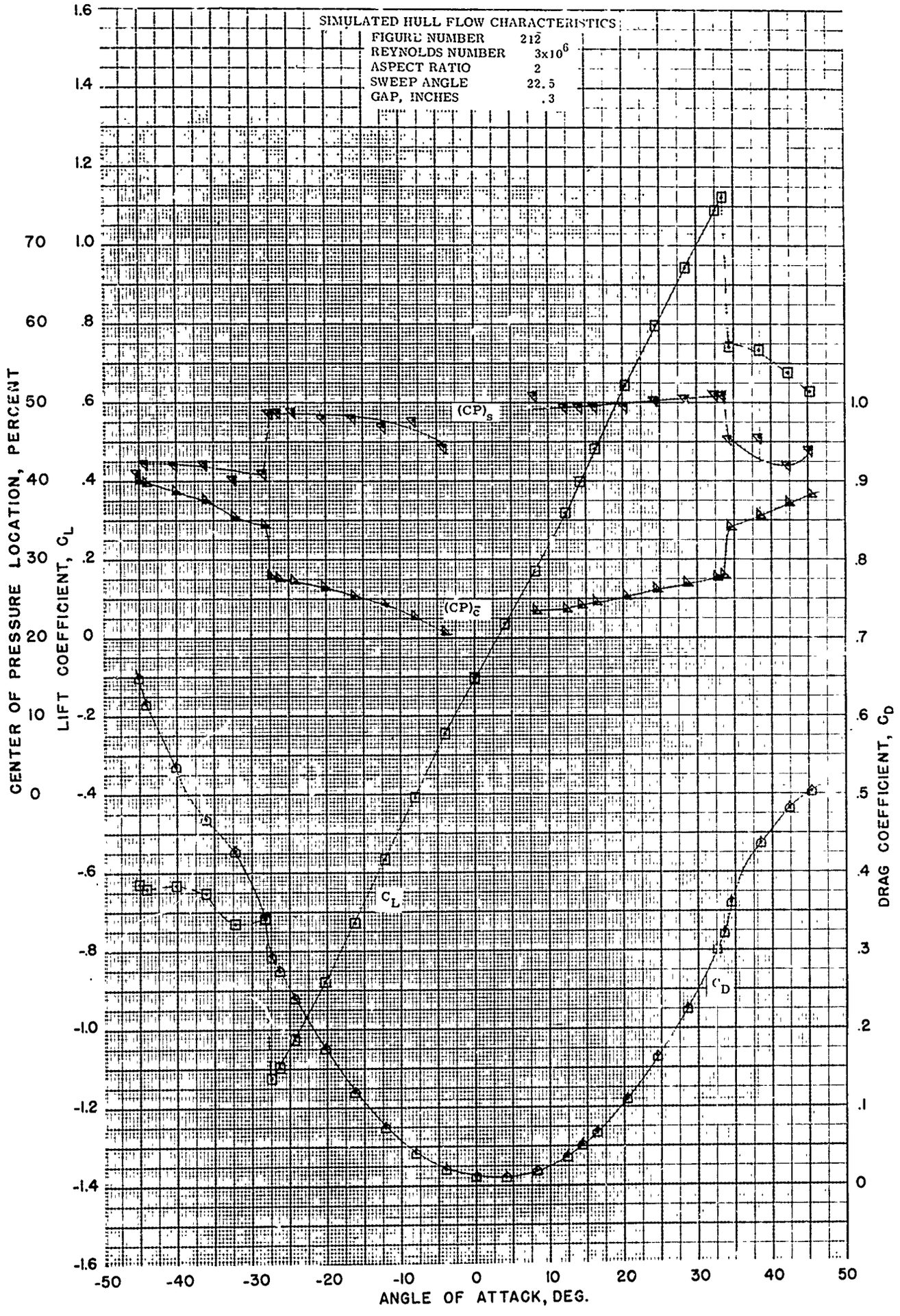
SIMULATED HULL FLOW CHARACTERISTICS
FIGURE NUMBER 212
REYNOLDS NUMBER 3x10^6
ASPECT RATIO 2
SWEEP ANGLE 22.5
GAP, INCHES .3
CENTER OF PRESSURE LOCATION, PERCENT
LIFT COEFFICIENT, C_L
DRAG COEFFICIENT, C_D
ANGLE OF ATTACK, DEG.
$(CP)_s$
$(CP)_{\bar{c}}$
C_L
C_D
70
60
50
40
30
20
10
0
1.6
1.4
1.2
1.0
.8
.6
.4
.2
0
-.2
-.4
-.6
-.8
-1.0
-1.2
-1.4
-1.6
1.0
.9
.8
.7
.6
.5
.4
.3
.2
.1
0
-50
-40
-30
-20
-10
0
10
20
30
40
50

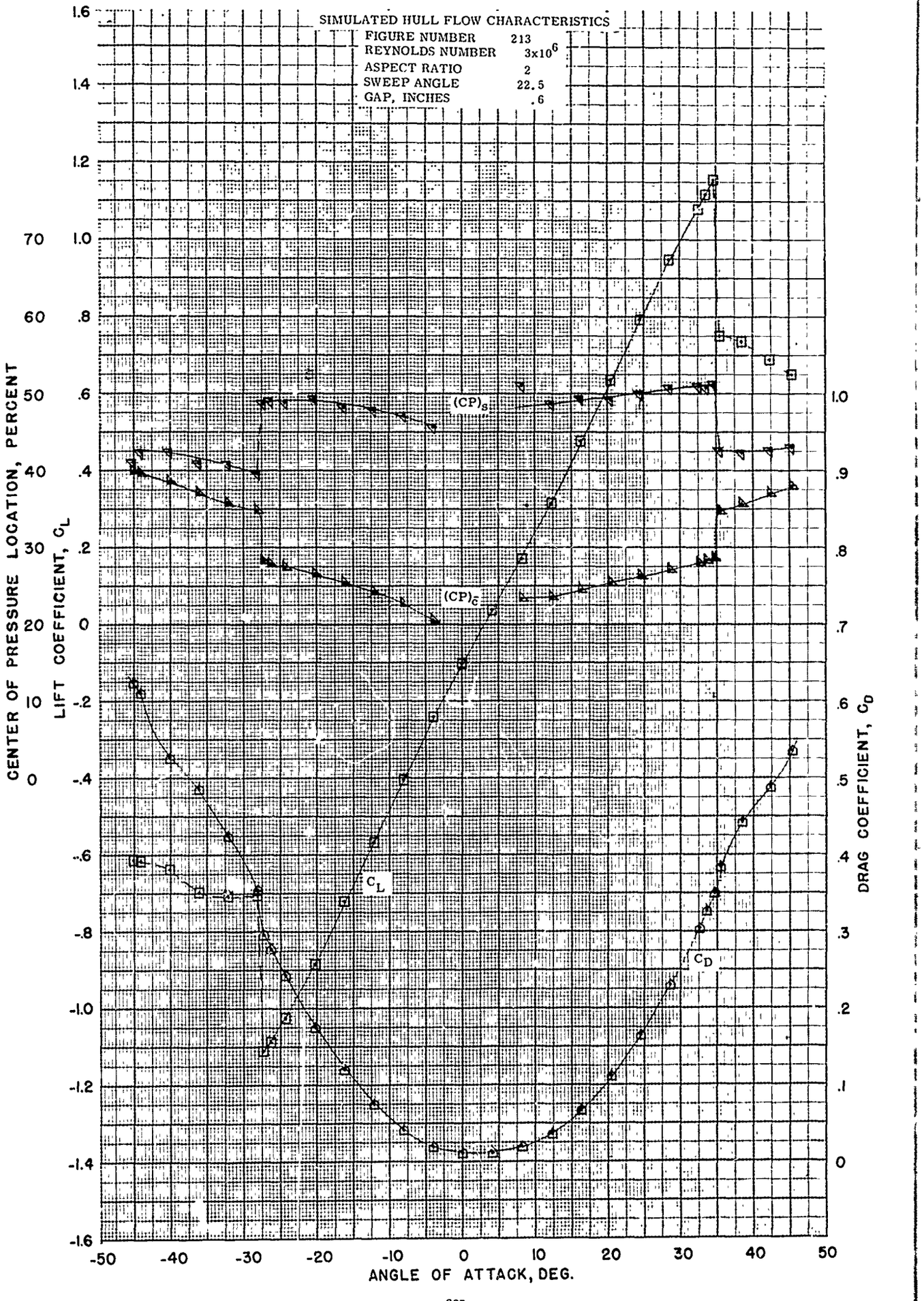
SIMULATED HULL FLOW CHARACTERISTICS
FIGURE NUMBER 213
REYNOLDS NUMBER 3×10^6
ASPECT RATIO 2
SWEEP ANGLE 22.5
GAP, INCHES .6
CENTER OF PRESSURE LOCATION, PERCENT
LIFT COEFFICIENT, C_L
DRAG COEFFICIENT, C_D
ANGLE OF ATTACK, DEG.
$(CP)_s$
$(CP)_c$
C_L
C_D
70
60
50
40
30
20
10
0
1.6
1.4
1.2
1.0
.8
.6
.4
.2
0
-.2
-.4
-.6
-.8
-1.0
-1.2
-1.4
-1.6
1.0
.9
.8
.7
.6
.5
.4
.3
.2
.1
0
-50
-40
-30
-20
-10
0
10
20
30
40
50

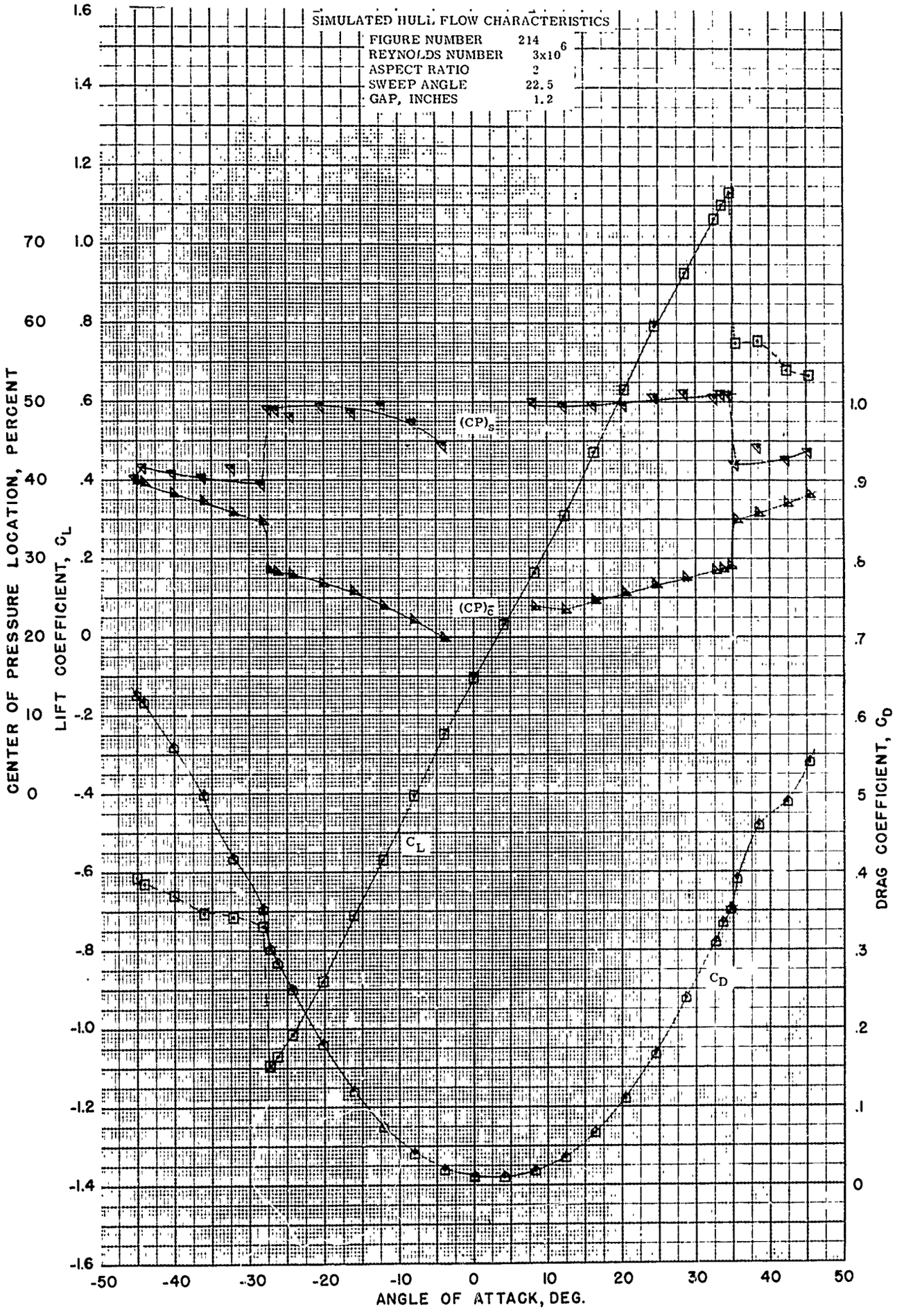
SIMULATED HULL FLOW CHARACTERISTICS
FIGURE NUMBER 214
REYNOLDS NUMBER 3x10^6
ASPECT RATIO 2
SWEEP ANGLE 22.5
GAP, INCHES 1.2
CENTER OF PRESSURE LOCATION, PERCENT
LIFT COEFFICIENT, C_L
DRAG COEFFICIENT, C_D
ANGLE OF ATTACK, DEG.
$(CP)_s$
$(CP)_c$
C_L
C_D
70
60
50
40
30
20
10
0
1.6
1.4
1.2
1.0
.8
.6
.4
.2
0
-.2
-.4
-.6
-.8
-1.0
-1.2
-1.4
-1.6
1.0
.9
.8
.7
.6
.5
.4
.3
.2
.1
0
-50
-40
-30
-20
-10
0
10
20
30
40
50

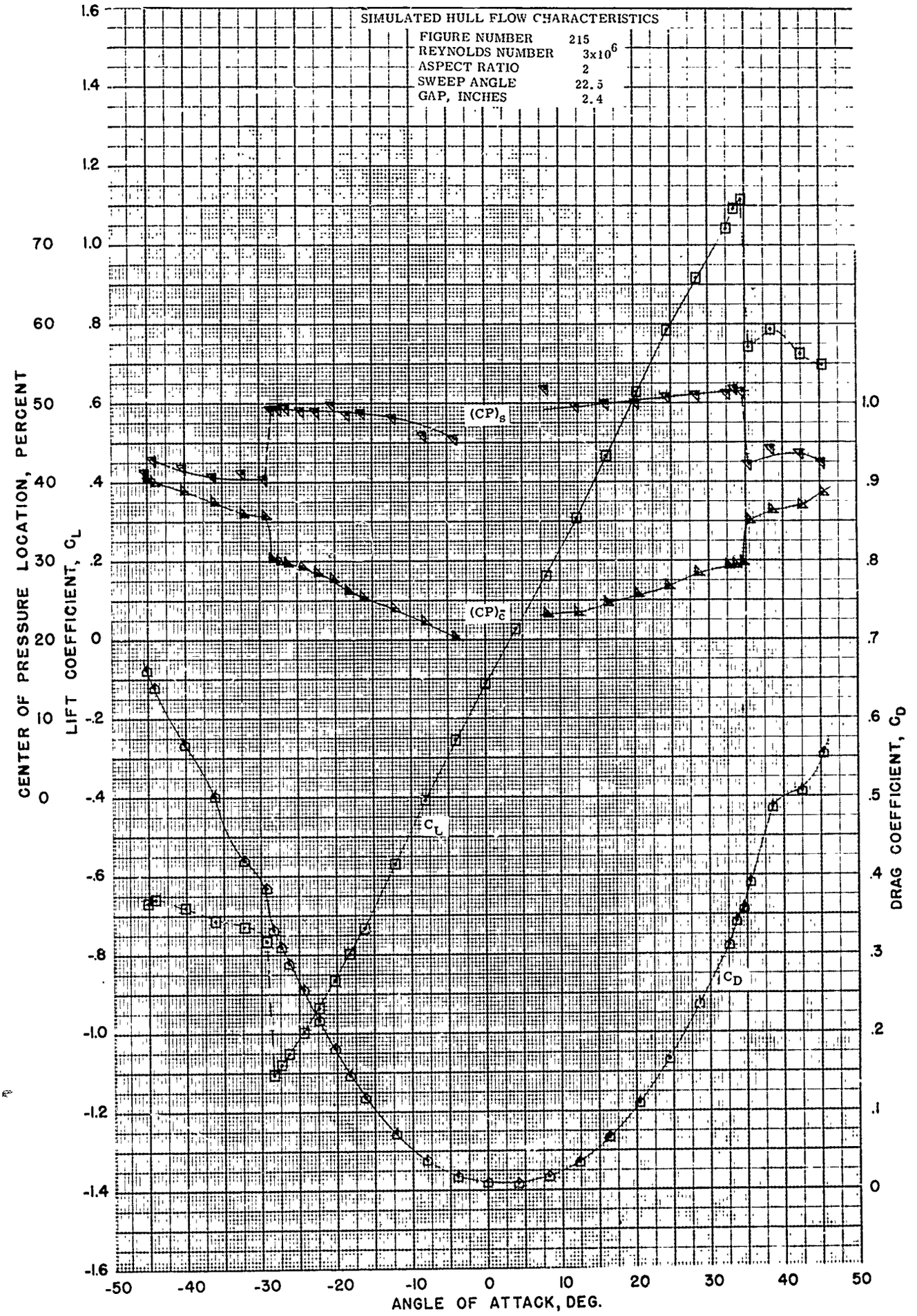
SIMULATED HULL FLOW CHARACTERISTICS
FIGURE NUMBER 215
REYNOLDS NUMBER 3x10^6
ASPECT RATIO 2
SWEEP ANGLE 22.5
GAP, INCHES 2.4
(CP)s
(CP)c
CL
CD
CENTER OF PRESSURE LOCATION, PERCENT
LIFT COEFFICIENT, CL
DRAG COEFFICIENT, CD
ANGLE OF ATTACK, DEG.
70
60
50
40
30
20
10
0
1.6
1.4
1.2
1.0
.8
.6
.4
.2
0
-.2
-.4
-.6
-.8
-1.0
-1.2
-1.4
-1.6
1.0
.9
.8
.7
.6
.5
.4
.3
.2
.1
0
-50
-40
-30
-20
-10
0
10
20
30
40
50

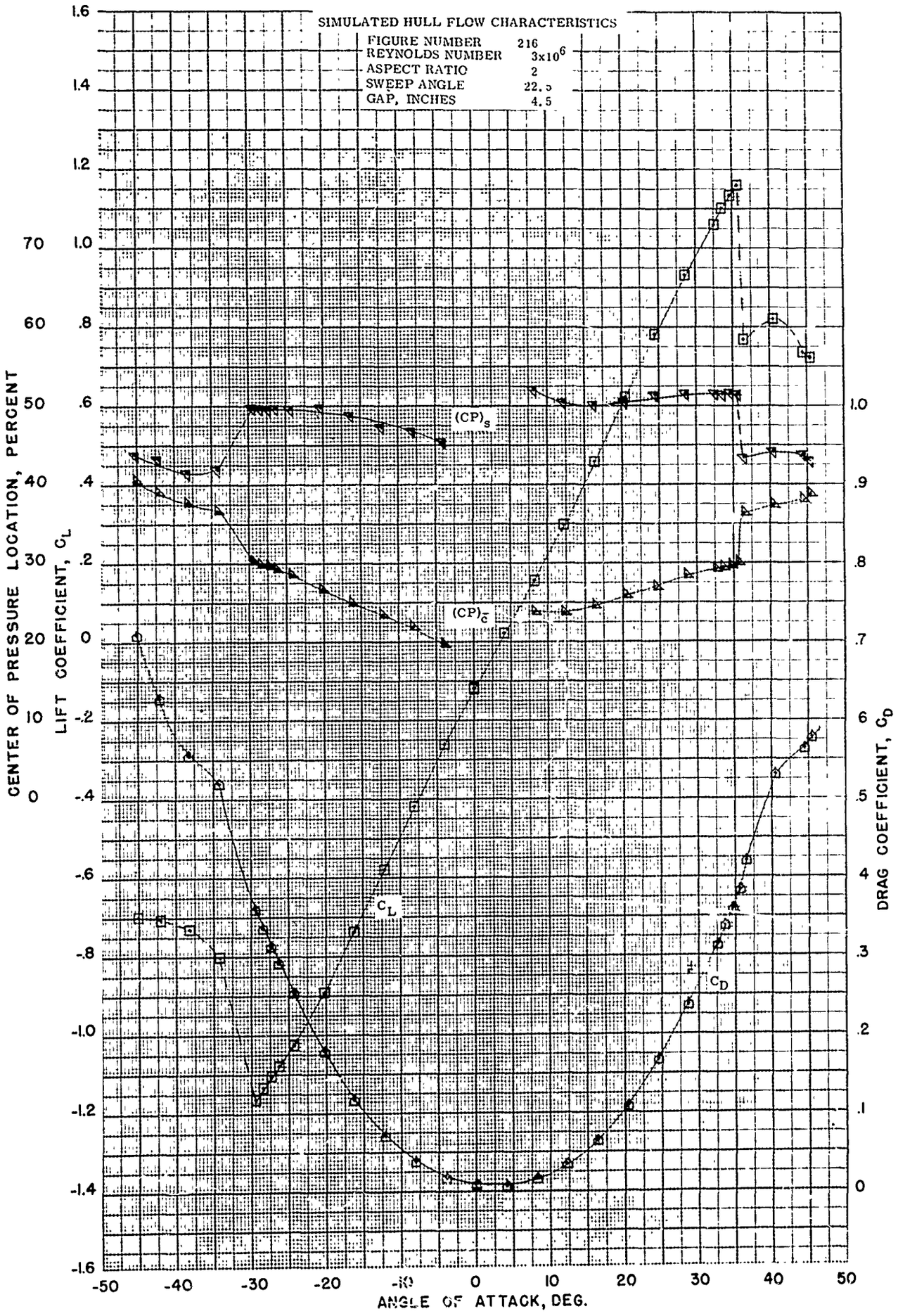
SIMULATED HULL FLOW CHARACTERISTICS
FIGURE NUMBER 216
REYNOLDS NUMBER 3x10^6
ASPECT RATIO 2
SWEEP ANGLE 22.5
GAP, INCHES 4.5
CENTER OF PRESSURE LOCATION, PERCENT
LIFT COEFFICIENT, C_L
DRAG COEFFICIENT, C_D
ANGLE OF ATTACK, DEG.
$(CP)_s$
$(CP)_{\bar{c}}$
C_L
C_D
70
60
50
40
30
20
10
0
1.6
1.4
1.2
1.0
.8
.6
.4
.2
0
-.2
-.4
-.6
-.8
-1.0
-1.2
-1.4
-1.6
1.0
.9
.8
.7
.6
.5
.4
.3
.2
.1
0
-50
-40
-30
-20
-10
0
10
20
30
40
50

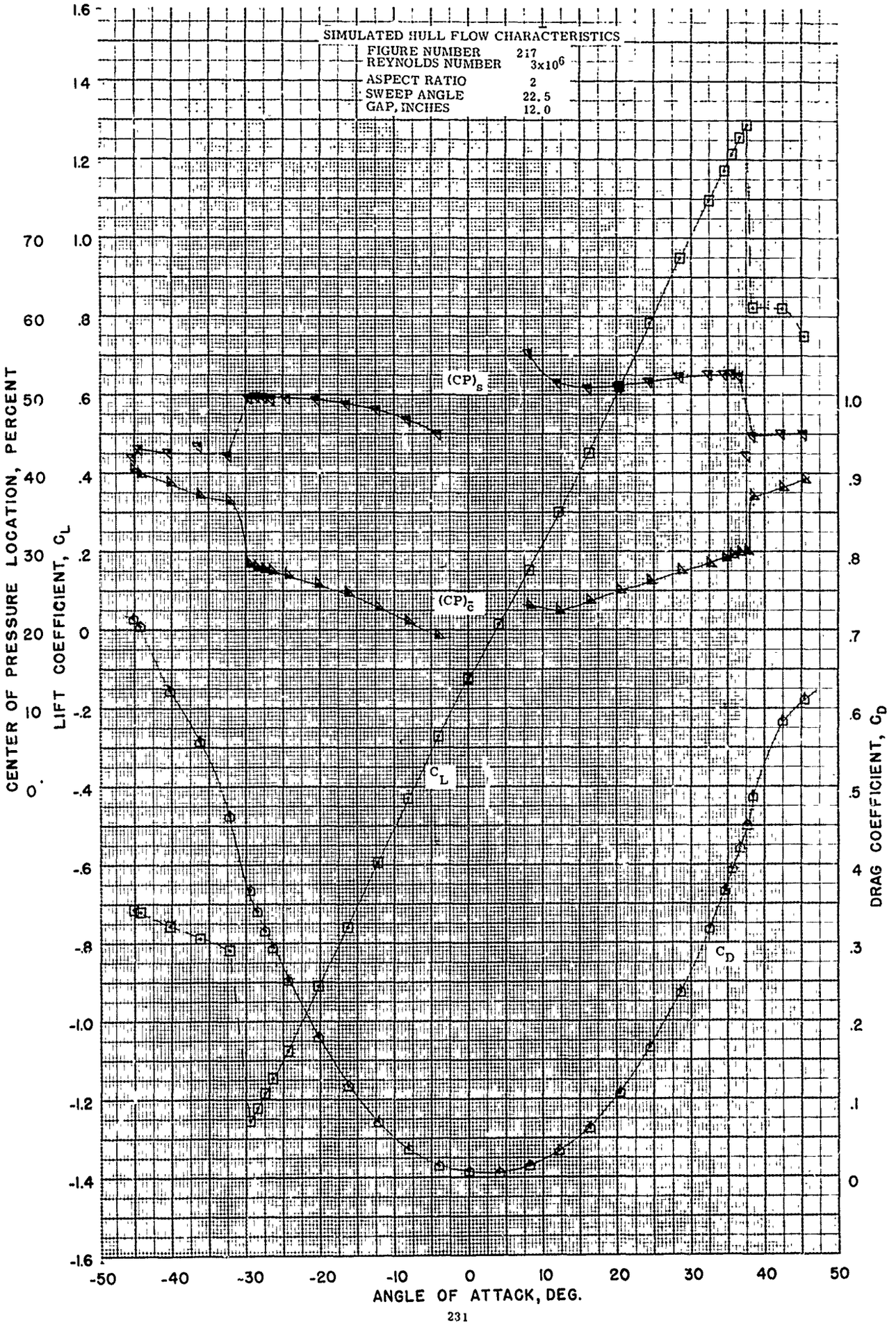
SIMULATED HULL FLOW CHARACTERISTICS
FIGURE NUMBER 217
REYNOLDS NUMBER 3x10^6
ASPECT RATIO 2
SWEEP ANGLE 22.5
GAP, INCHES 12.0
(CP)s
(CP)c
CL
CD
CENTER OF PRESSURE LOCATION, PERCENT
LIFT COEFFICIENT, CL
DRAG COEFFICIENT, CD
ANGLE OF ATTACK, DEG.
70
60
50
40
30
20
10
0
1.6
1.4
1.2
1.0
.8
.6
.4
.2
0
-.2
-.4
-.6
-.8
-1.0
-1.2
-1.4
-1.6
1.0
.9
.8
.7
.6
.5
.4
.3
.2
.1
0
-50
-40
-30
-20
-10
0
10
20
30
40
50

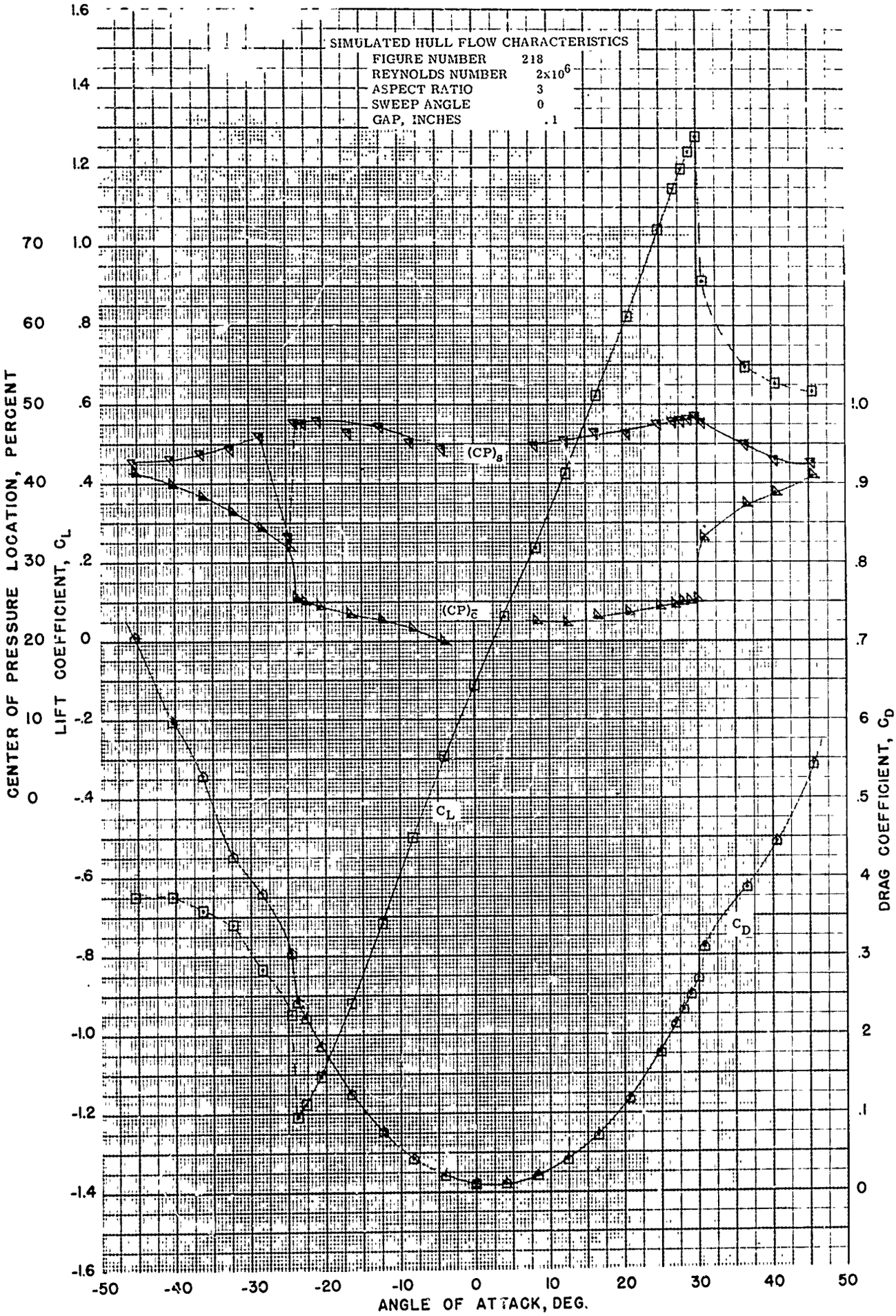
SIMULATED HULL FLOW CHARACTERISTICS
FIGURE NUMBER 218
REYNOLDS NUMBER 2x10^6
ASPECT RATIO 3
SWEEP ANGLE 0
GAP, INCHES .1
CENTER OF PRESSURE LOCATION, PERCENT
LIFT COEFFICIENT, C_L
DRAG COEFFICIENT, C_D
ANGLE OF ATTACK, DEG.
$(CP)_s$
$(CP)_{\bar{c}}$
C_L
C_D
70
60
50
40
30
20
10
0
1.6
1.4
1.2
1.0
.8
.6
.4
.2
0
-.2
-.4
-.6
-.8
-1.0
-1.2
-1.4
-1.6
1.0
.9
.8
.7
.6
.5
.4
.3
.2
.1
0
-50
-40
-30
-20
-10
0
10
20
30
40
50

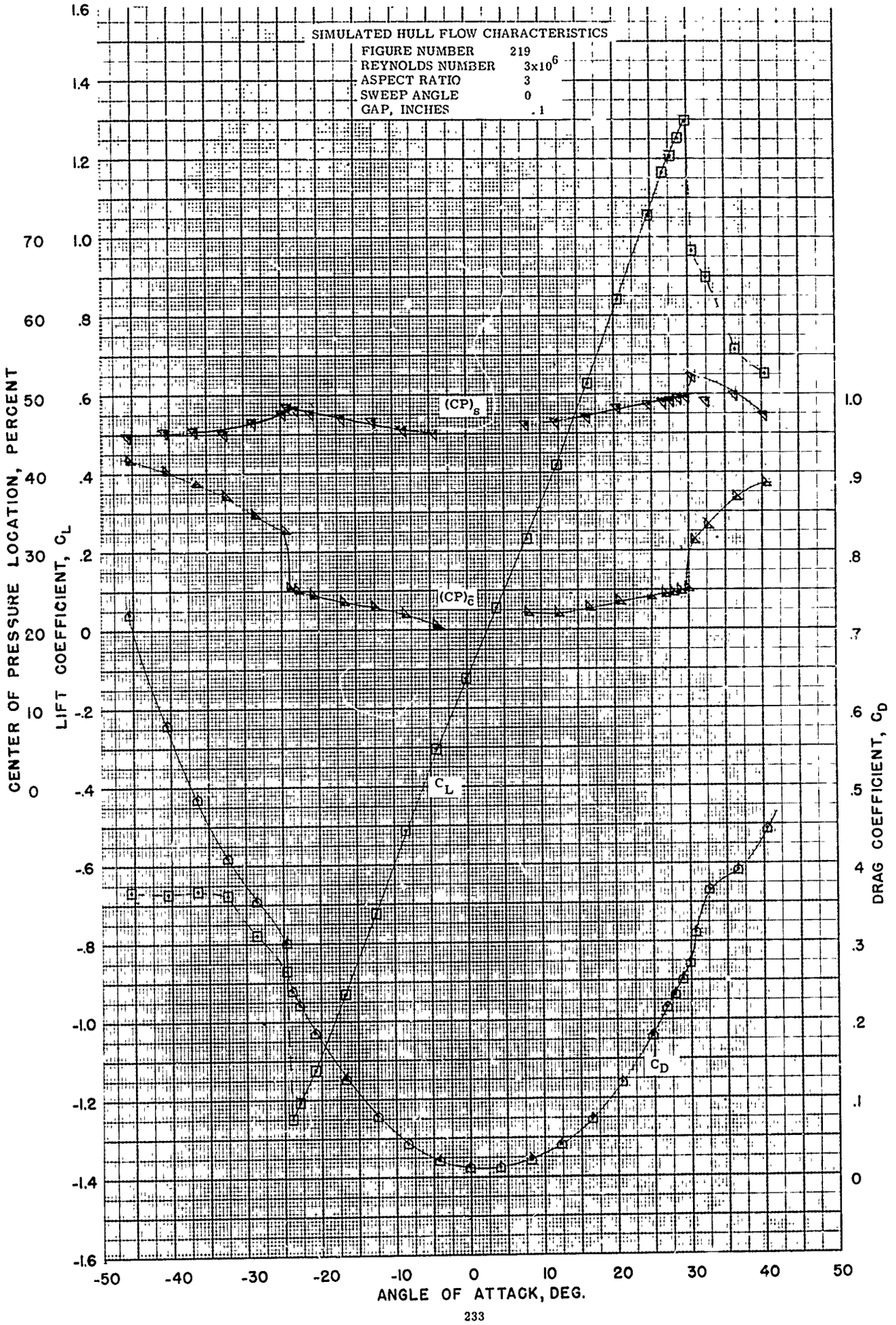
SIMULATED HULL FLOW CHARACTERISTICS
FIGURE NUMBER 219
REYNOLDS NUMBER 3x10^6
ASPECT RATIO 3
SWEEP ANGLE 0
GAP, INCHES .1
CENTER OF PRESSURE LOCATION, PERCENT
LIFT COEFFICIENT, C_L
DRAG COEFFICIENT, C_D
ANGLE OF ATTACK, DEG.
(CP)_s
(CP)_c
C_L
C_D
70
60
50
40
30
20
10
0
1.6
1.4
1.2
1.0
.8
.6
.4
.2
0
-.2
-.4
-.6
-.8
-1.0
-1.2
-1.4
-1.6
1.0
.9
.8
.7
.6
.5
.4
.3
.2
.1
0
-50
-40
-30
-20
-10
0
10
20
30
40
50

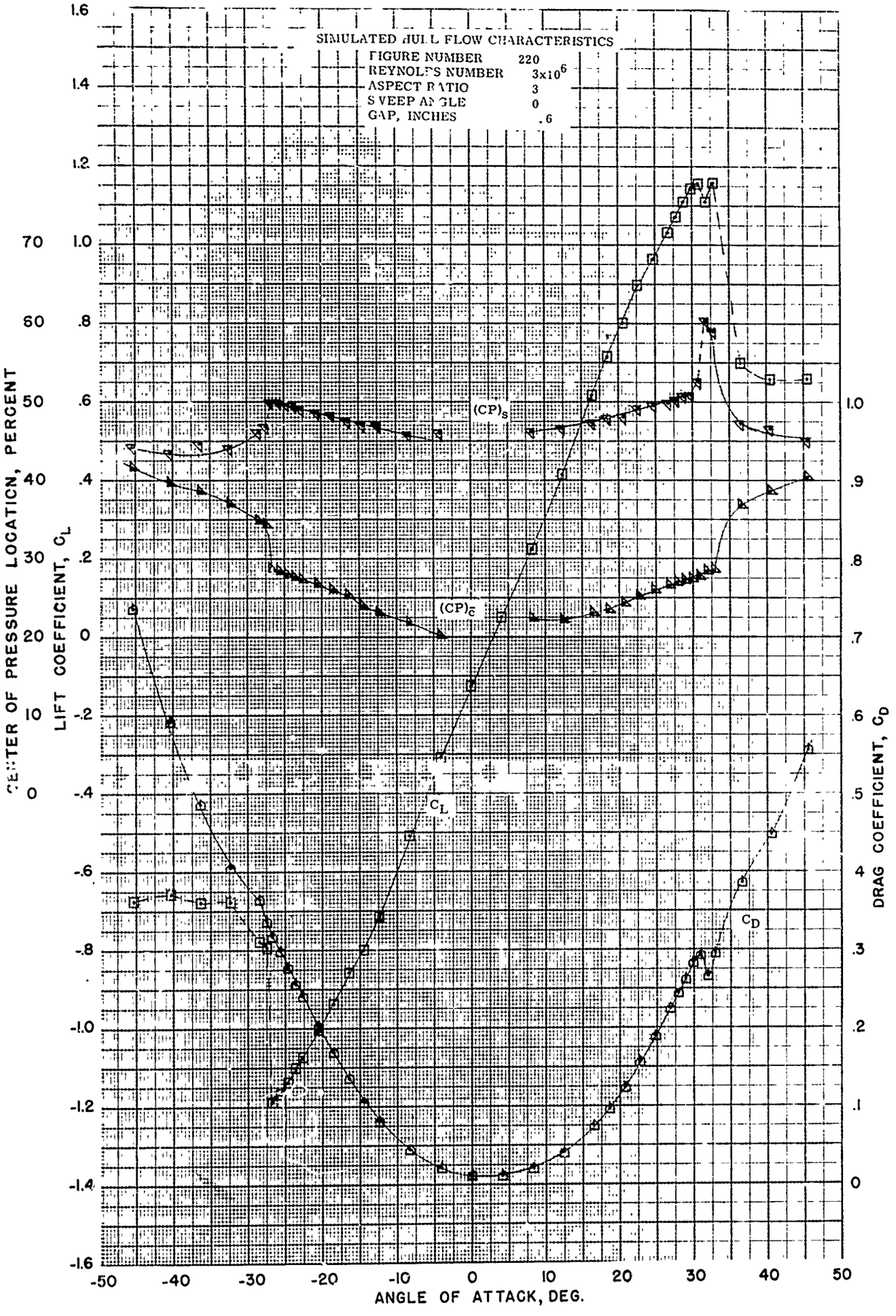
SIMULATED HULL FLOW CHARACTERISTICS
FIGURE NUMBER 220
REYNOLDS NUMBER 3x10^6
ASPECT RATIO 3
SWEEP ANGLE 0
GAP, INCHES .6
CENTER OF PRESSURE LOCATION, PERCENT
LIFT COEFFICIENT, C_L
DRAG COEFFICIENT, C_D
ANGLE OF ATTACK, DEG.
$(CP)_s$
$(CP)_{\bar{c}}$
C_L
C_D
70
60
50
40
30
20
10
0
1.6
1.4
1.2
1.0
.8
.6
.4
.2
0
-.2
-.4
-.6
-.8
-1.0
-1.2
-1.4
-1.6
1.0
.9
.8
.7
.6
.5
.4
.3
.2
.1
0
-50
-40
-30
-20
-10
0
10
20
30
40
50

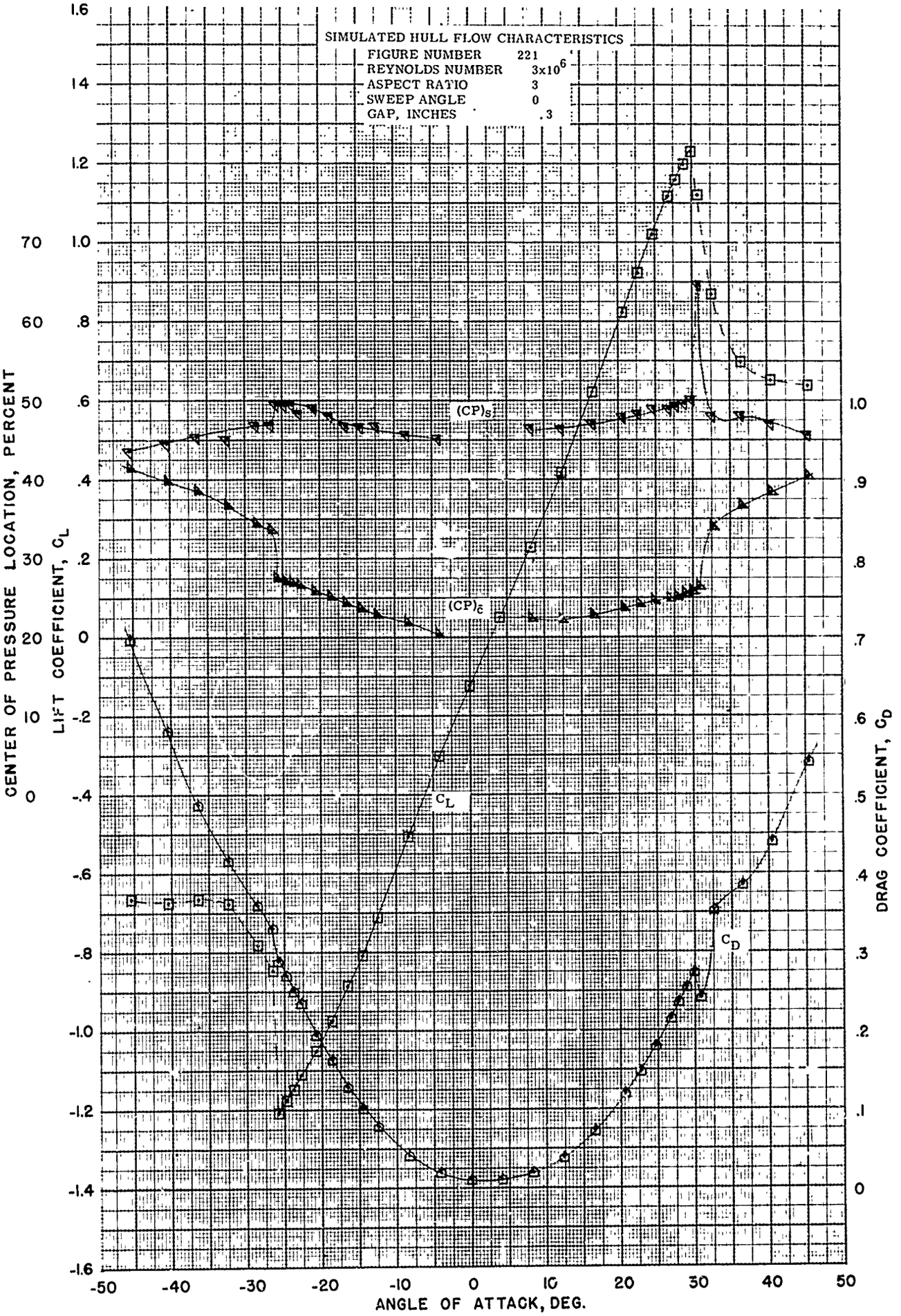
SIMULATED HULL FLOW CHARACTERISTICS
FIGURE NUMBER 221
REYNOLDS NUMBER 3×10^6
ASPECT RATIO 3
SWEEP ANGLE 0
GAP, INCHES .3
$(CP)_S$
$(CP)_{\bar{c}}$
C_L
C_D
CENTER OF PRESSURE LOCATION, PERCENT
LIFT COEFFICIENT, C_L
DRAG COEFFICIENT, C_D
ANGLE OF ATTACK, DEG.
70
60
50
40
30
20
10
0
1.6
1.4
1.2
1.0
.8
.6
.4
.2
0
-.2
-.4
-.6
-.8
-1.0
-1.2
-1.4
-1.6
1.0
.9
.8
.7
.6
.5
.4
.3
.2
.1
0
-50
-40
-30
-20
-10
0
10
20
30
40
50

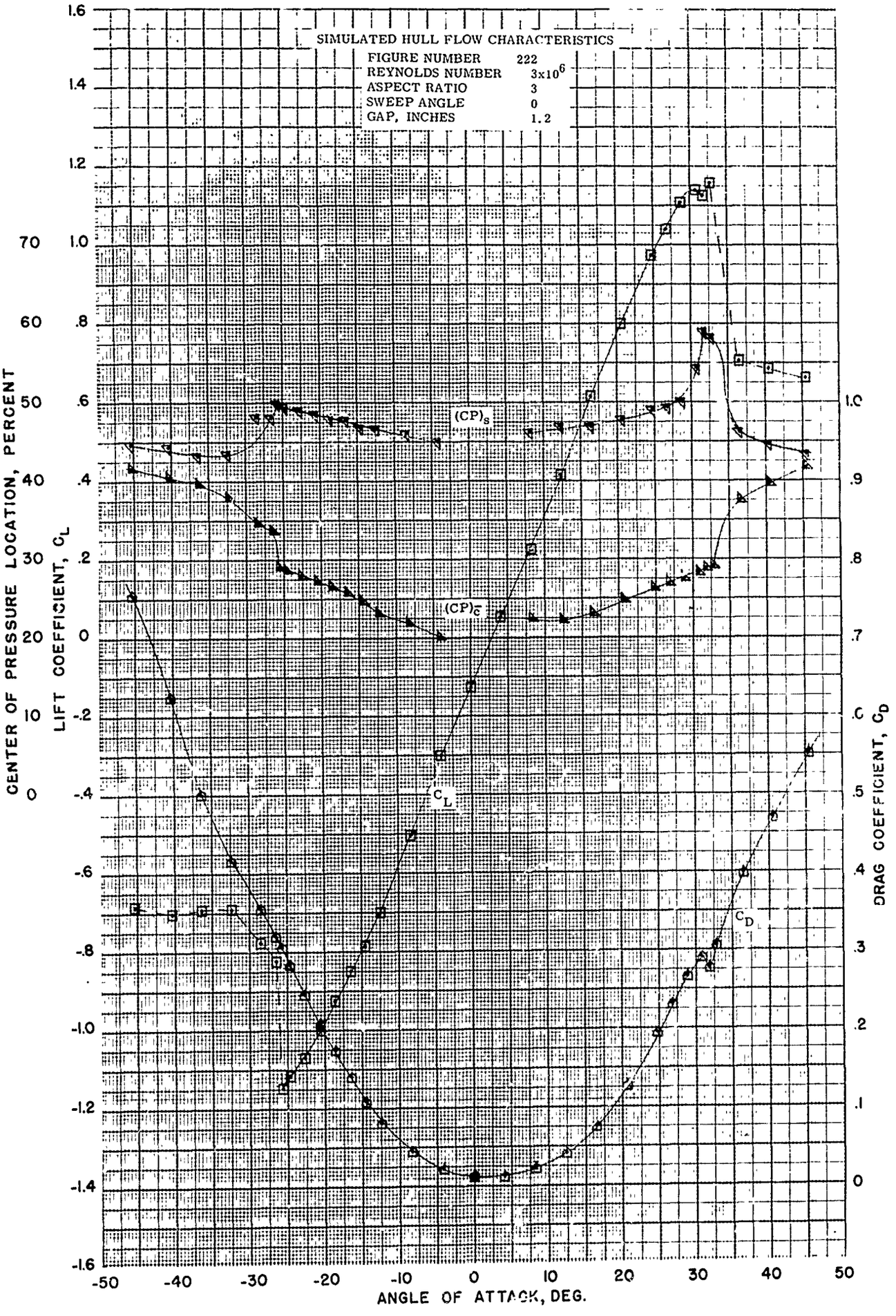
SIMULATED HULL FLOW CHARACTERISTICS
FIGURE NUMBER 222
REYNOLDS NUMBER 3x10^6
ASPECT RATIO 3
SWEEP ANGLE 0
GAP, INCHES 1.2
CENTER OF PRESSURE LOCATION, PERCENT
LIFT COEFFICIENT, C_L
DRAG COEFFICIENT, C_D
ANGLE OF ATTACK, DEG.
$(CP)_s$
$(CP)_{\bar{c}}$
C_L
C_D
70
60
50
40
30
20
10
0
1.6
1.4
1.2
1.0
.8
.6
.4
.2
0
-.2
-.4
-.6
-.8
-1.0
-1.2
-1.4
-1.6
1.0
.9
.8
.7
.6
.5
.4
.3
.2
.1
0
-50
-40
-30
-20
-10
0
10
20
30
40
50

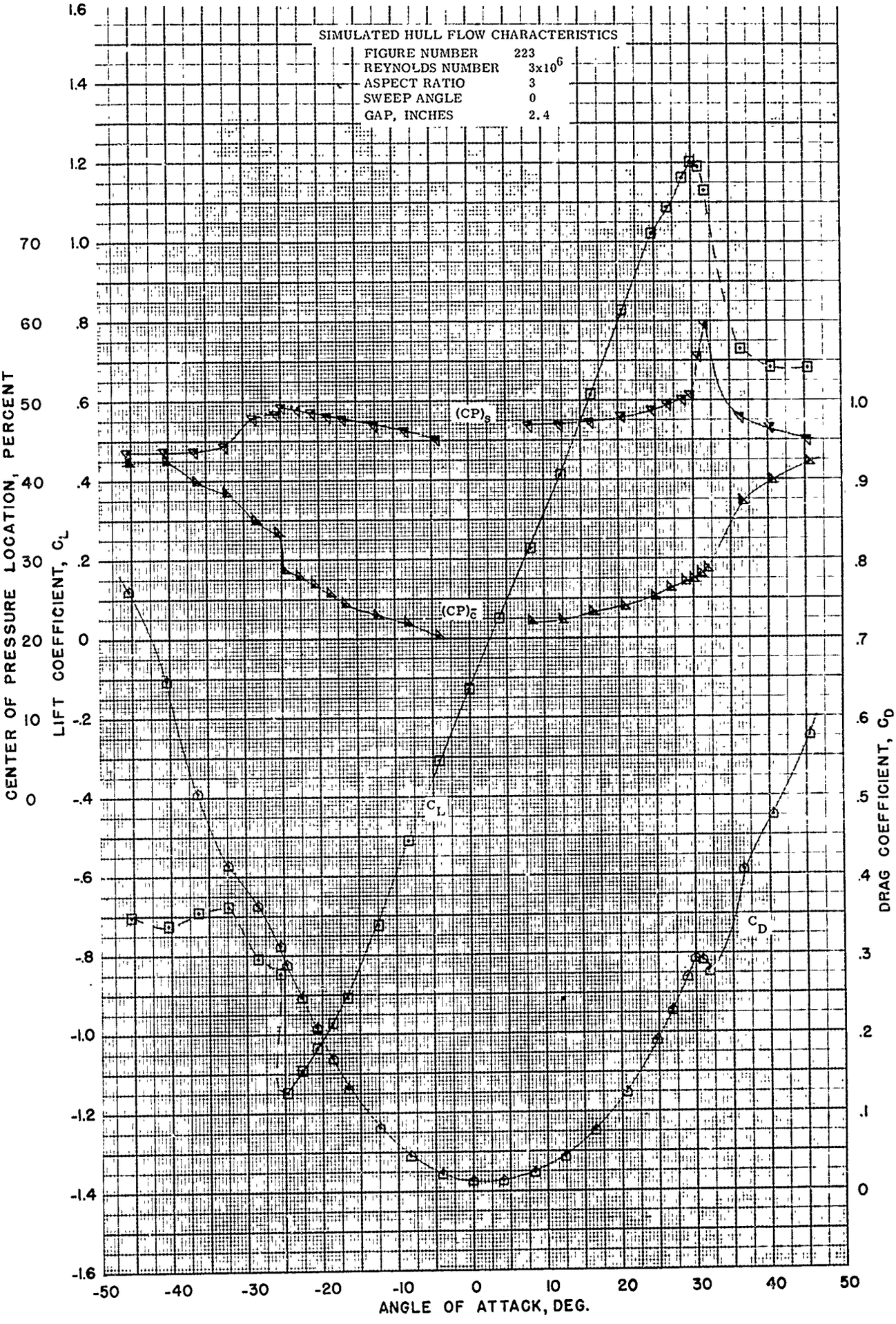
SIMULATED HULL FLOW CHARACTERISTICS
FIGURE NUMBER 223
REYNOLDS NUMBER 3x10^6
ASPECT RATIO 3
SWEEP ANGLE 0
GAP, INCHES 2.4
CENTER OF PRESSURE LOCATION, PERCENT
LIFT COEFFICIENT, C_L
DRAG COEFFICIENT, C_D
ANGLE OF ATTACK, DEG.
$(CP)_s$
$(CP)_{\bar{c}}$
C_L
C_D
70
60
50
40
30
20
10
0
1.6
1.4
1.2
1.0
.8
.6
.4
.2
0
-.2
-.4
-.6
-.8
-1.0
-1.2
-1.4
-1.6
1.0
.9
.8
.7
.6
.5
.4
.3
.2
.1
0
-50
-40
-30
-20
-10
0
10
20
30
40
50

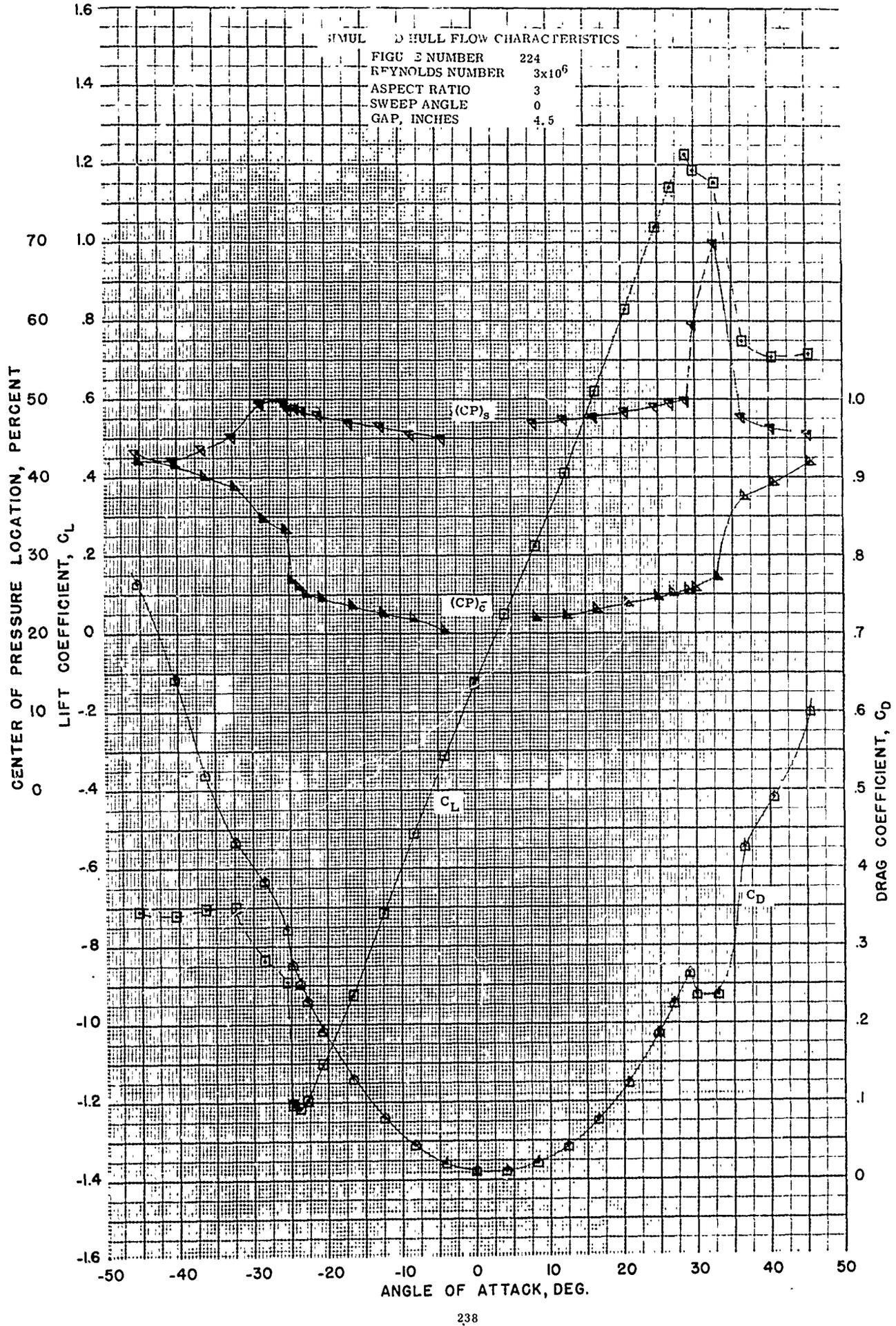
SIMUL D HULL FLOW CHARACTERISTICS
FIGU E NUMBER 224
REYNOLDS NUMBER 3x10^6
ASPECT RATIO 3
SWEEP ANGLE 0
GAP, INCHES 4.5
(CP)s
(CP)c
CL
CD
CENTER OF PRESSURE LOCATION, PERCENT
LIFT COEFFICIENT, CL
DRAG COEFFICIENT, CD
ANGLE OF ATTACK, DEG.
70
60
50
40
30
20
10
0
1.6
1.4
1.2
1.0
.8
.6
.4
.2
0
-.2
-.4
-.6
-.8
-1.0
-1.2
-1.4
-1.6
1.0
.9
.8
.7
.6
.5
.4
.3
.2
.1
0
-50
-40
-30
-20
-10
0
10
20
30
40
50

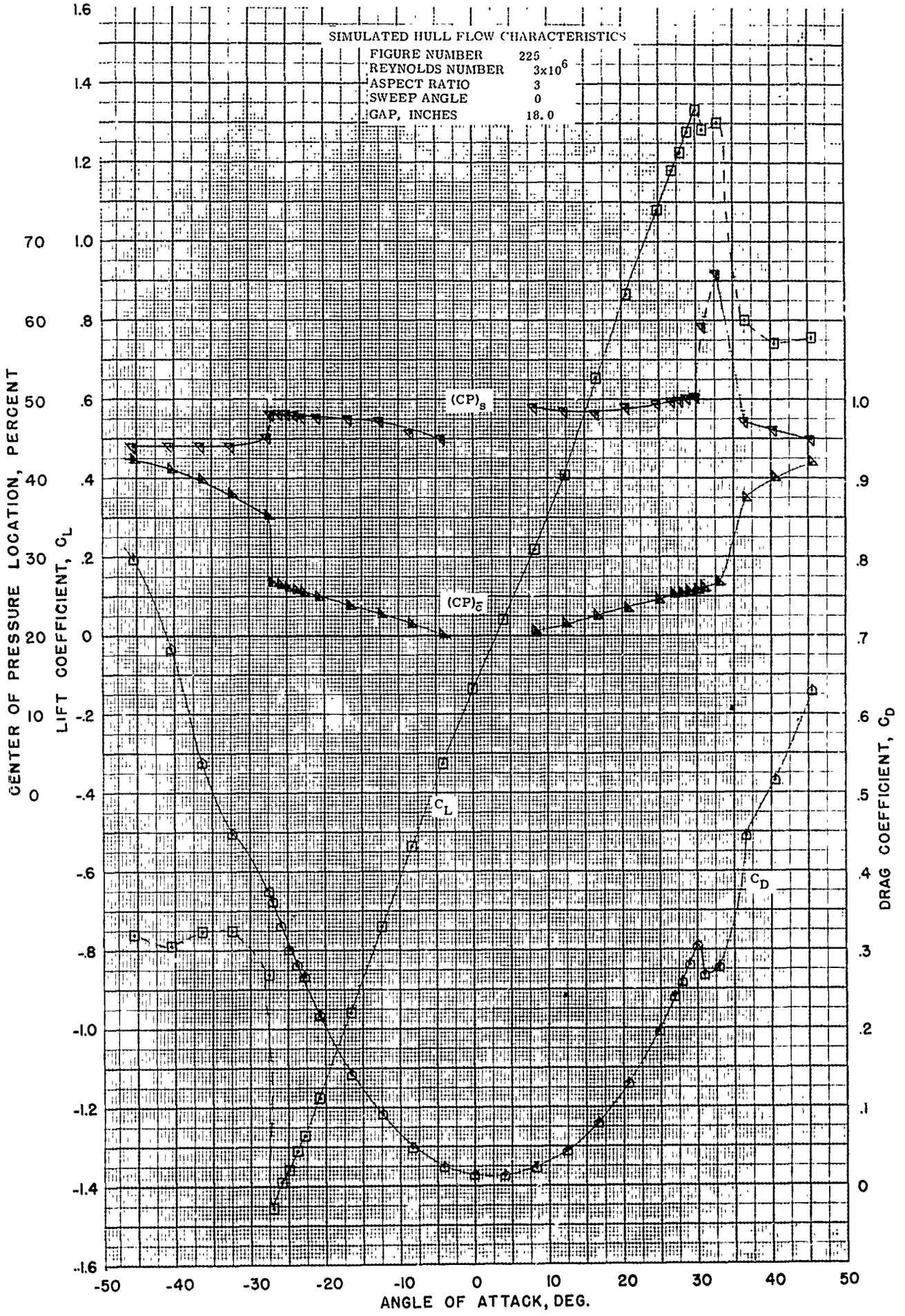
SIMULATED HULL FLOW CHARACTERISTICS
FIGURE NUMBER 225
REYNOLDS NUMBER 3×10^6
ASPECT RATIO 3
SWEEP ANGLE 0
GAP, INCHES 18.0
$(CP)_s$
$(CP)_\varepsilon$
C_L
C_D
CENTER OF PRESSURE LOCATION, PERCENT
LIFT COEFFICIENT, C_L
DRAG COEFFICIENT, C_D
ANGLE OF ATTACK, DEG.
70
60
50
40
30
20
10
0
1.6
1.4
1.2
1.0
.8
.6
.4
.2
0
-.2
-.4
-.6
-.8
-1.0
-1.2
-1.4
-1.6
1.0
.9
.8
.7
.6
.5
.4
.3
.2
.1
0
-50
-40
-30
-20
-10
0
10
20
30
40
50

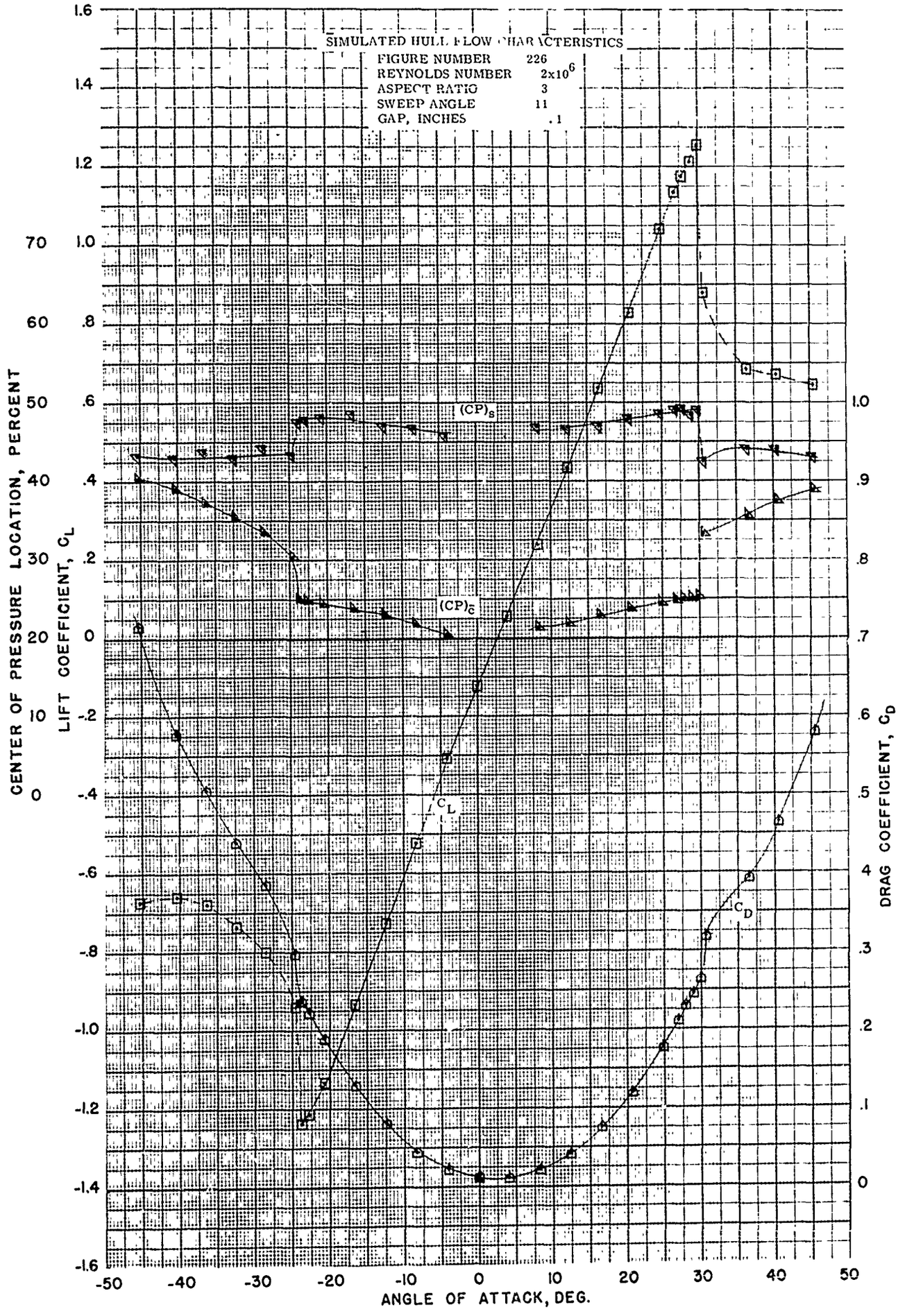
SIMULATED HULL FLOW CHARACTERISTICS
FIGURE NUMBER 226
REYNOLDS NUMBER 2×10^6
ASPECT RATIO 3
SWEEP ANGLE 11
GAP, INCHES .1
CENTER OF PRESSURE LOCATION, PERCENT
LIFT COEFFICIENT, C_L
DRAG COEFFICIENT, C_D
ANGLE OF ATTACK, DEG.
$(CP)_S$
$(CP)_{\bar{c}}$
C_L
C_D
70
60
50
40
30
20
10
0
1.6
1.4
1.2
1.0
.8
.6
.4
.2
0
-.2
-.4
-.6
-.8
-1.0
-1.2
-1.4
-1.6
1.0
.9
.8
.7
.6
.5
.4
.3
.2
.1
0
-50
-40
-30
-20
-10
0
10
20
30
40
50

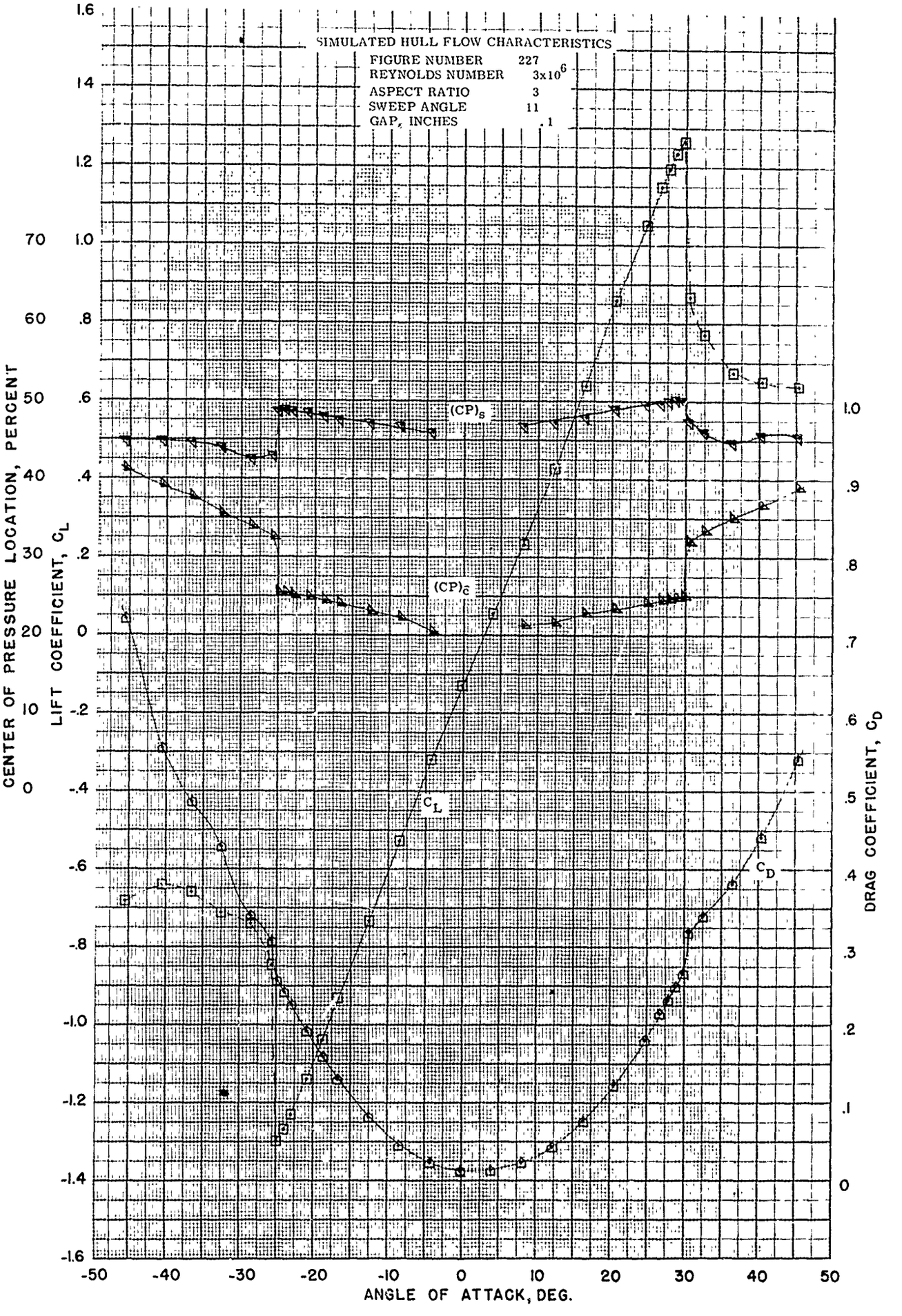
SIMULATED HULL FLOW CHARACTERISTICS
FIGURE NUMBER 227
REYNOLDS NUMBER 3x10^6
ASPECT RATIO 3
SWEEP ANGLE 11
GAP, INCHES .1
(CP)s
(CP)c
CL
CD
CENTER OF PRESSURE LOCATION, PERCENT
LIFT COEFFICIENT, CL
DRAG COEFFICIENT, CD
ANGLE OF ATTACK, DEG.
70
60
50
40
30
20
10
0
1.6
1.4
1.2
1.0
.8
.6
.4
.2
0
-.2
-.4
-.6
-.8
-1.0
-1.2
-1.4
-1.6
1.0
.9
.8
.7
.6
.5
.4
.3
.2
.1
0
-50
-40
-30
-20
-10
0
10
20
30
40
50

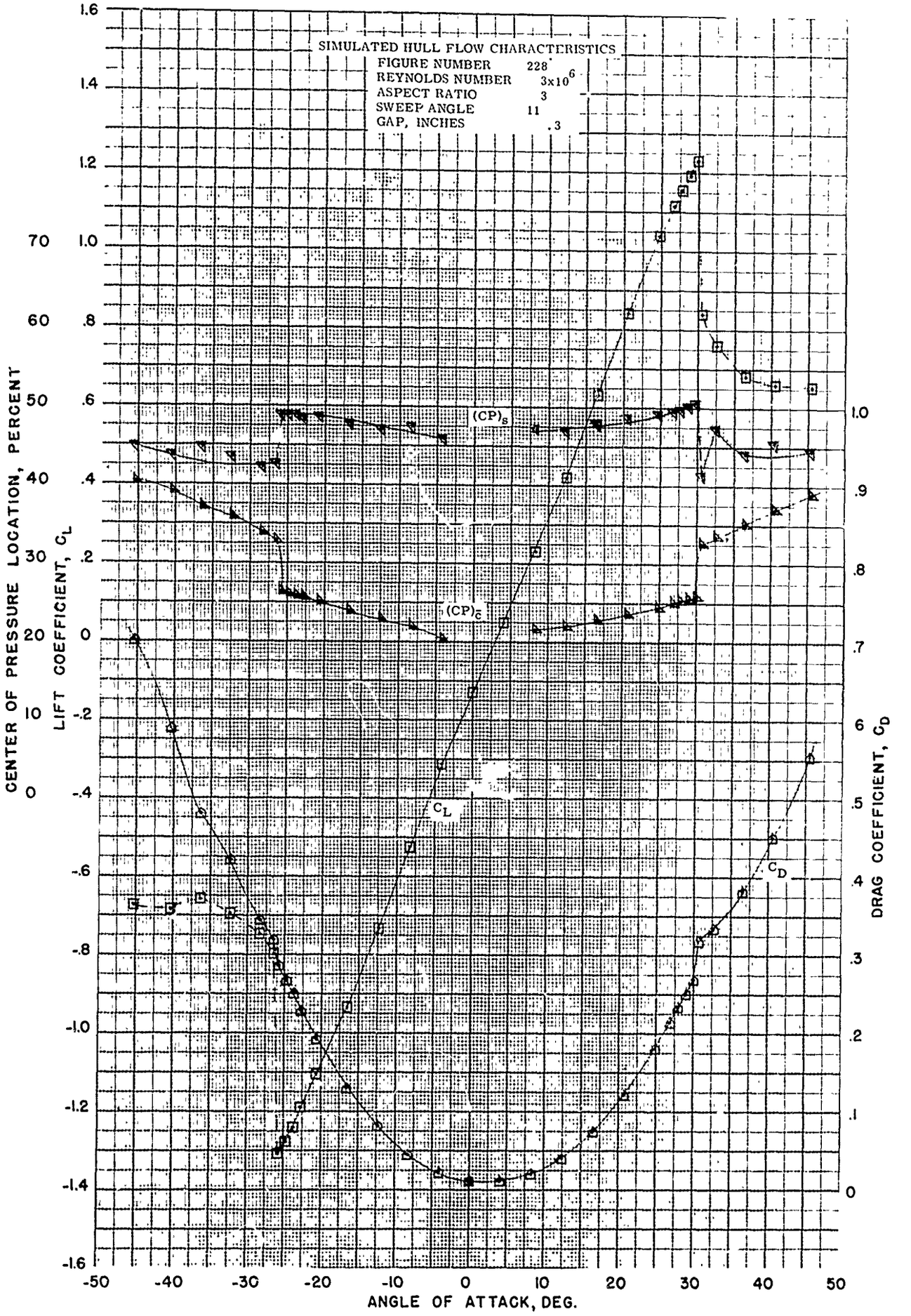
SIMULATED HULL FLOW CHARACTERISTICS
FIGURE NUMBER 228
REYNOLDS NUMBER 3x10^6
ASPECT RATIO 3
SWEEP ANGLE 11
GAP, INCHES .3
CENTER OF PRESSURE LOCATION, PERCENT
LIFT COEFFICIENT, C_L
DRAG COEFFICIENT, C_D
ANGLE OF ATTACK, DEG.
$(CP)_s$
$(CP)_{\bar{c}}$
C_L
C_D
70
60
50
40
30
20
10
0
1.6
1.4
1.2
1.0
.8
.6
.4
.2
0
-.2
-.4
-.6
-.8
-1.0
-1.2
-1.4
-1.6
1.0
.9
.8
.7
.6
.5
.4
.3
.2
.1
0
-50
-40
-30
-20
-10
0
10
20
30
40
50

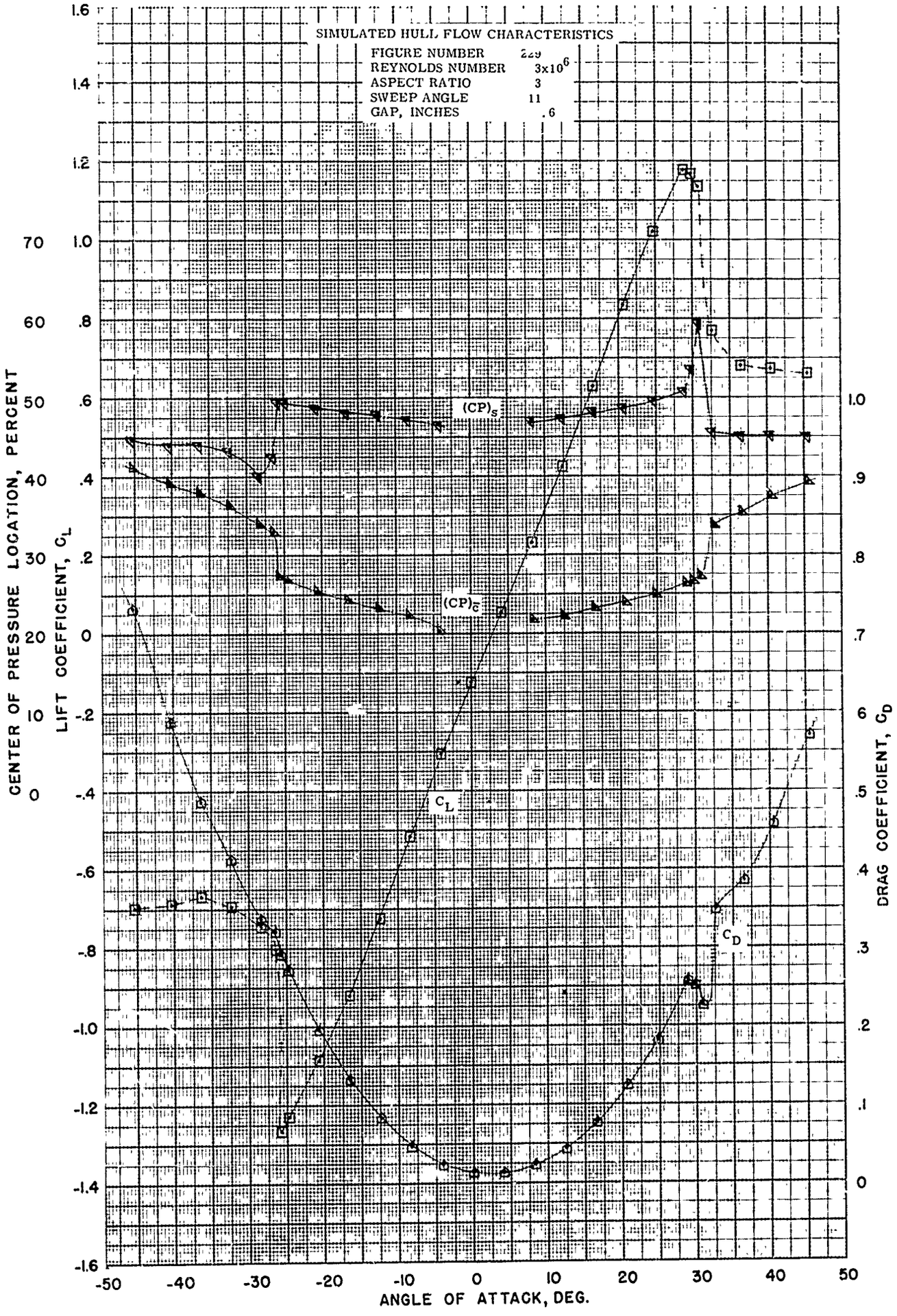
SIMULATED HULL FLOW CHARACTERISTICS
FIGURE NUMBER 229
REYNOLDS NUMBER 3x10^6
ASPECT RATIO 3
SWEEP ANGLE 11
GAP, INCHES .6
CENTER OF PRESSURE LOCATION, PERCENT
LIFT COEFFICIENT, C_L
DRAG COEFFICIENT, C_D
ANGLE OF ATTACK, DEG.
$(CP)_s$
$(CP)_{\bar{c}}$
C_L
C_D
70
60
50
40
30
20
10
0
1.6
1.4
1.2
1.0
.8
.6
.4
.2
0
-.2
-.4
-.6
-.8
-1.0
-1.2
-1.4
-1.6
1.0
.9
.8
.7
.6
.5
.4
.3
.2
.1
0
-50
-40
-30
-20
-10
0
10
20
30
40
50

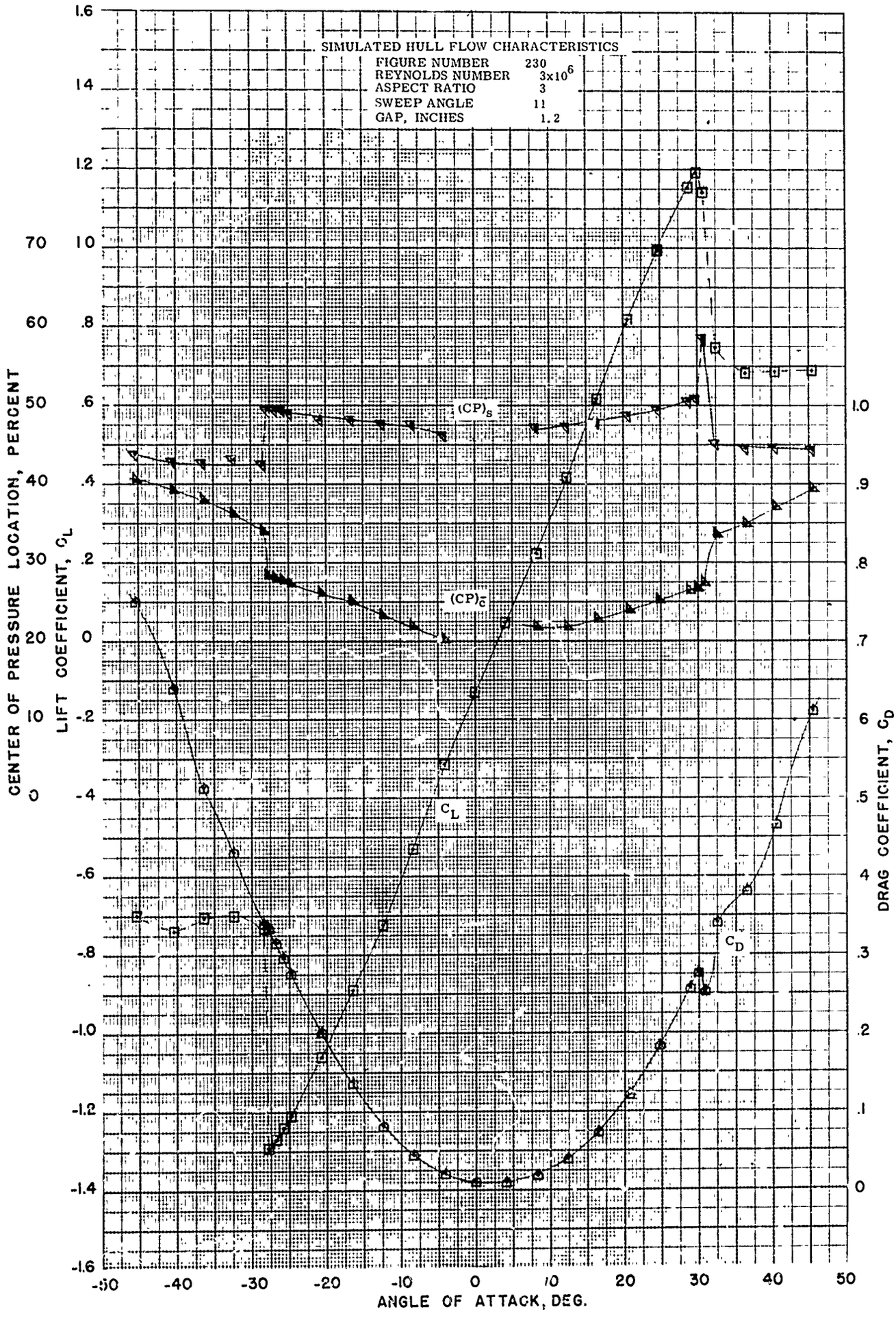
SIMULATED HULL FLOW CHARACTERISTICS
FIGURE NUMBER 230
REYNOLDS NUMBER 3x10^6
ASPECT RATIO 3
SWEEP ANGLE 11
GAP, INCHES 1.2
CENTER OF PRESSURE LOCATION, PERCENT
LIFT COEFFICIENT, C_L
DRAG COEFFICIENT, C_D
ANGLE OF ATTACK, DEG.
$(CP)_S$
$(CP)_{\bar{c}}$
C_L
C_D
70 60 50 40 30 20 10 0
1.6 1.4 1.2 1.0 .8 .6 .4 .2 0 -.2 -.4 -.6 -.8 -1.0 -1.2 -1.4 -1.6
1.0 .9 .8 .7 .6 .5 .4 .3 .2 .1 0
-50 -40 -30 -20 -10 0 10 20 30 40 50

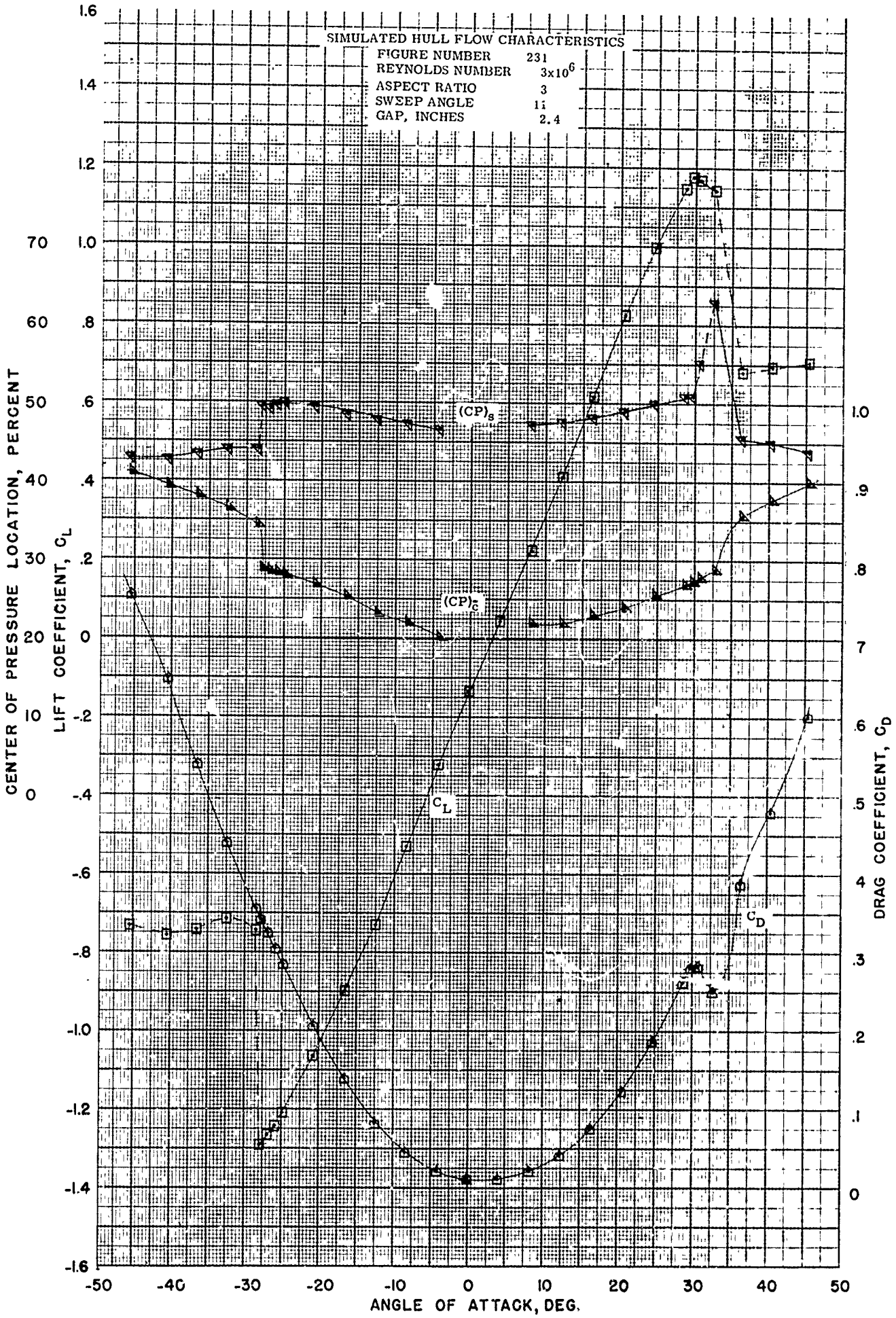
SIMULATED HULL FLOW CHARACTERISTICS
FIGURE NUMBER 231
REYNOLDS NUMBER 3x10^6
ASPECT RATIO 3
SWEEP ANGLE 11
GAP, INCHES 2.4
CENTER OF PRESSURE LOCATION, PERCENT
LIFT COEFFICIENT, C_L
DRAG COEFFICIENT, C_D
ANGLE OF ATTACK, DEG.
(CP)_S
(CP)_C
C_L
C_D
70
60
50
40
30
20
10
0
1.6
1.4
1.2
1.0
.8
.6
.4
.2
0
-.2
-.4
-.6
-.8
-1.0
-1.2
-1.4
-1.6
1.0
.9
.8
.7
.6
.5
.4
.3
.2
.1
0
-50
-40
-30
-20
-10
0
10
20
30
40
50

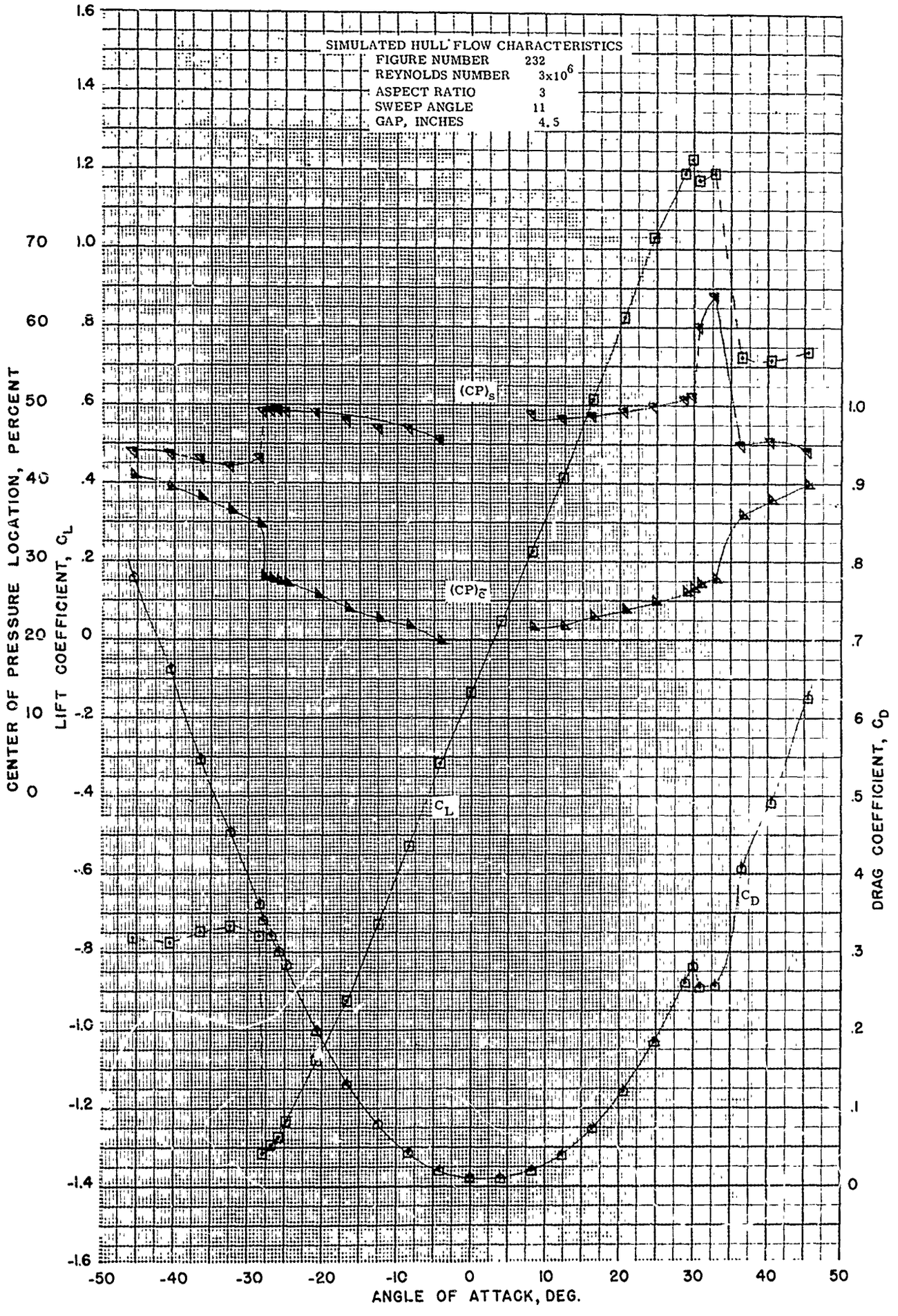
SIMULATED HULL FLOW CHARACTERISTICS
FIGURE NUMBER 232
REYNOLDS NUMBER 3x10^6
ASPECT RATIO 3
SWEEP ANGLE 11
GAP, INCHES 4.5
CENTER OF PRESSURE LOCATION, PERCENT
LIFT COEFFICIENT, C_L
DRAG COEFFICIENT, C_D
ANGLE OF ATTACK, DEG.
$(CP)_s$
$(CP)_{\bar{c}}$
C_L
C_D
70
60
50
40
30
20
10
0
1.6
1.4
1.2
1.0
.8
.6
.4
.2
0
-.2
-.4
-.6
-.8
-1.0
-1.2
-1.4
-1.6
1.0
.9
.8
.7
.6
.5
.4
.3
.2
.1
0
-50
-40
-30
-20
-10
0
10
20
30
40
50

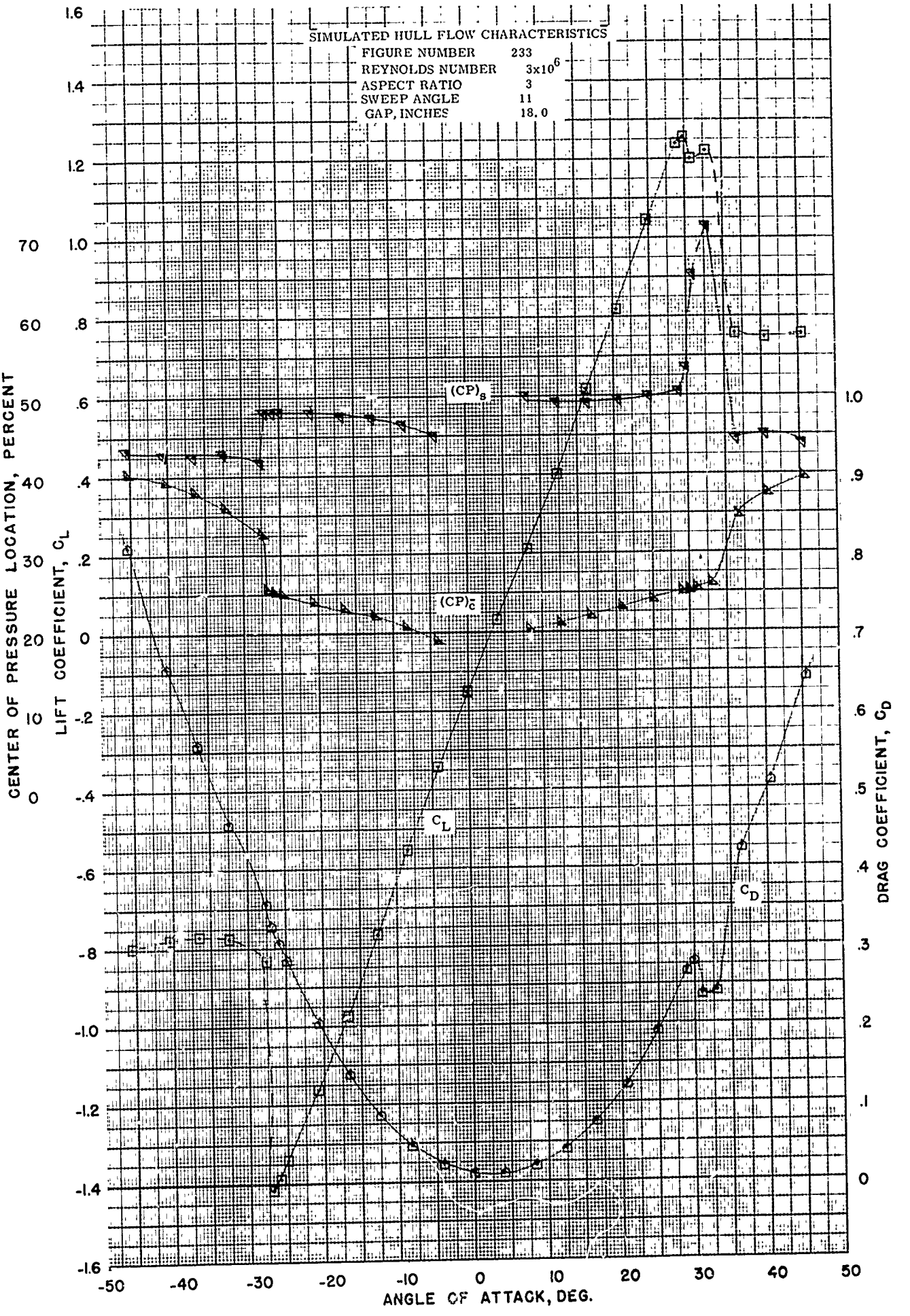
SIMULATED HULL FLOW CHARACTERISTICS
FIGURE NUMBER 233
REYNOLDS NUMBER 3x10^6
ASPECT RATIO 3
SWEEP ANGLE 11
GAP, INCHES 18.0
CENTER OF PRESSURE LOCATION, PERCENT
LIFT COEFFICIENT, C_L
DRAG COEFFICIENT, C_D
ANGLE OF ATTACK, DEG.
$(CP)_s$
$(CP)_c$
C_L
C_D
70
60
50
40
30
20
10
0
1.6
1.4
1.2
1.0
.8
.6
.4
.2
0
-.2
-.4
-.6
-.8
-1.0
-1.2
-1.4
-1.6
1.0
.9
.8
.7
.6
.5
.4
.3
.2
.1
0
-50
-40
-30
-20
-10
0
10
20
30
40
50

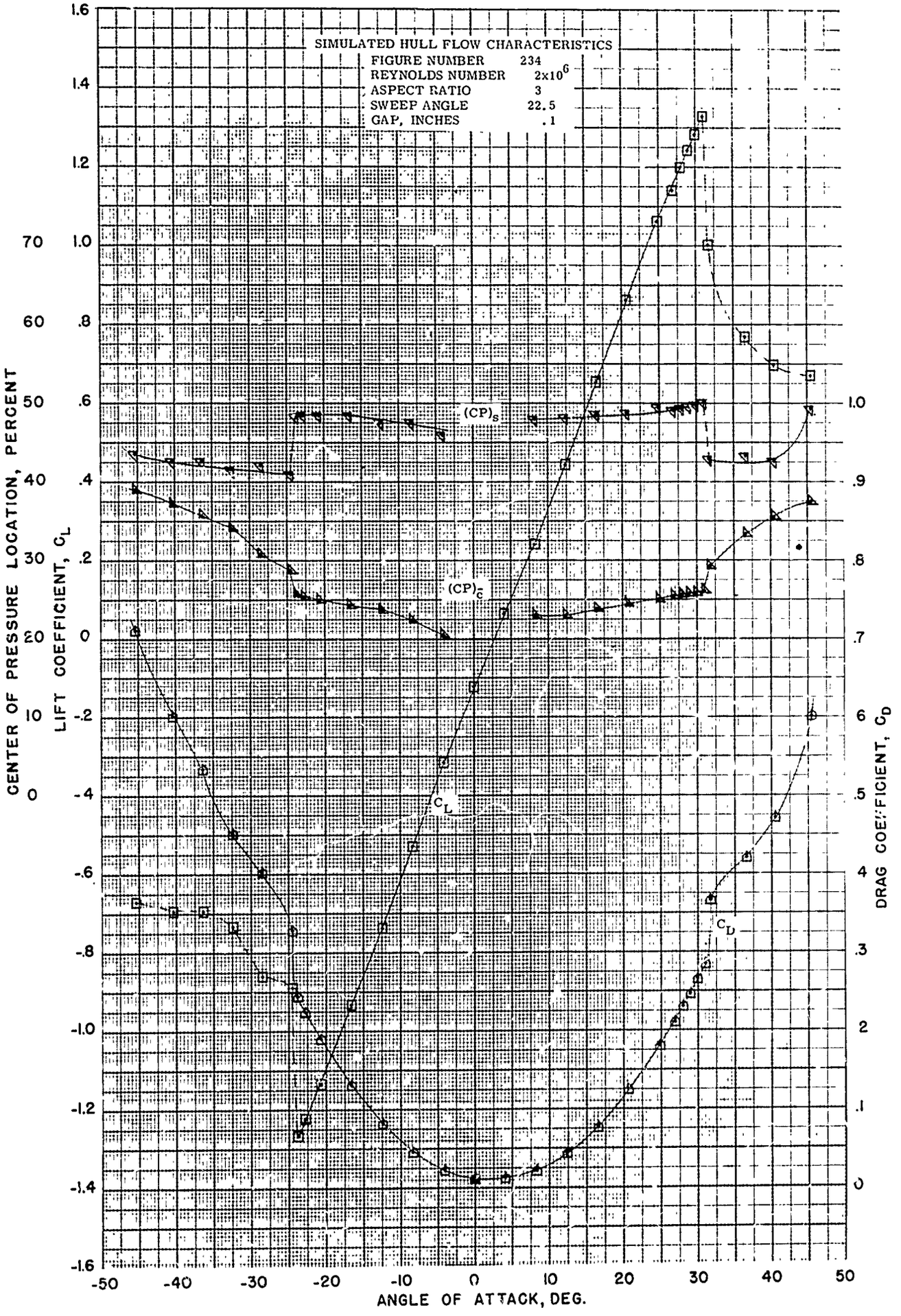
SIMULATED HULL FLOW CHARACTERISTICS
FIGURE NUMBER 234
REYNOLDS NUMBER 2x10^6
ASPECT RATIO 3
SWEEP ANGLE 22.5
GAP, INCHES .1
CENTER OF PRESSURE LOCATION, PERCENT
LIFT COEFFICIENT, C_L
DRAG COEFFICIENT, C_D
ANGLE OF ATTACK, DEG.
$(CP)_s$
$(CP)_{\bar{c}}$
C_L
C_D
70
60
50
40
30
20
10
0
1.6
1.4
1.2
1.0
.8
.6
.4
.2
0
-.2
-.4
-.6
-.8
-1.0
-1.2
-1.4
-1.6
1.0
.9
.8
.7
.6
.5
.4
.3
.2
.1
0
-50
-40
-30
-20
-10
0
10
20
30
40
50

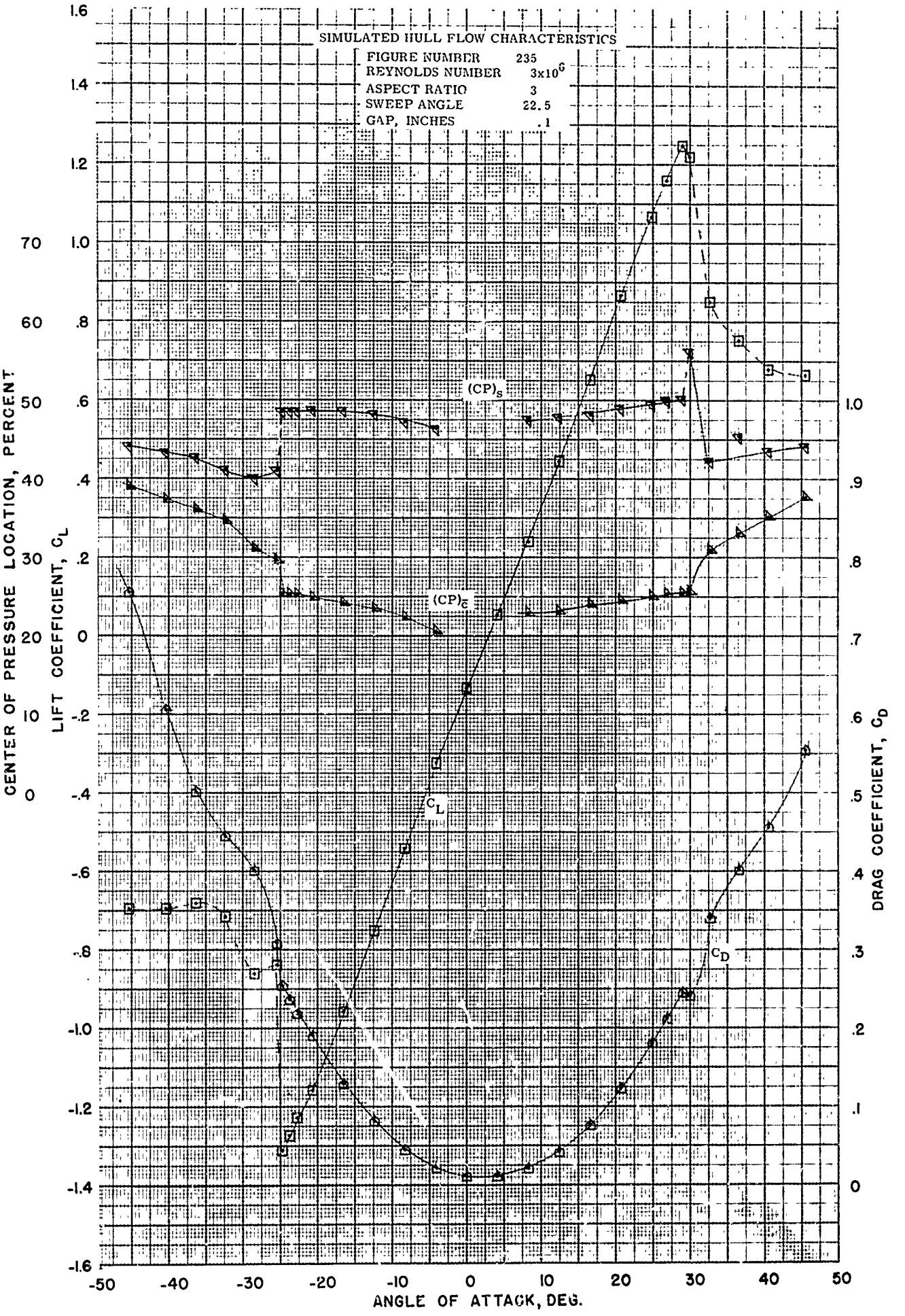
SIMULATED HULL FLOW CHARACTERISTICS
FIGURE NUMBER 235
REYNOLDS NUMBER 3x10^6
ASPECT RATIO 3
SWEEP ANGLE 22.5
GAP, INCHES .1
(CP)s
(CP)c̄
CL
CD
CENTER OF PRESSURE LOCATION, PERCENT
LIFT COEFFICIENT, CL
DRAG COEFFICIENT, CD
ANGLE OF ATTACK, DEG.
70
60
50
40
30
20
10
0
1.6
1.4
1.2
1.0
.8
.6
.4
.2
0
-.2
-.4
-.6
-.8
-1.0
-1.2
-1.4
-1.6
1.0
.9
.8
.7
.6
.5
.4
.3
.2
.1
0
-50
-40
-30
-20
-10
0
10
20
30
40
50

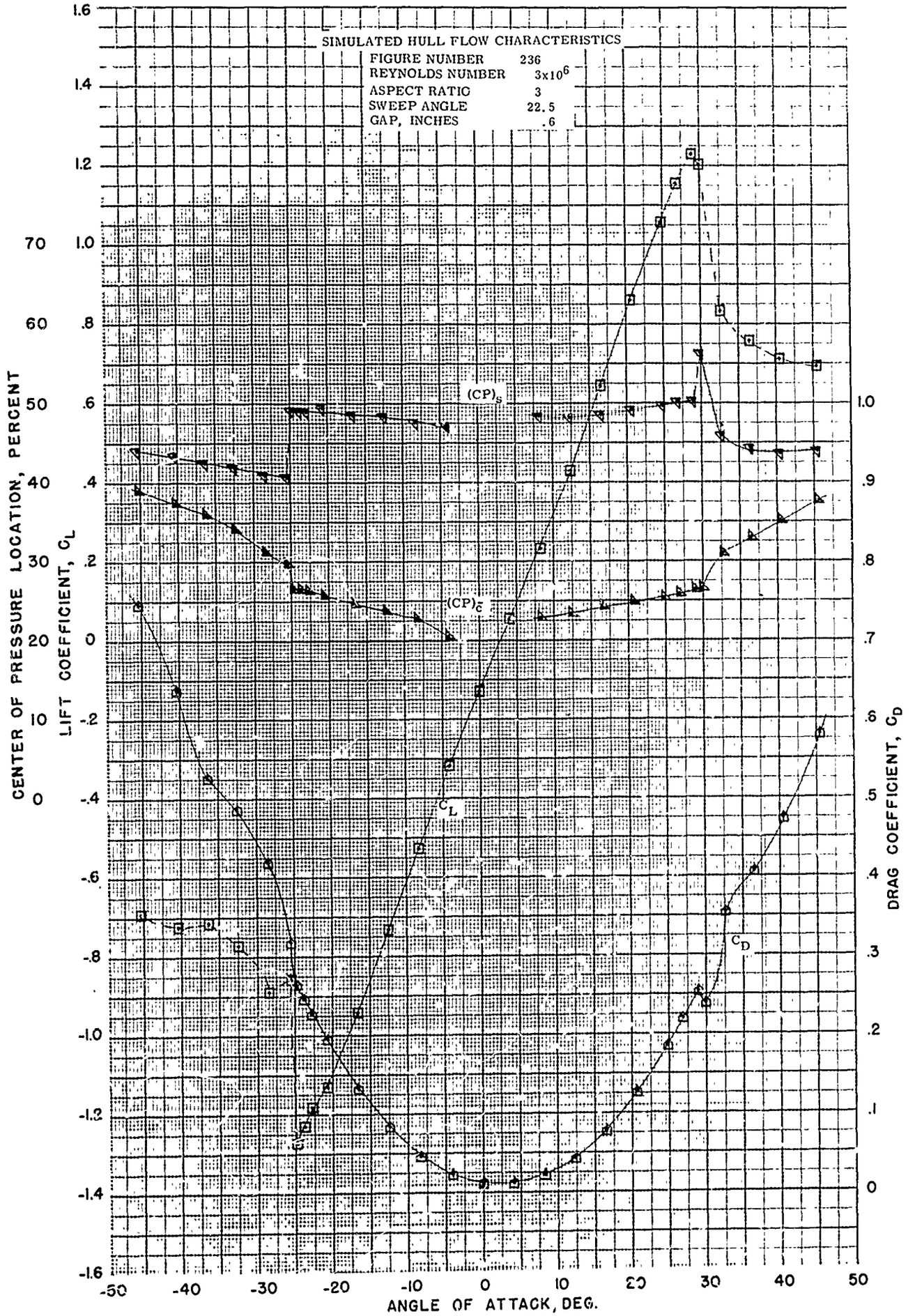
SIMULATED HULL FLOW CHARACTERISTICS
FIGURE NUMBER 236
REYNOLDS NUMBER 3x10^6
ASPECT RATIO 3
SWEEP ANGLE 22.5
GAP, INCHES .6
(CP)s
(CP)c
CL
CD
CENTER OF PRESSURE LOCATION, PERCENT
LIFT COEFFICIENT, CL
DRAG COEFFICIENT, CD
ANGLE OF ATTACK, DEG.
70
60
50
40
30
20
10
0
1.6
1.4
1.2
1.0
.8
.6
.4
.2
0
-.2
-.4
-.6
-.8
-1.0
-1.2
-1.4
-1.6
1.0
.9
.8
.7
.6
.5
.4
.3
.2
.1
0
-50
-40
-30
-20
-10
0
10
20
30
40
50

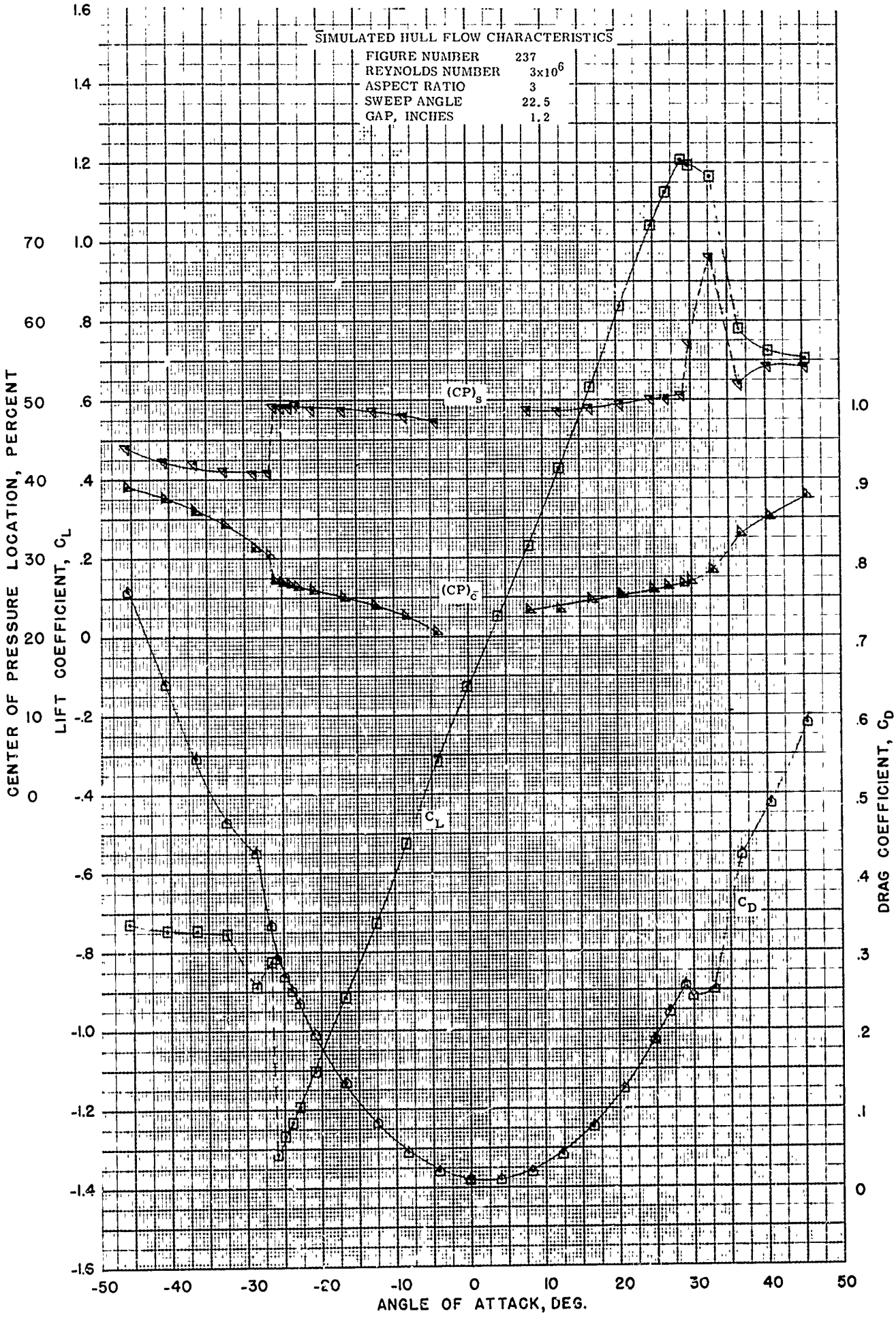
SIMULATED HULL FLOW CHARACTERISTICS
FIGURE NUMBER 237
REYNOLDS NUMBER 3x10^6
ASPECT RATIO 3
SWEEP ANGLE 22.5
GAP, INCHES 1.2
(CP)s
(CP)c
CL
CD
CENTER OF PRESSURE LOCATION, PERCENT
LIFT COEFFICIENT, CL
DRAG COEFFICIENT, CD
ANGLE OF ATTACK, DEG.
70
60
50
40
30
20
10
0
1.6
1.4
1.2
1.0
.8
.6
.4
.2
0
-.2
-.4
-.6
-.8
-1.0
-1.2
-1.4
-1.6
1.0
.9
.8
.7
.6
.5
.4
.3
.2
.1
0
-50
-40
-30
-20
-10
0
10
20
30
40
50

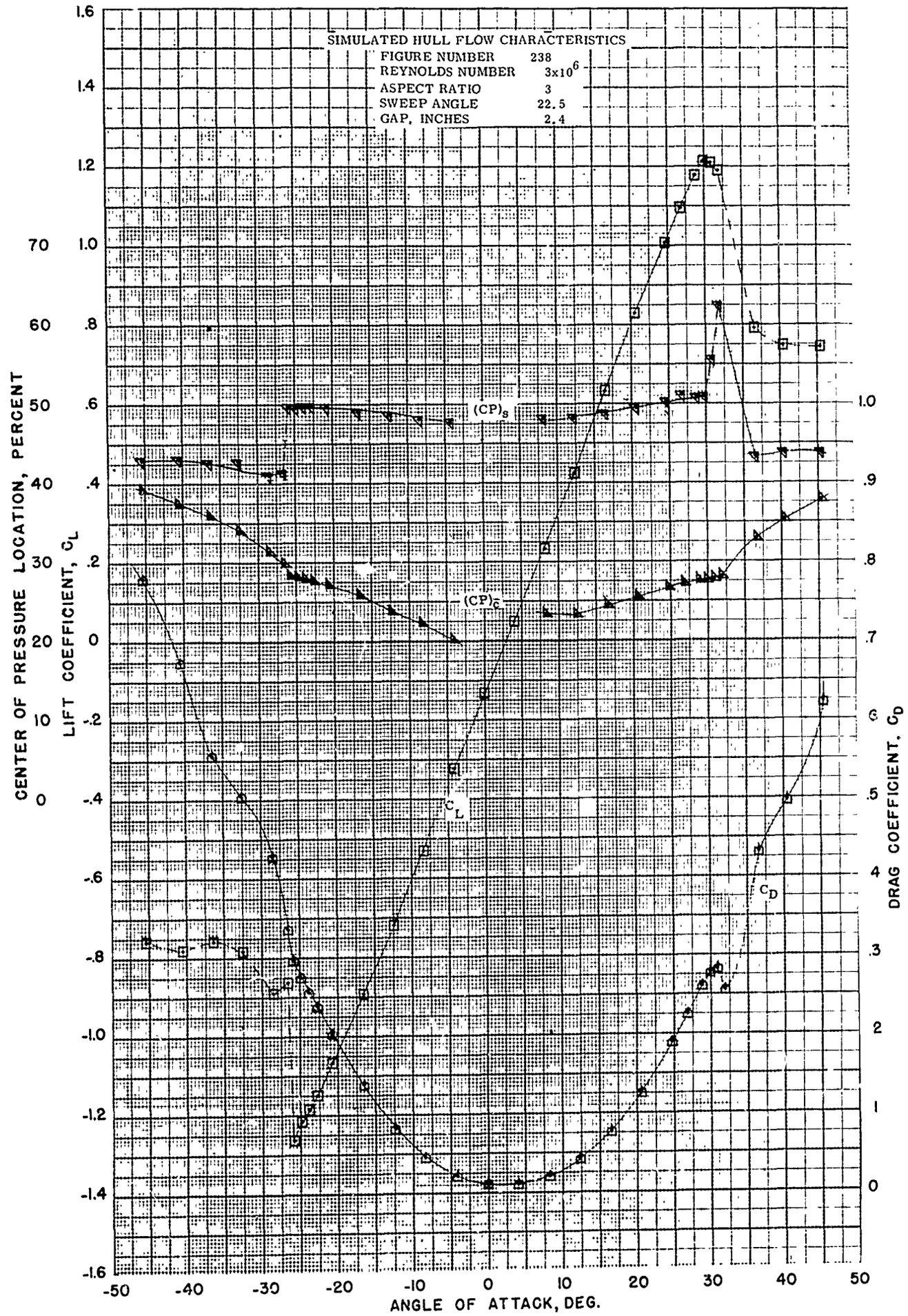
SIMULATED HULL FLOW CHARACTERISTICS
FIGURE NUMBER 238
REYNOLDS NUMBER 3x10^6
ASPECT RATIO 3
SWEEP ANGLE 22.5
GAP, INCHES 2.4
CENTER OF PRESSURE LOCATION, PERCENT
LIFT COEFFICIENT, C_L
DRAG COEFFICIENT, C_D
ANGLE OF ATTACK, DEG.
$(CP)_s$
$(CP)_c$
C_L
C_D
70
60
50
40
30
20
10
0
1.6
1.4
1.2
1.0
.8
.6
.4
.2
0
-.2
-.4
-.6
-.8
-1.0
-1.2
-1.4
-1.6
1.0
.9
.8
.7
.6
.5
.4
.3
.2
1
0
-50
-40
-30
-20
-10
0
10
20
30
40
50

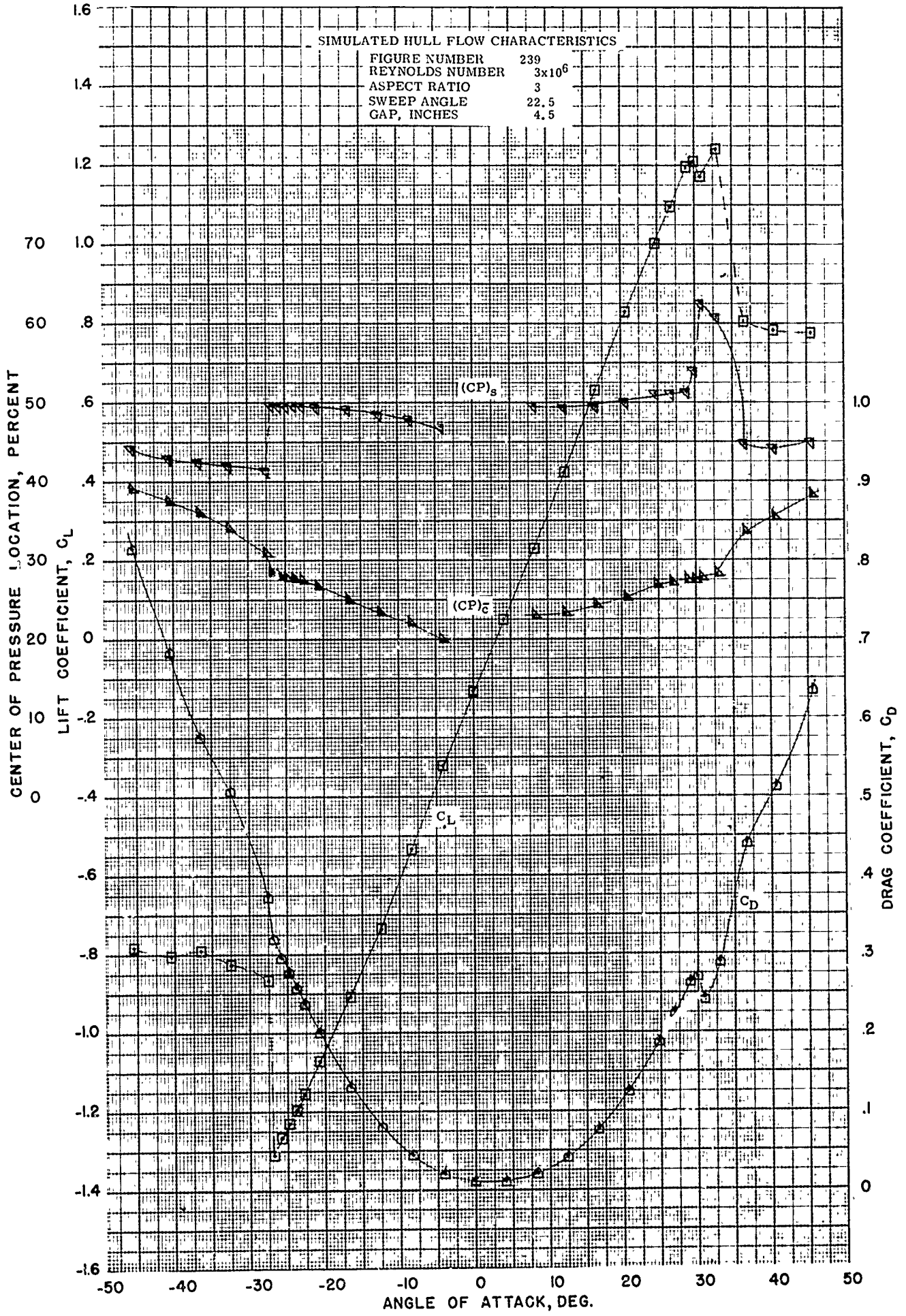
SIMULATED HULL FLOW CHARACTERISTICS
FIGURE NUMBER 239
REYNOLDS NUMBER 3x10^6
ASPECT RATIO 3
SWEEP ANGLE 22.5
GAP, INCHES 4.5
CENTER OF PRESSURE LOCATION, PERCENT
LIFT COEFFICIENT, C_L
DRAG COEFFICIENT, C_D
ANGLE OF ATTACK, DEG.
$(CP)_s$
$(CP)_{\bar{c}}$
C_L
C_D
70
60
50
40
30
20
10
0
1.6
1.4
1.2
1.0
.8
.6
.4
.2
0
-.2
-.4
-.6
-.8
-1.0
-1.2
-1.4
-1.6
1.0
.9
.8
.7
.6
.5
.4
.3
.2
.1
0
-50
-40
-30
-20
-10
0
10
20
30
40
50

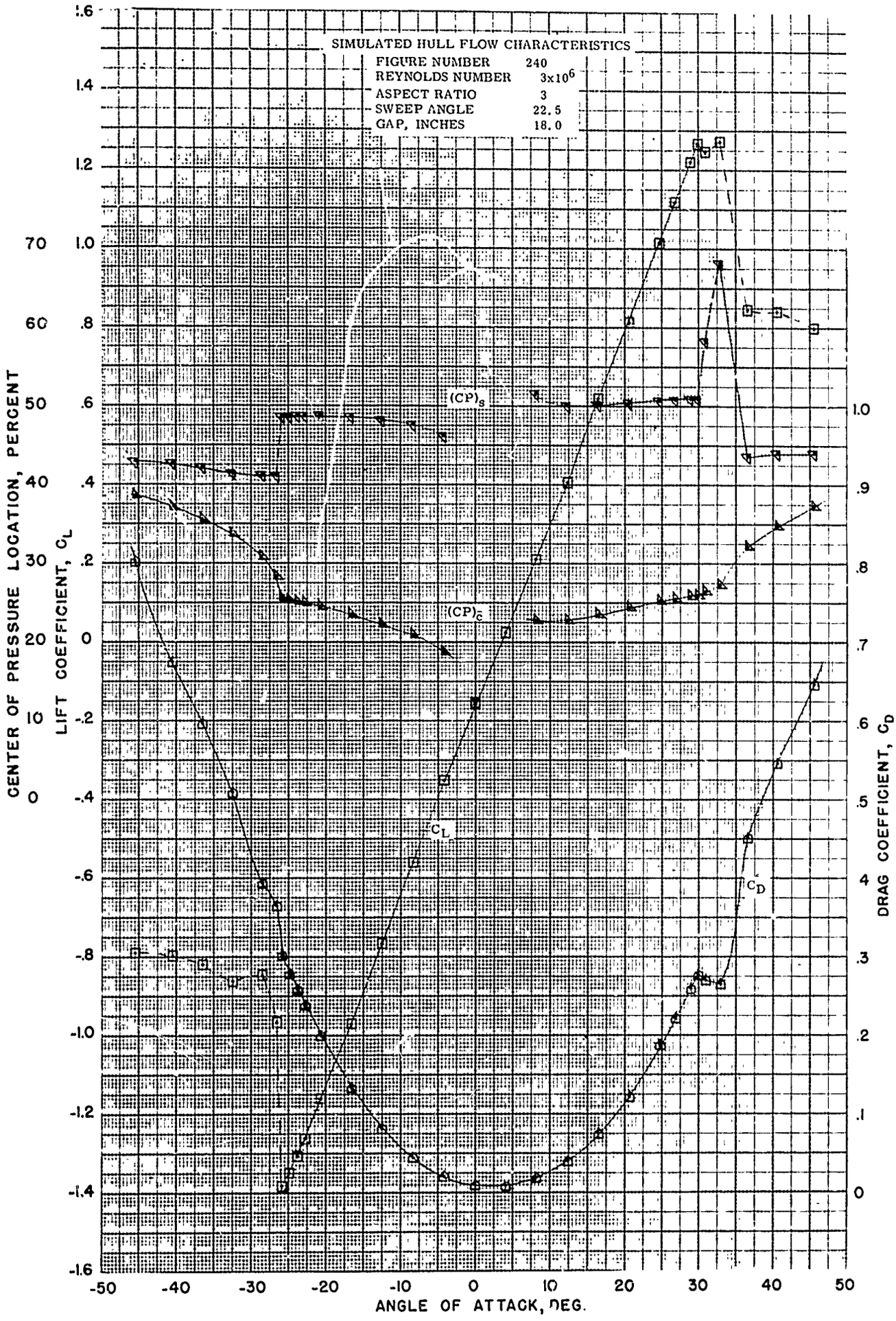
SIMULATED HULL FLOW CHARACTERISTICS
FIGURE NUMBER 240
REYNOLDS NUMBER 3x10^6
ASPECT RATIO 3
SWEEP ANGLE 22.5
GAP, INCHES 18.0
(CP)s
(CP)c
CL
CD
CENTER OF PRESSURE LOCATION, PERCENT
LIFT COEFFICIENT, CL
DRAG COEFFICIENT, CD
ANGLE OF ATTACK, DEG.
70
60
50
40
30
20
10
0
1.6
1.4
1.2
1.0
.8
.6
.4
.2
0
-.2
-.4
-.6
-.8
-1.0
-1.2
-1.4
-1.6
1.0
.9
.8
.7
.6
.5
.4
.3
.2
.1
0
-50
-40
-30
-20
-10
0
10
20
30
40
50

APPENDIX C

Combined Simulated Hull Flow And Propeller Slipstream Characteristics, Minimum Gap

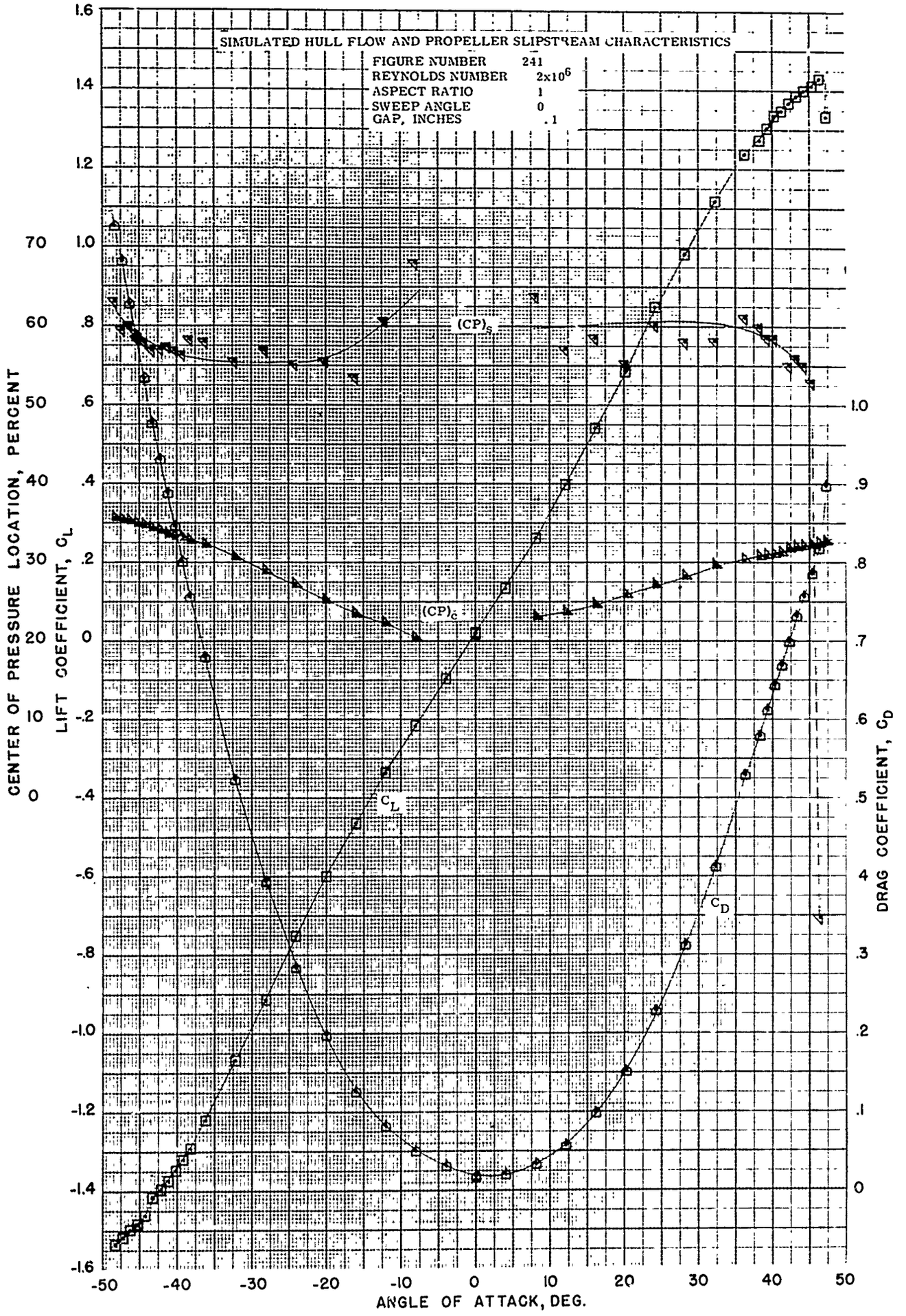
SIMULATED HULL FLOW AND PROPELLER SLIPSTREAM CHARACTERISTICS
FIGURE NUMBER 241
REYNOLDS NUMBER 2x10^6
ASPECT RATIO 1
SWEEP ANGLE 0
GAP, INCHES .1
CENTER OF PRESSURE LOCATION, PERCENT
LIFT COEFFICIENT, C_L
DRAG COEFFICIENT, C_D
ANGLE OF ATTACK, DEG.
$(CP)_s$
$(CP)_c$
C_L
C_D
70
60
50
40
30
20
10
0
1.6
1.4
1.2
1.0
.8
.6
.4
.2
0
-.2
-.4
-.6
-.8
-1.0
-1.2
-1.4
-1.6
1.0
.9
.8
.7
.6
.5
.4
.3
.2
.1
0
-50
-40
-30
-20
-10
0
10
20
30
40
50

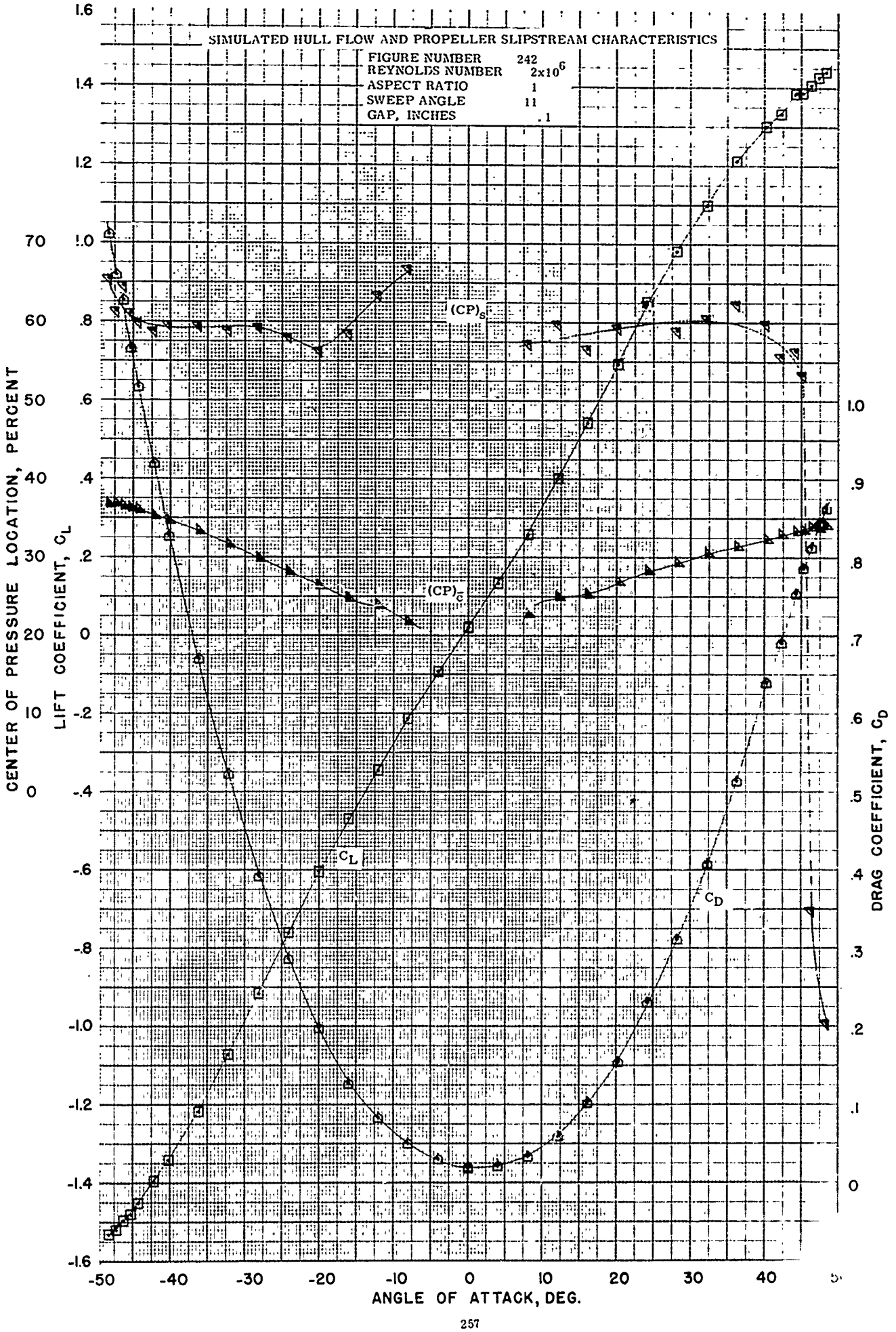
SIMULATED HULL FLOW AND PROPELLER SLIPSTREAM CHARACTERISTICS
FIGURE NUMBER 242
REYNOLDS NUMBER 2x10^6
ASPECT RATIO 1
SWEEP ANGLE 11
GAP, INCHES .1
CENTER OF PRESSURE LOCATION, PERCENT
LIFT COEFFICIENT, C_L
DRAG COEFFICIENT, C_D
ANGLE OF ATTACK, DEG.
$(CP)_S$
$(CP)_C$
C_L
C_D
70
60
50
40
30
20
10
0
1.6
1.4
1.2
1.0
.8
.6
.4
.2
0
-.2
-.4
-.6
-.8
-1.0
-1.2
-1.4
-1.6
1.0
.9
.8
.7
.6
.5
.4
.3
.2
.1
0
-50
-40
-30
-20
-10
0
10
20
30
40

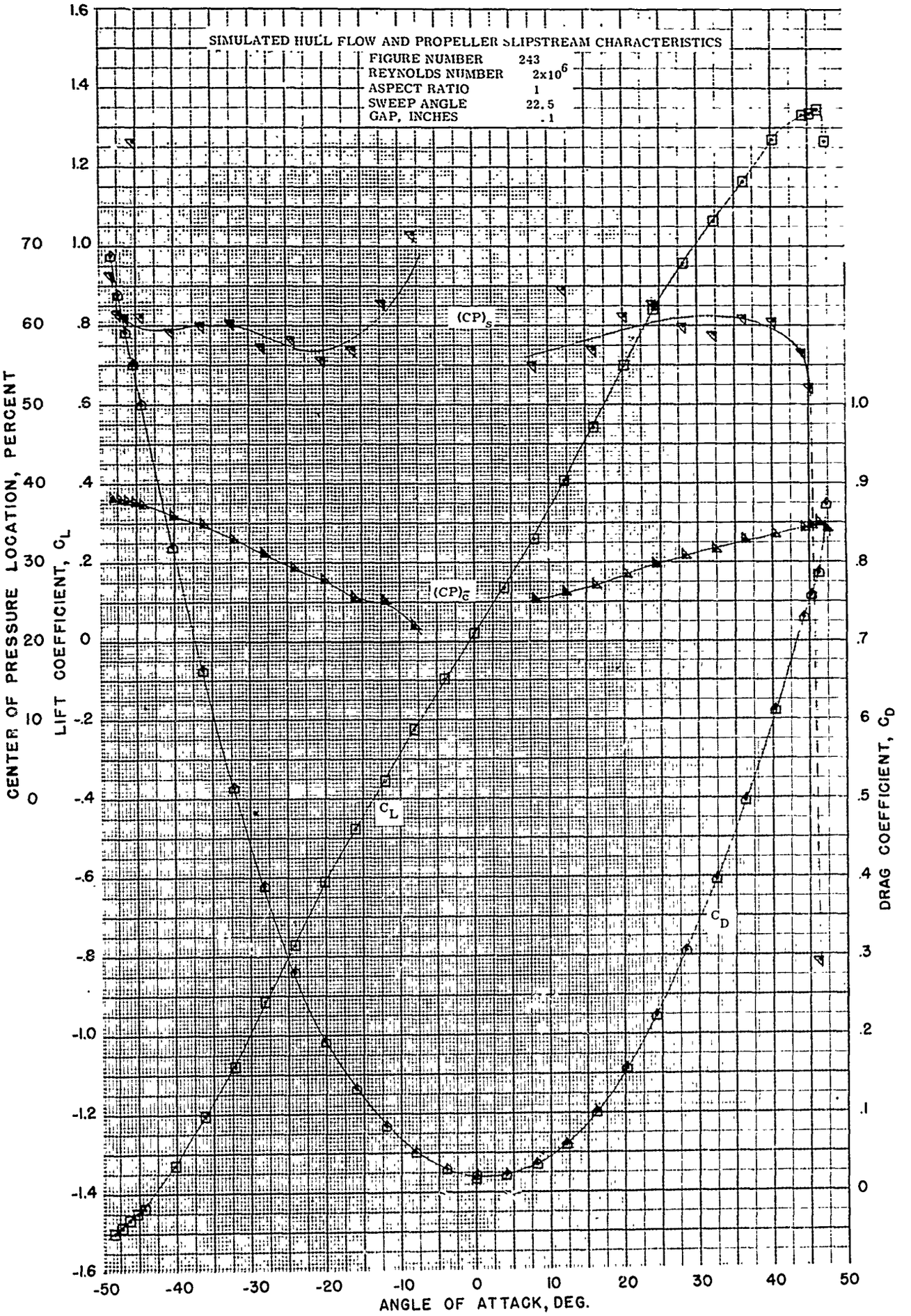
SIMULATED HULL FLOW AND PROPELLER SLIPSTREAM CHARACTERISTICS
FIGURE NUMBER 243
REYNOLDS NUMBER 2x10^6
ASPECT RATIO 1
SWEEP ANGLE 22.5
GAP, INCHES .1
CENTER OF PRESSURE LOCATION, PERCENT
LIFT COEFFICIENT, C_L
DRAG COEFFICIENT, C_D
ANGLE OF ATTACK, DEG.
$(CP)_s$
$(CP)_c$
C_L
C_D
70
60
50
40
30
20
10
0
1.6
1.4
1.2
1.0
.8
.6
.4
.2
0
-.2
-.4
-.6
-.8
-1.0
-1.2
-1.4
-1.6
1.0
.9
.8
.7
.6
.5
.4
.3
.2
.1
0
-50
-40
-30
-20
-10
0
10
20
30
40
50

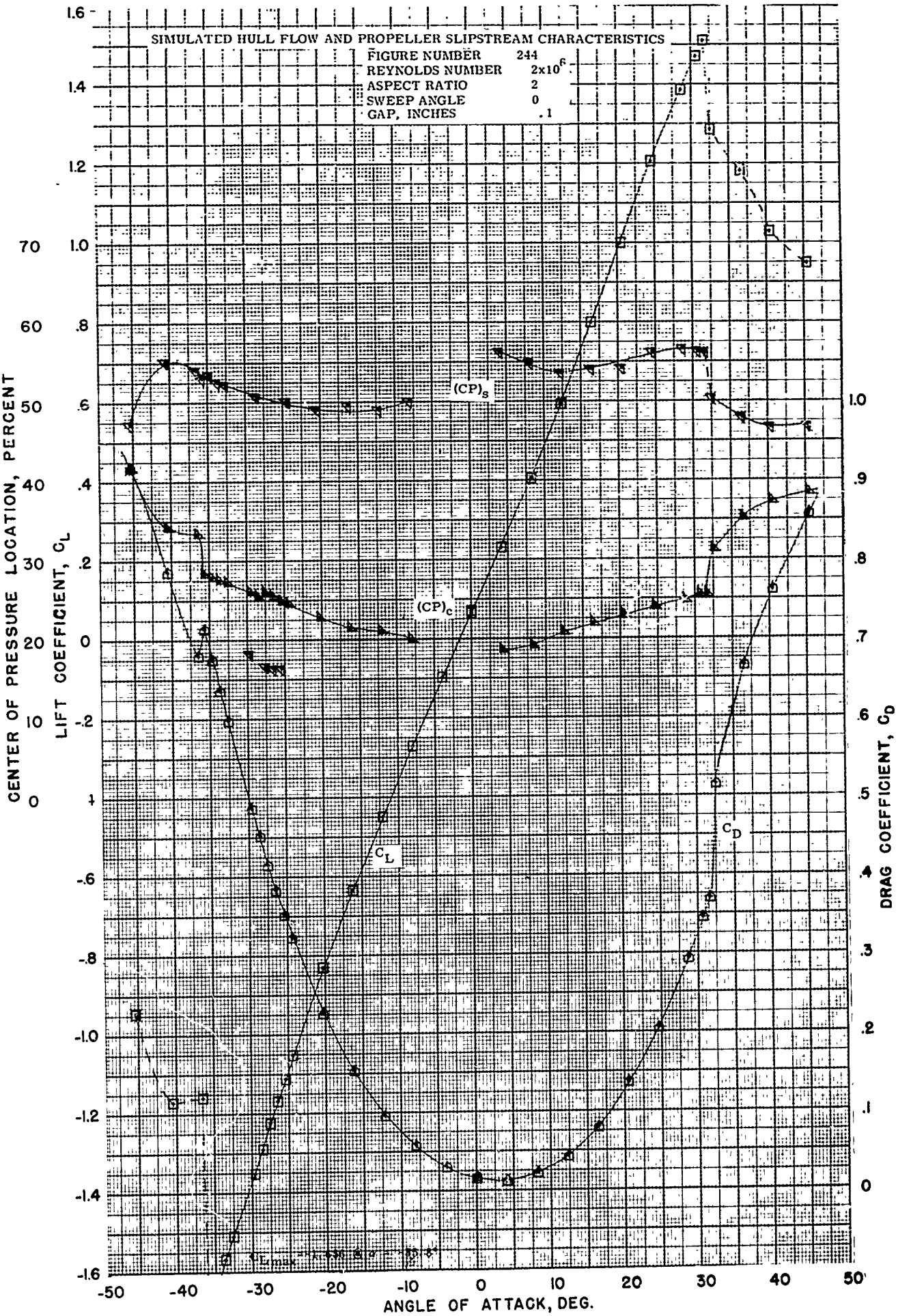
SIMULATED HULL FLOW AND PROPELLER SLIPSTREAM CHARACTERISTICS
FIGURE NUMBER 244
REYNOLDS NUMBER 2x10^6
ASPECT RATIO 2
SWEEP ANGLE 0
GAP, INCHES .1
CENTER OF PRESSURE LOCATION, PERCENT
LIFT COEFFICIENT, C_L
DRAG COEFFICIENT, C_D
ANGLE OF ATTACK, DEG.
$(CP)_s$
$(CP)_c$
C_L
C_D
$C_{L_{max}}$ = 1.530 @ α = 30.6°

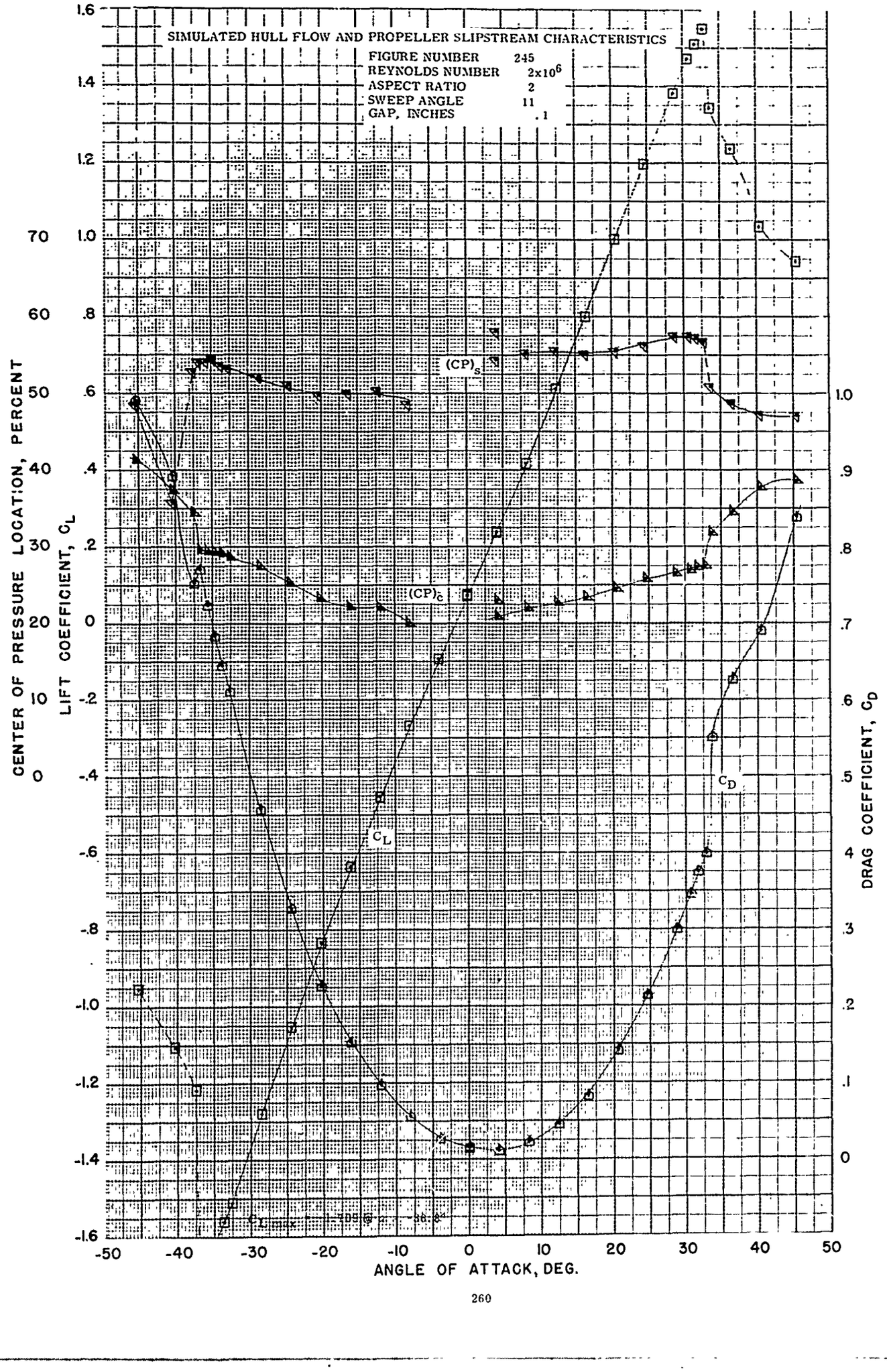
SIMULATED HULL FLOW AND PROPELLER SLIPSTREAM CHARACTERISTICS
FIGURE NUMBER 245
REYNOLDS NUMBER 2x10^6
ASPECT RATIO 2
SWEEP ANGLE 11
GAP, INCHES .1
CENTER OF PRESSURE LOCATION, PERCENT
LIFT COEFFICIENT, C_L
DRAG COEFFICIENT, C_D
ANGLE OF ATTACK, DEG.
$(CP)_s$
$(CP)_c$
C_L
C_D
$C_{L_{max}}$ = 1.309 @ α = 36.8°

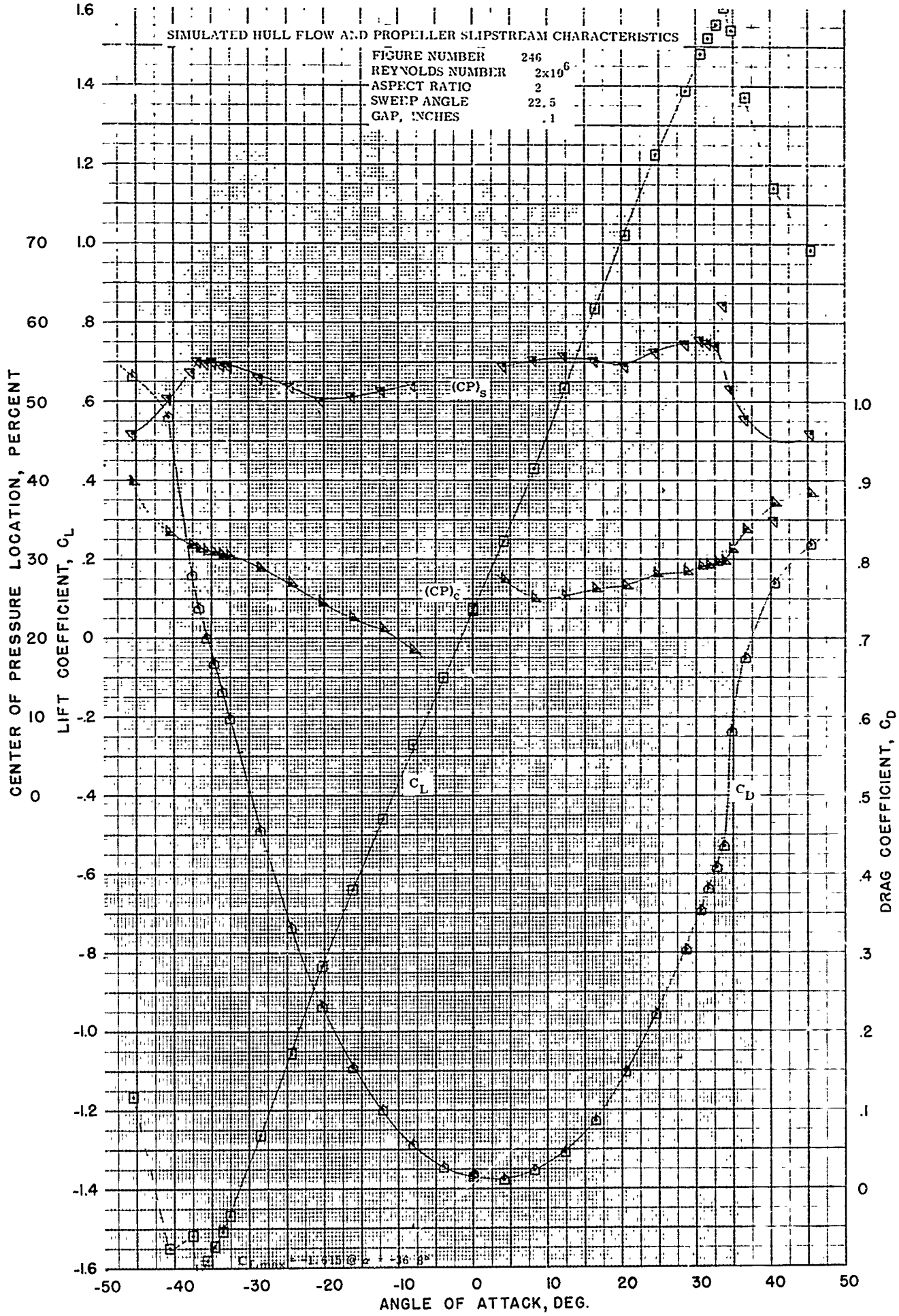
SIMULATED HULL FLOW AND PROPELLER SLIPSTREAM CHARACTERISTICS
FIGURE NUMBER 246
REYNOLDS NUMBER 2x10^6
ASPECT RATIO 2
SWEEP ANGLE 22.5
GAP, INCHES .1
CENTER OF PRESSURE LOCATION, PERCENT
LIFT COEFFICIENT, C_L
DRAG COEFFICIENT, C_D
ANGLE OF ATTACK, DEG.
$(CP)_s$
$(CP)_c$
C_L
C_D
$C_{L_{max}}$ = 1.615 @ α = -16.8°
70
60
50
40
30
20
10
0
1.6
1.4
1.2
1.0
.8
.6
.4
.2
0
-.2
-.4
-.6
-.8
-1.0
-1.2
-1.4
-1.6
1.0
.9
.8
.7
.6
.5
.4
.3
.2
.1
0
-50
-40
-30
-20
-10
0
10
20
30
40
50

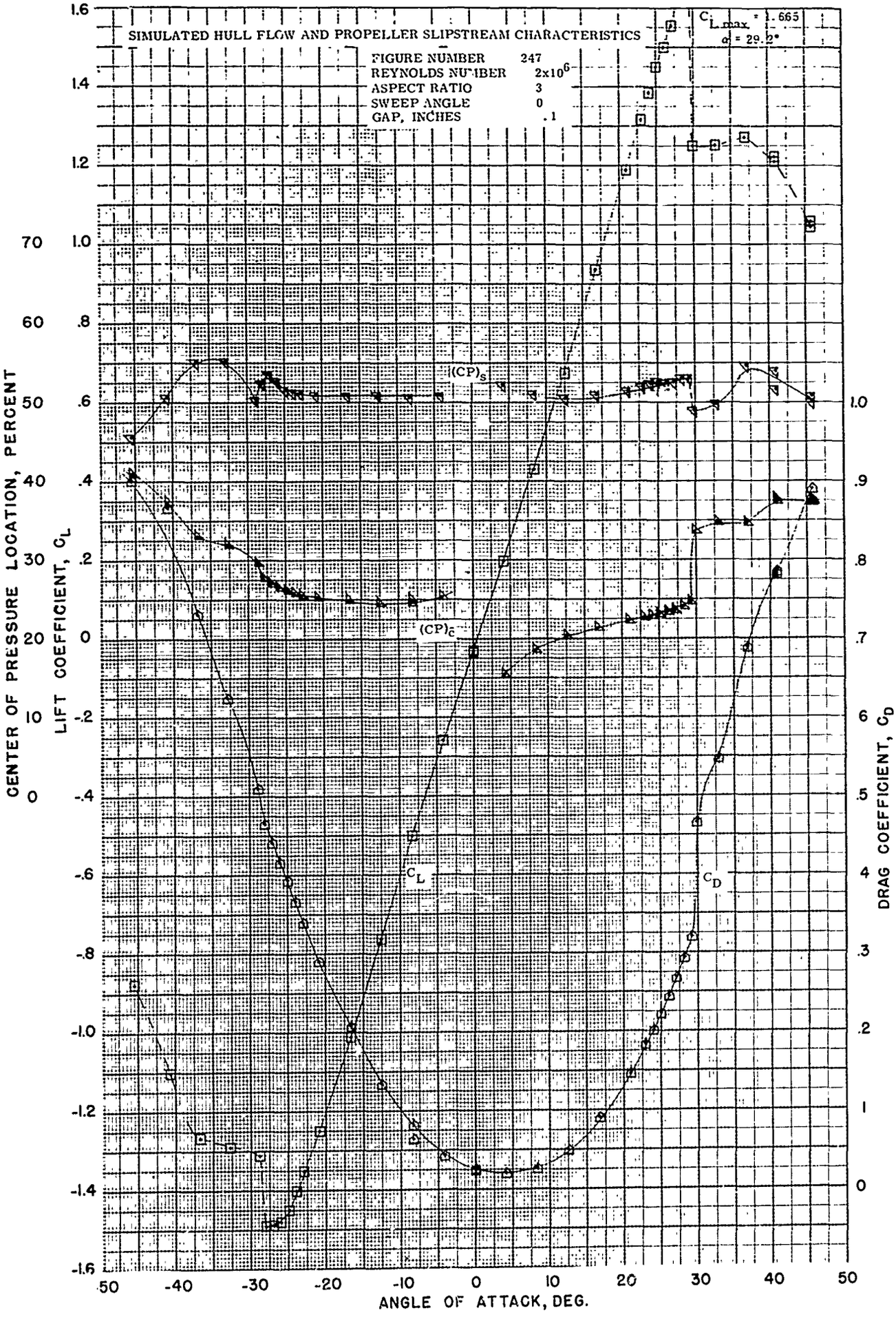
SIMULATED HULL FLOW AND PROPELLER SLIPSTREAM CHARACTERISTICS
FIGURE NUMBER 247
REYNOLDS NUMBER 2x10^6
ASPECT RATIO 3
SWEEP ANGLE 0
GAP, INCHES .1
C_L max = 1.665
α = 29.2°
(CP)_s
(CP)_c
C_L
C_D
CENTER OF PRESSURE LOCATION, PERCENT
LIFT COEFFICIENT, C_L
DRAG COEFFICIENT, C_D
ANGLE OF ATTACK, DEG.
70
60
50
40
30
20
10
0
1.6
1.4
1.2
1.0
.8
.6
.4
.2
0
-.2
-.4
-.6
-.8
-1.0
-1.2
-1.4
-1.6
1.0
.9
.8
.7
6
.5
4
.3
.2
1
0
-50
-40
-30
-20
-10
0
10
20
30
40
50

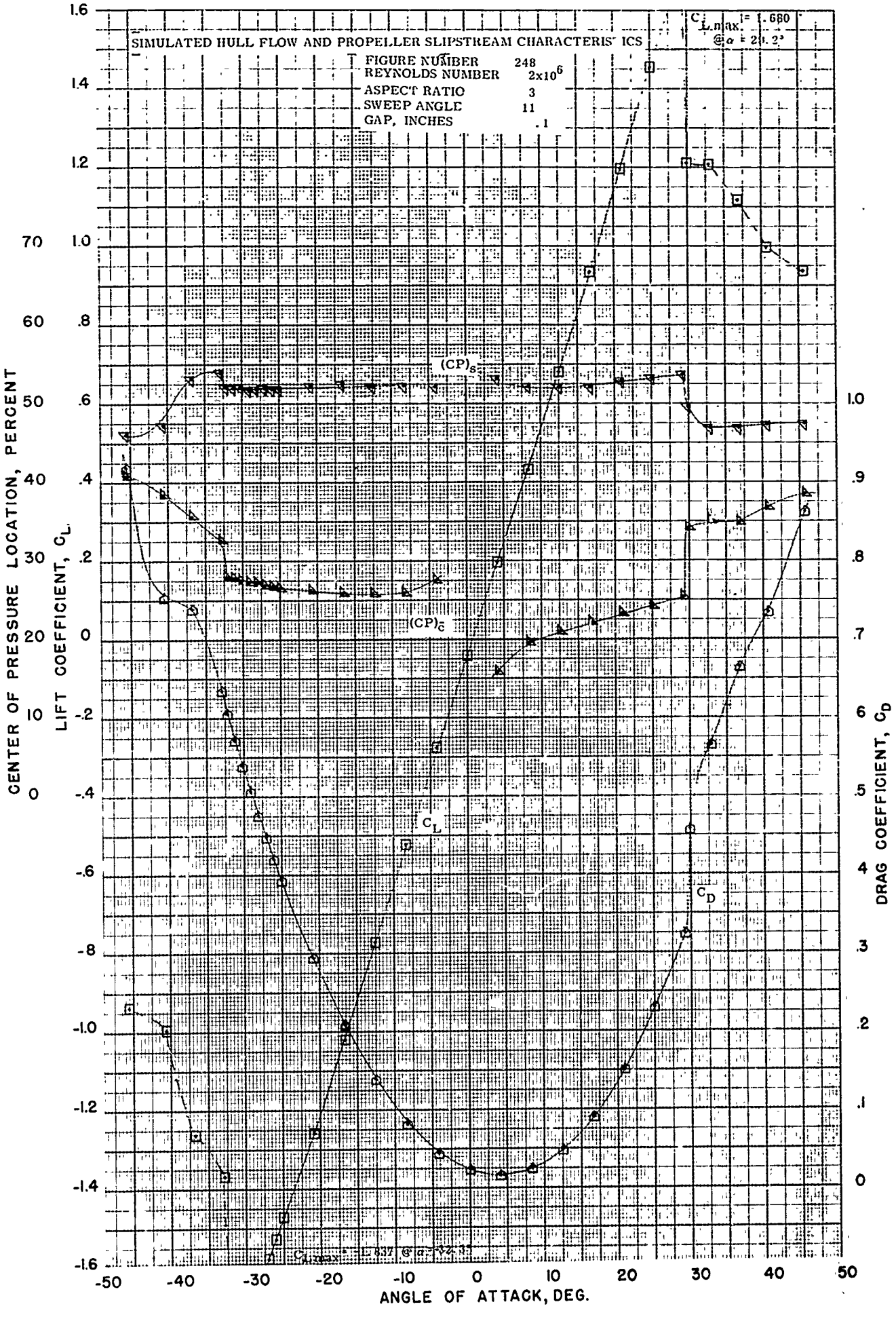
SIMULATED HULL FLOW AND PROPELLER SLIPSTREAM CHARACTERISTICS
FIGURE NUMBER 248
REYNOLDS NUMBER 2x10^6
ASPECT RATIO 3
SWEEP ANGLE 11
GAP, INCHES .1
C L,max = 1.680
@ α = 20.2°
(CP)s
(CP)c
CL
CD
CL,max = 1.837 @ α = 32.3°
CENTER OF PRESSURE LOCATION, PERCENT
LIFT COEFFICIENT, CL
DRAG COEFFICIENT, CD
ANGLE OF ATTACK, DEG.
70
60
50
40
30
20
10
0
1.6
1.4
1.2
1.0
.8
.6
.4
.2
0
-.2
-.4
-.6
-.8
-1.0
-1.2
-1.4
-1.6
1.0
.9
.8
.7
.6
.5
.4
.3
.2
.1
0
-50
-40
-30
-20
-10
0
10
20
30
40
50

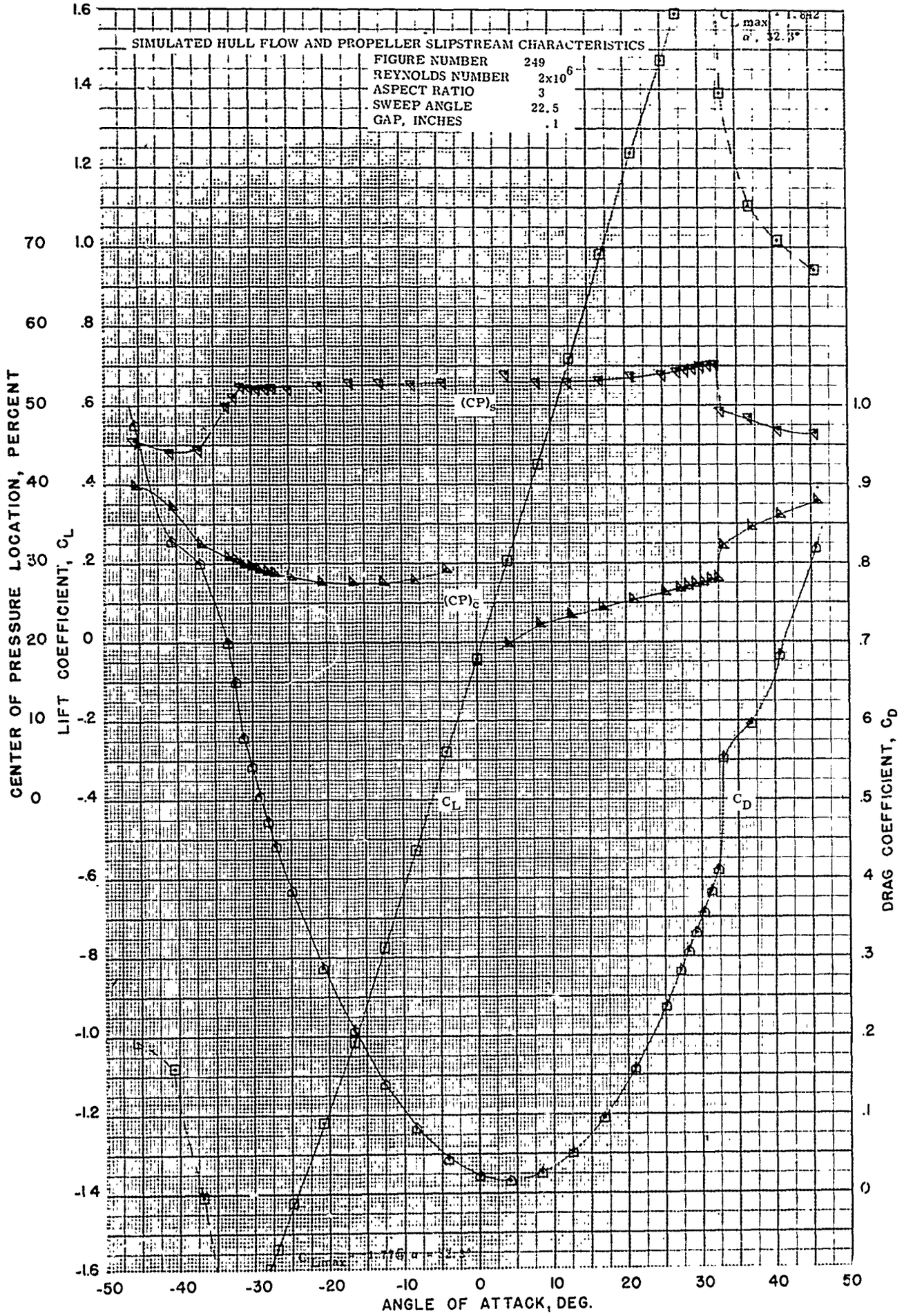
SIMULATED HULL FLOW AND PROPELLER SLIPSTREAM CHARACTERISTICS
FIGURE NUMBER 249
REYNOLDS NUMBER 2x10^6
ASPECT RATIO 3
SWEEP ANGLE 22.5
GAP, INCHES .1
$C_{L_{max}}$ = 1.682
α = 32.3°
$(CP)_s$
$(CP)_c$
C_L
C_D
$C_{L_{max}}$ = 1.776 α = 34°
CENTER OF PRESSURE LOCATION, PERCENT
LIFT COEFFICIENT, C_L
DRAG COEFFICIENT, C_D
ANGLE OF ATTACK, DEG.
70
60
50
40
30
20
10
0
1.6
1.4
1.2
1.0
.8
.6
.4
.2
0
-.2
-.4
-.6
-.8
-1.0
-1.2
-1.4
-1.6
1.0
.9
.8
.7
.6
.5
.4
.3
.2
.1
0
-50
-40
-30
-20
-10
0
10
20
30
40
50

UNCLASSIFIED
Security Classification

DOCUMENT CONTROL DATA - R&D
(Security classification of title, body of abstract and indexing annotation must be entered when the overall report is classified)

1 ORIGINATING ACTIVITY *(Corporate author)*
UNIVERSITY OF MARYLAND
WIND TUNNEL OPERATIONS DEPARTMENT

2a. REPORT SECURITY CLASSIFICATION
UNCLASSIFIED

2b. GROUP

3. REPORT TITLE
EFFECTS OF STREAMWISE GAPS, HULL FLOW AND PROPELLER SLIPSTREAM UPON THE AERODYNAMIC CHARACTERISTICS OF A FAMILY OF LOW-ASPECT RATIO, ALL-MOVEABLE CONTROL SURFACES

4. DESCRIPTIVE NOTES *(Type of report and inclusive dates)*
FINAL REPORT

5. AUTHOR(S) *(Last name, first name, initial)*
WINDSOR, RICHARD I.

6. REPORT DATE	7a. TOTAL NO. OF PAGES	7b. NO. OF REFS
MARCH 1968	264	7

8a. CONTRACT OR GRANT NO.	9a. ORIGINATOR'S REPORT NUMBER(S)
N00024-67-C-5149	UNIVERSITY OF MARYLAND WIND TUNNEL REPORT 485
b. PROJECT NO. 5F-13-02-64; Task 1712	9b. OTHER REPORT NO(S) *(Any other numbers that may be assigned this report)*
c.	
d.	

10. AVAILABILITY/LIMITATION NOTICES
QUALIFIED REQUESTERS MAY OBTAIN COPIES OF THIS REPORT FROM DDC

11. SUPPLEMENTARY NOTES	12. SPONSORING MILITARY ACTIVITY
	NAVAL SHIP SYSTEMS COMMAND WASHINGTON, D. C. 20360

13. ABSTRACT

Effects of faired, streamwise gaps upon the free stream characteristics of a family of low-aspect-ratio, all-moveable control surfaces are presented. The family of control surfaces consisted of three aspect ratios (1, 2, and 3) and three sweep angles (0, 11, and 3) and three sweep angles (0, 11 and 22.5 degrees), each having a NACA 0015 airfoil section and a taper ratio of 0.45. Gap effects were also investigated in conjunction with simulated hull effects. Propeller slipstream effects were determined for the minimum gap condition.

DD FORM 1 JAN 64 1473

UNCLASSIFIED
Security Classification

14. KEY WORDS	LINK A		LINK B		LINK C	
	ROLE	WT	ROLE	WT	ROLE	WT
CONTROL SURFACES MARINE RUDDERS LOW ASPECT RATIO WINGS STREAMWISE GAPS HULL EFFECTS PROPELLER SLIPSTREAM						

INSTRUCTIONS

1. ORIGINATING ACTIVITY: Enter the name and address of the contractor, subcontractor, grantee, Department of Defense activity or other organization *(corporate author)* issuing the report.

2*a*. REPORT SECURITY CLASSIFICATION: Enter the overall security classification of the report. Indicate whether "Restricted Data" is included. Marking is to be in accordance with appropriate security regulations.

2*b*. GROUP: Automatic downgrading is specified in DoD Directive 5200.10 and Armed Forces Industrial Manual. Enter the group number. Also, when applicable, show that optional markings have been used for Group 3 and Group 4 as authorized.

3. REPORT TITLE: Enter the complete report title in all capital letters. Titles in all cases should be unclassified. If a meaningful title cannot be selected without classification, show title classification in all capitals in parenthesis immediately following the title.

4. DESCRIPTIVE NOTES: If appropriate, enter the type of report, e.g., interim, progress, summary, annual, or final. Give the inclusive dates when a specific reporting period is covered.

5. AUTHOR(S): Enter the name(s) of author(s) as shown on or in the report. Enter last name, first name, middle initial. If military, show rank and branch of service. The name of the principal author is an absolute minimum requirement.

6. REPORT DATE: Enter the date of the report as day, month, year; or month, year. If more than one date appears on the report, use date of publication.

7*a*. TOTAL NUMBER OF PAGES: The total page count should follow normal pagination procedures, i.e., enter the number of pages containing information.

7*b*. NUMBER OF REFERENCES: Enter the total number of references cited in the report.

8*a*. CONTRACT OR GRANT NUMBER: If appropriate, enter the applicable number of the contract or grant under which the report was written.

8*b*, 8*c*, & 8*d*. PROJECT NUMBER: Enter the appropriate military department identification, such as project number, subproject number, system numbers, task number, etc.

9*a*. ORIGINATOR'S REPORT NUMBER(S): Enter the official report number by which the document will be identified and controlled by the originating activity. This number must be unique to this report.

9*b*. OTHER REPORT NUMBER(S): If the report has been assigned any other report numbers *(either by the originator or by the sponsor)*, also enter this number(s).

10. AVAILABILITY/LIMITATION NOTICES: Enter any limitations on further dissemination of the report, other than those imposed by security classification, using standard statements such as:

(1) "Qualified requesters may obtain copies of this report from DDC."

(2) "Foreign announcement and dissemination of this report by DDC is not authorized."

(3) "U. S. Government agencies may obtain copies of this report directly from DDC. Other qualified DDC users shall request through _____."

(4) "U. S. military agencies may obtain copies of this report directly from DDC. Other qualified users shall request through _____."

(5) "All distribution of this report is controlled. Qualified DDC users shall request through _____."

If the report has been furnished to the Office of Technical Services, Department of Commerce, for sale to the public, indicate this fact and enter the price, if known.

11. SUPPLEMENTARY NOTES: Use for additional explanatory notes.

12. SPONSORING MILITARY ACTIVITY: Enter the name of the departmental project office or laboratory sponsoring *(paying for)* the research and development. Include address.

13. ABSTRACT: Enter an abstract giving a brief and factual summary of the document indicative of the report, even though it may also appear elsewhere in the body of the technical report. If additional space is required, a continuation sheet shall be attached.

It is highly desirable that the abstract of classified reports be unclassified. Each paragraph of the abstract shall end with an indication of the military security classification of the information in the paragraph, represented as *(TS), (S), (C), or (U)*

There is no limitation on the length of the abstract. However, the suggested length is from 150 to 225 words.

14. KEY WORDS: Key words are technically meaningful terms or short phrases that characterize a report and may be used as index entries for cataloging the report. Key words must be selected so that no security classification is required. Identifiers, such as equipment model designation, trade name, military project code name, geographic location, may be used as key words but will be followed by an indication of technical context. The assignment of links, roles, and weights is optional.